Addis Ababa University

Ethiopian Institute of Water Resources

PhD Program in Water Resources Engineering and Management

Non-Point Source Pollution Modelling: Leveraging SWAT with Remote Sensing and GIS Technologies

Endaweke Assegide Chebude

Addis Ababa University

Addis Ababa Ethiopia

December 2024

Non-Point Source Pollution Modelling: Leveraging SWAT with Remote Sensing and GIS Technologies

Endaweke Assegide

A Dissertation Submitted to the Ethiopian Institute of Water Resources, Addis Ababa University

Presented in Fulfilment of the Requirements for the Degree of Doctor of Philosophy in Water Resources Engineering and Management (Surface Water Management)

Supervisors:
Gete Zeleke (Ph.D.)
Water and Land Resource Centre, Addis Ababa University

Tena Alamirew (Ph.D.)
Ethiopian Institute of Water Resources, Addis Ababa University

Addis Ababa University
Addis Ababa Ethiopia
December 2024

Declaration

I, the undersigned, declare that this dissertation has been composed solely by myself and that it has not been submitted, in whole or in part, in any previous application for a degree or any other qualification. Except where duly stated by references or acknowledgments, the work presented in this dissertation is entirely my own.

This Dissertation has been submitted for examination with my approval as the student's supervisor.

Supervisor Name:	Signature:	Date:
Gete Zeleke (PhD)		12/02/2024
Tena Alamirew (PhD)		12/02/2024

Dissertation approval

This is to certify that the dissertation prepared by Endaweke Assegide Chebude entitled, "**Non-Point Source Pollution Modelling Using SWAT and Remote Sensing and Geographic Information System,**" is submitted in fulfillment of the requirement of the Degree of Doctor of Philosophy (Ph.D.) in Water Resources Engineering and Management (Surface Water Management) complies with regulation of the University and meets the accepted standard concerning originality and quality.

Examining committee signature

Niguse Tekle (PhD)	
Chair, examining committee	Signature
Mulugeta Dadi (PhD)	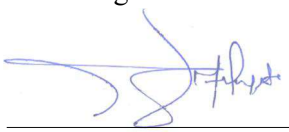
External examiner	Signature
Sirak Tekleab (PhD)	
Internal examiner	Signature
Agizew Niguse (PhD)	
Internal examiner	Signature
Gete Zeleke (PhD)	
Major advisor	Signature
Tena Alamirew (PhD)	
Co-advisor	Signature

List of Original Papers

Assegide, E., Alamirew, T., Bayabil, H., Dile, Y. T., Tessema, B., & Zeleke, G. (2022). Impacts of Surface Water Quality in the Awash River Basin, Ethiopia: A Systematic Review. *Frontiers in Water*, *3*(790900), 1–15. https://doi.org/10.3389/frwa.2021.790900 (Published)

Assegide, E., Alamirew, T., Dile, Y. T., Bayabil, H., Tessema, B., & Zeleke, G. (2022). A Synthesis of Surface Water Quality in Awash Basin, Ethiopia. *Frontiers in Water*, *4*(782124), 1–17. https://doi.org/10.3389/frwa.2022.782124. (Published)

Assegide, E., Shiferaw, H., Tibebe, D., Peppa, M. V., Walsh, C. L., Alamirew, T., & Zeleke, G. (2023). Spatiotemporal Dynamics of Water Quality Indicators in Koka Reservoir, Ethiopia. *Remote Sensing*, *15*(4), 1155. https://doi.org/10.3390/rs15041155. (Published)

Assegide, E., Alamirew, T., and Walsh, C. L., and Gete, z., "Prioritizing Watersheds for Intervention Design Using GIS and Remote Sensing," J. Environ. Earth Sci., vol. 07, no. 01, pp. 167–195, 2025, doi: https://doi.org/10.30564/jees.v7i1.6887. (Published)

Assegide, E., Alamirew, Kassew, B., & Zeleke, G. (2024). Assessing Non-Point Source Pollution in a Rapidly Urbanizing Sub-Basin to Support Intervention Panning. Manuscript ID: water-3131210. (Published)

Table of Contents

LIST OF TABLES

List of Figures

List of Appendixes

Abbreviations and Acronyms

AGWA	Automated Geospatial Watershed Assessment
ARS	Agricultural Research Institute
BASIN	Better Assessment Science Integrating Point and Nonpoint Sources
BMPs	Best Management Practices
CA	Cluster Analysis
CCME	Canadian Council of Ministers of the Environment
CFSR	Climate forecast system analysis
DDT	Dichlorodiphenyltrichloroethane
DPC	Dissolved Phosphorus Concentration
DWG	Drinking water guideline
EDWQ	European drinking water quality
EEPA	Ethiopia Environmental Protection Authority
EMC	Event mean concentration
WFD	Water Framework Directive
FEPA	Federal Environmental Protection Authority
HSPFEXP	Expert system for calibration of HSPF
KINEROS	Kinematic runoff and erosion model
MUSLE	Modified Universal Soil Loss Equation
NEQS	National Environmental Quality Standards
NOAA	National Oceanic and Atmospheric Administration
PCA	Principal component analysis
PLI	Pollution load index
RSC	Residual Sodium Carbonate
SDG	Sustainable Development Goal
STD	Secchi disc Transparency Depth
TAC	Total Aerobic Count
TAN	Total Ammonium Nitrogen
USEPA	United Sates Environmental Protection Agency
WQP	Water Quality parameter

Acknowledgments

I want to express my gratitude to Dr. Gete Zeleke and Dr. Tena Alamirew, my supervisors, for all of their patient advice, support, and direction. I consider myself very fortunate to have a supervisor who genuinely cares about my work and who always gets back to me with concerns. Their unwavering commitment to the topic and support have been extremely helpful to my growth as a researcher and the development of this dissertation. They also gave me the chance to transform the scant and data-poor opportunity of researching typical environmental issues in the upper Awash sub-basin into this Ph.D. Dissertation.

I also want to express my gratefulness to those of the Water and Land Resource Centre who assisted directly with the process of producing this dissertation and indirectly by facilitating the fieldwork data collection. Finally, I would like to thank the Water and Land Resource Centre, not only for providing the funding which allowed me to undertake this research but also for allowing me to go to international conferences and interact with a wide range of wonderful individuals.

A special appreciation goes to the EIWR staff for supporting me with my research and helping me with all my needs during my stay as a student. I want to express special thanks to my colleagues for their encouragement and kindly sharing their opinions.

My family has shown me so much love, support, encouragement, and prayers during this journey that words cannot describe. I must express my gratitude to Yeshizer Muche, my wife, for her continued support and encouragement. I want to express my appreciation to Arsema, Bethlehem, and Afomia Endaweke, my children, for tolerating and giving me time during my study and the completion of the dissertation.

Abstract

In many places across the world, non-point source pollutants (NPSP) are the primary threat to aquatic ecology and the primary cause of surface water deterioration. Because pollutants and waste may be dumped easily into the surface waters, they are especially vulnerable to pollution. NPSs contaminate surface water more than point sources do. Fertilizers, herbicides, oil, silt, and nutrients from animals and malfunctioning septic tanks can all contribute to NPSP. It has several negative impacts on aquatic life, including their invasion and a rise in the amount of suspended matter that blocks light and damages plant life in water. Eutrophication is the outcome of an increase in the rate at which ecosystems receive organic materials. For example, Koka Reservoir regularly experiences algal blooms due to the reservoir's nutrient load. Remedial measures are complex due to their widespread nature.

To assess the problem of water quality and the effects of water quality (WQ), a systematic review was conducted using PRISMA (Preferred Reporting Items for Systematic Review and Meta-Analysis Statement). The synthesis points out the following gaps: Inadequate evidence-based research on the effects of contaminated water on agriculture, health, and socioeconomics; a lack of combined spatial and temporal surface water quality data and monitoring; a lack of relative contribution from non-point sources; a lack of detailed integrated spatial and temporal water quality impact; and policy responses for surface water quality drivers for the case studies have received scant attention nationally and in the basin for the identified gaps.

This research work is designed to evaluate the non-point source pollutants load, prioritize the sub-watersheds based on the sediment load, LULC, and morphometric characteristics using hydrologic modeling, and develop a remote sensing-based water quality model. Several strategies were used to accomplish the designated goals. We used a variety of primary and secondary data sources. Analysis was done on the land use and land cover in 2023 and 2003. Primary data was gathered, including modeling work data and lake water quality analysis from the Koka Reservoir. For a year, water quality data for non-point source pollution modeling was collected every month from the Melka Kunture gauging stations.

The remote sensing technology was used to determine the spatiotemporal water quality condition of the Koka reservoir and develop a water quality model. To study the spatiotemporal dynamics of water quality indicators at Koka Reservoir, a Sentinel-2 satellite remote sensing data collection was used to develop a water quality monitoring model. For the annual scale, the temporal studies of water quality parameters were carried out from 2017 to 2022; for the monthly scale, it was carried out from June 2021 to May 2022. Regression analysis and empirical model development were used to develop algorithms that correlated satellite reflectance data with in situ measurements of turbidity (TU), total suspended matter (TSS), and chlorophyll-a (Chl-a). The determination coefficients (R^2) for each of the examined parameters are higher than 0.67, suggesting that they can all be used to develop predictive models. Good correlations between field-based and calculated Chl-a, TU, and TSS have been found, as indicated by the developed algorithms' respective R^2 values of 0.91, 0.92, and 0.67.

The multi-criteria decision-making, AHP-VIKOR, and hydrological modelling were used for sub-watershed prioritizing. The findings indicated that 2524.6 km^2 (25.45%) is in the high sensitivity class, 2722.14 km^2 (27.44%) is in the moderate sensitivity class, 854.35 km^2 (8.61%) is in the low sensitivity class, 2205.48 km^2 (22.23%) is in the very low sensitivity class, 1611.43 km^2 (16.25%) is in the class of very high erosion sensitivity. We evaluated and created linear function models to estimate WQ indicators, including Chl-a, turbidity, and TSS, using the Sentinel-2 image band ratios of B5/B4, B4/B3, and B4, respectively. The built-up area and agricultural land grew by 80.15% and 147.29%, respectively. There was a reduction of 47.55%, 96.7%, and 74.37% in forest, grassland, and shrubland, respectively.

The BASIN and SWAT models are the most effective for assessing point and NPS contamination in various basins. SWAT was used to examine the spatial and temporal variation of the non-point source pollutants NO_3^-, PO_4^{3-}, TN, and TP. The 2003 and 2023 LULCs were the main data sources used to evaluate the change in NPSP loads. The Melka Kunture gaging station non-point source pollution modeling was calibrated and validated between 2009 and 2014 and 2015 and 2019, respectively. The sensitivity analysis led to the selection of nine nutrient-related parameters for calibration. The most critical parameters are the phosphorus uptake distribution (R_P_UPDIS.bsn), the phosphorus percolation coefficient (10 m3/Mg) (R_PPERCO.bsn), and the organic P settling rate (R_RS5.swq). For the calibration and the validation periods, the results revealed good and very good performance. While the mean annual increase in surface runoff ranges from 183.1 mm to 487.9 mm, the mean annual increase in sediment yield ranges from 25.46 to 27,298.75 t. Runoff ranged from a minimum of 10.69 mm (5.1%) to a maximum of 223.3 mm (66.5%). The PO_4^{3-} load went from 3.12 to 2459.7 kg, and the NO_3^- burden went from 127.6 to 20,739.7 kg. The TP load went up from 1383.5 to 133,641.3 kg, and the TN load went up from 4465.5 to 482,014.5 kg. According to the monthly nitrate loading analysis, the “Belg” season, the second rainy time from February to May when rainfall is highly variable in time and space, has a higher nitrate load than the rainy season, probably due to nitrification. The LULC alteration increased surface runoff and NPSP loads (nitrate, phosphate, total nitrogen, total phosphorous, and sediment).

The study demonstrated that Sentinel-2A-derived regression models can support the spatiotemporal estimation and mapping of the annual and monthly patterns of Chl-a, TU, and TSS over the Koka reservoir. This enables improved capacity to analyze reservoir status and strategies for water resource management. The algorithms could potentially be useful as a monitoring tool for water quality in other regions in the country or other data-scarce areas of the world with comparable environmental and hydro-climatic contexts. The low operational cost of using freely available remotely sensed imagery is a strong incentive for water agencies to complement their field campaigns and produce spatially distributed maps of some water quality parameters. A more complete indicator of erosion risk in a watershed is the multiple values of morphometric parameters, LULC, and sediment load. For planners and decision-makers to comprehend the morphological, LULC, and sediment load characteristics of any particular sub-watershed for

planning at the sub-catchment level, AHP-VIKOR, GIS, and remote sensing approaches are more effective. LULC changes at a sub-watershed level by varying ranges of load had an impact on runoff and non-point source pollutant loading, including sediment, PO_4^{3-}, NO_3^-, TP, and TN, as results revealed. The growth of built-up areas in response to the need for settlement and the rising change in agricultural land were the main causes of the increases in runoff volume, sediment, PO_4^{3-}, NO_3^-, TP, and TN over two decades.

Keywords: sub-watershed prioritization, water quality, surface water, Koka reservoir, upper Awash, morphometric parameters, VIKOR, remote sensing.

Chapter 1 GENERAL INTRODUCTION

1.1. Background

Water resources are important natural resources essential to the production, the advancement of society, the long-term sustainability of food supplies, and playing a bigger role in the growth of many sectors (Kılıç, 2020). Despite Ethiopia's reputation as the "water tower of Africa," pressures on water security pose a threat to the country's growth and advancement. Growing and conflicting water needs can also result from economic expansion in all areas of the economy. (Lin et al., 2022).

The Awash Basin, due to its advantageous position, accessible highways, and plenty of land and water resources, is the most heavily used river basin. Nonetheless, the basin has several challenges, including significant environmental deterioration, yearly floods, inappropriate use of land and water resources, socioeconomic limitations, subpar agricultural methods, low yields, and issues with community health (Taddese et al., 2004). The basin is home to the majority of Ethiopia's extensive, heavy machinery-based governmental and private irrigated fields. The available water in the basin is under growing pressure due to the rapid expansion of industry, growing cities, the agriculture sector, and population. Due to more demand for water than there is supply, the basin is currently facing water stress (Taye et al., 2018). Upper Awash is the home of major agricultural investments as well as more than three-fifths of the nation's industries. The upper Awash sub-basin is one of Ethiopia's most significant sources of water supply due to the past and present use of water for different purposes, like domestic, industrial, and animal needs (Birhanu et al., 2021).

Numerous studies have been conducted on the issue of surface water quality in Ethiopia, generally and in the Awash Basin, specifically. These studies, as well as their data, weren't organized to give a comprehensive picture of the problem with water quality and the state of the surface water in the various basins across the nation and the study area. Due to this, it was difficult to identify gaps that needed to be filled and reduce or prevent duplication of research on nearly identical topics and issues in one particular area. So that the review section of this research work tried to synthesize the status and impact of surface water quality in the basin to justify the proposed research title acceptable to be done. Similarly, in the scientific community, choosing the best research method is a challenging and perplexing task, which helps figure out what kind and how much data the research requires (Opoku et al., 2016). To solve such a gap thirteen hydrological models of water quality were assessed in order to achieve the objective of the study.

Surface water resources are easily accessible for the dumping of waste and contaminants because they are particularly prone to contamination. The contamination of water will worsen as a result of both natural processes like soil erosion and sedimentation and human-caused activities like industry, urbanization, runoff from farming, building, and residential activities (Wondim, 2016). Assessing the water's suitability for a certain application requires monitoring its quality. Urban places in Africa where the lack of adequate testing equipment and capacities significantly limits attempts to monitor water quality (Chen et al., 2022). Over the last several decades, there has been a growing need to regularly evaluate different water quality factors to monitor the quality of surface water (Wondim, 2016). However, the basin lacks sufficient monitoring and data at both the location and time-based levels.

Rapid population growth, uncontrolled industrialization, urban sprawl, and poor waste management practices have left Addis Ababa extremely polluted, endangering both human health and the health of the ecosystem as a whole. About 25% of homes in the city lack a toilet (Welde, 2016). About 30% of city residents lack access to a facility for the dumping and treatment of liquid waste (Yohannes & Elias, 2017). The Akaki River is the country's most contaminated river system by untreated and insufficiently treated industrial wastewater, domestic wastes, residential and commercial operations, and sewage released into rivers. The Mojo River sub-basin in the Awash River basin is also another contaminated river, which consists of several industries disposing directly into the river and then to the Koka reservoir without appropriate treatment (Gebeyehu & Bayissa, 2020).

Non-point source (NPS) pollution is the consequence of excessive use of pesticides, fertilizers, animal manure, untreated waste water and solid waste. It is caused by agricultural growth, rural land use, and unregulated urban runoff (Liu et al., 2015). In many parts of the world, NPS pollution is now the main hazard to the aquatic ecosystem. For instance, NPS contamination has been the main factor causing impairments in over 33,000 waterways in the United States; these waters account for about 75% of all impaired waters (Zheng et al., 2014). Currently, the main factor causing surface water degradation in many nations, including the UK, USA, and China, is NPS pollution. Because of its complex nature and development, NPS pollution is challenging to regulate and control, particularly in data-sparse areas (Liu et al., 2015).

Surface water is more polluted by non-point sources of pollutants than by point sources of pollutants (Jones-lee et al., 2000). In sub-Saharan Africa, comparatively little is understood regarding non-point source contamination (Lee & Jones-Lee, 1999). According to (Moges et al., 2017a), in the Ethiopian context, non-point source sediment and nutrient influx to Lake Tana, together with a high rate of erosion from the watersheds, were the causes of the lake's declining water quality trend. Assegide (2022) states that determining the relative contributions from diffuse and point sources is a significant area of unmet research need in both the country and the Awash River basin. Research on non-point-source pollution, from urban or agricultural sources, is lacking both nationally and in the basin.

Land degradation and soil erosion are one of the most common issues in Ethiopia's highlands, where a significant quantity of productive soil is lost annually (Gela, 2018). Due to substantial livestock density, large population, and extensive cultivation, soil erosion is one of the main deteriorating processes that cause soil loss and diminish crop production in Ethiopia (Anteneh, 2022). Wide-ranging off-site effects of soil erosion include water quality degradation, the deposition of sediments, consequent diversion of stream channels, and the breakdown of infrastructure. Ethiopia loses almost 1.5 billion tons of topsoil annually from its highlands due to erosion. Soil erosion is a major issue that damages dams and reservoirs, wetland regions, lakes, and aquatic ecosystems in Ethiopia. It also causes issues with the water level, volume, and surface area of reservoirs. For example, the Koka Dam reservoir's yearly storage capacity loss was 17 million cubic meters due to sedimentation. Since soil erosion lowers the land's potential for production and exacerbates poverty and food insecurity, it is one of the many issues impacting the livelihoods of farmers, crop yield, and sustainability (Gela, 2018). One method utilized to decrease

erosion and the resulting nutrient loss is the conservation of soil and water, which lowers the risk of production (Anteneh, 2022).

Development programs for natural resources (land and water) must begin at the micro-watershed level, where all hydrological processes start. This is due to the following reasons: cost savings through resource allocation optimization and a reduction of the need for large infrastructure investments necessary for larger-scale developments; increased community involvement in development programs, as residents are more likely to participate in projects that directly affect their immediate environment; and greater implementation flexibility compared to larger-scale initiatives. It is imperative to commence development-oriented management operations with the most vulnerable sub-watersheds. As a result, the sub-watersheds that are part of the main watershed must be given priority (Welde, 2016). The research area is generally experiencing all of the previously described problems.

1.2. Statement of the Problem

Excessive grazing and crop production are major causes of water body pollution through runoff that carries harmful substances into aquatic ecosystems. This issue is worsened by poor farming practices that release harmful chemicals into the environment, such as the improper use of fertilizers, pesticides, and herbicides (Ahuja, 2013). The infiltration of fertilizers into water systems due to rainwater runoff from agricultural fields exacerbates this issue, leading to increased concentrations of phosphorus, nitrogen, and both suspended and dissolved sediments in surface waters. These changes contribute significantly to eutrophication (Ahuja, 2013). This has several effects, like the overgrowth of aquatic plants and increases in total suspended particles that obstruct light are harmful to aquatic plants (Karatas, 2015). Water quality is further compromised by urban waste disposal methods, which raise pollution levels (MoWIE, 2017). The prevalence of non-point source pollutants (NPSP) originating from agricultural practices poses a substantial threat to drinking water sources. The chemical pollution resulting from NPSP has emerged as a critical issue in water resource management (Karamouz et al., 2008; Burwell et al., 1975). Furthermore, non-point sources of pollutants are a source of pollution for surface water, and their contribution was not quantified, or their spatial variation was not examined; this problem is underscored by the extensive distribution of these pollutants, their potential long-term impacts on human health, and the degradation they cause to aquatic ecosystems (Corwin et al., 1998), these are the major gaps identified in the basin's assessment. Given the complexity of remediation efforts required to address NPSP contamination and its far-reaching consequences on both human health and environmental quality, there is an urgent need for comprehensive research aimed at the specific contributions of NPSPs to water contamination in the Upper Awash Sub-basin.

The lakes and reservoirs in Ethiopia, and specifically in the study area, are not regularly and continuously monitored to know their state of quality (Babiso et al., 2023). The reservoir receives contaminated water from the upstream areas of the main Awash and Mojo rivers because of its position as trapping for these rivers. The major Awash River is joined by the highly polluted Big and Little Akaki Rivers. Because of the reservoir's nutrient load, blue-green algal blooms frequently occur (Assegide et al., 2023). The Koka reservoir is currently experiencing these difficulties. There hasn't been any research done on the issues in the past with the lake's continious

monitoring or the reservoir's overall spatiotemporal water quality status. Given its significancefor the health of the aquatic ecosystem and for the dawn stream areas and the local population, where it serves as a supply of water for many reasons, scientific research is crucial to resolving the problems.

In developing countries, the development of water resources and sustainable land management are threatened by problems with soil erosion and sedimentation (Adhami & Sadeghi, 2016). Soil erosion is a prevalent problem in Ethiopia that affects lakes and results in problems with water level, volume, surface area dams and reservoirs, harmed wetland areas and disrupts aquatic ecosystems (Abhachire, 2014; Girma, 2016; Issaka & Ashraf, 2017; Tuppad et al., 2017). Every year, erosion causes Ethiopia to lose more than 1.5 billion tons of topsoil from its highlands (Tamene & Vlek, 2008). Although few studies have investigated erosion rates and dynamics, it is thought that catchment erosion quickly causes storage loss and nutrient loss. On agricultural land, soil erosion reduces the quality of surface water, ruins drainage systems, and diminishes crop yield potential (Desta, 2005). Changes in certain plant types and species coverage significantly affect the change in the sediment load (Miao et al., 2012). To develop suitable corrective actions, land use changes must be evaluated as a significant sediment loading factor (Babel et al., 2021). Sediment yield increases when agricultural land expands and forest area decreases (Miao et al., 2012) (Sinha & Eldho, 2018).

Most rivers have high sediment loads due to soil erosion, negligent agricultural methods that permit plows to reach the riverbanks, and a lack of terrace construction to reduce water runoff. As a result of this, the majority of rivers have muddy brown water (Ahuja, 2013). This is the state of situations in different rivers in the research area as shown in Figure 1-1. No research or action takes into account different variables for prioritizing the Upper Awash Sub-basin. These kinds of problems can be resolved by the application of watershed management techniques, however, it is highly challenging to address each sub-watershed simultaneously. Watersheds must be ranked according to how vulnerable they are to soil erosion to solve the issues. Scientific studies that take into account many factors should be conducted in order to address the aforementioned problems and suggest which sub-watersheds should receive priority attention for planning and action.

(a)

19 July 2020

(b)

19 March 2020

(c)

20 May 2020

Figure 1-1 Photograpgh taken from different rivers in the study area: Awash river and Akaki river junction (a), Jala river (b), Hombole river (c), main Awash river (d), Alito river (e). Photo taken by Endaweke Assegide.

1.3. Research questions

The following research questions were formulated:

1. What are the key morphometric and hypsometric characteristics that influence soil erosion susceptibility in sub-watersheds within the Upper Awash Sub-Basin, and how can these

characteristics be quantitatively analyzed to prioritize sub-watersheds for conservation efforts?
2. How can a remote sensing data set be utilized to model and predict key water quality indicators such as chlorophyll-a, TDS, and TU in Koka reservoir using Sentinel-2 remote sensing data?
3. How severely does the land use/cover transformation impact non-point source pollution and hydrological processes?

1.4. Objectives

1.4.1 General Objectives

To use cutting-edge remote sensing and GIS technologies to conduct thorough evaluations of water quality, watershed characterstics, and pollution dynamics in order to enhance sustainable water resource management.

1.4.2 Specific Objectives

1. To apply Sentinel-2 imagery for water quality assessment, map the spatiotemporal dynamics of chlorophyll-a, turbidity, and total suspended solids of the Koka reservoir, and develop a model that can be adopted as a future application as a water quality monitoring tool.
2. To prioritize sub-watersheds based on their LULC, sediment load, and morphometric parameters.
3. To model and examine LULC change and its impact on runoff and non-point source pollutants, map the sub-watersheds based on pollutant load and quantify spatiotemporal non-point source pollutants.

1.5. Significance of the study

The knowledge gained from this research will be crucial for managing, preserving, protecting, and/or restoring natural resources in settings with comparable stress. Therefore, it provides reliable information for policymakers to formulate rules and regulations to safeguard natural resources and balance competing social, economic, and environmental demands.

Research into linear regression empirical model development for water quality monitoring using sentinel 2A remote sensing data has significantly advanced our understanding and capabilities in environmental monitoring. It provides a systematic approach to assess and predict water quality across vast regions efficiently. Applying linear regression empirical models in conjunction with sentinel 2A remote sensing data provides a powerful tool for monitoring water quality over large spatial scales efficiently and effectively. In addition to this, it is used to design options for a water quality monitoring tool for data-scared areas to consistently assess the quality of lakes and reservoirs across various locations. By leveraging statistical relationships derived from historical data, researchers and environmental managers can gain insights into aquatic ecosystems' health and make informed decisions regarding conservation efforts.

The key knowledge contributed by integrating AHP-VIKOR with morphometric analysis, LULC considerations, and sediment yield assessments lies in its ability to provide a comprehensive

framework for prioritizing watershed management strategies. This methodology not only identifies vulnerable areas but also supports informed decision-making aimed at sustainable land use practices. The method contributed by AHP-VIKOR research incorporates morphometric parameters along with Land Use/Land Cover (LULC) considerations and sediment yield analysis, providing a robust framework for prioritizing sub-watersheds at risk of erosion.

The SWAT model research will significantly advance our understanding of how land use changes impact non-point source pollutants by providing quantitative data on pollutant loads, identifying critical areas for intervention, and predicting future trends under various land use change scenarios. The study will be a crucial baseline for further study in the identified gaps and using the research results in watersheds with similar agro-ecologies.

1.6. Scope of the study

The upper Awash sub-basin, where 37 sub-watersheds were identified during the modelling setup, served as the study's site. The sub-watersheds with an area of greater than 8000 ha were the minimum thresholds applied during the watershed delineation. The study takes into account the state of water pollution and the significant impact of the Awash Basin's water quality. This served as justification for the issues raised in the research area for future investigation. Only the three parameters of turbidity, total suspended sediment, and chlorophyll-a were considered in the modelling and evaluation of remote sensing-based water quality analysis in the Koka reservoir. The SWAT model was employed for the non-point source pollutant modelling, and analyses were conducted on runoff, sediment, nitrate (NO_3^-), phosphate (PO_4^{-3}), total nitrogen (TN), and total phosphorous (TP) loading. Other parameters like biological parameters, pesticides, and heavy metals were not taken as part of the modelling work. In addition to this, point source pollutants are not part of this study. This study is generally limited to surface water quality-related issues.

1.7. Structure of the dissertation

There are six chapters in this dissertation. Chapter 1 presents the general introduction, statement of the problem, research questions, general and specific objectives, the significance of the study, the scope of the study, a description of the study area, and the overall structure of the dissertation. With a specific objective of identifying gaps in the status of surface water quality, Chapter 2 addresses surface water quality issues as well as the state of surface water quality in the basin at specific and national levels. This chapter tried to point out the status of water quality monitoring, the details of surface water quality impairment indicators, and the causes of water quality impairment. In particular, it discourses the knowledge gap regarding surface water quality's effects in various contexts, including biological, socioeconomic, toxic, health, vegetable, and soil contexts, and it identifies issues and gaps for future research. Moreover, it addresses the appropriate water quality model selection for non-point source pollutant modelling. Using input data, strengths, limitations, spatial extent, temporal variability, capabilities in simulation, the components they have, type, nature, complexity, time step, hydrology, system, model category, intended usage, development, fundamental principle, supported land and water features, total maximum daily load (TMDL) support, operation, and pollution handling, this chapter attempted to evaluate thirteen hydrological water quality models. Chapter 3 is devoted to the second objective of the dissertation. This chapter mainly focused on evaluating the spatiotemporal water

quality using three water quality indicators: chlorophyll-a, turbidity, and total suspended matter. In addition to this, it discusses the water quality model development. Chapter 4 discusses the fourth specific objective of sub-watershed prioritization. This chapter mainly focused on the application of combined methods like GIS and Remote Sensing (RS), SWAT model, multi-criteria decision making (MCDM), Analytic Hierarchy Process (AHP), and Vlse Kriterijumska Optimizacija Kompromisno Resenje (VIKOR) by considering multi parameters for watershed prioritization. It also showed the spatial distribution of the sensitivity of watersheds. Chapter 5 discusses the last specific objective, which deals with the impact of the LULC on non-point source pollution, the spatial and temporal variations of the non-point source pollutants, and the mapping of the sub-watersheds based on surface runoff, sediment, nitrate, phosphate, total nitrogen, and total phosphorous loads. Chapter 6 is the concluding chapter, which discusses and integrates the results of the previous chapters. The problems and unmet research needs in the basin, the benefit of using publicly accessible remote sensing data for surface water quality monitoring, and conclusions for the potential future use of the findings looked into by planners and decision-makers. Figure 1-2 shows the general structure of the research.

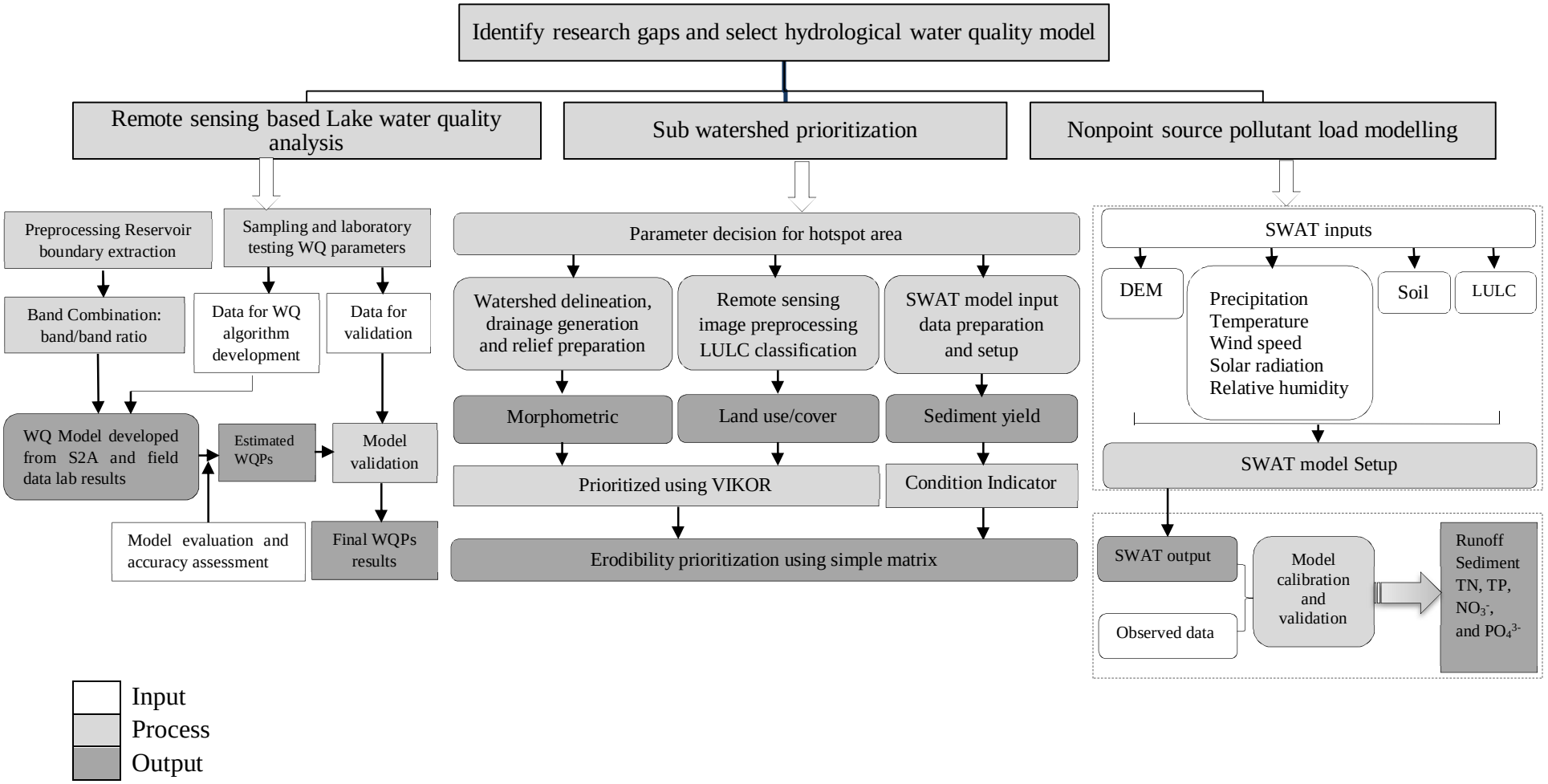

Figure 1-2 Schematic diagram illustrating the comprehensive research work employed in this study

1.8. Research methods

Awash is fed by several major tributaries in the upper, middle, and lower parts of the basin. Ginchi, Berga, Holleta, Bantu, Leman, Akaki, Mojo, Hombole, Arba I, Arba II, Keleta, Kesem, Najeso, and Logia are the major tributaries of the upper Awash (Amenu, 2013). The Awash River Basin is one of Ethiopia's 12 major river basins, which is shared by five administrative regions (Amhara, Oromia, Somali, Afar, and the Southern Region) (Mersha et al., 2018). The Upper Awash River Basin is the upper part of the Awash River Basin, one of the twelve major basins of Ethiopia, covering an area of 9918.1 km^2. Upper Awash basin (upstream to Koka reservoir), located in Central Ethiopia at the upper Awash Basin between 8° 23' 09'' and 9° 18' 14'' latitude and 37° 57'15'' and 38° 41' 08'' longitude. There are thirteen major settlements, including the capital city, located at the northern end of the basin, in order of largest to smallest: Addis Ababa, Bishoftu, Mojo, Dukem, Koka, Ginchi, Addis Alem, Sebeta, Holeta, Teji, Asgori, Tulubolo, and Wolenkomi. Addis Ababa city is located in the Akaki catchment; Mojo, Dukem, and Bishoftu are located in the Mojo catchment; Holeta, Teji, Asgori, Tulubolo, Addis Alem, Ginchi, and Wolenkomi are located in the Melka Kunture catchment and Koka in the Koka catchment (Birhanu et al., 2021). Some of the main streams that comprise the upper Awash River basin are the Holeta, Berga, Akaki, and Melka Kuntire streams, each of which flows into the main Awash River Figure 1-3 (Tessema et al., 2015).

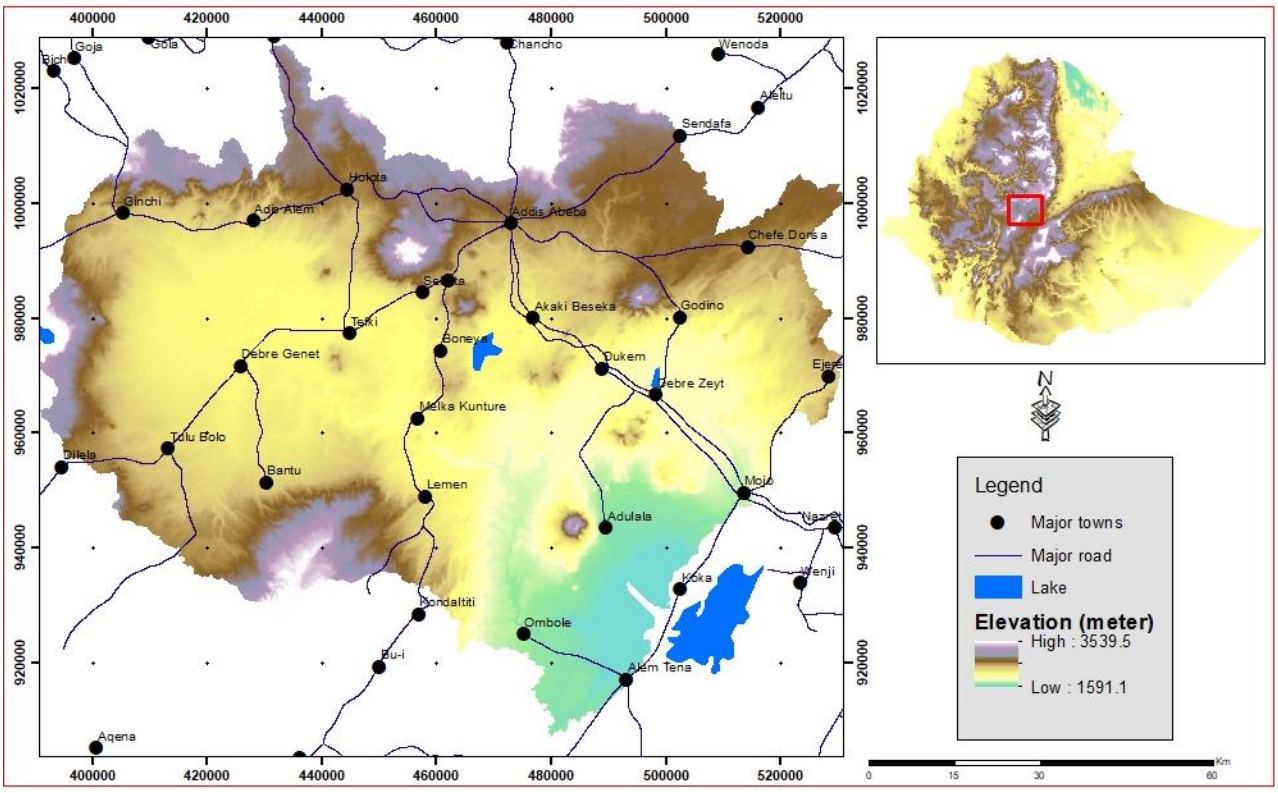

Figure 1-3 Map of the study area

1.8.1 Systematic review

The purpose of the systematic review was to identify research gaps related to the problem of water quality and the effects of that quality in various socioeconomic and environmental contexts, particularly in the Awash basin and throughout Ethiopia. A useful method for conceptualizing and synthesizing results from massive volumes of data is systematic review (SR) (Özerol et al., 2018). PRISMA (Preferred Reporting Items for Systematic Review and Meta-Analysis Statement) (Moher et al., 2009) was used to conduct the systematic review paper. The PRISMA Checklist 2009 literature search, evaluation process, and inclusion decision-making served as the foundation for the selection criteria (in Figure 1-4).

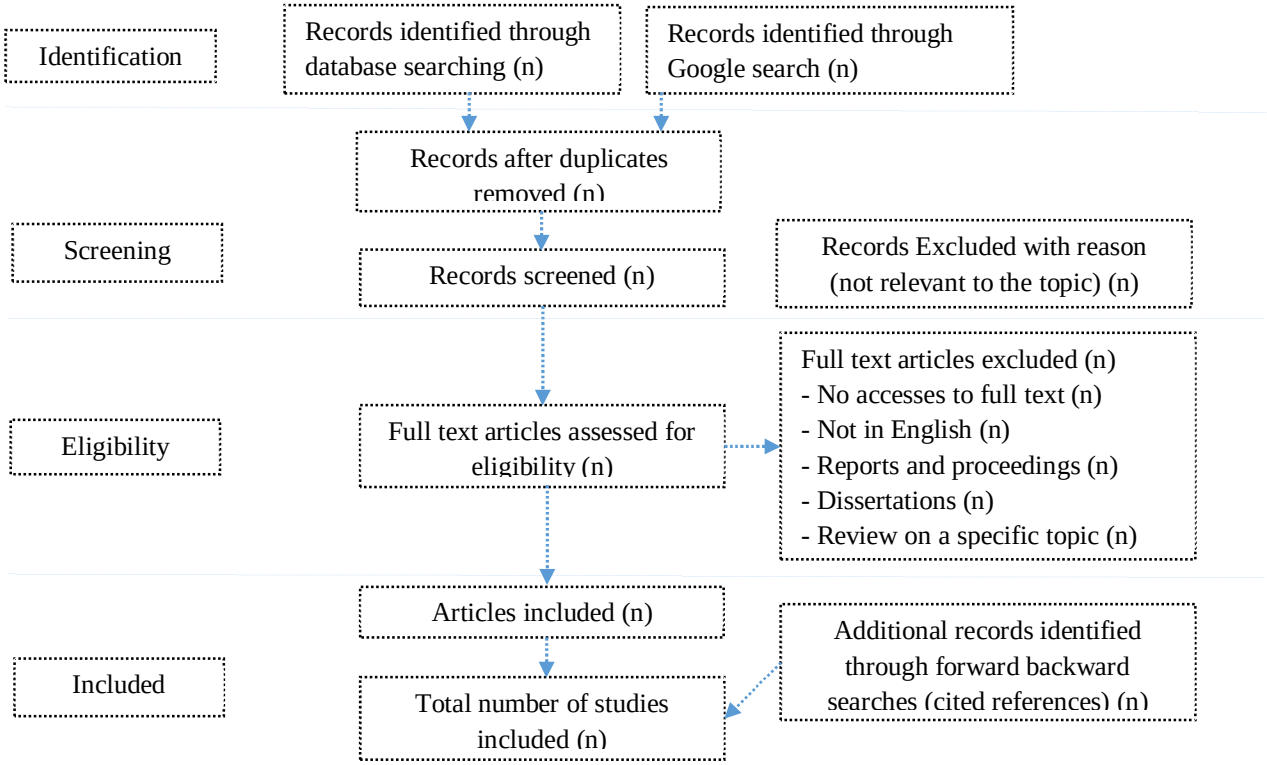

Figure 1-4 Schematic diagram for a systematic review

1.8.2 Remote sensing based water quality Analysis

The spatiotemporal water quality indicators were taken into consideration in this study objective, which was carried out in the Koka Reservoir. To develop a water quality monitoring model as well as to evaluate the spatiotemporal variation of water quality indicators (Chlorophyll-a, turbidity, and total suspended matter). For this research, remote sensing data was analyzed with observed water quality data. The building of the model took into account every potential pairing of imagery obtained from ACOLITE, i.e., after the atmospheric correction process (Angelats & Fern, 2019) using the linear regression method. Four main steps comprise the methodological approach employed in this study were in situ water sampling and laboratory analysis, Sentinel-2 image preprocessing and band combinations; empirical analysis for the development of the WQP model (Chl-a, TSS, and TU) with performance evaluation; and time-series derivation of WQP maps.

1.8.3 Sub-watershed prioritization

To identify hotspots of soil erosion in watersheds, this research also attempted to address the sub-watershed prioritization based on various parameters. To do this, it used GIS and RS in conjunction with MCDM, VIKOR (Ploskas & Papathanasiou, 2019), AHP (Pant et al., 2022), and the SWAT model (Adu & Kumarasamy, 2018). The VIKOR approach was used to prioritize the weighted normalized decision matrix for morphometric parameters. Sub-watersheds were graded based on their unique features and morphometric criteria. The VIKOR method was also used to account for the weighted normalized decision matrix for land use/cover. The sub-watersheds were ranked according to degradation using the VIKOR approach and a pairwise comparison matrix. Watersheds were ranked in this study according to how prone they were to erosion. The condition indicator for morphometric, land use/cover, and sediment load parameter values for priority index classification was used to rate the vulnerability.

1.8.4 Non-point source pollutant modelling using SWAT

To investigate the spatiotemporal variation of the non-point source pollutant as well as to evaluate the impact of LULC change on surface runoff, sediment, and nutrient load the SWAT model was used. The Calibration and Uncertainty Procedures (SWAT-CUP) software (Maroneze et al., 2014) was used to perform sensitivity evaluations, calibrations, validations, and uncertainty assessments of flow, sediment, and nutrient loads. A number of measures, such as the p-factor, r-factor, coefficient of determination (R2), Nash–Sutcliffe (NSE), percent bias (PBIAS), and observation standard deviation ratio (RSR), were used to assess the model's effectiveness and performance in simulating observed streamflow (Takele & Kebede, 2018).

Chapter 2 LITERATURE REVIEW

2.1 Introduction

Nonpoint source (NPS) pollution is a significant environmental issue characterized by the diffuse nature of its origins. Unlike point source pollution, which can be traced back to a single, identifiable source such as a pipe or discharge outlet, NPS pollution arises from multiple sources over large areas. This type of pollution typically occurs when rainfall or snowmelt moves over and through the ground, picking up various pollutants along the way before depositing them into water bodies like rivers, lakes, wetlands, and groundwater. The primary contributors to NPS pollution include agricultural runoff, urban runoff, construction sites, forestry practices, livestock waste, faulty septic systems, and atmospheric deposition. The consequences of NPS pollution are far-reaching: water quality degradation, ecosystem disruption, sedimentation issues, and public health risks (Baerenklau, 2014; Lian et al., 2019).

The Awash River originates from the Ethiopian central highlands and drains some parts of the endorheic river system in Ethiopia. It has no outlet to an ocean; it joins Lake Abe at the Ethio-Djibouti border. The catchment area of the Awash basin upstream of Lake Abe is ~113,304 km^2, which is almost within the Ethiopian boundary with negligible contribution from Djibouti. Its elevation is between 250 and 3,000 meters above sea level (masl). The main river length is about 1,200 km (Taye et al., 2018).

The Awash River basin is divided into four major stretches based on altitudinal variation, i.e. Upper basin which represents the areas from the headwater to the Koka Dam (>1,500 masl); Upper Awash Valley which ranges from Koka Dam to Awash Station (1,500 – 1,000 masl); Middle Awash Valley which represents the area from Awash Station to Gewane (1,000 – 500 masl), and; Lower Awash Valley which is the area that extends from Gewane to Lake Abe (<500 masl) (Duguma et al., 2021; Jin et al., 2021).

The Awash basin has varied landscapes, vegetation, rainfall, temperature, and soils across the basin. For example, the climate ranges from semi-arid lowlands to cold highland mountains. The mean annual rainfall varies from ~1600 mm at Ankober to ~160 mm at Asayita (Tufa, 2021). Land use in the basin is mainly rain-fed agriculture, which is used for rain-fed crops, shrubland, and grazing land. There are some irrigated lands in the basin, which are mainly developed by the government. A large part (~60%) of the large-scale irrigated agriculture in Ethiopia is located in the Awash basin (Keraga et al., 2017a). Crops cultivated in the basin include cereals (e.g., teff, beans, wheat, barley, and oil seeds), vegetables, flowers, cotton, perennial fruit trees, and sugarcane (Tufa, 2021). The other land use includes urban areas, industrial zones, forest, and swamps. Major cities in Ethiopia (e.g. Addis Ababa, Dire Dawa, Nazert, Debrezeit, Dessie, and Semera) are located in the Awash basin. More than 65% of the national industries in Ethiopia are located in the Awash basin (Keraga et al., 2017a) . Administratively, the basin is shared by Afar, Amhara, Oromia, and Somali Regional States, and Addis Ababa and Dire Dawa City Administrations Figure 1-4 Schematic diagram for a systematic review Figure 2-1. The population

and Necha, 2018). Such evidence shows that the Awash basin is enduring extensive socio-economic pressure that threatens the surface water quality and quantity in the basin.

The Awash basin is home to extensive smallholder rainfed and large-scale agricultural farms and large industries; it has been exposed to severe pollutant sources (Eliku and Leta, 2018). Although the pollution situation in the Awash basin is severe, pollution of freshwater systems in developing countries is becoming prevalent due to rapid urbanization and industrialization (Amde et al., 2016; Keraga et al., 2017b; Tamiru, 2001). Such surface water quality degradation issues are alarming in developing countries as limitations to access to clean water exist, and people will be compelled to consume such polluted water for domestic consumption (Keraga et al., 2017a; Tamiru, 2001), which has critical public health consequences.

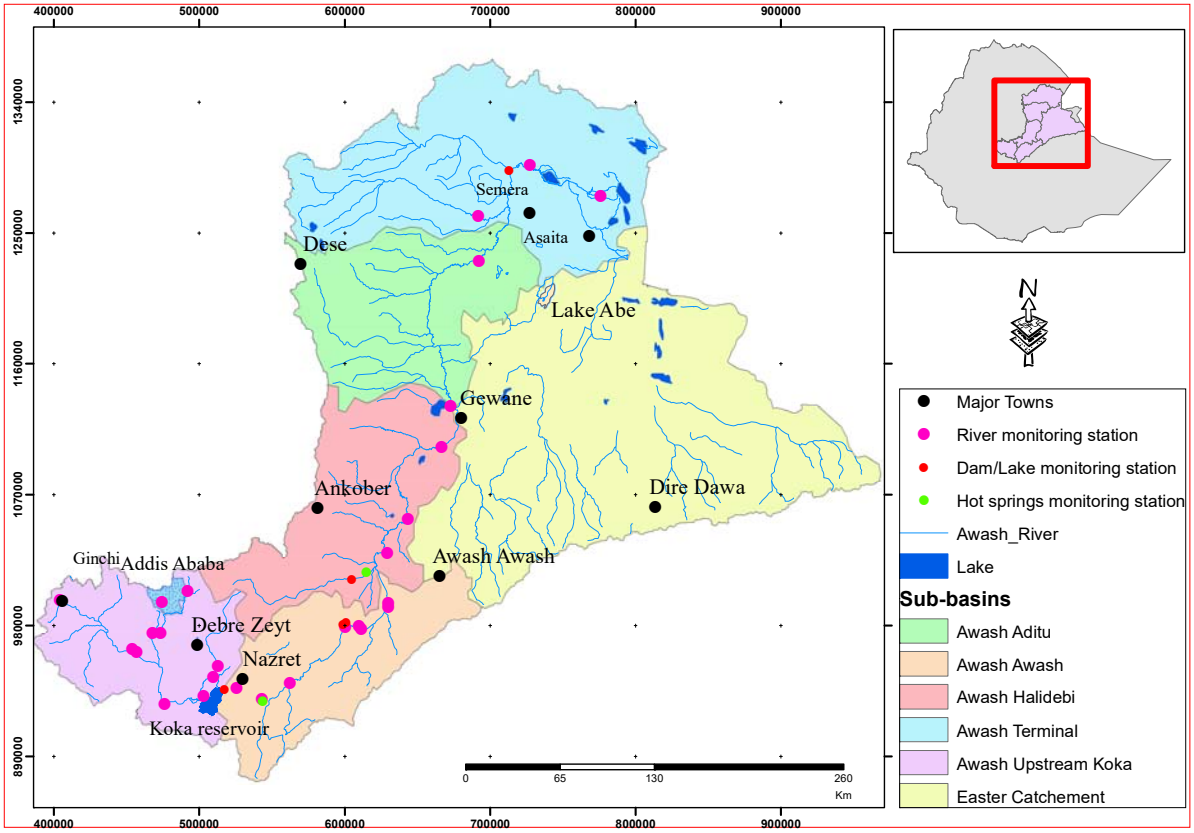

Figure 2-1 Map of Awash Basin with administrative, monitoring sites, and sub-basin boundaries

The Little and Tiliku Akaki Rivers are major tributaries of the Awash River which joins the Awash river system at the Aba-Samuel lake. Tinishu Akaki includes Burayu, Gefersa, Leku, Qille, Gerbeja, Worenchiti, Melka Qorani, Kera as its tributaries and while Ginfile, Kebena, Kechene, Kurtume and Yeka are tributaries to the Tiliku Akaki (Tufa, 2021).

2.2 A synthesis of surface water quality in the Awash Basin

For this systematic review (SR), we developed a search strategy to identify relevant literature. This search strategy was tailored to three databases: Web of Sciences, Scopus, Google, and Google Scholar, and the search terms used were the following: water quality, water pollution,

2.2 A synthesis of surface water quality in the Awash Basin

For this systematic review (SR), we developed a search strategy to identify relevant literature. This search strategy was tailored to three databases: Web of Sciences, Scopus, Google, and Google Scholar, and the search terms used were the following: water quality, water pollution, point source pollutants, and non-point source pollutants. All searches included journal articles, books, and book chapters. The selection criteria were based on the PRISMA Checklist 2009. The search mainly focused on mapping existing literature on water quality, water pollution, and sources of pollution in the fields of environmental sciences and earth sciences. The search span was from the year 2000-2021 in English only. The search was mainly focused on Ethiopia. The search from any other country was considered accordingly. A total of 12 research articles were excluded at this stage. There were 171 records extracted at this stage.

We extracted information on the following subtopics from each study: status of surface water quality monitoring, status of surface water quality, causes of surface water quality impairment, and surface water quality impairment indicators in the Awash basin. All data extraction and coding were performed using Microsoft Excel and Medley Reference Manager.

All duplications were extensively examined to maintain the review's quality. For the analysis and purification of the papers, the abstracts were checked deeply to ensure the quality and relevance of the research papers included in the review process. We read the abstracts of the 159 studies to see if they were relevant to the study topic and research questions. We got the full-text article for quality assessment after a total of 135 studies were deemed relevant. At a later stage, a careful examination of each study publication was carried out. We looked through the full-text publications to assess the studies' quality and relevance. 34 more publications were excluded from the study once the duplicate records were filtered out. After evaluating each article against the aforementioned inclusion and exclusion criteria, we chose 101 papers. The literature inclusion and removal at each level is depicted in Figure 1-4. 101 papers were chosen for data extraction, and the following aspects were extracted: articles must be published journal articles. Reports, dissertations, and unpublished documents were excluded. Through cited references, we discovered an additional 9 studies. In total, 110 studies were considered in this review.

Water is an essential requirement for all living forms on Earth, as well as the most crucial irreplaceable natural resource on which a country's socio-economic growth and long-term development are heavily reliant. Despite its importance to humans, water is the world's most poorly managed resource, particularly in developing countries, and is under serious threat from a wide range of anthropogenic activities (Kumar et al., 2021). The water quality degradation is exacerbating in Ethiopia due to increasing urbanization, and agricultural intensification. Poor urban water quality remains a concern, especially with the rising population, the presence of new and uncontrolled substances, a higher value attributed to ecosystem services, and uncertainty about the effects of climate change on controlling factors of water quality such as temperature and environmental flows (Miller & Hutchins, 2017). The effects of urbanization on water quality vary widely, depending on a variety of factors such as the age/type of urbanization (existing urban

center versus suburban development), the existence of wastewater treatment, stormwater infrastructure, legacy land use, vegetation, and hydrologic regime (O'Driscoll et al., 2010). Urbanization degrades water quality in three ways: point source pollution discharge, diffuse source pollution mobilization, flow changes, and temperature changes in receiving watercourses. Each of these will be determined by the shape and function of future urbanization, as well as the controls and management of potential pollutant discharges (Miller & Hutchins, 2017). for example, the population and built-up area of Addis Ababa are rapidly expanding as a result of urbanization. The area downstream of the city that is affected by industrial and domestic pollution seems to be growing as well (Mekonnen et al., 2020).

Land and surface water quality degradation in Ethiopia was minimal before the last 30 years due to the low population density that practices slash-and-burn agriculture with minimum agricultural inputs (Ligdi et al., 2010). However, due to natural and anthropogenic sources, Ethiopia's land and surface water quality has recently been vulnerable to a wide range of pollution, including organic matter, salts, nutrients, sediments, heavy metals, and so on. Recent increases in sedimentation biodiversity loss in Ethiopia have been driven by rapid ecosystem loss and land use change, which is partly attributable to agricultural intensification (Moges et al., 2017a). Although the United Nations General Assembly resolution 45/94 (1990), which reaffirmed the Stockholm declaration, advises that "all individuals are entitled to live in an environment adequate for their health and well-being", most of the Ethiopian people could not have access to clean water due to increasing environmental degradation. The right to have clean water and a healthy environment for all is also included as part of the Federal Democratic Republic of Ethiopia (FDRE's) constitution (Article 44(1)). Accordingly, developing countries like Ethiopia have policies, laws, and formal administrative mechanisms in place to monitor and manage pollution, but they fail to put them into practice and enforce them to safeguard the environment (Awoke et al., 2016). Likewise, the Ethiopian Public Health Proclamation (EFDR, 2000) prohibited the discharge of untreated waste generated from domestic and industrial sources into freshwater bodies. Although the freshwater policies are in place, the enforcement is weak and freshwater pollution has been predominant in Ethiopia (Berg et al., 2019). Despite the severity, no systematic and comprehensive surface water quality assessment in Ethiopia presents surface water quality challenges to policymakers and practitioners.

Agriculture releases non-point source pollutants, causing significant pollution of the aquatic ecosystems (Aymer et al., 2016). The main source of pollution in agricultural fields is the increased use of fertilizer and pesticides that are aimed at improving agricultural production (Wondie et al., 2007; Emama et al., 2010). The average annual fertilizer use in Ethiopia increased from 2.5 million decitonnes in 2003/4 to about 8.5 decitonnes in 2015/6 (Legesse et al., 2019), which is a fivefold increase in less than 10 years. Subsequent demand for pesticides in the agriculture and flower sectors pesticide use also increased significantly (3327.7 metric tons per year (mt/y) from 2006 to 4211.5 mt/y in 2010), in which the country imports more than 3346.32 mt annually (Begna, 2014). There is also an increase in land use conversion to agricultural land (from natural or native

vegetation), which reduces biodiversity in the landscape and undermines other ecosystem services such as pollination, medicinal plants, etc.

A growing number of evidence showed the severity of non-point source pollution in Ethiopia (Tafesse et al., 2015; Moges et al., 2016). Tafesse et al. (2015) showed that the contribution of overland flow to dissolved phosphorus is high in most of Lake Tana Basin catchments, mainly due to fertilizer application in agricultural fields. Similarly, (Moges et al., 2016) reported substantial amounts of available phosphorus in the Awramba watershed in the Lake Tana basin, which was related to the use of Di-ammonium Phosphate (DAP) fertilize. Alemu et al. (2017) measured dissolved phosphorous (DP) concentration at various sampling locations at the tributaries of the Lake Tana basin, in which the DP concentration was 0.09 mg/l for samples from the lake and 0.51 mg/l for the headwater tributaries.

DP of greater than 0.15 mg/l is considered to cause an adverse water quality problem responsible for the eutrophication in freshwater. Studies highlight that such non-point source pollution flowing into the Lake Tana basin may contribute to the existing water hyacinth infestation in the Lake (Moges et al., 2016). Water hyacinth infestation is also observed in other lakes in Ethiopia, for example, the Aba-Samuel Dam, Koka Reservoir, Lake Ellen, and Wonji in the Awash River system alone (Alemu et al., 2017). The surface water quality problem is, however, severe in some basins in Ethiopia. For example, the water quality of the Rift Valley Lakes is severely compromised due to horticultural, soda abstraction, and industrial activities (Ayenew and Legesse, 2007).

Textile pollution has a particularly negative impact on freshwater environments, with certain parts of the world being more affected than others. Streams and rivers often provide huge volumes of water for textile manufacturing while also acting as key consumers of industrial effluents, carrying contaminants to groundwater and marine habitats (Stone et al., 2020). Most of the industries in Ethiopia often discharge their wastewater into the freshwater system without any treatment (Girma, 2016). (Mehari et al., 2015) conducted a study to determine the effects of Bahir Dar textile factory effluents on the water quality of the Blue Nile River and reported that dissolved oxygen was higher at the upstream site where the effluent joins the river, whereas biological oxygen demand (BOD), total dissolved solids (TDS), and total alkalinity values were higher at a site downstream of the site where the wastewater effluent joins the river.

Awoke et al., (2016), applying physicochemical and biological analysis, showed that there is significant surface water quality deterioration in agriculture, coffee processing, and urban landscapes in the Nile, Omo-Gibe, Tekeze, and Awash River basins compared to corresponding pristine (or reference sites) in basins (Aymer et al., 2016). The total nitrogen (TN) and total prosperous (TP) estimates in the impacted sites were 100- to 1000-fold that of the European WFD and US-EPA standards, respectively. The exhaustive list of Ethiopia's surface water quality studies is summarized in Appendix B Table 2. The table also presents the study sites with the studied parameters and standards for evaluating the parameters. This indicates river water pollution in the

agricultural and urban environment in Ethiopia is a growing challenge and needs urgent action to avoid negative environmental consequences.

2.2.1 Status of surface water quality monitoring

Water quality monitoring provides a reliable assessment of water quality, enabling decision-makers to understand, interpret, and apply this information in support of management activities aimed at conserving the resource (Behmel et al., 2016). Surface and groundwater quality monitoring in Ethiopia has been incipient in most of the rivers (Graichen, 2011). If monitoring exists, the monitoring is very infrequent, for example, twice a year in the Ginchi River at Ginchi town and the Awash River at Asaita. For proper surface water quality monitoring, samples should be collected at least once a month to have a better understanding of the surface water quality situation in the watershed (Graichen, 2011). To monitor water quality, the following factors must be taken into account: determining a sampling site network for lakes and rivers; determining monitoring objectives (e.g., the information that must be provided); selection of water quality parameters (WQP); frequency and recurrence of sampling; estimation of human, technical, and financial resources; logistics planning (e.g., fieldwork, laboratory work, quality control and assessment, data handling, data storing, data analysis); and the identification of information dissemination pathways (Behmel et al., 2016). In Ethiopia, poor technical and financial capabilities restrict the monitoring of rivers and sediments and the understanding of the effects of pollutants (Zinabu et al., 2019). Moreover, consistent monitoring over a long period helps to acquire extensive surface water quality data that can be used to better understand the surface water quality status of river basins (Vega et al., 1998) and thereby helps to take appropriate measures.

Currently, relatively better surface water quality monitoring exists in a few water and environmental agencies, such as the Ethiopian Environmental Protection Agency (EPA) and the Addis Ababa City Environmental Protection and Green Development Commission. The Awash Basin Authority (AwBA) also started monitoring surface water quality in the Awash Basin in 2004 over 35 sites. Of the selected thirty-five monitoring stations, three trend, three impact, and seven flux monitoring stations have collected data monthly since July 2011. Quarterly surface water quality monitoring has been conducted in eight trends, four impact, and five flux monitoring stations since July 2011. Some stations measure twice per year and are located in Ginchi, Saburie, Deho, Logia, and Affambo towns (Figure 1-3), but all these efforts are not comprehensive, as stated by Jin (2021).

Surface water quality parameters collected in the Awash basin include pH, turbidity, electric conductivity, TDS, TS, TH, Alkalinity, Na^+, K^+, Ca^{2+}, Mg^{2+}, Fe, Mn, Cl^-, F^-, NH_3, NO_3^-, NO_2^-, SO_4^{2-}, PO_4^{3-}, HCO_3^-, and CO_3^{2-} The data collection was conducted both in the wet and dry seasons although there is an emphasis to the dry season data collection. Fifty percent of the researchers collected their data both in dry and wet seasons e.g. (Masresha et al., 2011; Prabu et al., 2011; Kassegne et al., 2018; Eliku and Leta, 2018; Keraga et al., 2017b; Yosef, 2017; Adugna et al., 2019; Aymer et al., 2016) while about the remaining 50% collected only dry season (Maschal and Zomaneh, 2018; Jebessa and Bekele, 2018; Kassegne et al., 2018). However, few studies monitor

surface water quality only in the wet season (e.g. (Eskinder, 2019)). Some studies do not report periods of monitoring of their surface water quality data (e.g. (Bedada et al., 2019; Itanna, 2002; Zinabu, 2019; Awol, 2018)).

There is limited surface water quality monitoring at a finer temporal resolution, e.g. at biweekly (Akalu et al., 2011), monthly (Degefu et al., 2011; Abhachire, 2014; Tesfay, 2007; Keraga et al., 2017b; Dirbaba et al., 2018; Yimer and Jin 2020), quarterly in Ginchi and Awash Below towns and in Awash river at the inlate of koka reservoir stations (Akalu et al., 2011; Chernet et al., 2001; Degefu et al., 2013). (Dirbaba et al., 2018) collected 10 years of monthly surface water quality data, which helped assess trends of Hg, As, Pb, Ni, Cu, Cr, Zn, and Cd at different stations of the Awash River in Awash-Awash, Awash Halidebi, and upper Awash sub-basins. There is also seasonal basis (both dry and wet season) surface water quality monitoring as shown in Appendix A Table 2.

2.2.2 Surface water quality status

Recent studies on freshwater and river basins all around the world have found that river water pollution from organic and inorganic contaminants has gotten significantly worse over time (Kumar et al., 2021). Although water quality problems are apparent in most Ethiopian Rivers, Awash leads to the extent of impairment due to its service as a sink for the basin-wide urban, industrial, and rural wastes. Land deterioration, high population density, natural water degradation, salinity, and wetland degradation are all problems in the Awash River Basin (Tufa, 2021). Due to repeated and poor irrigation practices and the increasing amount of Beseka Lake water flow to the downstream area, soil salinity becomes a challenge, especially in the middle and lower Awash River Basin areas (Aregahegn & Zerihun, 2021).

Some of the most important services given by the Awash River water are irrigation, electric power generation, fish production, and serving as a water source for domestic consumption for residents living near the river course, as well as for domestic and wild animals in the area (Degefu et al., 2013). However, water quality index-based evaluation showed that the water is below the standard for these purposes e.g. WHO and Canadian water quality ranking (Keraga et al., 2017a). Keraga et al., (2017a) showed that drinking and irrigation water quality indices of the upper basin were 34.79 and 46.39, respectively, which were in the poor and marginal categories of the Canadian water quality ranking. While the drinking and irrigation water quality indices of the middle/lower basin (which were 32.25 and 62.78) fall in the poor and fair ranges of the ranking. Surface water quality is frequently threatened or impaired; conditions often depart from natural or desirable levels of the ratings (Davies, 2006).

Nonpoint source pollution was severe in the Awash basin due to the presence of several irrigation schemes that produce bananas, sugar, and cotton. Because of poor irrigation practices and drainage in these irrigation schemes, salt and hazardous materials have accumulated in the irrigated fields, where they were easily carried into freshwater habitats (Tufa, 2021).

Untreated domestic, industrial, commercial, and institutional liquid waste discharged into rivers harmed the rivers' water quality. Because the city's solid and liquid waste treatment systems are poor and ineffective, all point and nonpoint sources in the city release their effluents directly or indirectly into surrounding rivers, which eventually join the Awash River (Yohannes and Elias, 2017). About 30% of the City's inhabitants do not have liquid waste disposal and treatment facilities. Of the total waste generated in the City, only 65% is collected and disposed of while about 10% of the waste is recycled and composted; and the remaining 25% joins freshwater systems without any treatment. Besides the liquid waste, the City produces about 0.45 kg/capita/day of solid waste (Mohammed and Elias, 2017).

The Akaki River is the country's most contaminated river system. Almost all of the assessed locations along the Akaki rivers had poor water quality and did not meet the river water quality criterion. This degradation was caused by a variety of contaminants from both point (factory discharge, urban wastewater discharges, garage wastes, hospital wastes, etc.) and non-point sources (e.g. different sewage runoff, agricultural runoff). The most common sources are industrial wastes (Yohannes and Elias, 2017). Water pollution in the Tinishu Akaki River is higher than in the Tiliku Akaki River, owing to industrial units located in and around the city, intense farming activities along riverbanks, and indiscriminate disposal of domestic and municipal wastes (Melaku et al., 2004). Similar to the Tinishu and Tiliku Akaki rivers, the Mojo River sub-basin in the Awash River basin consists of several industries, which dispose directly into the river and subsequently to the Koka reservoir without appropriate treatment (Gebeyehu & Bayissa, 2020). However, the water quality deterioration of the Tinishu Akaki River is more severe than the Mojo River due to alarming municipal and industrial waste from Addis Ababa (Mulu et al., 2013).

2.2.3 Surface Water Quality Impairment Indicators

Evaluations of the water quality in the Awash rivers using indicators showed that it is above global and Ethiopian minimum standards of water quality. For example, the mean value of phosphate, ammonia, nitrite, COD, and BOD of the upper stream of Gullele in the Shankela River was above the permissible limit of the WHO and Ethiopian standards. Likewise, TDS in the Shankela River exceeded the permissible limit. Concentration levels of the nitrogen and phosphate compounds of PO_4^{-3}, NH_3, and NO_2^- ion in the Shankela River were above the standard limit of WHO and Ethiopian EPA standards (Maschal and Zomaneh, 2018).

Turbidity, DO, BOD, COD, NH_3, and TH did not meet the WHO's requirement for DWQG. F^-, alkalinity, and PO_4^-. Likewise, TN, SO_4, NH_3, and TH in the UB and F^-, alkalinity, HCO_3^-, and PO_4^-, did not meet FAO's irrigation water quality guideline Figure 2-2. It is generally believed that the water quality of the Awash River is below the required standard. As such, the Awash River water did not meet the surface water standard of Ethiopia (Maschal and Zomaneh, 2018).

Bussi et al., (2021) examined under population growth scenarios, water quality is expected to deteriorate significantly, particularly in the Akaki River, which drains Addis Ababa, where nutrient loads could increase by up to one-third (nitrate) and more than 50% (phosphorus) compared to

baseline conditions, greatly increasing the risk of eutrophication. In the eutrophication of aquatic bodies, dissolved phosphorus plays a critical role (Moges et al., 2016). Phosphates from detergents, urban areas, industrial waste (such as sugar cane production), and intensive agriculture (Moges et al., 2016; Girma, 2016) can cause nutrient levels in the water to rise, resulting in algal blooms (Girma, 2016).

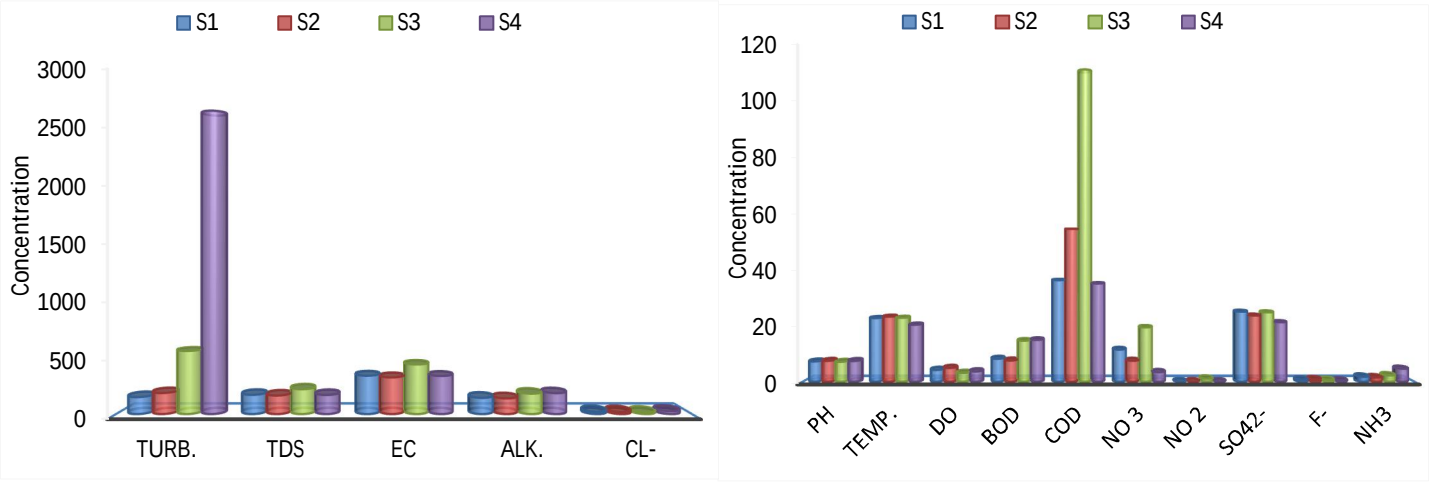

Figure 2-2 Mean concentrations of water quality parameters in five sites of upper Awash River (S1 = after Lake Koka, S2 = at Koka Dam, S3 = before Lake Koka, S4 = at Melka Kuntire). Source: (Maschal and Zomaneh, 2018).

Yosef (2017) reported that nitrite, phosphate, COD, and BOD concentrations from sampling sites on the Akaki River exceeded the minimum standard levels. Likewise, a study in the Tinishu and Tiliku Akaki Rivers showed that the dissolved oxygen was very low for aquatic species to survive (Melaku et al., 2007; Eshetu et al., 2004; Angello et al., 2021). Major pollutants of concern are sediments, nutrients, biodegradable organic wastes, and salt. According to studies, the Lake expansion has impacted the soil salinization of a nearby sugarcane plantation (Yimer and Jin 2020).

The concentrations of phosphate and total ammonia nitrogen in the rivers of Addis Ababa (e.g., Kebena, Little, and Tiliku Akaki rivers) reported that the nutrient levels can lead to eutrophication (Eriksson and Sigvant, 2019). The study showed that concentrations of total ammonia nitrogen, NO_3, and PO_4 were lower in the upstream part of the city, higher within the dense parts of the city, but lower in the downstream part of the city around the Akaki-Kaliti area. High concentrations of TAN and NO_3-N were found in the Kebena River in station 22, locally known as the Abuara area near Abune Gorgorios School (**Error! Reference source not found.**). Similarly, the mean concentrations of NH_3-N, PO_4^{3-} and BOD_5 levels were significantly lower in the headwaters than the other sites, especially the dense part of the city; the mean concentrations of NH_3-N, PO_4^{3-}, and BOD_5 decreased in the lower reaches of the city (Akalu et al., 2011). The primary cause of this spatial variation is the densely populated area of the city, which lacks adequate sanitation facilities and solid waste collection systems. The lower concentration downstream may also be due to the dilution effects of increasing discharge. The main reason for this spatial variation is the dense part

of the city poorly served with sanitation facilities and solid waste collection systems; second, the lower concentration downstream possibly from dilution effects of increasing discharge. Usher and van Biljon (2006) pointed out that the dominance of impervious surfaces, coupled with the altitude difference between upper and lower reaches, increased the discharge of rivers in the lower reaches of the city.

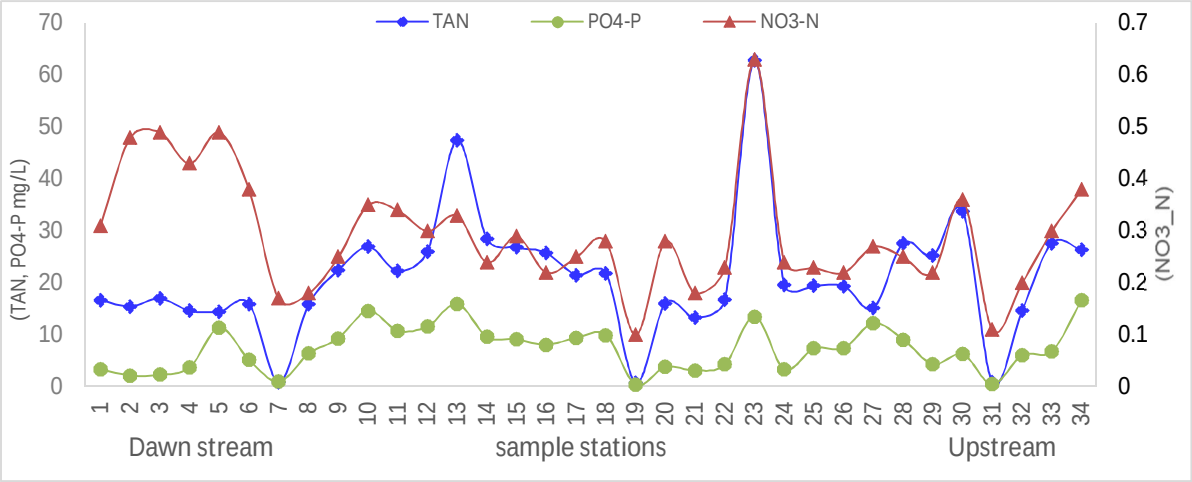

Figure 2-3 Addis Ababa rivers water quality in terms of total ammonia nitrogen (TAN), NO3-N, and PO4-P. Source: (Eriksson and Sigvant, 2019)

The accumulation of the nutrients translated into eutrophication in some freshwater systems in the Awash Rriver basin. For example, a blue-green algal bloom was observed in the Koka reservoir (Abhachire, 2014). Samples from Koka reservoir offshore zone at a depth of 6 m, littoral station at a depth of 2 m, and Awash River mouth station at a depth of 2 m showed that the chlorophyll *a* (Chl *a*) concentration was relatively high in the littoral station (

Figure *2-4*), which indicates there is spatial and temporal variation in the Chl *a* concentration in the reservoir. In addition to this, there is a high concentration of chlorophyll *a* in all stations in the month of December (Tesfay, 2007).

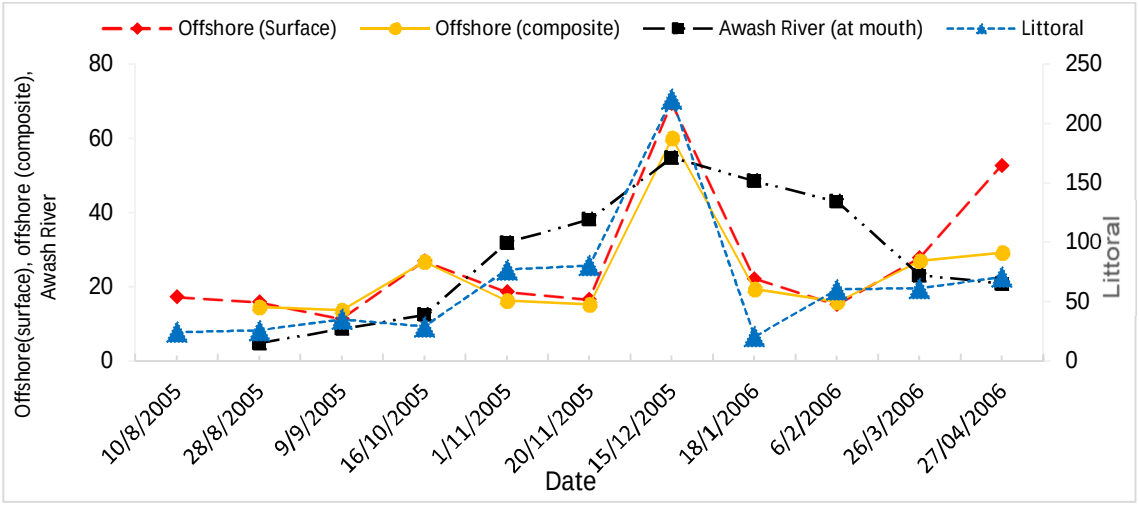

Figure 2-4 Samples from the Koka reservoir offshore zone and mouth of the Awash River

S1 = after Lake Koka, S2 = at Koka Dam, S3 = before Lake Koka, S4 = at Melka Kuntire. Source: (Tesfay, 2007)

The algal biomass (chl a, 446.55 µg/l) in the Koka reservoir may likely occur due to high concentrations of nitrate (NO_3, 7.15 mg/l), (NO_3-N, 0.69 mg/l), phosphate (PO_4-P, 3.13 mg/l), and ammonia (NH_3-N, 8.21 mg/l). Stations of the Littoral and Awash River (at the mouth) showed an increment in Chl a concentration from September to December. Awash River (at the mouth) showed a decreasing trend from January to July. The offshore (surface) and offshore (composite) sites showed fluctuating concentrations in different periods.

The concentration of some water quality parameters of the Koka reservoir showed a temporal increment. Some of the evidence by different researchers in Table 2-1 showed that the parameters were in different periods.

Table 2-1 Status of water quality in the Koka Reservoir

Parameter	Unit	Concentration (range)	Reference [#]
Tem	(^oC)	21- 26	(Abhachire, 2014)
		20.6/24*	(Masresha et al., 2011)
pH	-	6.13 - 8.6	(Abhachire, 2014)
		8/7.4*, 8.4	(Masresha et al., 2011), (Mesfin et al., 1988)
DO	(mg/l)	4 -11.6	(Abhachire, 2014)
EC	(µs/cm)	200 - 380	(Mesfin et al., 1988)
		274, 480/251*	(Wood and Talling, 1988), (Masresha et al., 2011)
NH_3-N	(mg/l)	89.3(µg/l)	(Degefu et al., 2011)
NO_3 -N	(mg/l)	0.69/1.43*, 44.4 (µg/l), 47-200	(Masresha et al., 2011), (Degefu et al., 2011), (Tesfay, 2007)
NO_2-N	(mg/l)	16.86 - 81.01	(Tesfay, 2007)
PO_4-P	(mg/l)	36.10(µg/l)	(Degefu et al., 2011)
TP	(mg/l)	477.2(µg/l)	(Degefu et al., 2011)
		NIL - 0.14	(Mesfin et al., 1988)
SO_4^{2-}	(mg/l)	0.24, 6.4/6.24*	(Wood and Talling, 1988), (Masresha et al., 2011)
		4-56	(Abhachire, 2014)
$CaCO_3$	(mg/l)	2.59 - 289	(Mesfin et al., 1988)
HCO_3	(mg/l)	3.22, 272/83*	(Wood and Talling, 1988), (Masresha et al., 2011)
CO_3	(mg/l)	0.2-6.6	(Abhachire, 2014)
CO_2	Mg/l	2.8-32, 0.25-0.49	(Abhachire, 2014), (Mesfin et al., 1988)
Cl^-	(mg/l)	0.16, 15.6/5.9*	(Wood and Talling, 1988), (Masresha et al., 2011)
		24-221.01	(Tesfay, 2007)
Chl *a*	µg/l	214.1, 22.4**	(Degefu et al., 2011), (Mesfin et al., 1988)

**- Dry/wet time data; **-1984; # - reference arranged in respected order of concentration (range)*

The Mojo River serves as a good example to demonstrate water pollution due to industries since it has water quality monitoring stations (Figure 2-5 and Table 2-2) along the river course at eight industries (i.e., Kolba Tannery, Ethio-Japan Textile, Soap Ffactory, Gelan Tannery, Organic Export Abattoir, Derartu Tannery, Mojo Tannery, and Food and Oil Complex). Most of the measured water quality indicators showed that the minimum acceptable limit was exceeded (Gebre et al., 2016). The mean concentrations of NH_4–N and NO_2–N in all stations exceeded Ethiopian EPA and WHO standards.

Table 2-2 Mean concentration of different parameters from Mojo River

St.	NH_4–N (mg/L)	NO_3-N (mg/L)	NO_2-N (mg/L)	PO_4-P (mg/L)	pH	TDS (ppm)	BOD* (mg/L)	COD (mg/L)	Temp (°C)	EC (mS/cm)	Turbidity (NTU)
1	0.11	0.74	0.12*	0.29	7.7	384	61.2	86.3	-	-	-
2	0.18	3.23	0.22*	0.69	6.69	487	132	181	-	-	-
3	35.12*	5.44	0.12*	0.63	8.83	388	354	461	22	419.5	366.6
4	0.36*	0.726	0.14*	0.77	8.28	263	111	151	22.6	211.4	438.4
5	0.43*	0.71	0.22*	0.75	8.16	550	81.7	95.7	22.6	236.2	830.45
6	0.35*	4.23	0.18*	0.18	8.46	549	85.8	131	23.6	218.4	718.45
7	0.24*	3.44	0.08	0.27	8.14	506	61.8	111	23	307.3	669.85
8	39.1*	6.45	0.35*	0.88	9.93*	566	162	254	23.5	394.3	564.6
9	29.85*	7.84	0.08*	19.15	11.1*	395	231	342	23.8	427.6	763.95
10	4.45*	5.92	0.58*	0.52	8.85	855	221	342	23.2	238.2	619.25

** - above Ethiopian EPA and WHO standards*

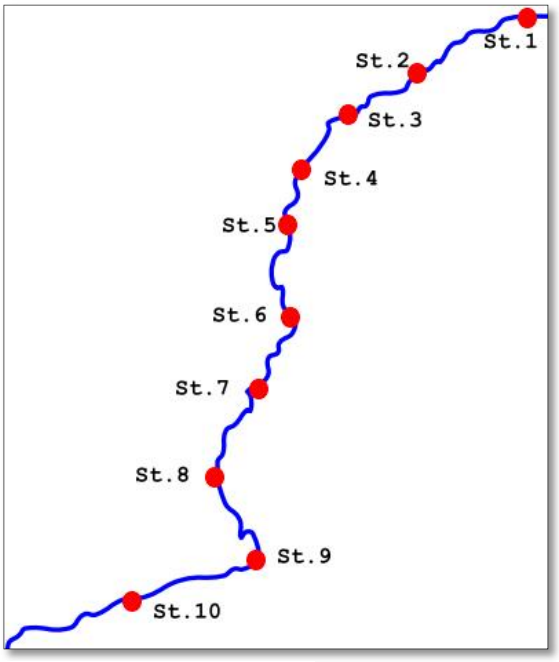

Figure 2-5 Sketch map of Mojo river.

St.1-upstream, st.2-food oil complex, st.3-Mojo tannery, st.4-Japan textile, st.5-Soap factory, st.6-Derartu tannery, st.7-Organic export abattoirs, st.8-Gelan tannery, st.9-Kolba tannery, st.10-Dawn stream

There is a distinct seasonal variability in water quality in the Awash Rriver basin. During the dry season, all the sampling sites of the basin showed a decrease in EC, TH and Cl^- from the upper to lower parts of the basin (Keraga et al., 2017a). However, TDS, Cl^-, and SO_4^{2-} decreased in the rainy season. Both seasons, maximum Cl^- and EC/TDS/SO_4^{2-} were observed at Beseka and before Beseka Lake, respectively. On the other hand, in both seasons, TH was at its absolute minimum at Beseka station. Beseka, before Beseka and Sodere spring sites were accountable for the spatial variation of water quality, for example, EC, TDS, TH, Cl, and SO_4^{2-} showed major differences in these sites (Figure 2-6).

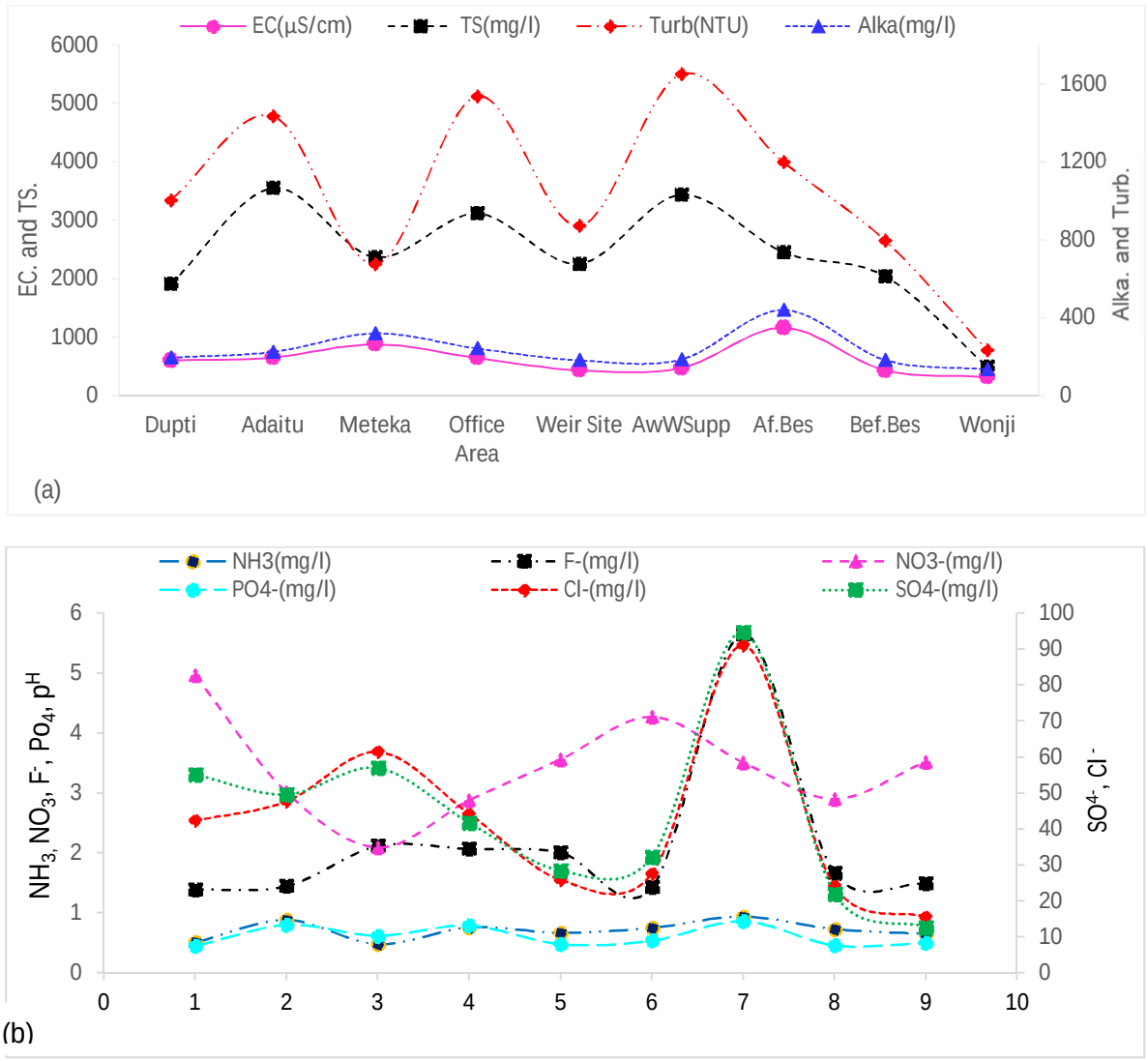

Figure 2-6 Spatial variation of water quality in the Awash River

Mean values of water quality parameters for nine sampling sites of Awash river from 2005 to 2013: 1-Dupti, 2-Adaitu, 3-Meteka, 4-Office area, 5-Weir site, 6-Awash water supply, 7-after Lake Beseka, 8-before Lake Beseka, 9-Wonji. Source: (Keraga et al., 2017a).

2.2.4 Causes of Surface Water Quality Impairment

The Awash River Basin is Ethiopia's most developed, and extensively utilized river basin. Furthermore, the Awash River basin contains the bulk of irrigated farmland in the country (Keraga et al., 2017a), with a variety of small-, medium-, and large-scale irrigation projects, industries positioned along the river, a significant rural population, and rapid urban development (Aregahegn & Zerihun, 2021). The water quality of the Awash River has been harmed by numerous types of pollution resulting from waste generated from various socioeconomic activities, poor farming practices, and large-scale irrigation, intensified irrigation schemes throughout the basin (Keraga et al., 2017b; Tamiru, 2001). This is due in part to the fact that the main sources of water pollution in the Awash River Basin include excessive irrigation pumping and overflowing, discharge of

saline Beseka Lake water and hot spring water from various places to the river, urbanization, and industrial waste (Aregahegn & Zerihun, 2021; Taddese, 2019).

The Awash River is polluted by liquid and solid effluents released from industries (Eliku & Leta, 2018) and households (Abebe, 2019) and runoff from agricultural and urban areas, irrigation drainage, and Lake Beseka (Elias et al., 2016). One of the major sources of pollution for the Awash River is untreated domestic discharge from the city of Addis Ababa (Worku & Giweta, 2018) and upstream effluents from industries (Itanna, 2002). For example, large and small factories around Addis Ababa, Mojo and Adama, Wonji, and Metehara sugar factories are among the upper basin's industrial operations, while Kesem Kebena and Tendaho sugar factories are the middle and lower basin's important industrial activity, respectively (Aregahegn & Zerihun, 2021).

The water quality of the Awash River has been affected by various types of pollution caused by waste produced from various socioeconomic activities, as well as inadequate agricultural and irrigation management in the basin. Excess pumping and overflowing during irrigation, discharge of saline Beseka. Lake water and hot spring water from various places to the river, urbanization, and industrial waste are the main sources of water pollution in the Awash River Basin (Taddese 2019; Aregahegn and Zerihun 2021; Yimer and Jin 2020).

The Upper Awash River Basin has poor water quality, which was largely mainly due to poor farming, untreated industrial effluents, and a lack of sanitation facilities for riparian communities (Degefu et al., 2013). There is extensive agricultural intensification (Alemu et al., 2017) and industrialization (Degefu et al., 2013), which has been exacerbating the surface water quality impairment. Besides receiving all industrial and domestic pollutants from the Upper Awash region, the Middle Awash experiences substantial soil erosion and other nonpoint source pollution due to inappropriate agricultural practices.

Addis Ababa's water resource is extremely polluted as a result of rapid population increase, unregulated urbanization and industrialization, and inadequate waste management methods, affecting human health and ecosystem function as a whole. Addis Ababa's rivers are simply used as a dumping ground for all of the city's waste (Yohannes & Elias, 2017). Several studies have found that untreated and inadequately treated industrial wastewater, household wastes, residential and commercial activities, and sewage discharged into waterways pollute Akaki river (Mekuria et al., 2021). According to Maschal and Zomaneh (2018), the causes include indiscriminate dumping of refuse into the river, indiscriminate dumping of industrial waste, scattering settlements or urbanization, and others like vehicle washing effluents released into the Shankila river.

Anthropogenic activities account for the lion’s share of surface water quality deterioration in several rivers (Abhachire, 2014; Degefu et al., 2011) where indiscriminate dumping of domestic and industrial wastes, and wastes from other sources such as agriculture, petrol stations, health facilities, and garages, etc. are rampant. Textiles, slaughterhouses, tanning, leather products, and other activities, among others, are located in this basin (Aregahegn & Zerihun, 2021).

Water pollution sources could be point sources (directly identifiable sources) and nonpoint sources (different non-identifiable sources of origin and number of ways that contaminants enter into the water body) (Singh and Gupta, 2017). Nutrients in surface water have been mainly related to land use activities (Eliku and Leta, 2018). Anthropogenic activities of point and nonpoint sources of pollution are the major causes of nutrient enrichment of surface water (Singh & Gupta, 2017).

A. Point sources

Wastewater generated from a single source like industrial influents and municipal wastewater/wastewater treatment facilities as well as leaking septic systems, chemical and oil pills and illegal dumping (Kebede et al., 2012), and certain agricultural activities, such as animal husbandry (Gebre et al., 2016) are point sources of pollution.

Historically the establishment of modern industries in Ethiopia started one hundred years ago (in the 1920s) (Gebreeyesus, 2013). However, Many Ethiopian leather processing industries, for example, lack suitable waste treatment methods. By its very nature, leather processing entails soaking, fleshing, washing, and other water-based methods for removing dirt, flesh, salt, and other foreign substances (Wassie, 2020). Many textile and garment industries in Ethiopia lack waste treatment plants, making it difficult to properly dispose of their waste. They just discharge their waste into the environment, which in most cases is freshwater. As a result of several studies conducted on a small number of individual textile factories, it has been suggested that the textile and garment sector's wastewater is perhaps the major source of water pollution in Ethiopia (Menbere, 2019).

Along the Awash River and its tributaries, particularly the Akaki River, several polluting industries and flower farms have been developed in the previous two decades. In addition, these companies discharge highly polluted sewage into Lake Koka's waters (Girma, 2016). According to Yohannes and Elias (2017), Addis Ababa hosts about 65% of the country's industries, and more than 90% of the industries discharge their waste to nearby rivers without proper treatment. In recent years, the expansion of industries around the cities of Akaki, Mojo, and Adama has increased the influence of industrial pollution on the Awash River water (Aregahegn & Zerihun, 2021). Addis Ababa Tannery, Tikur Abay Sshoe Factory, Gulele Soap Factory, Ethio Marble Industry, and Gulele Shirt Factory discharge their waste into Kera Rriver with little or no treatment applied (Itanna, 2002). Most industries in Gelan and Dukem have established neither treatment plants nor adequate storage or discharge channels for their wastes. As a result, polluted liquids are directly discharged into the open landscape (Dadi et al., 2017). No monitoring system follows if industries treat their effluents before discharging them into the Awash River system.

Jebessa and Wondemagegnehu (2018) studied physicochemical characteristics and impacts of raw and treated effluents from the Anmol Product Paper factory on upstream and downstream water qualities at the factory and 5 different sampling stations on the upper Awash River and showed that both raw and treated effluents had water quality levels that are above the WHO and Ethiopian standards (Appendix A Table 1).

Chemical wastes and byproducts from industry, as well as mismanaged urban trash disposal at open dump sites in major cities, continue to pollute the environment (Wassie, 2020). Despite generating large amounts of solid waste from domestic activities, Addis Ababa does not have adequate waste management facilities. As a result solid waste is often piled on available open grounds, stream banks, and near bridges, where it is washed off into rivers (Yohannes and Elias, 2017). The 29 hospitals in Addis Ababa produce 430.7 tons of infectious waste each year. Laboratory cultures, wound dressings, blood and other human fluids, and needles are examples of contagious clinical waste. Even though most hospitals have waste treatment facilities, some clinical waste makes its way into neighboring tributaries (Yohannes and Elias, 2017).

B. Non-point sources

Nonpoint source pollution (NPS) is polluting that does not originate from a single, easily identified source and is caused by the scouring effect of rainfall and dissolved pollutant solids entering recipient water bodies (such as rivers, lakes, reservoirs, and bays) by runoff (Liu et al., 2015). Non-point sources contribute more pollution to surface water than point source pollution sources. Relatively little is known about the nonpoint source pollution in sub-Saharan Africa (Jones-lee et al., 2000).

Water quality of surface waters is impaired by several factors such as non-point source contaminants through runoff (Carpenter et al., 1998). This affects the impairment of surface water quality and the aquatic life in lakes, especially in developing countries like Ethiopia (Awoke et al., 2016)

C. Agriculture

Agriculture is intensifying in Africa, increasing pressure on the environment. Agriculture is a large contributor of nonpoint source pollution to the aquatic environment. The degradation of water quality caused by widespread agricultural activities released into river water puts extra pressure on surface water (Islam et al., 2020). The interaction between agricultural malpractices and the environment in Ethiopia results in relentless pollution of freshwater. Agriculture-induced pollution contributes significantly to damaging aquatic ecosystem health in the country (Awoke et al., 2016).

Pollution from agricultural activities includes nitrogen and phosphorous-based chemical fertilizers, insecticides, herbicides, and organic matter. Large farms are the primary users of pesticides and herbicides (Girma, 2016). As a result of runoff or irrigation return flows, these pollutants end up in waterways (Awoke et al., 2016). For example, presumably due to pollution of the whole stream reached by the catchment nutrient sources in upper Awash (Degefu et al., 2013).

Both the main Awash River and its tributaries in Upper Awash have substantial rain-fed and commercial agricultural farms, high vegetable production, and animal husbandry activities (Eliku & Leta, 2018). Animal husbandry is dominantly found in the surrounding parts of Addis Ababa, Nazreth, and Debre Zeit. As a result of these activities, it is expected that a significant amount of organic waste is generated on rainy days (in runoff). Stormwater runoff or debris blown into

waterways from agricultural land, inorganic fertilizers in agricultural fields, and animal manure are non-identifiable sources of pollution that are responsible for nutrient enrichment in aquatic environments (Keraga et al., 2017a; Tamiru, 2001). Agricultural wastes have been polluting freshwater systems jeopardizing socio-economic and ecological assets in the river basin (Mengistie et al., 2017).

The chemical constituents of irrigation water can affect plant growth directly through toxicity or deficiency, or indirectly by altering plant availability of nutrients (Belay, 2019). The rising concentration of salt and toxic elements in the drainage waters from irrigated lands is a common awareness in the Middle Awash. The availability of good quality water in the Middle Awash Valley due to agro-industries has created great concern for surface water quality (Taddese, 2019; Taddese et al., 2007). Loiskandl et al., (2005) point out that community-based irrigation schemes are more feasible at highlands than in lowlands due to surface water quality deterioration, this is probably linked to the original water quality of the source.

D. Erosion by water

Soil erosion is very common and some of the lakes are affected by the consequences of sedimentation and increased turbidity (Girma, 2016; Abhachire, 2014). Anthropogenic forces that alter the physical landscape cause substantial soil erosion which has an adverse impact on surface water bodies (Issaka & Ashraf, 2017). Soil erosion and other sediment sources can also be significant nutrient sources, as nutrients often tend to be found in particulate form. Sediment that comes from active construction sites and washes off of particulate materials from impervious surfaces is one of the most common and potentially damaging pollutants found in urban runoff (Shaver et al., 2007).

According to Moges et al., (2017a), the decreasing water quality trend of Lake Tana was attributed to the non-point source sediment and nutrient inflow to the lake with a high erosion rate from the watersheds.

One of the major pollutants concerning agriculture is associated with erosion of the soil in the upper catchments of the Awash River. This is especially intense in the rainy season when there is high surface runoff. Chemical fertilizers used to boost production enter streams as a result of soil erosion. The erosion process is linked to pollution of local water bodies and wetlands. On cropland, soil erosion causes a reduction in yield potential, a decrease in surface water quality, and a breakdown in drainage systems. Nonpoint nutrient contaminants and chemicals are also transported with soil particles, resulting in greater sediment levels and, ultimately, water eutrophication and disruption of fragile aquatic ecosystems (Issaka & Ashraf, 2017).

E. Urbanization

Stormwater or urban runoff contains a mixture of constituents: sediment, nutrients (nitrogen and phosphorus), Chlorides, Petroleum hydrocarbons, and Organic chemicals (pesticides, herbicides, and industrial) (Shaver et al., 2007). The pollution sources of the Shankila River, one of the most

dominant causes were domestic wastewater releases along the entire river course (Maschal and Zomaneh, 2018).

Urbanization and industrialization significantly reduce the agricultural land and cause environmental damage in the basin. Urban areas like Addis Ababa, Dukem, Mojo, Debrezeit, and Nazert increase the influence of domestic pollution to the Awash and the Mojo rivers; and Lake Koka (Melaku et al., 2020). As the number of hotels, commercial establishments, and factories grows, the amounts of solid and liquid wastes being generated are also growing (Girma, 2016).

Even though Addis Ababa is the only city with sewer networks, it has a very limited sewer network coverage that accounts for 7.5% of the built-up areas. Since only parts of the older sections of the city are connected to the central sewer system, both residential and business premises use septic tanks. There is a high amount of waste disposal in the river and riverbanks from municipal sources (municipal solid and liquid wastes), liquid wastes from toilets, and houses that are built at the edges of the city's rivers link their toilets directly to them (as a result, the residents use the river as a toilet), open urination and defecation in and around Addis Ababa, 25% of the city's residence do not have a toilet. Therefore, the status of river pollution is increasing as time elapses (Yohannes and Elias, 2017).

F. Other sources

In addition to the socio-economic pressures, environmental pressures also play a major role in the surface water quality of the basin. This is evidenced by the high fluoride concentrations in Rift Valley soda springs, alkaline lakes, hot springs, and geological formations (Yimer and Jin 2020; Aregahegn and Zerihun 2021; Taddese 2019). Other waste sources come from construction buildings, roads and dams, fuel stations, garage operations, and congested settlements (Yohannes and Elias, 2017). Physical factors like heated water discharged from a power plant (Walker et al., 2019), for example it is observed that the discharge of an industry in Sebeta area (One Weha bottling and Balezafu Alcohol Industry) the temperature is about 28.2 and 32 ^{o}C respectively, contribute by changing the temperature of the water body. There are surface water quality studies in different parts of the Awash Basin by different researchers (as shown in Appendix B Table 3)

2.2.5 Gaps and problems identified

Surface water quality monitoring in Ethiopia has been incipient in most of the rivers this is due to poor technical and financial capabilities monitoring of rivers and sediments and understanding of the effects of pollutants becomes limited. In addition to this, the surface water quality status of river basins is not better understood and appropriate measures could not have been taken. There is limited surface water quality monitoring at a finer temporal resolution as well as appropriate locations so hydrological water quality modelling in the basin is very limited.

Some of the most important services given by the Awash River water are irrigation, and serving as a water source for domestic consumption for residents living near the river course, as well as for domestic and wild animals in the area. However, water quality index-based evaluation showed

that the water is below the standard for these purposes; conditions often depart from natural or desirable levels of the ratings.

The Awash Basin's surface water quality is degrading. Rapid urbanization and industrialization have resulted in substantial water pollution from untreated domestic, industrial, commercial, institutional liquid waste presence, and several irrigation schemes (both point and nonpoint sources). The bulk of the factories in the basin do not have wastewater treatment facilities; they have not built treatment plants, nor have they established appropriate storage or discharge paths for their waste; instead, they release their wastewater into neighboring rivers, lakes, and streams. The Akaki sub-basin (Tinishu Akaki river) is the country's most contaminated river system. Almost all of the assessed locations along the Akaki rivers had poor water quality and did not meet the river water quality criterion.

Water quality in the Awash rivers was assessed using various indicators and found to be above global and Ethiopian minimum standards for surface water quality. As such the Awash river water did not meet the surface water standard of Ethiopia.

Numerous types of pollution resulting from waste generated by various socioeconomic activities, poor farming practices, and large-scale irrigation intensified irrigation schemes throughout the basin have harmed the water quality of the Awash River. The surface water in Addis Ababa is an example of this. As a result of rapid population growth, unregulated urbanization and industrialization, and inadequate waste management systems, it is very polluted, impacting human health and ecosystem function as a whole. The rivers of Addis Ababa are simply used as a dumping ground for the city's waste. Several studies have found that untreated and inadequately treated industrial wastewaters, household wastes, residential and commercial activities, and sewage discharged into waterways pollute Akaki river.

Agriculture is a large contributor of nonpoint source pollutants to aquatic environment. Pollution from agricultural activities includes nitrogen and phosphorous based chemical fertilizers, insecticides, herbicides, and organic matter. Large farms are the primary users of pesticides and herbicides. Both the main Awash River and its tributaries in Upper Awash have substantial rain-fed and commercial agricultural farms, high vegetable production, and animal husbandry activities. As a result of these activities, it is expected that a significant amount of organic waste is generated on rainy days (in runoff) which are responsible for nutrient enrichment in aquatic environments. As agriculture erosion by water, storm water or urban runoff and other natural sources of pollutants like soda springs, alkaline lakes, hot springs and geological formations are sources of pollutants for surface water quality impairment.

The majority of the papers are either distinct graduate theses, unpublished reports, or studies focused on a specific location and/or time period. Furthermore, the majority of research projects are located in upper Awash this is due to the high population number and high population density (like Addis Ababa, Mojo, Debrezit, and Adama), high urbanization and comparatively large number of industries. Assessing the relative contribution from diffuse and point sources is a major

research gap in the basin. There is lack of nonpoint source pollution (urban based or agricultural based) investigation in a basin.

This review identifies several water quality research efforts, but it also identifies research gaps. The most important relates to the scope and delimitation of the study. Much of the reports are either separate graduate thesis, unpublished reports, or research limited to specific locations and/or time. For example, there is no comprehensive surface water quality study, and there is a lack of detailed combined spatial and temporal surface water quality data to show the overall picture of the sub-watershed or the basin in general. In addition to this, there is no sound and comprehensive surface water quality information system or database at federal and local levels that is open and accessible for the public. This review work tries to focus some of these research gaps.

Assessing the relative contribution from diffuse and point sources is a major research gap in the basin. There is a lack of nonpoint source pollution (urban-based or agricultural-based) investigation at a basin or country level except (Eskinder, 2019) in the Kombolcha area. There is little evidence-based investigation into the influence of agriculture on surface water quality impairment, for example, organic compounds or chemicals like herbicides, insecticides, hydrocarbons, DDT, lindane, and other forms of chemicals are not investigated. For the problem of surface water quality, there is no well-coordinated research and no meaningful discussion between researchers and the community.

There is inadequate good spatial and temporal scale surface water quality data and/or monitoring in the basin. Biological parameter monitoring is very limited in the research works. This could be probably becuse some surface water quality parameters to be monitored are too expensive (some not available in the country) to be monitored so as to make scientific research and to provide policy direction recommendations. In addition to this, the existing laboratory facilities are not fully equipped and not well organized to analyze the overall surface water quality parameters unless they are upgraded. Economic and financial pressures dominate other concerns, and the impact of pollutants on water is neglected (Zinabu et al., 2019).

Policy responses for surface water quality drivers for the case studies have received little attention. The analysis of the legal, policy, and institutional framework showed a lack of cooperation between stakeholders, a lack of knowledge of the policy documents, an absence of enforcement strategies, unavailability of appropriate working guidelines, and a disconnected institutional setup at the grass root level to implement the set strategies as the major problems (Awoke et al., 2016).

2.3. Impacts of water quality in the Awash River Basin

2.3.1 Introduction

For this SR, we developed a search strategy to identify relevant literature. This search strategy was tailored to three databases: Web of Sciences, Scopus, Google, and Google Scholar, and the search terms used were the following: water quality, Impact of water quality, water pollution, industrial pollutants, and heavy metals. All searches included journal articles, books, and book chapters. The

selection criteria were based on the PRISMA Checklist 2009. The search mainly focused on mapping existing literature on the impact of water quality, water pollution, and heavy metals in the fields of environmental sciences, and earth sciences. The search span was from the year 2000-2021 in English only. The search was mainly focused on Ethiopia. The search from any other country was considered accordingly. A total of 85 research articles were excluded at this stage. There were 105 records extracted at this stage.

All duplications were extensively examined to maintain the review's quality. For the analysis and purification of the papers, the abstracts were checked deeply to ensure the quality and relevance of the research papers included in the review process. We read the abstracts of the 182 studies to see if they were relevant to the study topic and research questions. We got the full-text article for quality assessment after a total of 97 studies were deemed relevant. At a later stage a careful examination of each study publication was carried out. We looked through the full-text publications to assess the studies' quality and relevance. One article was not included in the study since it was written in a language other than English. In addition, 29 more publications were excluded from the study once the duplicate records were filtered out. After evaluating each article against the aforementioned inclusion and exclusion criteria, we chose 68 papers. The literature inclusion and removal at each level is depicted in Figure 1-4. 68 papers were chosen for data extraction, and the following aspects were extracted: articles must be published journal articles. Reports, dissertations, and unpublished documents were excluded. Through cited references, we discovered an additional 31 studies. In total, 99 studies were considered in this review.

We extracted information on the following subtopics from each study: (1) Water quality status of rivers in the Awash basin; (2) Seasonal fluctuations of trace metals in lakes and reservoirs in the Awash basin; (3) Point source pollutants (4) Health, vegetable, soil, biological, socio-economic, and toxic effects of water pollution. All data extraction and coding were performed using Microsoft Excel and Medley Reference Manager.

The role of clean water in social development, economic growth, and sustaining a healthy economic system has been well established (Katko & Hukka, 2015). The global community has been mainstreaming water supply and sanction as one of its core activities. Ensuring availability and sustainable management of water and sanitation for all sustainable development goals (SDG 6) is among 17 Sustainable development goals the global community is grabbling to achieve by 2030 (Kroll et al., 2019). Moreover, due to its cross-sectoral nature, improved water security has a catalyst role in the achievement of other SDG targets.

Despite this, water security particularly in developing countries tends to be at a crossroads (Yomo et al., 2019). Growing population, expansion of cities, rapid urbanization, and the expansion of industrial activities, the difference in inter-sectoral priorities, and the low enforcement capacity are threatening the rivers, and lakes (McGrane 2016; Berg et al. 2019). Environmental law enforcement in South Africa, as in other developing nations, has suffered significant setbacks due to a lack of technical expertise, insufficient finances, corruption, and penalties with low deterrent effects (Edokpayi et al., 2017).

Anthropogenic activities are responsible for the majority of water quality degradation in several rivers, where indiscriminate dumping of domestic and industrial wastes, as well as waste from other sources such as agriculture and health facilities, is common (P.U. et al., 2017; Amoatey and Baawain 2019) and justified in Ethiopia (Mekonnen et al., 2018), Bangladesh (Islam et al., 2021; Hasan et al., 2019; Islam et al. 2020) India (Kant et al., 2020; PR 2020), Rakiraki town in Fiji (Kumar et al., 2021), Kenya (Chebet et al., 2020) and South Africa (Edokpayi et al., 2017). Land and water quality degradation in Ethiopia, in general, was not impacted much by anthropogenic activities for the past decades due to the low population density that practices slash and burn agriculture with minimum fertilizer use (Ligdi et al., 2010). However, in the recent past, a wide range of pollutants including organic matter, salts, nutrients, sediments, heavy metals, etc. due to natural processes and anthropogenic sources are posing a serious threat to the land and water qualities of many of the basins in Ethiopia (Moges et al., 2017a). The problem is aggravated further due to climate change, rapid population growth, urbanization, and agricultural practices that put intense pressure on natural resources including the availability and quality of freshwater resources (Berg et al., 2019).

The environmental impact on local rivers increases as a city gets bigger, especially if the city cannot properly handle solid waste and wastewater. Untreated wastewater from industries and households may be discharged into rivers, where solid waste may accumulate along the river's course (Chebet et al., 2020; Adugna et al., 2019), especially in developing countries where wastewater treatment facilities are not well developed. Most cities of developing countries generate on the average 30-70mm^3 of wastewater per person per year (Edokpayiet al., 2017). Urban development interferes with water resources by altering the biophysical processes and fluxes of water, sediment, chemicals, microorganisms, and heat (McGrane, 2016). As cities develop in population, so does the total amount of water required for adequate municipal service. This rise in total municipal water demand is due to a combination of factors, including an increase in urban population and a trend toward economic development (McDonald et al., 2014). China's rapid economic development has come at a cost to the environment, increasing volumes of untreated wastewater from households, and industrial and agricultural runoff all contributing to severe pollution of the aquatic environment (Ma et al., 2020). Water quality is becoming a serious problem in some basins in Ethiopia. For example, the Rift Valley Lakes and their contributing rivers are used for irrigation, soda abstraction, fish farming, and recreation (Ayenew & Legesse, 2007).

Industries in developing countries generating volumetric wastes which are discharged without treatment into nearby water bodies. For example, most industries in Uganda use outdated manufacturing technologies and do not have functional effluent treatment plants (Srinivasan & Reddy, 2009) and in Bangladesh and Ethiopia often discharge their wastewater into the freshwater system without any treatment (Naser et al., 2014; Girma 2016). Therefore, raw and harmful wastes are discharged into the surrounding water bodies. Textile industries are huge industrial consumers of water and producers of wastewaters, with growing demand for textile products leading to an increase in textile wastewater output, making the textile sector one of the most serious sources of pollution globally (Mehari et al., 2015). Dadi et al., (2017) investigated the environmental and health impacts of effluents from four different textile and garment plants in Gelan and Dukem

areas around Addis Ababa and found that the bacteriological pollutants in the effluent are higher than the permissible limit given by the Federal Environmental Protection Authority (FEPA) (Dadi et al., 2017). Such practices lead to water quality deterioration of many freshwater systems making them unsuitable for irrigation, domestic or industrial purposes (Amare et al., 2017).

Point and non-point source pollutions from towns and cities contribute nutrient-rich effluents that are conducive for eutrophication where an upsurge of algae growth in the lakes will happen, and thereby depletes the oxygen needed by fish and other ecosystems (Girma 2016). Addis Ababa, which is part of the Akaki catchment, has a rapidly growing population, unregulated urbanization and industrialization, poor sanitation, and uncontrolled waste disposal, all of which contribute to a substantial deterioration in surface water quality (Kassegne et al., 2018). Rapid loss of ecosystems and land-use change, in part due to agricultural intensification, have been among the major drivers for recent increases in water in sedimentation and water quality issues in Ethiopia (Moges et al., 2017a).

The river basin is convenient for irrigated agriculture and industrial development due to its proximity to major cities such as Addis Ababa, Nazert, Debre Zeit, Dessie, and Dire Dawa. It has been impaired by pollutants from large-scale irrigation scheme (Amare et al., 2017; Tamiru 2001). On top of these, most of the industrial plants and cities do not have wastewater treatment plants (Rooijen & Taddesse, 2009) releasing their effluents directly to the river basin. Therefore, the discharges of these domestic, industrial, and agricultural wastes have been polluting freshwater systems jeopardizing socio-economic and ecological assets in the river basin (Mengistie et al., 2017).

The costs of water scarcity, misallocation, and pollution can be difficult to measure, and they are not always visible (Mekonnen 2018). Smallholder farmers grow a variety of vegetables in and around Addis Ababa. Without developed modern irrigation techniques, water scarcity is rampant and these farmers rely on the Akaki River as their primary source of water for irrigation. Due to a scarcity of freshwater, partially treated and untreated wastewater from a variety of industries, as well as gray water from the Addis Ababa city environment, are now used for irrigation (Mengesha et al., 2021). While water quality is a complex issue and involves multiple disciplines, this review focuses on water quality with respect cation, metals and heavy metals in surface water, and their impacts on vegetables, soil, biodiversity, human health, toxic and socio-economic effects. The river collects untreated and unmanaged domestic, industrial, and agricultural pollutants from the catchment immediately along its course, which could lead to a change in quality of water. As a result, among Ethiopia's major rivers, the Awash River is the most vulnerable to many types of serious pollution (Amare et al., 2017).

There has been little research on the impact of contaminated water on human and animal health, as well as the socio-economic implications on the riverine community, the downstream population, the basin, and the country as a whole. Although it is not complete and does not cover the entire basin and sub-basins, this systematic review provides valuable insight into the positive aspects of several studies that reveal the state of river pollution by heavy metals and their sources.

Although various initiatives have to investigate the state of pollution in Awash (Amare et al., 2017), basin-wide synthesis of the state of surface water pollution is lacking. Hence, the purpose of this article is to synthesize and generate information that captures the impact of contaminated water on human health, vegetables, and soil, as well as toxic, biological, and socio-economic effects that rely on river systems, as well as to identify knowledge gaps that are needed for the basin's long-term development and management. The following clear, logical, and well-defined research question was formulated: what is the impact of contaminated water in Awash Bain and the knowledge gap that is needed for the sustainable development and management of the basin.

2.3.2 Water Quality Issues in the Awash River Basin

The purpose of this systematic review was to discuss the current situation of water quality in the Awash basin. It evaluates the principal impacts of contaminated water in the Awash basin on the biological aquatic environment, toxicity, health, irrigated crops using contaminated surface water and soil, and socio-economic impacts of trace metals in lakes and reservoirs.

1. ***Water quality status of Rivers in the Awash basin***

The population living in the Awash River Basin was estimated to be more than 18.6 million (FAO and IHE Delft, 2020) with a population density greater than 6452.4 persons/km^2, in Addis Ababa and 0-10 persons/km2 in the lowland areas (Aklilu & Necha, 2018). Substantial rain-fed and commercial agricultural farms and several industries exist in the basin that are sources of pollutants (Eliku & Leta, 2018).

The basin is experiencing severe point source water pollution due to rapid urbanization and industrialization (Gebre et al., 2016) and non-point sources from agricultural fields (Amare et al., 2017; Tamiru 2001). The Akaki catchment is located in central Ethiopia along the western margin of the main Ethiopian Rift Valley. Addis Ababa, which lies within the Akaki catchment. Tinishu Akaki River contained a higher load of trace metals than the other regions, which is due to the existence of most of the industrial establishments and commercial activities (Kassegne et al., 2018). The Akaki River is heavily polluted, owing to the emission of harmful industrial effluents with little or no treatment (Amare 2019). Untreated pollutants from industries, residential, and commercial activities are discharged into the Tinishu Akaki River, which runs through the Addis Ababa City Administration. Several studies have found that discharges of inadequately treated and untreated industrial wastewater, residential wastes, and sewerages into waterways pollute rivers and streams (Amare, 2019; Mekuria et al., 2021). Figure 2-7 shows water quality monitoring stations used by different studies in the Akaki sub-basin. Another main tributary of the Awash River is the Mojo River. Shoa and Ethio-tanneries, Mojo oil mill plants, abattoir houses, and poultry farms are major sources of wastewater effluents downstream of the Awash River, which releases their raw effluent directly into the Mojo River, a tributary of the upper Awash and eventually into the Koka Reservoir. The Akaki River is a major tributary of the Awash River, which drains its effluents from its source to the Koka reservoir (Degefu et al., 2013).

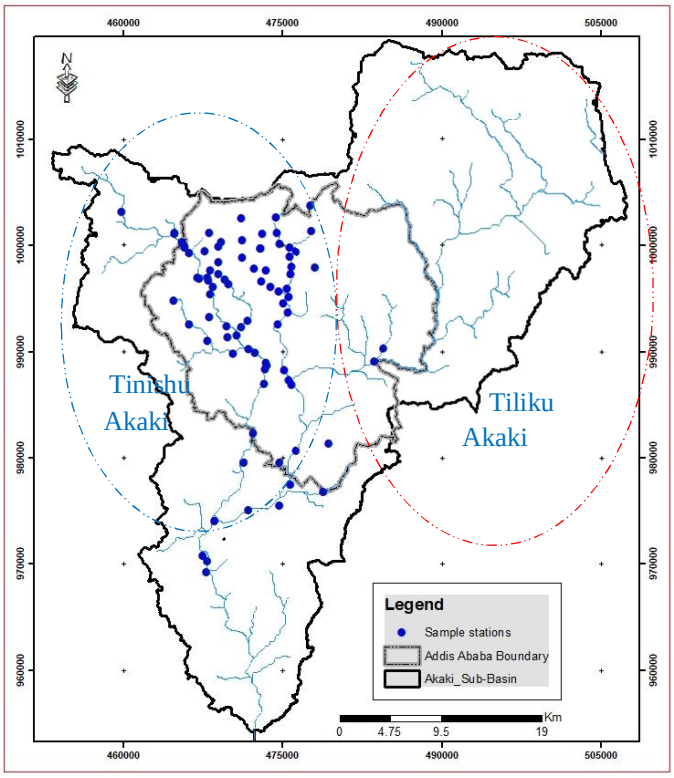

Figure 2-7 Akaki sub-basin water quality monitoring stations by several studies.

Source: (Aschale, 2015; Aschale et al., 2021; Mekuria et al., 2021; Melaku et al., 2007; Yard et al., 2015; Yilma et al., 2019)

Kassegne et al., (2018) reported that trace metals occurred in varying concentrations along the course of the sampling stations in Tinishu Akaki River and Aba Samuel reservoir. Relatively lower levels of trace metals were recorded at Aba Samuel reservoir due to the lower residence time of the sediment. Ecological risk assessment using USEPA sediment guidelines, geo-accumulation index, contamination factor, and pollution load index revealed the widespread pollution by Cd and Pb, these were followed by Mn, Ni, and Zn.

In addition, mean concentrations of heavy metals including Mn, Cr, Ni, Pb, As, and Zn were also above their allowable limits in these rivers (Amare et al., 2017) Arsenic and zinc were found higher in irrigated areas using water from the Akai River (Itanna, 2002) than rain-fed agricultural areas. Yosef (2017) on Tinishu and Tiliku Rivers reported that Cu, Cr, and Pb concentrations were greater than the standard limit set by the European directives for soil contaminants.

The water quality of the Tinishu and Great Akaki river basins has been classified, according to the WHO drinking water guideline (2004), as “badly polluted” to “very badly polluted,” making the water unsuitable for drinking. The presence of trace metals in the tested samples indicates that industries have a significant contribution to surface water pollution. Rooijen and Taddesse (2009) reported that E-coli bacteria concentrations in the Tinishu and Tiliku Akaki rivers were 6.68 x 10^9 and 6.61 x 10^9 CFU 100ml/L, respectively. The mean E.coli and Non-E.coli values in the measured water in Akaki River were 2.09 and > 3.48 log10 CFU 10 mL^{-1}, respectively, which were higher

than the WHO recommended standard (WHO, 2006) (Mengesha et al., 2021). The presence of trace metals in the tested samples indicates that industries have a significant contribution to surface water pollution and the high concentrations of E.coli bacteria indicate fecal pollution (Gebre, 2009).

Rooijen and Taddesse (2009) also reported that heavy metal concentrations that exceeded the natural levels were observed in vegetables grown in Tinishu and Tiliku Akaki Rivers and found that Cd, Cr, Cu, Hg, Ni, and Zn in potatoes; Zn and Hg in Cabbage; and Cr in onion and red beet. Water quality studies in different parts of Awash Basin are summarized in Appendix B Table 1. Another study by Itanna (2002) showed that cabbage was, in general, the least accumulator of metals/metalloids compared to other leafy vegetables except Ni and Cr. Lettuce had the highest concentrations of Cd, Co, Cr, Fe, and Mn; while Swiss chard contained the highest concentrations of As, Cu, Ni, Pb, and ZN (Itanna, 2002). Observed concentrations of As, Cr, Fe, and Pb were also greater than the maximum permitted levels in leafy vegetables and posed greater health concerns.

Fecal coliform levels in most vegetables in the Akaki River, except swish Chard, cabbage, and spinach in the wet season, were higher than the World Health Organization (WHO) and International Commission on Microbiological Specifications for Food (ICMSF) recommended level of 103 fecal coliform g/L fresh weights in both dry and wet season campaigns (Yosef 2017). This was attributed to the Akaki River water, which is higher than the WHO recommended standard used for irrigation of vegetables particularly in dry seasons due to flows from upstream through the town's major industrial, commercial, institutional, and residential areas. In addition, the application of organic manures is a common practice of farmers for the production of crops in that area.

2. Seasonal fluctuations of trace metals in lakes and reservoirs in the Awash basin

The presence, transport, and fate of toxic and persistent heavy metals and organic compounds in water bodies is a major area of concern around the world (Edokpayi et al., 2017). One of the world's greatest worries is the contamination of the environment with hazardous heavy metals. Because of their non-biodegradability, extended biological half-lives, and water solubility, the majority of heavy metals are extremely toxic (Naser et al., 2014). Most lakes and reservoirs in the Awash Basin are experiencing water quality degradation. There are twenty-two lakes and reservoirs within the Awash Basin. This section summarizes the water quality status of selected lakes and reservoirs within the basin. Speciation of selected trace elements on samples collected from the Koka reservoir showed that Cr, Mn, Co, Ni, Cu, Zn, and Pb were predominantly present at high molecular masses (HMM), i.e., greater than 10 kilo Daltons. The presence of trace elements at higher masses during the wet season suggests the reduced mobility of elements along with colloids and particles (Masresha et al., 2011).

Because Lake Beseka water is saline (EC~6.3 dS m^{-1}), sodic (SAR~300), or alkaline (pH~9.6), it cannot be used for irrigation or drinking (Dinka, 2012). The drastic expansion of the lake has led to many problems in the surrounding area, and is a severe threat to the wellbeing of the indigenous people and the economic welfare of the nation in general. Between 1960 to 2015, salinity and

alkalinity levels in Lake Beseka showed decreasing trends in ionic concentrations of quality parameters due to the dilution effect (Dinka, 2017). In general, the water quality of the Awash river downstream of Lake Beseka has deteriorated between 2013 and 2017 due to the release of unregulated Lake Water into the Awash River (Yimer & Jin, 2020). At the Awash inlet, Koka reservoir and Awash outlet, reported that the mean concentrations of metals ranked (high to low) was Fe > Cr > Cu > Zn > Pb > Cd > Ni and Fe > Cu > Zn > Pb > Cr > Cd > Ni during dry and wet seasons, respectively. Overall, concentration of heavy metals during dry season was higher than the wet season except for Fe. Increases in concentration of Fe during the wet season was attributed to increased runoff during the rainy season that eroded the soil particles containing iron (Eliku & Leta, 2018). Some heavy meatal related water quality studies in lakes, reservoirs and rivers in different parts of the Awash Basin Appendix B Table 1. Masresha et al., (2011) also observed differences in metal concentrations in Koka reservoir during dry/wet seasons with reported dry/wet season values (mg/L) of 46.6 /11, 6.4/1, 31.6/ 22, and 6.9/8.2 for Na^{++}, K^{++}, Ca^{++} and Mg^{++}, respectively. In addition, heavy metals like Fe, Cr, and Ni were in higher concentrations than the WHO limit Table 2-3. The lakes have primarily been used for commercial fishing, irrigation, recreation, and residential uses. Although these limited water resources are critical to the population's survival, there are signs that Koka reservoir is undergoing changes that could lead to water quality degradation.

The temporal and regional fluctuations of trace heavy metal concentrations in Mojo river in the extreme wet rainy season, semi-wet and semi-dry period (autumn), and extreme dry season (winter), according to Tamene and Seyoum (2015) showed that the level of As rises as the year progress from wet to dry, indicating dilution effects. Except for one result, all of the assessed Arsenic (As) results are higher than the WHO Drinking Water Guidelines (DWG) (0.01mg/L). In all study locations and sampling periods, the average Cd pollution load was found to be 0.12 ±0.075mg/L. All of the Hg experimental results are significantly higher than the WHO/FAO guidelines for fresh water (0.05 mg/L) and maximum allowable DW for livestock (0.003 mg/L), respectively. More than half of the examined results of Pb was above the WHO's maximum acceptable limit for DWG (0.01mg/L).

Adugna et al., (2019) observed higher concentrations of Cr(VI) in Tinishu Akaki and Jemo rivers. Figure 2-8 shows Cr(VI), CU, Mn, and Zn concentrations from studies conducted on different rivers. Overall, Cr(VI) and Mn concentrations exceeded the Ethiopian standard in both the dry and wet seasons in most locations. However, concentrations were greater during dry seasons compared to the wet season. This is probably due to the dilution effect of the wet season. In the different studies, there is very limited temporal heavy metal load analysis in rivers as well as in reservoirs/lakes in the different parts of the basin. The three rivers are the western side of the Akaki catchment Figure 2-7 which receives untreated wastewater from industries as well as from urban waste.

Table 2-3 Lake Koka cations and heavy metal study results by different studies.

Parameter	Unit	Parameter value	WHO standard
Ca^{++}	(mg/L)	31.6 dry season, 22 wet season (Masresha et al., 2011),	
Mg^{++}	(mg/L)	6.9 dry season, 8.2 wet season (Masresha et al., 2011)	
Na^{++}	(mg/L)	46.6 dry season, 11 wet season (Masresha et al., 2011)	
K^{++}	(mg/L)	6.4 dry season,11 wet seasons (Masresha et al., 2011)	
Fe	(mg/L)	6.8 dry season,37 wet season (Masresha et al., 2011)	(0.3)*
Cr	(µg/l)	27.8 dry season, 50.9 wet season (Masresha et al., 2011), 1.7-4.2 (Dsikowitzky et al., 2013)	(50)*
Mn	(µg/l)	303 dry season, 422 wet season, (Masresha et al., 2011)	(400)
Cu	(µg/l)	15.5 dry season, 20.8 wet seasons, (Masresha et al., 2011)	(2000)
Co	(µg/l)	4.8 dry season,7.7 wet season, (Masresha et al., 2011)	(110)
Zn	(µg/l)	48 dry season, 98.4 wet season, (Masresha et al., 2011)	(3000)
Pb	(µg/l)	4.9 dry season,8.5 wet season, (Masresha et al., 2011), 0.24-0.68 (Dsikowitzky et al., 2013)	(10)
Ni	(µg/l)	22.4 dry season,39.4 wet season, (Masresha et al., 2011)	(20)*
As	(µg/l)	2.8 dry season, 2.9 wet season (Masresha et al., 2011), 0.57-3.0 (Dsikowitzky et al., 2013)	(10)
Cd	(µg/l)	0.04 dry season, 0.06 wet season, (Masresha et al., 2011), < 0.1 (Dsikowitzky et al., 2013)	(3)
Se	(µg/l)	0.63 dry season, 1.2 dry season, (Masresha et al., 2011), < 0.1-0.12 (Dsikowitzky et al., 2013)	(50)
Hg	(µg/l)	< 0.1 (Dsikowitzky et al., 2013)	(6)
Viruses	(ml/l)	800E + 07 (Fasil et al., 2011)	
Bacteria	(ml/l)	502E + 06 (Fasil et al., 2011)	

**- higher than the WHO standard*

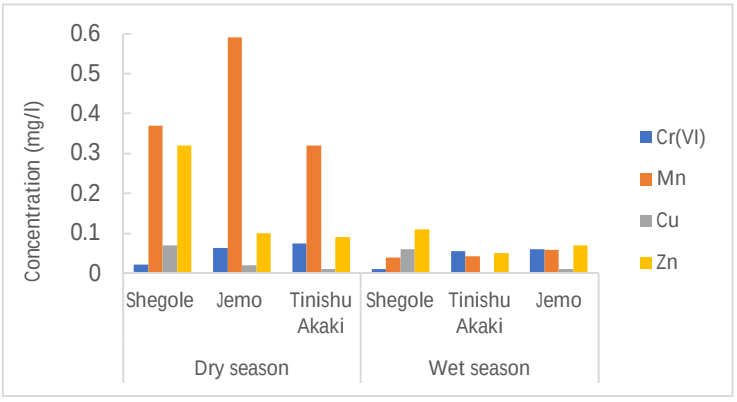

Figure 2-8 Trace metal content in Addis Ababa Rivers Sources (Adugna et al., 2019)

3. Point source pollution

Water contamination is caused by a variety of factors, including industrial wastewater and hazardous chemicals. Although Ethiopia has a small number of industries, its pollution impact is substantial. Industrial waste from poorly managed industries is a major source to water pollution, particularly in Ethiopian rivers. This is because most Ethiopian factories lack wastewater treatment

facilities (Menbere, 2019). In Ethiopia, most industries just dump their untreated toxic wastewater into adjacent rivers, lakes, and streams. Pollution from industrial wastewater discharge has increased as a result of hazardous chemicals (Alayu & Yirgu, 2018). The city of Addis Ababa hosts about 65% of industries in the country and more than 90% of those industries discharge their waste to the nearby river without proper treatment (Yohannes & Elias, 2017). However, in recent years, industrial activity is extending beyond Addis Ababa into towns like Mojo, Debrezeit and Nazret, increasing the influence of industrial pollution to the Awash and the Mojo rivers, and Koka reservoir as shown in Figure 2-7. The Awash River is polluted by liquid and solid effluents released from industries and households that release untreated their domestic and industrial effluents (Teshome, 2019). One of the major sources of pollution for the Awash River is untreated domestic discharge from the city of Addis Ababa. In Addis Ababa, for example, there are roughly 1200 significant industrial enterprises, which combined with institutions, commercial centers, and hotels generate 18 percent of the city's entire solid wastes (Menbere, 2019). The majority of the waste produced by residents and industries is deposited in the city's streams and rivers, which are consumed by livestock and also used for various purposes like as irrigating vegetables and crops (Weldegebriel et al., 2012)

Mengesha et.al., (2021) reported the Akaki River, like many Addis Ababa streams, is heavily contaminated by anthropogenic influences from upstream to downstream. The causes are specifically indiscriminate dumping of refuses into the river, indiscriminate dumping of industrial wastes (Mekonnen 2018). The majority of pollutants are discharged into a single collection location, such as reservoirs that can act as a sink for a variety of contaminants. Heavy metal concentrations in stream sediments are relatively high, according to several studies, due to significant anthropogenic metal loadings carried by tributary rivers. As a result, surficial sediments may act as a metal puddle, releasing metals into the underlying water and potentially harming riverine ecosystems (Astatkie et al., 2021).

Most industries in Gelan and Dukem have established neither treatment plants nor adequate storage or discharge channels for their wastes. As a result, polluted liquids are directly discharged into the open landscape (Dadi et al., 2017). A study by Dadi (2017) on the environmental and health impacts of effluents from textile industries in the Gelan and Dukem watersheds of the Upper Awash river showed the presence of substantial concentrations of Zn in industry effluents. (Feyissa and Bekele 2018) reported that both raw and treated effluents from the Anmol product paper factory contained higher concentrations of heavy metals that significantly deteriorated the water quality of the Awash River Table 2-4. The study found that, very high Na and Ca concentrations, greater than the national and WHO discharge limits, in both raw and treated effluents.

The Mojo watershed is one of the Awash Basin's sub-watersheds. The Mojo River Basin is experiencing rapid population growth, industrialization, and agricultural activities, all of which are potential causes of surface and groundwater contamination. Residents along the Mojo River use the river water for many purposes. However, the town's discharge of domestic and industrial pollutants severely restricts the use of surface water (Tamene & Seyoum, 2015). Kolba Tannery, Ethio-Japan Textile, Soap factory, Gelan Tannery, Organic Export Abattoir, Derartu Tannery, Mojo Tannery, and Food and Oil Complex drain their influent into the Mojo river. A study by

Gebre et al., (2016) found that mean concentration values of Cr in water samples ranged between 0-8.02 mg/L. Cr concentrations downstream of the Mojo, Kolba, Gelan and Derartu Tanneries were greater than NEQS standard (1 mg/L).

Table 2-4 Metals and heavy metals Anmol Product Paper Factory Sources: (Feyissa & Bekele, 2018)

	Concertation range (mg/L)		**Standards**	
Parameter	**Raw effluent**	**Treated effluent**	**WHO limit**	**EPA limit**
Na	140 – 900	130 – 800	400	400
K	2.9 – 12.1	2.1 – 11.6	-	-
Ca	11.09 – 1150	8.71 – 1104	200	200
Mg	5.23 – 110.4	6.18 – 66.24	150	150
Fe	0.27 – 2.77	0.18 – 1.67	-	-
Cu	0 – 0.03	0 – .03	2	2
Zn	0 – 0.59	0.13 – 0.55	10	6

2.3.3 Impacts of water pollution

Water quality affects the economic, social and political development of society (Mekonnen 2018). This paper focuses on the effects of water quality on biological, toxic, health as well as vegetable production and soil.

a. Biological effects

Nutrient loadings affect water quality throughout the world and have resulted in the eutrophication of many fresh water lakes (Alemu et al., 2017; Jonathan and Deniz, 2012). Water pollution in the basin is found to have contributed to the disappearance of aquatic species (Rooijen & Taddesse, 2009). Dissolved phosphorus plays an important role in the eutrophication of water bodies (Moges et al., 2016). Phosphates entering the water from detergents urban areas, industrial waste (such as sugar cane production), and intensive agriculture (Moges et al., 2016; Girma 2016; Rooijen and Taddesse 2009) can cause the nutrient levels in the water to rise and lead to algal blooms (Girma, 2016). A study by Ingwani et al., (2010) describes eutrophication from anthropogenic drivers as the main cause for the rapid spreading of water hyacinth over reservoirs. Water hyacinth is one of the biodiversity issues that contribute to the degradation of aquatic ecosystems. This is a case in Ethiopia where by degradation in water quality results in Water hyacinth (Eichhornia crassipes) invasion (Hailu et al., 2020). This can the incidental occurrence and spread of water hyacinths in Lake Tana (Moges et al., 2017a), as also observed in Lake Koka and Aba Samuel Lakes are indictors of the effect. Similarly, very high chlorophyll *a* values were observed upstream of Sebeta River (Tassew, 2007). The most severe area coverage by water hyacinths in Lake Tana was noticed at the mouth of the Megech River, which stretched both east and north with an estimated area coverage of 80-100 ha and wide distribution of daughter plants that pushed forward with the wave's assistance (Tewabe, 2015).

When nutrient-rich effluents enter a lake, it overloads the ability of the lake to provide oxygen to aquatic lives in it. This is a eutrophication process in which there is an upsurge of algae growth in the lake, which then results in the depletion of oxygen and fouling up of the lake water (Girma, 2016; Rooijen & Taddesse, 2009). This, in turn, can alter the food chain and ionic composition of

the water, increase organic matter in the sediment, decrease metalimnetic and hypolimnetic oxygen (which causes fish suffocation), and cause changes in the water temperature (Girma, 2016).

In many places of the world, the occurrence of harmful toxic algal occurrences has increased over the last three decades. Many bloom-forming algae species can produce biologically active secondary metabolites that are extremely harmful to humans and other animals (Radha and Mastan 2011; Edokpayi et al., 2017). Water pollution in the basin is found to have contributed to the disappearance of aquatic species (Amare et al., 2017)

Heavy metals concentrations in water and tissue samples from edible fish species from Hwassa and Koka lakes showed that metal concentration in Koka from highest to lowest was Cr>As >Pb>Cd>Se>Hg (Dsikowitzky et al., 2013). Metal concentrations in fish tissues also showed significant differences with average concentrations of metal in the gills from highest to lowest was: Cr>Pb>Hg>As>Cd>Se. In fish muscles, the rank was Cr>Hg>As>Pb>Cd>Se and in fish livers Cr>Hg>Cd>As>Pb>Se. Overall, Cr concentration was the highest in both water and fish tissue samples.

b. Toxicity effects

Toxic substances from farms, towns, and factories readily dissolve into and mix with it causing water pollution. Heavy metals are known to pose a variety of health risks such as cancer, mutation (Itanna 2002). Metals such as arsenic, lead, cadmium, nickel, mercury, chromium, cobalt, zinc and selenium present in natural waters are highly toxic even in minor quantities (Masindi & Khathutshelo, 2018). Some of the cations and heavy metal investigation results by different researchers in Lake Koka are shown in Table 2-3. For example, Fe, Cr, and Ni are higher than the maximum permissible limit of the WHO standard. The investigation made by Bahiru (2021) showed that concentrations (mg/L) of metals in the Akaki river water samples were found to be in the ranges of 0.18-0.28, 1.40-2.67, 0.97-1.40, 0.037-0.087, 0.037-0.080, and 01- 0.14 for Fe, Zn, Cu, Cd, Pb, and Cr, respectively. All are above the recommended limit of both WHO/FAO (2001).

The Tinishu Akaki catchment area has a high influx of trace metals. High levels of trace metals in sediments probably have adverse effects on the bottom-dwelling aquatic organisms as well as to the health of the people who depend on the water for various activities (Kassegne et al., 2018). Poor quality of river water in Addis Ababa cause and affect the production of different crops/vegetables (Bedada et al., (2019); this is justified by an investigation made by Rooijen and Taddesse (2009) trace metal content in vegetable leaves (Cd, Cr, Cu, Hg, Ni and Zn in potato and Cr in onion and red beet in Addis Ababa. The concentrations of trace metals in vegetables cultivated with wastewater are shown in **Error! Reference source not found.** (a) and (b) below. Although all of these metals have not yet reached phytotoxic levels, some plants have exceeded the normally occurring amounts. This is especially true in the case of Cd, Cr, Cu, Hg, Ni, and Zn in potatoes, as well as Cr in onion and red beet.

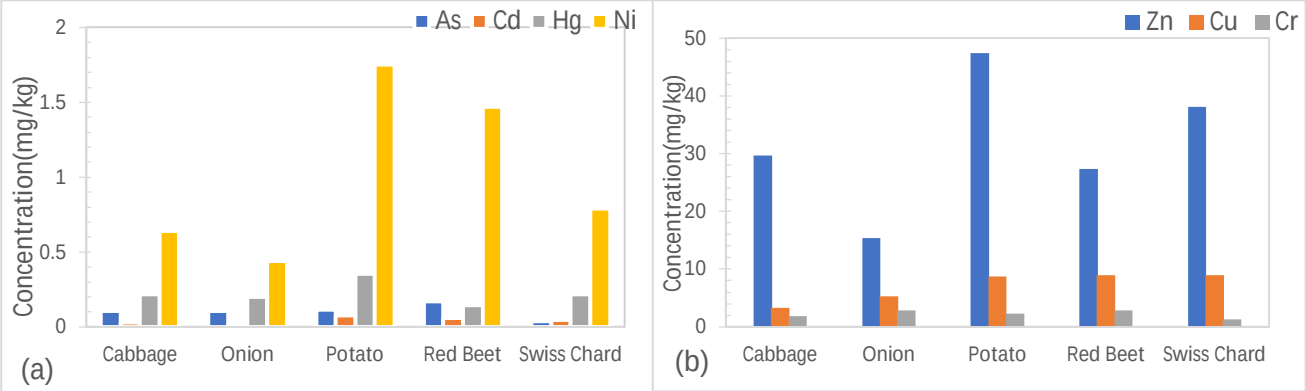

Figure 2-9 Concentration of trace metals produced by contaminated river water. Source: (Gebre, 2009)

c. Health effects

Virological Quality of Addis Ababa rivers and Hospitals total coliphages enumerations ranged from <1pfu/100ml to 5.2×103 pfu/100ml for urban rivers and <1pfu/100ml to 4.92×103 pfu/100ml for hospitals wastewaters. Coliphages were detected in 44 (52.4%) and 3 (10%) samples of 30 streams and rivers and four hospital waste waters, respectively.

Novel contaminants continue to pose new challenges to monitoring and treatment regimes in urban settings, where a variety of contaminants have an impact on water quality (McGrane, 2016). For example, as a result of fast population growth, uncontrolled urbanization and industrialization and poor waste management practices Addis Ababa's water resources are highly polluted which threatens human health and ecosystem function as a whole (Yohannes & Elias, 2017). Since downstream Addis river water is being used for various purposes such as drinking water supply (example, Nazareth town) and irrigation, public health risks are high (Rooijen & Taddesse, 2009). Contaminated drinking water has been linked to substantial illness and mortality around the world. It is used to spread communicable diseases such as diarrhea, cholera, dysentery, typhoid, and guinea worm infection (Wolde et al., 2020). For example, the negative impact on human health and the ecosystems as a result of the elevated level of several pollutants and irrigation products (vegetable) will ultimately affect the people that depend on the Akaki River water (Zinabu et al., 2002). An investigation conducted by (Bedada et al., (2019), in nine sub-Cities of thirteen rivers and four hospitals wastewaters of Addis Ababa, reported poor water quality in all rivers and one-half of the hospitals (detection of coliphages) will continue to cause a major health risk and will result in more number of deaths and also will affect the aquatic life and drinking water.

The overall mean count of E. coli and Non E. coli from water samples from Akaki River was 2.09 and >3.48 log10 CFU 10 mL−1 which is higher than the WHO recommended standard (Yosef 2017). A high level of total E. coli was recorded in effluents from ALSAR and ALMHADI textile industries in Gelan and Dukem (Dadi et al., 2017). Downstream residents use river water for domestic and agricultural purposes. Such practices have created major health risks to people who rely on the river for their livelihood. Despite the varied character of the Kebena River and its

neighboring buffer zones' environmental concerns, pollution remains the dominant worry (Asnake et al., 2021). Consumption of heavy metal-contaminated food crops is one of the most common routes for harmful compounds to enter the human body, with some symptoms appearing only after several years of exposure (Srinivasan & Reddy, 2009). The existence of total coliforms across the River has been a major threat to human health. Water pollution does not only have adverse health impacts, but it also imposes medical expenses on the population (Gebre, 2009)

Some research activities around Addis Ababa recognized there is a signal that human health and life are threatened due to crop production using polluted water (Regulation 2000). The negative impact on human health and the ecosystem as a result of the elevated level of several pollutants and irrigation products such as vegetables will ultimately affect the people who depend on the river water (Zinabu et al., 2002).

The local environment, people, and livestock of Gelan and Dukem towns are exposed to highly contaminated effluents. For example, related to skin allergies and stomach health problems in humans and bacteriological infections specifically “Salmonella” in cattle and donkeys diagnosed in veterinary clinics (Dadi et al., 2017).

d. Impact on Vegetable and Soil

Urban and industrial wastes are common sources of anthropogenic metal pollution in soils. Because of the negative impacts on food quality, crop growth, and soil environmental health, heavy metal deposition in soil is a key concern in agricultural production (Naser et al., 2014). The use of water with poor quality for agricultural activities can affect crop yield and cause food insecurity. Several studies have reported higher levels of heavy metal concentrations from different part of the country (Edokpayi et al., 2017). Heavy metals are easily accumulated in the edible parts of leafy vegetables compared to grain or fruit crops (Mapanda et al., 2005). Heavy metals accumulate in the edible and inedible sections of vegetables in sufficient concentrations to induce clinical issues in animals and humans who consume these metal-rich plants (Arora et al., 2008). Haile and Mohammed (2019) reported that Cr, Zn, Fe, K, Cu and Mn exceeded the WHO (2008) standards in lake Hawassa. Abate et al., (2015) stated that the concentration of Na^+ and K^+ greater than the 200mg/L permissible limit by WHO (1984). Worako (2015) also showed that Total Coliform and Fecal Coliform were greater than the acceptable limit of 1000 MPN/100ml set by WHO (1983) and CCME (1999); and above the 14MPN/100ml recommended limit by USEPA (1976).

Due to the high metal retention capacity of agricultural soil, it has been suggested that it is the most important sink for heavy metals. As a result of increased anthropogenic activity, there is evidence to suggest that agricultural soil has elevated amounts of heavy metals. Irrigation water's chemical contents can affect plant growth directly through toxicity or inadequacy, or indirectly by influencing plant nutrient availability (Belay, 2019). Heavy metals are inorganic pollutants with a wide range of negative effects on aquatic organisms, plants, and human (Inyinbor et al., 2018). The heavy metal concentration of irrigation water has been demonstrated to surpass the irrigation water standard (Amare et al., 2017).

Excessive accumulation of pollutants in soils, such as heavy metals, causes increased heavy metal uptake by crops, affecting food quality and safety (Srinivasan & Reddy, 2009). The mean

concentration of heavy metals including Mn, Cr, Ni, Pb, As, and Zn reported more in vegetables irrigated by the Awash River than their allowable limits (Amare et al., 2017). Vegetables like Ethiopian mustard, Lettuce, and Swiss chard, were collected and subsequently analyzed for selected heavy metals, Fe, Mn, Zn, Pb, Cr, and Cd. Zn was detected in all vegetable types, where around 51% of the samples exceeded the amount of Zn when compared to the standard limit of 99mg/kg in Akaki Rivers (Weldegebriel et al., 2012) Some of the vegetables tested in Tinishu and Tiliku Akakai Rivers have heavy metals exceeded the naturally expected levels. Based on the investigation, Cd, Cr, Cu, Hg, Ni, and Zn in potatoes, Zn and Hg in Cabbage, and Cr in onion and red beet (Gebre, 2009; Teshome, 2019).

The mean counts of TC, FC, and total aerobic count (TAC) on collected vegetables irrigated with Akaki River were 3.22, 1.37, and 4.72 in the dry season, and 3.87, 2.57, and 5.09 log10CFU per gram in the wet season, respectively. All fresh vegetables were contaminated with total coliform, fecal coliform, and total aerobics in the dry season (Yosef 2017). In addition to this, as stated by Bahiru (2021) Cd, Pb, Fe, Zn, Cr, and Cu concentration in lettuce samples irrigated by Akaki river water are in the range of (0.047-0.263), (0.42-6.55), (339.83-420.00), (2.96-13.44), (0.95-7.87) and (1.68-7.49) (mg /Kg) respectively, all heavy metal concentration is above-recommended level set by WHO (1999).

The investigation made by Itanna (2002) showed that Arsenic (As) and zinc (Zn) in soil irrigated by the Akaki River were higher than the normal limit. The concentrations of Pb, Cd, Mn, Ni, and Zn in sediments in the Tinishu Akaki River were relatively greater than other trace metals at levels that may have adverse biological effects on the surrounding biota (Kassegne et al., 2018). Similarly, a high concentration of tributary rivers and lakes (high concentration of salt) increases the pH level of the Awash River, and this affects the production of companies that engage in cotton production, wheat, and other cereal crops and vegetables (Teshome 2019). Akaki river water irrigated soil samples concentration (mg/kg) was found Cd (0.47-3.47), Pb (8.00-118.00), Fe (13557.30-16800.00), Zn (40.00-224.67), Cr (4.91-39.36) and Cu (35.00-149.88). All metals except Cd and Fe in the soil samples are below the recommended level set by FAO/WHO (2001) (Bahiru, 2021). Heavy metal levels in soil samples from Mojo sub-basin farmlands were measured. In soil samples from tomato cultivation, the mean concentration of arsenic (As) was found to be 21.00 mg/kg, and in soil samples from cabbage cultivation, it was found to be 30.73 mg/kg. Arsenic levels were found to be higher than the European Union's acceptable limit of 20 mg/kg in both soil samples tested (Gebeyehu & Bayissa, 2020). According to findings in Mojo River, the mean Cr value was 2.515.794mg/L, with half of the findings falling below the FAO standard for surface water irrigation (0.1mg/L) and WHO DWG (0.05mg/L) (Tamene & Seyoum, 2015).

Soil pH varied between 6.9 to 8.9 for Melka Sedi and 7.06 to 9.1 for Melka Werer farm areas. EC value ranges from 0.33- 82.1 deci Siemens per meter (dS/m) and 0.4 to 37.5 dS/m, respectively for soil samples taken from Melka Sedi and Melka Werer farms (Abebe et al., 2015). Soil salinity and sodicity assessment by Abebe et al., (2015) in the Amibara area revealed that substantial parts of farm areas were consistently and continuously affected by salinity problems.

e. Socio-Economic effects

The economic effect of water quality can be seen from different perspectives. A decrease in water quality can lead to increased treatment costs of potable and industrial process water. Crops will be prone to hunger and quality deterioration as a result of poor water quality, resulting in a drop in agricultural yield. Water contamination has a considerable impact on agricultural economic growth, as detailed by Li and Li (2021), which is a major roadblock to China's rural revitalization plan. China's water pollution has a cumulative effect on agricultural economic growth that is increasing in time and space, harming the agricultural ecology. Agricultural economic growth in China dropped by 27.994 units for every unit increase in wastewater discharge intensity.

In the case of Ethiopia, the mixing of Lake Beseka (extremely saline) water with Awash River (freshwater) was done to slow down Lake Beseka's rapid expansion rather than alleviate the basin's water scarcity problem. After the Lake Beseka mix, the Awash River serves as an important water source for cattle, domestic use, and irrigation water for nearby wheat, vegetable, cotton, and sugar plantations. These crops are extremely important economically for both the local community and the country. The water utilized for irrigation in the downstream community has a variety of negative consequences, including decreased crop yield and financial benefits, decreased irrigable or fertile land, and increased domestic water shortages (Yimer & Jin, 2020). For example, Tadesse et al., (2018) in their study Rebu River in the Oromia region reported that Cr, Zn, Fe, K, Cu, Na, Mn, and Pb concentrations were greater than the Ethiopian drinking water quality (EDWQ) (2010) and WHO (2008) standards as shown in the summary of major water quality studies from different parts of Ethiopia. Water pollution does not only have adverse health impacts but it also imposes medical expenses on the population (Gebre, 2009). The town of Awash with a population of 30,000 has to shift from abstracting water from river to groundwater primarily because of the pollution (Parker et al., 2016).

High concentrations of salt in tributary rivers and lakes increase the pH level of the Awash River and this affects the production of companies that engaged in cotton production, wheat, and other cereal crops and vegetables (Teshome, 2019).

2.3.4 Research Gaps and Problems Identified Future Agenda

The water quality of the Awash Basin's rivers, lakes and reservoirs is deteriorating. Rapid urbanization and industrialisation have resulted in serious point source water contamination in the basin and endangering the basin's socio-economic and ecological values. The majority of the factories in the basin lack wastewater treatment facilities, simply discharge their toxic wastewater into nearby rivers, lakes, and streams. There is also untreated domestic discharge. The industries in the Akaki and Mojo sub-basins discharge their waste into nearby rivers and streams. They haven't built any treatment plants, nor have they set up suitable storage or discharge pathways for their waste.

Heavy metal concentrations in rivers, as well as in plants irrigated by these river waters and in the soil, were beyond their permissible levels. Even in little amounts, heavy metals are extremely hazardous. This study found evidence of the presence of these harmful compounds over the WHO/FAO recommended limit in rivers, lakes, edible fish tissues, and vegetables, primarily in

upper Awash. Despite the fact that no previous study has been conducted to determine the influence on human and animal health, it is thought that they have negative impacts on aquatic organisms as well as the health of people who rely on water for various purposes. The amounts of cations, metals, viruses, and bacteria in most water sources of the basin exceed WHO and EPA legal limits, leaving them unsafe for human consumption. Water hyacinth (Eichhornia crassipes) invasion and harmful toxic algal occurrence owing to eutrophication caused by anthropogenic factors have been observed in the Koka and Aba Samuel reservoirs, as well as the Sebeta river. As a result, the food chain and ionic composition of the water can be altered, making people and other animals particularly harmful.

A comprehensive and systematic research spanning from identifying sources of pollution and its impact the health of humans, livestock and ecosystem at regular interval is vital. Moreover, a vulnerable ecosystem, it is vital to have an institutional arrangement responsible for regular monitoring and evaluation to protect vulnerable riparian communities and ecosystems. More research is needed to fully comprehend pollution dynamics and cleaning capacity of aquatic and wetland ecosystems. including a comprehensive study of the effects of contaminated water on human and livestock health, a comprehensive spatial extent investigation of the impact of contaminated water on growing vegetables, and the magnitude of the polluted water's socio-economic effects in the downstream community as well as the country as a whole.The novelty of this SR in that it is the first to combine information from many recognized research works on the impact of contaminated water on humans, vegetables, and soil, as well as toxic and socio-economic effects. The output will give background information for future research as well as preliminary policy direction for water resource managers and policymakers.

This SR is unique in that there has not been such a comprehensive including the accessing reports from different institutions in the country. The review also combines information from works on the impact of contaminated water on humans, vegetables, and soil, as well as toxic and socio-economic effects. The output will inform future research as well as plan management interventions. Building from narratives of different reports, the following immediate interventions: (1) Absence of accountability for industries that discharge effluents directly into water bodies without sufficient treatment; 2) widespread vegetable production in the upper Awash sub-basin using contaminated water. In the last decade, the Upper Awash River Basin has experienced rapid urbanization. If things keep going this way, the dawn stream's water quality will deteriorate dramatically. Wastewater reuse, such as that from Addis Ababa, is often used by the poor for vegetable growing. This is therefore water quality protection in the basin necessitates effective management and policy guidelines.

This SR is unique in that there has not been such a comprehensive including the accessing reports from different institutions in the country. The review also combines information from works on the impact of contaminated water on humans, vegetables, and soil, as well as toxic and socio-economic effects. The output will inform future research as well as plan management interventions. Building from narratives of different reports, the following immediate interventions: (1) Absence of accountability for industries that discharge effluents directly into water bodies without sufficient treatment; 2) widespread vegetable production in the upper Awash sub-basin

using contaminated water. In the last decade, the Upper Awash River Basin has experienced rapid urbanization. If things keep going this way, the dawn stream's water quality will deteriorate dramatically. Wastewater reuse, such as that from Addis Ababa, is often used by the poor for vegetable growing. This is therefore water quality protection in the basin necessitates effective management and policy guidelines.

This review identifies several impact-related contaminated water research efforts, but it also identifies research gaps. The most important relates to the scope and delimitation of the study. Much of the reports are either separate graduate thesis research limited to a specific location and or time. Consequently, there is no thorough integrated spatial and temporal water quality impact mapping to portray the overall picture of the sub-watershed or the entire basin. There is little evidence-based research on the effects of contaminated water on agriculture, health, and socio-economics. There is limited research on the socio-economic effects of water contamination and their estimated costs, human and animal health-related impacts of contaminated water, and all vegetables species grown by contaminated river waters. In addition to this, there is lack of regular biological water quality monitoring in the basin.

It is expected to participate in a comprehensive spatial and temporal study of the impact of contaminated water on irrigated vegetable production, human and animal health, socio-economic effects, and impact on living organisms living in the aquatic environment in the basin or sub-basin, utilizing the gaps identified in this review effort.

2.4. Hydrological /water quality model review

2.4.1 Introduction

Water, which causes erosion, transports chemicals, and is an uncontrolled common input, is the primary component of the system even though hydrology is only one part of the whole system (Menzel, 1980). Water supply, wastewater management, irrigation, flood control, erosion and sediment management, pollution abatement, recreational activities, and many more areas are only a few of the actual uses of hydrology (Jajarmizadeh et al., 2012). When evaluating a model's general applicability, it is important to keep in mind these changed circumstances (Menzel, 1980). The study of hydrology focuses on the movement, dispersion, and chemical and physical characteristics of earth's water as well as how it interacts with its environment, particularly how it affects living things.

According to (Jajarmizadeh et al., 2012), a model is a phrase used to depict a certain aspect of the natural or artificial environment. It might take the form of a physical, analog, or mathematical model. Every model has unique characteristics (Ganasri, 2015). Many hydrological models are being developed today, each with their own distinct and similar characteristics. As a result, classifications of hydrological models are crucial for precisely identifying each model's capabilities and constraints due to its distinctive and common properties.

The current state of environmental and water resource issues makes it difficult to solve them without using hydrological models of some form (Jajarmizadeh et al., 2012). It can be challenging to choose the best model for the transportation of water and pollutants because there are so many distinct options. Incorrectly applied models might produce incorrect outcomes and false information. The size and land use composition of the watershed under study, as well as the accessibility of local data, all influence the model type or methodology that is used (Ouma, 2018).

Many factors can be taken into consideration while selecting a hydrologic model. These requirements are always project-specific. Additionally, some criteria are subjective because they depend on the user. The many project-specific selection factors include the hydrologic processes that need to be modeled; the desired model outputs; the availability of input data; and the cost. The chosen models were then ranked based on several evaluation criteria. According to (Cunderlik & Simonovic, 2010), the important considerations included the temporal and spatial scales, processes modeled, pricing, technical assistance, setup time, required skill, available documentation, etc.

Since they represent various approaches to hydrologic modelling, lumped, semi-distributed, and distributed models should be compared independently (Cunderlik & Simonovic, 2010). The best model, according to (Ganasri, 2015), is the one that produces results that are similar to reality while using the fewest parameters and a low degree of model complexity.
This review study is a component of the water quality research being done in the Awash Basin, where there are a lot of knowledge gaps. A significant research gap in the basin is determining the relative contribution from diffuse and point sources. Except for the Kombolcha area (Eskinder, 2019), there is no non-point source contamination investigation at the national level. As a result, the best model must be chosen and used in the NPS pollutant study. Thirteen selected hydrological/water quality models with physical and conceptual foundations are therefore taken into consideration in this research. Each model's intended usage, nature, components, development, simulation aspects, fundamental principle, data requirements, and strengths and drawbacks are explored. So that this selection provides the scientific community with knowledge about the models to take into account when they are engaged in hydrological systems.

We created a search method to find relevant content for this SR. This search strategy was tailored to three databases: Web of Sciences, Scopus, Google, and Google Scholar, and the search terms used were the following: Hydrology, hydrological model, empirical model, water quality (WQ) model, and water pollution. Books, book chapters, and journal articles were all included in the searches. The 2009 PRISMA Checklist served as the foundation for the selection criteria Figure 1-4. The search mainly focused on mapping existing literature on the WQ, water pollution, and sources of pollution in the fields of environmental sciences, and earth sciences. The search span was from the year 1980-2023 in English only. A total of 32 research articles were excluded at this stage. There were 200 records extracted at this stage.

We extracted information on the following subtopics from each study: status of surface WQ monitoring, status of surface WQ, causes of surface WQ impairment, and surface WQ impairment indicators in the Awash basin. All data extraction and coding were performed using Microsoft Excel and Mendeley Reference Manager (Foeckler et al., 2020).

To preserve the caliber of the review, every duplicate was thoroughly inspected. For the analysis and purification of the papers, the abstracts were checked deeply to ensure the quality and relevance of the research papers included in the review process. We read the abstracts of the 200 studies to see if they were relevant to the study topic. We got the full-text article for quality assessment after a total of 185 studies were deemed relevant.

An in-depth examination of every study publication was done at a later point. We evaluated the quality and applicability of the research by reading the full-text articles. 15 more publications were excluded from the study once the duplicate records were filtered out. After evaluating each article against the aforementioned inclusion and exclusion criteria, we chose 160 papers. 160 papers were chosen for data extraction, and the following aspects were extracted: articles must be published journal articles. Reports, dissertations, and unpublished documents were excluded. Through cited references, we discovered an additional 6 studies. In total, 166 studies were considered in this review.

2.4.2 Types of models

According to different scholars, models can be categorized based on their use (groundwater, watershed) (Fares, 2008; Tsakiris & Alexakis, 2015), process description or parameter specification (deterministic vs. stochastic), timescale (single event vs. continuous), space scale (distribute vs. lumped) (Hossain et al., 2019), techniques of solution (analytical vs. numerical) (Fares, 2008; Jajarmizadeh et al., 2012; Tsakiris & Alexakis, 2015) and scale (single event vs. continuous). Watershed models can be divided into several groups according to the modelling techniques utilized (Patel et al., 2011). According to (Hossain et al., 2019)**,** the three key characteristics of watershed-scale modelling are the algorithms used (empirical, conceptual, or physically-based), the method used (a stochastic or deterministic approach for model input or parameter specification), and the spatial representation (lumped or distributed). However, the best classification, according to (Ganasri, 2015; Tsakiris & Alexakis, 2015), is the modelling that uses algorithms, specifically empirical, conceptual, and physically based models.

1. Empirical (Metric) models

Empirical (Metric) models are observation-oriented models that merely use the data that is already available, ignoring the characteristics and functions of the hydrological system (Devia et al., 2015). It uses equations derived from concurrent input and output time series rather than the catchment's physical processes. These models are only useful within these restrictions. Regression and correlation models are employed in statistically based methodologies to determine the functional relationship between inputs and outputs.

2. Conceptual (Parametric) Models

Without attempting to be precise replicas of physical reality, conceptual or parametric models depict all of the constituent hydrologic processes as a system of interconnected storages that are recharged and depleted in line with mass continuity (He & Croley, 2007). It is made up of several interconnected reservoirs that serve as a representation of the physical components of a watershed, which are replenished by precipitation, infiltration, and percolation and drained by evaporation, runoff, drainage, etc. This method employs semi-empirical equations, and the model parameters are evaluated both through calibration and field data. Numerous conceptual models of varying degrees of complexity have been developed.

3. Physically based model

A scaled-down version of a real system is what is meant by a physical model. According to (Jajarmizadeh et al., 2012), the analog model is the result of a simulated process that is utilized to imitate a natural process. The model is a mathematically idealized depiction of the actual phenomenon, according to (Abbott et al., 1986). These models, which incorporate the fundamentals of physical processes, are also known as mechanistic ones. It employs measurable state variables that are both time- and space-dependent. To prevent or reduce the requirement for calibration, physical models are based on the mathematical-physics equations of mass and energy transfer. A smaller- or larger-scale actual system is physically represented in the physical models. By conducting a small-scale experiment in the field or a lab, a physical model is used to represent a phenomenon on a big scale. Physical models' geometric and dynamic scales are crucial qualities (Fares, 2008).

Any model whose variables don't change randomly is said to be deterministic. A single set of input values will result in the same output for deterministic models, however, a single set of input values can result in multiple output values for stochastic models (Ganasri, 2015). Stochastic models have a certain amount of unpredictability and uncertainty, which are defined by statistical qualities such as trend, seasonality, mean, variance, skewness, covariance, correlation, and variance function. To add the dimension of spatial and temporal variability in some of the subprocesses, such as infiltration, some deterministic models may incorporate stochastic processes.

Event-based and continuous models both create output, but the former is only for discrete periods while the latter does it continuously. In contrast to a distributed model, a lumped model does not take into consideration the spatial variability of the input and output parameters. According to (Fares, 2008), a linear model is one in which the objective functions are represented by linear equations.

Distributed models, both physically based and conceptual, have been applied more frequently to understand the spatial and temporal variations of watershed processes and outputs due to the rapid

development of digital databases and computing technology as well as the growing requirements for knowledge of the distribution of water and material transport (He & Croley, 2007).

In general, empirical/statistical models are straightforward, require minimal data, and are especially helpful for comprehending hydrological responses on a geographically aggregated and/or temporally coarse resolution and ignoring spatial heterogeneity of hydrologic processes. Physically based models fully explain all significant hydrological elements and processes, but due to their high data and computing needs, their usage is only feasible in small, highly instrumented catchments (Zhang et al., 2016).

2.4.3 Hydrological /Water Quality Models

1. Soil and Water Assessment Tool (SWAT)

A continuous time, semi-distributed, basin-scale model called Soil and Water Assessment Tool (SWAT) was developed for the USDA's Agricultural Research Service (ARS) (Adu & Kumarasamy, 2018). The basin-scale model SWRRB (Arheimer & Olsson, 2001; Peterson & Hamlett, 1997) has been upgraded to SWAT. The SWAT model is a complex physical model that was designed to test and forecast water and sediment movement, as well as agricultural production on water, sediment, and agricultural chemical yields, in sizable, complex watersheds with a range of soil types, land uses, and management systems, in ungagged basins. Long-term simulations can be carried out using it successfully (Ganasri, 2015; Santhi et al., 2001; Yang & Wang, 2010).

Climate, soil type, sediment, nutrients, pesticides, vegetation growth, agricultural management, and surface and subterranean runoff are some of the major SWAT processes. Furthermore, it takes into account the water, sediments, and chemical yields from agricultural lands in intricate watersheds with a variety of soil types and management regimes (Santhi et al., 2001). In many watersheds, SWAT is utilized to estimate stream flow and nutrient loading (Adu & Kumarasamy, 2018). According to (Santhi et al., 2001), it can forecast changes in nutrient loadings from both nonpoint and point sources under various management circumstances.

SWAT is effective for simulating large basins with little effort and expense spent because of its high calculative efficiency. According to (Adu & Kumarasamy, 2018), it is susceptible to changes in the climate, plant cover, and management practices. When thinking about non-point source pollution and optimum management practices, SWAT is the model that is most frequently utilized (Nejadhashemi & Woznicki, 2011).

Topography, land use/cover, soil data, management conditions, daily rainfall data, maximum and minimum air temperature, solar radiation, relative air humidity, and wind speed are the inputs used by this model; and can describe water and sediment circulation, vegetation growth and nutrients circulation (Addis et al., 2016; Peterson & Hamlett, 1997; Setegn et al., 2008; Tuppad et al., 2011;

Xie & Lian, 2013) River discharge, sediment, and nutrient data are required for model calibration and validation (El-sadek & Irvem, 2014; Liu et al., 2014; Panagopoulos et al., 2011).

The model has the following strengths: provides a large amount of information even outside the boundary and can applied to a wide range of situations; predicts sediment load peaks, water and sediment circulation, vegetation growth, and nutrient circulation; used for large-scale water quantity investigations; predicts the long-term impact of rural and agricultural management practices; quantify and predict the impacts of land management practices on water, sediment, and agricultural chemical yields in large complex watersheds with varying soils, land use, and management conditions over long periods; modelling multiple functions at the same time in a dynamic way and incorporated with GIS. Moreover, it predicts peak sediment loads, water and sediment circulation, vegetation growth, and nutrient circulation; used for large-scale water quantity investigations; forecasts the long-term effects of rural and agricultural management practices; quantifies, and forecasts the effects of land management practices on water, sediment, and agricultural chemical yields in large complex systems. In addition to this, a large number of BMPs can be simulated within SWAT for use on agricultural watersheds; relatively accurate estimations of flow and WQ variables at the sub-basin scale over relatively short time intervals (daily or hourly) if the model is properly set up and calibrated (Glavan & Pintar, 2015; Mengistu et al., 2019; Gassman et al., 2007; Rostamian et al., 2008) It is physically based, has excellent documentation, makes use of easily accessible inputs with the help of the GIS interface, has detailed crop growth models and databases, good land management modules, and is ideal for studying watersheds of all sizes, from small to large (Nejadhashemi & Woznicki, 2011). According to (Shoemaker et al., 2005) SWAT uses a buildup and wash-off strategy similar to that of SWMM in urban settings.

The SWAT approach has some drawbacks: incapable of simulating single flood events (GAO & LI, 2015); uses equations with parameters that cannot be directly measured by using data (e.g., CN-equation, MUSLE); does not simulate sub-daily events like a single storm event; and cannot accurately evaluate processes such as extreme daily flow occurrences (Rostamian et al., 2008), the complex dynamic evolution of soil nitrogen and carbon, and simulation of runoff yield (Adu & Kumarasamy, 2018), scale-related issues affect just a small percentage of direct calibrations (Shoemaker et al., 2005), unable to simulate daily changes in dissolved oxygen in water bodies and has problems modelling floodplain erosion (Adu & Kumarasamy, 2018; GAO & LI, 2015; Nejadhashemi & Woznicki, 2011), unable to specify exact areas to apply fertilizers; only routes one pesticide at a time through the stream network (Yang & Wang, 2010), data-intensive, difficult to manage and alter when hundreds of data inputs are present. Only when conservative metal species are simulated from the input from a point source (Shoemaker et al., 2005).

2. Systeme Hydrologique European (MIKE SHE)

The hydrologic and WQ model MIKE SHE is deterministic, completely distributed, and physically based. It aims to model all significant land-phase hydrologic cycle phenomena. According to (He & Croley, 2007), the main purpose of MIKE SHE is to accurately model hydrologic processes at the micro scale (often less than 100 km2). According to (Golmohammadi et al., 2014; Graham & Butts, 2005; Jaber & Shukla, 2012) and others, the MIKE SHE modelling system simulates the movement of surface water, unsaturated subsurface water, evapotranspiration, overland channel flow, saturated groundwater, and exchanges between surface water and groundwater.

The MIKE SHE model, an advanced model of stream flow and WQ, can mimic the movement and modification of solutes in intricate river systems (Bakšić, 2019; Ganasri, 2015; GAO & LI, 2015). According to numerical stability, it operates at continuous, long-term, and storm event time scales with varied steps (Ouyang, 2013; Liu et al., 2014; Luo et al., 2015; Williams et al., 1985). At a variety of spatial and temporal scales, it can combine the treatment of multiple water management issues (Graham & Butts, 2005). By solving the advection-dispersion equation numerically for the specific regimes, conservative solutes were dissolved in surface, soil, and ground fluids in the case of chemical simulation (Ouyang, 2013).

The MIKE SHE model does not have a predetermined set of required input data. The hydrologic process that is included and the process model that is chosen, which in turn depend on the issue that MIKE SHE is intended to address, determine the necessary data. However, the following are necessary for almost every MIKE SHE model, including model extent (typically as a polygon, topography, precipitation, reference evapotranspiration including canopy interception (Shoemaker et al., 2005), air temperature, and sub-catchment delineation), river morphology, land use/land cover, soil and subsurface geology (DHI, 2017; Sandu & Virsta, 2015).

The flexibility of the MIKE SHE model to be linked to and coupled with other DHI (Danish Hydraulic Institute) models is one of its benefits (Jaber & Shukla, 2012). This allows researchers to evaluate the combined effects of land use management in urban and rural areas on broader hydrological systems. appropriate for researching both long-term trends and one-off storms (Borah & Bera, 2003). Similar to this, the model's merits include its ability to replicate various land-phase hydrologic cycle processes and its applicability to bigger watersheds. It covers solute transport as well as evapotranspiration, overland flow, unsaturated flow, groundwater flow, and channel flow and their interactions. There are no size restrictions on the system's watersheds (Golmohammadi et al., 2014). The MIKE SHE model also provides a GIS interface that enables the preparation of model input and the presentation of model output (Shoemaker et al., 2005).

The model has the following drawbacks: it is limited to use in smaller catchments due to the requirement for large data sets of physical parameters, which may not always be available and make model setup difficult; the MIKE SHE model lacks a more sophisticated module that would

model root zone processes (nitrification and denitrification) (Jaber & Shukla, 2012). Additionally, in order for the model to fully utilize the system, multiple modules must be purchased (Shoemaker et al., 2005). Lack of data makes it difficult to mimic some determinants accurately; for example, the need for channel cross-sections at reach borders makes calibrating and tracking the outcomes over time a laborious operation that necessitates a lot of computation effort (GAO & LI, 2015).

3. Agricultural Nonpoint Source Pollution (AGNPS)

AGNPS is a distributed, event-driven parameter model created by USDA ARS. For single-storm events, it simulates runoff and calculates the loads of sediment and nutrients from agricultural watersheds (Adu & Kumarasamy, 2018; Young et al., 1989). It is a physically based continuous and daily time step model used to simulate surface runoff, sediment, pesticides leaving the land areas, and nutrient yields and their subsequent passage through the watershed, according to (Ouyang, 2013; Shoemaker et al., 2005). To simulate surface runoff and pollution loads through rivers and streams within the watersheds, the sub-areas are combined. The AGNPS is a lumped-parameter model that produces a single value for each output variable using a one-time step (Adu & Kumarasamy, 2018; Borah & Bera, 2003).

The three primary parts of the AGNPS are hydrology, which determines peak flow rates and runoff volumes, chemical transport, which determines chemical concentrations like nitrogen (N) and phosphorus (P), and erosion and sediment movement. In addition, the model takes into account inputs from gullies, animal feedlots, springs, and other point sources of sediment, water, nutrients, and chemical oxygen demand (Adu & Kumarasamy, 2018; Yang & Wang, 2010; Young et al., 1989) The AGNPS's WQ components are determined by comparing discharge levels of nutrients and pesticides. Agricultural watersheds ranging in size from a few square kilometers to 200 square kilometers were the focus of the model's development (Young et al., 1989).

The model inputs include watershed delineation, cell (sub-watershed) boundaries, digital elevation model, land slope, slope direction, reach information and number of cells; daily precipitation, maximum and minimum temperature, dew point temperature, sky cover, and wind speed, if running for a single event, the storm type, duration and intensity; management information, land characteristics (land use), crop characteristics, field operation data, chemical operation data, feedlots, and soil information; point source information and management practices within the cell (Eriksson, 2003; Mohammed et al., 2004; Young et al., 1989).

The following are some advantages of the AGNPS model over experiments: it simulates the spatial distribution of catchment features (a distributed model); it responds immediately compared with experiments; it helps in understanding erosion processes (Adu & Kumarasamy, 2018; Shoemaker et al., 2005). It helps analyze watershed management strategies, particularly agricultural operations, ponds, grassed waterways, irrigation, tile drainage, vegetative filter strips, and riparian

buffers (Borah & Bera, 2003; Shoemaker et al., 2005; Shoemaker et al., 2005). It is also helpful in investigating single severe storms.

There are several restrictions with AGNPS. The model is unable to assess nutrient transformation and in-stream processes and is only capable of simulating single events (Adu & Kumarasamy, 2018; Yang & Wang, 2010) necessitating the need for exclusive and extensive data. Additionally, adaptation of the model necessitates a lot of work and programming expertise. Time-varying water, sediment, and chemical discharges, which are crucial in some analyses (Adu & Kumarasamy, 2018; Borah & Bera, 2003) cannot be predicted by it. An important drawback of the AGNPS model is its inability to estimate peak flow with any degree of accuracy (Babel & Najim, 2017). There are issues distinguishing storm runoff from the total discharge hydrograph, there are no clear accounts of the impact of the antecedent moisture conditions on runoff computation, and there are no simulations of subterranean flow. In addition, the model is unable to account for activities such as nutrient transformation and in-stream processes, pesticide handling, the need for additional field testing of the pollutant transport component, and more (Shoemaker et al., 2005; Yang & Wang, 2010) Before the next day's simulation, all runoff and related loads of sediment, nutrients, and pesticides for a single day are directed to the watershed outflow (Borah & Bera, 2003), (Cambien et al., 2020). Nutrients and pesticides associated with sediment deposited in stream reaches are not tracked from day to day. For the duration of the simulation, point sources are restricted to constant loading rates (for both water and nutrients). Rainfall that varies geographically is not permitted. Because the model does not take into account the spatially variable rainfall over the watershed, it is impossible to simulate base flow or frozen soil conditions (Cambien et al., 2020); the mass balance calculation for water inflow and outflow is also not provided; and the runoff simulation is not entirely based on physical laws (Patel et al., 2011; Shoemaker et al., 2005).

4. HSPF (Hydrologic Simulation Program FORTRAN)

Early in the 1960s, the Stanford Watershed Model was developed. Processes for ensuring WQ were added in the 1970s (Adu & Kumarasamy, 2018; Skahill, 2004) According to (WASEEM et al., 2018), the HSPF simulation model is semi-distributed and constant. According to (Fares, 2008; Guttierrez-Magness & Raffensperger, 2003) the HSPF is a comprehensive, conceptual, continuous watershed simulation model that simulates the processes that affect water quantity and quality in a watershed, including runoff flow rate, sediment loads, nutrients, pesticides, toxic chemicals, other water-quality constituent concentrations, and historical time series of water quantity and quality at any point in a watershed (Yang & Wang, 2010).

HSPF performs flow and WQ routings in the watershed channels by simulating NPS runoff and pollutant loadings, combining them with point source contributions (Tsai et al., 2017). HSPF covers the organic chemical sorption, volatilization, oxidation, hydrolysis, and photolysis transport and reaction mechanisms. The in-stream nutrient processes involve phytoplankton, zooplankton,

benthic algae, DO, BOD, nitrogen and phosphorus interactions, pH, and others (Yang & Wang, 2010).
Processes regulating water flow and chemical constituent concentrations can be modeled and simulated for land and in-stream (river reach, reservoir) environments using HSPF at different levels of detail (Shoemaker et al.,, 1997; Marcomini et al., 2001; Shoemaker et al., 2005; Singh et al., 2005; Skahill, 2004). By defining the HSPF modules and code compartments that are utilized, these decisions are established, and the decisions subsequently form the model structure used for every given case. For the HSPF calculations, additional forms of information must be provided in addition to the choice of modules and code compartments, such as model parameters and time series of input data (Angélica & Gutiérrez-Magness, 2003; Skahill, 2004).

For watershed simulation, meteorological records of precipitation and predictions of potential evapotranspiration are necessary. For the simulation of WQ, it may be necessary to consider factors such as air temperature, wind, solar radiation, humidity, cloud cover, tillage techniques, point sources, and pesticide application (Salah & Nelson, 2010). To calibrate and validate processes simulated by HSPF, empirical data are needed. These data are used to assess model performance but are not input to HSPF.

The HSPF model's capability to take into consideration the distribution of land use within a certain modeled watershed is one of its significant advantages. Part of the model parameterization process is based on this information, or a combination of this information and other data describing the watershed (Skahill, 2004). Its advantages include flexible design, thorough consideration of watershed-scale hydrologic and WQ processes, and broad applicability. With in-stream hydraulic and sediment-chemical interactions, it enables the integrated simulation of land and soil pollutant runoff processes. It accurately assesses sediment movement, runoff flow rate, and concentrations of nutrients and pesticides. It can simulate in-stream processes and makes accurate results predictions (Bakšić, 2019). One of the few watershed models that can simulate both land processes and receiving water processes at the same time. It can also simulate peak flows as well as low flows. It can simulate at different time scales, such as sub-hourly to one-minute, hourly, or daily. It can also simulate the hydraulics of complicated naturally occurring and artificial drainage networks. By defining the external targets block, the user-defined model output options are included. The setup can be made simple or complex, depending on the application, requirements, and data availability (Shoemaker et al., 2005). It also includes the ability to address a variable water table.

The shortcomings of the model are: it approaches a distributed model when smaller sub-watersheds are used, which may lead to an increase in model complexity and simulation time; lumped parameter approach at the sub-watershed does not take into account spatial variation of one land parcel relative to another in the watershed (Shoemaker et al., 2005; Yang & Wang, 2010). Additionally, it lacks detailed parameter suggestions, considerable data requirements, and the user

training that is normally needed to operate the model (Skahill, 2004). It also has limited handling of urban drainage systems and unidirectional flow hydraulics.

A thorough model parameterization effort for a watershed with mixed land uses is not supported by the guiding data and tools currently available. WQ model parameter estimate assistance is not provided by the expert system tool HSPEXP. It is confined to well-mixed rivers and reservoirs and one-dimensional flow, relies heavily on several empirical relationships to depict physical processes, requires significant calibration, and requires a high degree of knowledge for application (Bakšić, 2019; Shoemaker et al., 2005; Yang & Wang, 2010). For big sub-basins and long channels in particular, HSPF is inadequate for simulating powerful single-event storms (Patel et al., 2011). prevent them from being able to evaluate non-point source contaminants in aquatic bodies in a generalized, efficient, and simple way (Adu & Kumarasamy, 2018).

5. SWIM (Soil and Water Integrated Model)

To provide a thorough GIS-based tool for hydrological and WQ modelling in mesoscale watersheds (from 100 to 10,000 km2), the new watershed model SWIM was developed. The two previously developed tools SWAT and MATSALU serve as the foundation for the new model SWIM. According to (Gao et al., 2016; Krysanova et al., 1998), SWIM incorporates weather, hydrology, erosion, vegetation, and nitrogen/phosphorus dynamics at the watershed scale. The model was created primarily for usage in Europe and the region with temperate climates, although it could also be used in other places.

According to (WASEEM et al., 2018), SWIM is a time-continuous, spatially semi-distributed model. According to (Krysanova & Wechsung, 2000), the hydrological module is based on the water balance equation and accounts for precipitation, evapotranspiration, percolation, surface runoff, and subsurface runoff for the soil column separated into multiple layers. The following pools and flows are included in the nitrogen model: mineralization, fertilization, plant consumption, runoff with surface and subsurface flows, leaching into groundwater, loss with erosion, and de-nitrification (Krysanova et al., 1998). The nitrogen model also includes the following pools and flows: active and stable organic nitrogen, organic nitrogen in plant residue, and nitrate nitrogen in the nitrogen model's pools. The phosphorus module includes the following pools and flows fertilization, sorption/desorption, mineralization, plant uptake, loss with erosion, and wash-off with the lateral flow. The pools and flows include labile phosphorus, active and stable mineral phosphorus, organic phosphorus, phosphorus in the plant residue, and phosphorus in the pools.

The model simulates linked mesoscale phenomena such as erosion, nitrogen and carbon cycling, plant and agricultural growth, runoff generation, and so on. Numerous model outputs are provided by it, including river discharge, crop yield, and nutrient concentrations and loads (Krysanova & Wechsung, 2000). Using regionally available data (climate, land use, and soil) and taking feedback

into account, the approach enables the simulation of all associated processes inside a single model framework at a daily time step (Hesse & Krysanova, 2016; Krysanova & Wechsung, 2000). GIS interface support is provided for the model construction and post-processing. Basins, sub-basins, and hydrologic response units are the three levels of disaggregation used by the model (Gao et al., 2016; Krysanova et al., 1998). It was developed for river basin-scale impact analysis. It was specially created to investigate how climate and land use change impacts are seen at the regional scale, where adaptation efforts are made (Gao et al., 2016).

It uses input information including topography, land use, soil distribution, and parameters, the network of surface waterways and rivers, meteorological and precipitation stations, data on the management of water and land use, measured discharge data, and measured values of nutrient concentrations. Observed precipitation, temperature, river discharge, and nutrient concentrations in the basin outlet are required for the calibration and validation of SWIM (Gao et al., 2016). SWIM has the advantage of integrating sediment transport, nutrient cycling (C, N, and P), hydrological processes, and vegetation growth (crops, and natural vegetation) at the river basin scale. It can primarily be utilized for impact studies in large and mesoscale river basins (Krysanova et al., 1998; Krysanova & Wechsung, 2000). In addition, it is a model of intermediate complexity for the river basin and regional scale because, first, it is driven by commonly available data and can be parameterized more easily than more complex hydrological models; second, it is more comprehensive than purely hydrological and precipitation-runoff models due to a more accurate representation of interlinked hydrological, vegetation, and nutrient processes (Krysanova & Wechsung, 2000). The main drawbacks of SWIM are that it excludes several sub-models (such as pesticides, ponds and reservoirs, and lake WQ) and that the average sub basin area is limited to between 10 and 100 km^2.

6. Areal Nonpoint Source Watershed Environment Response Simulation (ANSWERS)

To represent the spatially variable processes of runoff, infiltration, subsurface drainage, and erosion for single-event storms, ANSWERS was developed at Purdue University in West Lafayette, Indiana (Borah & Bera, 2003; Yang & Wang, 2010) It is a lumped, deterministic model that can only simulate a single storm event. A conceptual model of the several processes that take place inside a watershed that is primarily agricultural was initially built to create and develop the model. WQ planners and other users would be able to simulate the effects of different combinations of land uses, management plans, and conservation strategies on the hydrologic and erosion responses of a watershed using the ANSWERS program (Beasley et al., 1980).

The ANSWERS program operates on the presumption that all significant parameters are constant inside an element. The runoff and erosion processes within each element are treated as independent functions of the hydrologic and erosion-related parameters within that element (such as slope direction and magnitude, vegetation, rainfall and infiltration rates, soil erodibility, and management factors, for example). The representation of topography, soils, and land use can have

a lot of spatial information when small elements are used (Beasley et al., 1980). A hydrological model, a sediment transport model, and many routing components make up the ANSWERS. The detachment, transport, and deposition of soil are described by a sediment continuity equation (Borah & Bera, 2003). Which inherently provides the ability to simulate the fate of any type of pollutant and to integrate the response of individual elements to yield a composite watershed simulation (Beasley & Huggins, 1991).

For analyzing the long-term effects of hydrological changes and watershed management techniques, particularly agricultural practices, ANSWERS is a continuous simulation model. Chemical simulation: Uptake, runoff, and sediment losses as well as the transport and modification of nitrogen and phosphorus through mineralization, ammonification, nitrification, and denitrification (Borah & Bera, 2003). The single-event ANSWERS model has just undergone a modification called ANSWERS-Continuous, which includes extensive upland process simulations. ANSWERS-Continuous lacks channel erosion and sediment transport routines, and therefore the sediment and chemical components are do not apply to watersheds (Borah & Bera, 2003).

According to (Beasley & Huggins, 1991), the ANSWERS model's input data consists of six different forms of data in general: Simulation requirements (Measurement unit and output control); Rainfall information (times and intensities); Soils information (moisture, infiltration, drainage response, and potential erodibility); Land use and surface information (crop type, surface roughness, and storage characteristics); Channel descriptions (width and roughness); Individual element information (location, topography, drainage, soils, land use, and BMPs); and Simulation requirements (Measurement unit and output control).

A surface runoff hydrograph is provided at both the watershed outlet and any other user-selected point within the watershed. The ANSWERS model's strengths include simulating transformations and interactions between four nitrogen pools, including stable organic N, active organic N, nitrate, and ammonium. In addition to this, a surface runoff hydrograph is provided at both the watershed outlet and any other user-selected point within the watershed (Beasley & Huggins, 1991).

The ANSWERS model has some drawbacks, such as the inability to replicate interflow and groundwater contributions to base flow; the inadequacy of its formulation to simulate powerful single-event storms; and the possibility of numerical issues in its solutions. The sediment and chemical components are not applicable to watersheds because there are no routines for channel erosion and sediment transport; the simulation is only available for medium-sized watersheds; and there is no chemical component and sediment simulation in stream channels (Adu & Kumarasamy, 2018; Beasley & Huggins, 1991) The WQ constituents that can be modelled for this storm event model include only nitrogen and phosphorous; pesticides cannot be included. Nitrogen and phosphorus are simulated using correlation relationships between chemical concentrations,

sediment yield, and runoff volume; no nitrogen or phosphorus transformation is taken into account (Yang & Wang, 2010)

7. Water Quality Analysis Simulation Program (WASP)

The US EPA developed the WASP surface WQ model for WQ modelling. WASP is a dynamic model in one, two, and three dimensions. A variety of interconnected systems, including those involving ammonia, nitrate, phosphate, phytoplankton, BOD, DO, organic nitrogen, and organic phosphorus, are developed in WASP. According to (GAO & LI, 2015; Yuceer & Coskun, 2016), a flexible compartmental modelling structure can be used to analyze a variety of WQ issues in ponds, streams, lakes, reservoirs, rivers, estuaries, and coastal waters. According to (Razdar et al., 2011), the WASP system is a generalized framework for simulating the fate and transport of contaminants in surface waters.

WASP may also be connected with hydrodynamic and sediment transport models that offer flows, depths, velocities, temperatures, salinities, and sediment fluxes (Wool et al., 2020). To address both conventional pollution (including DO, BOD, nutrients, and eutrophication) and toxic pollution (involving organic compounds, metals, and sediment), the most recent version of WASP7 includes two main kinetic modules: TOXI for toxicants and EUTRO for conventional WQ (GAO & LI, 2015). For various pollution management decisions, this model assists users in interpreting and forecasting WQ responses to natural events and man-made pollution (GAO & LI, 2015; Wool et al., 2006). Nitrogen, phosphorus, DO, BOD, sediment oxygen demand, algae, periphyton, organic compounds, nutrients, heavy metals, mercury, pathogens, eutrophication, bacterial contamination, and temperature are among the pollutants it can handle (Jayawardena, 2013; Razdar et al., 2011)

It is the most robust and complex model and successful implementation calls for more knowledge and experience. The model was widely used to evaluate the WQ in streams and rivers (Yuceer & Coskun, 2016). The input data consists of the following (Shoemaker et al., 2005): beginning conditions, point and NPS inputs, flow file, vertical mixing coefficients, open boundary conditions, and rates of chemical and biological reactions.

The most potent and sophisticated model is the WASP. WASP's integration with watershed and hydrodynamics models enables multi-year analysis in a range of meteorological and environmental circumstances. The model has been heavily used in the creation of TMDLs due to its versatility in managing various pollutant types. Users can use it to assess and forecast how changes in WQ will affect reactions to both natural and man-made pollution in various pollution control decisions. All sorts of water bodies, management assessments, and WQ factors can be handled (Borah & Bera, 2003; Shoemaker et al., 2005; Shukla, 2011; Wool et al., 2020) The model (Wool et al., 2006) represents the time-varying processes of advection, dispersion, point and diffuse mass loading, and boundary exchange.

The model has some drawbacks, including the inability to handle mixing zones or near field effects, the need for additional data and expertise for a successful application, the inability to handle sinkable/floatable materials, the need for a substantial amount of data for calibration and verification, and WASP's inability to accurately simulate suspended solid (SS) loading in the river (GAO & LI, 2015; Shoemaker et al., 2005) The model is based on the flexible compartment modelling approach rather than solving a set of multidimensional dynamical equations (Razdar et al., 2011). Requires an external hydrodynamic model to supply a flow file to solve the advection problem; dispersion coefficient and temperature are user-specified; the computation of the sediment flux is oversimplified; There is no periphyton or macroalgae; shear stress has little bearing on the mechanisms involved in transporting sediment (Shoemaker et al., 2005).

8. Distributed Large Basin Runoff Model (DLBRM)

The Great Lakes Environmental Research Laboratory of the U.S. National Oceanic and Atmospheric Administration (NOAA) and Western Michigan University collaboratively created the spatially distributed conceptual hydrology and water quality model known as the DLBRM. According to (Demarchi et al., 2009; L. Zhang et al., 2016), it simulates the geographical and temporal distributions of point and NPS materials in both the surface and subsurface. A daily time step is used for continuous operation (Gebremariam et al., 2014). A modified version of the LBRM (Large Basin Runoff Model) is used to create the DLBRM. The spatial response to hydrologic events cannot be simulated by the 1-D, conceptual parameter LBRM since it does not account for spatial heterogeneity. To overcome this limitation and to help researchers and resource planners to better understand the spatial distribution of hydrologic processes and their response a spatially DLBRM was developed (He & Croley, 2007). It was created in 2004 (Gebremariam et al., 2014).

DLBRM divides a watershed into a 1-km^2 homogeneous grid network and simulates hydrologic processes for the entire watershed sequentially (Cutts, 2013; Demarchi et al., 2009; He et al., 2008; He & Croley, 2007). Each watershed is made up of moisture storage from the upper soil zone, lower soil zone, groundwater zone, and surface, which are arranged as a serial and parallel cascade of "tanks" to correspond with the perceived basin storage structure (Cutts, 2013; Demarchi et al., 2009; Zhang et al., 2016) The snowpack absorbs water, which provides the basin surface with water (degree-day snowmelt). Partial-area infiltration is proportional to this supply and the saturation of the higher soil zone (Cutts, 2013; He et al., 2012) DLBRM calculates actual ET as proportional to both the potential and storage, using a heat balance that is indexed by the daily air temperature. In the DLBRM, river channel routing is not explicitly represented (Zhang et al., 2016).

It is difficult to build the input variables for each grid cell from numerous databases spanning vast watersheds because the DLBRM was developed for big-scale (> 103 km2) watersheds. An ArcView-DLBRM interface program has been created to help with the model's implementation to

simplify input and output processing for the DLBRM (Cutts, 2013; He et al., 2012). There are six modules: Soil Processor, DLBRM Utility, Parameter Generator, Output Visualizer, Statistical Analyzer, and Land Use Simulator are just a few of the tools available (Cutts, 2013; He et al., 2012; Lawrence, 2013). Land use, depths (cm) of USZ and LSZ, available water capacity (%) of USZ and LSZ, soil texture, permeability (cm/h) of USZ and LSZ, Manning's coefficient values, daily flows, and daily precipitation are some of the input variables (Cutts, 2013; He & Croley, 2007).

Snowmelt, evaporation, overland flow, infiltration, groundwater, and lateral flow are all DLBRM components. Compared to HSPF and SWAT, the DLBRM only requires 14-16 global optimizations during calibration (Gebremariam et al., 2014). The lumped-parameter LBRM was used to start the calibration process (Croley et al., 2005).

The DLBRM has several distinctive characteristics, including the following: (1) it applies to large watersheds; (2) it uses readily accessible climatological, topographical, hydrologic, soil, and land use databases; (3) mass continuity equations are used to govern the hydrologic processes and are solved analytically, making model solution tractable (Cutts, 2013).

9. GIS-PLOAD (GIS-based Pollutant Load model)

PLOAD was developed by CH2M Hill in Herndon, Virginia. PLOAD can assess different nonpoint pollution sources' seasonal or yearly average loads. It is not a continuous simulation model because it runs on an average annual basis (Duda et al., 2006; Nejadhashemi & Woznicki, 2011; USEPA, 2001). PLOAD is a streamlined, GIS-based model that estimates pollutant loads for watersheds (the simple method model is only applicable to watersheds less than 1 square mile) (USEPA, 2001). According to (Duda et al., 2006), the model makes it easy to compare various scenarios. According to (Ouma, 2018), PLOAD is a component of Better Assessment Science Integrating Point and NPSs (BASINS).

The Simple Method approach, an empirical technique created for predicting pollutant export from urban development sites, can be used by the user of the PLOAD model to compute the source pollution loads: the EC table lists loading rates for each pollutant type by land use type (Duda et al., 2006; Eskinder, 2019; Liu et al., 2017); typically used to calculate the pollutant loads for rural land use types; less than 260 ha is its limited application drainage area (Nejadhashemi & Woznicki, 2011).

For urban, suburban, and rural watersheds, PLOAD can estimate NPS pollution. It can calculate total suspended particles, nutrients, metals, and fecal coliform (Ouma, 2018). Additionally, best management practices (BMPs) for areas and specific sites are set up in PLOAD. Site-specific BMPs are displayed in GIS as points and include information on the type and area of influence.

Areal BMPs are displayed in GIS as polygons and solely contain data about the type of BMP (Nejadhashemi & Woznicki, 2011).

The PLOAD application requires pre-processed GIS and tabular input data including watershed/sub-watersheds boundary, land use, BMP location and reduction table, runoff coefficients, pollutant loading rate data tables event mean concentration (EMCs and/or EC for different land use types), point-source facility locations and loads, annual precipitation, bank erosion data tables, and impervious terrain factors (Duda et al., 2006; Nejadhashemi & Woznicki, 2011; USEPA, 2001).
PLOAD was created to be universally applicable as a screening tool for a variety of projects, such as storm water permitting under the National Pollutant Discharge Elimination System, watershed management, or reservoir preservation initiatives. Modification and customization are made easier by the application's structure and organization. It was designed to be an analytical tool for end users (USEPA, 2001).

PLOAD has the following advantages: it can estimate nonpoint-source pollution on an annual or seasonal average basis (Marcomini et al., 2001; Saleh & Du, 2004); it can study any user-specified pollutant if the loading rate data table is provided (Nejadhashemi & Woznicki, 2011); and it is useful in data-poor areas for planning industrial and agricultural development (Eskinder, 2019). On the other hand, the model contains the following flaws: A unique value (EMC or EC) is assigned depending on each land use, which does not take soil type into account. EMCs and/or ECs are necessary, which are variable based on area and frequently difficult to get. On the other hand, on different types of soil, the same land use types can produce varying levels of runoff and pollution (Moffitt, 2019; Nejadhashemi & Woznicki, 2011).

10. L-THIA (Long-Term Hydrologic Impact Assessment)

The Purdue University College of Engineering created the L-THIA model (Nejadhashemi & Woznicki, 2011). Its main function is to find out how changes in land use affect both the quality and amount of water. According to (Engel & Harbor, 2014; EPA, 2018; Ma, 2004), the model gives estimates of changes in runoff, recharge, and non-point source pollution arising from historical or planned land use changes. The curve number method, which is based on precipitation, land use, hydrologic soil group, and management practices (Bhaduri et al., 2000; Lim et al., 2001), is used to estimate annual runoff, whereas the pollutant EC or EMC used to calculate the average amount of various NPS pollutant loads. The NPS module, however, is constrained to a few contaminants and land uses (Lim et al., 2001). Land use, soil, hydrology, and daily rainfall data are needed to run this model (Lim et al., 2001; Mirzaei et al., 2017). Planners and managers of natural resources were the original target audience of L-THIA. L-THIA focuses on the average impact rather than an extreme year or storm by using many years of climate data in the analysis (Ma, 2004).

For agricultural areas, equivalent loading values are used, and dust and dirt accumulation in urban areas and its wash-off are used to assess NPS pollution. NPS pollutants for non-urban areas were not predicted by the NPS module in the original LTHIA/NPS GIS. The latest model version employed EMC data to forecast NPS pollution for both urban and non-urban areas. The Event Mean Concentration for an NPS pollutant for land use is calculated by dividing the total pollutant load by the runoff volume during a runoff event. However, some pollutant concentrations for rainfall events vary over time, therefore flow-averaged sample values were used in these situations as the event mean concentrations (Lim et al., 2001).

Advantages of L_THIA: easily set up with readily available data, and computation time is short; focuses on relative hydrologic and WQ impacts of different land use scenarios using long-term climate data; can estimate annual pollutant loadings for any user-specified pollutant (Nejadhashemi & Woznicki, 2011); does not require detailed data input; required data is readily available in most planning settings; available in GIS version and user friendly and Internet-accessible (Engel & Harbor, 2014).

Some of the drawbacks of L_THIA include: it only applies to areas where the curve number method is used; it does not analyze parameters such as political stability; it does not take into account snowfall contributions to precipitation for curve number value modification; it does not take into account effects of frozen ground in cold months and variation in antecedent moisture conditions to adjust curve number values; and it cannot evaluate the effectiveness of BMP implementation plans (Engel & Harbor, 2014; Nejadhashemi & Woznicki, 2011).

11. BASINS (Better Assessment Science Integrating Point and Nonpoint Sources)

The US EPA developed BASINS to integrate environmental data, analysis tools, and models of watersheds and WQ to support efforts to produce TMDLs and manage watersheds (Moffitt, 2019). To conduct watershed and WQ-based studies, regional, state, and municipal authorities can use the multipurpose environmental analysis system known as BASIN (Duda et al., 2006; Jayawardena, 2013; Zhang et al., 2016). It has always been a dynamic system that has gained more features as needed and as technology advances. BASINS made its debut in May 1996 (Marcomini et al., 2001). It was created to allow the analysis of point and NPS management approaches, to facilitate the investigation of environmental information, and to provide an integrated watershed and modelling framework (ROO et al., 1996; Saleh & Du, 2004).

It can support a range of analyses utilizing techniques that are simple to complex. By examining the combined effects of point and NPSs in a watershed, it was initially created to support the TMDL process (Duda et al., 2006; Moffitt, 2019). For some contaminants, BASINS can support watershed-based point and NPS analyses. Additionally, it enables the user to try various management settings. BASINS enables studies on watersheds and WQ by combining important data and analytical elements "under one roof" (Marcomini et al., 2001; Moffitt, 2019). BASINS is

a watershed assessment tool used for data download, watershed delineation, modelling projects, data management, data evaluation, various analyses, and report development (EPA, 2015).

The integrating framework for BASINS is provided by GIS. With the aid of GIS, BASINS has the adaptability to present and incorporate a variety of data at the user's selected scale. BASINS is a special and effective environmental study tool thanks to its "zooming" function (Duda et al., 2006; EPA, 2018; Moffitt, 2019). The primary watershed model in BASINS is HSPF. In addition, BASINS offers additional models including SWAT, SWMM, and WASP (EPA, 2015).

BASINS are a group of connected parts that work together to undertake several types of environmental investigation. The components are a simplified GIS-based model (PLOAD) that estimates nonpoint loads on an annual average basis, the Parameter Estimation (PEST) tool for model calibration, infrastructure to include watershed loading and transport models like HSPF, SWAT and Automated Geospatial Watershed Assessment (AGWA), assessment tools for watershed characterization based on observed data, utilities to facilitate organizing and evaluating data, tools for watershed delineation, and nationally derived databases with tools to build new projects (Duda et al., 2006; EPA, 2018; Moffitt, 2019).

The user can simulate the loading of pollutants and nutrients from the land surface using BASINS by integrating three models (SWAT, HSPF, and PLOAD). These three models can be used to analyze watersheds by separating the research region into homogenous sections because they are spatially distributed, lumped parameter models (Duda et al., 2006). BASINS integrates environmental data, analytical tools, and modelling programs to support the development of cost-effective approaches to watershed management and environmental protection, making it possible to swiftly assess significant amounts of data in a usable and understandable format (Duda et al., 2006). With the flexibility to facilitate research at a variety of scales using tools that range from simple to sophisticated, the BASINS system is set up to support environmental and ecological investigations in a watershed context (ROO et al., 1996). Point and NPS pollution are combined in the BASINS model. According to (Wang et al., 2013), BASINS models are appropriate for WQ study at the watershed scale.

A GIS framework is actively utilized in the present development and implementation of the BASINS model, particularly for TMDL analyses (Moffitt, 2019). Boundaries of hydrologic units, significant roads, census regions, and various political or administrative boundaries are all included in the cartographic data. The environmental data include information on soils, topography (DEM), land uses, and stream hydrography/river network, and is used to support watershed classification and environmental assessments. The data used for environmental monitoring includes rainfall records, statistical summaries of the outcomes, and data on a limited range of biological conditions. According to (Burton & Pitt, 2002; Duda et al., 2006), point source data

offer information on pollution loadings from authorized facilities as well as the locations of hazardous waste sites.

Since both developers and end users can access the source code for every component, BASINS has greater stability and transparency. Its architecture can be expanded to accommodate the addition of new tools and data types. Users of the system can investigate and research various methods for lessening the effects of those pollutants while evaluating alternative management scenarios. BASINS has capabilities that make it useful for TMDLs, particularly for differentiating and quantifying the impacts of point and NPSs. These capabilities also make it useful for other types of decisions. (Duda et al., 2006; Marcomini et al., 2001). Quantifying the loading contributions from various sources and locating the problematic elements throughout the watershed and related bodies of water serve as the basis for all of these decisions (Marcomini et al., 2001). A big dataset for the entire country, many watersheds or WQ models, automatic data downloads from the internet, good customer support, and an email listing service are all benefits of BASIN (Shoemaker et al., 2005).

While continuous simulation models are the most powerful instruments for analyzing watershed loadings, they have several important limitations. These models require enormous amounts of input data (Shoemaker et al., 2005), including observations over periods of many years. These models require a large amount of learning, and there is inherent uncertainty in the input data, techniques, and modelling assumptions (Duda et al., 2006). Despite being extremely powerful and essential for some applications, BASINS currently lacks the flexibility that the many different individual models do.
As a large-scale model, BASINS might be too complicated to focus on particular smaller areas or when in-depth analyses are required (Burton & Pitt, 2002). Setting up the model for sites outside of the United States is challenging, and using advanced modelling options may require training (Shoemaker et al., 2005).

12. Spatially Referenced Regressions on Watershed attributes (SPARROW)

According to (Benoy et al., 2016; Robertson & Saad, 2013), SPARROW is a spatially explicit watershed model that uses a mass-balance method to predict nutrient sources and non-conservative transport and transformation (i.e. losses) of nutrients throughout watersheds under long-term steady-state circumstances. SPARROW is a watershed modelling technique for relating water-quality measurements made at a network of monitoring stations to attributes of the watersheds containing the stations (Schwarz et al., 2006). The heart of the model consists of a nonlinear regression equation explaining the non-conservative movement of contaminants from point and diffuses sources on land to rivers and via the stream and river network (Benoy et al., 2016; USEPA, 2018). The regression equation's parameters are calculated by comparing publicly available stream water-quality records, such as those from State and Federal monitoring programs, with GIS data on pollutant sources, such as fertilizers, human and animal waste, and climatic and hydrogeologic

characteristics, such as precipitation, topography, vegetation, soils, and water routing (Robertson & Saad, 2013; Shoemaker et al., 2005). Measures of uncertainty in model coefficients and water-quality predictions are provided by the statistical estimate of parameters in SPARROW (Schwarz et al., 2006).

The model is intended to assess different hypotheses regarding significant contamination sources and watershed characteristics that regulate movement over broad spatial scales. It forecasts pollutant flux, concentration, and yield in streams. It is a method for modelling watersheds that estimates pollution sources and contaminant movement in watersheds and surface waters using a hybrid statistical and process-based approach (Preston et al., 2011; Schwarz et al., 2006).

The model is used to predict the "land-to-water" transport of nutrients to streams about statistically important landscape characteristics such as climate, soils, terrain, drainage density, and artificial drainage variables (Robertson & Saad, 2013). It is more accurate in large geographic areas than it is in small catchments, and it predicts long-term averages rather than short-term values. It can forecast WQ in both local and big river drainages. The model can be used to forecast changes in WQ as a result of management decisions or modifications to land use (Kathleen, 2010).

There are four major components of a SPARROW model: (1) a stream network and its catchments; (2) nutrient sources; (3) the land-to-water delivery and in-stream decay factors; and (4) measured estimates of long-term average annual nutrient loads, detrended to a specific year, at locations in the network for model calibration (dependent variables) (Benoy et al., 2016).

Four different types of data-all independent variables are used to set up the model: data about the stream network, which is used to define stream reaches and catchments; loading data for numerous sites inside the model boundaries; data about all the sources of the nutrient or other constituent being modelled; and data about the environment of the area being modelled (Robertson & Saad, 2013).

Using datasets at the national level, the model can simulate a range of pollutants at various spatial scales. With flexibility in the datasets and amount of information incorporated, the model can be used to describe both large- and small-scale systems (Shoemaker et al., 2005). The capability of SPARROW to map out model results is a crucial feature and strength. These findings contribute to actionable science by giving managers a tool to pinpoint problem regions and explain the issue in an understandable, visual fashion. The mass balance method has a lot of benefits. There is an expectation that the estimation of flux over spatial scales smaller and greater than those covered by the model's sample data would produce fairly accurate findings because flux and sources have a linear relationship (Mortensen, 2015).

The fundamental limitation of SPARROW is the quality of the model output depends entirely on the input data. Currently, there can be a lot of uncertainty when characterizing sources that are typically unregulated, such as animal feces. The precision of the model is constrained by the geospatial data for such activities, which may also have a coarse spatial or temporal resolution (Schwarz et al., 2006).

The model's calibration is a comparable restriction. The ability to calibrate a model depends on having enough observations to limit its parameters. Both temporal and spatial data of WQ must be taken into account during the calibration. SPARROW lacks an in-depth mechanistic knowledge of the major processes governing nutrient removal because it heavily relies on statistics and observations of stream flow and concentration (Mortensen, 2015). The model is only capable of rough estimates of pollutant loads and fate/transport traits (Shoemaker et al., 2005).

13. Storm Water Management Model (SWMM)

SWMM is a dynamic rainfall-runoff simulation model that is used to simulate runoff quantity and quality from primarily urban areas globally, either for a single event or over a long time (Moffitt, 2019; Shaver et al., 2007; Shoemaker et al., 2005). The runoff component of the model runs on some sub-catchment areas that produce runoff and pollutant loads in response to precipitation. It is still frequently applied in non-urban settings as well, with various applications in planning, analysis, and design relating to stormwater runoff, combined sewers, sanitary sewers, and other drainage systems in urban areas (EPA, 2018).

The simulation period consists of time steps, and SWMM may track both runoff quantity and quality for each time step. Conceptually, the model is divided into four main environmental compartments: the atmosphere compartment, which accounts for precipitation and air pollutants; the land surface compartment, which models areas receiving precipitation and generating runoff; the transport compartment, which routes flow from runoff source areas through a network of pipes, channels, etc.; and the ground-water compartment, which receives infiltration from the land. Many distinct parameters, some of which change from sub-catchment to sub-catchment, are included in a SWMM application. Inferred parameters include flow width, infiltration parameters, Manning's *n* for pervious and impervious areas, depression storage for pervious and impervious areas, imperviousness, and Manning's *n* for conduits. These parameters can be divided into measured parameters (sub-catchment area, pipe lengths, shapes, bed slopes, and diameters, manhole type, soil types, land-use types, and rainfall depth) and measured parameters (such as rainfall depth) (Tikkanen, 2013).

Six key environmental factors can be used to build a modelling project: external forcing data, such as precipitation, temperature, and evaporation; land surface runoff; subsurface groundwater; a conveyance system of pipes, channels, flow regulators, and storage units; contaminant buildup, wash-off, and treatment; and LID controls. A project does not necessarily need to incorporate each of these elements (Niazi et al., 2017).

Area, imperviousness, slope, roughness, width, depression storage, and infiltration characteristics are among the data needed for hydrologic simulation. For each model subarea, ground cover type is determined using land use data. Additional parameters may be required, depending on the settings selected for the loading calculations (for example, buildup coefficients would be required for the dry weather buildup simulation). If the user wants to model subsurface drainage and interflow, further information is required. Dimensions, slope, roughness coefficients, altitudes, and storage are necessary depending on the stormwater system. It is necessary to maintain ongoing records of evapotranspiration, temperature, and solar intensity (Shoemaker et al., 2005).

Strengths of the model include fully dynamic hydraulic routing, simulation of hydraulic structures (manholes, weirs, and orifices), overland flow routing between pervious and impervious areas within a sub-catchment (latest version), and a variety of options for quality simulation, including buildup and wash off, rating curves, and regression techniques. Limitations of the model include its inability to simulate groundwater and the fact that it only takes into account settling and first-order decay for in-stream pollutant transport and transformation (Shoemaker et al., 2005).

2.4.4 Considerations

Precipitation, air temperature, soil characteristics, topography, vegetation, hydrogeology, and other physical parameters are among the data sources that different models use. All of these models can be applied to very vast and complicated basins (Ganasri, 2015). According to (Engel et al., 2007), the problem definition, model application goals, objectives, and hypotheses, model selection, model sensitivity analysis, available data, data to be collected, model representation issues, model calibration, model validation, model scenario prediction, and results interpretation hypothesis testing should all be taken into account when conducting a hydrologic/water quality modelling process. Diverse hydrological models exhibit diverse model performances in the applications due to differing model topologies. Even the same hydrological model exhibits variable results when used in several catchments.

It is essential to ascertain "which models are most suitable for a particular application". The source and severity of point and NPS pollution problems in a watershed can thus be significantly better understood, which is a crucial step in the decision-making process, by choosing the appropriate parameter values and models (Nejadhashemi & Woznicki, 2011; Zhang et al., 2016).

Following Table 2-5 to Table 2-8 is a discussion of the capabilities and limitations of the models based on the model reviewed above and other sources. General land and water features supported model TMDL supported Table 2-5 considers the model’s ability like load vs. concentration. Characterizes the models to simulate typical TMDL target pollutants and expressions; depending on the time step of the simulation for the target steady state, storm event, annual, daily, or hourly.

Table 2-5 TMDL Supporting Models of Hydrological Water Quality

Model	TP load	TP conc.	TN load	TN conc.	Nitrate Conc.	Ammonia conc.	TN: TP mass ratio	DO	Chlorophyll a	Algal density	Net TSS load	TSS conc.	Sediment conc.	Sediment load	Sulfate conc.	Metals conc.	Pesticides conc.	Herbicides conc.	Toxics conc.
AGNPS	E	E	E	E	NS	NS	NS	E	E	NS	NS	E	E	E	NS	NS	E	E	NS
AnnAGNPS	D	D	D	D	NS	NS	NS	D	NS	NS	NS	D	D	D	NS	NS	D	D	NS
BASINS	H	H	H	H	H	H	H	H	H	D	H	H	H	H	NS	H	H	H	H
HSPF	H	H	H	H	H	H	H	H	H	D	H	H	H	H	NS	H	H	H	H
MIKE SHE	NS	NS	NS	NS	NS	NS	NS	NS	NS	NS	NS	NS	NS	NS	NS	NS	NS	NS	NS
SPARROW	A	A	A	A	NS	NS	A	NS	NS	NS	NS	NS	NS	A	NS	NS	A	A	NS
SWAT	D	D	D	D	D	D	D	D	D	NS	NS	D	D	D	NS	D	D	D	NS
SWMM	H	H	H	H	H	H	H	H	NS	NS	H	H	H	H	NS	H	NS	NS	NS
WASP	H	H	H	H	H	H	H	H	H	H	NS	H	H	NS	NS	NS	NS	NS	H

(NS) not supported, E- Event/storm, D- Daily, H – Hourly, A – Annually

Table 2-6 General Land and Water Features Supported Models

Model	Urban	Rural	Agriculture	Forest	River	Lake	Reservoir
AGNPS	NS	H	H	NS	NS	NS	NS
AnnAGNPS	NS	H	H	NS	NS	NS	NS
BASINS	M	H	H	H	H	M	M
HSPF	M	H	H	H	H	M	M
MIKE SHE	H	H	H	H	H	M	H
SPARROW	M	M	M	M	M	NS	NS
SWAT	M	H	H	H	L	L	L
SWMM	H	M	L	L	L	L	M
WASP	NS	NS	NS	NS	H	H	H

(NS) Not supported, L - Low, M - Medium, H - High

Table 2-7 Summary of Receiving Water Simulation Capabilities of Models

Model	Type			Complexity			Water Quality							
	Steady-state[1]	Quasi-dynamic[2]	Dynamic[3]	1-D	2-D	3_D	User-defined	Sediment	Nutrients	Toxics	Metals	BOD	Dissolved oxygen	Bacteria
BASINS	NS	NS	S	S	NS	NS	S	S	S	S	S	S	S	S
HSPF	NS	NS	S	S	NS	NS	S	S	S	S	S	NS	NS	S
SWAT	NS	S	NS	S	NS	NS	NS	S	S	S	S	S	S	NS
SWMM	NS	NS	S	S	NS	NS	S	S	S	S	S	NS	NS	S
WASP	NS	NS	S	S	S	S	S	S	S	S	S	S	S	NS

(NS) Not Supported, (S) - Supported

[1] *These models operate under a single non-variable flow condition. Steady state models are typically used to evaluate a design flow.*

[2] *Quasi-dynamic models allow for limited variation, typically a variation in meteorological conditions over the course of day, to examine variability.*

[3] *These models allow for variations in both flow and meteorological conditions on a small time step, typically shorter than daily.*

Table 2-8 Summary of Watershed Simulation Capabilities of models.

Model	Type		Complexity			Time Step				Hydrology		Water Quality											
	Grid -based	stream routing included	Export coefficients	Loading functions	Physically based	Sub-daily	Daily	Monthly	Annual	Surface	Surface & G.Water	User defined	Sediment	Nutrients	Toxics/pesticides	Metals	BOD	Bacteria	Watershed[4]	BMPs analysis[5]	System[6]	Statistical	Processed
AGNPS	S	S	NS	NS	S	S	NS	NS	NS	S	NS	NS	S	S	S	NS	NS	NS	S	S	NS	NS	S
AnnAGNPS	NS	S	NS	NS	S	NS	S	NS	NS	S	NS	NS	S	S	S	NS	NS	NS	S	S	NS	NS	S
BASINS	NS	S	S	S	NS	NS	S	NS	NS	S	S	S	S	S	S	S	S	S	S	S	S	NS	S
HSPF	NS	S	NS	NS	S	S	NS	NS	NS	NS	S	S	S	S	S	S	S	S	S	S	NS	NS	S
MIKE SHE	NS	S	NS	NS	S	S	NS	NS	NS	NS	S	NS	NS	NS	NS	NS	NS	NS	S	S	S	NS	S
SPARROW	NS	S	NS	NS	NS	NS	NS	NS	S	S	NS	NS	S	S	S	NS	NS	NS	S	NS	NS	S	NS
SWAT	NS	S	NS	NS	S	NS	S	NS	NS	NS	S	NS	S	S	S	S	NS	NS	S	S	NS	NS	S
SWMM	NS	S	NS	NS	S	S	NS	NS	NS	NS	S	S	S	S	S	S	S	S	S	S	NS	NS	S
WASP	NS	NS	NS	NS	NS	NS	NS	NS	NS	NS	NS	NS	NS	NS	NS	S	NS	NS	NS	NS	NS	NS	S

(NS) not Supported, S-Supported

[4] This group of models emphasizes the description of watershed hydrology and WQ, including runoff, erosion, and wash-off of sediment and pollutants. Simplified groundwater movement and surface-groundwater interconnections are included in certain models. Some also include internally linked river transport and WQ processes and reservoirs.

[5] BMP refers to models that can assess one or more individual BMPs and their influence on hydrology or WQ loading.

[6] Some models are identified as "systems" to recognize that these systems support multiple models (e.g., the EPA TMDL Modelling Toolbox includes linkages between watershed models and receiving water models). The list of models includes systems as a whole, which include the various functionalities of component models.

In this systematic review, thirteen selected hydrological/water quality models are reviewed. The models appraised depending on their input data, strengths, limitations, the area that can covered (spatial extent), their temporal variability, capabilities in the simulation (nutrient, heavy metals, toxicity, BOD, DO), the components they have (Hydrology, sediment, nutrient/chemical), type (grid, stream routing), the complexity of the model, the time step of the simulation, hydrology (surface, surface & groundwater), system, analysis (watershed, BMPs), Model category (physical, conceptual, etc.), land and water features supported (urban, rural, etc.), TMDL support, operation (grid, HRU, cell, lumped), and Pollution handling (point, non-point) the model selection has been done. So that this selection provides the scientific community with knowledge about the hydrological models to take into account when they are engaged in hydrological systems.

For simple screening of the models for a project for the different basins the following assessments have been done: the application of AGNPS and ANSWERS is limited to watersheds of about 200 km^2; SWRRB has a limited distributed parameter capability and can be used in agricultural basins of up to 600–800 km^2. SWIM can be applied at a mesoscale level it cannot be implemented on a basin scale. Similarly, models like DLBRM, PLOAD, and MIKE SHE have 1000 km^2, 3 km^2, and less than 100 km^2 respectively. BASIN is applicable for WQ analysis in a regional as well as in-country scale; whereas SWAT can be used from small watersheds on a basin scale (up to 25000 km^2). All these models are to a certain extent integrated with GIS tools (Krysanova et al., 1998).

L-THIA and PLOAD models are not capable of identifying high-priority areas except SWAT (Nejadhashemi & Woznicki, 2011). Comparing HSPF and SWAT found that HSPF has better river flow simulation and SWAT has better results in total phosphorus simulation. Although SWMM includes subsurface flow routing, the quality of subsurface water can only be approximated using a constant concentration (Yang & Wang, 2010). For the simulation of hydrology and water quality, the HSPF model is meteorologically data intensive. Unlike the DLBRM, the HSPF model has been applied widely to watersheds in many other parts of the world (Gebremariam et al., 2014).

Models like AnnAGNPS, HSPF, MIKE-SHE, and SWAT are long-term continuous simulation models having all three major components (hydrology, sediment, and chemical) that apply to watershed-scale catchments (Borah & Bera, 2003). Compared to the PLOAD and L-THIA models, SWAT more accurately represents the current understanding of watershed processes and their effects on pollution generation (Nejadhashemi & Woznicki, 2011). Among the models reviewed above, HSPF, and SWMM have persisted for a long period, while BASIN and SWAT are comparatively new (Yang & Wang, 2010).

DLBRM, PLOAD, L-THIA, ANSWER, and AGNPS in one way or another lack one of the three components (hydrology, sediment, nutrient/chemistry); hence, the three components are basic for NPSP. Some of the models are non-point source pollution (no room for point source pollution)

based simulations like L-THIA and AGNPS. The selection considers the model that is used to incorporate both the point and non-point pollution sources.

Water quality parameters like sediment, nutrients, toxin, BOD, and DO are supported by BASINS, SWAT, and WASP. The time step simulation of the BASIN and SWAT models in the WQ parameters is daily and is one of the selection measures for the model selection.

The TMDL of TP, TN, and sediment load and concentration, nitrate, ammonia, DO, BOD, chlorophyll *a*, TSS, metal, pesticide, herbicide, and toxic concentration is simulated daily by SWAT and AnnAGNPS. However, AnnAGNPS doesn't support metallic and BOD simulation in watersheds. It is also limited in rural and Agricultural watersheds.

As of the look over models above the BASIN and SWAT models are the best models that could be applied for point and NPS pollution in different basins. Different models in the BASINS suite have different temporal scales for example HSPF: is a user-defined time step, typically hourly, continuous simulation from days to years; SWAT: is a daily time step, continuous simulation for months to years; PLOAD: is an export coefficient model, annual; and KINEROS: single-storm event, part of AGWA, variable time step typically in minutes. However, in the case of adaptation of the models, the SWAT model is applied in all different corners of the world; and BASIN is dominantly applied in the USA, as discussed in the BASINS section in this review it is difficult to set the model for locations outside of the United States and may require training to use the advanced modelling options.

2.4.5 Case Study and New Technologies Applied

Almost all the research works in Ethiopia in this review dominantly used the statistical analysis and analytical method (laboratory analysis results) as revised in Table 2-9; another method of analysis like applying models (conceptual/parametric, physical) for different sources of pollutants (point and non-point sources) does almost not exist. This of course could be a lack of available data for calibration or other reasons. In addition to this, the statistical analysis of descriptive statistics and analytical analysis is the major share of the study in WQ analysis in Awash Basin and Ethiopia as well. The only studies that applied physically based semi-distributed SWAT model and new technologies (Remote sensing) are (Asmelash, 2017; Ayana et al., 2012a; Ayele et al., 2017; Chekol et al., 2007; Eskinder, 2019; Geleta, 2010; Gonfa, 2016; Gonfa & Kumar, 2016; Tilahun et al., 2017; Worku et al., 2017). These are the fundamental modelling and new technologies applied for WQ purposes.

Sediment is one of the diffuse sources that has a significant impact impairing the WQ of lakes and rivers. The research conducted by (Asmelash Tilahun, 2017; Chekol et al., 2007; Geleta, 2010; Gonfa, 2016a; Gonfa & Kumar, 2016; Tilahun et al., 2017; Worku et al., 2017) is related to the sediment load in Ethiopia. Other sediment load works using SWAT in different parts of the country are not exhaustively reviewed and included in this review.

A study conducted by (Eskinder, 2019) estimated total nitrogen and total phosphorus losses in a data-poor catchment of the Kombolcha area. The study used a PLOAD model (incorporated in the BASINS 4.1 System). A study conducted by (Moges et al., 2017a) in Lake Tana for WQ Assessment by Measuring and Using Landsat 7 ETM+ Images for the Current and Previous Trend Perspective. In this research work the following saptio-temporal WQ parameters have been analyzed: turbidity, Secchi disc Transparency Depth (STD), Dissolved Phosphorus Concentration (DPC), and Chl *a*. Using a sentinel 2 satellite image, a study by (Assegide et al., 2023) in the Koka reservoir model the spatiotemporal WQ indicators such as Chl-a, turbidity, and TSS. It is a good start to apply remote sensing technology in data-scarce areas due to the lack of continuous WQ monitoring of lakes in developing countries like Ethiopia.

Researchers like (Abate et al., 2015; Chernet et al., 2001; Degefu et al., 2013; Eliku & Leta, 2018; Haile & Mohammed, 2019; Jebessa & Bekele, 2018; Kassegne et al., 2018; Moges et al., 2016; Tadesse et al., 2018; Tassew, 2007; Tialye, 2018; Worako, 2015; Yimer & Jin, 2020; Zinabu, Kelderman, van der Kwast, et al., 2019) have used the ANOVA statistical model for WQ analysis. Except (Kassegne et al., 2018) and (Tialye, 2018) who applied ANOVA for WQ impact in soil and WQ impact on aquatic plants and animals the remaining research works are used for WQ of lakes and rivers.

Table 2-9 Water quality models used in Ethiopia.

Application	Statistical																	Other
	1	2	3	4	5	6	7	8	9	10	11	12	13	14	15	16	17	18	SWAT[7]
a	(Yimer & Jin, 2020), (Abate et al., 2015)		(Masresha et al., 2011)			(Haile & Mohammed, 2019), (Worako, 2015), (Chernet et al., 2001), (Yimer & Jin, 2020), (Moges et al., 2016)					(Dsikowitzky et al., 2013)	(Dsikowitzky et al., 2013)		(Tafesse et al., 2015), (Haile & Mohammed, 2019), (MoWE, 2013), (Brehan, 2017)	(Abhachire, 2014), (Degefu et al., 2011), (Ademe, 2014), (Dinka, 2017), (Mesfin et al., 1988), (Tesfay, 2007), (Abate et al., 2015), (MoWE, 2013), (Haile & Mohammed, 2019)			(Moges et al., 2016)	
b	(Keraga et al., 2017a)	(Keraga et al., 2017b), (Feyissa & Bekele, 2018)		(Keraga et al., 2017b), (Gebreyohannes et al., 2015)	(Keraga et al., 2017b)	(Jebessa & Bekele, 2018), (Eliku & Leta, 2018), (Tadesse et al., 2018) (Tassew, 2007), (Abate et al., 2015), (Degefu et al., 2013) (Zinabu, Kelderman, van der Kwast, et al., 2019)	(Jebessa & Bekele, 2018), (Feyissa & Bekele, 2018)	(Eskinder, 2019)	(Eliku & Leta, 2018), (Tadesse et al., 2018), (Gebre et al., 2016), (Tassew, 2007), (Salami, 2016), (Feyissa & Bekele, 2018)			(Bedada et al., 2019), (Awoke et al., 2016)		Eliku & Leta, 2018) (Masresha et al., 2011) (Mengesha et al., 2017) (Gebre et al., 2016) (Eskinder, 2019) (Salami, 2016) (Mulu et al., 2013) (Tafesse et al., 2015) (Tadesse et al., 2018) (B.Abate et al., 2015) (Gebreyohannes et al., 2015) (Awoke et al., 2016) (Olbasa, 2017),	(Nugusu, 2015), (Abhachire, 2014), (Mengesha et al., 2017),(Prabu et al., 2011), (Tarekegn & Truye, 2018), (Gebre et al., 2016), (Feyissa & Bekele, 2018), (Olbasa, 2017), (Haddis et al., 2014), (Olbasa, 2017), (Awoke et al., 2016), (Olbasa, 2017),	(Tadesse et al., 2018), (Haile & Mohammed, 2019), (Abate et al., 2015)	(Gebreyohannes et al., 2015)		
c										(Akalu et al., 2011)					(Tarekegn & Truye, 2018)				

[7] SWAT applied in Awash Basin for sediment load

h	g	f	e	d
			(Kassegne et al., 2018)	
			(Niguse Bekele Dirbaba, Xue Yan, Hongjuan Wu, 2018), (Kassegne et al., 2018)	
			(Niguse Bekele Dirbaba, Xue Yan, Hongjuan Wu, 2018), (Dirbaba et al., 2018)	
		(Tialye, 2018)	(Kassegne et al., 2018)	
			(Dirbaba et al., 2018), (Kassegne et al., 2018)	
		(Dsikowitzky et al., 2013)		
		(Dsikowitzky et al., 2013)		
		(Tialye, 2018)		
		(Teffera, 2009), (Tialye, 2018)		(Masresha et al., 2011), (Mengesha et al., 2017)
		(Teffera, 2009),(Abhachire, 2014), (Degefu et al., 2011)		(Mengesha et al., 2017), (Itanna, 2002)
(Adugna et al., 2019)				
	(Asmelash Tilahun, 2017),(Chekol et al., 2007),(Geleta, 2010), (Gonfa, 2016), (Worku et al., 2017), (Ayele et al., 2017), (Gonfa & Kumar, 2016)			

1. CCME WQI/geo-accumulation index/Pollution load index (PLI)/contamination factor/ Sodium Absorption Ratio (SAR), Residual Sodium Carbonate (RSC) index, trophic state index. 2. Multivariate statistical analysis Cluster Analysis (CA). 3. Monte Carlo permutation test. 4. Principal component analysis (PCA). 5. Mann-Kendall trend test. 6. ANOVA. 7. Least square difference test. 8. Shapiro-Wilk normality test. 9. Pearson's correlation. 10. Spearman bivariate correlation. 11. Levene's test. 12. Kruskal-Wallis test. 13. Kaplan-Meyer test. 14. Descriptive. 15. Analytical. 16. Post Hoc Tests/ Tukey Test. 17. t-test. 18. Regression Analysis. a) Lake WQ, b) River WQ, c) Impact of humans on WQ, d) Impact of WQ in Vegetable, e) Impact of WQ in Soil, f) Impact of WQ in Aquatic Animals and Plants, g) Sediment load, h) stormwater runoff on river WQ.*

Chapter 3 : SPATIOTEMPORAL DYNAMICS OF WATER QUALITY INDICATORS IN KOKA RESERVOIR, ETHIOPIA

Abstract

The science and application of the Earth observation system are receiving growing traction and wider application, and the scope is becoming wider and better owing to the availability of higher-resolution satellite remote sensing products. A water quality monitoring model was developed using a Sentinel-2 satellite remote sensing data set to investigate the spatiotemporal dynamics of water quality indicators at Koka Reservoir. L1C images were processed with an Atmospheric correction processor ACOLITE. The months from June 2021 to May 2022 and the years 2017 to 2022 were used for the temporal analyses. Algorithms were developed by using regression analysis and developing empirical models by correlating satellite reflectance data with in situ Chlorophyll-a (Chl-a), turbidity (TU), and Total suspended matter (TSS) measurements. All of the analyzed parameters have determination coefficients (R2) greater than 0.67, indicating that they can be turned into predictive models. R2 for the developed algorithms were 0.91, 0.92, and 0.67, indicating that good correlations have been found between field-based and estimated Chl-a, TU, and TSS, respectively. Accordingly, the mean monthly Chl-a, TU, and TSS levels have ranged from (59.69 to 144.25 µg/L), (79.67 to 115.39 NTU), and (38.46 to 368.97 mg/L), respectively. The annual mean Chl-a, TU, and TSS vary from (52.86–96.19 µg/L), (71.04–83 NTU), and (36.58–159.26 mg/L), respectively, showing that the reservoir has been continuously polluted over the last seven years. The spatial study found that the distributions of Chl-a, TU, and TSS were heterogeneous, with Chl-a being greater in the south and southwest, and TU and TSS being higher on the western shore of the reservoir. In conclusion, these results show that there are spatial as well as temporal variations in water quality parameters. The proposed algorithms are capable of detecting optically active water quality indicators and can be applied in similar environmental situations.

Keywords: linear regression; remote sensing; Sentinel 2A; Chlorophyll-a; turbidity; total suspended matter

3.1 Introduction

Water security and sustainable management of water resources are critical; responsible policies that protect ecological and economic health are needed (Ashok & Singh, 2010). The United Nations has designated the provision of clean water and sanitation as one of the Sustainable Development Goals (SDGs), recognizing the importance of water security in global development (SDG 6) (Chawla et al., 2020). To achieve the SDGs, integrated management of water resources has become the scientific paradigm. Water resource management requires continuous monitoring of water quality, availability and vulnerabilities over time and space (Ashok & Singh, 2010). Information is a necessary prerequisite if target 6.3, to improve water quality, is to be accomplished by 2030. The proportion of water bodies with good ambient water quality is monitored by SDG indicator 6.3.2 (UNEP, 2021). At present in Ethiopia not all urban and rural areas have access to clean water. In most towns, rivers provide the main source of water for personal and household consumption as well as for any other activities. However, effluents from some industries are discharged into these rivers (Ademe, 2014).

The two biggest threats to environmental water quality worldwide are pollution from agriculture and untreated wastewater, which release excess nutrients into rivers, lakes, and aquifers and impair ecosystem function (UNEP, 2021). Due to increased urbanization, agricultural intensification (Assegide et al., 2022), and industrialization (Abhachire, 2014) Ethiopia's water quality is deteriorating at an alarming rate, and freshwater contamination is a major problem (Abhachire, 2014; Assegide et al., 2022)

Nutrient loadings affect water quality throughout the world and have resulted in the eutrophication of many fresh water lakes (Abell et al., 2012; Alemu et al., 2017; Ligdi et al., 2010). In Koka Reservoir there was regular occurrence of blue-green algal bloom during the high temperature period (Abhachire, 2014). The Mojo and the Akaki Rivers are heavily contaminated by anthropogenic influences from upstream to downstream and are deteriorating the Koka reservoir’s water quality (Assegide et al., 2022) particularly affecting the reservoir’s aquatic life. The causes are specifically indiscriminate dumping of refuses into the river, indiscriminate dumping of industrial wastes (Tarekegn & Truye, 2018).

Fixed-site hydrological monitoring, in-situ reconnaissance investigations, physical models, numerical simulation, remote sensing (RS), and other methods are useful to monitor and understand concentrations of water quality parameters (WQPs) and to assess spatial and temporal fluctuations (Toming et al., 2016). In-situ monitoring involves water sampling and laboratory analysis, which can be time-consuming and resource intensive (Karaoui et al., 2019; Yepez et al., 2018) especially when sampling across large water bodies and monitoring on a regular basis (Ansper & Alikas, 2019; Mamun et al., 2021), both also requires highly specialized technical skills (Giardino et al., 2010). With the emerging high resolution Earth Observation datasets, monitoring water quality parameters using satellite imagery can effectively reduce the aforementioned costs while providing the advantages of wide coverage (Wang et al., 2021; Zhao, 2020), spatially distributed estimates with a higher temporal frequency (Pizani et al., 2020; Wang et al., 2021),

traceable history (Wang et al., 2021) and access to inaccessible water bodies (Govedarica & Jakovljevic, 2019). Furthermore, the possibility of composing time series from remotely sensed historical data allows the evaluation of water quality variations over time (Ansper & Alikas, 2019) which can potentially support monitoring and management of pollution levels in the water bodies (Karaoui et al., 2019).

Studies on physicochemical and biological characteristics (Abhachire, 2014), speciation of specific trace elements (Masresha et al., 2011), limnological observations (Fasil et al., 2011; Mesfin et al., 1988), and spatiotemporal dynamics of phytoplankton have previously been conducted in the Koka reservoir (Tesfay, 2007). However, the data collected lacks a spatiotemporal representation of the reservoir's water extent and only covers a very narrow time span. Furthermore, there are only a few scientific data concerning the pollution level and the threats posed to this reservoir (Fasil et al., 2011). There is no monitoring system and no regular water quality observations (Assegide et al., 2022). There is also a lack of effective tools, that allow assessment of the spatial and temporal water quality status of reservoirs and lakes in Ethiopia (Assegide et al., 2022). There has not been any prior remote sensing-based research undertaken in the study site specifically or indeed in the country as a whole.

In this study, we address this data scarcity gap by applying a RS-based water quality assessment. The objectives of this study are: (1) To evaluate the applications of Sentinel-2 imagery for water security quality assessment and to map the spatiotemporal variations of chlorophyll-a (Chl-a), Turbidity (TU) and Total Suspended Solid (TSS) of Koka reservoir; (2) to develop an empirical-based regression model that can be adopted as a future application as a water quality monitoring tool for sustainable water management in other inland lakes and reservoirs in Ethiopia, as well as to other data-scarce areas.

3.2 Related Work

Since the advent of satellite technology about 50 years ago, remote sensing methods have been used to measure the quality of inland waters (Sent et al., 2021; Topp et al., 2020). In the last decades, hundreds of RS publications have proposed solutions to overcome the challenges previously described and accurately quantify the WQPs (Sent et al., 2021). Sentinel-2 multi-spectral imager (S2A-MSI) has shown some intriguing results when used for WQ analysis. For example, (Buma & Lee, 2020) investigated the potential applicability of S2A for estimating Chl-a concentrations in Lake Chad which represented the concentrations in their study area. In (Lins et al., 2017), the authors findings suggested that empirical models based on optical properties involving water constituents have strong potential to estimate Chl-a using multispectral data in the northeastern Brazil. Chl-a was retrieved from S2A-MSI in Estonian lakes, and (Ansper & Alikas, 2019) came to the conclusion that the sensor could be used for WQ monitoring parameters from small areas. Remote sensing-based alternatives to traditional techniques have recently found popularity because they may be more practical and cost-effective. For example, semi-analytical modelling techniques have been utilized to accurately and successfully forecast Chl-a concentrations in Brazil from S2A-MSI (Borges et al., 2020). In (Subiyanto et al., 2018), the

authors concluded that Chl-a and TU can be estimated through remote sensing technology using multispectral S2A satellite images. (Kupssinskü et al., 2020) estimated Chl-a and TSS, their assessment of the machine learning systems, and S2A spectral images showed the robustness of the method for different types of water bodies. Despite the numerous applications for S2A images, there are some limitations as cloud cover, particularly during rainy seasons, frequently obscures the view of the area, making it hard to use satellite imagery for monitoring water quality.

Models that control the relationship between the optical qualities of a waterbody and its concentration of optically active water quality constituents are commonly referred to as bio-optical algorithms. Among various algorithms for estimating Chl-a, algorithms based on the relationship between Chl-a and reflectance at the "red edge (RE)" of the visible spectrum have shown a strong correlation between Chl-a and the difference of reflectance between NIR and red regions (Malthus et al., 2012). These regions correspond to low and high absorption ranges of Chl-a, even in waters with high presences of suspended sediment loads and colored dissolved organic matter (CDOM) (Malthus et al., 2012; Schalles, 2006).

Examples of band ratios and band combinations from previous studies applied to Sentinel-2 and/or Landsat imagery for modelling Chl-a, TU, and TSS are listed in *Table 3-1*. As indicated in the table, visible and vegetation red edge (VRE) bands are the predominant bands that most studies employed for chlorophyll-a TU, and TSS estimation of surface water quality analysis.

Table 3-1 Bands, band combinations, and band ratios in previous studies

Band combination or band ratio	**Reference**
Chlorophyll *a* (Chl-a)	
VRE (B5)/Red (B4)	(Ansper & Alikas, 2019), (Borges et al., 2020; Buma & Lee, 2020; Lins et al., 2017), (Cairo et al., 2020; Ha et al., 2017)
Green (B3)/ Red (B4)	(Ha et al., 2017)
Blue (B2)/ Green (B3)	(Lins et al., 2017), (Ansper & Alikas, 2019)
Red (B4)/ Green (B3)	(Cairo et al., 2020), (Mishra & Mishra, 2012)
VRE (B5)/ Green (B3)	(Cairo et al., 2020)
VRE (B6)/ Green (B3)	
VRE (B6)/ Red (B4)	
VRE (B6)/ Red (B4)	(Ha et al., 2017)
VRE (B7)/ Red (B4)	
VRE (B8a)/ Red (B4)	
NIR (B8)/ Red (B4)	
Blue (B2)-SWIR (B11)	(Ouma et al., 2020)
Green (B3)	
(Red (B4)-1-VRE (B5)-1)*VRE (B6)	(Lins et al., 2017), (Ansper & Alikas, 2019), (Borges et al., 2020)
(Red (B4)-1-VRE (B5)-1)*VRE (B6)	(Cairo et al., 2020)

(1/Red (B4) - 1/(VRE (B5)) * VRE (B8a)	(Rodríguez-Benito et al., 2020)
(1/Red (B4) - 1/VRE (B5)) * (VRE (B8))	(Buma & Lee, 2020)
(VRE (B5) + VRE (B6)) / Red (B4)	(Ha et al., 2017)
VRE (B5) (Red (B4)+ VRE (B6))/2	(Grendaitė et al., 2018), (Toming et al., 2016)
VRE (B5)/(Green (B3) + Red (B4))	(Ansper & Alikas, 2019)
(Red (B4)-1-VRE (B5)-1)*VRE (B7)	
Green (B3) + (SWIR (B12)- SWIR (B11)	(Ouma et al., 2020)
Total Suspended matter (TSS)	
Blue (B2)/ Green (B3)	(Ouma et al., 2020)
Green (B3)/ Blue (B2)	
Red (B4)/ Green (B3)	
Blue (B2)/ Red (B4)	
Coastal aerosol (B1)+ Coastal aerosol (B1)/ Blue (B2))	
Red (B4)	(Quang et al., 2017)
Green (B3)	
VRE (B5)/ Red (B4)	
VRE (B5)/ Green (B3)	(Ma et al., 2021)
Turbidity (TU)	
Green (B3)/VRE (B7)	(Premkumar et al., 2021)
VRE (B7)/ Blue (B2)	
Blue (B2)/VRE (B7)	
VRE (B7)/ Green (B3)	
VRE (B7)/ Red (B4)	
VRE (B5)/ Blue (B2)	(Sòria-Perpinyà et al., 2021)
Red (B4)	(Liu et al., 2017), (Caballero et al., 2018)
VRE (B5)	
VRE (B7)	
VRE (B8a)	
(Red (B4)+(NIR (B8)/ Red (B4)))/2	(Ouma et al., 2020)
(Red (B4) + Green (B3) – Blue (B2)) / (Red (B4) + Green (B3) + Blue (B2))	(Nguyen et al., 2020)
Blue (B2) + Green (B3) + Red (B4)	(Ouma et al., 2020)
(Red (B4)-1 – Green (B3)-1)*Blue (B2)	(Zhao, 2020)

SWIR-Short wave infrared. Bands, band combinations, and band ratios applied to Sentinel-2 and/or Landsat imagery in previous studies for the development of water quality models.

For low biomass, oligotrophic to mesotrophic water bodies, the Chl-a spectrum is characterized by a sun-induced fluorescence peak around 680 nm (Dierssen et al., 2006; Gitelson et al., 1994). For high biomass, eutrophic water bodies, the florescence signal is masked by absorption features and backscatter peaks centred at 665 nm and 710 nm respectively (Gitelson et al., 1994). The ratio between these two wavelengths has been used to accurately estimate Chl-a concentration in

numerous studies (Matthews et al., 2012). Beyond basic constituent retrieval, research focusing on chlorophyll includes the detection of harmful cyanobacteria (Topp et al., 2020). The height of the reflectance peak between 700 and 720 nm has been used for estimating the Chl-a concentration in lake waters for more than two decades (Blaustein, 1992; Gower et al., 2005). These reflectance peaks have been used in many studies by researchers (Ansper & Alikas, 2019; Borges et al., 2020; Buma & Lee, 2020; Cairo et al., 2020; Ha et al., 2017; Lins et al., 2017).

There are a large number of studies (e.g. Table 3-1), where all the bands of the entire visible wavelength region are analysed either individually or in combination for turbidity estimation. Literature suggests that even a single band, if chosen appropriately, can provide a robust estimate of turbidity (Gholizadeh et al., 2016). Studies also mentioned the use of red and NIR together for better turbidity assessment (Toming et al., 2016). Previous studies indicate that empirical models that estimate TSS as a function of RS reflectance (Rrs) in the visible and near-infrared (NIR) bands perform well in single-band adjusted linear regressions and with the NIR and Red bands ratio (Marinho et al., 2021; Martinez et al., 2015).

3.3 Materials and Methods

3.3.1 Study Site

The Koka reservoir is located (08°26` N; 39° 10` E) at an altitude of about 1588 meter above sea level (masl) at the dam outlet, 1625 masl in the north, 1882 masl in the east, 1965 masl in the south, and 1620 masl in the west. 90 km southeast of the capital city, Addis Ababa, Ethiopia. The reservoir covers a total area of 90 km2 at the end of the dry season (June), this expands to about 152 km2 just after the rainy season (October). Besides the Awash River, other sources of water to the reservoir are the Mojo and Akaki Rivers, as seen in Figure 3-1 (a). The Koka dam is 458 m long and rises to a maximum of 47 meters in height. The storage capacity of the reservoir was 1,850 million m3, when the dam was constructed in 1961 (Masresha et al., 2011), but now it has been reduced by 35% due to sedimentation. The dam has also become useful to regulate high flows during the flood season, to supply water for the downstream irrigated land, to the fishing industry, with some 625 tons of fish landed each year (SWECO, 2008), for recreation (Fasil et al., 2011), as well as to supply water for downstream towns and villages from which they generate electricity, although this was not originally planned for (SWECO, 2008). There is a variety of wildlife and birds around the reservoir (Fasil et al., 2011), which makes it an important biodiversity ecosystem.

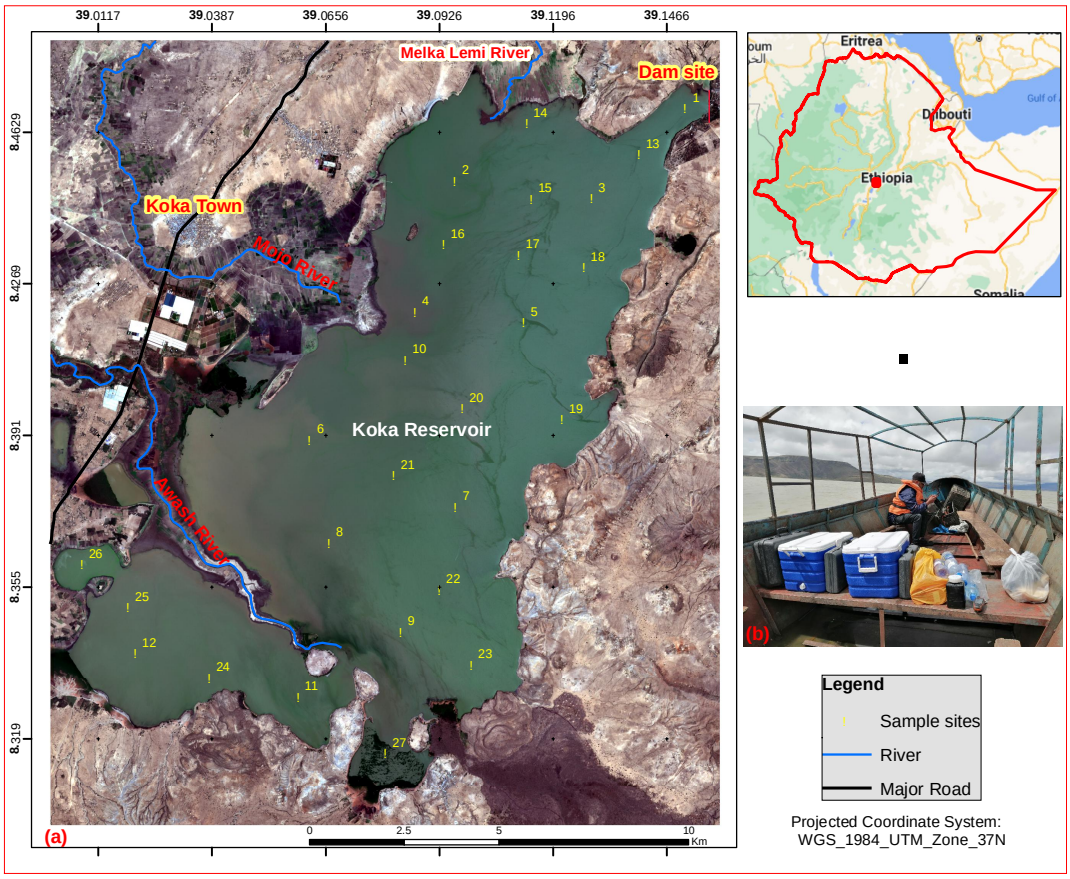

Figure 3-1 Overview of the Koka reservoir

The 27 sampling locations(a), superimposed over a Sentinel-2 image retrieved on 20th March 2017, as surveyed with a handheld GPS receiver on a boat seen in (b).

In Ethiopia there are three major seasons, particularly the "Kiremt" (June-September), Bega (October-January), and "Belg" (February-May); and inter-annual rainfall variability in "Kiremt" and "Belg" can lead to droughts and flooding in the basin where the reservoir is found. The basin has an annual average rainfall of 832 mm. The rainfall in the study area is unimodal with main rainfall from June to September and low rainfall from February to May (Adane et al., 2020; Gebremichael et al., 2022). Rainfall during the "Belg" season is highly variable in time and space and high maximum temperature values are common (Legese et al., 2018). This basin has a mean annual temperature of 27.18 ^{o}C. The mean minimum and mean maximum temperature are 25.87 and 28.98 ^{o}C, respectively (Duguma et al., 2021).

3.3.2 Methodology

The methodological approach used in this study is shown in Figure 3-2 and consists of four main stages of analysis: 1) In-situ water sampling and laboratory analysis; 2) Sentinel-2 image pre-processing and band combinations; 3) Empirical analysis for the development of the WQP model (Chl-a, TSS and TU) with performance evaluation; and 4) time-series derivation of WQP maps.

The developed equations were used to investigate the spatio-temporal variation in WQPs in the Koka reservoir from 2017 to 2022. Sentinel-2A_MSIL1C images from the month of March were selected and processed, this was on different dates due to cloud cover and image clearance; the area of interest, the Koka Reservoir, was extracted from the images. Sentinel 2A satellite images from the years 2021 (June, November-December) and 2022 (January-May) were also used to track the temporal variability of WQPs monthly.

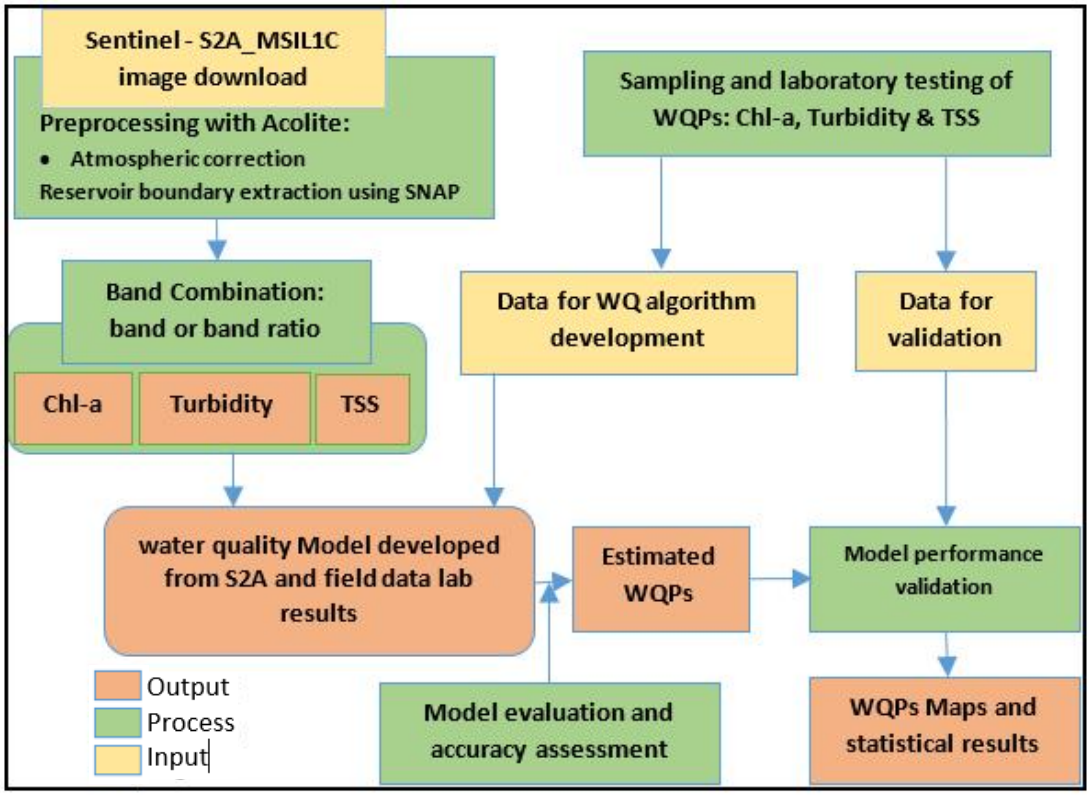

Figure 3-2 A general framework of WQP model development

To minimize error propagation, the satellite images were selected based on image quality. Satellite images with a sign of turbulence or water current on the reservoir were excluded based on visual inspection. As a result, each month's images have a distinct date. Values of WQPs were computed in ArcMap Raster Calculator tool from their band/band combination values and evaluated for the change detection study on both an annual and monthly basis.

3.3.3 In-Situ Water Sampling and Laboratory Analysis

On February 25-26, 2022, ground monitoring datasets were collected from 27 sample sites within two days. It was not possible to take and complete sample collection on the same day of the satellite overpass due to the turbulence. We collected the data the same day of the satellite overpass over the area and one day after the S2A images were acquired for the local scenes. The number of water quality samples and sites have been determined by examining the satellite image while taking into account inlets, outlets, noticeably turbid areas, visibly green areas, and area representation of the reservoir. Figure 3-1 shows the lake extent as seen in Sentinel-2 true color image composite on

20th March 2017 together with the in-situ sampling locations, that were surveyed with a handheld Garmin 60s global positioning system (GPS) receiver. The samples were taken using a Van Dorn water sampler (Alpha Bottle Kit-2.2L Horizontal) (WILDCO, 2013) at a depth of 0.50 m. For Chl-a, the water sample was filtered on site, double wrapped in aluminum foil, and kept in a cold ice box.

In the laboratory, Chl-a, TU and TSS were determined from the water samples. To determine Chl-a, 0.1L water sample was passed through Whatman GF/F 47 mm glass fibre filter at the time of sampling and then extracted into 90% acetone. The Chl-a of the extracts was determined spectrophotometrically at a wavelength of 663, 665, and 750 nm using a SP-2000 spectrophotometer, which utilized 50 mm optical path, 10*10*45 mm standard glass cuvettes and a 5 nm spectral bandwidth. Chl-a was calculated based on (EPA, 1991), as seen in Equ. (1).

$$Chl-a\ (\mu g/L)\ =\ \frac{26.73(663_b-665_a)E(F)}{V(L)}, \qquad (1)$$

Where:
F = Dilution Factor (if the extract requires dilution)
E = The volume of acetone used for the extraction (mL)
V = The volume of water filtered (L)
L = The cell path length (cm)
665 a = The turbidity corrected Abs at 665 nm after acidification
663 b = The turbidity corrected Abs at 663 nm before acidification

TSS analysis was performed by collecting the total solids portion on a Whatman 47 mm microfiber filter, which has a nominal pore size of 1.5 μm. The filters were weighed before the samples were filtered. A volume of 100 ml was passed through the filter using a vacuum flask continuing suction for about three minutes after filtration was completed. The filter was placed in a drying oven set at 104±1°C for at least one hour. After the filter was dried, filters/pans were removed from the oven and placed in a desiccator until they reached room temperature. Each filter was weighted after the samples were filtered and dried up. Finally, the concentration of TSS was calculated by dividing the difference in weight before and after filtering from the water sample volume equation, according to Kersley (2006) as seen in Equ. (2).

$$\mathrm{TSS}\ \left(\frac{\mathrm{mg}}{\mathrm{L}}\right) = \frac{Weight_{final\,(g)}-Weight_{initial\,(g)}}{Sample\ volume(L)}, \qquad (2)$$

3.3.4 Sentinel 2A spatial, spectral, radiometric, and temporal resolution

The Sentinel-2A satellite has distinct spatial, spectral, radiometric, and temporal resolutions that contribute to its effectiveness in Earth observation. The spatial resolution of the Sentinel-2A satellite varies across its 13 spectral bands. Four specific bands, which include the three classical RGB bands (Blue at approximately 493 nm, Green at 560 nm, and Red at 665 nm) along with a Near Infrared band at approximately 833 nm have 10-meter resolution. Six bands that include four

narrow bands in the vegetation red edge spectral domain (approximately 704 nm, 740 nm, 783 nm, and 865 nm) as well as two wider short-wave infrared (SWIR) bands (1610 nm and 2190 nm) that have 20-meter resolution. This lower resolution is designated for three bands primarily focused on atmospheric corrections and cirrus-cloud screening (443 nm for aerosols, 945 nm for water vapor, and 1374 nm for cirrus detection), which have 60-meter resolution (Bramich et al., 2021; Caballero et al., 2020; Du et al., 2016; Molkov et al., 2019; Sent et al., 2021).

The spectral resolution of Sentinel-2A is defined by its ability to distinguish features in the electromagnetic spectrum across its 13 spectral bands. The bands cover a range from visible light through near-infrared to short-wave infrared: The combination of these bands allows for detailed analysis of land cover types, vegetation health assessments, and water quality evaluations (van der Werff & van der Meer, 2016)

Sentinel-2A has a radiometric resolution of 12 bits, which enables it to capture brightness intensity values ranging from 0 to 4095. This high level of detail allows for accurate differentiation between various levels of reflectance. The radiometric accuracy goal is less than 5%, with an ideal target of around 3% (Huang et al., 2016).

The temporal resolution refers to how frequently the satellite revisits a specific location on Earth: Each Sentinel-2 satellite has a revisit frequency of 10 days. However, due to the operation of two satellites (Sentinel-2A and Sentinel-2B), the combined revisit frequency improves to every 5 days, allowing for more timely monitoring of changes on the Earth's surface. These resolutions collectively enhance the capabilities of Sentinel-2A in providing high-quality imagery for various applications, such as agriculture monitoring, land use classification, environmental management, and disaster response efforts (Li & Roy, 2017).

3.3.5 Atmospheric Correction (AC)

Cloud-free Sentinel-2 images (Level 1C processing) were downloaded from the ESA Sentinels Scientific Data hub. Sentinel-2 L1C scenes in the SAFE format contain orthorectified, geolocated, and radiometrically calibrated top-of-atmosphere reflectance in Universal Transverse Mercator (UTM) projection with the WGS84 datum (Vanhellemont & Ruddick, 2016). All Sentinel-2 level-1C data were atmospherically corrected with ACOLITE software, which is completely image-based. Level-2A's main output is an ortho-image Bottom-Of-Atmosphere (BOA) corrected reflectance product, as produced by ACOLITE (Saberioon et al., 2020).

The ACOLITE processor and atmospheric correction developed in the EC-FP7 HIGHROC project (Vanhellemont & Ruddick, 2016). It bundles the atmospheric correction (AC) algorithms and processing software developed by the Royal Belgian Institute of Natural Sciences (RBINS) for aquatic applications (Angelats & Fern, 2019). Model development was carried out considering all possible combinations of ACOLITE-derived imagery (Angelats & Fern, 2019). ACOLITE is an AC processor developed for coastal and inland waters (Ansper & Alikas, 2019; Vanhellemont, 2019) and applicable for processing high-resolution Landsat 8 OLI and S2 MSI images to give results (water-leaving reflectance) over extremely turbid, narrow, and small water bodies (Ansper & Alikas, 2019).

ACOLITE was chosen because it better reproduces the shape of the reflectance spectra. Additionally, ACOLITE is more flexible in configuration than SNAP plugins. It has the ability to apply coefficients for vicarious calibration, choose AC algorithms (SWIR-SWIR or dark spectrum), and select bands for AC (Molkov et al., 2019).

3.3.6 Sentinel-2 Analysis and Boundary Extraction

The first of a series of Multi-Spectral Imager (MSI) instruments was launched in June 2015 by the European Space Agency (ESA) on board Sentinel-2A (Warren et al., 2019). MSI optical sensors are a promising tool for studying inland freshwater ecosystems (Molkov et al., 2019). Sentinel-2A Level-1C images were selected for the month of March 2017 to 2022 as March typically includes cloud-free images over the Koka reservoir to analyze WQPs on an annual basis. In addition to this, Sentinel-2 imagery was downloaded for a monthly based analysis in June 2021, October-December 2021, and January-May 2022. A total of 14 Sentinel-2 images (path/row: 116/34 and 115/34) were retrieved from the Copernicus Open Access Hub (https://scihub.copernicus.eu/). Sentinel-2 imagery was captured at approximately 3:40 GMT (corresponding to 10:40 Ethiopia's local time) over the Koka Reservoir. The Sentinel-2 Level-1C product is ortho-images providing top-of-atmosphere (TOA) reflectance along with the parameters to transform them into radiances in WGS84 UTM zone 37 N. Level-1C products are resampled with a constant Ground Sampling Distance (GSD) of 10, 20 and 60 m depending on the native resolution of the different spectral bands. ACOLITE converts the bands internally to the same resolution. For bands at lower resolution than the processing resolution, values are replicated by nearest neighbor resampling, i.e. no new pixel values are computed, and for bands at higher resolution, pixels are spatially mean averaged. By default, the 10 m grid is used, which means the values from the 20 and 60 m bands are replicated 4 and 36 times to form a 10 m grid (Vanhellemont & Ruddick, 2016).

In this study, the water surface boundary was extracted from the RS image by the modified normalized difference water index (MNDWI) Equation (3), and the reservoir area boundary was masked out using the QGIS software package. MNDWI was developed by (Xu, 2006) and can enhance open water features while efficiently suppressing and even removing built-up, land noise, vegetation, and soil noise. (Singh et al., 2014) showed that MNDWI outperformed the normalized difference water index (NDWI) in extracting water features mixed with vegetation when the depth of standing water varied from 0.60 m to 0.75 m. Equation 3 shows how to calculate the MNDWI using Sentinel-2 image bands, with IR referring to infra-red (Singh et al., 2014).

$$MNDWI = \frac{(green - middle\_IR)}{(green + middle\_IR)}, \quad (3)$$

3.3.7 Empirical Analysis for the WQPs Model Development

Firstly, pixel values of the processed Sentinel-2 images were extracted from each sampling location based on the GPS surveyed coordinates. To address GPS positional inaccuracies and

potential boat drifting, the mean of a 3×3-pixel window was calculated, and then compared with resampled mean observed data and mean Sentinel-2 spectra.

To construct the model expression between Sentinel-2 image bands and the measured Chl-a, TU, and TSS concentration of the Koka Reservoir, an empirical analysis was adopted. Based on the measured and estimated values of the model, descriptive statistics such as R2, RMSE, MAE, and MAPE were calculated and used to evaluate the accuracy and stability of the regression model. The calculations of R2, RMSE, SI, MAE, and MAPE are described in Equations 4, 5, 6, 7and 8 respectively, as follows:

$$R^2 = \frac{\sum\left(x_i^{measured} - \bar{x}^{estimated}\right)(y_i - \bar{y})}{\sqrt{\sum(x_i^{measured} - \bar{x})^2 \sum(y_i - \bar{y})^2}}, \quad (4)$$

$$RMSE = \sqrt{\frac{\sum_{i=1}^{N}(X_i^{estimated} - X_i^{measured})^2}{N}}, \quad (5)$$

where x- represents the average value of Chl-a, TU and TSS measured, y-represents the average value of the water surface reflectance on the image, y_i is the value of the water surface reflectance on the image, $x_i^{estimated}$ represents the simulated value of Chl-a, TU and TSS concentration, $x_i^{measured}$ represents the measured value of Chl-a, TU and TSS concentration, and N is the number of test points (Lai et al., 2021).

The RMSE gives the absolute scattering of the retrieved remote sensing reflectance as well as water quality parameter concentration (Jaelani et al., 2016). A term called scatter index (SI) is defined to judge whether RMSE is sufficient or not. SI is RMSE normalized to the measured data mean, providing it gives the percentage of expected error for the parameter. If SI is less than one, estimations are considered acceptable (Bryant et al., 2016).

$$SI = \frac{RMSE}{\bar{X}} * 100, \quad (6)$$

Where $\bar{x}$ is measured data mean.

$$MAE = \frac{|Y\_observed - Y\_estimated|}{n}, \quad (7)$$

$$MAPE = \frac{100\%}{n}\sum_{y_i}^{n}\left|\frac{Y\_observed - Y\_estimated}{Y\_observed}\right|, \quad (8)$$

3.4 Results

3.4.1 In-Situ Data

Chl-a, TU, and TSS of the surveyed sampling points exhibited high variability over time and space, as seen in Table 3-2. Chl-a ranged from 3.475 to 396.14 µg/L, with an average value of 26.172 µg/L and a standard deviation of 75.96 µg/L. TU varies from 34 to 148 mg/L with an average value of 54.09 mg/L and a standard deviation of 26.04 mg/L, and TSS varies from 192 to 860 mg/L with an average value of 328 mg/L and a standard deviation of 178.89 mg/L.

Table 3-2 Laboratory water quality parameter results, sample taken February 25-26, 2022

Sample ID	Chl-a (µg/L)	TU (NTU)	TSS (mg/L)	Sample ID	Chl-a (µg/L)	TU (NTU)	TSS (mg/L)
1	3.475	38	218	15	19.112	36	246
2	18.243	38	286	16	16.062	-	197
3	12.162	-	222	17	20.849	40	247
4	23.456	44	288	18	19.112	52	212
5	21.718	52	228	19	17.375	46	402
6	16.506	46	308	20	18.687	40	226
7	21.718	64	210	21	19.112	52	223
8	17.031	100	338	22	14.768	52	827
9	18.849	48	860	23	17.012	48	235
10	10.425	42	192	24	52.718	-	318
11	105.98	-	514	25	77.375	44	606
12	49.517	34	436	26	396.14	148	317
13	15.212	-	247	27	-	72	227
14	17.819	-	226				

3.4.2 Remote Sensing Reflectance Rrs (λ) in Sampling Locations

The RS reflectance Rrs(λ) from the 27 sampling locations was extracted from the Sentinel-2 using the spatial analyst tool in ArcGIS software package. As presented in Figure 3-3, the reflectance across the Sentinel-2 bands ranges from 0.1123 to 0.2783 Sr-1. The red (B4) and red edge band (B5) show characteristically higher reflectance compared with other bands over the reservoir. The B5 band of the red edge spectral region shows the highest reflectance in all the sampling sites compared with the other bands. With the except the sampling sites B2, B3, B11, and B12, all bands show characteristically higher reflectance at station 8 than the other sampling points. Similarly, Except B2, B3, B4, B11 and B12 all bands show high reflectance at sampling sites 12, 24, 25, and 26, B2, B3, B4, B11, and B12 show lower reflectance at sampling sites 11.

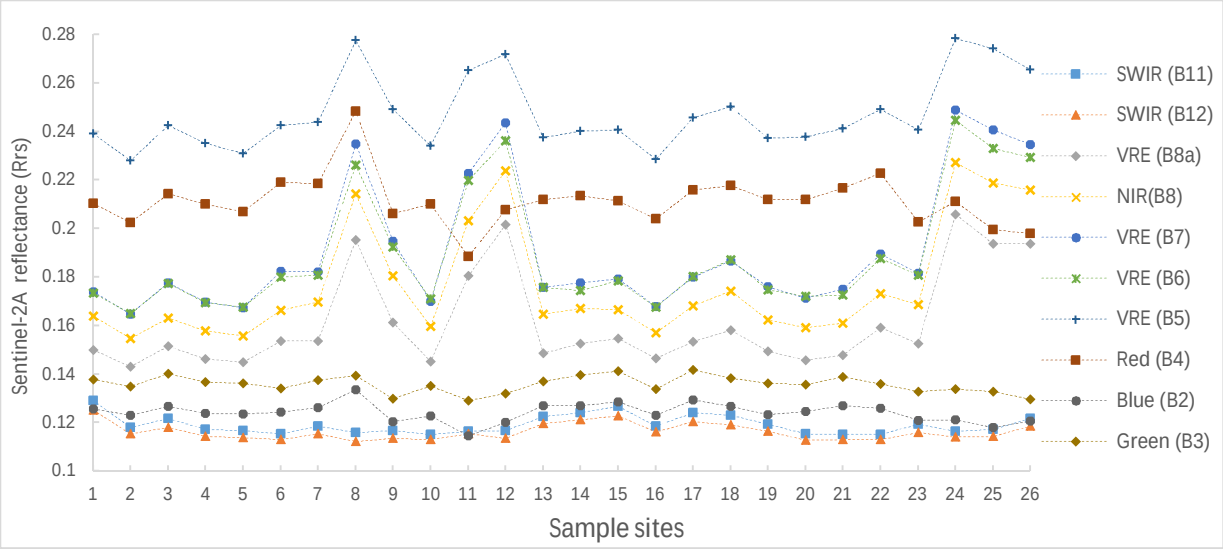

Figure 3-3 RS reflectance variations over sampling points across Sentinel-2 bands.

Almost all bands show low reflectance at sampling sites 16. Similarly, except B2, B3, B4, B11, and B12 all bands show low reflectance at sampling site 10. In general, the reflectance pattern within the dam follows the same pattern from sampling site 1 to sampling site 12, but not under the visible spectral region (B2, B3, B11 and B12).

3.4.3 Empirical Model Development for Chlorophyll a

After arranging the data as seen in Table 3-2, two outliers were identified for Chl-a (sampling site 1 3.475 µg/L and sampling site 26 and 396.14 µg/L). In the development of the empirical models, these outliers were omitted.

The central wavelength of Sentinel-2 band 5 is 705 nm, which is useful for mapping phytoplankton biomass (Chl-a). Therefore, we calculated the height of the peak against band 4 (665 nm), band 6 (740 nm), band 7 (783 nm), and band 8A (865 nm) and determined its correlation with the observed Chl-a in the Koka reservoir.

All band combinations found in previous studies (see Table 3-1) were tested in this study. However, few of them provided the strongest correlations, those are B5/B4, (1/B4 - 1/B5) * B8A, (1/B4 - 1/B5) * B7, (1/B4 - 1/B5) * B6, and (1/B4 - 1/B5) * B8. Figure 3-4 shows the selected regression of in-situ Chl-a and Sentinel-2 bands, band ratios and band combinations, with the strongest correlation detected between Chl-a and (1/B4 - 1/B5) * B8A (R^2 = 0.887 and P = 0.09); (1/B4 - 1/B5) * B6 (R^2 = 0.886 and P = 0.07), B5/B4 (R^2 = 0.9127 and P = 0.037); (1/B4 - 1/B5) * B7 (R^2 = 0.8762 and P = 0.083), and (1/B4 - 1/B5) * B8 (R^2 = 0.8692 and P = 0.075).

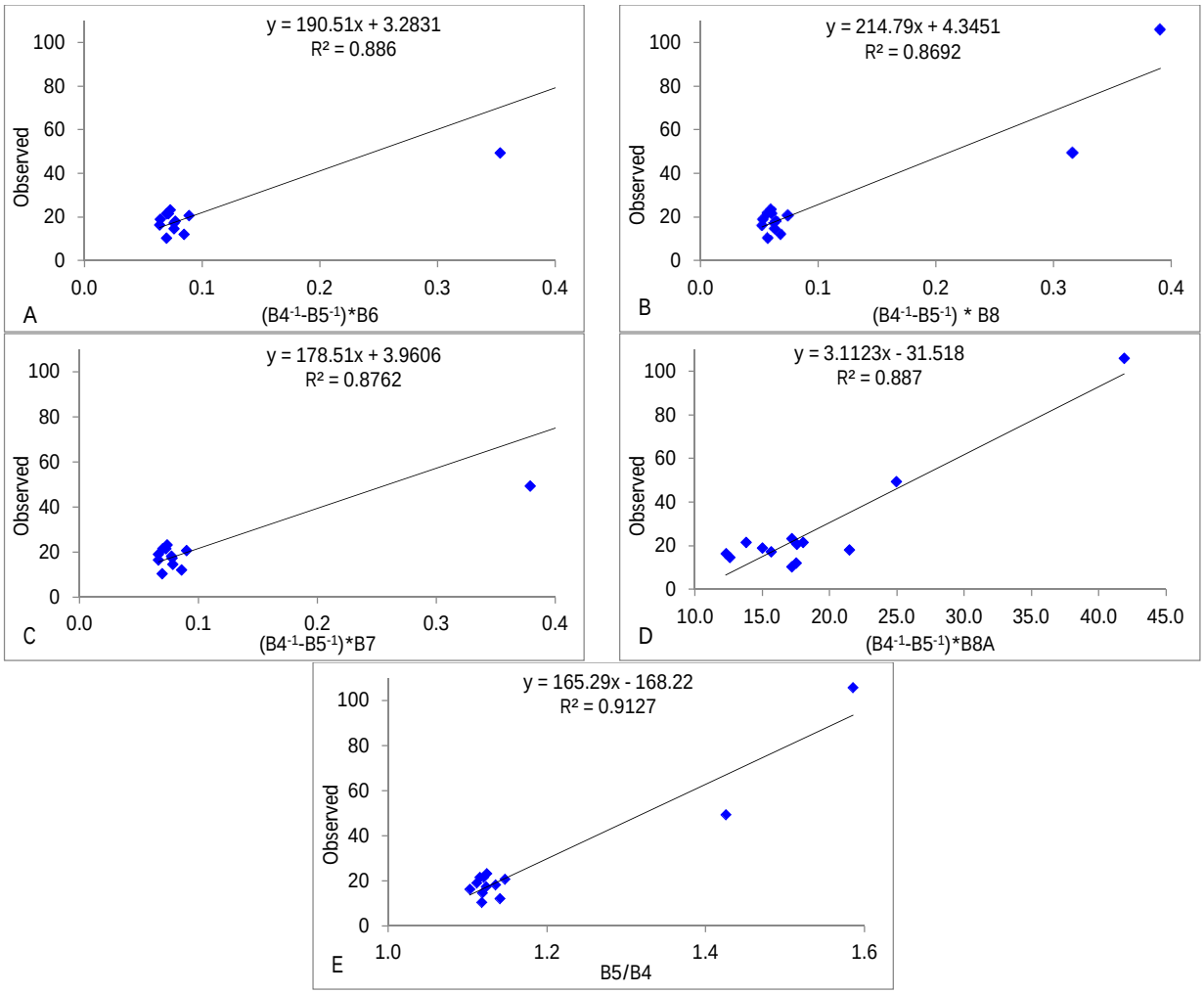

Figure 3-4 Regression analysis of in-situ Chl-a and corresponding S2A reflectance to estimate Chl-a

*Abbreviations of the Sentinel-2 band 1 to band 8a corresponded to B1 to B8a. (a) Observed and estimated (band ratio (B4-1-B5-1) *B6) Chl-a, (b) Observed and estimated (band ratio (B4-1-B5-1) *B8) Chl-a. (c) Observed and estimated (band (B4-1-B5-1) *B7) Chl-a; (d) Observed and estimated (band ratio (B4-1-B5-1) *B8A) Chl-a. (d) Observed and estimated (band ratio B5/B4) Chl-a.*

The highest correlation and the smallest error of S2A (B5/B4) with in-situ Chl-a confirmed the appropriateness of using this two-band ratio for estimating Chl-a in the Koka reservoir (Figure 3-4). The standard error (µg/L) of the estimate Chl-a of selected band combinations (ratio) B5/B4, (1/B4 - 1/B5) * B8A, (1/B4 - 1/B5) * B7, (1/B4 - 1/B5) * B6, and (1/B4 - 1/B5) * B8 equals to 0.34, 0.11, 0.60, 0.53, and 0.55, respectively, corresponded to 5 % of the mean value of in-situ Chl-a; see Table 3-3 (a). Therefore, (B5/B4) was selected as the best ratio for estimating Chl-a in the Koka reservoir in this study. Based on this selection, Chl-a can be calculated by equation (9) below. Sentinel-2 derived Chl-a showed a linear correlation with in-situ Chl-a R^2 = (0.9127), RMSE =

(9.86) which has SI 0.31, CI = (0.037) also confirming a relatively good similarity between satellite and field observed data as shown in Figure 3-4 (E).

$$\text{Chl-a} = 165.29 * (B5/B4) - 168.22, \quad (9)$$

3.4.4. Empirical Model Development for Turbidity

The selected regression of in-situ turbidity and Sentinel-2 bands and band ratios, with the strongest correlation detected between TU and B3/B2 (R^2 = 0.8578 and P = 0.028); B4/B3 (R^2 = 0.9156 and P = 0.04); B2/B4 (R^2 = 0.8851 and P = 0.074), and B2/B3 (R^2 = 0.8617 and P = 0.06) as shown in Figure 3-5. The B3/B2, B2/B4 and B2/B3 of the TU and Sentinel-2 bad model results showed that model was not statistically significant with p-values for each variable tested being greater than 0.05.

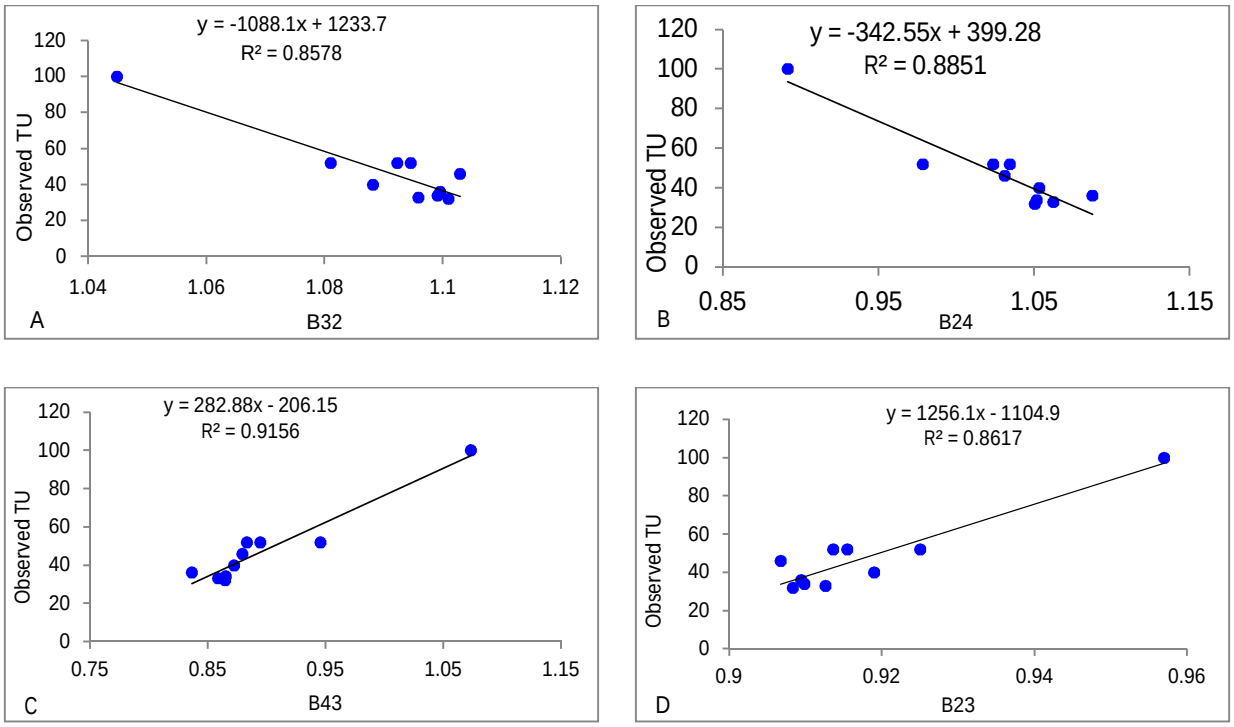

Figure 3-5 Turbidity and Sentinel-2 band ratio analysis.

Observed and estimated (band ratio B3/B2) turbidity (a), Observed and estimated (band ratio B2/B4) turbidity (b), Observed and estimated (band B4/B3) turbidity (c), and Observed and estimated (band ratio B2/B3) turbidity (d).

The standard error (NTU) of the estimate TU of selected band ratio (B3/B2), (B2/B4), B4/B3, and band B2/B3 equals 4.536, 4.81, 3.421, and 4.112, respectively, corresponded to 5% of the mean value of in-situ TU, (see Table 3-3 (b)). The highest correlation and the smaller error of Sentinel-2 band ratio is B4/B3 ratio with in-situ TU confirming the appropriateness of using this two-band

ratio for estimating TU. Therefore, B4/B3 was selected as the best ratio for estimating TU in the Koka reservoir water in this study. Sentinel-2 derived TU showed a linear correlation with in-situ TU R^2 of 0.9156 and RMSE of 17.94 and which has SI of 0.24; also confirming a relatively very good similarity between satellite and field observed data as shown in Figure 3-5 (C). TU can be calculated by using equation (equation 10).

$$TU = 282.88 * (B4/B3) - 206.15, \quad (10)$$

3.4.5 Empirical Model Development for TSS

The TSS in the reservoir ranges between 150 mg/L and 860 mg/L, with an average of 331 mg/L. Adopting a regression model-based approach, the best results for the estimation of TSS concentration were obtained from Sentinel-2 using a linear regression function of a band ratio. The overall performance of the satellite sensors in the retrieval of TSS within the reservoir is summarized in Table 3-3 (c) where the top R^2 estimations are 0.3067, 0.2979, 0.5892, and 0.6717. The standard error (mg/L) of the estimated TSS of selected band combination (B7/B3), band (B7/B2), band (B4/B3), and band (B4), equals 25.45, 86.25, 48.97, and 18.46 respectively, corresponded to 5 % of the mean value of in-situ TSS. Therefore, B4 was selected as the best band ratio for estimating TSS in the Koka reservoir. The results from the current study show the significance of the red and vegetation red edge band wavelengths in the estimation of TSS in shallow reservoir inland water bodies. TSS can be calculated by equation (11).

Sentinel-2 derived TSS showed a linear correlation with in-situ TSS R^2 of 0. 6717, and RMSE of 65.38, which has SI of 0.23, and Confidence level (CL) of 0.02; confirming a relatively very good similarity between satellite and field observed data as shown in Figure 3-6 (D).

$$TSS = 3938.9(B4) - 536.9, \quad (11)$$

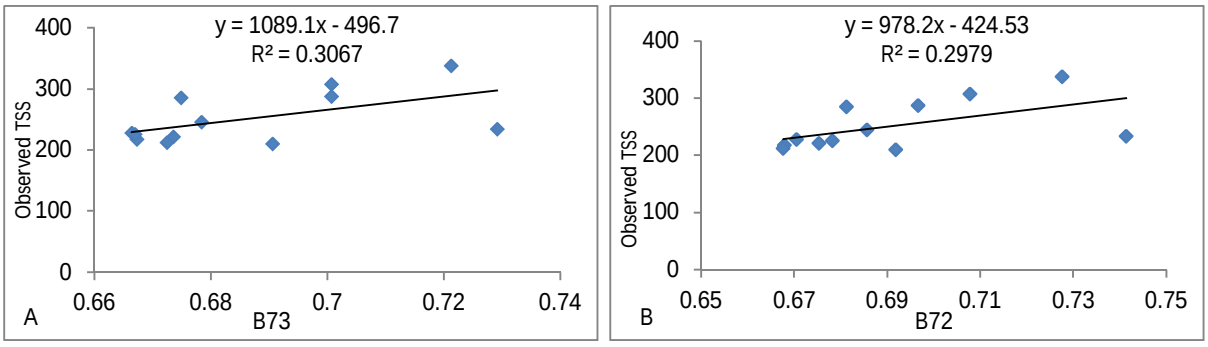

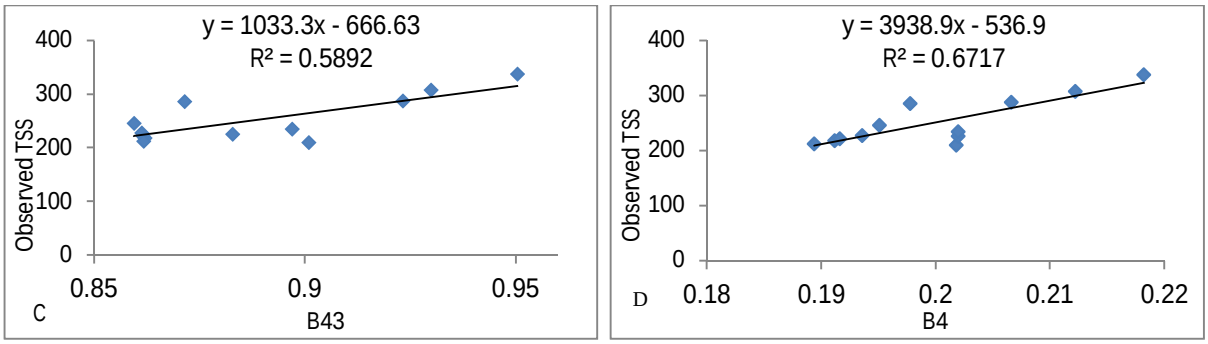

Figure 3-6 Cross-relationships of in-situ TSS and corresponding S2A reflectance band ratios.

Base on the estimated TSS in the reviewed literature (Table 3-1), the highest correlation and the smallest error of S2A band (B4) with in-situ TSS confirmed the appropriateness of using this band for estimating TSS in Koka reservoir water Figure 3-6 (D).

Table 3-3 Selected regression model from Sentinel 2A and in-situ-measured data

	Model* (Chl-a =)	Band (Band ratio) #	R^2	SE	CL (95%)	SD	RMSE	SI
	190.51x + .2831	$(B4^{-1}-B5^{-1})*B6$	0.886	6.54	0.07	21.7	10.14	0.31
	178.51x+ 3.9606	$(B4^{-1}-B5^{-1})*B7$	0.876	6.60	0.083	21.9	9.58	0.30
	214.79x + 4.3451	(1/B4 - 1/B5) * B8	0.869	6.55	0.075	21.7	10.24	0.31
	3.1123x - 31.518	(1/B4 - 1/B5) * B8A	0.887	6.11	0.09	20.3	10.29	0.60
(a)	165.29x - 168.22	B5/B4	0.913	6.34	0.037	21.00	10.30	0.3

	Model* (TU=)	Band (Band Ratio) #	R^2	SE	CL (95%)	SD	RMSE	SI
	1256.1x - 1104.9	B2/B3	0.8617	4.536	0.06	12.05	16.48	0.31
	-1088.1x + 1233.7	B3/B2	0.8578	4.81	0.03	14.43	17.28	0.32
	-342.55x + 399.28	B2/B4	0.8851	4.112	0.74	12.34	20.19	0.47
(b)	282.88x - 206.15	B4/B3	0.9156	3.421	0.04	10.26	17.94	0.24

	Model* (TSS =)	Band (Band ratio) #	R^2	SE	CL (95%)	SD	RMSE	SI
	540.34x - 55.362	B7/B3	0.3067	25.45	0.27	84.41	88.21	0.43
	425.27x - 26.859	B7/B2	0.2979	86.25	0.37	286.07	572.7	0.40
	-357.43x + 816.34	B4/B3	0.5892	48.97	0.34	162.43	239.86	0.41
(c)	481.06x - 48.746	B4	0.6717	18.46	0.02	61.23	65.38	0.23

** regression model equation for estimation of Chl-a, TU, and TSS from the Sentinel 2A MSI sensor;*
 # Band combination for deriving x. (a) regression model for the retrieval of Chl-a, (b) regression model for the retrieval of TU, (c) regression model for the retrieval of TSS.

Overall, as shown in Figure 3-4, Figure 3-5, and Figure 3-6, in all regression analysis of Chl-a, TU and TSS with reflectance that corresponded to the selected Sentinel-2 bands or band ratios or band combinations, the linear function obtained smaller errors.

3.4.6 Model Performance Validation with In-Situ Measurements.

Based on previously developed equations 9, 10, and 11, Chl-a, TU and TSS concentrations were predicted for the validation dataset. The accuracy of the model prediction was assessed by comparing the estimated and the observed Chl-a, TU and TSS concentration. Validation of the developed regression models was carried out using randomly selected sampling sites of twelve (12) sampling stations for Chl-a, nine (9) sampling sites for TU, and fifteen (15) sampling sites for TSS, with all observations collected on the same day. Table 3-4 includes the validation results, including the statistics from the selected stations which were used in the model development.

The results of the regression model assessment in Figure 3-4, Figure 3-5, and Figure 3-6 show the correlation between measured Chl-a, TU and TSS and Sentinel-2 imagery band or band ratio, respectively. The regression model has significant descriptive statistics attributable to four parameters consists of R^2, RMSE, MAE, and MAPE to characterize the performance of the models. In this study, water samples were used to evaluate or validate the accuracy of the regression model for each parameter. Comparison between concentration of Chl-a, TU, and TSS at the measurement points and the results calculated from different bands or band ratios or band combinations was made.

Table 3-4 Descriptive statistics of the observed and predicted water quality parameters

Parameters and Sentinel-2		Sample (*n*)	Min	Max	Mean	SD	SE	CV	RMSE	MAE	MAPE (%)
Chl-a (µg/L)	Observed	13	13.47	77.37	25.21	18.59	5.60	0.77	9.00	6.9	20
	Estimated	12	15.18	83.39	31.73	21.01	6.34	0.69			
Turbidity (NTU)	Observed	10	38.00	78.0	52.00	11.7	3.89	0.23	17.94	14.79	24.09
	Estimated	11	24.08	57.74	37.72	13.6	3.42	0.27			
TSS (mg/L)	Observed	12	192.0	450.0	286.4	42.61	12.3	0.35	65.38	49.28	22.68
	Estimated	11	133.8	332.0	220.4	61.23	18.4	0.28			

Comparisons of analysed Chl-a and estimated Chl-a from Sentinel-2 using equation (9) are shown in Figure 3-7(a). Estimated Chl-a has a relatively greater minimum and maximum value compared to in-situ Chl-a; the mean value of the estimated and observed Chl-a is 31.7 (µg/L) and 25.2 (µg/L), respectively. It is clear that the RMSE=9, MAE=6.9, and MAPE=20, corresponded to 18.6 (observed) and 21 (estimated) of standard deviation as well as 5.6 (observed) and 6.34 (estimated) of standard error with CV 0.77 (observed) 0.69 (estimated) confirming the appropriateness of equation for estimating Chl-a in the Koka reservoir using Sentinel -2 images. These comparisons show that the Sentinel-2 satellite image particularly the vegetation red (B4) and red edge (B5) band ratio are suitable for the prediction of Chl-a in land water bodies confirming the appropriateness of the developed empirical model. It is confirmed that the developed empirical model is

appropriate for Chl-a monitoring using Sentinel-2 satellite imagery although the predicted Chl-a for two sampling sites was underestimated (sample site 8 and 20) and overestimated for other sites as compared to observed Chl-a, with MAE of 6.9 μg/L.

Evaluations of analysed turbidity and estimated turbidity from Sentinel-2 using equation (10) obtained are shown in Figure 3-7(b). Also, the bands through blue to NIR were analysed for model development in their spectral response to estimate turbidity concentrations. It is evident that estimated turbidity has small MAE (14.79), MAPE (24.09), and RMSE (17.94) when compared to the observed turbidity, corresponded to 11.7 (observed) and 13.6 (estimated) of standard deviation as well as equal (3.89) observed and (3.42) estimated of standard error with CV 0.23 (observed) 0.27 (estimated) confirming the appropriateness of the developed empirical model for estimating TU in the Koka reservoir.

Comparisons of analysed TSS and estimated TSS from Sentinel-2 using equation (11) are shown in Figure 3-7(C). It is shown that estimated TSS has MAE = 49.28, MAPE = 22.68, and RMSE = 65.38 values, corresponded to 42.61 (observed) and 61.23 (estimated) of standard deviation as well as 12.3 (observed) and 18.4 (estimated) of standard error with CV 0.35 (observed) 0.28 (estimated) confirming the appropriateness of the developed empirical model for estimating TSS in the Koka reservoir.

In addition to the descriptive and other statistical measures, the graphical assessment of the validation results is presented in Figure 3-7. For Chl-a, TU, and TSS it shows that for their respective number of samples and validation sampling sites, the retrieval of Chl-a, TU and TSS relatively matched with the observed measurements for Sentinel-2 image bands or band combination model results, with the exception of some sampling sites 1, and 20 where Sentinel-2 band combinations underestimated Chl-a by 1.85 and 0.96 μg/L, and the remaining sites overestimated the Chl-a ranging from 22.02 μg/L and 0.24 μg/L, see Figure 3-7(A). Overall predicted TU from Sentinel-2 was overestimated in some sampling sites (1, 2, and 6) and underestimated for other sites as compared to observed TU between satellite and field observed data, with MAE of 7.3 NTU as shown in Figure 3-7(b); in addition, sampling sites 10, 14, 16 and 21 overestimated TSS by 80.9, 18.2, 108.4 and 109.2 mg/L, respectively. Other sample stations underestimated TSS concentrations ranging from 32.2 mg/L to 274.2 mg/L as shown in Figure 3-7(C).

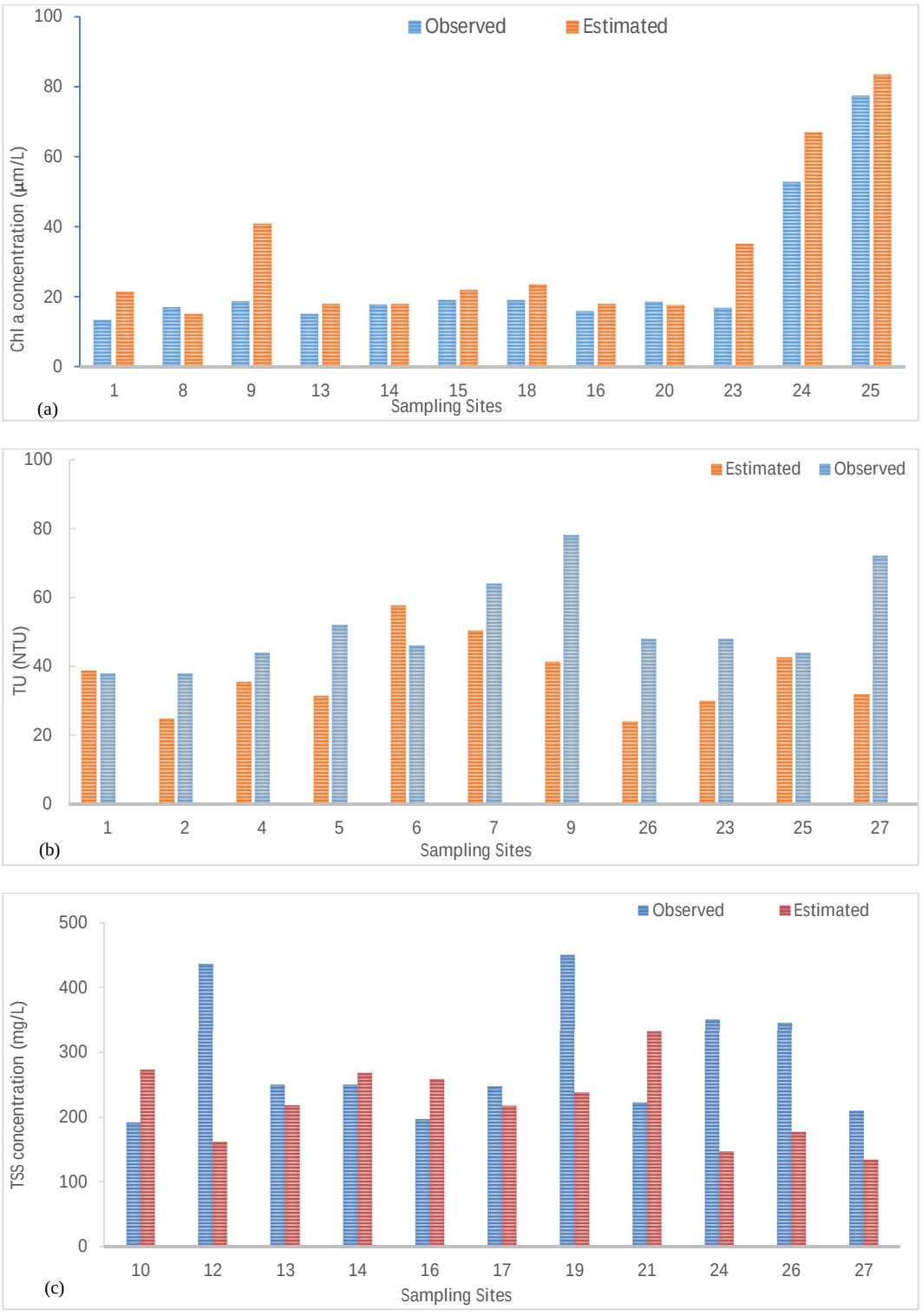

Figure 3-7 Prediction and validation of Chl-a, TU, and TSS with Sentinel-2A band (band ratio).

Observed and estimated Chl-a concentration band ratio (B5/B4) (a), Observed and estimated Turbidity (band ratio B4/B3) (b), and Observed and estimated TSS (B4) (c), within the reservoir using equation (9), (10) and (11), respectively

3.4.7 Spatial and Temporal Patterns of Water Quality Parameters Mapping

a. Temporal Variation of Water Quality Parameters

The monthly mean, minimum, maximum, SD, and CV for Chl-a, TU, and TSS values are reported in Table 3-5. When satellite image assessment results were compared across a year (January 2021 to May 2022), the minimum and maximum values of Chl-a were widely dispersed. In the analysed months, the mean value ranged from 59.69 µg/L in May to 144.25 µg/L in December (Appendix D Figure 4 (A) and Table 3-5). From November to February, the maximum concentration of Chl-a decreased (354.64, 340.53, 287.34, and 205.29 µg/L, respectively). In March, April, and May the maximum Chl-a (254.24, 246.08, and 155.47 µg/L) showed a decreasing trend. The mean Chl-a concentration showed a decreasing order or trend from December to March. November had the highest Chl-a concentration (354.64 µg/L) followed by December (340.53) and January (287.34 µg/L).

The highest concentration of TSS was obtained in April 2022 (574.51 mg/L) followed by May 2022, and June 2021 478.94 and 387.56 mg/L, respectively. The lowest minimum TSS concentration (0.05 mg/L) was observed in March 2022. The maximum lower concentration of TSS was observed in April 2022 (9.81 mg/L). From January to April, TSS showed an increasing trend (124.58, 128.77, 135.07, and 574.51mg/L), respectively. This stretch starts the transition time of the dry season to the Belg season in the area. The mean concentration of TSS ranges from 38.46 to 368.97 mg/L. The mean TSS concentrations in the respective months follow a decreasing trend from June 2021 to February 2022 (Appendix D Figure 4 (C) and Table 3-5).

The minimum and maximum turbidity showed a decreasing trend by 36.72 NTU from June to December 2021 and the maximum turbidity showed an increasing trend from February to May 2022 by 37.33 NTU. There is a similar trend of the mean turbidity as the maximum turbidity showed in the respected months. However, there was no consistent pattern in the lowest turbidity of the years studied (Appendix D Figure 4 (B) and Table 3-5.

As seen in Table 3-5, for the whole reservoir, monthly mean, Chl-a (59.69 µg/L) levels were at their lowest in May 2022 and their highest level (144.25 µg/L) in December 2021. The average TU was low in December 2022 (79.67 NTU) and high in June 2021 and May 2022 (about 115 NTU). The monthly mean of TSS ranged from 38.46 mg/L in February 2022 to 368.97 mg/L in April 2022. Similarly, for the whole reservoir, the yearly mean Chl-a was low in 2021 (52.86 µg/L) and high in 2017 (96.19 µg/L); mean TU was low in 2018 (71.04 NTU) and high in 2022 (83 NTU) and the mean TSS was low in 2018 (36.58 mg/L) and high in 2020 (159.26 mg/L).

Maximum concentration of Chl-a levels dropped by 123.39 µg/L from 2020 to 2021 and increased by 149.53 µg/L from 2021 to 2022. In contrast, from 2019 to 2020 maximum Chl-a concentration increased by 72.66 µg/L and from 2018 to 2019, maximum concentration of Chl-a decreased by 63.94 µg/L.

Table 3-5 descriptive statistics of the in-situ-measured and predicted water quality parameters

Descriptive statistics	2021			2022				
	June	November	December	January	February	March	April	May
(Chl-a)								
Minimum	8.67	0.67	0.98	0.07	0.53	0.35	0.79	6.02
Maximum	235.58	354.64	340.53	287.34	205.29	254.24	246.08	155.47
Mean	64.75	115.08	144.25	124.58	84.52	81.80	114.80	59.69
(TSS)								
Minimum	1.96	0.83	0.91	0.93	0.58	0.05	9.81	0.02
Maximum	387.56	159.49	302.48	124.05	128.77	135.07	574.51	478.94
Mean	191.72	64.27	66.38	59.65	38.46	62.30	368.97	210.81
(TU)								
Minimum	38.44	0.88	0.48	0.71	0.36	0.18	0.52	41.02
Maximum	209.85	209.66	173.13	176.06	165.48	172.44	180.76	202.81
Mean	115.07	98.24	79.67	84.82	82.18	82.77	90.64	115.39

Selected regression model for the retrieval of WQPs from Sentinel 2A MSI bands and descriptive statistics of the in-situ-measured and predicted water quality parameters.

In 2020, the lowest maximum (12.46 µg/L) and mean (94.53 µg/L) concentrations of Chl-a were recorded, with the lowest margin of maximum concentration. In comparison to previous years, 2022 had the highest maximum (254.24 µg/L) and mean (83.2 µg/L) of Chl-a concentration followed by 2020, the maximum Chl-a concentration of 228.1 µg/L. The annual mean Chl-a fluctuates between 52.86 µg/L in 2021 and 96.19 µg/L in 2017. As illustrated in Appendix D Figure 5 (A) and Table 6, the annual minimum Chl-a ranges from 0.28 µg/L in (2017 and 2022) to 12.46 µg/L in 2020.

TU is the highest in 2022 (172.44 NTU). The mean turbidity ranges from 72.82 in 2017 to 83 in 2022. Similarly, the maximum TU ranges from 149.73 NTU in 2021 to 172.44 in 2022. The minimum TU ranges from 0.03 NTU in 2018 to 12.18 NTU in 2021. The minimum, maximum, and mean turbidity not show a regular trend. The minimum turbidity concentration showed the highest turbidity value in the year 2021 (12.18 NTU) Appendix D Figure 5 (B) and Table 3-6.

The satellite-based TU model results showed that the higher whole reservoir mean turbidity in the month of June 2021 and May 2022 was about 115 NTU. In contrast, the whole reservoir satellite-based data showed mean TU in month of April 2022 (90.64 NTU) and November 2021 (98.24 NTU) lower than in the months of June 2021 and May 2022 (215 NTU). Lower turbidity was observed in the dry season than in “Belg” and “Kiremt” season (June) was significant in the analyses of the evaluated months Appendix D Figure 5 (C) and Table 3-6.

TSS concentrations are highest in 2020 (358.41 mg/L), followed by 2019 (279.63 mg/L). From 2018 to 2020 TSS revealed an increasing trend (170.13, 279.63, and 358.41 mg/L). The mean

value of the year 2020 was higher (159.26 mg/L) than the mean value of the remaining evaluated years. The maximum concentration of TSS ranges from 120.89 mg/l in 2021 to 358.41 mg/l in 2020. Similarly, the mean concentration of TSS ranges from 36.58 mg/l in 2018 to 159.26 in 2020.

Table 3-6 Descriptive statistics of model predicted water quality parameters

Year	Chlorophyll *a* (µg/l)			Turbidity (NTU)			TSS (mg/l)		
	Min	Max	Mean	Min	Max	Mean	Min	Max	Mean
2017	0.28	211.58	96.19	0.24	161.15	72.82	0.77	217.39	51.04
2018	0.33	219.38	68.67	0.03	163.53	71.04	1.13	170.13	36.58
2019	7.71	155.44	77.95	0.28	167.06	72.42	0.64	279.63	67.97
2020	12.46	228.10	94.53	0.65	153.04	79.96	1.61	358.41	159.26
2021	4.22	104.71	52.86	12.18	149.73	80.42	0.23	120.89	54.12
2022	0.28	254.24	83.20	0.67	172.44	83.00	0.85	135.08	57.84

b. Spatial Distribution of Chl-a, TU and TSS and Time Series Analysis

The annual spatial distribution maps of Chl-a, TU and TSS developed through time derived observations from the Sentinel-2 are illustrated in Figure 3-8, Figure 3-9, and Figure 3-10, with monthly maps of Chl-a TU and TSS presented in Appendix D Figure 1, Appendix D Figure 2, and Appendix D Figure 3, respectively.

Spatial patterns reflected the inlets of Mojo and Awash rivers (Figure 3-9 and Figure 3-10) have high TSS and TU. Similarly, the south and south-western side of the reservoir which is left side of the Awash river showed the highest concentration of Chl-a. There is no spatial heterogeneity in all the months as well as the years of all the analysed Sentinel-2 images for all WQ indicators.

The annual variation in Chl-a concentrations across the lake was noticeable (Figure 3-8). Chl-a concentrations were higher in the south and south western sections of the reservoir in all the studied years than in 2017. Except for the north and north-eastern tip of the reservoir, the Chl-a was highly spread across the reservoir were found in 2017, regardless of concentration. The minimum concentration of Chl-a in all the examined years except 2017 had a large area coverage than the maximum Chl-a concentration. The highest concentrations of Chl-a were found in the south and south western part of the reservoir. This may be related to the prevailing wind in the study area. It is observed that the wind direction during fieldwork (reconnaissance survey) and water quality sample collection from the reservoir the wind blows from the southeast to the southwest. We have also justified this in the rainy season (July to Semptember) the concentration of waterhysciene in the dam covers very large area (southeastern part of the reservoir) and when we visit the site in October the waterhysciene 100% move to the southwester direction (lake inlate of the Awash river). This indicates there is a a relation ship between the wind and the concentration of the chlorophyll a as researches indicate that wind plays a significant role in influencing chlorophyll a concentration in lakes through its effects on mixing dynamics, nutrient resuspension, light

availability, and temperature regulation (George & Edwards, 1976; Lake & Small, 1948; Zhang et al., 2021).

The distribution of relatively lower TSS concentrations on the south and southwest sides of the reservoir were observed from 2018, 2019, 2021 and 2022. TSS and TU distributions in all years studied followed a similar trend (Figure 3-9, and Figure 3-10). Overall, the spatial pattern during the monitoring period showed a high concentration upstream (Awash river inlet to the reservoir) and decreased downstream (the Awash river outlet from the reservoir). This is consistent with the pattern observed in Chl-a, TU and TSS in Figure 3-8, Figure 3-9, and Figure 3-10.

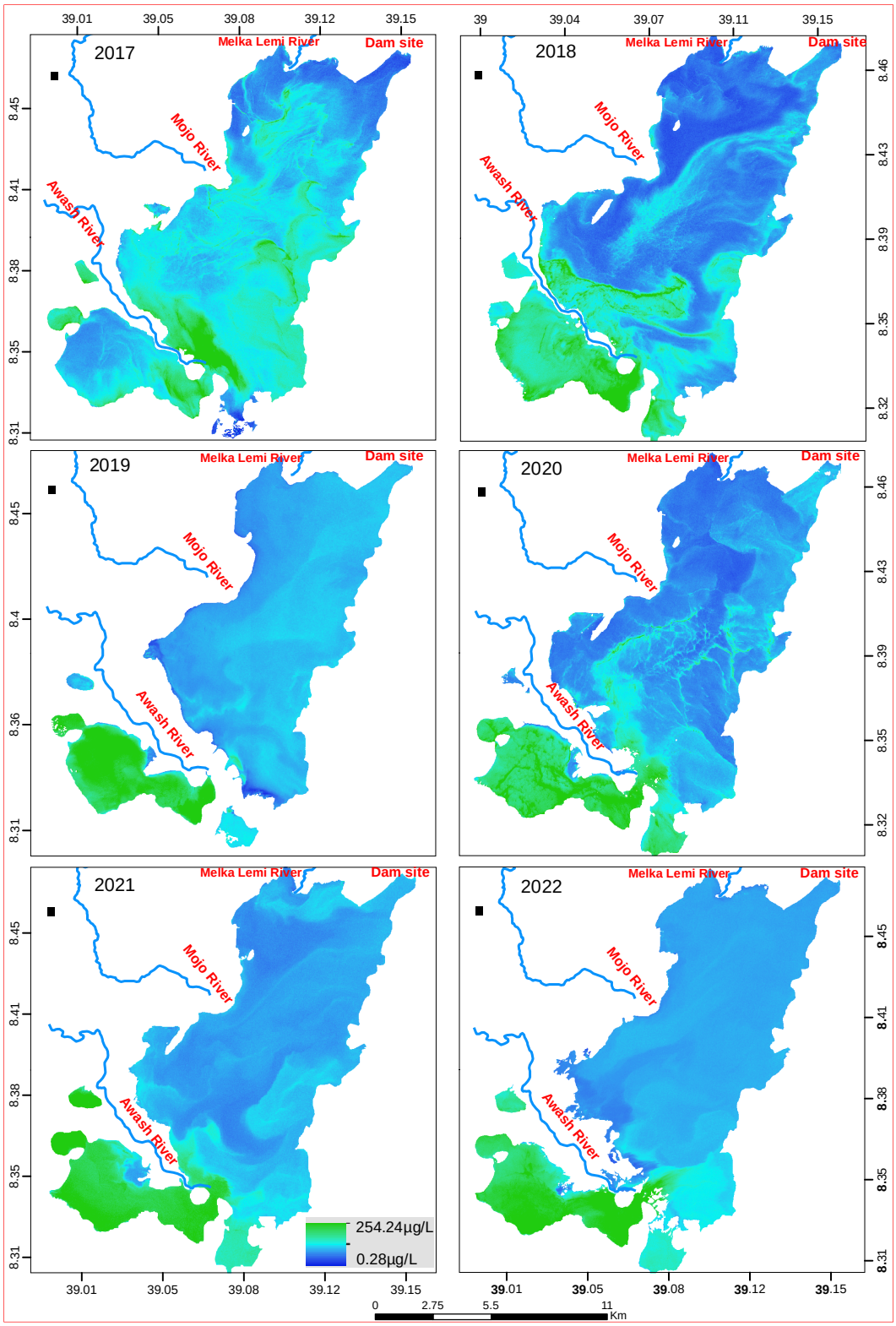

Figure 3-8 Map of Chl-a (µg/L) using linear regression models (2017-2022).

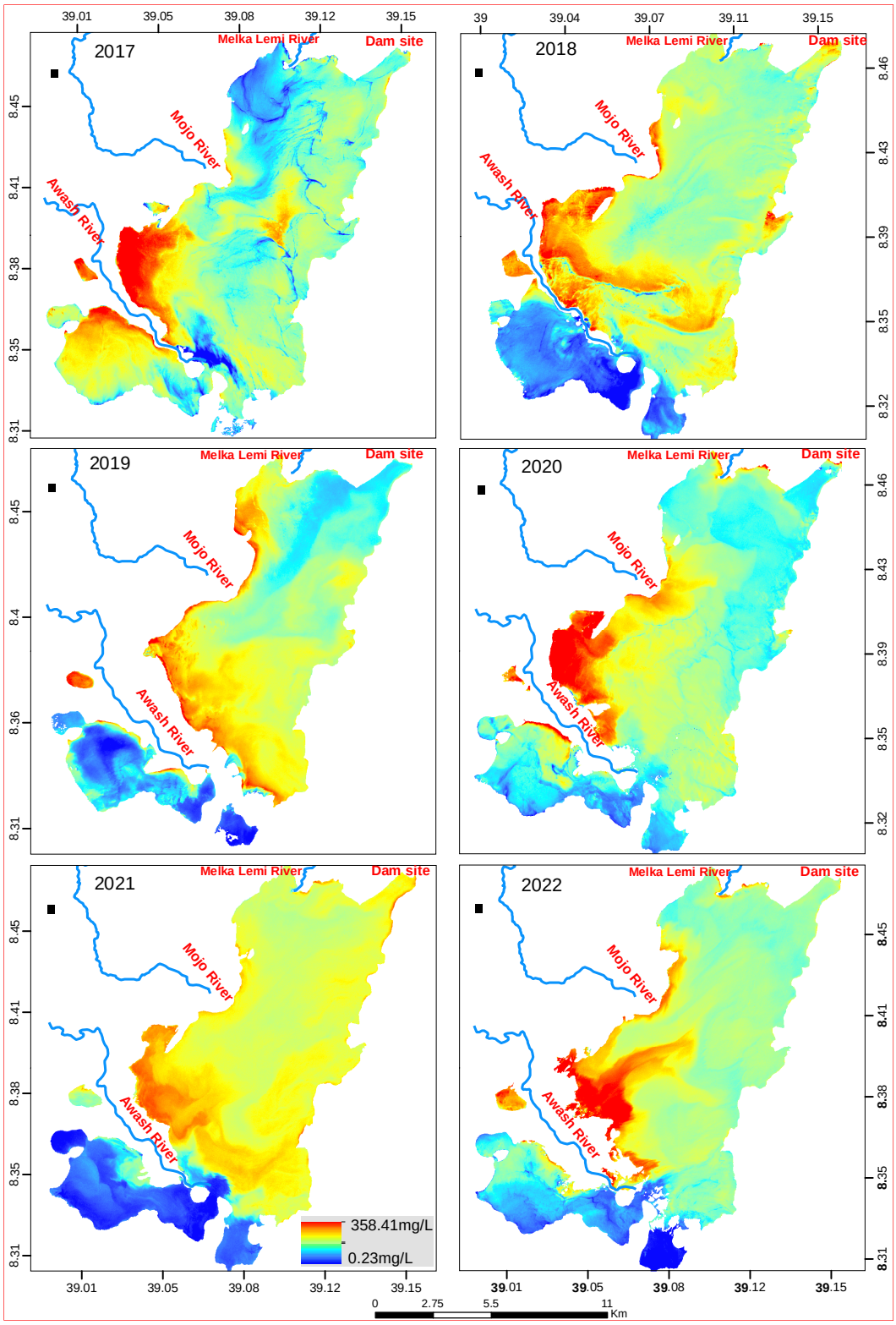

Figure 3-9 Map of TSS(mg/L) using linear regression models (2017-2022).

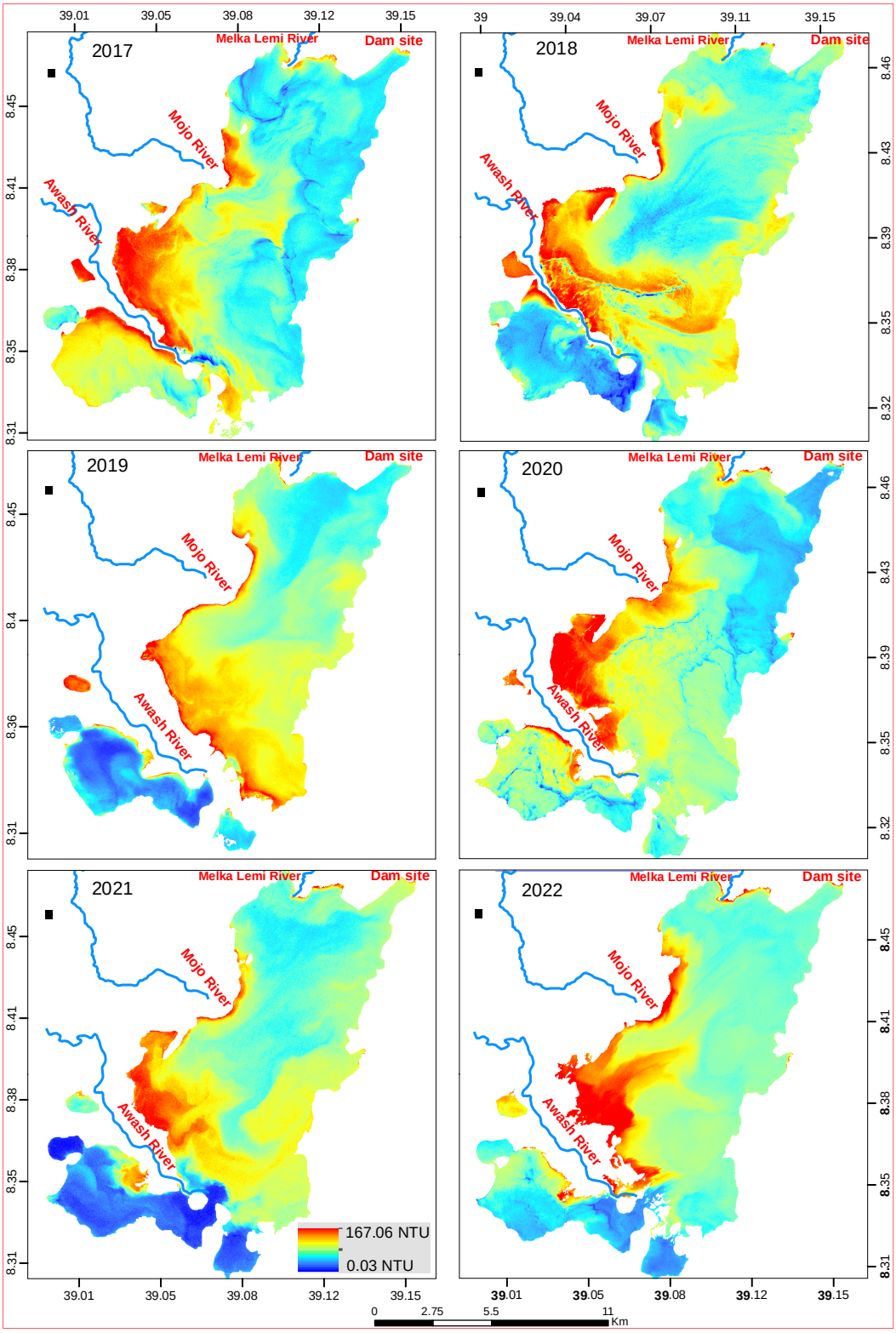

Figure 3-10 Map of TU (NTU) using linear regression models (2017-2022).

3.5 Discussion

In the absence of ground-based observations, reflectance data, and lack of handheld radiospectrometer at the reservoir in Koka, we have developed an indirect method of extracting and validating Chl-a, TU, and TSS satellite data. We used the reflectance and reflectance ratios at different wavelengths and compared the abridged set of in-situ data for Chl-a (µg/L), TU (NTU), and TSS (mg/L), which was obtained concurrently with the images (2017-2022 and June 2021, October-December 2021, January-May 2022). The best linear regressions for the calculation and mapping of Chl-a, TU, and TSS from Sentinel-2 imagery are discussed in sections 3.4.3 to 3.4.5.

Considering the performance of the extracted bands of Sentinel-2 and the developed water quality models, the specific spectral band of B4 (665 nm) provided the strongest correlations with both Chl-a, TU, and TSS. The findings of this investigation reveal that Sentinel-2 products can efficiently predict, quantify, and visualize temporal and spatial Chl-a, TU, and TSS trends in small water bodies. Furthermore, it was found that using interactions between optical and water quality parameters, the linear regression method can accurately predict Chl-a, TU, and TSS as developed equations (9-11).

For low biomass, oligotrophic to mesotrophic water bodies, the Chl-a spectrum is characterized by a sun-induced fluorescence peak around 680 nm (Dierssen et al., 2006; Gitelson et al., 1994). For high biomass, and eutrophic waterbodies, the fluorescence signal is masked by absorption features and backscatter peaks centered at 665 nm and 710 nm respectively (Gitelson et al., 1994). The ratio between these two wavelengths has been used to accurately estimate Chl-a concentration in numerous studies. The height of the reflectance peak between 700 and 720 nm has been used for estimating the Chl-a concentration in lake waters for more than two decades (Blaustein, 1992; Gower et al., 2005).

Among the many band-reflectance ratio algorithms that have been proposed for Chl-a estimation in lake waters, algorithms based on spectral band ratios (Table 3-3 (a)) are the more preferred because they help reduce the irradiance, atmospheric and air-water surface effects on reflectance (Ha et al., 2017; Ruddick et al., 2008; Schalles, 2006). In comparison to other studies, such as (Katlane et al., 2020) in Tunisia, the water-leaving radiance reflectance for the 705/665 nm band ratio (B5/B4) showed the best regression coefficient with the in-situ Chl-a data with an R2 value of 0.72. Similar results were reported by Matthews et al., (2010) and Liu et al., (2017), showing a good agreement between field and modelled Chl-a for the analysed sites with R2 values of 0.925 and 0.87, respectively. The regression validation indicated successful correlations with R2 of 0.9127 for Chl-a estimations. The results showed that the blue, green, red, vegetation red edge bands and band ratios yielded the best results with R2 greater than 0.8 for the estimation of Chl-a concentrations. In general, Chl-a concentrations rose in June with the start of algal bloom.

The distribution of Chl-a in a monthly analysis can be seen in Appendix D Figure 1. Smaller lakes were formed in June 2021, April and May 2022 due to lower river flow into the reservoir (the dry

season). The major portion of the formed lake had a low Chl-a concentration in June 2021. In April and May 2022, however, this reservoir's segment had a higher Chl-a concentration than the main reservoir waterbody. Except for the shore areas (in May 2021) and south-western section of the reservoir (June 2021), nearly every region of the reservoir had a large coverage of Chl-a distribution in November and December 2021 and April and May 2022. The reservoir's western, south-western, and southern portions had the largest coverage of higher concentration of Chl-a in November and December 2021. From January to March 2022, the south and south western parts of the reservoir had a larger area coverage of Chl-a than the rest of the reservoir., peaked in November, and then dropped in February. It showed decreases from November to February. In addition, Chl-a showed a decreasing trend from March to May. Chl-a concentrations ranged from 0.07 µg/L in January to 354.64 µg/L in November. January had the minimum lowest concentration (0.07 µg/L) of Chl-a, which was followed by March (0.35 µg/L). Appendix D Figure 1 shows that the mean highest and lowest concentrations followed a similar pattern. The highest maximum, minimum, and mean turbidity were recorded in June 2021, at the start of the rainy season, and in May 2022, at the middle of the “Belg” season.

The Koka Reservoir was reported to have hazardous concentrations of toxic cyanobacteria (Willén, 2011). Lake water quality issues related to algal blooms are a serious problem in basins with abundant agricultural land, causing harmful effects on freshwater ecosystems such as taste and odor issues in drinking water, oxygen depletion causing fish kills, and water exceeding safe drinking water standards (Ambrose-igho, 2020). In addition to this, water hyacinth (Eichhornia crassipes) invasion and harmful toxic algal occurrence owing to eutrophication caused by anthropogenic factors have been observed in the Koka reservoir (Assegide et al., 2022).

Clear water has low reflectance in the visible spectrum and has no reflection in NIR region, as this wavelength is absorbed by clear water. However, high reflectance measurements in red (600-700 nm) and NIR region (750-1400 nm) show a strong correlation with TSS concentrations (Cahyono et al., 2019). Organic-dominated systems derive their spectral signatures from algae concentrations and can share the pronounced absorption features and backscatter peaks described above for chlorophyll (Shi et al., 2013). As inorganic TSS concentrations increase within a waterbody, the location of the spectral maximum moves from around 550 nm into the red or near-infrared wavelengths (Doxaran et al., 2002) with waterbody specific variation dependent on chlorophyll and CDOM concentrations (Topp et al., 2020). This study confirms that sentinel 2 image red (B4), and green (B3) band ratio is suitable for the prediction of TU inland water bodies.

Caballero et al., (2018) predicted TSS for in the Guadalquivir estuary based on the band calculated from 664 nm (band 4) with R2 value of 0.70 as the model developed by this study. The reflectance in visible region specifically red region increases with increase in sediments in the water or turbidity, as also evidenced in (Garg et al., 2020).

In November to December 2021, January to March 2022, with the exception of the south and south-western parts of the reservoir, and the north-western part (June 2021), and the northern tip

(April 2022) TSS was spread more or less consistently in all areas of the reservoir, regardless of concentration value. TSS concentrations and distributions were lowest in the southern and south-western sections of the reservoir in November and December 2021, and from January to March 2022. In April and May 2022, the highest concentrations of TSS were found in the reservoir's western and central areas. TSS concentrations were highest in the western and south western parts of the reservoir in June 2021 and May 2022. The increasing concentration of TSS from February to April is related to the Belg rainfall which wash the exposed soil from agricultural lands from upstream watersheds as well as urban areas. Ethiopia is characterized by three distinct seasons. These are locally known as Bega (October to January), Belg (February to May) and Kiremt (June to September) (Zhao, 2020).

Soil erosion is very common in Ethiopia, and some of the lakes are affected by the consequences of sedimentation and increased turbidity (Assegide et al., 2022). In almost all the years studied, there was a high concentration of TSS in the reservoir's eastern area, which is where the Awash River enters the reservoir. The highest concentrations are attributed to the water inflow from the Awash and Mojo rivers (Figure 3-9 and Figure 3-10) at an area of low depth which leads to the agitation of the settled sediment. The higher degree of settling of sediment therefore leads to low turbidity in the reservoir.

With in-situ turbidity varying from 34 NTU to 168 NTU and averaging at 54.09 NTU, low turbidity could be attributed to low flows into the reservoir, especially during the period in which the water samples were collected. As the reservoir is relatively deeper in the outlet, the sediment tends to settle faster leading to generally low concentrations of particulate matter, with minimal potential for resuspension (Ouma et al., 2020) by water currents and waves. The higher degree of settling of sediments therefore leads to low turbidity in the reservoir however, the reservoir is shallow causing this scenario. In all of the years studied the spatial distribution of TU and TSS followed a remarkably similar pattern.

From July to October, it is difficult to get cloud-free satellite images to examine the circumstances and to compare dry and rainy season WQPs. Furthermore, acquiring steady and consistent RS Top of Atmosphere (TOA) reflectance for the purpose in all 5 days' interval satellite image is particularly difficult due to the shallowness of the reservoir, water turbulence, and water current. To overcome these limitations, further verification should be done using a drone or a handheld spectroradiometer instrument.

There are factors that influence the spatiotemporal WQPs in the reservoir. The Koka reservoir is one of the direct recipients of sedimentation increased turbidity and algal blooms (toxic cyanobacteria) (Tilahun et al., 2019), as well as excessive chemicals and fertilizers washed from the nearby farms, and disposed by industries (Zewde et al., 2018). For example, phosphates entering the water from detergents urban areas like Addis Ababa, Dukem, Mojo, and Debrezeit (Girma, 2016; Moges et al., 2016; Rooijen & Taddesse, 2009) can cause the nutrient levels in the water to rise and lead to algal blooms (Girma, 2016). Furthermore, the surrounding agricultural

land use has been a major source of nutrient input to the reservoir (Willén, 2011; Zewde et al., 2018). However, temporal shifts in water quality can be influenced by factors such as stream flow, which influences seasonal variability in the delivery of the constituent to the rivers and the reservoir, and rainfall and air temperature (Guo et al., 2019).

3.6 Conclusions

This study demonstrated that Sentinel-2 derived regression models can support the spatiotemporal estimation and mapping of the annual and monthly patterns of Chl-a, TU and TSS over the Koka reservoir. This enables improved capacity to diagnosis reservoir status and strategies for water resource management.

This research also confirmed the appropriateness of the linear function model for estimating WQ indicators, such as Chl-a, Turbidity, and TSS in shallow waters from the Sentinel-2 image band ratio of B5/B4, B4/B3 and band 4 (B4), respectively. In addition to this, it has tested the suitability of Sentinel-2 data for mapping reservoir water quality parameters (Chl-a, turbidity and TSS) by means of empirical models, which complement the traditional methods of WQ monitoring. This work will greatly expand the use of these procedures, not only by researchers but also by water management agencies and interested members of the public, with the long-term goal of improving societal knowledge and understanding of surface water resources and helping to improve data-driven resource management.

A unique water quality assessment method is here recommended, which breaks through the traditional water quality point sampling and analysis, taking advantage of remote sensing and open satellite datasets. The presented Sentinel-2-based method can directly associate the concentration level of Chl-a, TU, and TSS with the degree of progress to quantify the dynamic change process of Chl-a, TU, and TSS in multiple time series. The low operational cost of using freely available remotely sensed imagery is a strong incentive for water agencies to complement their field campaigns and produce spatially distributed maps of some water quality parameters. The algorithms could potentially be useful as a monitoring tool for water quality in other regions in the country or in other data-scarce areas of the world with comparable environmental and hydro climatic context.

Chapter 4 : PRIORITIZING WATERSHEDS FOR INTERVENTION DESIGN USING REMOTE SENSING AND GEOGRAPHIC INFORMATION SYSTEM.

Abstract

In many developing countries with poorly managed landscapes, soil erosion poses a threat to the sustainability of water bodies. Sedimentation severely affects the storage capacity, and turbidity threatens aquatic biodiversity in many of the water bodies in Ethiopia. Poor land use policy and resource management in the Upper Awash Sub-basin leads to soil erosion and sedimentation of hydrological infrastructure, particularly artificial reservoirs. The first step in planning watershed management for soil and water conservation undertakings is to prioritize watersheds based on their vulnerability to degradation, as it is not pragmatic to develop all the watersheds simultaneously due to logistical reasons. This research aims to prioritize the Upper Awash Sub-Basin by its morphometric, land use and cover (LULC), and sediment yield characteristics. The integrated AHP-VIKOR multi-attribute decision-making method was used to prioritize watersheds, incorporating morphometry, LULC, and sediment load attributes in the simple matrix approach. The findings showed the following classes of erosion: exceedingly high (2722.14 km2), high (2524.46 km2), moderate (2205.48 km2), low (1611.43 km2), and extremely low (854.35 km2). Sub-watersheds WS6, WS8, WS10, WS13, and WS24 are the top priorities for watershed management. This study prioritizes watersheds based on various attributes, but the lack of daily observed sediment data is its limitation. It can be concluded that decision-makers and planners may successfully combine GIS and RS approaches alongside multi-attribute decision-making (MCDM) tools like AHP-VIKOR with a risk assessment matrix to prioritize activities related to conserving water and soil.

Keywords: Morphometric Analysis, Soil Erosion, MCDM, VIKOR, AHP, SWAT

4.1 Introduction

Soil erosion and sediment-related challenges constitute a challenge for developing water resources and sustainable land management in many emerging nations (Morris & Fan, 1997). Problems with soil loss and sedimentation threaten the sustainability of land management and the development of water resources (Adhami & Sadeghi, 2016). Soil erosion is common in Ethiopia, and increased turbidity and sedimentation have an impact on some lakes (Assegide et al., 2023; Abhachire, 2014; Girma, 2016); soil erosion and sedimentation of hydrological infrastructure, especially artificial reservoirs used for power generation and water supply, as a result of the lack of a land use policy and poor resource management. In the Upper Awash Sub-basin, which has seen significant urbanization and deforestation, this is a common phenomenon (Argaw & Yohannes, 2024). Because of the increasing amounts of silt deposition, lakes in the country's highland areas also confront issues with surface area, volume, and water level (Getaneh et al., 2022). Both the anticipated advantages of the dams and the significant costs made in their construction are lost as a result of reservoirs that were intended to deliver irrigation water and rapid sedimentation. On agricultural land, soil erosion affects water quality, ruins drainage systems, and reduces crop yield potential (Assegide, Alamirew, Dile, et al., 2022). Even though watershed degradation is believed to be the cause of the fast storage loss of Ethiopia's water-harvesting scheme and the loss of vital nutrients, few studies have been done to measure erosion rates and comprehend the dynamics of erosion-siltation processes at the catchment scale in terms of space (Desta, 2005).

According to Hurni (1993), erosion in Ethiopia results in soil loss from cropland of 42 t/ha/y. However, the complexity and unpredictability of the related land characteristics, for example, landscape, LULC, soils, and climate, affect the link between yearly sediment yield and drainage area. This implies that if two catchments of comparable size have distinct geomorphologies and climatic conditions, their sediment yield may vary (Verstraeten et al., 2003). Depending on the local conditions and the geographical extent we are working with, the association between sediment yield and area may even alter between neighboring places if the associated erosion processes and environmental variables are different (Verstraeten et al., 2003). This indicates that before implementing practical connections discovered in other environmental conditions, it is necessary to evaluate the association between the catchment area and the measured area-specific sediment yield for local conditions (Boer & Crosby, 1996; Getaneh et al., 2022; Houser & Hamilton, 2009; Schiefer et al., 2001). The drainage pattern and runoff time necessary for a micro-watershed to focus at the outlet are controlled by the watershed's shape, which also influences the rate at which soil erosion and sediment generation occur (Rymbai, 2012).

Because of soil erosion and sedimentation problems, the watersheds' ability to store water is reduced, dams and reservoirs are harmed, and surface waters are polluted (Tuppad et al., 2017). Consequently, sustaining and increasing resource production requires excellent planning and management of watersheds, especially making the best use of land in high-risk locations. The development, exploitation, and management of water and land resources are crucial for the future generation's food security and population growth. It has previously been shown that this approach of all-encompassing watershed management heavily relies on watershed-based soil and water conservation techniques (Biswas et al., 1999). SWC, if properly designed and carried out, had multiple positive effects on the environment and socio-economic system, in addition to lowering

runoff and soil erosion, which is the main objective of tangible conservation measures (Degfe et al., 2023).

Ethiopia's highlands are some of Africa's most degraded regions (Shawul & Chakma, 2019a). Ethiopia is experiencing alarming LULC changes, primarily driven by cultivation, leading to soil erosion and a decline in forests and grasslands (Bekele, 2019). LULC in Ethiopia has changed significantly in the last 5 decades due to the higher population growth rate and socioeconomic fluxes. The changes in population growth, overgrazing, and agricultural expansion in the highland areas have caused a drastic increase in the rate of LULC changes. LULC change causes significant impacts on water resources by causing alterations in the hydrological cycle (Shawul & Chakma, 2019a). The LULC change detection study in upper Awash revealed declining trends in pasture, woodlands, and shrubland coverage and a notable increase in cropland and urban areas, along with a higher conversion rate from shrubland to cropland. Urban area and farmland increased by 606.2% and 47.3%, respectively, between 1972 and 2014; in contrast, forests, pasture, shrubland, and water experienced declines of around 25%, 87%, and 29%, respectively. Many researchers have investigated the impact of LULC change on sediment yield dynamics in the Upper Awash. For example, according to Bihonegn (2019), streamflow, surface runoff, and sediment output increased by 4.55%, 12.68%, and 8.84%, respectively, due to the rapid change of LULC from 2000 to 2015.

The Upper Awash Sub-basin is one of the most densely populated and urbanized parts of the country where the most populous cities, such as Addis Ababa and Adama, are located (Shawul & Chakma, 2019a). If proper land use planning is not followed, the notable development in built-up regions and unplanned human settlements may increase the danger of environmental impairments (Dewan & Yamaguchi, 2009). Higher urban sprawl is primarily brought about by the rapid rate of population growth, economic expansion, and accessibility to resources and essential infrastructure (Wilson et al., 2003). In addition to this, a high rate of soil erosion and a decline in the amount of arable land available are the results of a growing population (Bekele, 2019).

According to a study by Mitiku (Mitiku et al., 2023) the upper Awash Sub-basin's hydrological response to environmental and climate change has been impacted by increased annual and wet season river flows, with land use changes potentially leading to flooding. The results indicate that the annual and wet season monthly river flows increased by up to 77.5% and 100.5%, respectively, as a result of climate change. On the other hand, the change in land use affects river flow in a percentile increment or decrease of one.

Problems with soil erosion and water scarcity in the upper Awash Basin harm livelihoods and productivity. Even though some SWC interventions have been put into place in the region, it is unclear how beneficial these initiatives are, and their impact is not extensively documented. Many smallholder farmers who depend on agriculture for their livelihoods live in this basin (Moges et al., 2024).

Current land treatment procedures may not be feasible for large watersheds, making it difficult to manage the entire basin in a watershed management program (Kumar & Ramaraj, 2021). Since reducing the effects of natural disasters, management of all natural resources, including land and water, is essential to attaining sustainable development (Ranjan et al., 2013). Sub-watershed units

are prioritised based on the degree of denudation caused by soil erosion and the criticality of drainage areas (Pandey et al., 2007). Thus, the integration of spatial analysis and satellite image approaches demonstrated a well-organized means that many researchers have successfully employed for studies on watershed management and development, along with the characterization and prioritizing of watersheds (Beven et al., 1988).

A watershed's prone areas can be identified and ranked in order of priority for mitigation measures using a variety of methodologies, including morphometric analysis, multi-criteria decision analysis, field surveys, and expert assessment (Duressa et al., 2024; Okoli et al., 2023). Every approach has advantages and disadvantages. A field survey is a very precise method, but it has limitations since collecting the required data takes a lot of expense and effort (Saha et al., 2019). Based on familiarity with and knowledge of the area, an expert view is an effective method for determining the locations affected by soil erosion. However, it's critical to remember that the output quality may suffer from insufficient data and competent specialists (Sahour et al., 2021). A more straightforward and affordable approach is morphometric analysis, which results in reliable findings (Duressa et al., 2024).

Rather than relying on watershed morphometry analysis, a more comprehensive approach that includes LULC and sediment load estimation is needed to characterize and prioritize sub-watersheds (Abdeta et al., 2020). Additionally, the prioritising approach permits the addition of LULC as a component to the morphometric parameters that may be introduced and that can have both direct and inverse impacts on the potential for erosion risk (Meshram & Sharma, 2017; Javed et al., 2009; Suji et al., 2015; Shekar & Mathew, 2022). Ranking criteria may include morphometric variables, LULC, the average yearly soil loss, and other pertinent variables. To characterize and prioritize watersheds based on morphometric properties, LULC, and the degree of erosion or a load of sediment, remote sensing and GIS are essential (Dabral et al., 2008).

An appropriate approach is required to integrate different parameters of multi-attributes for sub-watershed prioritization. The widely used multi-attribute decision-making (MADM) model, known as the Vlse Kriterijumska Optimizacija Kompromisno Resenje (VIKOR), was first proposed by Opricovic (2004) and stressed the ranking and selection of numerous competing sets of criteria (J. J. Huang et al., 2009). Rather than delivering an ideal answer for a problem, the VIKOR technique finds a compromise solution for the conflicting attributes among numerous options (Opricovic & Tzeng, 2004). The VIKOR model is more accurate for prioritizing sub-watersheds, according to (Ameri et al., 2018; Kang & Park, 2014). Due to this and the measure of ‘closeness to the ideal, it was selected and implemented for this research work.

It is crucial to evaluate the amount of soil lost due to water erosion and its geographical distribution to successfully implement land and water conservation practices. In several regions of the world like the Pohru Watershed of the Jhelum Basin (Northwestern Himalayas) (Mir & Ahmed, 2021), the Nagwan watershed, the Upper Damoder Valley Corporation (India) (Tripathi et al., 2003), the Banha watershed (India) (Mishra et al., 2007), the Ribb watershed (Ethiopia) (Admas et al., 2022), and Finchaa Catchment (Ethiopia) (Dibaba et al., 2021), SWAT has been used to analyze soil loss due to water erosion for watershed prioritizing purposes (Mir & Ahmed, 2021). The study also takes this research as a reference to implement the SWAT model.

The soil erosion in the upper catchments of the Awash River is one of the non-point pollution sources concerning agriculture. Water body and wetland pollution in the area are related to the erosion process. On crops, soil erosion lowers the yield potential, lowers the quality of the surface water, and damages the drainage network (Issaka & Ashraf, 2017). Diffused pollutants and chemicals are also transported with soil particles, leading to increased sedimentation, eutrophication of the water, and tampering with fragile aquatic habitats (Assegide et al., 2022). In addition to the previously noted issues, a watershed priority research project has never been done in the study area. Therefore, to identify hotspots of soil erosion in watersheds and rank sub-watersheds according to their LULC, sediment yield, and morphometric characteristics of several drainage parameters for intervention design, the main objective of this research is to apply GIS and RS techniques in conjunction with multi-criteria decision-making (MCDM) like the AHP-VIKOR and SWAT model.

4.2 Study area

One of Ethiopia's twelve major basins, the upper part of the Awash River Basin is the Upper Awash River Basin., which has an area of 9918.1 km^2. The upper Awash Sub-basin is situated between longitudes 37° 57'E and 39° 17'E and latitudes 8° 17'N and 9° 18'N (Takele & Kebede, 2018). The Omo Gibe and Rift Valley Lake Basins share the basin's western and southwest borders. The Abbay Basin to the north and the Wabi Shebele Basin to the southeast. The river begins in a location known as Elam near Ginchi town, south of Mount Warqe, at an elevation of 3000 meters above mean sea level (amsl). It then ascends to Koka Reservoir, located at an elevation of 1559.1 meters amsl. Its altitude variation range is between 1,591.1 and 3539.5 amsl. The Upper Awash River is a meandering river that flows for over 200 kilometers before entering Koka Reservoir (Figure 4-1) (Mekonnen et al., 2023). Holeta, Alito, Teji, Gilo and Kelina, Kebena, Akaki, and Mojo are some of the river's principal tributaries. Upper Awash is home to significant agricultural farms, high vegetable production, and animal husbandry activities, primarily found in Addis Ababa, Adama, and Bishoftu (Assegide et al., 2022).

This area is near the western escarpment of the major Ethiopian rift in the Ethiopian Highlands. This sub-basin is home to the significant Palaeolithic site Melka Kunture, which is well-known for its abundance of early hominid remains. The oldest documented use of obsidian, which comes from many outcrops surrounding the location, is Melka Kunture. The area is characterized by its flat plateau terrain, with slopes primarily reaching 10° (High- et al., 2016). The Awash River drains the research region to the east and southeast. The river flows into a canyon, Knick Point (a waterfall), because of head-ward erosion occurring in the rift valley at a base level. Tectonic activity associated with rifting, including explosive volcanism, erosion, and sedimentation, was responsible for the creation of the terrain (Salvini et al., 2012). Scarps that are visible display layers of ignimbrites and extensive lava flows. That area is characterized by a structural rift pattern, or graben and horst structure, which runs parallel to the semi-graben fault system (Gallotti, 2013). The surrounding area of Melka Kunture has morphological evidence of the tectonic structure (Raynal & Kieffer, 2004).

The study area has a humid to sub-humid climate in the highlands and a semiarid environment in the lowlands, with an average annual temperature of 15-20 ◦C. The mean annual precipitation,

strongly controlled by elevation, varies from 800 to 1400 mm. In Ethiopia, the primary wet season, Kiremt, typically occurs between June and September. It is followed by "Belg," which occurs from March to May (Tolera et al., 2018).

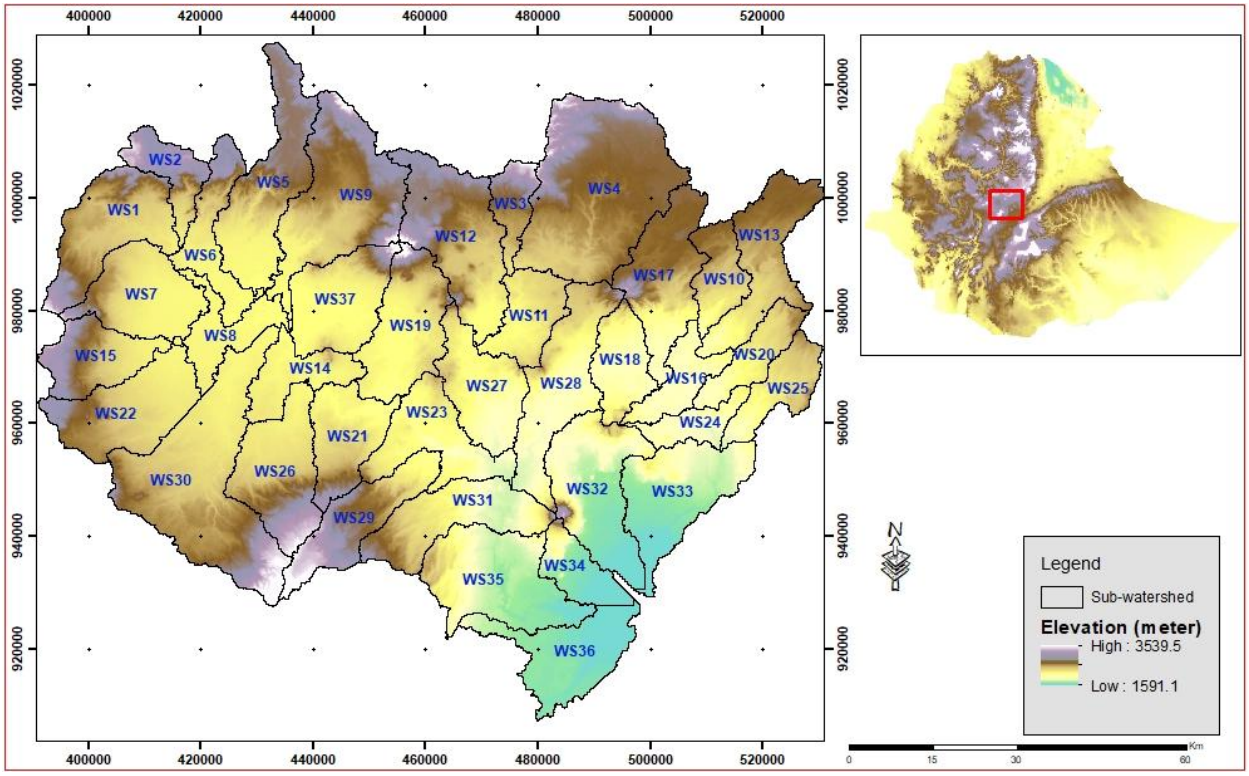

Figure 4-1 Study area, Upper Awash sub-basin

4.3 Data and Method

4.3.1 Input data

Different input data were used for this sub-watershed prioritization LULC *is* one of the features used for watershed prioritization. The major LULC is cropland followed by shrubland

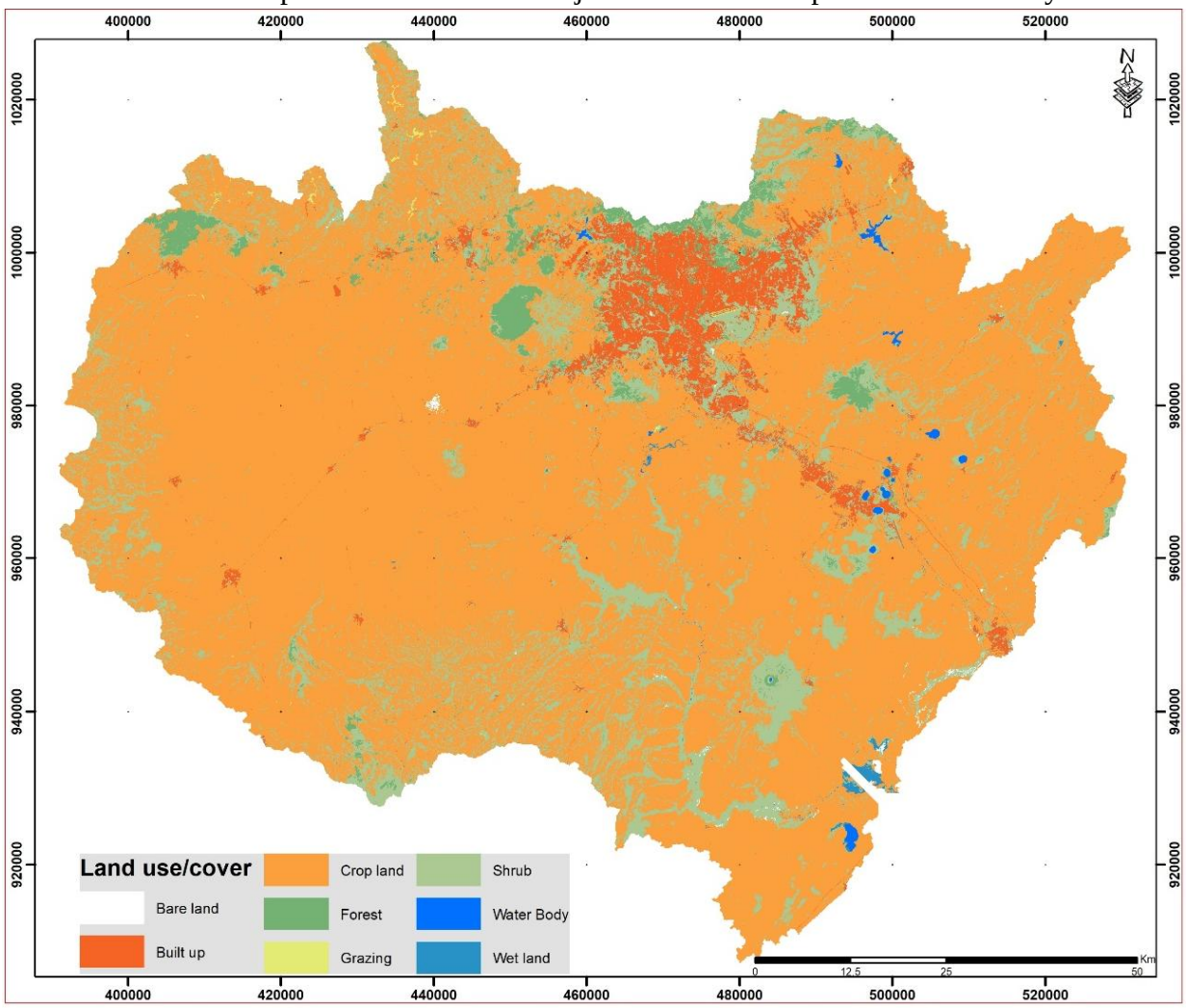

Figure *4-2*.

Table 4-1. The strength of calibration is judged relative to these benchmark values. Data on daily river flows were used to validate and calibrate the model (Takele & Kebede, 2018). Sediment calibration and validation were conducted using monthly sediment data. It could be necessary to use different datasets to assess the SWAT model's performance in different environmental scenarios (Moriasi et al., 2007). However, site-to-site variations may exist in the quantity of attributes and duration of observation needed for a suitable assessment of the driving processes of the watershed. There is a dearth of reliable, long-term data on the Ethiopian highlands. The full simulation period in this work is restricted to field observation data from 2002 to 2018 (validation) and 1979 to 2001 (calibration). To reduce the impact of non-equilibrium beginning circumstances, a five-year warm-up time was used for the split-sample calibration and validation (Veltman et al., 2018).

LULC is one of the features used for watershed prioritization. The major LULC is cropland followed by shrubland

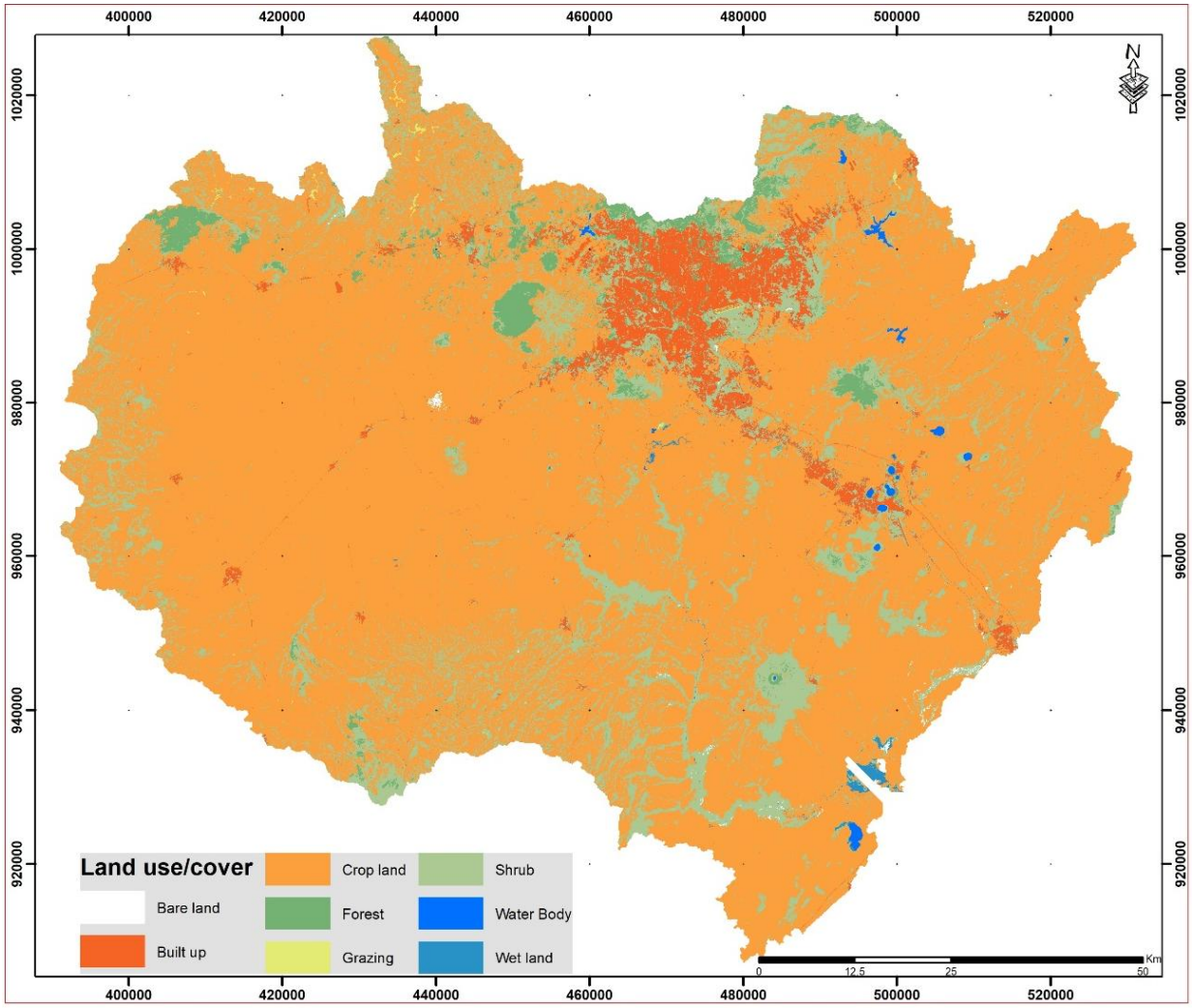

Figure *4-2*.

Table 4-1 Input data for the SWAT model and their sources

Data	Resolution/ period	Source
Digital elevation model	30 meters	http://earthexplorer.usgs.gov/ accessed on 31 October 2021
Land cover	10-meters (2023)	https://earthexplorer.usgs.gov/ accessed on 17 February 2023 https://scihub.copernicus.eu/ accessed on 16 February 2023
Soil map	1:250000	Water and Land Resource Center
Climate	Rainfall, temperature	National meteorological agency
	wind speed, relative humidity, and solar radiation	https://climatedataguide.ucar.edu/climate-data accessed on 18 July 2023
Stream flow data	Observed daily	Ministry of Water and Energy
Sediment	Observed monthly	Ministry of Water and Energy

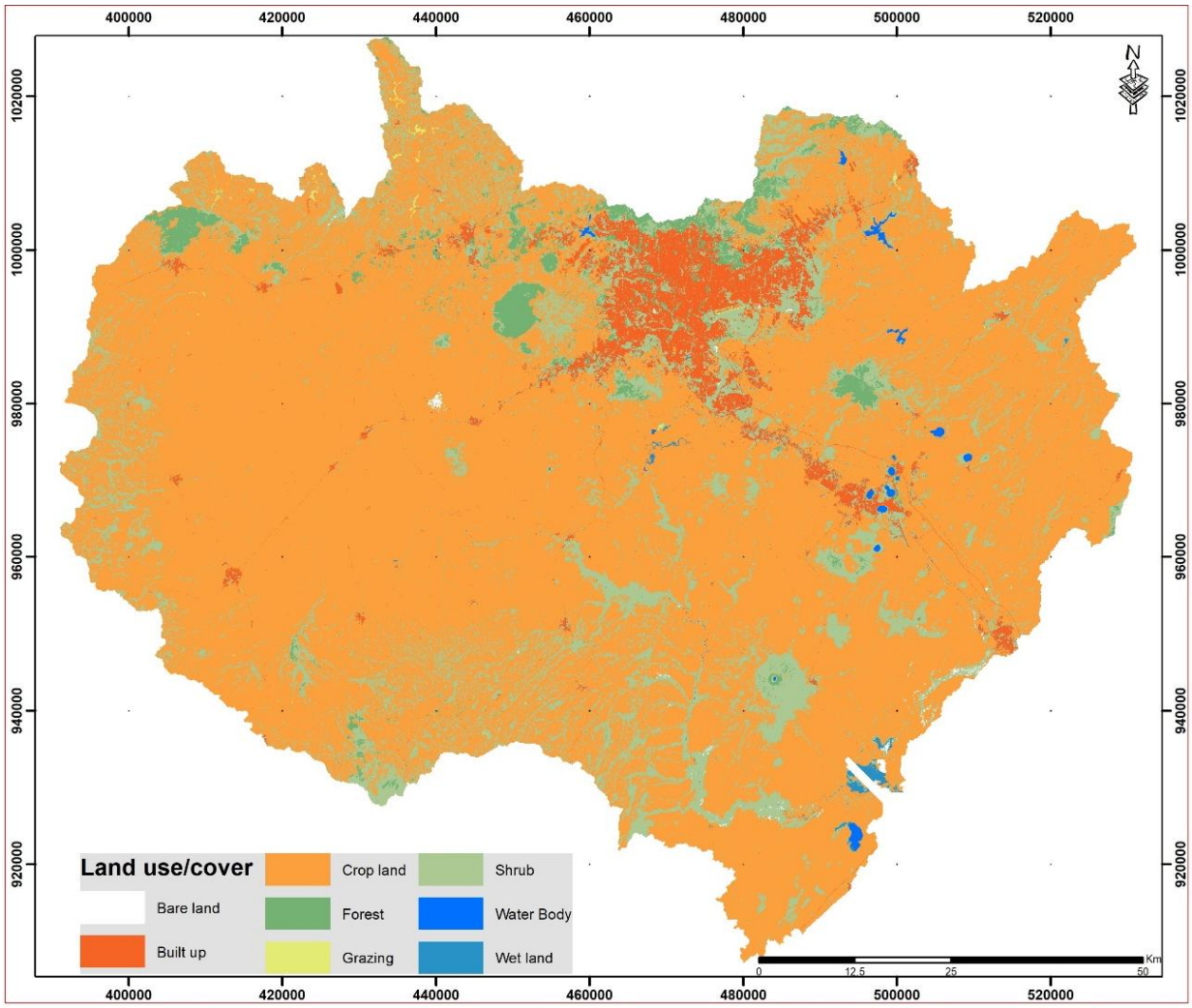

Figure 4-2 Map of land use and cover in the research area

Different soil physicochemical and textural characteristics, such as bulk density, organic carbon content, hydraulic conductivity, and soil texture for various soil types' layers, are needed for the SWAT hydrological model. This has been prepared and incorporated in the SWAT database for further analysis in the SWAT model. The dominant soil type in the study site is pellic vertisols (*Figure 4-3*).

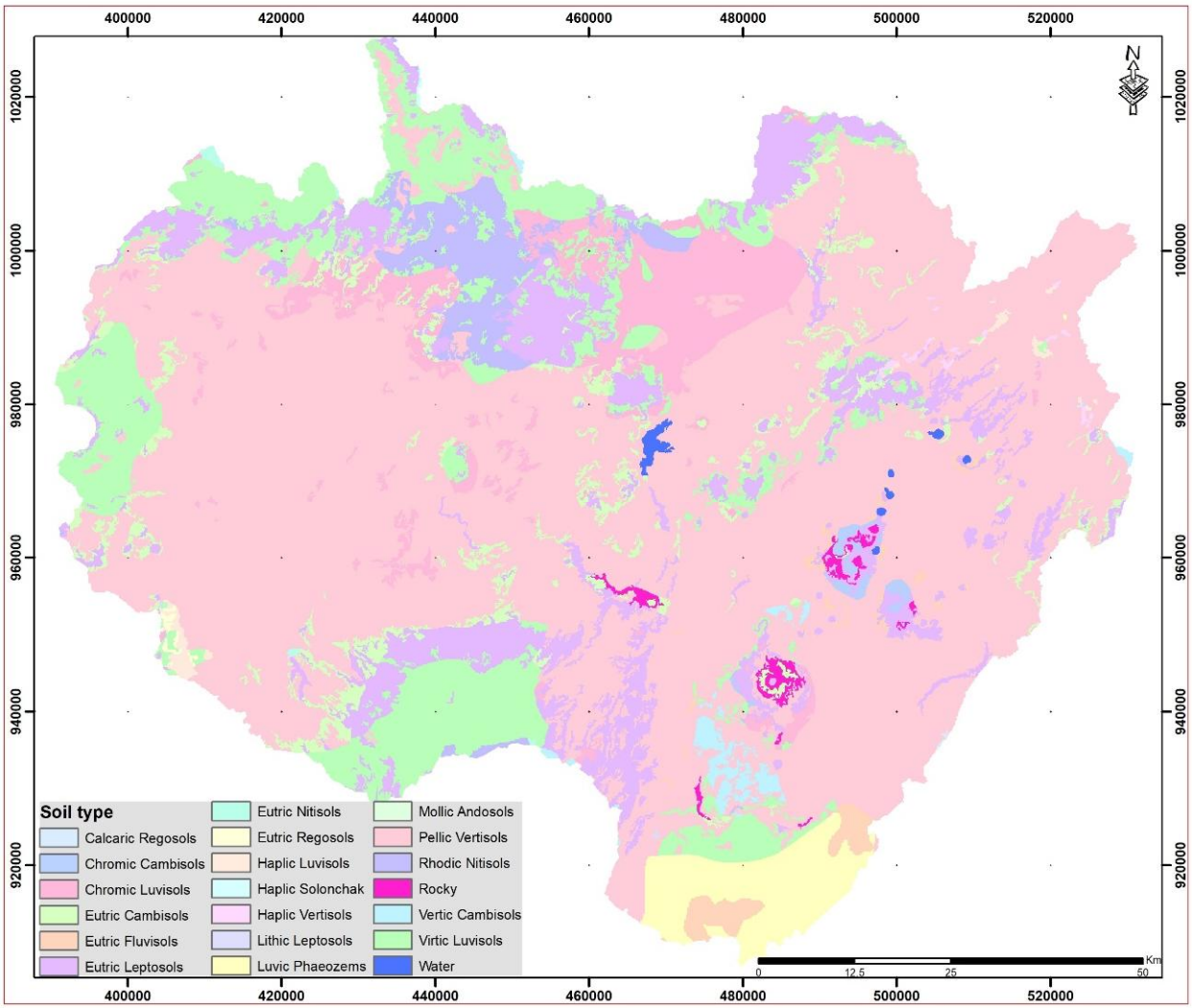

Figure 4-3 The research area soil map

4.3.2 Watershed Delineation and Morphometric Analysis

The sub-watershed ranking is the process of breaking down an entire watershed under investigation into smaller watershed units and assigning a score to each one based on priority for treatment (Ali & Ikbal, 2015). In ArcGIS software, the minimum area choice for sub-watersheds was set to 80 km^2 for watershed delineation. The Upper Awash sub-basin comprises 37 sub-watersheds, from SW01 to SW37. The SW24 and SW04 sub-watersheds, which are the smallest and largest, respectively measure 98.35 and 681.71 km^2. The sub-watershed threshold area's average value is about 2.7% of the sub-basin total area. No detailed investigation and comparison were done to set the threshold value of sub-watershed delineation in this research. The basis for choosing watershed delineation thresholds was based on other research works. Streamflow is not significantly affected by increasing the number of sub-watersheds. This is because the surface runoff is directly related to the CN, and CN is not markedly affected by the size of the sub-

watersheds (Jha et al., 2004). Nevertheless, different study projects have varying threshold values for the size of the watershed area concerning soil erosion. Arabi (2006) proposed an optimal watershed subdivision level for representation of the best management practices, corresponding to 2% of the total watershed areas and an average sub-watershed area of approximately 4%. Lin (B. Lin et al., 2020) reported that the average sub-watershed area was approximately 1.6% of the entire watershed. For instance, the watershed area threshold proposed by Jha (2004) indicates ranging between 2% and 6% of the total drainage area with a median value of 3%.

Three categories -linear, areal, and relief- generally comprise the morphometric characteristics. "Stream order, number of streams, length, bifurcation ratio, drainage texture, relief ratio, drainage density, frequency, basin shape, form factor, circularity ratio, elongation ratio, and length of overland flow" are among the subcategories. Based on the stream hierarchy presented by Farhan (2015) and Rahaman (2015). The morphometric evaluation of drainage basins begins with the identification of stream order. The morphometric characterization of the designated sub-watersheds was computed using the method illustrated (Table 4-2).

Table 4-2 Algorithms used to calculate morphometric parameters and descriptions of parameters

	Parameters	Algorisms /Definition	Source
Shape aspects	Watershed area (A)	Area within a watershed boundary (km^2)	(Strahler, 1973)
	Perimeter (P)	The perimeter of the watershed (km)	(Horton, 1945)
	Basin length (L*b*)	Length of the stream (km)	(Horton, 1945)
	Form factor (Rf)	Rf = A/Lb, where A = area of the basin (km^2) Lb^2 = square of the basin length	(Horton, 1945)
	Elongation ratio (Re)	Re =1. 128 A L e b = , where, A = area of the basin (km^2) Lb = basin length	(Schumm, 1956)
	Circularity ratio (Rc)	$Rc = 4 \times \pi \times A/P^2$ where, π= 3.14 A = area of the basin (km^2) P = perimeter (km)	(Patton & Baker, 1976)
Linear aspects	Mean stream length (L*sm*)	Lu/Nu (km) = Lsm, where Lsm is the mean stream length and Lu is the total length of each order's stream. Nu = total number of segments in the stream of order "u"	(Schumm, 1956)
	Stream order (U)	Hierarchical rank	(Strahler, 1957)
	Stream length ratio (R*L*)	RL is equal to Lu/Lu-1, and Lu-1 is the whole stream length of its next lower-order	(Horton, 1945)
	Bifurcation ratio (R*b*)	Rb=Nu/Nu+1, where Nu+1 is the number of segments of the next higher order	(Schumm, 1956)
	Mean bifurcation ratio (R*bm*)	Rbm is the average of all orders' bifurcation ratios.	(Strahler, 1957)
	Drainage density (D*d*)	Dd is the ratio of the total stream length of all orders (km) with the area of the watershed (km^2)	(Horton, 1945)
	Stream frequency (Fs)	Fs is the ratio of the total number of streams across all orders with the basin's area (km^2)	(Horton, 1932)

	Drainage texture (Dt)	Dt is the ratio of the total number of stream segments of order "u" with a perimeter of the watershed (km)	(Smith, 1950)
Relief aspect	Relief ratio (Rr)	Rr is H/L*b*, where, H is the total relief, L*b* is the basin length	(Schumm, 1963)
	Basin relief (Bh) or Total relief (H)	Bh = h – h_1, where, h = maximum height (m) h_1 = minimum height (m)	(Schumm, 1956)
	Dissection index (Dis)	Dis = Bh/Ra, where, Ra = absolute relief Bh = basin relief	(Mishra, et al., 2017)
	Ruggedness number (Rn)	Rn = Dd*(Bh/1000), where, Bh = basin relief, Dd = drainage density	(Patton & Baker, 1976)

4.3.3 Land use land cover (LULC) analysis

LULC variations were mapped using the supervised classification method. Primarily, layer stacking and image subsetting using the study area boundary were made for Sentinel 2A image bands with 10 m spatial resolution satellite imagery. Secondly, before the image classification, the LULC categories were decided from previous knowledge and field observation experiences as well as the visual inspection of the image. Then typical training areas for each LULC class were selected from homogeneous pixels of the satellite imagery. Finally, the maximum likelihood classification was implemented using the area of interest, and their areas were estimated. The 2023 LULC data was used as one factor to prioritize the sub-watersheds.

4.3.4 Sediment load analysis using SWAT Model

The Soil and Water Assessment Tool (SWAT) is a continuous time, semi-distributed, basin-scale model developed for the USDA's Agricultural Research Service (ARS). The model was used to analyze the sediment load for sub-watershed priority (Adu & Kumarasamy, 2018); to evaluate and forecast the flow of water and sediment in large, ungagged basins; and to assess the impacts of agricultural output on water, sediment, and agricultural chemical yields. It successfully enables the execution of long-term simulations (Ganasri, 2015; Santhi et al., 2001; Yang & Wang, 2010).

For conservation planning in a watershed, modelling, and mapping of soil loss as well as risk assessment are crucial. The sub-watersheds are prioritized using how much soil loss occurs in each catchment. An empirical model MUSLE is used to determine annual upland soil erosion (Renard et al., 1997). Five parameters are included in the MUSLE (Modified Universal Soil Loss Equation) that relate to rainfall, soil, landscape, LULC, and conservation efforts. SWAT integrates MUSLE with temporal elements of climate, base flow, and direct runoff to estimate sediment loading into streams (Arnold et al., 2012).

MUSLE is a model that determines the maximum amount of sediment that can be routed in a reach based on peak channel velocity.

$$Sed_i = 11.8\ (Q_{surf} * q_{peak} * A_{hru})^{0.56} * K_{USLE} * C_{USLE} * P_{USLE} * LS_{USLE} * CFGR$$

The ArcGIS 5.1 extension, the graphical user interface for SWAT, and ArcSWAT version 10.21.10_5.24, released on August 19, 20, were used to develop the model setup. The stream

definition was determined using the threshold area option, which specifies the minimum area of a sub-watershed, which was set at 8000 ha. To verify the comparability of observed and simulated data, one catchment outlet was manually inserted at this point to calibrate and validate flow and sediment data. Second, multiple HRUs were determined by applying a threshold of 20-10-20 (Winchell et al., 2018) for the LULC, soil, and slope as the most suitable standard to ascertain the quantity and kind of HRUs in every sub-watershed. The HRU definition was based on the user-defined minimum percentage requirement determined by the user for each category. Thirdly, meteorological data was added to create data tables and an integrated database required for model setup and to mimic soil, weather, plant cover, management chores, and urban activities. Lastly, the start and end dates for the SWAT set-up from January 1979 to December 2019 were determined.

Sequential Uncertainty Fitting Version 2 (SUFI-2) is an automated system that assesses the sensitivity and uncertainty analysis, parameterization, and calibration and validation of the hydrological parameters. The computational speed of this algorithm is very high. According to earlier tests, it performs better than the other algorithms in assessing uncertainty (Mekonnen et al., 2023; High et al., 2016; Salvini et al., 2012). In this study, the SUFI-2 algorithm was utilized to evaluate the sensitivity of the model inputs (Gholami et al., 2016), before calibration as shown in the supplementary material Table S1.

The P-factor in SUFI-2, which indicates the percentage of observations, runs from 0 to 100% in the calibration and validation, while the r-factor, which shows the thickness of the 95PPU, ranges from 0 to infinity (Abbaspour, 2012). A simulation that exactly matches observed data has a p-factor of 1 and an r-factor of zero (Abbaspour et al., 2007), with a desirable r-factor value of less than 1 (Abbaspour, 2012). The strength of calibration is judged relative to these benchmark values. The model calibration and validation were conducted using daily river flow data (Takele & Kebede, 2018). Monthly sediment data was utilized for calibration and validation purposes. Firstly, the hydrological component was calibrated, and then the sediment component (Im et al., 2007).

4.3.5 VIKOR method

The decision support system presented in this study employs the VIKOR technique, which tries to collect data on all information about several qualities and criteria (Sasanka & Ravindra, 2015). The VIKOR approach is applied as it makes it possible to choose extremely effective and efficient criteria when deciding how to proceed when there are multiple attributes and different criteria (Sasanka & Ravindra, 2015; C. Wang & Pang, 2011; Xue et al., 2016). As the name indicates, the analytic hierarchy process (AHP) begins with the multi-attribute decision-making issue being broken down into a hierarchy mode. From there, weights are found by mathematical calculations (Pant et al., 2022). Pair-wise comparisons are the basis of AHP, while Saaty (1977) provides its specifics.

Using the specified weights, VIKOR computes the compromise ranking list, compromise solution, and weight stability intervals for preference stability. When there are competing criteria, this strategy focuses on ranking and choosing from a group of choices. It presents the multi-criteria ranking index, which considers the relative importance of the distance to the ideal (J. J. Huang et

al., 2009; Suh et al., 2019; Topno et al., 2022), and is determined by a specific metric for "closeness" to the "ideal" response (Opricovic & Tzeng, 2004).

In the VIKOR approach, the steps below can be used to define options for rating (J. J. Huang et al., 2009):

1. Choosing the best decision among several options (Decision matrix):

$$D = \begin{bmatrix} a_{11} & a_{12} & \dots & a_{1n} \\ a_{21} & a_{22} & \dots & a_{2n} \\ . & . & & . \\ . & . & & . \\ a_{m1} & a_{m2} & \dots & a_{mn} \end{bmatrix}$$

2. The linear approach to calculate the normalized decision matrix Eq. (1):

$$n_{ij} = \frac{x_{ij}}{\sqrt{\sum_{i=1}^{m} {x_{ij}}^2}} \quad (1)$$

   Where n_{ij} is the element of the normalized matrix and a *ij* is i^{th} alternative in j^{th} criteria.
3. Calculating the criteria's weight. The advantage of the VIKOR framework is that raw data can be used in addition to the elimination of the need for expert assessment of all criteria. The AHP approach was utilized in this study to determine the weight assigned to each criterion (Ren et al., 2015).

The comparisons of two options pairwise using the given criteria can be used to create these weights. According to the specific criterion, the decision-maker evaluates the preference as weak, strong, very weak, or very strong (Saaty, 1987; Saaty & Vargas, 1987). As a result, it may be misleading to rank watersheds using a compound parameter. In this study, the weights of each morphometric parameter were determined using the AHP approach. AHP includes creating a matrix objectively and comparing each probable match. The elicitation of pairwise comparison judgments was the second step. Pairwise comparisons carried out at the fundamental scale shown in Table 4-3 utilize the procedure outlined by Saaty (1990), which provides the scale to be applied in the assessments. The effectiveness of this scale has been attested by many users in numerous applications and theoretical comparisons with a vast array of other scales (Saaty, 1990). Finally, ArcGIS was used to perform the spatial distribution of erodibility prioritizing sub-watersheds by the VIKTOR technique using morphometric characteristics.

4. Computation of a weighted normalized matrix by multiplying the normal matrix by the weight of each criterion as Eq. (2)

$$V_{ij} = n_{ij} \times w_j \quad (2)$$

   where V_{ij} is the weighted normalized decision matrix element, R_{ij} is a normalized decision matrix element, and w_j is the weight of criteria calculated using the AHP model.

Table 4-3 The basic AHP rating used for pairwise comparison assessment. Source: (Saaty, 1990)

Level of significance	Meaning	Description

1	*Equally significant*	*Each of the two activities contributes equally to the goal.*
3	*Moderately significant of one over another*	*One activity is moderately preferred over another by experience and judgment.*
5	*Strongly significant*	*Judgment and experience strongly preferred one activity over another*
7	*Very strong significant*	*Activity is highly encouraged, and its superiority is shown practically*
9	*Extreme significant*	*The strongest level of affirmation is seen in the data that supports a particular action over another.*
2, 4, 6,8	*Values in the middle of the two adjacent judgments*	*While finding the middle ground is required*

5. Find the top (Vj^*) and the lowest (Vj^-) value: then $Vj^+ = \max V_{ij}$ and $V_J{}^- = \min V_{ij}$. The top value (Vj^*) and the lowest value (Vj^-) are determined by picking the min and max values calculated by Eq. (2) above. The best value (Vj^*) is the calculated max and the worst value (Vj^-) is the calculated min value.
6. Using Equations (3) and (4), respectively, to calculate the values of Si (Utility Index) and Ri (Regret Index):

$$S_i = L_{1,i} = \sum_{i=1}^{n} W_j \left(V_j^* - V_{ij}\right) / \left(V_j^* - V_j^-\right) \quad (3)$$

$$R_i = L_{\infty,i} = \max \left[\sum_{i=1}^{n} W_j \left(V_j^* - V_{ij}\right) / \left(V_j^* - V_j^-\right) \right] \quad (4)$$

Where, $V_j{}^* = \max V_{ij}$ and $V_j{}^- = \min V_{ij}$ for maximizing criteria, and W_j is the weight of the criterion j.

7. Computing the values Q by Eq. (5)

$$Q_i = V \times \frac{(S_i - S^-)}{(S^* - S^-)} + (1 - V) \times \frac{(R_i - R^-)}{(R^* - R^-)} \quad (5)$$

where, S^-=min S_i, S^*=max S_i, R^-=min R_i, R^*=max R_i, and v is the weight of the strategy of maximum group utility, whereas (1-*v*) is the weight of the individual regret. Here, when *v* is larger than 0.5, the index of Q_i follows the majority rule

The strategy of maximum group utility, with v representing the strategy's maximum group utility and (1-v) representing individual regret, follows the majority rule when v exceeds 0.5. Within each sub-watershed, a high Qj designates a higher priority, and a lesser Qj shows a less significant priority (Topno et al., 2022).

The ranking index in VIKOR is determined using the opponent's least individual regret and maximum group utility (Kang & Park, 2014; Suh et al., 2019). In other words, the degree of similarity to the ideal choice may be compared to establish the compromise rating, provided that each alternative can be assessed using each criterion.

8. Prioritising the options included considering S, R, and Q values. Out of these three parameters, the optimal choice has the lowest value.

4.3.6 Priority index

Evaluating watersheds in order of importance or degradation involves analyzing each unique characteristic. Based on how susceptible they are to erosion, watersheds were given priority in this study. Erosion risk assessment parameters are the morphometric variables Rb, Dd, Fs, Dt, Re, Cc, Bs, Rr, R, Rn, Rf, Lo, If, and SW (Biswas et al., 1999). While form characteristics are inversely proportional to erodibility, linear morphometric parameters are directly proportional to it (Ratnam et al., 2005). The VIKOR approach was used to prioritize the weighted normalized decision matrix for morphometric parameters. The weighted normalized decision matrix for the land use/cover was also taken into account using the VIKOR approach.

Sub-watersheds were ranked according to their morphometric parameters, taking into account their unique features. The VIKOR technique and a pairwise comparison matrix were used to rank the sub-watersheds in order of relevance or degradation. In this study, watersheds were prioritized based on their susceptibility to erosion (Meshram & Sharma, 2017). The susceptibility was rated based on the condition indicator for morphometric, land use/cover, and sediment load parameter values for five priority index classifications as specified in Table 4-4.

The specifics of the complete procedure for ranking sub-watersheds along with morphometric factors were done while taking into account their unique properties. Based on how susceptible they are to erosion, watersheds were given a higher priority in this study (Meshram & Sharma, 2017). For example, watersheds with higher levels of several linear and relief morphometric criteria, including drainage density, stream frequency, overland flow length, basin relief, relief ratio, and roughness number, are particularly vulnerable to erosion due to high runoff and steeper slopes (Duressa et al., 2024).

To extrapolate a particular and related category, LULC was further processed. For instance, all types of agricultural land were combined into a single attribute and given the name "cropland." The six LULCs that were taken into account throughout the ranking procedure were built-up, cultivated, forest, shrub, grass, and bare land. Wetlands and water bodies were not taken into account in this work's rating process. The same process used to apply the morphometric parameters was used to apply the ranking technique for sub-watershed priority based on LULC. Additionally, as part of watershed prioritization, the sediment load from each watershed was taken into account. Prioritization of each sub-watershed was completed using priority index classification and quantitative data for each sub-watershed morphometric, LULC, and sediment load characteristics.

By taking two parameters at a time, the two-dimensional overlay matrices from the qualitative rating had been developed. First, morphometric data and land use/cover were analyzed as a matrix, and the results were divided into five classes that were then used for a second matrix analysis that included sediment load. Finally, they were divided into five qualitative categories once more. The group was chosen based on the risk assessment matrix Table 4-4 and Table 4-5, which categorized all 37 sub-watersheds into five groups.

Besides the literature expert's knowledge and experiances have been considered. The following approach was used to incorporate the experts knowledge and experience. These procedures were taken in order to properly take into account the opinions of pertinent specialists when conducting the pairwise comparison for soil erosion-related watershed prioritization: Establish the criteria and sub-criteria pertinent to sub-watershed prioritization, covering aspects of morphometric and LULC parameters (listed in Tables 4-8 and 4-11); second, identify pertinent experts (two from soil science, one from hydrology, two agricultural specialists, and one environmentalist); and third, use the AHP to enable pairwise comparisons among the identified criteria. Pairs of criteria were assessed by each expert according to their relative significance. After each expert's evaluation is finished, add up all of their scores to determine each criterion's overall rating. The arithmetic mean can be used to determine the average score for each criterion among all experts. Finally, the assessment of the consistency of judgments made by experts through consistency ratio calculations.

Table 4-4 Risk assessment matrix for identifying and determining priority aspects: Based on their ordinal values of arithmetic operation (Krisper, 2021)

	*Ordinal	1	2	3	4	5
*Ordinal	Rating	VLP	LP	MP	HP	VHP
1	VLP	1	2	3	4	5
2	LP	2	4	6	8	10
3	MP	3	6	9	12	15
4	HP	4	8	12	16	20
5	VHP	5	10	15	20	25

**Ordinal scale values refer to 1-management not required in all cases, 2-management not required in most cases, 3-management required in some cases, 4-most cases require management attention, and 5-requires immediate management attention. The numbers resulted from the product of ordinal values 1-3 Very low (VLP), 4-6 Low (LP), 8-10 Medium (MP), 12-15 High (HP), and >16 Very high (VHP).*

Table 4-5 Risk matrix with categories at the priority level determined by their qualitative value (NASA, 2020).

Rating	VLP	LP	MP	HP	VHP
VLP	VLP	VLP	VLP	LP	LP
LP	VLP	VLP	LP	MP	MP
MP	VLP	LP	MP	HP	HP
HP	LP	MP	HP	VHP	VHP
VHP	LP	MP	HP	VHP	VHP

When employing a simple matrix method for prioritization, the morphometric, land use/cover, and sediment load variables were considered. The range of quantitative values for the qualitative value has been defined to create this matrix. The qualitative values of the morphometric, land use/cover and sediment load parameter values are shown in Table *4-6* as a condition indicator.

Five priority index classes (Gumma et al., 2016; Nitheshnirmal et al., 2019) were established, with the sub-catchment with the lowest rating value indicating good environmental condition. In contrast, the sub-catchment, having the best rating value in Table *4-6* was provided with a very high priority designation and advised to undergo treatment immediately to control erosion.

Table 4-6 Condition indicator for morphometric, land use/cover, and sediment load parameter values

Rank	Morphometric (Qi)	Land use (Qi)	Sediment yield (t/ha/year)
Very Low	> 0.8	> 0.9	0-5
Low	0.7-0.8	0.9-0.8	5-20
Medium	0.6-0.7	0.8-0.7	20-50
High	0.6-0.5	0.7-0.6	50-100
Very High	< 0.5	< 0.6	> 100

The Q_i value indicates the morphometric and land use parameter values calculated using the VIKOR approach as condition indicators.

4.4 Results and Discussion

Priority analysis was carried out in this work using satellite imagery, DEM data, and the output of the SWAT model. Using various erosion hazard parameters, including morphometric parameters, LULC parameters, and sediment load, the multi-attribute decision-making (MADM) approach has been used in this investigation to identify priority sub-watersheds (Ranjan et al., 2013).

4.4.1 Sub-Watersheds Prioritization Using Morphometric Analysis

In the study location, dendritic and sub-dendritic drainage patterns were identified. The delimited layer area (presented in Table 4-7 and Figure 4-4) was used to generate several fundamental parameters for the 37 watersheds.

Table 4-9 shows the output of the morphometric analysis. Prior research applying morphometric parameters for watershed prioritization led to the selection of each morphometric parameter employed in this study (Dofee et al., 2024; Gela, 2018; Makhdumi & Dwarakish, 2019; Nasir et al., 2023; Ren et al., 2015).

A. Fundamental criteria

Area (A) is an area of a watershed as projected onto a horizontal plane. As it accurately reveals the water within a catchment, it is an important watershed property. Greater size intercepts more rainfall, more runoff, and higher peak discharge. Smaller sizes have occasionally also seen the highest levels of flooding and sedimentation. Other watershed morphometric properties, such as stream networks, relief parameters, and shape and length, are accountable. The area of the current

study runs from 98.35 to 681.72 km2, with SW04 having the least and SW24 having the greatest Table 4-7.

The watershed perimeter (P) is the length of the defined watershed border. It also shows the extent of the catchment. The perimeter is between 241.55 and 78.09 km; the smallest is SW30, while the longest is SW34.

Watershed length (Lb) refers to the longest dimension of the basin in parallel with the principal discharge channel (Schumm, 1956); it shows the primary waterway in the watershed, which transports most of the water. The longest sub-watershed in this regard is at SW03 (53.75 km), and the shortest is at SW24 (17.9 km)

Watershed relief (Bh) is the elevation between a catchment outlet and the highest point on its perimeter, varying from 1591.11 to 3538.6 amsl.

Stream order (U) is a measure of a stream's position in the hierarchy of tributaries. The first stage in morphometric analysis is to organize or categorize streams based on the quantity and kind of tributary connections. The rivers are assigned an order using the (Farhan et al., 2015) approach. Since six is the highest stream order found in the catchment; the Upper Awash Basin belongs to the sixth order (Figure 4-4). The sixth order is seen at SW23, SW31, SW34, and SW24. In the study area SW08, SW14, SW16, SW21, SW23, SW24, SW27, and SW33 are of fifth order, whereas, SW23, SW31, and SW35 have sixth order. The entire upper Awash basin falls under the sixth order.

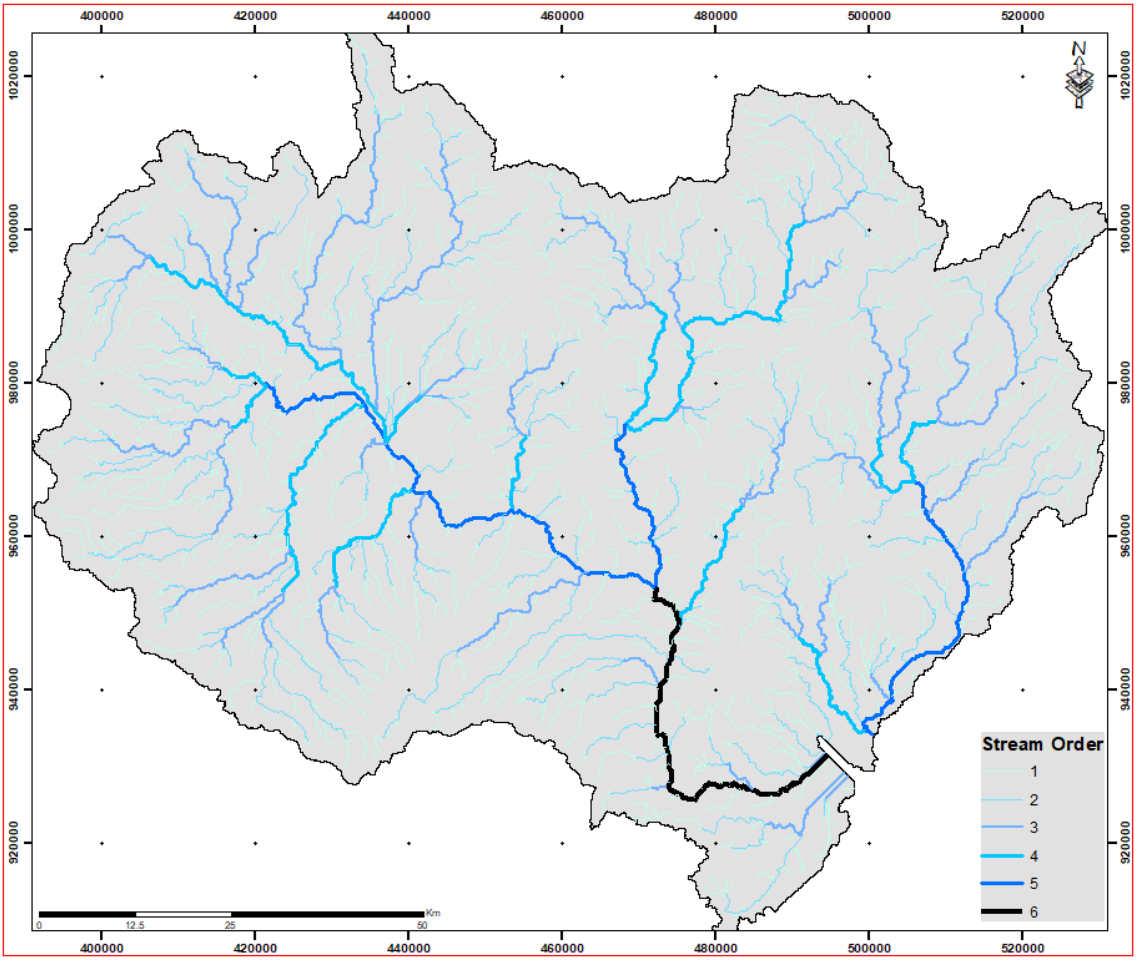

Figure 4-4 Stream order of Upper Awash sub-basin

Stream number (Nu) is used to describe how many stream segments are present in each sequence. An inverse geometric series is formed as a link between the stream order and the number of streams of a particular order (Horton, 1945). For instance, a watershed with a higher proportion of uppermost channels often has a topography that is highly permeable and permeable to infiltration. Soft shale and slate rocks are typical of a watershed where the quantity and arrangement of streams are increased (Biswas, 2016). With 71 first-order streams, WS04 was found to have the most, while WS03 had the fewest, with just 10 first-order streams (Table 4-7).

Table 4-7 Computation of basic parameters of sub-watersheds.

WSID	Area (A) (Km^2)	Perimeter (p) (km)	Stream number (Nu)	Stream Length (Lu) Total	Basin Length (Lb)
WS1	320.15	132.41	67	161.1	34.99
WS2	130.73	96.78	29	58.4	21.04
WS3	101.52	83.88	19	49.8	18.22
WS4	681.72	177.29	141	342.4	53.75
WS5	366.14	187.91	85	190.5	37.76
WS6	185.06	151.91	31	94.4	25.63

WS7	275.09	120.84	55	170.5	32.10
WS8	153.32	160.79	27	89.0	23.03
WS9	472.60	204.29	97	235.9	43.65
WS10	137.05	90.18	25	67.2	21.61
WS11	167.42	104.40	37	83.9	24.21
WS12	395.84	163.91	87	206.1	39.47
WS13	284.69	164.33	53	134.7	32.73
WS14	156.70	121.56	32	72.0	23.32
WS15	203.10	111.24	47	127.8	27.02
WS16	130.66	111.06	29	63.6	21.03
WS17	308.41	152.99	69	150.7	34.26
WS18	166.62	91.98	40	89.5	24.15
WS19	301.11	135.05	67	154.8	33.79
WS20	136.44	94.74	27	73.1	21.55
WS21	218.69	110.22	36	110.0	28.18
WS22	316.64	133.43	55	194.8	34.77
WS23	252.38	158.15	50	122.6	30.57
WS24	98.35	94.08	23	48.9	17.90
WS25	151.23	96.12	31	83.2	22.85
WS26	309.31	131.75	65	180.6	34.31
WS27	245.15	123.60	55	113.9	30.07
WS28	338.04	175.43	72	188.2	36.09
WS29	241.22	136.73	42	116.8	29.79
WS30	656.66	241.55	131	366.7	52.62
WS31	284.76	135.23	48	161.0	32.74
WS32	350.96	145.37	67	193.4	36.86
WS33	328.11	144.77	68	198.1	35.48
WS34	130.16	78.90	18	83.7	20.99
WS35	377.57	165.89	73	193.6	38.43
WS36	271.38	161.63	46	132.2	31.85
WS37	273.08	106.74	62	185.4	31.97

Stream length (Lu) is the mean distance of streams to each of the various orders. Since uppermost channels have the largest lengths, stream orders go up (Horton, 1945). Stream length varies with the topography; longer streams are found in places with more coarse textures and lower slopes, while shorter streams are found in areas with finer textures and steeper slopes (Farhan et al., 2015). Additionally, it evaluates the hydrologic features and rock formation of the area. A lesser number of streams with longer lengths are formed relative to the porous rock layer and well-drained catchment, and vice versa (Sethupathi et al., 2011). The stream lengths of all orders, both longest and shortest in the current research, are SW30 (366.7 km) and SW24 (48.93 km), respectively Table 4-8.

B. Linear parameters

The bifurcation ratio (Rb) is a proportion of all rivers in an order (Nu) to all rivers in the next order (Nu + 1) (Schumm, 1956). Horton (1945) asserts that Rb is connected to the drainage system's branching pattern, indicating the level of integration between streams of various orders. In basins

without any structural influence and nearly level terrain, the Rb value is less than 3. When the Rb number falls between three and five, it indicates that the rock structure of the basin has less impact on the drainage network (Singh et al., 2020). Less structurally disrupted watersheds without any deformation in the river network are indicated by lesser Rb (Suji et al., 2015). In the current study, SW31 (5.83) and SW24 (0.79) have the greatest and lowest Rb values, respectively. This suggested that SW24 and SW16 are comparatively sustainable sub-watersheds, while SW31 and SW27 are relatively more disturbed than the others. This implies that structural disruptions have not impacted the drainage network in nearly every catchment (Hindersah et al., 2018).

Stream length ratio (Rl) is calculated by dividing the average river length of a given order (Lu) by the average river length of the subsequent lowermost order (Lu-1) (Rl) (Horton, 1945). The relative rock formation permeability within a watershed and the historical evolution of stream segments are shown by the mean length of a stream's order remains longer than that of its below it. Two main principles govern how many streams and how long each stream order should be in a catchment area (Horton, 1945).

Stream frequency (Fs) is the ratio of the area of a watershed to all of its streams in all stream orders (Horton, 1945). Since they often vary with drainage area size, the stream frequency values and drainage density for large and small drainage areas cannot be directly compared. However, drainage density and stream frequency are positively correlated, which suggests stream population and drainage density are increasing concurrently (Paghadal et al., 2019; Suji et al., 2015). High values of Fs are used to represent steep surfaces with more surface runoff. A high Fs value indicates an impermeable underlying material, high relief conditions, and low infiltration capacity. That is to say, the larger value of Fs shows greater soil erosion (increased runoff) (Horton, 1932). The watersheds' Fs values varied from 0.14 (SW18) to 0.24 (SW34), signifying substantial to moderate relief. It was discovered that in the watershed, Fs and Dd directly correlate.

Drainage density (Dd) is the proportion of the total length of the current river to the area of the catchment (Horton, 1945), which is influenced by plant cover, permeability, and runoff potential. It represents the development of a watercourse and the closeness of proximity inside a sub-watershed. High Dd indicates a steep slope, low plant cover, fine drainage texture, mountainous relief, and high runoff in a watershed and subsurface with low permeability, whereas low Dd represents watersheds with low relief and extremely permeable underlying plant cover. Because of the quick runoff in the canals, such basins are in danger of flooding (Langbein, 1947). Among the 37 watersheds, WS37 had the highest drainage density (Dd = 0.68) and WS02 the lowest (Dd = 0.45). Extremely coarse drainage density in the studied area suggests that the watershed has poor hydrologic response and insufficient drainage. Gully erosion and flooding are major risks due to surface runoff not quickly removed from the watershed (Sukristiyanti et al., 2018).

Drainage Texture (Rt) indicates the comparative spacing of river channels. Mathematically, it is the total number of streams per perimeter of a watershed (Horton, 1945; Smith, 1950). Rainfall, slope, subsurface permeability, vegetation, and climate all affect Rt. Based on the drainage texture, the sub-basin has been classified into four groups [63]: coarse (Rt < 4), intermediate (Rt = 4–10), fine (Rt = 10–15), and ultra-fine (Rt >15). Rt varied from 0.8 to 0.17 in the current study, and all watersheds were categorized as coarse. Low infiltration capacity, an impermeable soil layer, and

excessive runoff in the basins are indicated by the coarse drainage texture (Rt) values. The more stream segments in a basin, the more impermeable the surface is (Rai et al., 2018).

Length of overland flow (Lo), equal to drainage density reciprocal divided by half. This quantity is essentially equivalent to the length of sheet flow and has a significant inverse connection with the mean channel slope. It describes how long water travels across the terrain before condensing into certain river channels. Greater surface runoff enters the stream when Lo is less. Even little rainfall is adequate to provide a large volume of surface runoff to stream discharge in terrain that is generally regular (Horton, 1945; Sakthivel et al., 2019). The fact that the SW02 sub-catchment overland flow distance is lower than that of the other sub-watersheds suggests that the water travels through the land surface over a shorter distance. In contrast, the sub-catchment SW37 takes the highest value, suggesting that before being concentrated in stream channels, the water in SW37 tends to go farther across the land surface.

Infiltration number (If) is the product of stream frequency and drainage density. Greater infiltration numbers are correlated with higher surface runoff and low infiltration rates. The ratio of drainage density to stream frequency can be used to calculate the infiltration number (Umrikar, 2017). It and the infiltration rate have an inverse relationship. If values highlight areas of high relief and impermeable bedrock in the watershed and give information about infiltration characteristics (Umrikar, 2017). A low infiltration rate is indicated by a larger infiltration number, and vice versa.

The highest infiltration number is found in SW02; this is associated with increased drainage density and overall stream frequency. This indicates that SW02 may have more opportunity for overland flow and a much lower rate of infiltration compared to the other sub-watersheds. The lowest infiltration value, on the other side, is found in SW34, which denotes a lower total stream frequency and drainage density. This implies that SW34 may have a significantly greater penetration rate and a lower danger of overland flow than the sub-watershed.

C. Areal parameters

Elongation ratio (Re) is the proportion of the watershed's greatest length to its circular diameter (Schumm, 1956). It is used to evaluate a watershed's form. A lower value denotes a lengthy basin and a steep slope. It ranges from 0.4 to 1.0. Extremely low relief areas are characterized by Re values near 1.0 (Farhan et al., 2015). Re can be divided into four classes: circular (>0.9), oval (0.8-0.9), less elongated (0.7-0.8), and elongated (<0.7) (Sukristiyanti et al., 2018). Typically, Re has a value between 0 and 1, with 1 denoting a circular shape catchment and 0 denoting a severely elongated shape catchment. Among the 37 watersheds, WS24 (Re = 0.63) had the greatest value, while WS04 and WS30 (Re = 0.55) had the lowest. The study area is grouped as a low value of Re (elongated watershed) and has high relief and a steep slope. The area can be characterized by a poor rate of infiltration with high runoff.

Circularity ratio (Rc) is affected by the sub-watershed relief, slope, LULC, climatic change, stream length, stream frequency, and geological conditions. High Rc values indicate the catchment's stronger resemblance to a circular shape, which promotes consistent infiltration and a flow of excess water that lasts for a long time. Low Rc values indicate an extended watershed. Since a circular watershed will have the shortest concentration period, it is most vulnerable to peak

discharge. Lower, medium, and higher values of Rc represent the young, mature, and ancient phases of watershed development (D. P. Patel et al., 2013; Schumm, 1956). In the research area, SW37 has greater circulatory ratio values (0.30). The Rc value for Watershed WS8 was 0.07, which was the lowest. The sub-basin exhibits a range of Rc values from 0.07 to 0.3, which suggests that the geologic materials are homogeneous, highly permeable, and free of structural disturbances.

Form Factor (Rf) depicts the catchment shape and has an inverse relationship with erosion susceptibility (Horton, 1932). Higher Rf values indicate higher peak flows over shorter periods, while lower Rf values indicate lower peak flows over longer periods (Chopra et al., 2005; Horton, 1945). Lower Rf values imply stretched watersheds where water flows for extended periods with a flatter peak, while higher Rf values have high peak flows for shorter periods (Nautiyal, 1994). Watershed form factor values <0.78 are elongated, whereas > 0.78 are circular (Sukristiyanti et al., 2018). The Rf ranged from 0.31 (WS24 and WS03) to 0.24 (WS04 and WS30) in the research sub-basin. Sub-watersheds with low form factors have high peak flows over shorter periods, which increases their vulnerability to water-induced mechanical erosion.

Compactness Coefficient (Cc) the compactness coefficient represents the ratio of a watershed's perimeter to and the circumference of a comparable circular area (Horton, 1945). The watershed's slope influences it, but not its extent. A lower Cc value denotes greater runoff and erodibility. In a circular basin, the drainage system will provide the least concentration time before the peak flow event becomes a greater risk (Javed et al., 2009; Ratnam et al., 2005). In the current investigation, SW37 (1.82) has a lower compactness coefficient value than SW08 (3.66) but a higher compactness coefficient overall. The sub-watershed area and shape of SW04 and SW34 have lower values, while SW05, SW13, and SW23 take substantially greater values. The lower value of Cc indicates that WS37, WS04, and SW34 are most susceptible to erosion.

D. Relief parameters

The relief ratio (Rh) is basin relief (the variation in height between the highest and lowest) divided by the longest drainage distance of the catchment. It evaluates a watershed's overall steepness and measures the rate and severity of erosion on its slopes (Schumm, 1956). Channel gradient and relief are directly correlated. Rh of the watershed is strongly associated with several hydrological features. Rh values that are higher indicate severe slopes and higher relief. Rh=66.81 was discovered to be the highest value that corresponds to WS34.

Rh increases when drainage/stream area and watershed size decrease. It ties the overall slope of the drainage area to the steepness and soil erosion in the basin. Numerous studies have found a strong relationship between Rh and loss of sediment (Ahmed et al., 2010; Rai et al., 2018; Schumm, 1956). The steepness (high slope) (Vittala et al., 2004) and elevated relief within the watershed are higher values of Rh. The runoff increases the likelihood of erosion in the basins with steeper slopes. The lower Rh value, on the other side, denotes a low slope (steepness) and low relief.

Ruggedness number (Rn) is drainage density multiplied by basin relief (Patton & Baker, 1976). Rn measures how uneven the catchment's surface is and illustrates the clear relationship between erosion and Rn. It combines the length and steepness of the slope. It makes a relation between the

slope's length and steepness (Chaubey, et al., 2017; Rai, Mishra, et al., 2017). An extraordinarily high value of Rn arises under steep slopes (Umrikar, 2017) and high Dd values when both factors are large. These basins have been assessed to be at risk of flooding. Rn's value ranged from 0.05 (for WS08) to 0.9 (for WS34 and WS37). Slopes have a higher value when they are steep and longer. The study area has high values at SW29, SW30, SW34, and SW37, and lower values at SW08, SW14, and SW36.

4.4.2 Pairwise comparison matrix using AHP

Comparisons between pairs of options under the specified standard in Table 4-8, it is possible to define the weights of the morphometric factors. The decision-maker judges each preference according to the criterion: very strong, strong, weak, or very weak. Apply inverses, that is, from 1/9 ("extremely not preferred") to 1 ("equally not preferred"). Table 8, if we think one choice is less desirable than another on a criterion *Table 4-8* (Saaty, 1987; Saaty & Vargas, 1987). The elicitation of pairwise comparison judgments and scale was, as mentioned in Section 6.3.5 and Table 4-4.

Table 4-8 Calculated criterion weight values (using AHP) for morphometric parameters

	Rb	Fs	Dd	Dt	Rc	Re	Rf	Cc	Rr	R	Bs	SW	Rn	Lo	If
Rb	1	2	2	5	5	6	5	5	9	9	9	9	5	9	9
Fs	0.50	1	3	5	3	5	5	6	4	5	9	9	5	9	9
Dd	0.50	0.33	1	3	5	4	3	3	3	2	9	9	2	9	5
Dt	0.20	0.20	0.33	1	3	5	2	2	2	3	5	5	3	5	5
Rc	0.20	0.33	0.20	0.33	1	2	2	2	2	2	3	3	1	3	5
Re	0.17	0.20	0.25	0.20	0.50	1	2	2	2	2	3	3	2	3	9
Rf	0.20	0.20	0.33	0.50	0.50	0.50	1	2	2	2	5	5	2	5	4
Cc	0.20	0.17	0.33	0.50	0.50	0.50	0.50	1	2	2	3	3	2	3	3
Rr	0.11	0.25	0.33	0.50	0.50	0.50	0.50	0.50	1	2	3	3	2	3	2
R	0.11	0.20	0.50	0.33	0.50	0.50	0.50	0.50	0.50	1	3	3	2	3	2
Bs	0.11	0.11	0.11	0.20	0.33	0.33	0.20	0.33	0.33	0.33	1	2	1	2	2
SW	0.11	0.11	0.11	0.20	0.33	0.33	0.20	0.33	0.33	0.33	0.5	1	1	2	2
Rn	0.20	0.20	0.50	0.33	1.00	0.50	0.50	0.50	0.50	0.50	1	1	1	2	2
Lo	0.11	0.11	0.11	0.20	0.33	0.33	0.20	0.33	0.33	0.33	0.5	0.5	0.5	1	2
If	0.11	0.11	0.20	0.20	0.20	0.11	0.25	0.33	0.50	0.50	0.5	0.5	0.5	0.5	1
Weight*	22.4	18.5	12.5	8.5	5.6	5.6	5.6	4.3	3.8	3.5	2	1.8	2.9	1.5	1.4

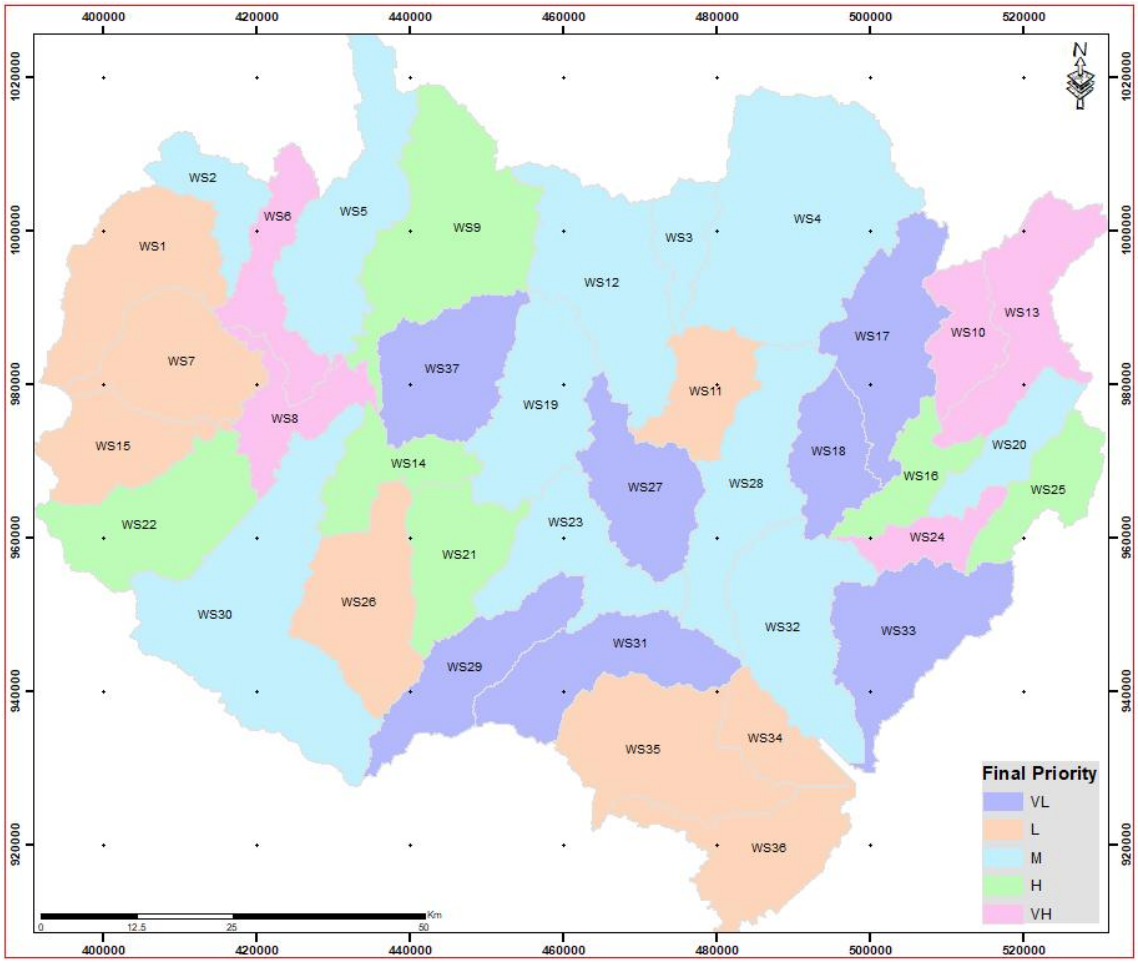

Figure 4-5 Sub-watershed priority map based on morphometric parameter

The bold font in

Table 4-9, the column value derived according to the equation in **Error! Reference source not found.**, shows the sub-watersheds greater and lower values for every variable. The higher Qi value indicates the highest priority and the most vulnerable to soil loss; however, the lowest Qi value indicates the lowest priority and the least susceptible to soil erosion. Finally, ArcGIS is used to complete the spatial distribution of erodibility priority of each drainage area by the AHP-VIKTOR technique using LULC parameters.

Table 4-9 prioritizing sub-watersheds using morphometric parameters.
(Tthe AHP-VIKTOR technique prioritizes the erodibility of sub-watersheds at v = 0.5.)

WSID	Rn	Rr	Rb	Dd	Fs	Bs	Dt	Rc	Re	Rf	Cc	R	Lo	If	S_i	R_i	Q_i
WS01	0.55	31.01	2.18	0.50	0.21	3.82	0.51	0.23	0.58	0.26	2.09	1085.1	0.99	0.42	0.56	0.16	0.54
WS02	0.43	46.29	1.63	**0.45**	0.22	3.39	0.30	0.18	0.61	0.30	2.39	973.9	1.12	**0.50**	0.56	0.19	0.66
WS03	0.52	58.14	1.83	0.49	0.19	3.27	**0.23**	0.18	0.62	**0.31**	2.35	1059.6	1.02	0.38	0.58	0.18	0.64
WS04	0.55	20.37	1.88	0.50	0.21	**4.24**	**0.80**	0.27	**0.55**	**0.24**	1.92	1094.9	1.00	0.41	0.56	0.18	0.61
WS05	0.45	22.76	1.54	0.52	0.23	3.89	0.45	0.13	0.57	0.26	2.77	859.4	0.96	0.45	0.58	0.19	0.69
WS06	0.41	31.55	1.61	0.51	0.17	3.55	0.20	**0.10**	0.60	0.28	3.15	808.7	0.98	0.33	**0.69**	0.19	0.84
WS07	0.68	34.36	2.02	0.62	0.20	3.75	0.46	0.24	0.58	0.27	2.06	1102.9	0.81	0.32	0.52	0.17	0.52
WS08	**0.05**	**4.10**	1.57	0.58	0.18	3.46	0.17	0.07	0.61	0.29	**3.66**	94.5	0.86	0.30	0.68	0.19	0.83
WS09	0.66	30.27	1.61	0.50	0.21	4.03	0.47	0.14	0.56	0.25	2.65	1321.5	1.00	0.41	0.61	0.19	0.72
WS10	0.31	29.17	1.58	0.49	0.18	3.41	0.28	0.21	0.61	0.29	2.17	630.3	1.02	0.37	0.66	0.19	0.80
WS11	0.19	15.78	2.09	0.50	0.22	3.50	0.35	0.19	0.60	0.29	2.28	382.0	1.00	0.44	0.58	0.17	0.59
WS12	0.70	33.87	1.67	0.52	0.22	3.94	0.53	0.19	0.57	0.25	2.32	1336.9	0.96	0.42	0.55	0.18	0.63
WS13	0.31	20.12	1.54	0.47	0.19	3.76	0.32	0.13	0.58	0.27	2.75	658.6	1.06	0.39	**0.69**	0.19	**0.85**
WS14	0.16	15.13	1.83	0.46	0.20	3.47	0.26	0.13	0.61	0.29	2.74	352.9	1.09	0.44	0.66	0.18	0.75
WS15	0.67	39.68	1.57	0.63	0.23	3.59	0.42	0.21	0.60	0.28	2.20	1072.0	0.79	0.37	0.47	0.19	0.53
WS16	0.27	26.32	**1.29**	0.49	0.22	3.39	0.26	0.13	0.61	0.30	2.74	553.5	1.03	0.46	0.61	0.20	0.78
WS17	0.59	35.13	2.36	0.49	0.22	3.80	0.45	0.17	0.58	0.26	2.46	1203.4	1.02	0.46	0.54	0.15	0.48
WS18	0.51	39.23	2.15	0.54	**0.24**	3.50	0.43	0.25	0.60	0.29	2.01	947.3	0.93	0.45	0.46	0.16	0.40
WS19	0.71	40.60	1.73	0.51	0.22	3.79	0.50	0.21	0.58	0.26	2.20	1372.1	0.97	0.43	0.54	0.18	0.60
WS20	0.36	31.08	1.68	0.54	0.20	3.41	0.29	0.19	0.61	0.29	2.29	670.0	0.93	0.37	0.60	0.18	0.69
WS21	0.46	32.61	1.94	0.50	0.16	3.63	0.33	0.23	0.59	0.28	2.10	919.0	0.99	0.33	0.68	0.17	0.75
WS22	0.49	22.79	1.78	0.62	0.17	3.82	0.41	0.22	0.58	0.26	2.12	792.6	0.81	0.28	0.63	0.18	0.72
WS23	0.40	26.70	1.97	0.49	0.20	3.70	0.32	0.13	0.59	0.27	2.81	816.3	1.03	0.41	0.63	0.17	0.67
WS24	0.29	32.49	0.79	0.50	0.23	**3.26**	0.24	0.14	**0.63**	**0.31**	2.68	581.5	1.01	0.47	0.58	**0.22**	0.84
WS25	0.39	31.43	1.57	0.55	0.20	3.45	0.32	0.21	0.61	0.29	2.21	718.2	0.91	0.37	0.59	0.19	0.70
WS26	0.62	31.16	1.95	0.58	0.21	3.81	0.49	0.22	0.58	0.26	2.11	1069.3	0.86	0.36	0.54	0.17	0.55
WS27	0.47	33.80	5.03	0.46	0.22	3.69	0.45	0.20	0.59	0.27	2.23	1016.4	**1.08**	0.48	0.43	0.12	0.17
WS28	0.72	35.59	1.67	0.56	0.21	3.85	0.41	0.14	0.57	0.26	2.69	1284.5	0.90	0.38	0.57	0.18	0.65
WS29	0.81	56.23	3.75	0.48	0.17	3.68	0.31	0.16	0.59	0.27	2.48	1675.3	1.03	0.36	0.55	0.13	0.39
WS30	0.83	28.27	1.69	0.56	0.20	4.22	0.54	0.14	**0.55**	**0.24**	2.66	1487.6	0.90	0.36	0.59	0.18	0.68
WS31	0.66	35.59	**5.83**	0.57	0.17	3.76	0.35	0.20	0.58	0.27	2.26	1165.2	0.88	0.30	0.45	0.13	0.25
WS32	0.77	38.12	1.82	0.55	0.19	3.87	0.46	0.21	0.57	0.26	2.19	1405.3	0.91	0.35	0.58	0.18	0.65
WS33	0.32	14.85	2.54	0.60	0.21	3.84	0.47	0.20	0.58	0.26	2.25	527.0	0.83	0.34	0.54	0.15	0.45
WS34	**0.90**	**66.81**	3.92	0.64	**0.14**	3.38	**0.23**	0.26	0.61	0.30	1.95	1402.0	0.78	**0.22**	0.49	0.19	0.55
WS35	0.39	19.72	2.41	0.51	0.19	3.91	0.44	0.17	0.57	0.26	2.41	757.9	0.97	0.38	0.63	0.15	0.59
WS36	0.18	11.58	2.86	0.49	0.17	3.74	0.28	0.13	0.58	0.27	2.77	369.0	1.03	0.35	**0.69**	0.13	0.59
WS37	**0.90**	41.38	3.34	**0.68**	0.23	3.74	0.58	**0.30**	0.58	0.27	**1.82**	1323.0	**0**.74	0.33	**0.33**	**0.11**	**0.00**

The study area drainage has not been impacted by structural disturbances, as seen by low bifurcation ratio values and very low drainage densities for nearly all of its sub-watersheds. Additionally, the area is primarily covered by permeable and resistant formations (Das & Mukherjee, 2005). The loss of soil is influenced by morphometric factors such as form factor, elongation ratio, circularity ratio, and compactness coefficient in an inverse manner, and directly by bifurcation ratio, overland flow length, drainage density, texture, and stream frequency. This

might be taken to suggest that for morphometric factors that have a direct correlation with soil erosion, larger values should be allocated a greater rank (lower values). The ruggedness number and relief ratio measures are directly correlated with soil degradation (Puno & Puno, 2019). As previously stated, sub-watersheds with higher soil erodibility are assigned higher priorities, and the other way around.

4.4.3 Defining Sub-Watershed Priorities Using LULC Analysis

Eight main classifications comprise the LULC categories: bare ground, cropland, shrubland, water body, forest, built-up area, and grassland. A LULC classification accuracy assessment for the respective periods was made using local familiarity with the research area and Google Earth visuals. The overall accuracy of the classification was 91.2%. These are the classes that were taken into consideration for sub-watershed prioritization, except the water body and wetland classifications.

Table 4-10 displays the ranking of thirty-seven sub-watersheds based on LULC using the AHP-VIKOR method. The VIKOR index (Qi) ranges from 0.37 in WS03 to 1.0 in WS08. The watershed prioritization LULC parameter was based on the value range of the condition indicator Table *4-6*. Sub-catchments with high Qi values are most susceptible to soil loss (high priority), while those with low Qi values are least vulnerable (low priority). Finally, the spatial distribution of erodibility ranking of catchments by the AHP-VIKTOR technique using LULC parameters was done using ArcGIS Figure 4-5.

Table 4-10 Erodibility prioritization of sub-watershed by AHP-VIKTOR method (at v = 0.5) using LULC

WSID	Fst	Grl	Shl	Crl	Bar	Bup	Si	Ri	Qi
WS01	9.34	0.06	10.80	78.75	-	1.06	0.81	0.28	0.72
WS02	2.73	0.74	17.31	78.27	-	0.95	0.79	0.28	0.70
WS03	20.05	0.24	22.14	6.53	0.06	50.96	0.45	0.28	0.37
WS04	4.27	0.20	25.30	55.98	0.07	13.44	0.80	0.28	0.71
WS05	1.79	1.01	14.72	81.30	0.03	1.16	0.77	0.28	0.68
WS06	0.77	0.50	9.85	88.27	0.08	0.54	0.87	0.28	0.83
WS07	-	0.04	3.82	95.99	-	0.15	0.96	0.30	0.99
WS08	-	-	0.70	98.67	-	0.63	0.97	0.30	1.00
WS09	8.54	0.01	18.25	70.06	0.07	3.06	0.81	0.28	0.72
WS10	-	-	10.44	87.93	0.16	1.45	0.95	0.30	0.98
WS11	-	-	19.41	60.62	0.17	19.49	0.84	0.30	0.88
WS12	6.77	0.05	23.95	29.49	0.04	39.12	0.68	0.25	0.44
WS13	-	-	10.40	88.69	0.00	0.45	0.94	0.30	0.97
WS14	0.05	-	2.67	97.11	-	0.17	0.97	0.29	0.99
WS15	-	-	18.50	80.92	-	0.58	0.94	0.30	0.97
WS16	0.07	-	12.77	83.88	-	2.82	0.94	0.29	0.97
WS17	1.89	-	13.38	82.00	0.01	1.54	0.91	0.27	0.76
WS18	3.28	-	19.50	59.32	0.02	15.63	0.84	0.27	0.71

WS19	1.88	-	11.20	81.60	-	5.26	0.91	0.27	0.79
WS20	-	-	7.65	92.08	-	0.27	0.96	0.30	0.99
WS21	-	-	7.14	92.63	-	0.21	0.96	0.30	0.99
WS22	0.00	-	8.66	90.68	-	0.65	0.96	0.30	0.99
WS23	-	-	19.01	80.46	0.01	0.45	0.94	0.30	0.97
WS24	0.06	-	8.92	89.82	0.11	1.09	0.95	0.29	0.98
WS25	0.67	-	8.48	90.14	0.03	0.67	0.95	0.29	0.91
WS26	0.09	-	9.94	89.51	0.00	0.43	0.95	0.29	0.97
WS27	0.16	-	12.59	86.59	-	0.14	0.91	0.29	0.93
WS28	2.34	-	12.69	82.14	-	2.82	0.91	0.28	0.81
WS29	0.39	0.05	28.52	70.23	0.03	0.79	0.91	0.29	0.91
WS30	1.05	0.02	12.00	86.34	-	0.59	0.93	0.28	0.87
WS31	0.09	0.02	23.68	75.76	0.10	0.29	0.93	0.29	0.95
WS32	0.99	-	18.93	77.36	0.57	0.44	0.73	0.28	0.67
WS33	0.00	-	13.58	81.98	1.09	2.92	0.87	0.29	0.91
WS34	0.16	-	20.17	77.09	0.01	0.03	0.66	0.29	0.69
WS35	0.02	-	29.73	69.62	0.45	0.07	0.92	0.29	0.95
WS36	-	-	6.60	91.05	0.00	0.34	0.90	0.30	0.94
WS37	5.33	-	5.99	86.93	-	0.92	0.79	0.22	0.33

4.4.4 Pairwise comparison matrix using AHP

The researcher generates weights through pairwise comparisons of two alternatives, judging weak, strong, very weak, or very strong preferences under specific criteria (Saaty, 1987; Saaty & Vargas, 1987), as discussed in Sections 4.3.5, Table 4-4, and Section 4.4.2.

Table 4-11 Pairwise comparison matrix and calculated criteria weight (using AHP) for LULC

	Bup	Wel	Fst	Grl	Shl	Crl	Bar
Bup	1	1	2	2	7	9	9
Wel	1.00	1	2	2	7	9	9
Fst	0.50	0.50	1	1	5	9	9
Grl	0.50	0.50	1.00	1	5	9	9
Shl	0.14	0.14	0.20	0.20	1	2	2
Crl	0.11	0.11	0.11	0.11	0.50	1	1
Bar	0.11	0.11	0.11	0.11	0.50	1.00	1
Weight (%)	17.5	27.5	29.5	14.6	5.5	3.1	2.3

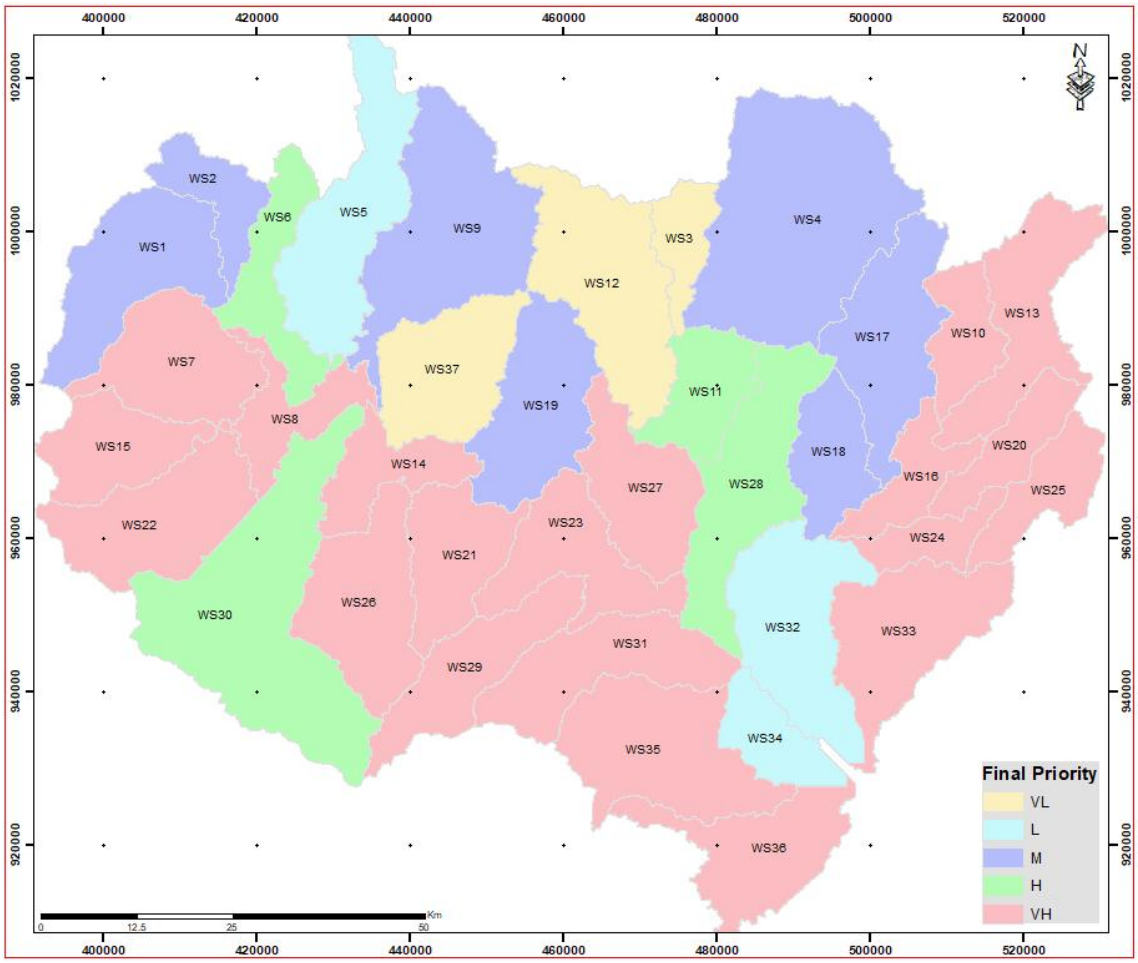

Figure 4-6 Priority map of sub-watersheds based on LULC parameter

4.4.5 Sub-Watershed Prioritization Using Sediment Load Analysis

In this study, measured monthly suspended sediment and daily streamflow were used to validate and calibrate the model. The hydrological component was calibrated, followed by the sediment component (Im et al., 2007).

According to Abbaspour (2015), the result indicates that the model accurately simulates streamflow (Table 4-12). In line with the evaluation standards suggested by Moriasi (2015), for the calibration and validation period, the PBIAS was very good, the NSE was good, and the RSR was good (Table 4-12).

Once the performance of the SWAT hydrological model was deemed satisfactory, it was calibrated and used to evaluate the sediment yield modelling. The p-value indicates that 0.82 of the monthly sediment for the calibration period and 0.76 of the validation period. The calculated r-factors for the monthly sediment yield were 0.71 for the calibration and 0.63 for the validation periods (Table 4-12).

Table 4-12 The performance of the SWAT model for streamflow and sediment

Observatory		Period	p-factor	r-factor	PBIAS	RSR	R2	NSE
Flow	Calibration	1979-2001	0.94	0.94	4.6	0.58	0.68	0.67
	Validation	2002-2018	0.92	0.8	5.4	0.57	0.68	0.67
Sediment	Calibration	1979-2001	0.82	0.71	-14.9	0.69	0.65	0.70
	Validation	2002-2018	0.76	0.63	20.8	0.55	0.63	-1.4

Watershed ranking was done using the results of the model sediment load study. The sediment load varies from 2.09 (t/ha/yr.) in WS18, which has an area of 166.62 km2, to 174.02 (t/ha/yr.), which has an area of 271.38 km^2 as shown in Table 4-13. The watershed ranking sediment load parameter was according to the value range of the condition indicator Table 6. Finally, the spatial distribution of erodibility was determined using ArcGIS based on the sediment load parameter (*Figure 4-7*).

Table 4-13 Prioritization of sub-watershed using sediment load (t/y)

WSID	**Sediment load (t/y)**	**WSID**	**Sediment load (t/y)**	**WSID**	**Sediment load (t/y)**
WS01	1168.9	WS14	15125.5	WS26	2090.9
WS02	512.2	WS15	1884.6	WS27	11907.1
WS03	217.6	WS16	2547.4	WS28	835.5
WS04	3922.6	WS17	3751.5	WS29	2508.3
WS05	7157.9	WS18	348.9	WS30	7480.5
WS06	1478.7	WS19	717.8	WS31	12269.9
WS07	824.8	WS20	1273.1	WS32	979.3
WS08	3247.1	WS21	33031.9	WS33	13214.5
WS09	8308.2	WS22	3226.1	WS34	644.8
WS10	1601.7	WS23	40703.9	WS35	59823.9
WS11	3811.9	WS24	10816.5	WS36	47226.8
WS12	5617.9	WS25	1721.9	WS37	15475.5
WS13	3044.9				

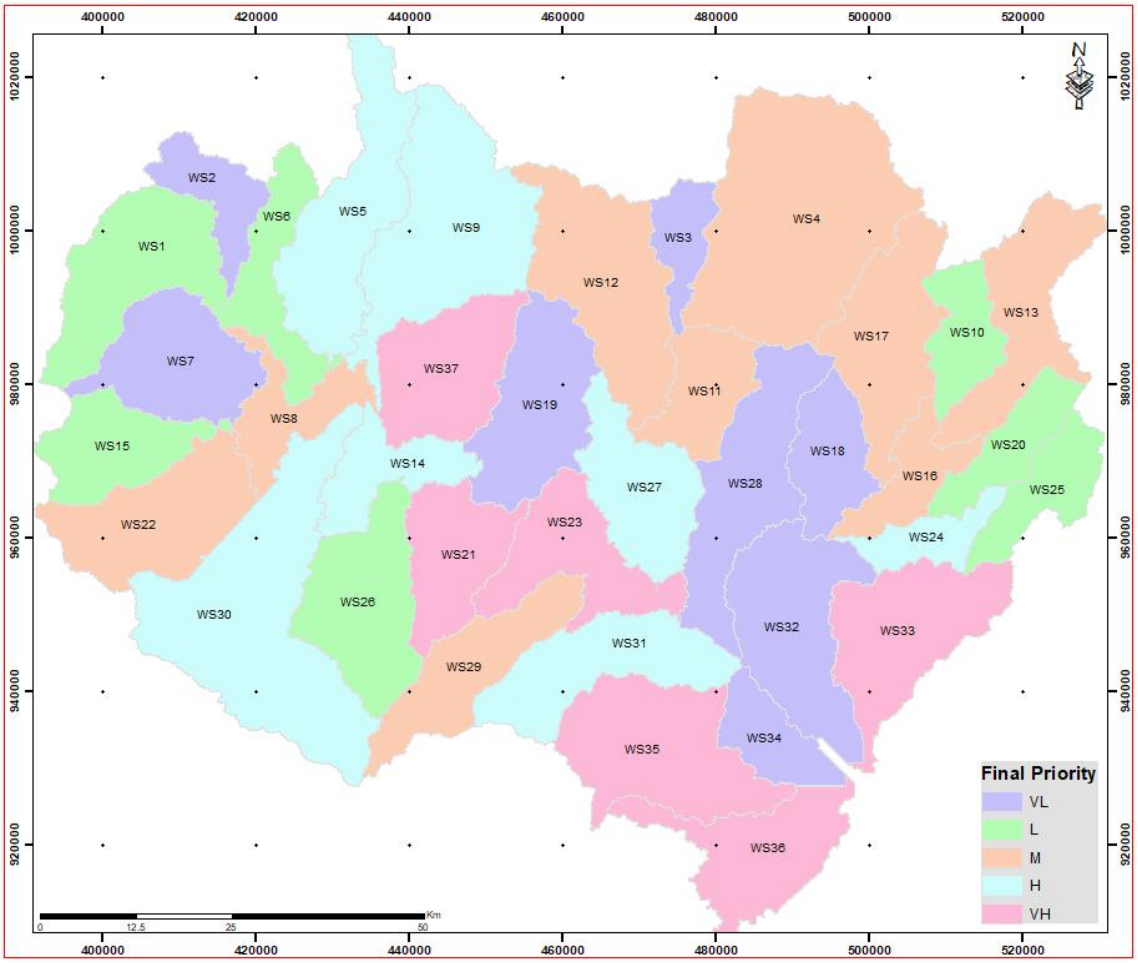

Figure 4-7 Priority map for sub-catchments based on the sediment load parameter

4.4.6 Consistency ratio (CR)

The consistency ratio is an index that shows the reliability of the decision-making. The concept of a consistency metric is useless without the corresponding standards; according to Pant (2022), the limit is 0.10. To guarantee the judgments' credibility, the decision maker makes revisions to the decisions until a CR of less than 0.10 (Saaty, 1990).

A pairwise comparison matrix was created by selecting fifteen morphometric factors directly or indirectly related to soil erosion and runoff for ranking sub-watersheds, as shown in Table 4-8 for morphometric analysis and Table 4-11 for LULC analysis, respectively. Next, to get the criterion weight values, all pairwise comparison matrix values were standardized for morphometric and LULC, respectively. For morphometric analysis and LULC analysis, the consistency ratio from the AHP analysis was determined to be 0.087 and 0.06, respectively. This indicates clearly that the criterion weight values are consistent and are less than 0.1.

In addition, the equation was used in the VIKOR approach to determine the best and worst values of the morphometric parameters. To determine Qi values, utility, and regret metrics were then

computed, and the result revealed that SW17, SW18, SW27, SW29, SW31, SW33, and SW37 are the most vulnerable watersheds to soil loss and other erosive factors, as shown in

Table 4-9 and Figure 4-5. Similarly, the analyzed LULC parameters, SW03, WS12, and WS37, are the most vulnerable watersheds to soil loss and other erosive factors, as revealed in Table 4-10 and Figure 4-6. The VIKOR method's Qi values were utilized to determine the final prioritizing.

4.4.7 Erodibility prioritization

Setting priorities is a crucial component of any plan for managing watersheds to achieve beneficial outcomes and locating problem areas so that appropriate remedies using various soil and water conservation techniques can be found. Characterizing and prioritizing sub-watersheds requires a more comprehensive methodology that contemplates alterations to the LULC and estimates of runoff and sediment production (Abdeta et al., 2020). In this research, based on the morphometric, LULC, and sediment load data, the combined AHP-VIKOR technique is used to prioritize the watersheds. The morphometric, LULC, and sediment load values in Table *4-6* were taken as a condition for prioritization using a simple matrix method. The integration process prepared a prioritized map by rescaling theme maps to five classes using the scores. Based on the range of condition indicator Qi value (VIKOR method), these micro-watersheds were classified as very high, high, medium, low, and very low.

The results for ranking of sub-watersheds indicated that SW8, SW13, SW14, SW16, SW21, SW22, SW23, and SW24 categorized under very high priority, whereas WS01, WS02, WS03, WS12, WS17, WS18, WS19, WS32, WS34, and WS35 characterized that very low priority as illustrated in Table 4-14 and Figure 4-8.

Sub-watersheds with Qi values for morphometric and LULC parameters ranging from 0.0 to 0.85 and 0.3 to 1.0, respectively. The final sub-watershed prioritized rank is shown in Table 4-14. The map in Figure 4-8 shows the spatial distribution of the sub-catchments for land and water management work according to the grouped matrix evaluation of the morphometric, LULC, and sediment load parameters.

Table 4-14 VIKOR index value and ranking for prioritization of sub-watersheds

WSID	Morphometric				Land use/cover (LULC)				Sediment Load (SL)		Final rank*
	S*i*	R*i*	Q*i*	Rank	S*i*	R*i*	Q*i*	Rank	SL (t/y)	Rank	
WS01	0.56	0.16	0.54	L	0.81	0.28	0.72	M	1169.0	L	VL
WS02	0.56	0.19	0.66	M	0.79	0.28	0.70	M	512.2	VL	VL
WS03	0.58	0.18	0.64	M	0.45	0.28	0.37	VL	217.6	VL	VL
WS04	0.56	0.18	0.61	M	0.80	0.28	0.71	M	3922.6	M	M
WS05	0.58	0.19	0.69	M	0.77	0.28	0.68	L	7157.9	H	M
WS06	0.69	0.19	0.84	VH	0.87	0.28	0.83	H	1478.7	L	H
WS07	0.52	0.17	0.52	L	0.96	0.30	0.99	VH	824.8	VL	L
WS08	0.68	0.19	0.83	VH	0.97	0.30	1.00	VH	3247.1	M	VH

WS09	0.61	0.19	0.72	H	0.81	0.28	0.72	M	8308.2	H	H
WS10	0.66	0.19	0.80	VH	0.95	0.30	0.98	VH	1601.7	L	H
WS11	0.58	0.17	0.59	L	0.84	0.30	0.88	H	3812.0	M	M
WS12	0.55	0.18	0.63	M	0.68	0.25	0.44	VL	5617.9	M	VL
WS13	0.69	0.19	0.85	VH	0.94	0.30	0.97	VH	3045.0	M	VH
WS14	0.66	0.18	0.75	H	0.97	0.29	0.99	VH	15125.5	VH	VH
WS15	0.47	0.19	0.53	L	0.94	0.30	0.97	VH	1884.6	L	M
WS16	0.61	0.20	0.78	H	0.94	0.29	0.97	VH	2547.4	M	VH
WS17	0.54	0.15	0.48	VL	0.91	0.27	0.76	M	3751.5	M	VL
WS18	0.46	0.16	0.40	VL	0.84	0.27	0.71	M	349.0	VL	VL
WS19	0.54	0.18	0.60	M	0.91	0.27	0.79	M	717.8	VL	VL
WS20	0.60	0.18	0.69	M	0.96	0.30	0.99	VH	1273.1	L	M
WS21	0.68	0.17	0.75	H	0.96	0.30	0.99	VH	33031.9	VH	VH
WS22	0.63	0.18	0.72	H	0.96	0.30	0.99	VH	3226.1	M	VH
WS23	0.63	0.17	0.67	M	0.94	0.30	0.97	VH	40703.9	VH	VH
WS24	0.58	0.22	0.84	VH	0.95	0.29	0.98	VH	10816.5	H	VH
WS25	0.59	0.19	0.70	H	0.95	0.29	0.91	VH	1721.8	L	H
WS26	0.54	0.17	0.55	L	0.95	0.29	0.97	VH	2090.9	L	M
WS27	0.43	0.12	0.17	VL	0.91	0.29	0.93	VH	11907.1	H	M
WS28	0.57	0.18	0.65	M	0.91	0.28	0.81	H	835.5	VL	L
WS29	0.55	0.13	0.39	VL	0.91	0.29	0.91	VH	2508.4	M	L
WS30	0.59	0.18	0.68	M	0.93	0.28	0.87	H	7480.5	H	H
WS31	0.45	0.13	0.25	VL	0.93	0.29	0.95	VH	12269.9	H	M
WS32	0.58	0.18	0.65	M	0.73	0.28	0.67	L	979.3	VL	VL
WS33	0.54	0.15	0.45	VL	0.87	0.29	0.91	VH	13214.5	VH	M
WS34	0.49	0.19	0.55	L	0.66	0.29	0.69	L	644.8	VL	VL
WS35	0.63	0.15	0.59	L	0.92	0.29	0.95	VH	59823.9	VH	H
WS36	0.69	0.13	0.59	L	0.90	0.30	0.94	VH	47226.8	VH	H
WS37	0.33	0.11	0.00	VL	0.79	0.22	0.33	VL	15475.5	VH	L

**The final rank is based on the value given in* Table 4-5 and Table *4-6* at *v = 0.5*

Soil erosion is a complex process influenced by various factors including land use, climate, geology, and management techniques. Prioritization using sediment load, LULC, and morphometric analysis showed that SW8, SW13, SW14, SW16, SW21, SW22, SW23, and SW24 sub-watersheds fall under very high priority, suggesting that the most susceptible watersheds and more vulnerable to soil erosion and other erosive agents; WS06, WS09, WS10, WS25, WS30, WS35, WS36, and WS37 under high priority; WS04, WS05, WS11, WS15, WS20, WS26, WS27, WS31, and WS06, WS09, WS10, WS25, WS30, WS35, WS36, and WS37 medium priority; WS07, WS28 and WS29 low priority and WS01, WS02, WS03, WS12, WS17, WS18, WS19, WS32, WS34, and WS35 fall under very low priority concerning soil erosion, signifying that low-priority sub-watersheds natural resources are less vulnerable to the damaging impacts of precipitation and other erosive agents.

The major reason behind this research is to identify and categorize hotspots of soil erosion sub-watersheds. However, the result will contribute to makeing remedial measures by planners and decision-makers for different environmental issues like flood management, preventing soil

erosion, improving water quality, natural resource management, and applying different conservation treatments. In addition to this, this research is crucial for major schemes, allowing planners to select approaches based on catchment area size, problem severity, funding constraints, and local and political system demands. When implementing conservation techniques for soil and water, extra attention needs to be given to the high-priority sub-catchments. To stop soil loss, rapid soil and water conservation techniques such as contour binding, bench terracing, gully control structures, and grass waterways are needed in sub-watersheds with high and very high erosion susceptibility. By slowing down runoff, preventing gully erosion, and holding onto sediment, these actions help stop water runoff and soil erosion (Hindersah et al., 2018; Liu et al., 2019).

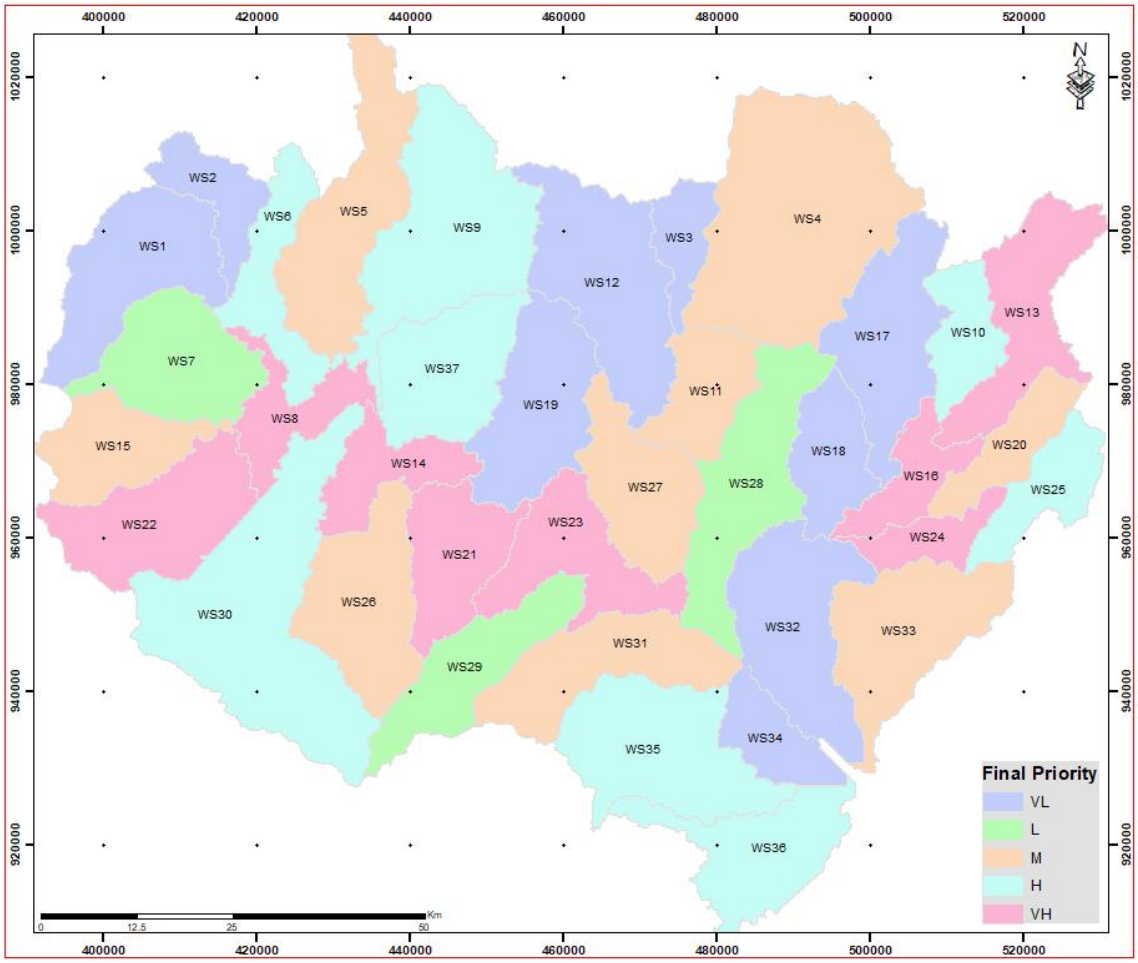

Figure 4-8 Erodibility prioritization of sub-watersheds

4.5 Discussion

The Upper Awash Sub-basin is one of the most densely populated and urbanized parts of the country where the most populous cities such as Addis Ababa are located (Shawul & Chakma, 2019a). If proper land use planning is not followed, the notable development in built-up regions and unplanned human settlements may increase the danger of environmental impairments (Dewan & Yamaguchi, 2009). Higher urban sprawl is primarily brought about by the rapid rate of population growth, economic expansion, and accessibility to resources and essential infrastructure

(Wilson et al., 2003). Moreover, a high rate of soil erosion and a decline in the amount of arable land available are the results of a growing population (Bekele, 2019).

Studies on sub-watershed prioritizing in Ethiopia apply various techniques or methodologies. For example, Welde (2016), Dibaba et al., (2021), Kefay et al., (2022) and Admas et al., (2022) prioritise Tekeze Dam watershed, Fincha catchment Blue Nile Basin, the middle Awata watershed in southern Ethiopia and Ribb watershed in Blue Nile Basin using SWAT, respectively; Jothimani et al., (2020) prioritized Megech River catchment, Blue Nile Basin, using morphometric analysis; Terefe et al., (2024) prioritized Ayu watershed, Abay basin, using the Revised Universal Soil Loss Equation (RUSLE) model and the Sub-Watershed Prioritization Tool (SWPT); Ketema and Dwarakish (2020) did prioritization in Tikur Wuha watershed based on soil loss rate; using the RUSLE model; Gashaw et al., (2018) and Abro (2021) defined priority to the Geleda watershed in the Blue Nile basin and the Gotu watershed in the Awash River basin, respectively; Godif and Manjunatha (2022) and Duressa et al., (2024) prioritized Geba river basin in Tigray and Dabus watershed in Blue Nile basin using morphometric parameters of the compound factor calculation approach, respectively; Gela (2018) prioritizes Gilgel Abay watershed, Blue Nile Basin using RUSLE model and morphometric parameters using compound factors approach.

While various Ethiopian watersheds have been prioritized using the aforementioned methodologies, the Upper Awash sub-basin, the research area, has not undergone any prioritizing efforts, furthermore, there is extremely little. Three distinct criteria - morphometric, LULC, and sediment load (as determined by the SWAT model)-are crucial in this case for watershed prioritizing using the AHP-VIKOR technique. GIS and RS approach alongside multi-attribute decision-making (MCDM) tools like AHP-VIKOR with a risk assessment matrix were used to prioritize the Upper Awash sub-basin, Ethiopia.

Prior research applying morphometric parameters for watershed prioritization led to the selection of each morphometric parameter employed in this study (Dofee et al., 2024; Ren et al., 2015; Makhdumi & Dwarakish, 2019; Nasir et al., 2023; Gela, 2018). Some of the fundamental criteria considered in the morphometric parameters are area, perimeter, watershed length, watershed relief, stream order, stream number, stream length, bifurcation ratio, stream length ratio, stream frequency, drainage density, drainage texture, length of overland flow, infiltration number, elongation ratio, circularity ratio, form factor, and compactness coefficient. As it accurately reveals the amount of water within a catchment, the area is extremely important watershed property. Greater size intercepts more rainfall, more runoff, and higher peak discharge. Smaller sizes have occasionally also seen the highest levels of flooding and sedimentation. Other watershed morphometric properties, such as stream networks, relief parameters, and shape and length are accountable.

The first stage in morphometric analysis is to organize or categorize streams based on the quantity and kind of tributary connections. Since six is the highest stream order found in the sub-basin, the Upper Awash Basin belongs to the six-order type. An inverse geometric series is formed as a link between the stream order and the number of streams of a particular order (Horton, 1945). For instance, a watershed with a higher proportion of uppermost channels often have a topography that

is highly permeable to infiltration. Soft shale and slate rocks are typical of a watershed where the quantity and arrangement of streams are increased (Biswas, 2016).

The uppermost channels have the largest lengths, and stream orders go up from there (Horton, 1945). Stream length varies with the topography; longer streams are found in places with more coarse textures and lower slopes, while shorter streams are found in areas with finer textures and steeper slopes (Farhan et al., 2015). Additionally, it evaluates the hydrologic features and rock formation of the area. A lesser number of streams with longer lengths are formed relative to the porous rock layer and well-drained catchment, and vice versa (Sethupathi et al., 2011). The study measures a total stream length of 366.7 km, 342 km, 235 km, and 206 km, corresponding to SW30, SW04, SW2, and SW12, in that order. These watersheds are the uppermost channels and it is considered that sediment can be carried out downstream. Because water flows more slowly in longer streams, sediment can settle out of the water column and be transferred downstream over longer distances (Duressa et al., 2024).

Horton (1945) asserts that the bifurcation ratio (Rb) is connected to the drainage system's branching pattern, indicating the level of integration between streams of various orders. In basins without any structural influence and nearly level terrain, the Rb value is less than 3. When the Rb number falls between three and five, it indicates that the rock structure of the basin has less impact on the drainage network (Singh et al., 2020). Less structurally disrupted watersheds without any deformation in the river network are indicated by lesser Rb (Suji et al., 2015; Hindersah et al., 2018). This implies that, in the study area, structural disruptions have not impacted the drainage network in nearly every catchment. SW16 is nearly flat and less structurally disturbed compared to SW31 which is highly dissected and structurally disturbed resulting in extensive erosion and sediment transportation.

High values of stream frequency (Fs) are used to represent steep surfaces with more surface runoff. A high Fs value indicates an impermeable underlying material, high relief conditions, and low infiltration capacity. That is, the larger the Fs value, the greater the soil erosion (increased runoff) (Horton, 1932).

In the current study, drainage texture varied from 0.8 to 0.17, and all watersheds were categorized as coarse. The coarse drainage texture (Rt) values indicate low infiltration capacity, an impermeable soil layer, and excessive runoff in the basins. The more stream segments in a basin, the more impermeable the surface is (Rai et al., 2018).

The fact that the SW02 sub-catchment overland flow distance is lower than that of the other sub-watersheds suggests that the water travels through the land surface over a shorter distance. In contrast, the sub-catchment SW37 takes the highest value, suggesting that before being concentrated in stream channels, the water in SW37 tends to go farther across the land surface.

The highest infiltration number is found in SW02, this is associated with increased drainage density and overall stream frequency. This indicates that SW02 may have more opportunity for overland flow and a much lower rate of infiltration compared to the other sub-watersheds. The lowest infiltration value, on the other side, is found in SW34, which denotes a lower total stream frequency and drainage density. This implies that SW34 may have a significantly greater

penetration rate and a lower danger of overland flow than the sub-watershed. The study area is grouped as a low value of Re (elongated watershed) and has high relief and a steep slope. The area can be characterized by a poor rate of infiltration with high runoff.

In the research area, SW37 has greater circulatory ratio values (0.30). The lowest Rc value for Watershed WS8 was 0.07. The sub-basin exhibits a range of Rc values from 0.07 to 0.3, which suggests that the geologic materials are homogeneous, highly permeable, and free of structural disturbances.

The Watershed form factor ranged from 0.31 (WS24 and WS03) to 0.24 (WS04 and WS30) in the research sub-basin. Sub-watersheds with low form factors have high peak flows over shorter periods, which increases their vulnerability to water-induced mechanical erosion. Watershed form factor values < 0.78 are elongated whereas > 0.78 are circular (Sukristiyanti et al., 2018). Higher Rf values indicate higher peak flows over shorter periods, while lower Rf values indicate lower peak flows over longer periods (Horton, 1945; Chopra et al., 2005).

In the current investigation, SW37 (1.82) has a lower compactness coefficient value than SW08 (3.66) but a higher compactness coefficient overall. The sub-watershed area and shape of SW04 and SW34 have lower values, while SW05, SW13, and SW23 take substantially greater values. The lower value of Cc indicates that WS37, WS04, and SW34 are most susceptible to erosion.

Relief Ratio (Rh) increases when drainage/stream area and watershed size decrease. It ties the overall slope of the drainage area to the steepness and soil erosion in the basin. Numerous studies have found a strong relationship between Rh and loss of sediment (Schumm, 1956; Ahmed et al., 2010; Rai et al., 2018). The steepness (high slope) (Vittala et al., 2004) and elevated relief within the watershed are shown by the higher values of Rh. The runoff increases the likelihood of erosion in the basins with steeper slopes. The lower Rh value, on the other side, denotes a low slope (steepness) and low relief. Rh values that are higher indicate severe slopes and higher relief. Rh=66.81 was discovered to be the highest value that corresponds to WS34.

An extraordinarily high value of Rn arises under steep slopes (Umrikar, 2017) and high Dd values when both factors are large. These basins have been assessed to be at risk of flooding. Rn's value ranged from 0.05 (for WS08) to 0.9 (for WS34 and WS37). Slopes have higher value when they are steep and longer. The study area has high values at SW29, SW30, SW34, and SW37, and lower values at SW08, SW14, and SW36.

The higher VIKOR index (Qi) value (Table 8) for morphometric parameters indicates the highest priority and the most vulnerable sub-watershed to soil loss, however the lowest Qi value indicates the lowest priority and the least susceptible sub-watershed to soil erosion. The study area drainage has not been impacted by structural disturbances, as seen by low bifurcation ratio values and very low drainage densities for nearly all of its sub-watersheds. Additionally, the area is primarily covered by permeable and resistant formations (Das & Mukherjee, 2005). The loss of soil is influenced by morphometric factors such as form factor, elongation ratio, circularity ratio, and compactness coefficient in an inverse manner, and directly by bifurcation ratio, overland flow length, drainage density, texture, and stream frequency. This might be taken to suggest that for morphometric factors that have a direct correlation with soil erosion, larger values should be

allocated a greater rank (lower values). The ruggedness number and relief ratio measures are directly correlated with soil degradation (Puno & Puno, 2019). As previously stated, sub-watersheds with higher soil erodibility are assigned higher priorities, and the other way round.

In the VIKOR approach to determine the best and worst values of the morphometric parameters, to determine Qi values, utility, and regret metrics were computed, and the result revealed that SW17, SW18, SW27, SW29, SW31, SW33, and SW37 are the most vulnerable watersheds to soil loss and other erosive factors, as shown in

Table 4-9 and Figure 4-5. Similarly, The Qi ranges from 0.37 in WS03 to 1.0 in WS08 for the LULC parameter at v = 0.5. the result showed that SW03, WS12, and WS37 are the most vulnerable watersheds to soil loss and other erosive factors, as revealed in Table 4-10 and Figure 4-6.

According to Abbaspour (Abbaspour et al., 2015), the result indicates that the SWAT model accurately simulates streamflow. In line with the evaluation standards suggested by Moriasi et al., (2015), for the calibration and validation period, the PBIAS was very good, NSE was good and RSR was good, Table 4-12. WS18 had the lowest sediment load (2.09 t/ha/yr) and an area of 166.62 km^2, while WS35 had the highest sediment load (174.02 t/ha/yr.) and an area of 271.38 km^2.

Soil erosion is a complex process influenced by various factors including land use, climate, geology, and management techniques. Prioritising using sediment load, LULC, and morphometric analysis showed that SW8, SW13, SW14, SW16, SW21, SW22, SW23, and SW24 sub-watersheds fall under very high priority, suggesting that the most susceptible watersheds and more vulnerable to soil erosion and other erosive agents; WS06, WS09, WS10, WS25, WS30, WS35, WS36, and WS37 under high priority; WS04, WS05, WS11, WS15, WS20, WS26, WS27, WS31, and WS06, WS09, WS10, WS25, WS30, WS35, WS36, and WS37 medium priority; WS07, WS28 and WS29 low priority and WS01, WS02, WS03, WS12, WS17, WS18, WS19, WS32, WS34, and WS35 fall under very low priority concerning soil erosion, signifying that low-priority sub-watersheds natural resources are less vulnerable to the damaging impacts of precipitation and other erosive agents as illustrated in Table 4-14 and Figure 4-8.

The major purpose of this research is to identify and categorize hotspots of soil erosion sub-watersheds. However, the result will contribute to planners and decision-makers making remedial measures for different environmental issues like flood management, preventing soil erosion, improving water quality, natural resource management, and applying different conservation treatments. In addition to this, this research is crucial for major schemes, allowing planners to select approaches based on catchment area size, problem severity, funding constraints, and local and political system demands. When implementing conservation techniques for soil and water, extra attention needs to be given to the high-priority sub-catchments. To stop soil loss, rapid soil

and water conservation techniques such as contour binding, bench terracing, gully control structures, and grass waterways are needed in sub-watersheds with high and very high erosion susceptibility. Slowing down runoff, preventing gully erosion, and holding onto sediment help stop water runoff and soil erosion (Liu et al., 2019; Hindersah et al., 2018).

4.6 Conclusion

This research focuses on prioritizing sub-watersheds for intervention design using GIS and remote sensing techniques and the AHP-VIKOR Method. This approach is very important to identify and categorize hotspots of soil erosion sub-watersheds for planners and decision-makers for different environmental management purposes. Land managers may develop specific measures that reduce soil erosion and safeguard water resources after determining each sub-watershed's susceptibility to soil erosion.

Natural and human-caused degradation in drainage can affect water resource initiatives and a nation's economy by lowering crop yield. As a result, a more complete indicator of erosion risk in a watershed is the multiple values of morphometric parameters, LULC, and sediment load. For planners and decision-makers to comprehend the morphological, LULC, and sediment load characteristics of any particular sub-watershed for planning at the sub-catchment level, GIS and remote sensing approaches are more effective. The linear, areal, and relief features illustrated the watershed's hydrological characteristics, and their features were very helpful in demonstrating how each sub-watershed should be prioritized.

The morphometric parameters' accuracy and specificity may have been limited by low-resolution DEM (30 meters), which might have led to an underestimating or incorrect description of erosion-prone locations. As a result, further research is advised to use higher resolution DEM data than 30 meters to improve accuracy for conservation efforts, acquire more accurate physical data for sediment yield simulations that are more trustworthy, and capture more detail that can offer a more realistic representation of fine-scale features like small gullies, ridges, and ephemeral streams, which are essential for comprehending erosion patterns. The study prioritized watersheds based on various attributes but faced limitations like the absence of daily sediment data, geological structure, and lithology.

The results showed that 1611.43 km^2 (16.25%) in the category of extremely susceptible erosion, 2524.6 km^2 (25.45%) in the high susceptible class, 2722.14 km^2 (27.44%) in the moderate susceptible class, 854.35 km^2 (8.61%) in the class of low susceptible, and 2205.48 km^2 (22.23%) in the class of very low susceptible. The percentage of sub-watersheds classified as low and very low priority for soil erosion is just 30% (12 sub-watersheds). High and extremely high-priority areas require immediate management solutions, covering about 42% (16 sub-watersheds) of the sub-watersheds to decrease the potential for degradation. It is recommended that conservation action be taken to lower soil erosion and sediment yield in the sub-watersheds and reduce sedimentation in the Koka reservoir, which is the study area's final outlet. This is due to the very high susceptibility of the Upper Awash Basin to soil erosion.

Chapter 5 : NON-POINT SOURCE POLLUTANT LOAD MODELLING

Abstract

Non-point sources of pollution (NPSPs) originating from runoff from contaminated agricultural and populated areas are becoming a growing concern in developing countries, endangering the environment and public health. This requires systematic investigation, including modelling the likely impact using an appropriate hydrological model. This study quantified the spatiotemporal variation of the NPSP and prioritised the most vulnerable sub-watersheds. We investigated the effects of land use and cover (LULC) conversion on runoff generation and NPSP loads in terms of sediment, phosphate, total nitrogen, total phosphorus, and nitrate loading using the SWAT model. The principal source of data utilised to assess the change in NPSP loads was the 2003 and 2023 LULC. The analysis of the results showed that grassland and shrubland substantially changed, with 96.7% and 74.4% reductions, respectively, while the increase in agricultural land was 147.3% and that of built-up areas increased by 80.14%. The mean yearly increase in sediment yield ranges from 25.46 to 27,298.75 t, while the mean yearly increase in surface runoff ranges from 150.1 mm to 466.7 mm. The minimum recorded runoff was 10.69 mm (5.1%) in WS03, while the highest was 223.3 mm (66.5%) in WS02. The NO_3^- load increased from 127.6 to 20,739.7 kg, and the PO_4^{3-} load increased from 3.12 to 2459.7 kg. The TN load increased from 4465.5 to 482,014.5 kg, and the TP load increased from 1383.5 to 133,641.3 kg. The monthly analysis of nitrate loading revealed that the “Belg” season has the highest nitrate load than the rainy season, probably due to nitrification. The findings clearly showed that the inputs applied to the farms were not effectively utilised for the intended purpose. Hence, efforts must be made to ensure that nutrients remain in the catchment through an appropriate land management intervention

Keywords: nutrient load; sediment; diffuse source pollution; SWAT; Awash Basin; land use/cover change

5.1 Introduction

For aquatic ecosystems and related functions, clean water availability and quality are critical (Pulighe et al., 2020). Throughout human history, rivers have been of utmost importance. They are essential in providing the water needed for many industries, including the agricultural sector and human consumption; water is considered an important socioeconomic artery of society (Sharifinia et al., 2017). River water is a fundamental natural resource, important to many human endeavours, and is at the heart of modern society's environmental problems. Rivers and lakes are known to be more vulnerable due to contamination. To safeguard these resources, it is crucial to identify the source of pollutants and implement effective methods for their prevention or elimination. Some activities relating to human activities degrade the quality of surface waters and impair their use for households, farming, productive enterprises, and other purposes (Sharifinia et al., 2013). The release of diffuse sources of pollutants has a major impact on the river water quality of the river system. The interplay of watershed characteristics, hydrological processes, and agricultural practices ultimately influences the loss of nutrients to surface waterways (Vagstad et al., 2004). Controlling non-point source contamination is challenging because many different factors cause it. The most polluted surface waters are typically caused by diffuse sources of pollutants, which usually consist of other forms of phosphorus and nitrogen (Liu et al., 2020).

Numerous studies have demonstrated that surface and groundwater contamination may be significantly worsened by natural processes controlled by river flow, including salt, erosion, and releases of nitrogen and phosphorus (Sorando et al., 2019). During the rainy season, surface runoff collects contaminants that pollute and alter surface water's biophysical and sometimes chemical characteristics (Li et al., 2011). When contaminants from identifiable sources find their way into rivers, they are quickly identified and provided with the proper care. However, diffuse source contamination occurs when contaminants from the soil, farming lands, slums, and polluted lands (Hou et al., 2022) enter water bodies because of scouring and leaching from rainfall-runoff occurrences (Han et al., 2011). According to Assegide et al. (2022), diffuse source contamination studies in Ethiopia are limited. There has not been much research using the proof to determine how agriculture affects water quality. One of the main study gaps in the country in general and in the basin in specific is determining the relative contributions from diffuse and point sources. There has not been much research using evidence to determine how agriculture affects the quality of surface waters. Additionally, one of the main causes of Ethiopia's recent increases in water sedimentation and problems with water quality is the country's rapidly disappearing ecosystems and changing land use as a result of intensifying agriculture. Nevertheless, no study has measured how much the LULC variation affects the NPSP load (Assegide et al., 2022).

Ethiopia's recent rise in the deposition of soil and water pollution problems is mainly driven by agricultural intensification, which is causing the swift destruction of ecosystems and land-use

dynamics (Assegide et al., 2022). The increase in the use of pesticides and fertilisers to improve crop production is the primary cause of contamination (Ligdi et al., 2010). The average annual use of fertiliser in Ethiopia has been reported to have increased from 250 million kg in 2003/4 to about 850 million kg. in 2015/6 (Legesse et al., 2019), about a 3.4-fold increase in less than 10 years. Diffuse contaminants pose a significant threat to water quality and pose an uncontrollable water pollution issue (Ongley et al., 2010). Varying temporal and spatial contaminant loads, intricate systems, and random as well as uneven events are characteristics of NPS (Wang et al., 2016).

As Sebilo (2013) stated, "the soil organic matter pool and soil microbial biomass" absorb the leftover nitrogen fertiliser in cropland; of the fertiliser, 40–60% is absorbed by the crops and eliminated before harvesting (Sebilo et al., 2013). Jenkinson (Jenkinson & Parry, 1989) reports that 71% of all N input fertiliser and non-fertiliser is harvested annually, while the soil–plant system loses 29%. In the context of the study area, cereal nitrogen uptake is typically low; about thirty to forty percent of the N fertilisers used are harvested. The remaining nitrogen applied is lost through absorption and washed into the soil, where the frequent over-application of nitrogen can pollute natural ecosystems. Additionally, high N fertiliser costs lead to significant direct economic losses for growers due to the loss of N (Belete et al., 2018). Nitrate is removed from soil layers by irrigation and rain. Consequently, the weather, soil structure, and texture affect its prevalence in the soil. In sandy soils, it might be higher than in clay soils. According to Giordano (2021), some irrigated vegetables, such as lettuce plants, only absorbed 38.4% of the 150 kg/ha of nitrogen applied; the remaining 61.6% remained in the soil. It is more detrimental when vegetable-growing areas are located near waterways.

Complex and unpredictable diffuse source pollutants are very challenging to model due to their restricted capacity. However, due to the need for massive amounts of input data, modelling becomes prohibitively expensive, and calibration becomes very challenging; as a result, the usage of the physically based model is limited (Han et al., 2011). The compiled monitoring data merely show the output and do not go into detail about the reasons behind the alterations, so they fail to clarify the processes in and of themselves. Hence, SWAT can provide a full description of watershed processes through simulations, convert input data into output indications, and determine the quantity and quality of water (Neitsch et al., 2011).

The implementation of nutrient management strategies in the Upper Awash basin faces several significant challenges. These challenges stem from a combination of environmental, social, and governance factors that complicate effective management of nutrient loads in this critical region. (Mortazavi-Naeini, 2019; Taye, 2018). Effective nutrient management strategies must address both the sources of nutrient pollution and the methods for mitigating its impacts on water quality. The primary sources of nutrient pollution in the Upper Awash basin include: Agricultural Runoff, Urbanization and Industrial Discharges and Domestic Waste. Agricultural practices contribute significantly to nutrient loading in rivers through fertilizers and pesticides. Approximately 29% of surface water pollutants originate from agricultural activities (Bussi, 2021). Urban growth has led to increased wastewater production, which often enters waterways without adequate treatment.

This contributes to nutrient loads, particularly nitrogen and phosphorus (Degefu, 2013). Domestic waste disposal practices contribute significantly to nutrient loading, with contamination from household waste being a major concern (Alemayehu, 2001). By addressing both anthropogenic and natural sources of nutrients through comprehensive management strategies, it is possible to improve the overall health of the Upper Awash basin's ecosystems while ensuring safe drinking water for local communities.

Understanding the degree of geographical variation in erosion and related causes can be aided by describing the main methods for assessing soil erosion and the corresponding erosion rates. On cultivated LULC, average erosion rates are estimated to be between 50 and 179 t/ha/year (Adimassu et al., 2017). In the Ethiopian highlands, extreme cases can result in soil loss of up to 300 t/ha (Hurni et al., 2015). According to Tamene (2022), Ethiopia's rate of yearly soil loss varies from 0 to 220 t/ha. Ethiopia loses 1.5 billion tonnes of topsoil annually (Bihonegn & Awoke, 2023), with an average sediment production of 21.43 tonnes/ha/year in the middle and upper Awash (Jilo et al., 2022).

The hydrodynamic properties of the water largely determine the spatiotemporal variation in water quality that various types of lakes and rivers exhibit (Rothman et al., 1982). To address the environmental problems of the current land administration, decision-makers should use modelling techniques on a sub-catchment basis to evaluate the potential implementation of top management techniques and alternative scenarios (Pulighe et al., 2020). The primary goal of the current investigation is to examine changes in LULC and their effects on runoff and non-point source pollutant loads (sediment, total nitrogen, total phosphorus, and nitrate). Further, it has also attempted to quantify spatiotemporal diffuse source pollutants and map the sub-watersheds according to pollutant loads.

5.1 Study Area

The western edge of the main Ethiopian Rift is where the upper Awash basin (upstream of Koka Reservoir) is situated in central Ethiopia, between 8°23′09″ and 9°18′14″ latitude and 37°57′15″ and 38°41′08″ longitude. The climate is considered humid to sub-humid in the highlands and semiarid in the lowlands, with an average yearly temperature range of 15 to 20 °C. An average annual precipitation, strongly controlled by elevation, varies from 800 to 1400 mm. In Ethiopia, the primary wet period, Kiremt, typically lasts from June to September. It is followed by "Belg", which occurs from March to May (Tolera et al., 2018). At least 15.7 million people, or almost 17% of Ethiopia's total population, live in the upper Awash basin (UAB), which also contains Addis Ababa, the country's capital (Chan et al., 2020) (see Figure 5-1). This has put pressure on the catchment of resources related to land and water (Arnold et al., 1998).

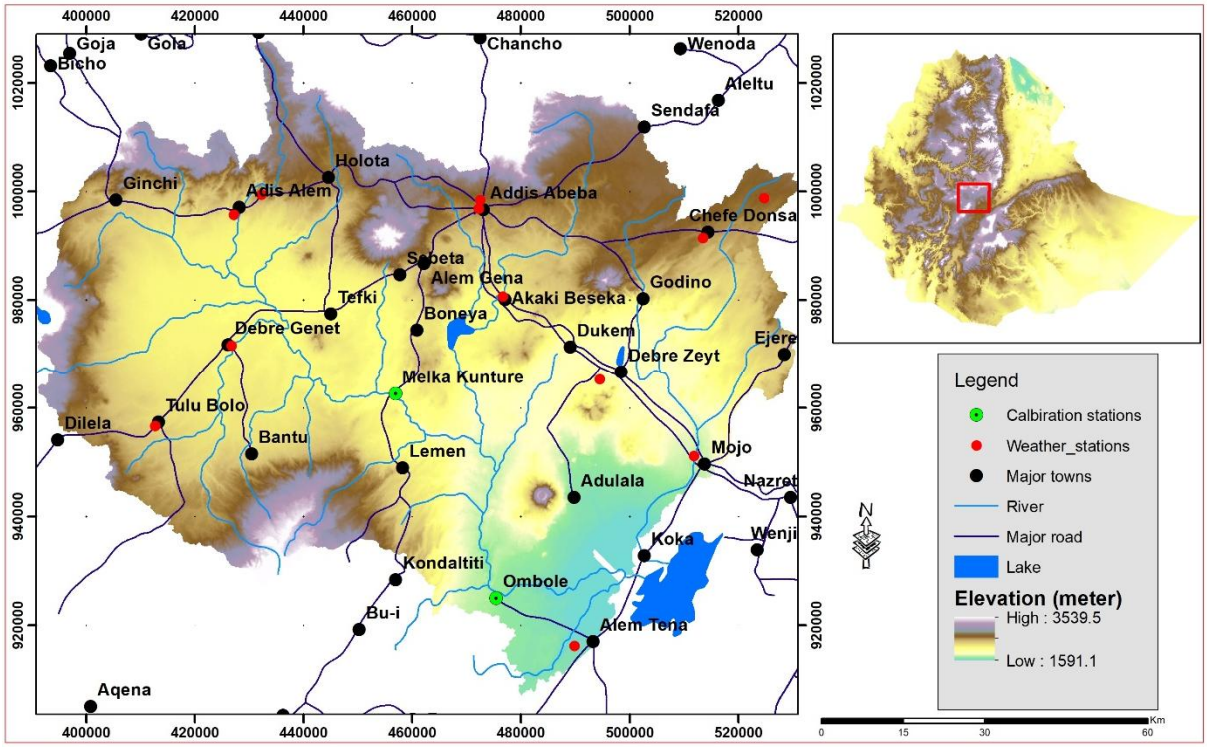

Figure 5-1 Map of the study area

5.2 Data and Methods

5.3.1 SWAT model

Arnold (1998) created the physically grounded, geographically semi-distributed SWAT watershed model (Alves et al., 2019). It operates continuously and facilitates the modelling of physical processes inside a watershed. SWAT simulates and predicts runoff, sediment load, and use of agricultural chemicals for big and intricate watersheds using different soil and LULC overextended times (Green & Ampt, 2011). The hydrological and pollutant processes of precipitation, streamflow, sediments, and loads of phosphorus and nitrogen are all simulated by SWAT (Uribe et al., 2018). Each hydrological response unit's (HRU) hydrological components are computed using water balance, which also provides the main streamflow and hydrological balance. In the model, hydrology is separated into two stages: the land phase regulates water flow to the main channel, while the routing phase governs water movement within the network of channels (Neitsch et al., 2011).

$$\mathrm{SW}_t = \mathrm{SW}_o + \sum_{i=1}^{t}\left(R_{\mathrm{day}} - Q_{\mathrm{surf}} - E_a - w_{\mathrm{seep}} - Q_{gw}\right) \quad \text{……..(1)}$$

As mentioned by Tessema (2015), "SW_t is the final soil water content (mm), SW_o is the initial soil water content on day i (mm), t is the time (days), R_{day} is the amount of precipitation on day i (mm), Q_{surf} is the amount of surface runoff on day i (mm), E_a is the amount of evapotranspiration on day i (mm), w_{seep} is the amount of water entering the vadose zone from the soil profile on day i (mm), Q_{gw} is the amount of return flow on day i (mm)".

The model offers two approaches to surface runoff computation: as Alves stated, the "Soil Conservation Service (SCS) curve number (CN)" method (Alves et al., 2019) and the "Green & Ampt infiltration" method (Green & Ampt, 2011). Since the second approach needs sub-daily precipitation data, the SCS CN technique was applied in this investigation. The CN is a comparison parameter between 0 and 100. For a specific landscape status, it depicts the soil, LULC, and antecedent soil moisture conditions. Based on mean "antecedent soil moisture conditions" (CN2), the typical SWAT technique employs CNs for different soils and land cover situations. Two distinct approaches to computing the retention parameter are incorporated into the model. Field capacity, wilting point, and saturation water content are indicators of the amount of water in the soil horizon, and these can be used to adjust the retaining parameter as part of the initial procedure. As with the other approach, the retention parameter can be allowed to alter in line with the total plant evapotranspiration, which determines the daily curve number mainly depending on the previous climate. This study used the latter approach (Tessema et al., 2015).

Potential evapotranspiration (PET) can be estimated using three methods: Hargreaves, Priestley–Taylor, and Penman-Monteith, which require air temperature, solar radiation, relative humidity, and wind speed (Attanasi et al., 1973; Hargreaves & Samani, 1985; Li et al., 2011). The Penman-Monteith and variable storage (Williams, 1969) coefficient methods were used to estimate runoff and ET, respectively.

Because the curve number approach was applied, the difference between runoff and precipitation determines how much water passes through the soil horizon. Modelling the infiltration rate in fewer time steps is problematic because of the daily timeframe of the rainfall data. Kinematic storage models compute lateral subsurface flow from a saturated area of soil horizons, contributing to streamflow, but base flow, part of streamflow, has its origin from recharged shallow aquifers through percolation. Water that enters the shallow aquifer is considered removed from the system; in SWAT, base flow is only allowed to enter the reach if the volume of water stored in the shallow aquifer surpasses the minimum limit the user has selected. The Manning equation defines the flow's velocity and rate (Tessema et al., 2015).

According to Zhang and Wu (2013) and Neitsch (2011), SWAT simulates the transformation and movement of nitrogen and phosphorus in several organic and inorganic pools (Figure 5-2). The soil nitrogen cycle is simulated by using five different pools; two are inorganic forms (ammonium and nitrate) while the other three are organic forms (fresh, stable, and active). The SWAT model simulates movement between N pools, such as mineralization, decomposition and immobilization, nitrification, denitrification, and ammonia volatilization. Other soil N processes - such as plant uptake, N fixation by legumes, and NO_3^--N movement in water are also included in the model. Nitrates are removed from soil with surface and subsurface runoff, while the amount of organic N transported with sediments is calculated as a function of organic N in the topsoil layer and the sediment yield. The loading function estimates daily organic nitrogen runoff loss based on the concentrations of constituents in the topsoil layer, the sediment yield, and an enrichment ratio. Nitrate export with runoff, lateral flow, and percolation are estimated as products of the volume of water and the average concentration of nitrate in the soil layer. Once N enters channel flow, the SWAT model partitions N into four pools: organic N, NH_4^+-N, Nitrite-N (NO_2^--N), and NO_3^--N.

The SWAT model simulates N changes that result in N movement between pools. SWAT simulates six different pools of phosphorus in soil; three are inorganic forms, and the rest are organic forms. Transformations of soil P among these six pools are regulated by algorithms that represent mineralization, decomposition, and immobilization. The solution (labile) pool is considered to be in rapid equilibrium (days to weeks) with active pools that subsequently are considered to be in slow equilibrium with stable pools. The amount of soluble P removed in runoff is predicted by using labile P concentration in the topsoil layer, the runoff volume, and a phosphorus soil partitioning factor. The sediment transport of P is simulated with a loading function similar to the organic N transport. In-stream P dynamics in SWAT are also simulated by using two state variables, inorganic and organic P, adopted from the QUAL2E model (Brown & Barnwell, 1987).

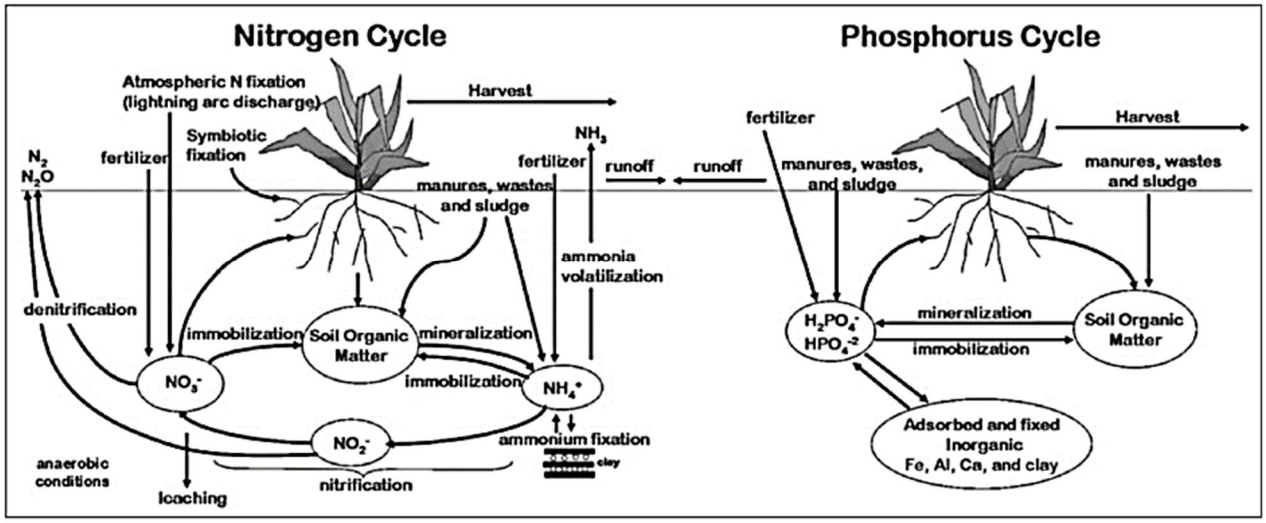

Figure 5-2 Figure Nitrogen and phosphorus cycles modeled by SWAT (Neitsch et al., 2011; Zhang & Wu, 2013)

The SWAT model simulates the movement of P from the landscape into surface runoff as:

$$P_{surf} = \frac{P_{solution,surf}\ Q_{surf}}{\rho_b\ depth_{surf}\ k_{d,surf}}$$

Where P_{surf} is the amount of soluble P transported by surface runoff (kg P ha^{-1}), $P_{solution,\ surf}$ is the amount of labile P in the top 10 mm (kg P ha^{-1}), Q_{surf} is the amount of surface runoff on a given day (mm), and $k_{d,\ surf}$ is the P soil partitioning coefficient (m^3mg^{-1}) (Neitsch et al., 2002).

5.3.2 Model setup

The model configuration was carried out utilising ArcSWAT version 10.21.10_5.24, released on 19 August 2020, an ArcGIS extension of a menu-driven interface for SWAT. Using the 30 m

DEM, the watershed was first defined, then split into 37 sub-watersheds, and the drainage patterns were examined. Using the limit area choice to define a sub-watershed's minimum area, the stream definition was created, which was 8000 ha. Due to the availability of calibration and validation data and the nested-scale gauging sites, at the moment, two sub-catchment pour points were manually created: Hombole station for the calibration and validation of flow and sediment data and Melka Kunture for the validation of flow and sediment data and calibration and validation of nutrients to confirm the model performance. Second, HRUs were defined using LULC, soil, and slope datasets, with multiple HRUs defined using a 20-10-20 (Winchell et al., 2018) threshold for optimal criteria in each sub-watershed. Third, to simulate soil, weather, plant cover, management operations, and urban activities, meteorological data were inserted to build data tables, and a built-in database was needed for model setup. In addition to this, the amount at which fertilisers are applied was updated by editing a default input table for plant growth. Finally, to conduct the SWAT modelling procedure, dates ranging from January 1979 to December 2019 were set up; see Table 5-1 for the input data. For every sub-watershed, the SWAT auto-irrigation choice was implemented.

Table 5-1 Sources, spatial resolution, and type of input data for the SWAT model.

Data Type	Spatial Resolution/Period	Source
DEM	30 m	https://earthexplorer.usgs.gov/ accessed on 31 October 2021
LULC	10 m (2023), 30 m (2003)	https://earthexplorer.usgs.gov/, accessed on 17 February 2023 https://scihub.copernicus.eu/, accessed on 16 February 2023
Soil map	1:250,000	Water and Land Resource Center (WLRC)
Rainfall and temperature	1979–2019	National Meteorological Agency (NMA)
Solar radiation, relative humidity, and wind speed	1979–2019	https://climatedataguide.ucar.edu/climate-data accessed on 18 July 2023
Observed stream flow	Daily	Ministry of Water and Energy
Observed sediment	Monthly	Ministry of Water and Energy
Observed nutrient quality	Monthly (2009–2019)	Ethiopian Construction Design and Supervision; field observation by the researcher.

5.3.3 Data Collection and processing

Data quality is crucial for the accuracy and reliability of the SWAT (Soil and Water Assessment Tool) model outputs. Poor-quality input data can lead to incorrect simulations, which may affect decision-making processes related to water resource management. The SWAT model requires various types of input data, including climate, soil, land use/cover, topographic, hydrological, sediment, and nutrient data.

Before researching detailed assessments, preliminary checks are performed on the datasets. Completeness (ensure that all required data fields are present without missing values), consistency (verify that data formats are uniform across datasets (e.g., date formats), and timeliness (confirm that the data is up-to-date and relevant for the study period). Additionally, graphical observations

are performed to check for outliers, which indicate mistakes in data gathering, and minimum and maximum values are reviewed to comprehend data distributions. In addition, sensitivity analyses are conducted to determine how variations in input parameters affect model outputs. This can highlight which inputs are most critical for model performance and warrant closer scrutiny regarding their quality. By following these steps systematically, researchers can ensure that their SWAT model inputs are of high quality, leading to more reliable modeling outcomes.

Monthly sediment from 1992 to 2018 was calculated using sediment data from two chosen surface-water observation points in the upper Awash River Basin (Hombole and Melka Kunture gauging stations). LOADEST can be a useful tool for estimating loads and filling in those gaps and missing data (Ouyang, 2022). Using the Load Estimator (LOADEST) tool, data gaps or missing data were filled using regression techniques describing the data on stream flow and suspended material gathered at the chosen observation points (Kaleab et al., 2013), as revealed in

Figure ***5-3***. LOADEST aids in the creation of regression models that estimate nutrient loads over a user-defined time interval. It is used to generate the continuous time series of each constituent load. These models are based on streamflow, time, and additional user-specified variables (Noori et al., 2020; G. Wang et al., 2016). Regression techniques are statistical methods used to model the relationship between a dependent variable and one or more independent variables. Among the statistical techniques in the LOADEST, simple linear regression was used to estimate sediment based on the observed data; Simple linear regression is employed in LOADEST due to its effectiveness in modeling the relationship between two variables: the concentration of sediment and the corresponding discharge (flow rate) of water. The basic premise of simple linear regression is that it can identify a linear relationship between these two variables, allowing for predictions about sediment load based on measured flow rates. This could be used to relate the dependent variable (sediment concentrations) and the independent variable (flow rates) (Kim et al., 2018). In SWAT modelling, LOADEST has been widely used to estimate monthly or annual loads and to create continuous data from discrete data (Han et al., 2023; Lee et al., 2018; Noori et al., 2020).

5.3.4 LULC Mapping and LULC Change Analysis

Utilising the supervised classification approach, LULC variations were mapped. Sentinel 2A image bands with 10 m spatial resolution satellite imagery were the primary source for layer stacking and image sub-setting using the study area boundary. Second, before image classification, the LULC categories were determined by field observation experiences, previous knowledge, and visual inspection of the image and the Google Earth images. Subsequently, representative training areas for every LULC category were chosen from uniform pixels in the satellite image. Lastly, their areas were determined, and the maximum probability classification was applied using the area of interest. The LULC change in the study region was analysed using the LULC data from 2003 and 2023 as input for the change detection analysis. A Sankey diagram is a visualisation used to depict the change from the 2003 set of values to 2023.

5.3.5 Calibration, parameterization and uncertainty analysis

SWAT-CUP is a freeware package developed by Abbaspour (2007) that allows applying distinct methods to improve the SWAT model. Additionally, the SWAT-CUP software version 5.1.6 allows for uncertainty and sensitivity analysis of various hydrological parameters (Narsimlu et al., 2015; Thavhana et al., 2018). As stated by (Abbaspour et al., 2007; Gholami et al., 2016; Kaleab et al., 2013; Narsimlu et al., 2015; Thavhana et al., 2018; Winchell et al., 2018), "the optimizing algorithms include Generalized Likelihood Uncertainty Estimation (GLUE), Parameter Solution (PararSol), Markov Chain Monte Carlo (MCMC), and Sequential Uncertainty Fitting version 2 (SUFI2)". The computational speed of the SUFI2 algorithm is very high, and previous studies have found it to be better than the other algorithms in determining uncertainty (Cui et al., 2015; Emiru et al., 2022; Maroneze et al., 2014). In this study, the SUFI-2 algorithm was utilised to assess the sensitivity of the model inputs (Gholami et al., 2016) before calibration.

A. Sensitivity analysis

Finding the important parameters that influence model performance during calibration is the primary goal of the sensitivity analysis (Emiru et al., 2022). By measuring how quickly model outputs alter in response to given modifications in the parameters of the model, sensitivity analysis aids in observing the parameters that are most sensitive and, consequently, the driving watershed processes (Srinivasan et al., 2012). Equation (2) represents the multiple regression used in SUFI2 for calculating the parameters' sensitivity, which uses Latin hypercube sampling from user-defined parameter ranges versus the objective function values (Maroneze et al., 2014).

$$g = \alpha + \sum_{i=1}^{m} \beta_i b_i \qquad \ldots\ldots\ldots\ldots\ldots\ldots\ldots 2$$

where g is the objective function, α and β are the variables, and b_i is the parameter. The sensitivity of b_i is determined using the *t*-test, and the significance of parameter sensitivity is determined by the value of p (Cui et al., 2015; Maroneze et al., 2014).

The sensitivity analysis considered 14 input parameters, including flow, sediment, nitrate, total nitrogen, and total phosphorus and started with baseline values gathered from the literature (Misaghi et al., 2020).

The p-factor, computed at the 2.5% and 97.5% levels of the cumulative dispersion of the output variable obtained using Latin hypercube sampling, is the proportion of the historical data related by the 95% prediction uncertainty (95PPU) (Abbaspour, 2015). The r-factor is the product of the standard deviation of the observed data and the mean width of the 95PPU band (Abbaspour, 2015). According to Misaghi et al. (2015), based on the circumstances, an r-factor value of roughly 1.0 and a "P-factor" value of >0.7 are acceptable for streamflow simulation.

The parameters calculated by the SWAT and the monitored data must be included because this process is executed in tandem with the calibration process. This is required because the sensitivity is determined based on the objective function variations that assess the efficacy of the model

calibration (Maroneze et al., 2014). Unlike one-at-a-time sensitivity analysis, SWAT-CUP employs global sensitivity analysis, which involves altering the parameters (Misaghi et al., 2020). We considered observed and simulated data as well as the most sensitive parameters to alter streamflow, sediment, and water quality in the area; the greater value of the t-stat and the smaller *p*-value were taken as more sensitive parameters during the analysis.

B. Calibration and validation

In SUFI-2, theoretically, the value for P-factor ranges between 0 and 100% (the percent of observations bracketed by the 95PPU), while that of r-factor ranges between 0 and infinity (the thickness of the 95PPU) (Abbaspour, 2012). A p-factor of 1 and r-factor of zero is a simulation that exactly corresponds to observed data (Abbaspour et al., 2007). A value of less than 1 is a desirable measure for the r-factor (Abbaspour, 2012). The strength of calibration is judged relative to these benchmark values. Daily river flow data were used for model calibration and validation (Takele & Kebede, 2018). Monthly sediment and nutrient data were used sediment and nutrient calibration and validation.

Different datasets may be required to evaluate model performance for different environmental conditions (Moriasi et al., 2007). However, the number of attributes and the observation period required for proper consideration of the driving watershed processes may vary from site to site. Long-term and good-quality data is especially rare for the Ethiopian highlands. In the present study, the entire simulation period is limited to field observation data from 1979 to 2001 (calibration) and 2002-2018 (validation),

Figure ***5-3***. The split-sample calibration/validation was performed with a warm-up period of five years to minimize the effect of non-equilibrium initial conditions (Veltman et al., 2018). In this research, daily streamflow, sediment yield, and nutrient load recorded at the outlet of the watershed were used for model calibration/validation. Calibration was performed for sub-watershed number 33 (Hombole station) and for watershed outlet number 23 (Melka Kunture) using observed monthly average stream flow and sediment data (Figure 5-1). Nutrients were calibrated at Melka Kunture, no water quality data were available at Hombole (Migliaccio & Chaubey, 2010).

Firstly, the hydrological component was calibrated then the sediment component (Im et al., 2007) and finally the nutrient component.

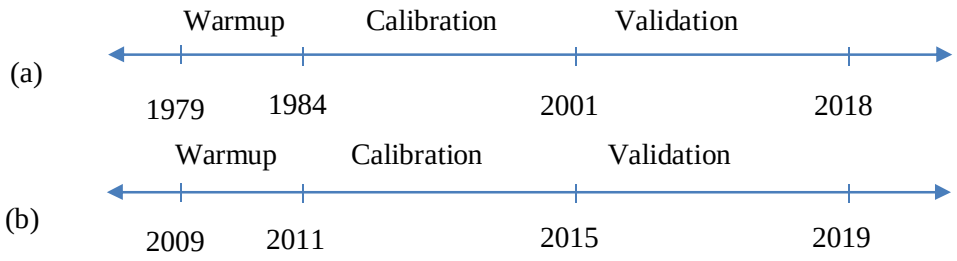

Figure 5-3 The calibration and validation periods for stream flow, sediment (a), and nutrient (b).

5.3.6 SWAT Model Performance Assessment

The degree of a model's accuracy, consistency, and flexibility must be taken into consideration while assessing its performance (Takele & Kebede, 2018). The evaluation of SWAT hydrologic and pollutant estimations can be performed using a wide range of statistical methods; for example, Moriasi (2007) lists around 15 statistical tests that can be used to evaluate the accuracy of watershed simulation models. Statistical evaluation should carefully consider daily and monthly data characteristics as well as other properties of the model output to customise statistical analysis for the given application. To simulate observed streamflow, the model's efficiency and performance were evaluated by a variety of metrics, including the p-factor, r-factor, coefficient of determination (R2), Nash–Sutcliffe (NSE), percent bias (PBIAS), and observation standard deviation ratio (RSR) (Moriasi et al., 2007). Earlier SWAT research usually used the Nash–Sutcliffe coefficient and the R2 coefficient for evaluation (Coffey et al., 2004). In addition, graphical techniques were used in this study. Legates and McCabe (Legates, 2007) assert that graphical methods are necessary for a proper model evaluation. Model bias, variations in peak flow timing and amplitude, and recession curve form can all be detected with the use of visual analysis (Mendez et al., 2022).

The NSE ranges from $-\infty$ to +1, where a value of 1 indicates full agreement between the observed and simulated results. The overall likelihood of the simulation results to differ from the observed data, either more or less, is measured by PBIAS. Zero demonstrates accurate simulation; positive values show underestimation bias and negative values signify overestimation bias (Moriasi et al., 2007). The ratio of the root mean square error (RMSE) to the observed data's standard deviation is known as the standard deviation ratio (RSR). It ranges from a high positive value to the ideal value of 0. The model simulation performance improves with decreasing RSR and decreasing RMSE (Golmohammadi et al., 2014). The suggested ranges explain the model's performance, as shown in Table 5-2 (Almeida et al., 2018).

$$\mathrm{NSE} = 1 - \frac{\sum_{i=1}^{N}(Q_{i,m} - Q_{i,s})^2}{\sum_{i=1}^{N}(Q_{i,m} - \overline{Q_m})^2} \tag{3}$$

$$\mathrm{RSR} = \frac{\sqrt{\sum_{i=1}^{n}(Q_m - Q_s)^2}}{\sum_{i=1}^{n}(Q_m - \bar{Q})^2} \tag{4}$$

$$\mathrm{PBIAS} = 100^* \frac{\sum_{i=1}^{N}(Q_{i,s} - Q_{i,m})}{\sum_{i=1}^{N}(Q_{i,m})} \tag{5}$$

While Q_s *is simulated runoff,* Q_m *is measured runoff.*

Table 5-2 Classification of statistical indices for model evaluation.

Performance Rating	PBIAS			RSR	NSE
	Stream Flow	Sediment	N and P		
Very good	PBIAS ≤ ±10	PBIAS ≤ ±15	PBIAS ≤ ±25	0.00 ≤ RSR ≤ 0.50	0.75 < NSE ≤ 1.00
Good	±10 < PBIAS ≤ ±15	±15 < PBIAS ≤ ±30	±25< PBIAS ≤ ±40	0.50 < RSR ≤ 0.60	0.60 < NSE ≤ 0.75
Satisfactory	±15 < PBIAS ≤ ±25	±30 < PBIAS ≤ ±55	±40 < PBIAS ≤ ±70	0.60 < RSR ≤ 0.70	0.36 < NSE ≤ 0.60
Bad	≥±25	PBIAS ≥ ±55	PBIAS ≥ ±70	RSR > 0.70	≥±0.36

5.3 Results and Discussion

5.4.1 Change in the Land use land cover

With Google Earth images and local knowledge of the area, an accuracy assessment of the LULC classification was performed for each of the corresponding periods. The classification's overall accuracy was 91.2%. The proportion of the entire area, as well as its spatial variation of the eight LULC types for 2003 and 2023, are shown in Figure 5-4. The results show that agricultural land covers 31.46% and 77.9%, shrub land covers 58.4% and 14.9%, forest covers 4.06% and 2.13%, and the built-up area covers 2.52% and 4.54% for 2003 and 2023, respectively. In the study area, cropland has the major contribution with a loss of grassland, shrub, forest, and wetland, respectively (Figure 5-4 and Figure 5-5), showing the LULC.

The study area experienced a decrease in forest land due to agricultural expansion, while the built-up area gradually increased from 2.01% to 15.51% throughout the study period. This is due to the rise in urbanisation and interest in land for commercial or industrial purposes. The overall LULC change between 2003 and 2023 statistics for each year and sub-catchment is presented in Appendix C Table 1. The analysis shows that during the past 20 years, there has been an increase in built-up area and agricultural land while there has been a significant reduction in wetlands, water, forests, shrubs, and grasslands. Agricultural land increased by 147.29% throughout the study period, followed by built-up area by 80.15%. This results from population growth, which raises the demand for land for investment, legal and unofficial settlements, and various agricultural products like cereal crops. The forest, grassland, and shrubland were diminished by 47.55%, 96.7%, and 74.37%, respectively. This might be due to deforestation activities and the clearing of shrubland that have been made for investment, urbanisation, and farming. The direction of transformation from one LULC to another LULC, the percentage of transformation, and the change matrix are presented in Figure 5-4, Figure 5-5, and Table 5-3.

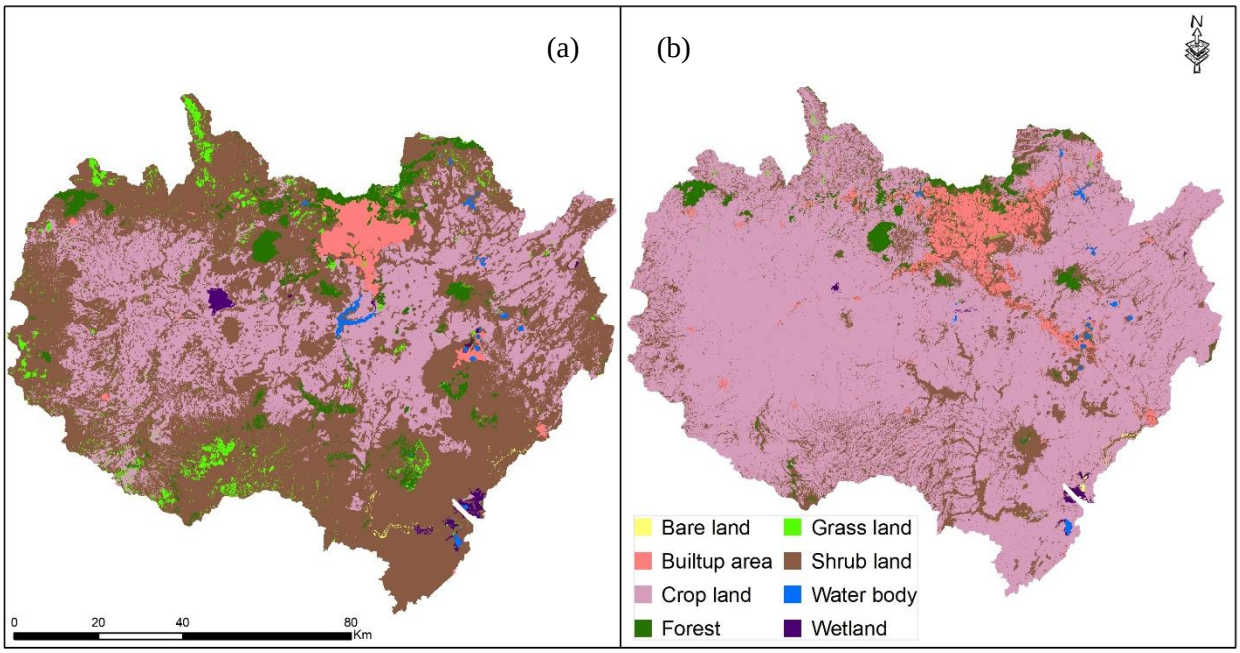

Figure 5-4 Land use land cover map of 2003 (a) and 2023 (b)

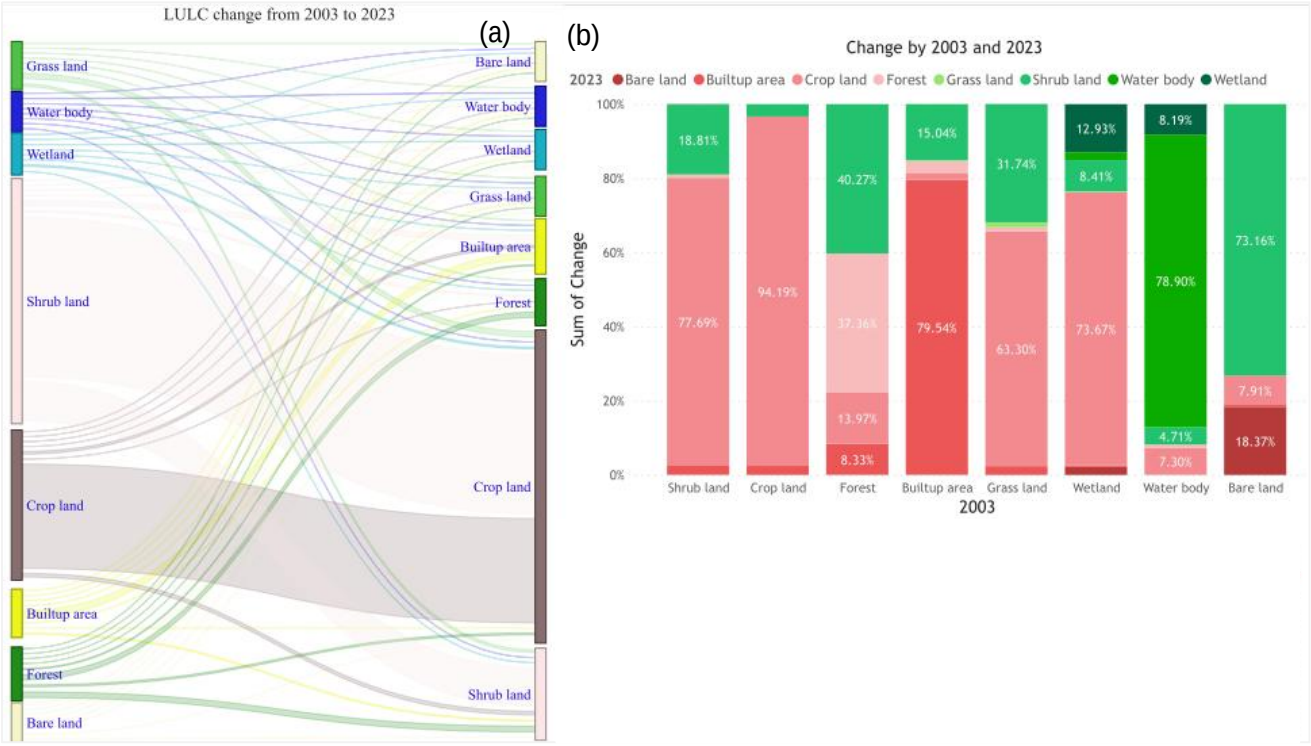

Figure 5-5 LULC change of upper Awash sub-basin(2003-2023)The figure shows direction of transformation (a), and sum of change (b)

Table 5-3 Land use land cover change matrix of Awash sub-basin (2003-2023)

	2023							
2003	Bare land	Builtup area	Crop land	Forest	Grass land	Shrub land	Water body	Wetland
Bare land	170.27	4.70	73.31	0.00	0.00	678.17	0.47	0.00
Builtup area	18.16	19,885.96	475.02	788.05	55.88	3,760.13	18.40	0.01
Crop land	79.61	7,516.64	293,848.17	87.01	29.47	10,379.77	39.90	9.35
Forest	16.95	3,353.61	5,627.43	15,048.11	0.00	16,218.20	7.82	1.52
Grass land	2.32	582.95	15,503.08	267.24	338.77	7,773.57	5.04	18.18
Shrub land	517.85	13,651.25	450,243.33	4,896.71	367.07	108,985.91	319.82	572.35
Water body	0.01	1.42	142.88	16.13	0.00	92.27	1,544.75	160.35
Wetland	155.22	33.11	5,385.90	1.67	16.91	614.73	157.29	945.55

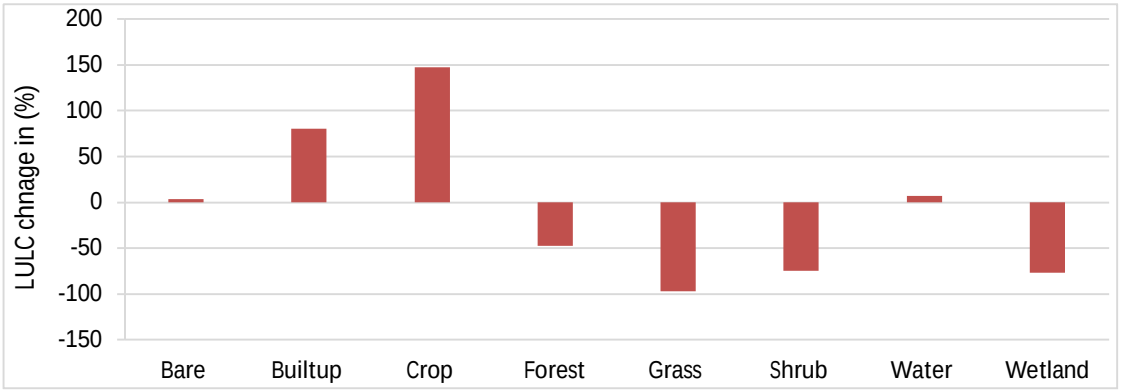

Figure 5-6 LULC rate of change from 2003 to 2023 in percent

The results of this study's land use/cover analysis align with prior research in the region. Alemayehu (2019) reports that the LULC change detection study showed declining trends in the covering of pasture, woodlands, and shrublands, and a notable increase in the amount of cropland and urban areas. LULC change matrices of the research showed that throughout the sixteen years (1984-2000), a higher rate of conversion from shrubland to farmland area was noted. According to (Tadese et al., 2020)**,** cropland grew by 12% between 1988 and 2002 and by 15% by 2018; in the same way, the research revealed that between 1988 and 2002, the built-up area increased by 184%, reaching 225% by 2018. According to the data, throughout the 30-year study period, forest and shrubland decreased by 4% and 25%, respectively, as farmland and built-up area increased at the expense of these natural resources. Therefore, this desertation research analysis makes it evident that the shift in land use and cover will continue as the population grows and there is a direct correlation between the demand for residential and agricultural land. This will have a significant socioeconomic and environmental impact in general.

5.4.2 Hydrological Model output

1. Sensitivity analysis

Thirteen hydrological, ten sediment-related, and nine nutrient-related factors were chosen for further SWAT calibration as a result of the sensitivity analysis. Table 5-4 lists the ranking of 14 parameters based on their smaller p-value and a higher absolute value of the t-stat. The identified parameters broadly correspond to previous studies in this geographical region (Tang et al., 2012).

Each parameter's relative significance is determined using the t-test and p-value values. The t-stat is the ratio of the parameter coefficient to its standard error. Parameters with a p-value less than 0.05 are taken as sensitive. The relative significance of each parameter is ascertained using the t-test and p-value. With a p-value of less than 0.05, parameters are considered sensitive. The t-stat measures the ratio of a parameter coefficient to its standard error.

Table 5-4 Descriptions of calibrated parameters; the statistical index values of "p-value" and "t-stat"

Flow Parameter	Parameter Description	t-Stat	*p*-Value
V_RCHRG_DP.gw	Deep aquifer percolation fraction	−7.363	0.000
V_CH_K2.rte	Effective channel hydraulic conductivity (mm/h)	6.386	0.000
R_CN2.mgt	SCS curve number for moisture condition II	−2.062	0.040
V_ALPHA_BF.gw	Base flow alpha factor (days)	1.203	0.230
V_SURLAG.bsn	Surface runoff lag time	−1.120	0.263
V_CANMX.hru	Maximum canopy storage	−1.103	0.271
R_USLE_K(..).sol	Soil erodibility factor in USLE	−0.955	0.340
V_GW_DELAY.gw	Groundwater delay (days)	−0.863	0.389
V_REVAPMN.gw	Threshold depth of water in the shallow aquifer (mm)	−0.733	0.464
V_GW_REVAP.gw	Groundwater revap coefficient	0.589	0.556
R_OV_N.hru	Overland Manning roughness	−0.529	0.597
R_SOL_BD(..).sol	Moist bulk density (Mg/m^3 or g/cm^3)	−0.469	0.639
V_GWQMN.gw	Threshold depth of water in the shallow aquifer (mm)	0.321	0.749
R_SOL_AWC(..).sol	Available water capacity of the soil layer (mm/m)	−0.072	0.943
Sediment			
V_CH_D.rte	The average depth of the main channel	12.411	0.000
R_SLSUBBSN.hru	Average slope length (m)	2.868	0.004
A_CH_COV2.rte	Channel cover factor	−2.554	0.011
R_HRU_SLP.hru	Average slope steepness (m/m)	−2.072	0.039
A_CH_ERODMO(..).rte	Channel erodibility factor	1.023	0.307
V_CH_W2.rte	Average width of channel at the top of the bank (m)	−0.997	0.320
V_SPEXP.bsn	Exponent parameter for calculating the channel sediment routing	0.951	0.343
A_USLE_P.mgt	The USLE equation supports the parameter	−0.489	0.625
A_USLE_C{..}.plant.dat	Min value of USLE C factor applicable to the land cover/plant	−0.003	0.998
R_CH_BED_TC.rte	Critical shear stress of channel bed (N/m^2)	−0.001	0.999
Nutrient parameter			
R_RS5.swq	The organic P settling rate	1.822	0.069
R_PPERCO.bsn	Phosphorus percolation coefficient (10 m^3/Mg)	−1.532	0.127
R_P_UPDIS.bsn	Phosphorus uptake distribution parameter	−1.369	0.172
R_ERORGP.hru	P enrichment ratio with sediment loading	−1.098	0.273
R_GWSOLP.gw	Concentration of soluble phosphorus in groundwater (mg P/l	0.888	0.375
R_USLE_P.mgt	USLE support practice factor	0.825	0.410
V_PSP.bsn	Phosphorus availability index	−0.410	0.682
R_BC4.swq	Rate constant for mineralisation of organic P to dissolved P in the reach at 20 °C (1/day)	0.115	0.908
R_PHOSKD.bsn	Phosphorus soil partitioning coefficient	0.011	0.991

2. Flow Calibration and Validation

The calibration and validation were conducted using daily streamflow data at the Hombole gauging station with the fourteen most influential model parameters, as shown in Table 5-5 (Leta et al., 2022). The monthly runoff calibration and validation results (Figure 5-7 a) show a p-factor of 0.94 and r-factor of 0.94 during the calibration period (1979–2001) and a p-factor of 0.92 and r-factor of 0.8 during the validation period (2002–2018). The Melka Kunture gauging station, used for validation, had a p-factor of 0.63 and an r-factor of 0.94 from 2002 to 2018, as shown in Figure 5-7 b.

A p-factor of above 0.70 and an r-factor of under 1.5, according to Abbaspour (Abbaspour et al., 2015), indicate that the model accurately simulates streamflow. During the calibration and validation phases, a significant portion of the data was enclosed by the 95PPU at Melka Kunture, 0.63. For the calibration and validation period at Hombole, the PBIAS was very good, the NSE was good, and the RSR was good, following the evaluation criteria proposed by Moriasi (2015), as shown in Table 5-5.

Visually, flow models at calibration sites generally compared well to observed flow data, except in 1986 and 1994, as shown in . Similarly, the flow simulations for the validation periods generally matched the measured flow records, except for the years 2013 and 2016–2018 at Hombole (Figure 5-7). The input uncertainty connected to rainfall data and measured flow data is most likely the cause of differences between simulated and measured flows.

The model, according to the results, accurately represents the flow characteristics in the upper Awash basin. The scatter plot (Figure 5-8a) shows the relationship between observed and simulated flows, with moderate correlation at Hombole during calibration.

Table 5-5 Calibration and validation statistics of Hombole and Melka Kunture gauging stations

	Period	**Observatory**	**p-Factor**	**r-Factor**	**PBIAS**	**RSR**	**R^2**	**NS**
Calibration	1979–2001	Hombole	0.94	0.94	4.6	0.58	0.68	0.67
Validation	2002–2018		0.92	0.8	5.4	0.57	0.68	0.67
Validation	2002–2018	Melka Kunture	0.63	0.94	−4.3	0.58	0.69	0.66

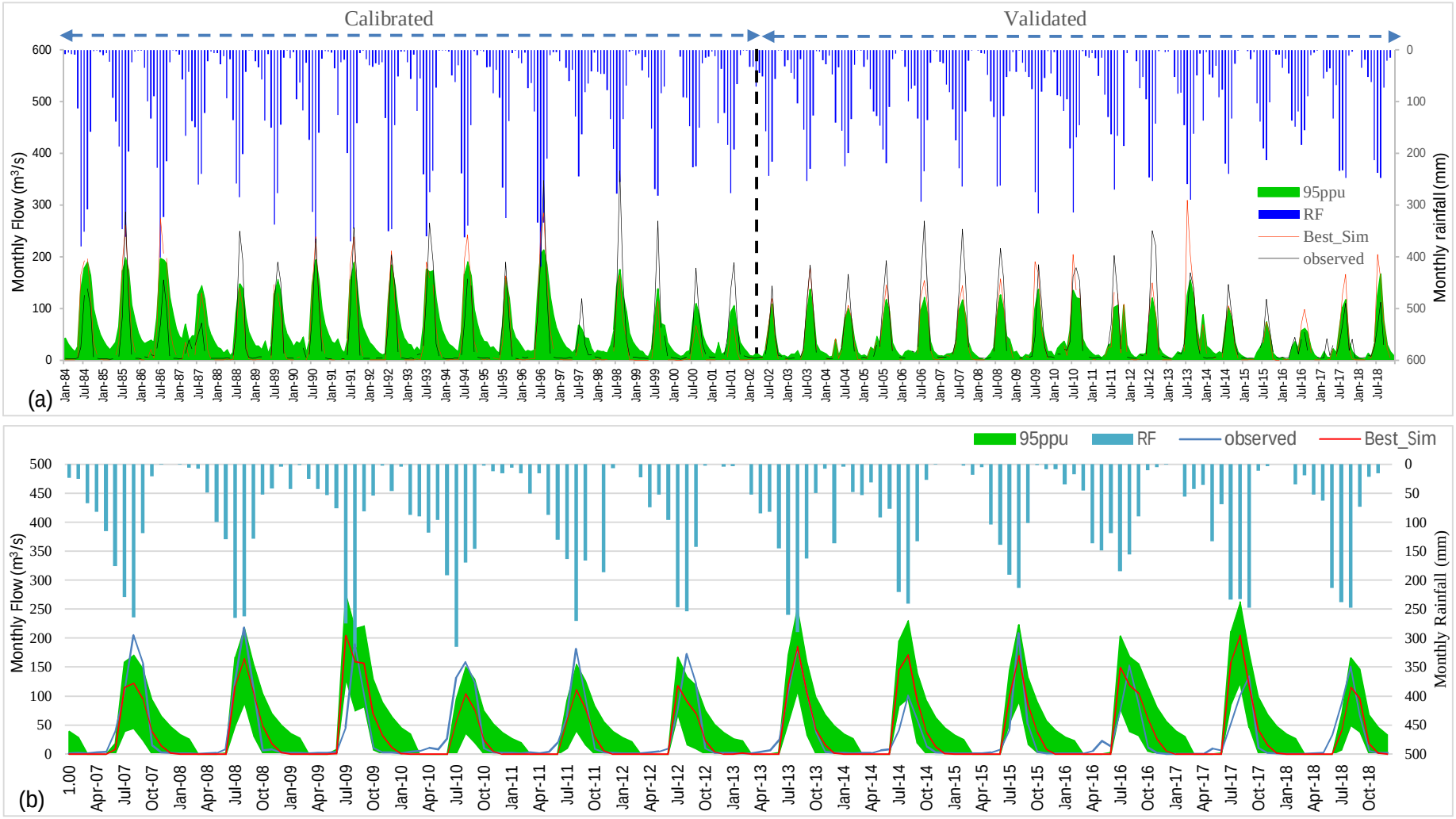

Figure 5-7 Flow calibrated and validated at Hombole (1984–2018) (a) and flow validated at Melka Kunture (2007–2018) (b) gauging stations

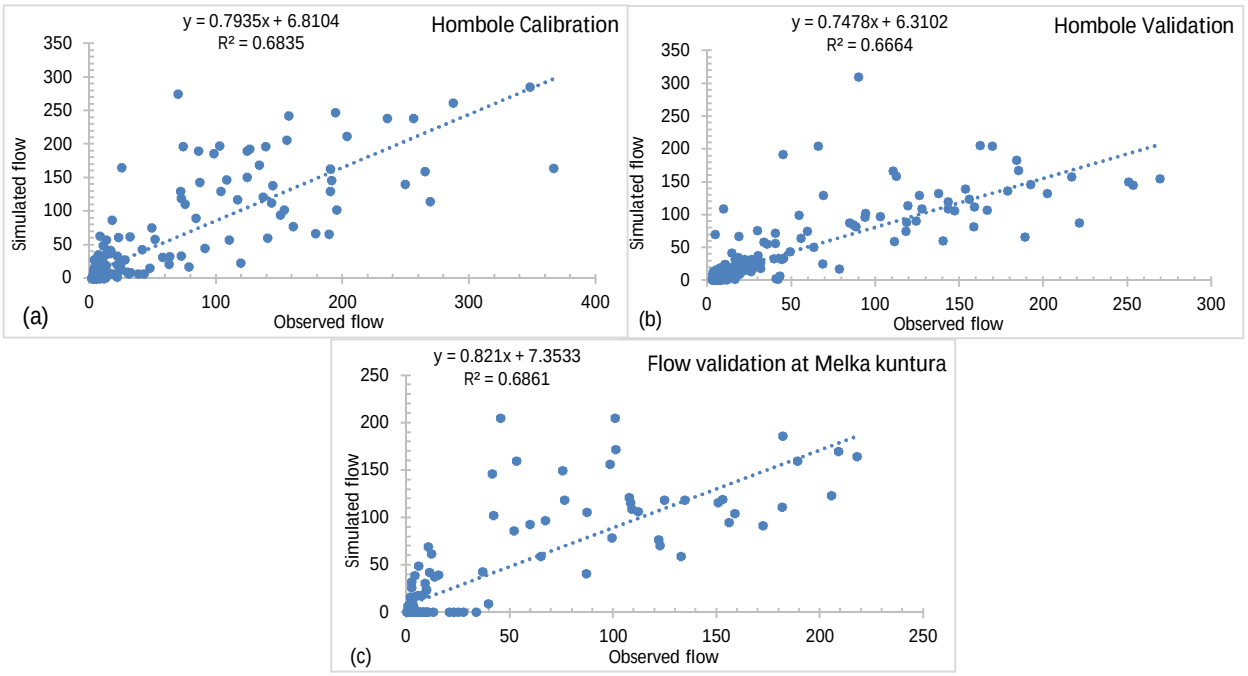

Figure 5-8 The flow simulated and observed at Hombole during calibration (a) and validation (b) and Melka Kunture during validation (c).

3. Sediment Load Calibration and Validation

Once the SWAT hydrological model performance was deemed satisfactory, it was calibrated and was used to evaluate the sediment and nutrient yield modelling in the upper Awash.

The data were bracketed for calibration and validation periods at the Hombole gauge station, with 0.82 and 0.76 as the p-values of the monthly sediment data, respectively. The Melka Kunture observatory recorded a 0.74 p-value of the data being bracketed during the validation period. The calculated R-factors for the monthly sediment yield were 0.71 for the calibration, 0.63 for the validation periods at the Hombole gauge station, and 0.94 for the validation period at the Melka Kunture gauge. Except for the validation PBIAS value, which is within the satisfactory range, the indicators at the Melka Kunture gauge station are within the range of good to very good performance levels (Figure 5-9. Table 5-6). All statistical indices obtained values during the calibration period were higher, except the PBIAS.

Table 5-6 The performance of the SWAT model for sediment during the calibration and validation periods.

	Period	Observatory	p-Factor	r-Factor	PBIAS	RSR	R^2	NSE
Calibration	1979–2001	Hombole	0.82	0.71	−14.9	0.69	0.65	0.70
Validation	2002–2018		0.76	0.63	20.8	0.55	0.61	0.64
Validation	2002–2018	Melka Kunture	0.74	0.94	34.3	0.58	0.64	0.58

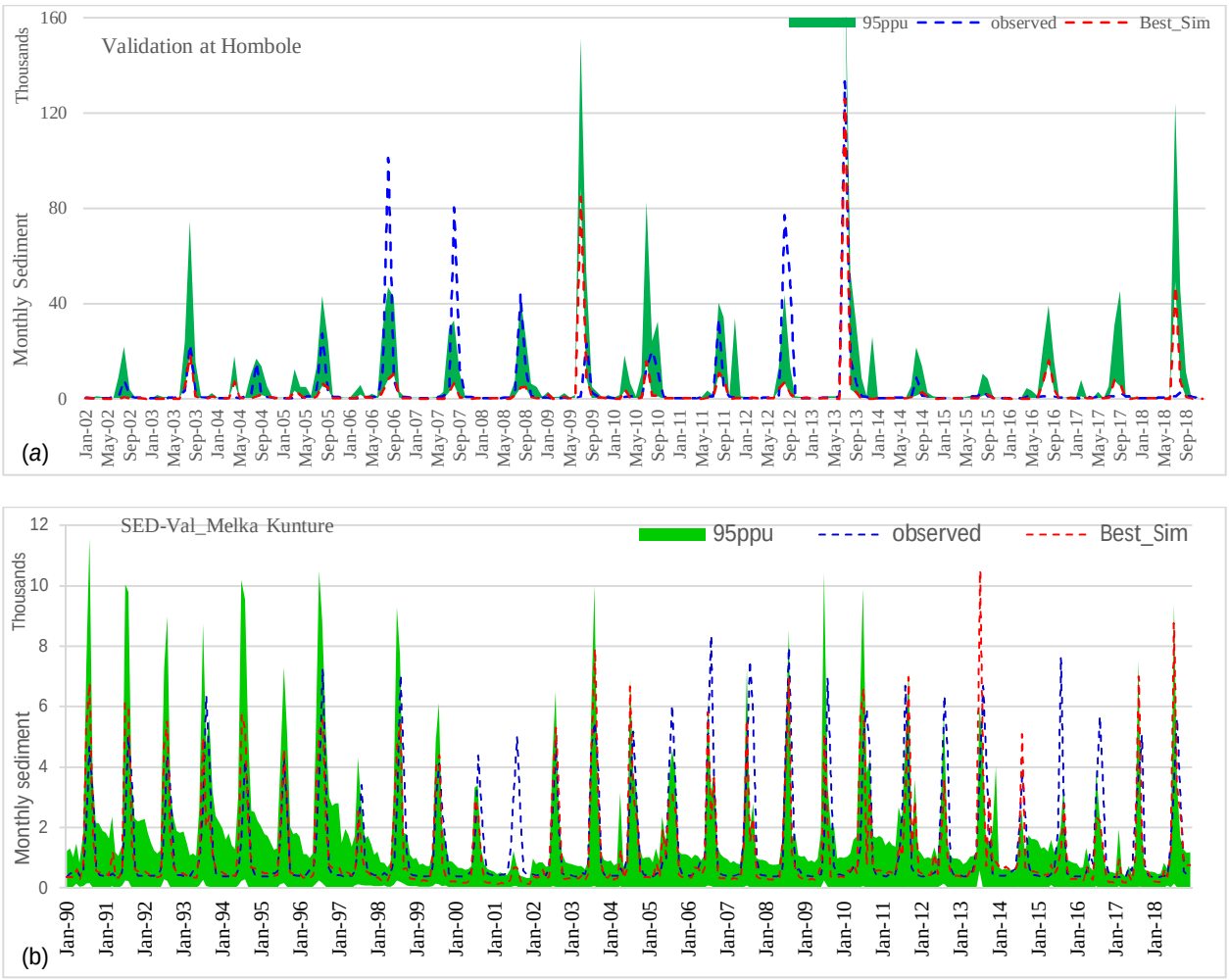

Figure 5-9 The calibration and validation of sediment: at Hombole (a) and Melka Kunture (b) gauging stations.

It is recognised that there is inherent uncertainty in the observed data (Moriasi et al., 2007). The simulated sediment load was compared to the observed sediment load on an annual basis. The observed sediment ranged from 1.16 t/ha/yr. to 70.41 t/ha/yr., whereas the calibrated model predicted values in the 9.9 t/ha/yr. to 81 t/ha/yr. The yearly mean sediment yield of upper Awash during the 1984–2018 period result shows about 33.01 t/ha/yr (Figure 5-10). The mean yearly sediment yield in this research at the sub-basin level is generally consistent with earlier findings. For instance, the final result agrees with Chekol (2007), upper Awash sub-basin, upstream of Koka dam, who reported an average annual sediment yield predicted in the range of 8 to 46 tonnes/ha/yr. with an eighteen-year average of 21.5 tonnes/ha/year Jilo (2019) in the lower Awash basin, indicated that the annual range of sediment output was 3.28 to 51.77 t/ha/year Gonfa (2016), in the Mojo sub-basin (WS10, WS13, WS16-WS18, WS20, WS24, WS25, WS32, and WS33), the estimated soil loss rate ranges from 2 to 204 t/ha/year. The upper limit of the sediment yield does

not agree with this study, but the annual average predicted rate of soil loss was 21.97 t/ha/year, which is relatively in agreement with the average value of this study.

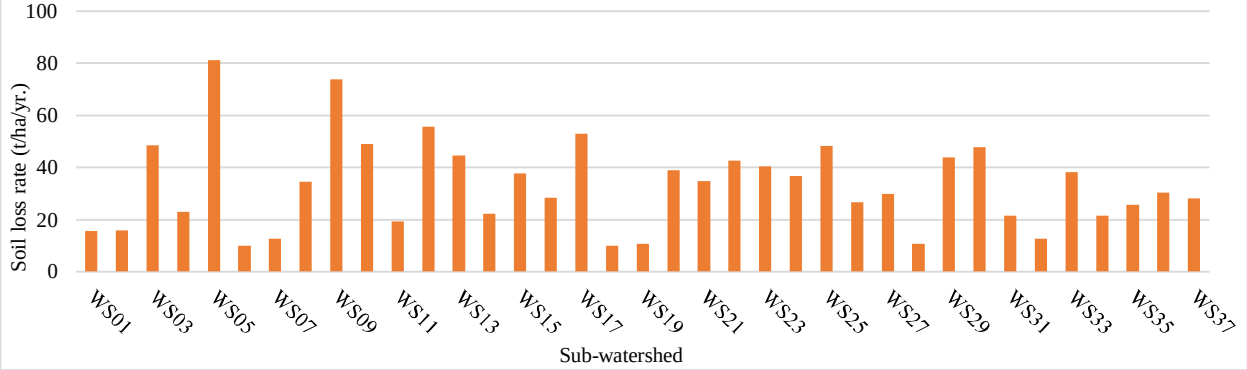

Figure 5-10 Average annual soil loss rate Awash basin sub-watershed between 2003 and 2023.

4. Soil Erosion Rates and Spatial Distribution

It is challenging to determine the proper erosion severity classes for all soil types and environments. Five classes are recommended (in Table 5-7) for soil management purposes and should ideally be further refined to describe the combination of erosion and deposition in a particular environmental setting. For example, in the case of gully and rill erosion, the depth and spacing may need to be recorded; for sheet erosion, the loss of topsoil; for dunes, the height; and for deposition, the thickness of the layer.

Figure 5-11 shows spatial variations of sediment load among the 37 sub-watersheds, WS03, SW05, SW09, SW10, SW12, SW17, and SW30, which cover about 27.9% of the area and are categorised into the severe class. This can be due to the steep topography nature of the watersheds. Sediment severity classes ranging from moderate to extremely severe are about 86% of the watershed, identified as hotspot areas for soil erosion. The remaining 14.4% is considered the low severity class.

Table 5-7 Description of coverage area, yearly rates of soil load, magnitude, and severity classes.

Soil Load Rate (t/ha/y)	Class Severity	Area (ha)	Area (%)	Average Annual Load (t/Year)	Average Annual Load (%)
<12	Low	33,804.1	14.4	99,083.2	10.0
12–20	Moderate	35,095.6	14.9	124,434.1	12.5
20–30	High	68,171.7	28.9	258,910.9	26.1
30–45	Very high	32,811.2	13.9	250,431.7	25.3
>45	Severe	65,666.1	27.9	258,944.5	26.1

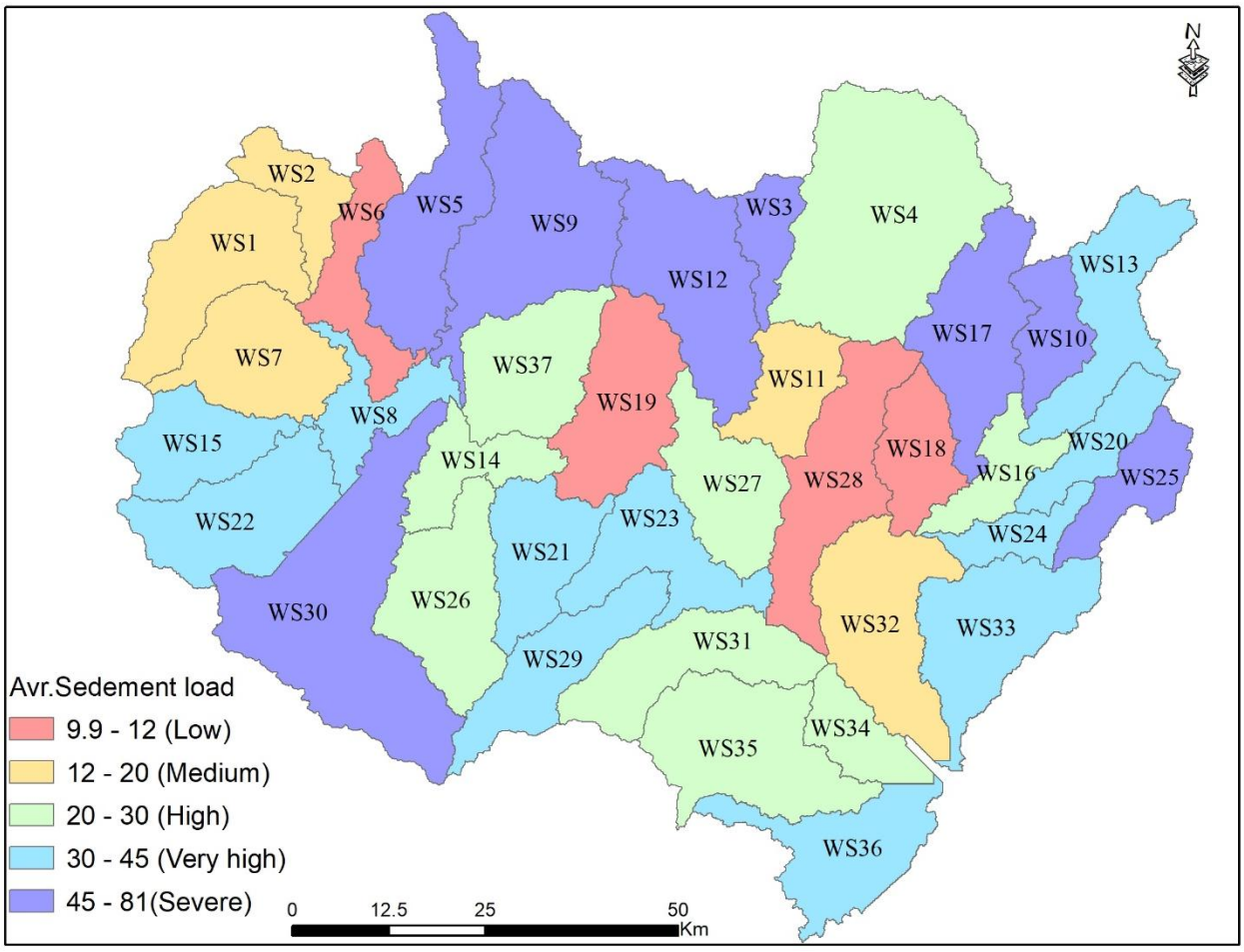

Figure 5-11 Map of average soil loss (t/h/y) severity class for the upper Awash sub-basin

5. Nutrient Load Calibration and Validation

Information regarding the application rates/timings of nitrogen and phosphorus fertiliser applications to row croplands was provided by local farmers. The local farmers indicated that, on average, 100–120 kg/ha of urea and 50–75 kg/ha of di-ammonium phosphate (DAP) were applied to the cropland throughout the growing period, respectively. Figures do not include fertiliser application in irrigated vegetable production. This study considers only the fertiliser application on cereal crop production lands. In addition to this, the nutrient loss resulting from applications of manure was believed to originate primarily from livestock. The LULC map of grazing land that is now in place, which designates grassland as the grazing area presented in Figure 5-4, was used to disperse the amount of manure in the watershed. The amount of manure applied to HRU was determined by looking at the area where the livestock were grazing.

The model predictions were evaluated for both the calibration and validation periods using the graphical comparisons and statistical methods mentioned and the performance rating (shown in Table 5-2). The model underestimated the TN and TP loads during high flow years, particularly in the upper Awash watershed at the Melka Kunture gauging station, as shown in Figure 5-1 and

Figure ***5-3***.

The nutrient loads for the period 2011–2019 were calibrated using the SWAT-CUP software to the observations available at Melka Kunture. According to Moriasi's (2007) evaluation criteria, the result showed good and very good metrics for the calibration period and good and very good metrics for the validation period. In the stages of the calibration phase, the PBIAS for NO_3^-, PO_4^{3-}, TN, and TP load indicated very good performance; over the validation time, the PBIAS again fell within the very good performance rating range. The PBIAS in the stage calibration phase for TN and the validation phase for TP showed better performance compared to the other nutrients.

Except for TP, which had a satisfactory simulation result of an NSE value of 0.54, the Melka Kunture gauging station's NSE data at the calibration stage revealed good simulations for the nutrients. Except for the NSE value of the NO_3^- simulation, the NSE values were higher in the validation period. PO_4^{3-} and TP RSR values demonstrated very good simulation performance throughout the calibration period; NO_3^- and TN RSR values, on the other hand, showed good simulation performance (shown in Table 5-8). During the validation period at Melka Kunture, the simulation performance for NO_3^- was very strong throughout, whereas PO_4^{3-}, TN, and TP demonstrated good performance.

Table 5-8 Details on the model's monthly performance for nutrients during its validation (2015–2019) and calibration (2011–2014) phases.

Nutrient	Calibration			Validation		
	PBIAS	**RSR**	**NSE**	**PBIAS**	**RSR**	**NSE**
NO_3^-	14.2	0.53	0.66	15.6	0.49	0.52
PO_4^{3-}	17.8	0.42	0.64	12.1	0.52	0.60
TN	7.8	0.54	0.61	13.9	0.57	0.65
TP	12.6	0.48	0.54	9.7	0.59	0.63

As the time series is provided in Figure 5-12, the surface runoff nitrate load simulation showed higher peak values in 2011 and 2014 than the observed nitrate during the calibration period. From May 2012 to July 2014, there was good concordance between the simulated surface runoff nitrate and observed nitrate. Through the validation phase, the surface runoff nitrate load simulation showed a higher peak load than the observed nitrate except from May 2018 through the end of 2019, (as shown in Figure 5-12 a). In the case of surface runoff phosphate and TP simulation load, the high peak simulation result was observed throughout the time for calibration and validation except in 2012 through the calibration phase and 2017 through the validation phase regarding phosphate simulation load (Figure 5-12 b, c). This discrepancy between predicted and measured runoff phosphate and TP load is likely due to input uncertainty and technical and instrumental errors propagated during the laboratory and field data collection and analysis process.

The results for TN in the surface run of load during calibration time are very good in contrast to the other nutrient parameter calibration results. There is less observed result in the lower range of

TN than simulated values from January to April 2011 and October 2011 to May 2012, and there is a high peak observed value in March to May 2013 and 2014 simulated surface runoff TN load during the calibration period. These periods are the second rainfall season in Ethiopia, known as the "Belg" season. Similarly, there are fewer observed results compared with the simulated TN load in 2015, 2016, 2017, and 2018 in the "Belg" season through the validation time. During the validation time, there is a higher observed total nitrogen load than the simulated surface runoff TN both in the "Belg" and the main rainy season (Figure 5-12 d).

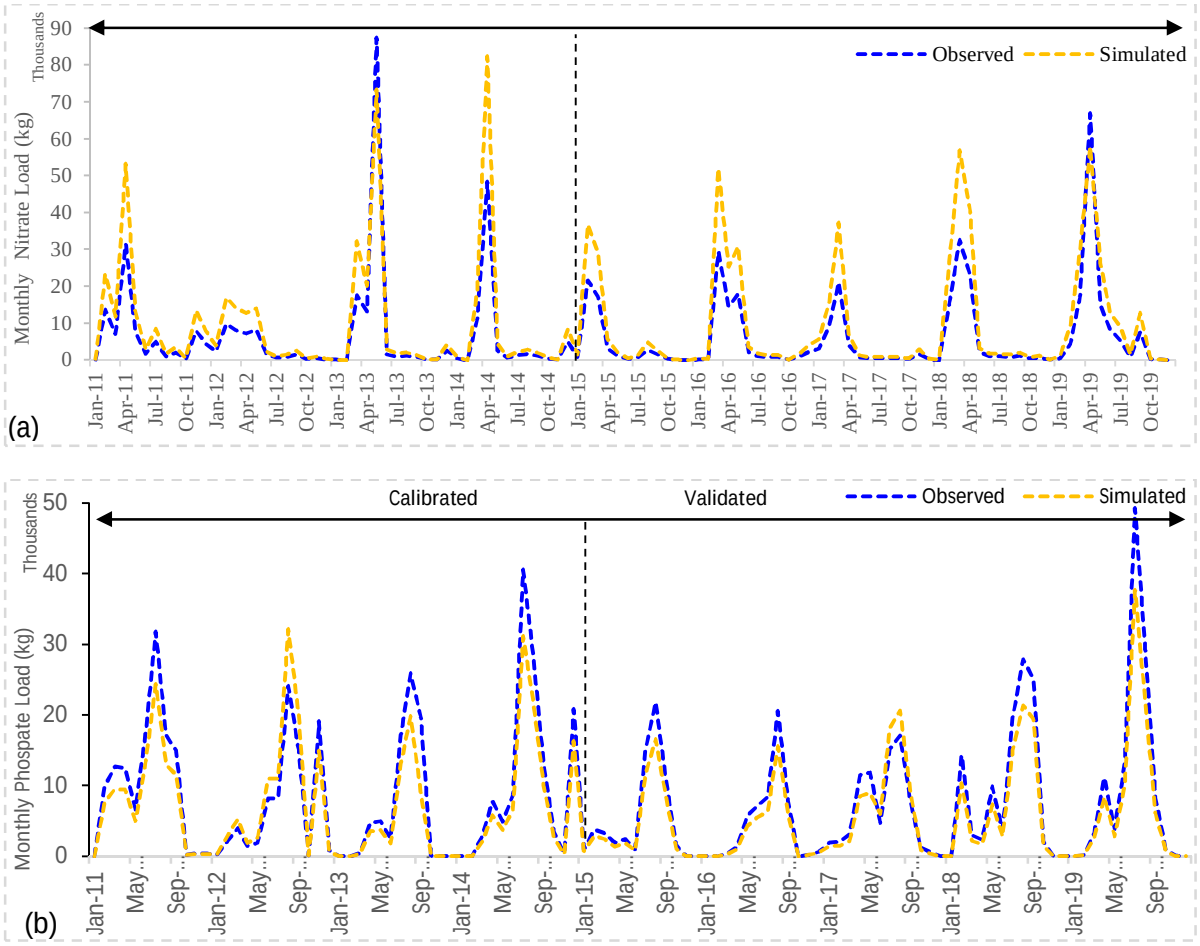

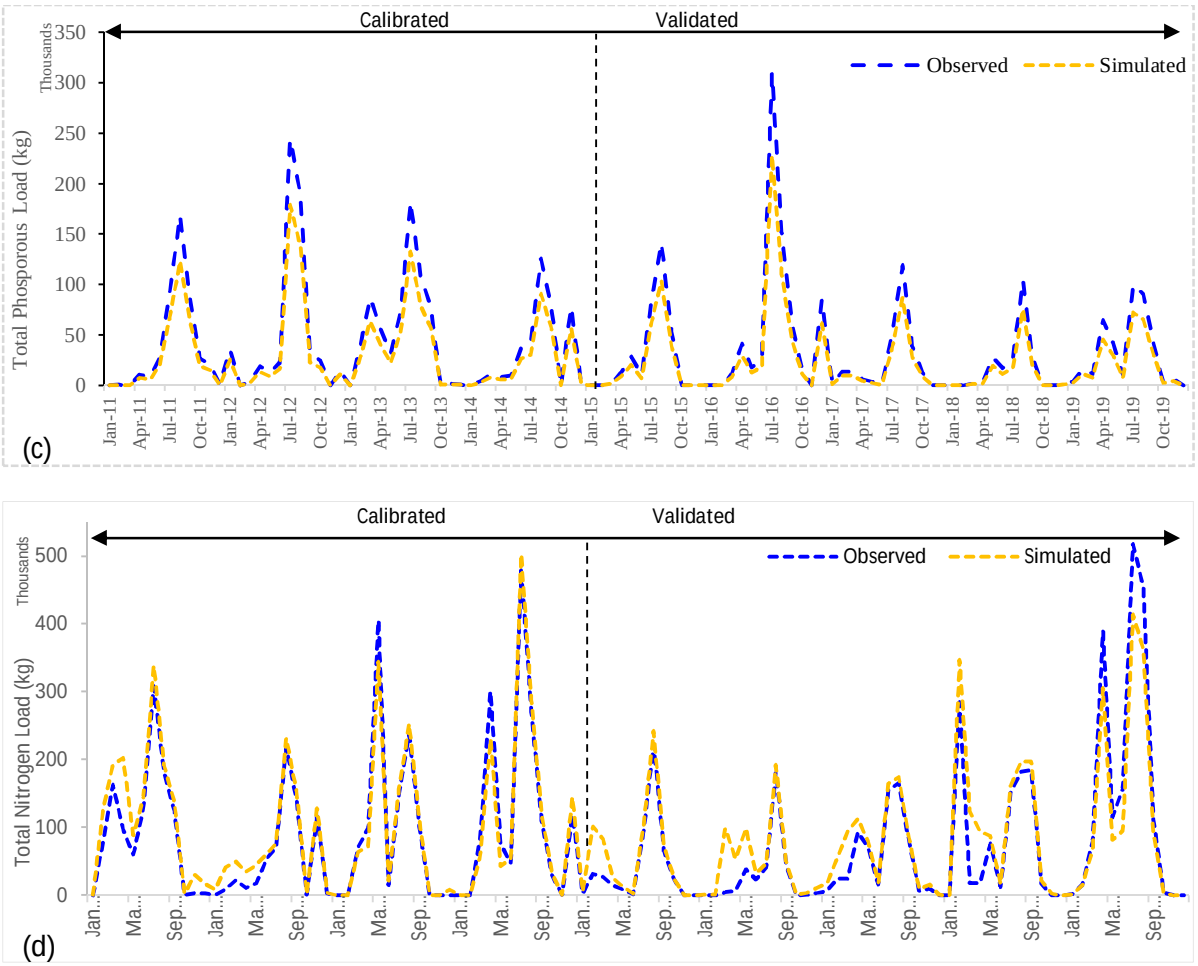

Figure 5-12 Melka Kuture gauging station monthly nitrate load (a), phosphate (b), total phosphorous (c), and total nitrogen (d) load calibration (2011–2014) and validation (2015–2019).

5.4.3 Variations in Surface Runoff, Sediment, and Nutrient Load in Space and Time

1. Soil and Nutrient Load Spatial Variations

At the sub-watershed scale, Figure 5-13 shows the spatial distributions of sediment load, phosphate, total phosphorus, nitrate, runoff, and total nitrogen. The average yearly surface runoff varies from 150.1 mm to 466.7 mm. About 26% of the average surface runoff per year is below 200 mm, with the low runoff shown in the central and northwest regions of the study area. A total of 28% of the area classified as high runoff (>350 mm) is located in the northern, western, southwestern (coinciding with high elevations shown in Figure 5-1), and southern tip of the sub-basin (Figure 5-13a).

At the sub-watershed scale, the average annual loads for nitrate, total nitrogen, phosphate, total phosphorus, and sediment load varied from 0.6 to 36.3 t/year, 9 to 901.3 t/year, 25 to 7048 kg/year, and 4.4 to 287.9 t/year, respectively, as shown in Figure 5-13.

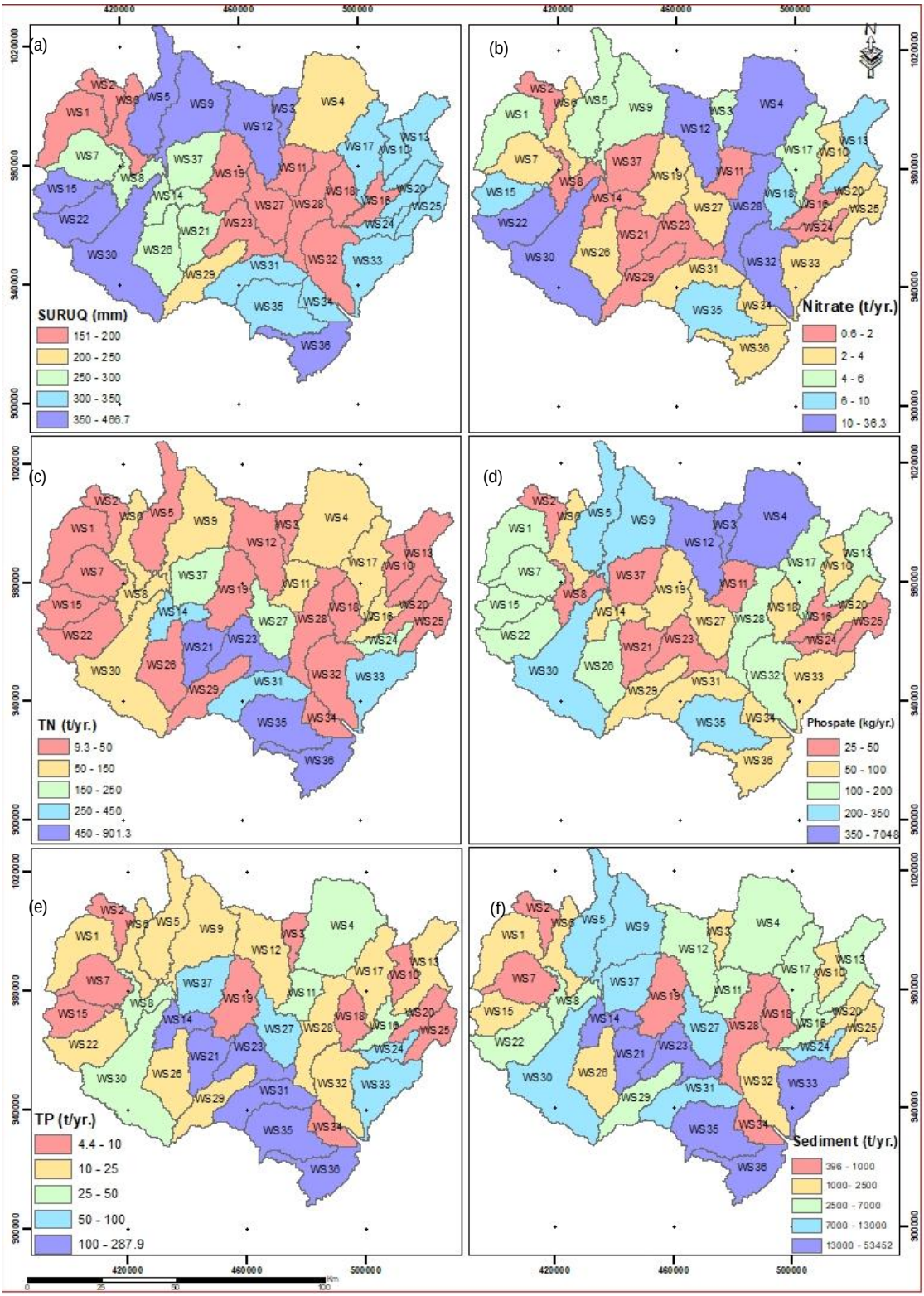

Figure 5-13 The runoff distribution and NPSP loads:runoff (a), nitrate (b), total nitrogen (c), phosphate (d), total phosphorous (e), and sediment (f).

Comparatively low nitrate loads occur in the central part of the sub-watersheds, which covers about 18.4% of the area, and high nitrate loads occur in the southwestern and a more central north–south belt, which takes up about 27.6% of the study area, as shown in Figure 5-13b.

The average annual TN loads, 46.7% of the area, are in the lower range of 9–50 t/year, with higher values in the south of the study area. High TN loads (>450 t/year) were found in the central and southern regions of the study area, covering an area of about 11%, as shown in Figure 5-13c.

The northern sub-watersheds contributed 11.8% of the total area, with phosphate exceeding 350 kg/year through surface runoff. The phosphate load with the maximum areal coverage was 27.2%, followed by 26.5%, 18.8%, and 15.8% with phosphate amounts of 100–200 kg/year, 50–100 kg/year, 200–350 kg/year, and 25–50 kg/year, respectively, as shown in Figure 5-13d.

The largest coverage of any load level ranging from 10 to 25 t/year was found in the average annual TP runoff loads, accounting for 39.2% of the area. Next in order of coverage are 25–50 t/year, 4–10 t/year, and total phosphorous load over 100 t/year, which account for 18.9%, 17.4%, and 15.9% of the area, respectively. On the other hand, the TP load covering between 50 and 100 t/year is relatively lower, taking up approximately 9.5% of the area, as shown in Figure 5-13e.

The spatial variation of sediment and nutrient loads within a watershed can be attributed to several interrelated factors that influence both the physical and biological processes occurring in these environments. Surface runoff, sediment, and nutrient load showed spatial variability in the Upper Awash Sub-basin. Urbanization and agriculture activities contribute significantly to runoff, sediment and nutrient loading through runoff. The spatial variability of these pollutants often correlates with land use patterns in the sub-watersheds. Vegetation plays a vital role in controlling both sediment transport and nutrient cycling within watersheds. Moreover, land use practices such as agriculture, urban development, and forestry play a critical role in determining sediment and nutrient loads. For example, areas with less vegetation cover are more susceptible to erosion, leading to higher sediment loads in nearby water bodies. Dense plant cover reduces the velocity of surface runoff, allowing sediments to settle before they reach waterways. Agricultural activities often involve soil disturbance through tillage, which can increase erosion rates (Renard et al., 1997; Heathcote et al., 2013; Mathieu et al., 2019). Intensive agricultural practices are often associated with increased sediment and nutrient loads in nearby water bodies (Maximus, 2025).

The application of fertilizers also contributes to nutrient loading in runoff water. In contrast, areas with natural vegetation or managed forests tend to have lower erosion rates due to root systems that stabilize the soil. In this study the cropland increased by 147% this indirectly indicates there is an increasing amount of feritilizer application as well. Studies have shown that areas with high agricultural intensity typically exhibit elevated phosphorus and nitrogen concentrations due to fertilizer runoff. Conversely, a reduction in intensive agricultural areas has been linked to decreased sediment loads corresponds with improved water quality (Maximus, 2025). Furthermore, areas with healthy vegetation will generally exhibit lower nutrient loads entering

aquatic systems compared to bare or poorly vegetated lands this is due to plants uptake nutrients from the soil (Firoozi, 2024). But in the study area the forest cover, grass land and shrub land showed a decreasing trained and there is a potential to increase the nutrient load and has an impact in the near by aquatic ecosystem in general.

The shrub land and grass land decreased by 74% and 96%, respectively, in the Upper Awash sub-basin, this indicates the land is exposed to soil erosion. Forests, grasslands, and shrublands are critical in mitigating sediment transport and nutrient loading. These ecosystems enhance soil stability through root structures that bind soil particles together, reducing erosion potential. Additionally, forested areas can act as buffers that filter out nutrients before they reach water bodies. The increase in forest cover in a catchment contributed to reduced sediment dynamics and improved ecological status of waters due to lower nutrient inflow (Szatten et al., 2024)

Urbanization introduces impervious surfaces such as roads and buildings, which can exacerbate runoff rates during precipitation events. This leads to increased sediment transport as well as higher concentrations of pollutants entering waterways due to the lack of natural filtration processes found in vegetated landscapes (Öztürk et al., 2024). In the study area, the builtup area coverage increased by 80% in twenty years of interval. This change has significant contribution for nutrient load.

2. Temporal variations of nutrient and soil load

The wet season is when the study area's runoff is at its maximum (June, July, and August), followed by the "Belg" season from March to May. From 2003 to 2023, the NPS pollutants changed both the wet and dry periods. The average monthly runoff values ranged from 5.56 to 384.86 mm in December and July. July and August contributed 32.3% and 31.5% of the runoff total, respectively. The lowest contributing months were December (5.56 mm) and November (6.79 mm). The study area's annual average runoff in 2020 and 2018 is depicted in Figure 5-14 with a range of 183.09 to 487.89 mm, respectively.

The temporal variation of monthly simulated sediment and nutrient loads of NO_3^-, PO_4^{3-}, TN, and TP are shown in Figure 5-14. The critical period of PO_4^{3-}, TN, TP, and sediment load occurs in July and August. The highest NO_3^- load occurs between March and May, which collectively contributes 67.5% of the annual load. From July to September, the NO_3^- load contributed 14.32% of the annual load. Unlike the other nutrients, the maximum NO_3^- load occurs before the wet season, the "Belg" season. The season is not a growing season in the study area. This could be due to one of the following reasons as other researches indicated. Possibly, it was noted by Sebilo (Sebilo et al., 2013) that 32–37% of the nitrate that was applied but not absorbed by the crops was quickly assimilated into the "soil organic matter pool". This pool of nitrogen created by fertilisers may accumulate nitrate, which can then build up and drain out of the soil, specifically during the off-growing period. During this season, when the production cycle concludes, the nitrate content of the soil increases (Giordano et al., 2021). Crop harvesting or nitrate leaching are two ways that nitrogen can escape agricultural systems (Giordano et al., 2021). To increase agricultural yield,

farmers may also apply fertiliser in higher amounts than is advised. As a result, leaching releases some of the remaining nitrogen from the fertiliser into the surface water environment after harvest in the form of NO_3^- (Giordano et al., 2021; Chotpantarat & Boonkaewwan, 2018). This could be the most likely reason for the elevated NO_3^- levels observed in the study area during this specific season. In addition, during the rainy season, several mechanisms contribute to a lower nitrate load in non-point source pollution. Heavy rainfall increases the volume of water in rivers and streams, which can dilute the concentration of nitrates in surface waters; When heavy rains occur, they can wash away topsoil that contains fertilizers and other nitrogen sources before they have a chance to leach into groundwater or reach surface waters as nitrate. This process can temporarily reduce the amount of nitrate entering water bodies. Similarly, crops only absorb 10–20% of the phosphorous fertiliser applied in the first year, and the majority of the phosphorous accumulates as leftover in the soil (Sattari et al., 2012). Moreover, Nitrification, the conversion of ammonia to nitrate by bacteria, is accelerated in nitrogen-rich environments. Synthetic fertilizers and agrochemicals are the most emphasized factors that influence the nitrification process. Over-fertilization can lead to nitrate leaching into waterways (Ayiti & Babalola, 2022). The abundance of nitrogen compounds supports the growth of nitrifying bacteria. In nutrient-rich environments, these bacteria can multiply rapidly, thereby increasing nitrification rates (Alfisah et al., 2022). The addition of nitrogen fertilizers to soils can lead to spikes in ammonia concentrations, creating a favorable environment for rapid nitrification (Ayiti & Babalola, 2022).

The months of July and August account for a TN loss of 24.46% and 25.25%, respectively, with about 69.06% of the overall TN loss occurring from June to September. The TN load for the “Belg” season (March-May) was 22.6%. In the upper Awash basin, this season marks the second important TN load period. Nonetheless, with 0.84 percent, November has the lowest TN load. This suggests that there were differences in yields between growing and non-growing seasons as well (Figure 5-14). Nitrate is a relatively easily produced form of nitrogen via nitrification, unlike TN. TN levels may take longer to show increases due to the more complex pathways involved in the breakdown of organic materials. Thus, under certain conditions, the supply of nitrate can be transient and highly dependent on specific environmental parameters. For example, seasonal factors, warmer temperatures can enhance nitrification rates, causing a spike in nitrate levels. which can result in earlier peaks in nitrate concentrations compared to total nitrogen levels that are influenced by various nitrogen forms (Németh et al., 2023; Auyeung et al., 2015). For example, high maximum temperature is a common characteristic of the “Belg” season in Ethiopia (Zegeye et al., 2022).

The highest simulated TP loss occurred in July and August, 29.17 and 29.07%, respectively. Of the total TP loss, the TP losses from June to September comprised about 79.89%. In the “Belg” season (March–May), the TP load showed 13.83%. This season is the second significant time for TP load in the upper Awash. However, November is the lowest TP load, which was below 1%. This also indicates that TP load differed between the crop-growing and non-growing seasons (Figure 5-14).

June to September's sediment yield constituted 83.2% of the average annual sediment yield. The average annual sediment load was in 2019, followed by 2011 and 2014, which had 623, 610, and 574.9 t/year, respectively. The lowest sediment load was observed in 2016, 2015, and 2013; their sediment load was 214.1, 279.1, and 292.3 t/year, respectively. The variation in annual sediment load could be the different climate variations that occurred in the local area as well as the influence of the global condition (Figure 5-14).

The year 2015 had the second-highest surface runoff (462.37 mm) in the sub-basin, with the greatest annual sediment, TN, and TP loads; in contrast, the year 2013 had the highest NO_3^- load and the third-lowest surface runoff. In addition to the LULC, the sediment, TN, and TP were related to the surface runoff in these circumstances. Despite what the monthly NO_3^- load indicates, the NO_3^- load was unrelated to surface runoff; the low nitrate load in the highest runoff throughout July and August justifies this. The surface runoff PO_4^{3-} load was higher in 2018, followed by 2019. Comparatively, the lowest sediment, TN, and TP load were observed in the year 2016, while in 2012, NO_3^- load showed the lowest load, and in 2012, PO_4^{3-} showed the lowest surface runoff load. With an average of 8407.5 tonnes, the yearly sediment load varied greatly, ranging from 396 to 53,452 tonnes. Unlike 2016, which showed the lowest sediment yield, 2019 saw the biggest annual soil loss. A significant flooding event with the second-highest yearly average surface runoff of 25.04 mm could be the cause. Similarly, the yearly result of TP and TN fluctuated; that is, TP varied from 4.4 to 287.9 t/year with a yearly mean of 49.55 t/year, and TN ranged from 9.3 to 901.3 t/year with an average value of 154.7 t/year (Figure 5-14).

Typically, crops only absorb 10–20% of the phosphorous fertiliser applied in the first year, and the majority of the phosphorous accumulates as leftover in the soil (Sattari et al., 2012).

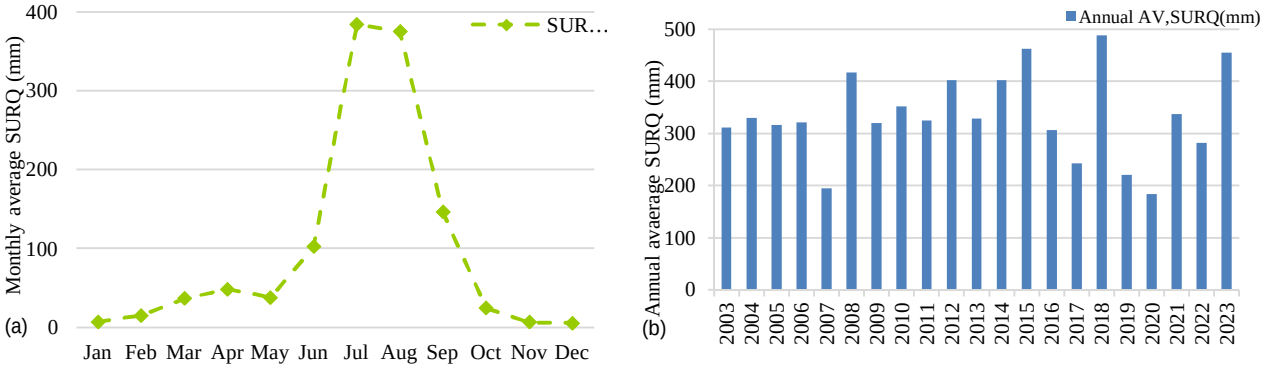

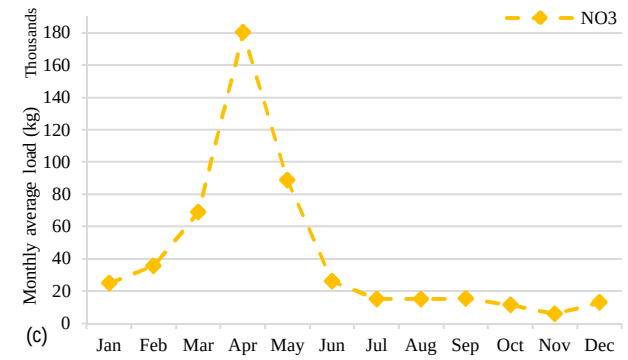
NO3
Thousands
Monthly average load (kg)
180
160
140
120
100
80
60
40
20
0
Jan Feb Mar Apr May Jun Jul Aug Sep Oct Nov Dec
(c)

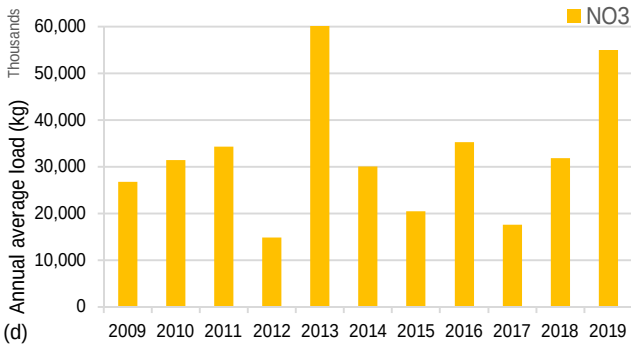
NO3
Thousands
Annual average load (kg)
60,000
50,000
40,000
30,000
20,000
10,000
0
2009 2010 2011 2012 2013 2014 2015 2016 2017 2018 2019
(d)

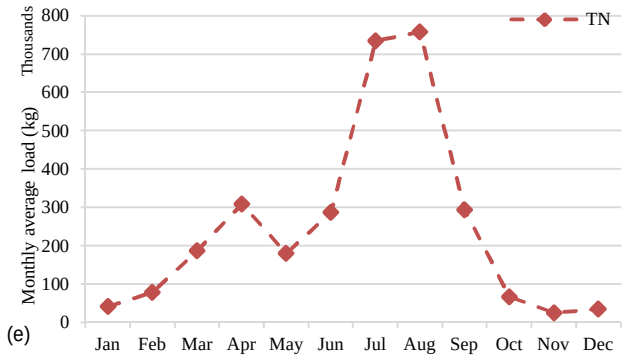
TN
Thousands
Monthly average load (kg)
800
700
600
500
400
300
200
100
0
Jan Feb Mar Apr May Jun Jul Aug Sep Oct Nov Dec
(e)

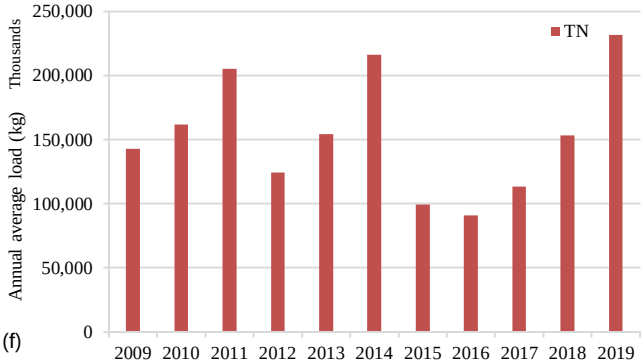
TN
Thousands
Annual average load (kg)
250,000
200,000
150,000
100,000
50,000
0
2009 2010 2011 2012 2013 2014 2015 2016 2017 2018 2019
(f)

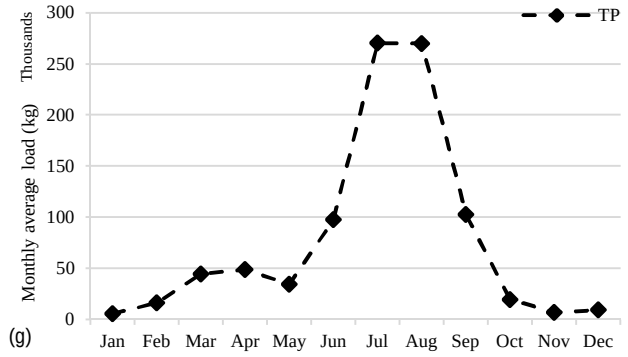
TP
Thousands
Monthly average load (kg)
300
250
200
150
100
50
0
Jan Feb Mar Apr May Jun Jul Aug Sep Oct Nov Dec
(g)

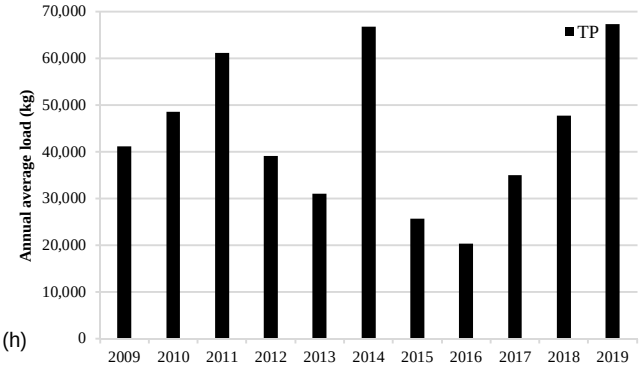
TP
Annual average load (kg)
70,000
60,000
50,000
40,000
30,000
20,000
10,000
0
2009 2010 2011 2012 2013 2014 2015 2016 2017 2018 2019
(h)

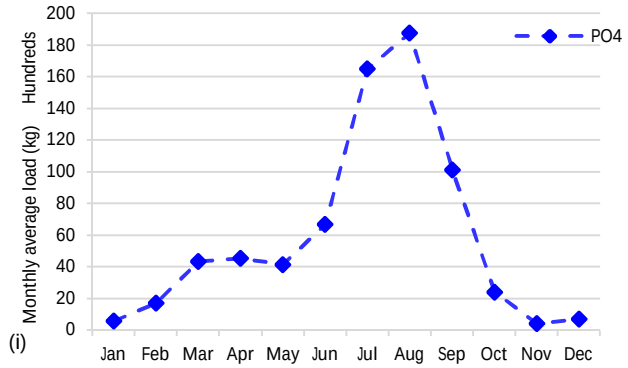
PO4
Hundreds
Monthly average load (kg)
200
180
160
140
120
100
80
60
40
20
0
Jan Feb Mar Apr May Jun Jul Aug Sep Oct Nov Dec
(i)

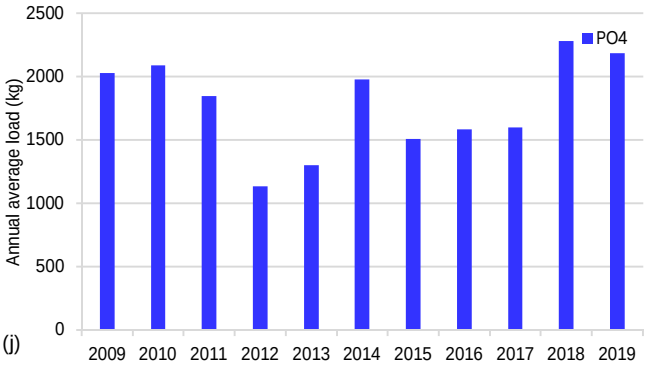
PO4
Annual average load (kg)
2500
2000
1500
1000
500
0
2009 2010 2011 2012 2013 2014 2015 2016 2017 2018 2019
(j)

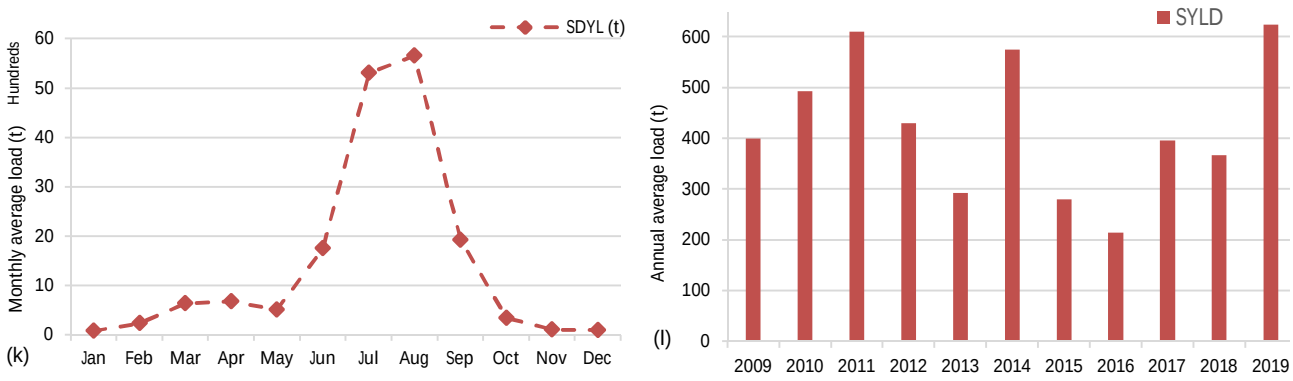

Figure 5-14 The temporal runoff and NPSP loads of upper Awash basin:

average monthly runoff (a), average annual runoff (b), average monthly nitrate load (c), average annual nitrate (d), average monthly total nitrogen (e), average annual total nitrogen (f), average monthly phosphate (g), average annual phosphate (h), average monthly total phosphorous (i), average annual total phosphorous (j), average monthly sediment (k), and average annual sediment (l).

5.4.4 Impact of LULC Change on Runoff, Sediment and Nutrient load:

There are two phases during the study period: 1986-2002 and 2003-2023 for the evaluation of the effect of LULC transformation on flow, sediment, NO_3^-, PO_4^{3-}, TN, and TP in the upper Awash basin. The calibrated model was run to simulate eight LULC each year by the "fixing-changing" technique (LULC adjustment while maintaining other inputs) using the 2003 and 2023 LULC data.

1. Surface Runoff

WS05 has a surface runoff value of 466.7 mm/year, followed by WS09, WS22, WS12, WS30, and WS15 with values of 433.7, 408.1, 405.6, 401.8, and 397 mm, respectively, in 2023. Differences in runoff water can be related to the different physical conditions between the thirty-seven catchments. According to the simulations, at stations WS02, WS36, WS31, WS29, and WS35, the annual runoff had increased by 66.5, 51.8, 48, 47.5, and 42.5%, respectively. Different characteristics in LULC provide different runoff values. The impact of the LULC change on the amount of runoff is shown in Figure 5-15 (a) and (b) and Supplementary Material Table S1. WS37 showed almost no change in flow in the 20 years; this sub-watershed serves as a wetland catchment region and is a flood plain that is flooded for an extended period following the rainy season. Consequently, runoff increased by 0–66.5% due to the change in LULC between 2003 and 2023. As a result, variations in LULC and surface runoff volume are strongly correlated. The effect of LULC alterations on hydrological responses has been modelled in several other studies. For instance, Chotpantarat (Chotpantarat & Boonkaewwan, 2018) revealed that runoff increased by 13–49% due to changes in land use. in part of the Yom River Basin, Thailand. Mishra (A. Mishra et al., 2007) used the SWAT model to characterise the impact of LULC change on runoff in the Banha watershed in India. According to his study, runoff showed an increment ranging from 1.7% to 5.6% in the different sub-watersheds. The study by Sajikumar (Sajikumar & Remya, 2015) performed similar work in the Manali and the Kurumali watersheds in India; the result showed

that the runoff increased by 15%. A similar work by Getu (2021) in the Upper Baro Basin, Ethiopia, showed an average increase in surface runoff by 46.64 mm over 20 years.

2. Sediment load

Figure 5-15 (c) and (d) show the annual average sediment load simulated for each sub-watershed using the pre- and post-change LULC (2003–2023) and the percentage change in sediment load, respectively. The conversion of shrubs, forests, and grassland to agriculture and built-up areas indicates an increase of 147.3% for agriculture and 80.2% for built-up areas; this causes the yearly average sediment load values to rise by 23.89% within 20 years. The primary components of surface runoff and sediment yields are cropland and areas with no vegetation cover. Built-up areas constitute a large source of surface runoff but a relatively small contributor to sediment yields relative to runoff (Chelkeba, 2023). The available sediment sources are severely eroded by the increased runoff in urban areas (Santos et al., 2020).

Thus, the change in LULC from the 2003 coverage to the 2023 coverage resulted in a 25-27298.7-tonnes increase in the average annual sediment yield at stations WS28 and WS35 (Figure 5-15). Similar to this study's findings, previous studies by Kalsido (2020) in Ethiopia, the effect of LULC dynamics on sedimentation in the Lake Ziway area showed that there is an increment of 1.5–2.03 mcm/yr. of sediment load within 30 years; a study by Tumsa (2023) in Blue Nile Basin, Guder, Ethiopia, indicated that there is an increment of sediment yield by 138.92 t/ha within 18 years (2003–2021); according to an investigation by Mamo (Tumsa et al., 2023) in Blue Nile Basin, Fincha, Ethiopia, the average yearly soil loss rose from 34.5 to 58.7 t/ha/yr. in 1991–2021 (Figure 5-15).

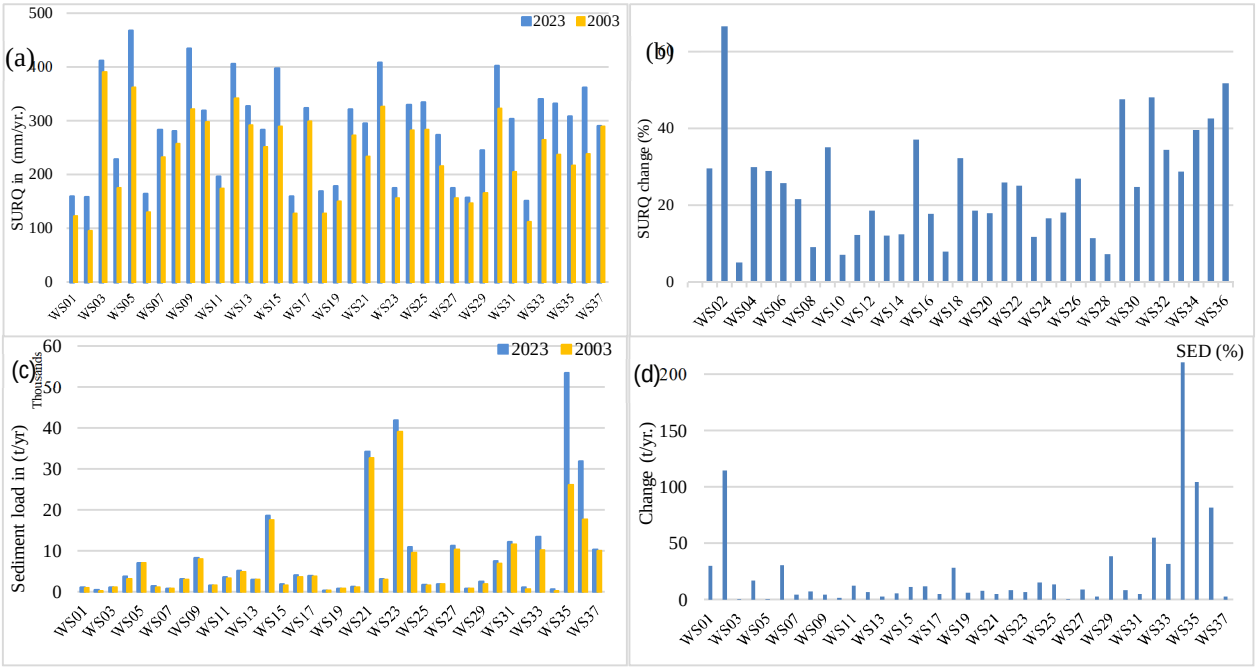

Figure 5-15 The yearly average surface runoff :(a), % change in surface runoff (b), sediment load (c), and percentage change in sediment load (d) from 2003 to 2023.

For example the sediment load in WS35, the change in the LULC in the watershed indicated (as it seen Appendix C) the Built-up area, cropland, increased by 24.8 ha, and 25166.6 ha, respectively; the forest land, grassland, shrub land, and wetland decreased by 339.3 ha, 294.4 ha, 23809.8 ha, and 374.6, respectively. These are significant changes for the incensement of the sediment load at this level. From our field observation, the watershed has an area of volcanic ash and a steep slope with the gorge area that the Awash River passes through. In addition to direct impacts on runoff volumes, changes in land use also influence sediment transport and water quality. Increased runoff often carries more sediments into waterways due to soil erosion from disturbed lands. This sedimentation can degrade aquatic habitats and affect water quality by introducing pollutants that were previously retained by natural vegetation (Maximus, 2025)**.** Studies showed that the conversion of natural landscapes, such as forests and grasslands, into agricultural lands or urban areas typically increases soil erosion. In the Upper Awash Sub-Basin, for example, agricultural practices increased by 6.7% from 2000 to 2015, while forested areas decreased by 5.47%. This shift leads to a reduction in vegetation cover that stabilizes soil, resulting in higher rates of erosion (Bihonegn et al.,2023).

3. Nitrate and phosphate load

According to the simulation, the NO_3^- load increased from 127.6 kg/yr. (29%) to 20,739.7 kg/year (133.5%), in sub-watersheds WS08 and WS04, in all sub-watersheds. The highest nitrate load is observed for sub-watersheds WS04, WS12, WS30, WS32, WS22, and WS28, in average 20,739, 16,445.7, 11,144, 12,616, 10,852.6, and 14,327 in kg/yr., respectively, as discussed below. However, the highest increment rate was observed in sub-watersheds WS04 (15,527%), WS12 (12,254%), and WS28 (11,400%) (Figure 5-16).

The NO_3^- load increased in the sub-watershed WS04, which is at high elevation and contains the major urban expansion area in Addis Ababa. The main LULC change is cropland, which covers about 16,430.8 ha, followed by built-up area and bare land, which cover 5488.6 ha and 42.1 ha, respectively. Meanwhile, shrubland, forest land, and grassland decreased by 17,814 ha, 2561 ha, and 1593 ha, respectively. The LULC change in sub-watershed WS30 increased cropland and built-up area by 33,958.7 ha and 201.9 ha, respectively. But shrubland, grassland, and forest areas decreased by 30,791.4 ha, 3054.5 ha, and 292.7 ha, respectively. Sub-watersheds WS32, WS28, WS22, and WS12 showed that built-up area and cropland increased while forest, shrubland, and grasslands decreased. Sub-watershed WS32 has most of its LULC transformed into agricultural land (about 8811 ha), built-up area (155.3 ha), and bare land (198.6 ha). In addition, in these sub-watersheds, in the last 6 to 7 years, there has been an expansion of irrigated farming, especially along the Awash River, Mojo River, and Koka Reservoir.

When $NO_3^-$is released into rivers from non-point sources, the resulting high load can be dangerous to human health when consumed through water. In addition to that, the south-eastern parts of the sub-watersheds in the study area are dominantly agricultural land, people grow vegetables and other crops using small-scale irrigation, and because of this, there is a growing tendency for

increased NO_3^- load in the river, which may lead to eutrophication in the future in the downstream areas more specifically in Koka reservoir.

The effect of LULC change from the 2003 to the 2023 map led to a simulated 4.27–349% increase in PO_4^{3-} levels of the net contribution, increasing by 31 t/yr. in WS27, and 2459.7 t/yr. in WS04 (Figure 5-16). WS27 built-up area and agricultural land increased by 100% and 45.5%, respectively, with forest area, grassland, and shrubland decreasing by 87.5%, 100%, and 65%. In the WS04 sub-watershed built-up area, agricultural land and bare land increased by 149.5% and 75.6%, respectively, with forest land, grassland, and shrubland decreasing by 46.8%, 92.1%, and 50.8% (see Appendix C Table 1). The model result shows that sub-watersheds W04 and WS12 showed high annual PO_4^{3-} load by 2459.7 t/yr. and 1553 t/yr.; in terms of high increment in PO_4^{3-} load, WS04 took the lead by 349% followed by WS32, WS18, and WS11 that showed an increment of 225.5%, 219%, and 185.6%, respectively. The quantity of phosphate in the study area generally increased; it was 5513 t/year for 2003 LULC conditions and 8215.4 t/yr. for 2023 conditions (Figure 5-16).

When NO_3^- is released into rivers from non-point sources, the resulting high load can be dangerous to human health when consumed through water. In addition to that, the study area's southeastern parts, predominantly cropland, are growing vegetables and other crops using small-scale irrigation, potentially leading to an increase in elevated NO_3^- load in the river that could eventually result in eutrophication in the downstream areas, more specifically in Koka Reservoir (Assegide et al., 2022; Assegide et al., 2022; Chotpantarat & Boonkaewwan, 2018).

In general, from the two nutrients (PO_4^{3-} and NO_3^-), it can be explained that most of the sub-watersheds showed the conversion of LULC from other uses to agriculture, and the built-up area contributed to the change and increase in the nutrients. This could be a release of wastewater and household sewerage effluents containing detergents and other cleaning products, in addition to being a major contributor to fertiliser application for crop production in rain-fed or irrigation practices.

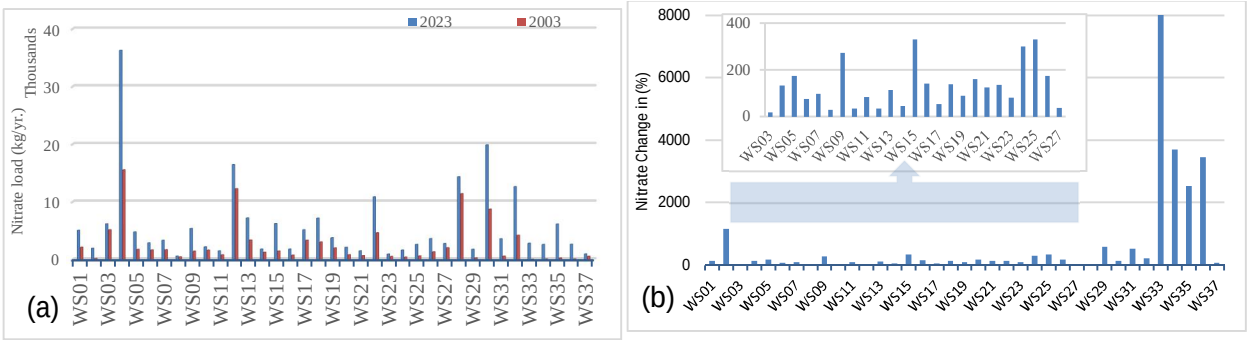

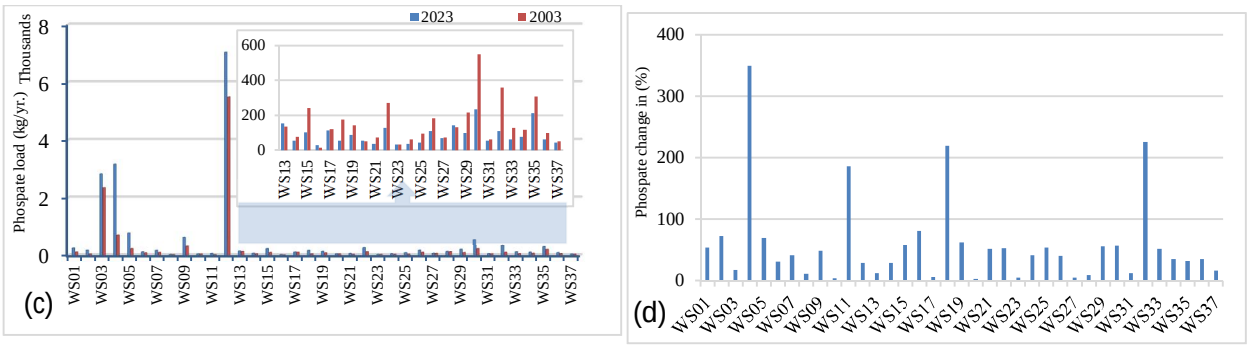

Figure 5-16 Impact of LULC change in:NO3 load (a), change in NO3 load (b), change in PO4 load (c), and change in PO4 (d).

4. Load of Total nitrogen and total phosphorous

The simulated output of total nitrogen ranged from an increase of 22.2% (8736 kg/yr.) to 1201.5% (20,615 kg/yr.) for 2003 and 2023 LULC conditions in WS02 and WS28 sub-watersheds, respectively. The sub-watersheds mentioned earlier demonstrated an increase of 106,667.8 ha and 972.78 ha, respectively, in cropland and built-up areas. The lowest TN load increment was observed in sub-watersheds WS10, WS19, WS27, and WS11, which contributed 26.7% (4466 kg/yr.), 41.3% (7452 kg/yr.), 49.9% (68,929 kg/yr.), and 50.6% (47,020 kg/yr.), respectively, as shown in Figure 5-16.

The model output of TP indicated increasing, ranging from 1383.5 kg/yr. (25.66%) to 133,641.2 kg/yr. (86.6%). For 2003 and 2023, LULC conditions in sub-watersheds WS10 and WS35, respectively. WS04, WS06, WS08, WS09, WS14, WS16, and WS21, WS23, WS24, WS27, WS30, WS31, WS33, and WS35 to WS37 TP load was greater than 10,000 kg/yr., which had comparatively the highest TP change. The output of the TP increase is related to the change in LULC change, as shown in Figure 5-16.

The lowest surface runoff TP load increment lower than 40% was observed in sub-watersheds WS10, WS11, WS12, WS19, WS27, and WS28, which contributed 25.6 (1383.4 kg/yr.), 32.4 (9711.3 kg/yr.), 35.1 (17,967.8 kg/yr.), 18.9 (1818.9 kg/yr.), 37.1 (2539.1 kg/yr.), and 37.6% (5556.1 kg/yr.), respectively. The LULC change in the six sub-watersheds showed an increment of 9443.8 ha built-up area and 28,289 ha agricultural land.

Built-up area in WS14, WS21, WS23, WS31, WS35, and WS36 increased by about 27, 45, 114, 75, 25, and 33 hectares, respectively; the cropland area in WS14, WS21, WS23, WS31, WS35, and WS36 increased by about 4468, 12682, 8814, 18729, 25167, and 24699 hectares; forest areas in WS21, WS23, WS31, and WS35 decreased by about 862, 2390, 1198, and 339 hectares, respectively; grassland area in WS14, WS21, WS23, WS31, WS35, and WS36 decreased by about 5, 562, 23, 635, 294, and 88 hectares, respectively; scrubland land in WS14, WS21, WS23, WS31, WS35, and WS36 decreased by about 4497, 11307, 6527, 16996, 23810, and 24542 hectares, respectively. The TN and TP load in the watersheds may rise noticeably as a result of these changes in land use and cover.

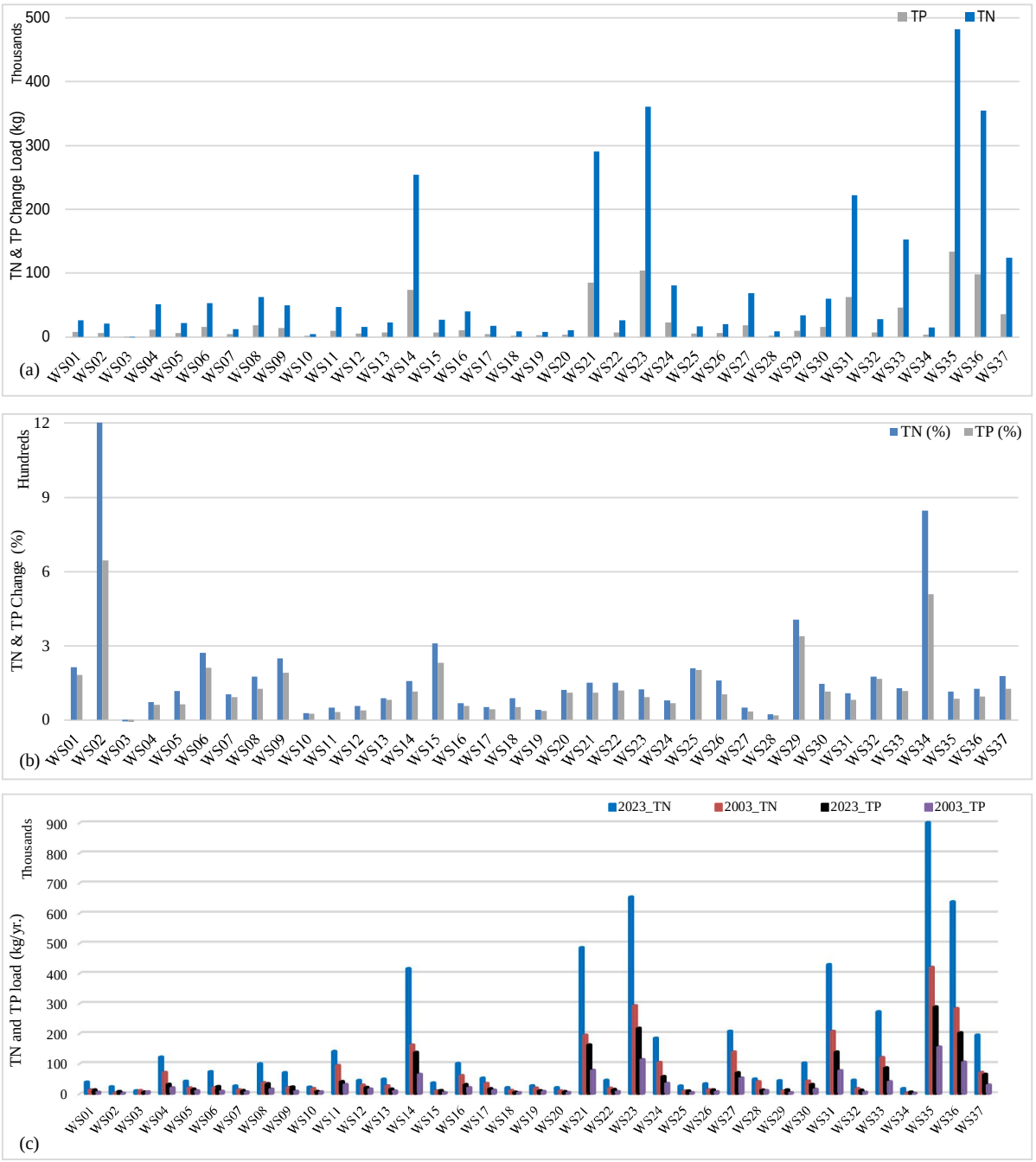

Figure 5-17 Sub-watershed level nutrient load; TN and TP change in (t/yr.) (a), TN and TP change in (%) (b), TN and TP load (t/yr.) (c).

5.4 Conclusions

A 991,804.6 ha in the study area was used to parameterise, calibrate, and validate the SWAT model to predict the effect of LULC transformation on runoff, sediment load, and surface runoff non-point source chemical pollutants load such as PO_4^{3-}, NO_3^-, TP, and TN. Following the recommendations made by Moriasi (2007) (Moriasi D. N. et al., 2007), statistical evaluation of the model output was approved following the calibration and validation procedures. To ascertain if the model satisfied the suggested thresholds, the following statistical measures were employed in

this study: P-factor, r-factor, R^2, RSR, PBIAS, and NSE. For instance, the NSE value of the sediment load throughout the calibration and validation periods is represented by the SWAT model performance indicator, which is 0.7 and 0.64, respectively. Similarly, throughout the calibration and validation period, the NSE values of NO_3^-, PO_4^{3-}, TN, and TP load were (0.66, 0.52), (0.64, 0.6), (0.61, 0.65), and (0.54, 0.63), respectively. The findings showed that SWAT can estimate the rate of changes in sediment and nutrient loads between 2003 and 2023 with adequate accuracy.

LULC changes at a sub-watershed level by varying ranges of load had an impact on runoff and non-point source pollutant loading, including sediment, PO_4^{3-}, NO_3^-, TP, and TN, as results revealed. The growth of built-up areas in response to the need for settlement and the rising change in agricultural land were the main causes of the increases in runoff volume, sediment, PO_4^{3-}, NO_3^-, TP, and TN over two decades. Higher nutrient loads resulted from increased cropland areas in 2023 compared to 2003 (77.9% and 31.46%, respectively) and increased built-up areas in 2023 compared to 2003 (4.54% and 2.52%, respectively). The non-point source result showed that agricultural areas contribute significantly to the creation of NPSP since crop fertilisation is primarily dependent on inorganic fertilisers and that priority source areas in the study area are mainly connected to densely populated human settlements.

The findings indicate there was a direct correlation between runoff and the occurrence of diffuse source pollution. However, this fact cannot be applied to all non-point source pollutants, as the nitrate load example illustrates. The monthly examination of nitrate load revealed that the “Belg” season had a high nitrate load. This is because the nitrogen pool process and the timing of nitrification cause a rise in nitrate levels during the off-growing season. This study indicated that diffuse source contaminant loads in the upper Awash generally happened during the rainy season, except for nitrate loads. Consequently, it is possible to view the wet season as a critical time for preventing nutrient loss.

The evidence generated can be used by planners and policymakers when developing management plans for reducing runoff and sediment yields in the watershed, as well as for managing fertiliser application in cropland areas to reduce diffused source chemical pollutants and increase the efficiency with which rain-fed crops use nutrients. Nutrient management and planning must be used to apply the right amounts of nutrients to the soil following crop nutrient requirements to avoid contaminating water bodies. To implement these practices, we must follow the principles of nutrient management, which include choosing and utilising the right rate, right place, right time, and a variety of organic sources of nutrients, such as organic manure amendments, understanding the soil and landscape features, identifying the soil fertility reserves, and recognising the crop’s nutrient requirements. We also need to adjust application tools to determine the appropriate amount to apply, use the best management techniques (preventive measures) while providing nutrients, and adopt the best soil and water conservation practices to prevent nutrient leaching. Furthermore, drip irrigation systems can distribute liquid fertilisers via the irrigation water on farms that use irrigation. By delivering nutrients straight to the root zone, this method lowers nutrient loss.

Chapter 6 : CONCLUSION AND RECOMMENDATION

6.1 Conclusion

From the results provided in the previous sections, the following conclusions have been made.

6.1.1 Water quality status, impact, and most suitable water quality model

Understanding biogeochemical pressures and identifying research gaps with an emphasis on biological parameters and non-heavy metals were the key objectives of Chapter 2. Seventy-seven research works were considered for this synthesis. While most Ethiopian rivers have water quality problems, Awash has the worst impairment because it serves as a sink for garbage from urban, industrial, and rural areas throughout the basin. WHO and Canadian water quality index-based evaluation showed that the water is below the standard for these purposes (Keraga et al., 2017a).

Due to inadequate financial and technical resources, Ethiopian surface water quality monitoring is limited, which results in a limited understanding of the effects of pollutants. Insufficient monitoring at appropriate and finer temporal scales leads to limited modelling of hydrological water quality (Zinabu et al., 2019). Water from the Awash River is crucial for domestic use and irrigation, but its quality is often poor and not in line with desired or natural levels. The Awash Rivers' water quality was found to be above Ethiopian and global minimum surface water quality standards. Large-scale irrigation, poor farming practices, and pollution from socioeconomic activities all degrade the quality of the water in the Awash River.

Untreated domestic, industrial, commercial, and institutional liquid waste discharged into the Awash River harmed the river’s water quality. Agricultural farms, vegetable production, and animal husbandry have a major impact on the Awash River and Upper Awash tributaries (Tufa, 2021). This has resulted in a significant generation of organic waste and nutrient enrichment in aquatic environments. Due to its high population density, high rate of urbanization, and relatively high number of industries, Uupper Awash is the major research area. Assessing the comparative impact of NPS pollutants and point sources, however, remains a significant area of unmet research in the basin.

In Chapter 3, knowledge gaps for long-term basin development and management are identified by examining the effects of contaminated water on soil, vegetables, human health, and river systems. The biological impact of water quality analysis revealed that the levels of heavy metals in rivers, lakes, edible fish tissues, soil, and plants that were irrigated by these river waters were above the WHO-recommended limit. The greatest quantities of heavy metals were discovered in Cr, followed by As, Pb, Cd, Se, and Hg in water and tissue samples from edible fish species in Koka Lake (Dsikowitzky et al., 2013).

In addition, eutrophication caused by urban detergents, agricultural, and industrial waste raises nutrient levels and produces algal blooms, which in turn create water hyacinths and a decrease in biodiversity. The food chain, ionic composition, organic matter in the sediment, oxygen levels, and water temperature are all changed by these contaminants, which causes fish suffocation. There are dangerous poisonous algae species present in the Sebeta River, the Koka and Aba Samuel reservoirs, and the water hyacinth invasion.

Exposure to heavy metals through the skin and ingested pathways can lead to significant toxicity. For instance, it was discovered that the levels of Fe, Cr, and Ni in Lake Koka exceeded the WHO's recommended limit. The Tinishu Akaki River has high quantities of heavy metals, which might affect aquatic life and those who depend on the water. Water samples from the Akaki River have varying quantities (mg/L) of Fe, Zn, Cu, Cd, Pb, and Cr: 0.18-0.28, 1.40-2.67, 0.97-1.40, 0.037-0.087, 0.037-0.080, and 01-0.14, in that order, above the recommended limit. The poor quality of the river water affects crop products; the leaves of potatoes, onions, red beet, and other crops contain trace amounts of Cd, Cr, Cu, Hg, Ni, and Zn. In addition to this, concentrations of Cd (0.47-3.47), Pb (8.00-118.00), Fe (13,557.30-6,800.00), Zn (40.00-224.67), Cr (4.91-39.36), and Cu (35.00-49.88) (mg/kg) were observed in soil samples irrigated by Akaki River water. In the soil samples, every metal (except Cd and Fe) is not within the recommended standard set (Bahiru, 2021).

Water quality has socio-economic impacts. The contamination of rivers has forced the 30,000-person municipality of Awash to switch from abstracting water from rivers to groundwater. Furthermore, the Awash River's pH level is raised by the high concentration of salt in its tributary rivers and lakes, which has an impact on the output of businesses that grow cotton, wheat, and other cereal crops as well as vegetables (Assegide et al., 2022). Studies are lacking comprehensive spatial and temporal water quality impact mapping and analysis. Evidence-based research on contaminated water's effects on agriculture, human and animal health, and socioeconomics is scarce. Regular biological water quality monitoring is also lacking.

The most effective model for the NPSP evaluation that can be employed in this research was the primary topic of discussion in the fourth chapter. This review discusses thirteen hydrological water quality models. Input data, strengths, limitations, spatial extent, temporal variability, capabilities in simulation, components they possess, type, nature, complexity, time step, hydrology, system, model category, intended usage, development, fundamental principle, supported land and water features, TMDL support, operation, and pollution handling are the main factors taken into consideration. So that this model selection has a crucial role in giving the scientific community information on the hydrological models that they should consider while working with hydrological systems.

Various models employ different data sources, such as precipitation, air temperature, soil properties, terrain, vegetation, hydrogeology, and other physical factors. These models can all be used for extremely large and complex basins. Applications of AGNPS and ANSWERS are restricted to watersheds of about 200 km^2, whereas SWRRB may be applied in agricultural basins up to 600–800 km^2 and has a limited distributed parameter capability (Young et al., 1989). While SWIM may be used at the mesoscale, it cannot be employed at the basin scale. Similar to this, models of 1000 km^2, 3 km^2, and less than 100 km^2 respectively are found in DLBRM, PLOAD, and MIKE SHE. SWAT may be utilized from small watersheds to basin scale (up to 25000 km^2), whereas BASIN can be used for WQ study at both the regional and national levels. Each of these models has some degree of integration with GIS tools (Cutts, 2013).

Long-term continuous simulation models with all three key components (hydrology, sediment, and chemical) suited to catchments at the watershed scale include AnnAGNPS, HSPF, MIKE-SHE,

and SWAT. SWAT more closely captures our current understanding of watershed processes and how they affect the creation of pollution than do the PLOAD and L-THIA models. Of the models discussed, BASIN and SWAT are relatively new, although HSPF and SWMM have endured for a long time. BASINS, SWAT, and WASP support water quality measures such as sediment, nutrients, toxics, BOD, and DO. SWAT and AnnAGNPS simulate the TMDL of TP, TN, and sediment load and concentration, nitrate, ammonia, DO, BOD, chlorophyll a, TSS, metal, pesticide, herbicide, and hazardous concentration daily basis. However, AnnAGNPS is unable to simulate BOD and metals in watersheds. Additionally, it is restricted to agricultural and rural watersheds.

The BASIN and SWAT models are now the most effective models that may be used to analyze point and NPS contamination in various basins.

6.1.2 Spatiotemporal variation of water quality indicators

The approach to collecting and verifying Chl-a, TU, and TSS satellite data is indirect because there is no reflectance data, ground-based observations, or handheld radiospectrometers at the reservoir in Koka. To compare the gathered and associated set of in situ data for Chl-a (µg/L), TU (NTU), and TSS (mg/L) concurrently with the images, the reflectance and reflectance ratios at different wavelengths were utilized.

After analyzing Sentinel-2's extracted bands and developing water quality models, the particular spectral band B4 (665 nm) showed the best relationships with TSS, TU, and Chl-a. The investigation shows that Sentinel-2 products are effective in predicting, measuring, and visualizing temporal and geographical patterns in Chl-a, TU, and TSS in small water bodies. Moreover, it was discovered that the linear regression approach can precisely predict Chl-a, TU, and TSS utilizing interactions between optical and water quality indicators.

Regression validation showed that the Chl-a estimations had satisfactory correlations, with an R^2 of 0.9127. The findings demonstrated that, for the assessment of Chl-a concentrations, the blue, green, and red vegetation red edge bands, and band ratios produced the best results, with R^2 greater than 0.8. The January value of Chl-a was the lowest (0.07 µg/L), whereas November's was the highest (354.64 µg/L). November (0.83 mg/L) and December 2021(0.91 mg/L), as well as January–March 2022 (0.93, 0.58, 0.5 mg/L), had the lowest TSS concentrations and dispersion. April and May 2022 were the months with the highest amounts of TSS (574.51, 478.94 mg/L). In 2021, the highest TSS concentrations were seen in June (387.56 mg/L). An increase in TSS content is associated with the “Belg” rains, which wash exposed soil from urban areas, agricultural fields in upstream watersheds, and bare lands from February to April. In June 2021, at the beginning of the rainy season, and May 2022, at the middle of the “Belg” season, recorded the greatest maximum (38.44, 44.02 mg/L), minimum (209.85, 202.81 mg/L), and mean (115.07, 115.39 mg/L) turbidity, respectively.

The results of the spatial analysis showed that the distributions of TSS, TU, and Chl-a were heterogeneous, with TSS and TU being higher on the reservoir's western side and Chl-a being more prevalent in the south and southwest. In summary, our findings demonstrate that water quality measures exhibit both temporal and spatial variability. The suggested algorithms may be

used in comparable environmental circumstances and can identify optically active water quality indicators.

In this case, a novel approach to water quality evaluation is suggested, one that utilizes open satellite datasets and remote sensing to overcome the limitations of traditional water quality point sampling and analysis. The Sentinel-2-based approach that has been described may directly correlate the level of concentration of TSS, TU, and Chl-a with the extent of advancement in measuring the dynamic change process of TSS, TU, and Chl-a across various time series.

6.1.3 Prioritizing watersheds for intervention design

To address the subject of where erosion hotspot sub-watersheds are located and how they are ranked in terms of susceptibility to erosion, Chapter 6 was created to rank sub-watersheds according to their LULC, sediment load, and morphometric characteristics.

This work employed a quantitative morphometric analysis using satellite images, DEM data, and the output of the SWAT model. Remote sensing and GIS technologies were consequently more successful in helping planners and decision-makers understand the morphological, LULC, and sediment load factors of the particular sub-watershed for planning at the sub-watershed level. Linear, areal, and relief features were used to depict the hydrologic behavior of the watersheds. Their attributes were particularly useful in showing the relative severity of each sub-watershed.

The findings indicated that 2524.6 km2 (25.45%) is in the susceptibility to soil erosion class, 2722.14 km^2 (27.44%) is in the moderate susceptible class, 854.35 km^2 (8.61%) is in the low susceptible class, and 2205.48 km^2 (22.23%) is in the very low susceptible class. About 1611.43 km^2 (16.25%) is in the class of very high erosion sensitivity. As the sub-watersheds final outlet, the Koka reservoir, it is advised that the appropriate conservation measures be implemented to decrease soil erosion, reduce sediment production in the sub-watersheds, and reduce sediment deposition in the reservoir. This is because the upper Awash basin is extremely vulnerable to erosion due to the transformation of forest grassland and shrubland to cropland in the last two decades.

Decision-makers and planners may successfully employ GIS and RS approaches to prioritize soil and water conservation activities when combined with multi-criteria decision-making (MCDM) methodologies like AHP-VIKOR with a risk assessment matrix.

6.1.4 Non-point source pollutant modelling

Examining LULC change and its effects on runoff and non-point source pollutant loads (sediment, nitrate (NO_3^-), total nitrogen (TN), and total phosphorus (TP)) has been the primary goal of the current study. Additionally, it has made an effort to map the sub-watersheds by pollution loads and quantify spatiotemporal non-point source contaminants.

The SWAT model was parameterized, calibrated, and validated on a 991804.6 ha area in the upper Awash sub-basin to estimate the effects of LULC change on runoff, sediment load, and non-point source chemical pollutants (PO_4^{3-}, NO_3^-, TP, and TN) in surface runoff. The results demonstrated

that SWAT could accurately predict the rate of changes in nutrient and sediment loads between 2003 and 2023.

According to the data, the built-up area covers 2.52% and 4.54% in 2003 and 2023, whereas agricultural land covers 31.46% and 77.9%, shrub land covers 58.4% and 14.9%, and forest covers 4.06% and 2.13%. Grassland, bushes, woods, and wetlands have contributed the most to sub-basin agricultural land in the research. The analysis shows that during the past 20 years, there has been a rise in built-up areas and agricultural land, while there has been a reduction in shrubs, forests, grassland, water, and wetland areas. During the research period, there was an increase of 147.29% in agricultural land and 80.15% in built-up areas, mainly Addis Ababa. Population growth drives up the need for land for investment, for formal and informal settlements, and for a range of agricultural goods, including cereal crops. In contrast, there was a 47.55%, 96.7%, and 74.37% decrease in the forest, grassland, and shrubland, respectively. This might be the result of investments, urbanization, and agriculture leading to the removal of shrublands and deforestation.

The upper Awash sub-basin had a 0-66.5% increase in runoff as a result of the LULC shift that occurred between 2003 and 2023. As a result, variations in LULC and surface runoff volume are strongly correlated. The average yearly sediment load increased by 25-27, 298.7 tons as a result of the conversion in LULC between 2003 and 2023. Within 20 years, the annual average sediment load values rise by 23.89% when built-up areas and agriculture replace grassland, shrubs, and forests. According to the simulations, there was an increase in the NO_3^- load of between 127.6 kg/yr. (29%) and 20739.7 kg/yr. (133.5%). The PO_4^{3-} levels of the net contribution increased by 4.27-349% as a result of the LULC modification, or 31 t/yr. The majority of the sub-watersheds exhibit the conversion of LULC from other uses to agriculture, as shown by the two parameters (PO_4^{3-} and NO_3^-), and the built-up area contributed to the change and growth of the nutrients. Between 2003 and 2023, the total nitrogen output of the model increased, with values ranging from 22.2% (8736 kg/yr.) to 1201.5% (20615 kg/yr.). From 1383.5 kg/yr. (25.66%) to 133641.2 kg/yr. (86.6%), the TP model output showed an increase between 2003 and 2023.

The results show that there was a direct relationship between the quantity of rainfall and runoff and the prevalence of non-point-source pollution. rising levels of precipitation, which cause runoff and consequent nutrient loss. As the nitrate load example shows, this fact does not apply to all non-point-source contaminants. The "Belg" season had a high nitrate load, according to the monthly analysis of nitrate load. This is because nitrate levels rise during the off-growing season due to the nitrogen pool process and the timing of nitrification. In addition to this, nitrate decomposed from domestic waste, malfunctioning septic systems, and other activities throughout dry periods. Except for nitrate load, this study showed that non-point source pollutant loads in the upper Awash basin typically occurred during the rainy season.

6.2 Recommendations

Policymakers can formulate laws and regulations to protect natural resources and establish a balance between conflicting social, economic, and environmental needs by using trustworthy data and information on the research results. Building capacity and strengthening training programs are critical if nations like Ethiopia can capitalize on the benefits of technical advancements like remote sensing-based water quality monitoring tools.

Sub-watershed prioritizing is a useful strategy for managing watersheds and preserving water resources. In addition to this, the remote sensing methods research results can also be used to monitor the continuous state of lakes and reservoirs by using the technology as an alternative water quality monitoring tool. Therefore, the results of this study project can be applied in different places and settings by planners and decision-makers dealing with soil and water resources.

The research findings can be used by planners and practitioners as a critical baseline for additional studies in the identified gaps and in watersheds with similar agro-ecologies to lower runoff and sediment loads in the watershed, control fertilizer in agricultural areas to lower non-point source chemical pollutants, and improve the efficiency with which rain-fed crops use nutrients.

REFERENCE

Abbaspour, K. C. (2012). *A package of calibration procedures linked to SWAT through a generic platform to perform calibration , validation , and uncertainty analysis SWAT-CUP*. https://envirogrids.net/envirogrids_d4.5_calibration_swat_cupdfb0.pdf?option=com_jdownloads&Itemid=13&view=finish&cid=145&catid=13

Abbaspour, K. C. (2015). SWAT-CUP: SWAT Calibration and Uncertainty Programs - A User Manual. In *Swiss Federal Institute of Aquatic Science and Technology: Eawag, Switzerland* (pp. 1–100).

Abbaspour, K. C., Rouholahnejad, E., Vaghefi, S., Srinivasan, R., Yang, H., & Kløve, B. (2015). A continental-scale hydrology and water quality model for Europe: Calibration and uncertainty of a high-resolution large-scale SWAT model. *Journal of Hydrology*, *524*, 733–752. https://doi.org/10.1016/j.jhydrol.2015.03.027

Abbaspour, K. C., Yang, J., Maximov, I., Siber, R., Bogner, K., Mieleitner, J., Zobrist, J., & Srinivasan, R. (2007). Modelling hydrology and water quality in the pre-alpine/alpine Thur watershed using SWAT. *Journal of Hydrology*, *333*(2–4), 413–430. https://doi.org/10.1016/j.jhydrol.2006.09.014

Abbott, M. ., Bathurst, J. C., Cunge, J. A., O'Connell, P. E., & Rasmussen, J. (1986). AN INTRODUCTION TO THE EUROPEAN HYDROLOGICAL SYSTEM - SYSTEME HYDROLOGIQUE EUROPEEN, "SHE", 1: As the cost of water resource development has increased , so there has been an increasing demand for a new approach to hydrolo. *Journal of Hydrology*, *87*, 45–59.

Abdeta, G. C., Tesemma, A. B., Tura, A. L., & Atlabachew, G. H. (2020). Morphometric analysis for prioritizing sub-watersheds and management planning and practices in Gidabo Basin, Southern Rift Valley of Ethiopia. *Applied Water Science*, *10*(7), 1–15. https://doi.org/10.1007/s13201-020-01239-7

Abebe, F., Alamirew, T., & Abegaz, F. (2015). Appraisal and Mapping of Soil Salinity Problem in Amibara Irrigation Farms, Middle Awash Basin, Ethiopia. *International Journal of Innovation and Scientific Research*, *13*(1), 298–314. http://www.secheresse.info/spip.php?article6480

Abell, J. M., Özkundakci, D., Hamilton, D. P., & Jones, J. R. (2012). Latitudinal variation in nutrient stoichiometry and chlorophyll-nutrient relationships in lakes: A global study. *Fundamental and Applied Limnology*, *181*(1), 1–14. https://doi.org/10.1127/1863-9135/2012/0272

Abhachire, L. W. (2014). Studies on Hydrobiological Features of Koka Reservoir and Awash River in Ethiopia. *International Journal of Fisheries and Aquatic Studies*, *1*(3), 158–162. www.fisheriesjournal.com

Abro, T. W. (2021). Licensed under a Creative Commons Multi-criteria based Watershed Prioritization for Soil and Water Conservation: The case of Gotu Watershed, Awash River Basin, Ethiopia. *Print) East African Journal of Sciences*, *15*(2), 115–128. http://earthexplorer.us

Adane, G. B., Hirpa, B. A., Song, C., & Lee, W. K. (2020). Rainfall characterization and trend analysis of wet spell length across varied landscapes of the upper awash river basin, ethiopia. *Sustainability (Switzerland)*, *12*(21), 1–14. https://doi.org/10.3390/su12219221

Addis, H. K., Strohmeier, S., Ziadat, F., Melaku, N. D., & Klik, A. (2016). Modeling streamflow and sediment using SWAT in ethiopian highlands. *International Journal of Agricultural and Biological Engineering*, *9*(5), 51–66. https://doi.org/10.3965/j.ijabe.20160905.2483

Ademe, A. S. (2014). Source and Determinants of Water Pollution in Ethiopia: Distributed Lag Modeling Approach. *Intellectual Property Rights: Open Access*, *2*(2). https://doi.org/10.4172/2375-4516.1000110

Adhami, M., & Sadeghi, S. H. (2016). Sub-watershed prioritization based on sediment yield using game theory. *Journal of Hydrology*, *541*(August), 977–987. https://doi.org/10.1016/j.jhydrol.2016.08.008

Adimassu, Z., Langan, S., Johnston, R., Mekuria, W., & Amede, T. (2017). Impacts of Soil and Water Conservation Practices on Crop Yield, Run-off, Soil Loss and Nutrient Loss in Ethiopia: Review and Synthesis.

Environmental Management, *59*(1), 87–101. https://doi.org/10.1007/s00267-016-0776-1

Admas, B. F., Gashaw, T., Adem, A. A., Worqlul, A. W., Dile, Y. T., & Molla, E. (2022). Identification of soil erosion hot-spot areas for prioritization of conservation measures using the SWAT model in Ribb watershed, Ethiopia. *Resources, Environment and Sustainability*, *8*(April), 100059. https://doi.org/10.1016/j.resenv.2022.100059

Adu, J. T., & Kumarasamy, M. V. (2018). Assessing non-point source pollution models: A review. *Pol. J. Environ. Stud*, *27*(5), 1913–1922. https://doi.org/10.15244/pjoes/76497

Adugna, D., Brook, L., Sahilu, G. G., Larissa, L., Kumelachew, Y., & Bergen, J. M. (2019). Stormwater impact on water quality of rivers subjected to point sources and urbanization – the case of Addis Ababa, Ethiopia. *Water and Environment Journal*, *33*(1), 98–110. https://doi.org/10.1111/wej.12381

Agizew, N., & Getaneh, Z. (2016). *Awash River Basin Water Allocation Modeling and Conflict Resolution Study Project, WP4 Water Quality Study Final Report*.

Ahmed, S. A., Chandrashekarappa, K. N., Raj, S. K., Nischitha, V., & Kavitha, G. (2010). Evaluation of morphometric parameters derived from ASTER and SRTM DEM - A study on Bandihole sub-watershed basin in Karnataka. *Journal of the Indian Society of Remote Sensing*, *38*(2), 227–238. https://doi.org/10.1007/s12524-010-0029-3

Ahuja, S. (2013). Monitoring Water Quality: Pollution Assessment, Analysis, and Remediation. In *Monitoring Water Quality: Pollution Assessment, Analysis, and Remediation*. https://doi.org/10.1016/C2011-0-05798-8

Akalu, S., Mengistu, S., & Leta, S. (2011). Assessing Human Impacts on the Greater Akaki River, Ethiopia Using macroinvertebrates. *Ethiop. J. Sci.*, *34*(2), 89–98.

Aklilu, A., & Necha, T. (2018). Analysis of the Spatial Accessibility of Addis Ababa's Light Rail Transit: The Case of East–West Corridor. *Urban Rail Transit*, *4*(1), 35–48. https://doi.org/10.1007/s40864-018-0076-6

Alayu, E., & Yirgu, Z. (2018). Advanced technologies for the treatment of wastewaters from agro-processing industries and cogeneration of by-products: a case of slaughterhouse, dairy and beverage industries. *International Journal of Environmental Science and Technology*, *15*(7), 1581–1596. https://doi.org/10.1007/s13762-017-1522-9

Alemayehu, F., Motuma, T., & Gizaw, T. (2019). Land Use Land Cover Change Trend and Its Drivers in Somodo Watershed South Western, Ethiopia. *African Journal of Agricultural Research*, *14*(2), 102–117. https://doi.org/10.5897/ajar2018.13672

Alemu, M L., Geset, M, Mosa, H M., Zemale, F A., Moges, M A., Giri, S K., Tillahun, S A., Melesse, A., Ayana, E K., Steenhuis, T. S. (2017). Spatial and Temporal Trends of Recent Dissolved Phosphorus Concentrations in Lake Tana and its Four Main Tributaries. *Land Degradation and Development*, *28*(5), 1742–1751. https://doi.org/10.1002/ldr.2705

Alfisah, R. K., Rusmana, I., Widiyanto, T., & Affandi, R. (2022). The Abundance and Potential Activity of Nitrifying, Denitrifying, and Nitrate-ammonifying Bacteria in the Vanamae Shrimp Culture in Karawang. *IOP Conference Series: Earth and Environmental Science*, *1062*(1). https://doi.org/10.1088/1755-1315/1062/1/012011

Ali, S. A., & Ikbal, J. (2015). Prioritization based on geomorphic characteristics of Ahar watershed, Udaipur district,Rajasthan, India using Remote Sensing and GIS. *Journal of Environmental Research And Development*, *10*(1), 187–200. https://www.researchgate.net/publication/281856622_Prioritization_based_on_geomorphic_characteristics_of_Ahar_watershed_Udaipur_districtRajasthan_India_using_Remote_Sensing_and_GIS

Almeida, R. A., Pereira, S. B., & Pinto, D. B. F. (2018). Calibration and validation of the SWAT hydrological model for the Mucuri river basin. *Engenharia Agricola*, *38*(1), 55–63. https://doi.org/10.1590/1809-4430-

Eng.Agric.v38n1p55-63/2018

Alves, G. J., Rogério de Mello, C., Beskow, S., Junqueira, J. A., & Nearing, M. A. (2019). Assessment of the soil conservation service–curve number method performance in a tropical oxisol watershed. *Journal of Soil and Water Conservation*, *74*(5), 500–512. https://doi.org/10.2489/jswc.74.5.500

Amare, A. (2019). Corporate environmental responsibility in Ethiopia: a case study of the Akaki River Basin. *Ecosystem Health and Sustainability*, *5*(1), 57–66. https://doi.org/10.1080/20964129.2019.1573107

Ambrose-igho, G. (2020). *Spatiotemporal Analysis Of Lake Water Quality Indicators On Small Lakes, Lake Bloomington And Evergreen Lake In Central Illinois, Using Satellite Remote Sensing* [Illinois State University]. https://ir.library.illinoisstate.edu/etd/1190

Amenu, K. (2013). Assessment of water sources and quality for livestock and farmers in the Rift Valley area of Ethiopia: Implications for health and food safety. In *Psychology Applied to Work: An Introduction to Industrial and Organizational Psychology, Tenth Edition Paul* (Vol. 53, Issue 9). https://doi.org/10.1017/CBO9781107415324.004

Ameri, A., Pourghasemi, H., & Cerda, A. (2018). Erodibility prioritization of sub-watersheds using morphometric parameters analysis and its mapping: A comparison among TOPSIS, VIKOR, SAW, and CF multi-criteria decision making models. *Science of the Total Environment*, *613–614*, 1385–1400. https://doi.org/10.1016/j.scitotenv.2017.09.210

Amoatey, P., & Baawain, M. S. (2019). Effects of pollution on freshwater aquatic organisms. *Water Environment Research*, *91*(10), 1272–1287. https://doi.org/10.1002/wer.1221

Angelats, E., & Fern, M. (2019). *First Results of Phytoplankton Spatial Dynamics in Two NW-Mediterranean Bays from Chlorophyll- a Estimates Using Sentinel 2 : Potential Implications for Aquaculture*.

Angélica L., Gutiérrez-Magness, and J. J. P. R. (2003). *Development, Calibration, and Analy sis of a Hydrologic and Water-Quality Model of the Delaware Inland Bay s Watershed*.

Angello, Z. A., Tränckner, J., & Behailu, B. M. (2021). Spatio-temporal evaluation and quantification of pollutant source contribution in little akaki river, Ethiopia: Conjunctive application of factor analysis and multivariate receptor model. *Polish Journal of Environmental Studies*, *30*(1), 23–34. https://doi.org/10.15244/pjoes/119098

Ansper, A., & Alikas, K. (2019). *Retrieval of Chlorophyll a from Sentinel-2 MSI Data for the European Union Water Framework Directive Reporting Purposes*. https://doi.org/10.3390/rs11010064

Anteneh, A. (2022). Review on the role of soil and water conservation practices on soil properties improvement in Ethiopia. *International Journal of Agricultural Science and Food Technology*, *8*(3), 225–231. https://doi.org/10.17352/2455-815x.000168

Anteneh, W. (2014). *Water hyacith coverage survey report on Lake Tana technical report series 1*.

Arabi, M., Govindaraju, R. S., Hantush, M. M., & Engel, B. A. (2006). Role of Watershed Subdivision on Modeling the Effectiveness of Best Managemen ... *Water Resources*, *45268*, 513–528.

Aregahegn, & Zerihun. (2021). Study on Irrigation Water Quality in the Rift Valley Areas of Awash River Basin, Ethiopia. *Applied and Environmental Soil Science*, *2021*. https://doi.org/10.1155/2021/8844745

Argaw, M., & Yohannes, H. (2024). Impact of land use/land cover changes on surface water and soil-sediment export in the urbanized Akaki River catchment, Awash Basin, Ethiopia. *Journal of Hydrology: Regional Studies*, *52*(February 2023), 101677. https://doi.org/10.1016/j.ejrh.2024.101677

Arheimer, B., & Olsson, J. (2001). *Integration and Coupling of Hydrological Models with Water Quality Models : Applications in Europe*. 53. http://www.wmo.int/pages/prog/hwrp/documents/RAVI/Water Quality_FINAL2.pdf

Arnold, J. G., Moriasi, D. N., Gassman, P. W., Abbaspour, K. C., White, M. J., Srinivasan, R., C. Santhi, R., Harmel, D., Griensven, A. van, Liew, M. W. Van, & N. Kannan, M. K. J. (2012). SWAT: Model use, calibration, and validation. *Transactions of the ASABE*, *55*(4), 1249–1260. https://doi.org/10.13031/2013.42256

Arnold, J. G., Srinivasan, R., Muttiah, R. S., & Williams, J. R. (1998). Large area Hydrologic Modeling and Assessment Part I: Model development. *American Water Resources Association*, *34*(February), 73–89. https://doi.org/10.1111/j.1752-1688.1998.tb05961.x

Arora, M., Kiran, B., Rani, S., Rani, A., Kaur, B., & Mittal, N. (2008). Heavy metal accumulation in vegetables irrigated with water from different sources. *Food Chemistry*, *111*(4), 811–815. https://doi.org/10.1016/j.foodchem.2008.04.049

Aschale, M. (2015). *Assessment of Potentially Toxic Elements in Vegetables Grown along Akaki River in Addis Ababa and Potential Health Implications*. *40*, 42–53.

Aschale, M., Sileshi, Y., Kelly-Quinn, M., & Hailu, D. (2021). Multivariate analysis of potentially toxic elements in surface waters in Ethiopia. *Applied Water Science*, *11*(5). https://doi.org/10.1007/s13201-021-01412-6

Ashok K., M., & Singh, V. P. (2010). A review of drought concepts. *Journal of Hydrology*, *391*(1–2), 202–216. https://doi.org/10.1016/j.jhydrol.2010.07.012

Asmelash Tilahun, H. A. S. and B. G. (2017). Sediment inflow estimation and mapping its spatial distribution at sub-basin scale: the case of Tendaho dam, Afar regional state, Ethiopia. *University of Twente*, *44*(3), 389–397. https://doi.org/10.11698/PED.2017.03.08

Asnake, K., Worku, H., & Argaw, M. (2021). Integrating river restoration goals with urban planning practices: the case of Kebena river, Addis Ababa. *Heliyon*, *7*(7). https://doi.org/10.1016/j.heliyon.2021.e07446

Assegide, Alamirew, Bayabil, H., Dile, Y. T., Tessema, B., & Zeleke, G. (2022). Impacts of Surface Water Quality in the Awash River Basin, Ethiopia: A Systematic Review. *Frontiers in Water*, *3*(790900), 1–15. https://doi.org/10.3389/frwa.2021.790900

Assegide, Alamirew, T., Dile, Y. T., Bayabil, H., Tessema, B., & Zeleke, G. (2022). A Synthesis of Surface Water Quality in Awash Basin, Ethiopia. *Frontiers in Water*, *4*(782124), 1–17. https://doi.org/10.3389/frwa.2022.782124

Assegide, Shiferaw, H., Tibebe, D., Peppa, M. V., Walsh, C. L., Alamirew, T., & Zeleke, G. (2023). Spatiotemporal Dynamics of Water Quality Indicators in Koka Reservoir, Ethiopia. *Remote Sensing*, *15*(4), 1155. https://doi.org/10.3390/rs15041155

Astatkie, H., Ambelu, A., & Mengistie, E. (2021). Contamination of Stream Sediment With Heavy Metals in the Awetu Watershed of Southwestern Ethiopia. *Frontiers in Earth Science*, *9*(July), 1–13. https://doi.org/10.3389/feart.2021.658737

Attanasi, E. D., Johnson, S. R., Leduc, S., & McQuigg, J. D. (1973). Forecasting Work Conditions for Road Construction Activities: An Application of Alternative Probability Models. *Monthly Weather Review*, *101*(3), 223–230. https://doi.org/10.1175/1520-0493(1973)101<0223:fwcfrc>2.3.co;2

AwBA. (2017). *Executive Summary of Strategic River Basin Plan for Awash Basin*.

Awoke, A., Beyene, A., Kloos, H., Goethals, P. L. M., & Triest, L. (2016). River Water Pollution Status and Water Policy Scenario in Ethiopia: Raising Awareness for Better Implementation in Developing Countries. *Environmental Management*, *58*(4), 694–706. https://doi.org/10.1007/s00267-016-0734-y

Awol, A. (2018). Physicochemical Analysis of Hora and Spring Water Bodies in AnderachaWoreda, Sheka Zone, South West Ethiopia. *International Journal of Current Research and Academic Review*, *6*(4), 48–53. https://doi.org/10.20546/ijcrar.2018.604.007

Ayana, A. B., Edossa, D. C., & Kositsakulchai, E. (2012a). Simulating of sediment yield using swat in Fincha. *Kasetsart J. (Nat. Sci.)*, *46*(2).

Ayana, A. B., Edossa, D. C., & Kositsakulchai, E. (2012b). Simulation of sediment yield using SWAT model in Fincha watershed, Ethiopia. *Kasetsart Journal - Natural Science*, *46*(2), 283–297.

Ayele, G. T., Teshale, E. Z., Yu, B., Rutherfurd, I. D., & Jeong, J. (2017). Streamflow and sediment yield prediction for watershed prioritization in the upper Blue Nile river basin, Ethiopia. *Water (Switzerland)*, *9*(10). https://doi.org/10.3390/w9100782

Ayenew, T., & Legesse, D. (2007). The changing face of the Ethiopian rift lakes and their environs: Call of the time. *Lakes and Reservoirs: Research and Management*, *12*(3), 149–165. https://doi.org/10.1111/j.1440-1770.2007.00332.x

Ayiti, O. E., & Babalola, O. O. (2022). Factors Influencing Soil Nitrification Process and the Effect on Environment and Health. *Frontiers in Sustainable Food Systems*, *6*(2), 1–12. https://doi.org/10.3389/fsufs.2022.821994

B., P., & Ouyang, Y. (2013). Watershed-Scale Hydrological Modeling Methods and Applications. In *Current Perspectives in Contaminant Hydrology and Water Resources Sustainability*. https://doi.org/10.5772/53596

B.Abate, A.Woldesenbet, & D.Fitamo. (2015). Water quality assessment of lake Hawassa for multiple designated water uses. In *Water Utility Journal* (Vol. 9, Issue 11). TC.

Babel, M. S., Gunathilake, M. B., & Jha, M. K. (2021). Evaluation of ecosystem-based adaptation measures for sediment yield in a tropical watershed in Thailand. *Water (Switzerland)*, *13*(19), 1–25. https://doi.org/10.3390/w13192767

Babel, M. S., & Najim, M. M. M. (2017). *Assessment of Agricultural NonPoint Source Model for a Watershed in Tropical Assessment of Agricultural NonPoint Source Model for a Watershed in Tropical Environment*. *9372*(December). https://doi.org/10.1061/(ASCE)0733-9372(2004)130

Babiso, W. Z., Ayano, K. K., Haile, A. T., Keche, D. D., Acharya, K., & Werner, D. (2023). Citizen Science for Water Quality Monitoring in the Meki River, Ethiopia: Quality Assurance and Comparison with Conventional Methods. *Water (Switzerland)*, *15*(2). https://doi.org/10.3390/w15020238

Baerenklau, K. A. (2014). Nonpoint Source Pollution. *Environmental and Natural Resource Economics: An Encyclopedia*, *December*, 232–335. https://doi.org/10.2175/106143016x14696400495497

Bahiru. (2021). Evaluation of Heavy Metals Uptakes of Lettuce (Lactuca sativa L.) Under Irrigation Water of Akaki River, Central Ethiopia. *American Journal of Environmental Science and Engineering*, *5*(1), 6. https://doi.org/10.11648/j.ajese.20210501.12

Bakšić, N. (2019). *SHORT TERM SCIENTIFIC MISSION (STSM) REPORT : Cost action 15206 PESFOR- W , STSM title : Reviewing available pollutant models and decision support tools for informing the design and ma ... SHORT TERM SCIENTIFIC MISSION (STSM) SCIENTIFIC REPORT*. *January*.

Beasley, D. B., L. F. Huggins, & E. J. Monke. (1980). ANSWERS: A Model for Watershed Planning. *Transactions of the ASAE*, *23*(4), 0938–0944. https://doi.org/10.13031/2013.34692

Beasley, & Huggins, L. F. (1991). *ANSWERS - Users Manual*.

Bedada, T. L., Eshete, T. B., Gebre, S. G., Dera, F. A., Sima, W. G., Negassi, T. Y., Maheder, R. F., Teklu, S., Awoke, K., Feto, T. K., & Tullu, K. D. (2019). Virological Quality of Urban Rivers and Hospitals Wastewaters in Addis Ababa, Ethiopia. *The Open Microbiology Journal*, *13*(1), 164–170. https://doi.org/10.2174/1874285801913010164

Begna, D. (2014). Assessment of Pesticides Use and its Economic Impact on the Apiculture Subsector in Selected Districts of Amhara Region, Ethiopia. *Journal of Environmental and Analytical Toxicology*, *05*(03), 3–6.

https://doi.org/10.4172/2161-0525.1000267

Behmel, S., Damour, M., Ludwig, R., & Rodriguez, M. J. (2016). Water quality monitoring strategies — A review and future perspectives. *Science of the Total Environment*, *571*, 1312–1329. https://doi.org/10.1016/j.scitotenv.2016.06.235

Bekele, T. (2019). Effect of Land Use and Land Cover Changes on Soil Erosion in Ethiopia. *International Journal of Agricultural Science and Food Technology*, *5*, 026–034. https://doi.org/10.17352/2455-815x.000038

Belay, T. (2019). Assessment of Pollution Status of Soils and Vegetables Irrigated by Awash River and its Selected Tributaries. *International Journal of Environmental Sciences & Natural Resources*, *18*(5), 163–168. https://doi.org/10.19080/ijesnr.2019.18.556000

Belete, F., Dechassa, N., Molla, A., & Tana, T. (2018). Effect of nitrogen fertilizer rates on grain yield and nitrogen uptake and use efficiency of bread wheat (Triticum aestivum L .) varieties on the Vertisols of central highlands of Ethiopia. *Agriculture & Food Security*, 1–12. https://doi.org/10.1186/s40066-018-0231-z

Benoy, G. A., Jenkinson, R. W., Robertson, D. M., & Saad, D. A. (2016). Nutrient delivery to Lake Winnipeg from the Red—Assiniboine River Basin – A binational application of the SPARROW model. *Canadian Water Resources Journal*, *41*(3), 429–447. https://doi.org/10.1080/07011784.2016.1178601

Berg, H. van den, Rickert, B., Ibrahim, S., Bekure, K., Gichile, H., Girma, S., Azezew, A., Belayneh, T. Z., Tadesse, S., Teferi, Z., Abera, F., Girma, S., Legesse, T., Truneh, D., Lynch, G., Janse, I., & Husman, A. M. de R. (2019). Linking water quality monitoring and climate-resilient water safety planning in two urban drinking water utilities in Ethiopia. *Journal of Water and Health*, *17*(6), 989–1001. https://doi.org/10.2166/wh.2019.059

Beven, K., Wood, E., & Sivapalan, M. (1988). Catchment morphology and hydrological processes are inextricably linked through the geomorphic processes of soil development , erosion and deposition . Water provides the major driving force in the development of morphology through its role as a transport. *Journal of Hydrology*, *100*, 353–375.

Bhaduri, B., Harbor, J., Engel, B., & Grove, M. (2000). Assessing watershed-scale, long-term hydrologic impacts of land-use change using a GIS-NPS model. *Environmental Management*, *26*(6), 643–658. https://doi.org/10.1007/s002670010122

Bihonegn, B. G., & Awoke, A. G. (2023). Evaluating the impact of land use and land cover changes on sediment yield dynamics in the upper Awash basin, Ethiopia the case of Koka reservoir. *Heliyon*, *9*(12), e23049. https://doi.org/10.1016/j.heliyon.2023.e23049

Birhanu, B., Kebede, S., Charles, K., Taye, M., Atlaw, A., & Birhane, M. (2021). Impact of Natural and Anthropogenic Stresses on Surface and Groundwater Supply Sources of the Upper Awash Sub-Basin, Central Ethiopia. *Frontiers in Earth Science*, *9*(May). https://doi.org/10.3389/feart.2021.656726

Biswas, S. S. (2016). Analysis of GIS Based Morphometric Parameters and Hydrological Changes in Parbati River Basin, Himachal Pradesh, India. *Journal of Geography & Natural Disasters*, *6*(2), 1–8. https://doi.org/10.4172/2167-0587.1000175

Biswas, S., Sudhakar, S., & Desai, V. R. (1999). Prioritisation of subwatersheds based on morphometric analysis of drainage basin: A remote sensing and GIS approach. *Journal of the Indian Society of Remote Sensing*, *27*(3), 155–166. https://doi.org/10.1007/BF02991569

Blaustein, A. (1992). The peak near 700 nm on radiance spectra of algae and water: Relationships of its magnitude and position with chlorophyll. *International Journal of Remote Sensing*, *13*(17), 3367–3373. https://doi.org/10.1080/01431169208904125

Borah, & Bera. (2003). *WATERSHED-SCALE HYDROLOGIC AND NONPOINT-SOURCE POLLUTION MODELS: REVIEW OF MATHEMATICAL BASES*. *46*(6), 1553–1566.

Borges, H. D., Cicerelli, R. E., De Almeida, T., Roig, H. L., & Olivetti, D. (2020). Monitoring cyanobacteria occurrence in freshwater reservoirs using semi-analytical algorithms and orbital remote sensing. *Marine and Freshwater Research*, *71*(5), 569–578. https://doi.org/10.1071/MF18377

Bramich, J., Bolch, C. J. S., & Fischer, A. (2021). Improved red-edge chlorophyll-a detection for Sentinel 2. *Ecological Indicators*, *120*, 106876. https://doi.org/10.1016/j.ecolind.2020.106876

Brehan, M. (2017). Fisheries , water quality status and management challenges of Lake Gudera Wetland , West Gojjam Zone , Sekela district Ethiopia. *International Journal of Fisheries and Aquatic Studies*, *5*(3), 21–26.

Bryant, M. A., Hesser, T. J., & Jensen, R. E. (2016). *Evaluation Statistics Computed for the Wave Information Studies (WIS)*. *July*, 1–10. https://apps.dtic.mil/sti/citations/AD1013235

Buma, W. G., & Lee, S. Il. (2020). Evaluation of Sentinel-2 and Landsat 8 images for estimating Chlorophyll-a concentrations in Lake Chad, Africa. *Remote Sensing*, *12*(15). https://doi.org/10.3390/RS12152437

Burton, G. A., & E.Pitt, R. (2002). *Stormwater Effects Handbook, A Toolbox for Watershed Managers, Scientists, and Engineers*. A CRC Press Company Boca Raton London New York Washington, D.C. LEWIS PUBLISHERS A.

Bussi, G., Whitehead, P. G., Jin, L., Taye, M. T., Dyer, E., Hirpa, F. A., Yimer, Y. A., & Charles, K. J. (2021). Impacts of climate change and population growth on river nutrient loads in a data scarce region: The upper awash river (Ethiopia). *Sustainability (Switzerland)*, *13*(3), 1–15. https://doi.org/10.3390/su13031254

Caballero, I., Fernández, R., Escalante, O. M., Mamán, L., & Navarro, G. (2020). New capabilities of Sentinel-2A/B satellites combined with in situ data for monitoring small harmful algal blooms in complex coastal waters. *Scientific Reports*, *10*(1), 1–14. https://doi.org/10.1038/s41598-020-65600-1

Caballero, I., Steinmetz, F., & Navarro, G. (2018). Evaluation of the first year of operational Sentinel-2A data for retrieval of suspended solids in medium- to high-turbiditywaters. *Remote Sensing*, *10*(7). https://doi.org/10.3390/rs10070982

Cahyono, B. E., Jamilah, U. L., Misto, Nugroho, A. T., & Subekti, A. (2019). Analysis of Total Suspended Solids (TSS) at Bedadung River , Jember District of Indonesia Using Remote Sensing Sentinel 2A Data. *Singapore Journal of Scientific Research*, *9 (4): 117*. https://doi.org/10.3923/sjsres.2019.117.123

Cairo, C., Barbosa, C., Lobo, F., Novo, E., Carlos, F., Maciel, D., Jnior, R. F., Silva, E., & Curtarelli, V. (2020). Hybrid chlorophyll-a algorithm for assessing trophic states of a tropical brazilian reservoir based on msi/sentinel-2 data. *Remote Sensing*, *12*(1). https://doi.org/10.3390/RS12010040

Cambien, N., Gobeyn, S., Nolivos, I., Eurie Forio, M. A., Arias-Hidalgo, M., Dominguez-Granda, L., Witing, F., Volk, M., & Goethals, P. L. M. (2020). Using the soil and water assessment tool to simulate the pesticide dynamics in the data scarce guayas River Basin, Ecuador. *Water (Switzerland)*, *12*(3), 1–21. https://doi.org/10.3390/w12030696

Carpenter, S. R., Caraco, N. F., Correll, D. L., Howarth, R. W., Sharpley, A. N., & Smith, V. H. (1998). Nonpoint pollution of surface waters with phosphorus and nitrogen. *Ecological Applications*, *8*(3), 559–568. https://doi.org/10.1890/1051-0761(1998)008[0559:NPOSWW]2.0.CO;2

Chan, W. C. H., Thompson, J. R., Taylor, R. G., Nay, A. E., Ayenew, T., MacDonald, A. M., & Todd, M. C. (2020). Uncertainty assessment in river flow projections for Ethiopia's Upper Awash Basin using multiple GCMs and hydrological models. *Hydrological Sciences Journal*, *65*(10), 1720–1737. https://doi.org/10.1080/02626667.2020.1767782

Chawla, I., Karthikeyan, L., & Mishra, A. K. (2020). A review of remote sensing applications for water security: Quantity, quality, and extremes. *Journal of Hydrology*, *585*. https://doi.org/10.1016/j.jhydrol.2020.124826

Chebet, E. B., Kibet, J. K., & Mbui, D. (2020). The assessment of water quality in river Molo water basin, Kenya.

Applied Water Science, *10*(4), 1–10. https://doi.org/10.1007/s13201-020-1173-8

Chekol, D. A., Tischbein, B., Eggers, H., & Vlek, P. (2007). Application of SWAT for assessment of spatial distribution of water resources and analyzing impact of different land management practices on soil erosion in Upper Awash River Basin watershed. *FWU Water Resources Publications*, 110–117.

Chelkeba Tumsa, B. (2023). The Response of Sensitive LULC Changes to Runoff and Sediment Yield in a Semihumid Urban Watershed of the Upper Awash Subbasin Using the SWAT+ Model, Oromia, Ethiopia. *Applied and Environmental Soil Science*, *2023*. https://doi.org/10.1155/2023/6856144

Chen, S. S., Kimirei, I. A., Yu, C., Shen, Q., & Gao, Q. (2022). Assessment of urban river water pollution with urbanization in East Africa. *Environmental Science and Pollution Research*, *29*(27), 40812–40825. https://doi.org/10.1007/s11356-021-18082-1

Chernet, T., Travi, Y., & Valles, V. (2001). Mechanism of degradation of the quality of natural water in the lakes region of the Ethiopian Rift Valley. *Water Research*, *35*(12), 2819–2832. https://doi.org/10.1016/S0043-1354(01)00002-1

Chopra, R., Dhiman, R. D., & Sharma, P. K. (2005). Morphometric analysis of sub-watersheds in Gurdaspur district, Punjab using remote sensing and GIS techniques. *Journal of the Indian Society of Remote Sensing*, *33*(4), 531–539. https://doi.org/10.1007/BF02990738

Chotpantarat, S., & Boonkaewwan, S. (2018). Impacts of land-use changes on watershed discharge and water quality in a large intensive agricultural area in Thailand. *Hydrological Sciences Journal*, *63*(9), 1386–1407. https://doi.org/10.1080/02626667.2018.1506128

Coffey, M. E., Workman, S. R., Taraba, J. L., & Fogle, A. W. (2004). STATISTICAL PROCEDURES FOR EVALUATING DAILY AND MONTHLY HYDROLOGIC MODEL PREDICTIONS. *ASABE*, *47*(1992), 59–68.

Corwin, D. L., Letey, J., & Carrillo, M. L. K. (1998). Modeling non-point source pollutants in the vadose zone: Back to the basics. *Geophysical Monograph Series*, *108*(March), 323–342. https://doi.org/10.1029/GM108p0323

Croley, T. E., He, C., & Lee, D. H. (2005). Distributed-Parameter Large Basin Runoff Model. II: Application. *Journal of Hydrologic Engineering*, *10*(3), 182–191. https://doi.org/10.1061/(asce)1084-0699(2005)10:3(182)

Cui, X., Sun, W., Teng, J., Song, H., & Yao, X. (2015). Effect of length of the observed dataset on the calibration of a distributed hydrological model. *IAHS-AISH Proceedings and Reports*, *368*(August 2014), 305–311. https://doi.org/10.5194/piahs-368-305-2015

Cunderlik, J., & Simonovic, S. P. (2010). Hydrologic models for inverse climate change impact modeling. *18th Canadian Hydro-Technical Conference*, *June*, 1–9.

Cutts, B. (2013). Geospatial Tools for Urban Water Resources Geotechnologies and the Environment. In *Geospatial Tools for Urban Water Resources*.

Dabral, P. P., Baithuri, N., & Pandey, A. (2008). Soil erosion assessment in a hilly catchment of North Eastern India using USLE, GIS and remote sensing. *Water Resources Management*, *22*(12), 1783–1798. https://doi.org/10.1007/s11269-008-9253-9

Dadi, D., Stellmacher, T., Senbeta, F., Van Passel, S., & Azadi, H. (2017). Environmental and health impacts of effluents from textile industries in Ethiopia: the case of Gelan and Dukem, Oromia Regional State. *Environmental Monitoring and Assessment*, *189*(1). https://doi.org/10.1007/s10661-016-5694-4

Das, A. K., & Mukherjee, S. (2005). Drainage morphometry using satellite data and GIS in Raigad district, Maharashtra. *Journal of the Geological Society of India*, *65*(5), 577–586.

Davies, J. M. (2006). Application and tests of the canadian water quality index for assessing changes in water quality in lakes and rivers of central North America. *Lake and Reservoir Management*, *22*(4), 308–320. https://doi.org/10.1080/07438140609354365

De Boer, D. H., & Crosby, G. (1996). Specific sediment yield and drainage basin scale. *IAHS-AISH Publication*, *236*(236), 333–338.

DE ROO, A. P. J., WESSELING, C. G., & RITSEMA, C. J. (1996). Lisem: a Single-Event Physically Based Hydrological and Soil Erosion Model for Drainage Basins. I: Theory, Input and Output. *Hydrological Processes*, *10*(8), 1107–1117. https://doi.org/10.1002/(SICI)1099-1085(199608)10:8<1107::AID-HYP415>3.0.CO;2-4

Degefu, F., Lakew, A., Tigabu, Y., & Teshome, K. (2011). Some limnological aspects of Koka reservoir, a shallow tropical artificial lake, Ethiopia. *J. Recent Trends Biosci.*, *1*(1), 94–100.

Degefu, F., Lakew, A., Tigabu, Y., & Teshome, K. (2013). The water quality degradation of upper Awash River, Ethiopia. *Ethiopian Journal of Environmental Studies and Management*, *6*(1). https://doi.org/10.4314/ejesm.v6i1.7

Degfe, A., Tilahun, A., Bekele, Y., Dume, B., & Diriba, O. H. (2023). Adoption of soil and water conservation technologies and its effects on soil properties: Evidences from Southwest Ethiopia. *Heliyon*, *9*(7), e18332. https://doi.org/10.1016/j.heliyon.2023.e18332

Demarchi, C., Ii, T. E. C., & Hunter, T. S. (2009). *APPLICATION OF A DISTRIBUTED WATERSHED HYDROLOGY AND WATER QUALITY MODEL IN THE GREAT LAKES BASIN*.

Desta, L. T. (2005). *Reservoir siltation in Ethiopia: Causes, source areas, and management options* (Issue 15). https://www.zef.de/fileadmin/webfiles/downloads/zefc_ecology_development/ecol_dev_30_text.pdf

Devia, G. K., Ganasri, B. P., & Dwarakish, G. S. (2015). A Review on Hydrological Models. *Aquatic Procedia*, *4*(Icwrcoe), 1001–1007. https://doi.org/10.1016/j.aqpro.2015.02.126

Dewan, A. M., & Yamaguchi, Y. (2009). Using remote sensing and GIS to detect and monitor land use and land cover change in Dhaka Metropolitan of Bangladesh during 1960-2005. *Environmental Monitoring and Assessment*, *150*(1–4), 237–249. https://doi.org/10.1007/s10661-008-0226-5

DHI. (2017). Mike She Volume 1: User Guide. The Experts in WATER ENVIRONMENTS. *DHI Software Licence Agreement*, *27*(1), 91–95.

Dibaba, W. T., Demissie, T. A., & Miegel, K. (2021). Prioritization of sub-watersheds to sediment yield and evaluation of best management practices in highland ethiopia, finchaa catchment. *Land*, *10*(6). https://doi.org/10.3390/land10060650

Dierssen, H. M., Kudela, R. M., Ryan, J. P., & Zimmerman, R. C. (2006). Red and black tides: Quantitative analysis of water-leaving radiance and perceived color for phytoplankton, colored dissolved organic matter, and suspended sediments. *Limnology and Oceanography*, *51*(6), 2646–2659. https://doi.org/10.4319/lo.2006.51.6.2646

Dinka, M. O. (2012). Analysing the extent (size and shape) of Lake Basaka expansion (Main Ethiopian Rift Valley) using remote sensing and GIS. *Lakes and Reservoirs: Research and Management*, *17*(2), 131–141. https://doi.org/10.1111/j.1440-1770.2012.00500.x

Dinka, M. O. (2017). Analysing the temporal water quality dynamics of Lake Basaka, Central Rift Valley of Ethiopia. *IOP Conf. Ser.: Earth Environ. Sci*, *52*, 12057. https://doi.org/10.1088/1755-1315/52/1/012057

Dirbaba, N. B., Li, S., Wu, H., Yan, X., & Wang, J. (2018). Organochlorine pesticides, polybrominated diphenyl ethers and polychlorinated biphenyls in surficial sediments of the Awash River Basin, Ethiopia. *PLoS One*, *13*(10), e0205026. https://doi.org/10.1371/journal.pone.0205026

Dofee, A. A., Chand, P., & Kumar, R. (2024). Prioritization of soil erosion-prone sub-watersheds using geomorphometric and statistical-based weighted sum priority approach in the middle Omo-Gibe River basin, Southern Ethiopia. *International Journal of Digital Earth*, *17*(1), 1–32. https://doi.org/10.1080/17538947.2024.2350198

Doxaran, D., Froidefond, J.-M., Lavender, S., & Castaing, P. (2002). Spectral signature of highly turbid waters. *Remote Sensing of Environment*, *81*(1), 149–161. https://doi.org/10.1016/s0034-4257(01)00341-8

Dsikowitzky, L., Mengesha, M., Dadebo, E., De Carvalho, C. E. V., & Sindern, S. (2013). Assessment of heavy metals in water samples and tissues of edible fish species from Awassa and Koka Rift Valley Lakes, Ethiopia. *Environmental Monitoring and Assessment*, *185*(4), 3117–3131. https://doi.org/10.1007/s10661-012-2777-8

Du, Y., Zhang, Y., Ling, F., Wang, Q., Li, W., & Li, X. (2016). Water bodies' mapping from Sentinel-2 imagery with Modified Normalized Difference Water Index at 10-m spatial resolution produced by sharpening the swir band. *Remote Sensing*, *8*(4). https://doi.org/10.3390/rs8040354

Duda, P. B., Jr., J. L. K., Donnigian, A. S., & Kinerson, R. (2006). *BASINS:Better Assessment Science Integrating Point and Nonpoint Sources*. 273–290.

Duguma, F. A., Feyessa, F. F., Demissie, T. A., & Januszkiewicz, K. (2021). Hydroclimate trend analysis of upper awash basin, Ethiopia. *Water (Switzerland)*, *13*(12), 1–17. https://doi.org/10.3390/w13121680

Duressa, A. A., Feyissa, T. A., Tukura, N. G., Gudeta, B. G., Fekadu Gechelu, G., & Bibi, T. S. (2024). Identification of soil erosion-prone areas for effective mitigation measures using a combined approach of morphometric analysis and geographical information system. *Results in Engineering*, *21*(December 2023). https://doi.org/10.1016/j.rineng.2023.101712

Edokpayi, J. N., Odiyo, J. O., & Durowoju, O. S. (2017). Impact of Wastewater on Surface Water Quality in Developing Countries: A Case Study of South Africa. *Water Quality*. https://doi.org/10.5772/66561

EFDR. (2000). Federal negarit gazeta of the federal democratic republic of Ethiopia, Public Health Proclamation. *BERHANENA SELAMPRINTING ENTERPRISE*.

El-sadek, A., & Irvem, A. (2014). *Evaluating the impact of land use uncertainty on the simulated streamflow and sediment yield of the Seyhan River basin using the SWAT model Evaluating the impact of land use uncertainty on the simulated streamflow and sediment yield of the Seyhan River ba*. *May*. https://doi.org/10.3906/tar-1309-89

Elias, K. H., Brook, A., & Tilahun, H. (2016). Effect of blended irrigation water quality on soil physico-chemical properties and cotton yield in Middle Awash Basin Ethiopia. *International Journal of Water Resources and Environmental Engineering*, *8*(1), 1–10. https://doi.org/10.5897/ijwree2015.0613

Eliku, T., & Leta, S. (2018). Spatial and seasonal variation in physicochemical parameters and heavy metals in Awash River , Ethiopia. *Applied Water Science*, *8*(6), 1–13. https://doi.org/10.1007/s13201-018-0803-x

Emiru, N. C., Recha, J. W., Thompson, J. R., Belay, A., Aynekulu, E., Manyevere, A., Demissie, T. D., Osano, P. M., Hussein, J., Molla, M. B., Mengistu, G. M., & Solomon, D. (2022). Impact of Climate Change on the Hydrology of the Upper Awash River Basin, Ethiopia. *Hydrology*, *9*(1). https://doi.org/10.3390/hydrology9010003

Engel, B., & Harbor, J. (2014). Long-Term Hydrological Impact Analysis (L-THIA). In *Purdue University* (pp. 1–10). https://engineering.purdue.edu/mapserve/LTHIA7/documentation/LTHIAFactSheet2.htm

Engel, B., Storm, D., White, M., Arnold, J., & Arabi, M. (2007). A hydrologic/water quality model application protocol. *Journal of the American Water Resources Association*, *43*(5), 1223–1226. https://doi.org/10.1111/j.1752-1688.2007.00105.x

EPA. (1991). *ESS Method 150.1: Chlorophyll - Spectrophotometric* (Issue September). Environmental Sciences

Section Inorganic Chemistry Unit Wisconsin State Lab of Hygiene 465 Henry Mall Madison, WI 53706. http://polk.wateratlas.usf.edu/upload/documents/methd150.pdf

EPA. (2015). *Application of BASINS/HSPF to Data-scarce Watersheds*. *February*, 88. https://www.epa.gov/ceam/hydrological-simulation-program-fortran-hspf#Application

EPA. (2018). *Nutrient and Sediment Estimation Tools for Watershed Protection*.

Eriksson, M., & Sigvant, J. (2019). *Causes and impact of surface water pollution in Addis Ababa, Ethiopia* (Issue June).

Eriksson, N. (2003). Adaptation of the Agricultural Non-point Source Pollution Model to the Morsa Watershed. *Researchgate.Net*. http://www.researchgate.net/publication/2476324_Adaptation_of_the_Agricultural_Non-point_Source_Pollution_Model_to_the_Morsa_Watershed/file/9fcfd508e83650d820.pdf

Eshetu, G., Worku, L., Alemayehu, H., & Wondwossen, B. (2004). Assessment of factors contributing to eutrophication of aba samuel water reservior in Addis Ababa, Ethiopia. *Ethiop J Health Sci*, *14*, 109–117.

Eskinder, Z. B. (2019). *Estimating Combined Loads of Diffuse and Point- Source Pollutants into the Borkena River, Ethiopia* (Issue February). https://doi.org/10.18174/466828

FAO and IHE Delft. (2020). *Water accounting in the Awash River Basin REMOTE SENSING FOR WATER PRODUCTIVITY*. the Food and Agriculture Organization of the United Nations and IHE Delft Institute for Water Education. www.fao.org/publications

Fares, A. (2008). *Overview of the hydrological modeling of small coastal watersheds on tropical islands* (Vol. 33). https://doi.org/10.2495/978-1-84564-091-0/01

Farhan, Y., Anbar, A., Enaba, O., & Al-Shaikh, N. (2015). Quantitative Analysis of Geomorphometric Parameters of Wadi Kerak, Jordan, Using Remote Sensing and GIS. *Journal of Water Resource and Protection*, *07*(06), 456–475. https://doi.org/10.4236/jwarp.2015.76037

Fasil, D., Kibru, T., Gashaw, T., Fikadu, T., & Aschalew, D. (2011). Some limnological aspects of Koka reservoir, a shallow tropical artificial lake, Ethiopia. *J. Recent Trends Biosci.*, *1*(1), 94–100.

Feyissa, Z., & Bekele, E. (2018). Physicochemical Characterization of Upper Awash River of Ethiopia Polluted by Anmol Product Paper Factory. *International Journal of Water and Wastewater Treatment*, *4*(2). https://doi.org/10.16966/2381-5299.154

Foeckler, P., Henning, V., & Reichelt, J. (2020). *Mendeley Reference Manager For Desktop Windows*. Version 1.19.8 [Software]. https://www.mendeley.com/download-reference-manager/windows

G. Gebre, D. V. R. (2009). Urban water pollution and irrigated vegetable farming. *Water, Sanitation and Hygiene: Sustainable Development and Multisectoral Approaches - Proceedings of the 34th WEDC International Conference*, 166. https://doi.org/https://hdl.handle.net/2134/30512

Gallotti, R. (2013). An older origin for the Acheulean at Melka Kunture (Upper Awash, Ethiopia): Techno-economic behaviours at Garba IVD. *Journal of Human Evolution*, *65*(5), 594–620. https://doi.org/10.1016/j.jhevol.2013.07.001

Ganasri, B. P. (2015). *A Review on Hydrological Models ENGINEERING (ICWRCOE 2015) A Review on Hydrological Models*. *July*. https://doi.org/10.1016/j.aqpro.2015.02.126

Gao, C., Yao, M. T., Wang, Y. J., Zhai, J. Q., Buda, S., Fischer, T., Zeng, X. F., Yao, M. T., Wang, Y. J., Zhai, J. Q., Buda, S., Fischer, T., & Zeng, X. F. (2016). Hydrological model comparison and assessment : criteria from catchment scales and temporal resolution. *Hydrological Sciences Journal*, *61*(10), 1941–1951. https://doi.org/10.1080/02626667.2015.1057141

GAO, L., & LI, D. (2015). A review of hydrological/water-quality models. *Frontiers of Agricultural Science and Engineering*, *1*(4), 267. https://doi.org/10.15302/j-fase-2014041

Garg, V., Aggarwal, S. P., & Chauhan, P. (2020). Changes in turbidity along Ganga River using Sentinel-2 satellite data during lockdown associated with COVID-19. *Geomatics, Natural Hazards and Risk*, *11*(1), 1175–1195. https://doi.org/10.1080/19475705.2020.1782482

Gashaw, T., Tulu, T., & Argaw, M. (2018). Erosion risk assessment for prioritization of conservation measures in Geleda watershed, Blue Nile basin, Ethiopia. *Environmental Systems Research*, *6*(1), 1–14. https://doi.org/10.1186/s40068-016-0078-x

Gebeyehu, H. R., & Bayissa, L. D. (2020). Levels of heavy metals in soil and vegetables and associated health risks in Mojo area, Ethiopia. *PLoS ONE*, *15*(1), 1–22. https://doi.org/10.1371/journal.pone.0227883

Gebre, A. E., Demissie, H. F., Mengesha, S. T., & Segni, M. T. (2016). The Pollution Profile of Modjo River Due to Industrial Wastewater Discharge, in Modjo Town, Oromia, Ethiopia. *Environmental & Analytical Toxicology*, *6*(3), 1–5. https://doi.org/10.4172/2161-0525.1000363

Gebreeyesus, M. (2013). Industrial policy and development in Ethiopia: Evolution and present experimentation. In *Soils and Foundations* (Vol. 38, Issue 4). https://www.brookings.edu/wp-content/uploads/2016/07/L2C_WP6_Gebreeyesus-1.pdf

Gebremariam, S. Y., Martin, J. F., DeMarchi, C., Bosch, N. S., Confesor, R., & Ludsin, S. A. (2014). A comprehensive approach to evaluating watershed models for predicting river flow regimes critical to downstream ecosystem services. *Environmental Modelling and Software*, *61*, 121–134. https://doi.org/10.1016/j.envsoft.2014.07.004

Gebremichael, H. B., Raba, G. A., Beketie, K. T., Feyisa, G. L., & Siyoum, T. (2022). Changes in daily rainfall and temperature extremes of upper Awash Basin, Ethiopia. *Scientific African*, *16*, e01173. https://doi.org/10.1016/j.sciaf.2022.e01173

Gebreyohannes, F., Gebrekidan, A., Hedera, A., & Estifanos, S. (2015). Investigations of Physico-Chemical Parameters and its Pollution Implications of Elala River, Mekelle, Tigray, Ethiopia. *Momona Ethiopian Journal of Science*, *7*(2), 240. https://doi.org/10.4314/mejs.v7i2.7

Gela, A. G. (2018). Watershed Prioritization Using Morphometric Analysis & RUSLE Model for Soil Conservation Planning , in Gilgel Abay Watershed , Ethiopia. *Research Square*, 1–21.

Geleta, H. I. (2010). *Watershed Sediment Yield Modeling for Data Scarce Areas*.

George, D. G., & Edwards, R. W. (1976). The Effect of Wind on the Distribution of Chlorophyll A and Crustacean Plankton in a Shallow Eutrophic Reservoir. *The Journal of Applied Ecology*, *13*(3), 667. https://doi.org/10.2307/2402246

Getaneh, Y., Abera, W., Abegaz, A., & Tamene, L. (2022). A systematic review of studies on freshwater lakes of Ethiopia. *Journal of Hydrology: Regional Studies*, *44*(October), 101250. https://doi.org/10.1016/j.ejrh.2022.101250

Getu Engida, T., Nigussie, T. A., Aneseyee, A. B., & Barnabas, J. (2021). Land Use/Land Cover Change Impact on Hydrological Process in the Upper Baro Basin, Ethiopia. *Applied and Environmental Soil Science*, *2021*. https://doi.org/10.1155/2021/6617541

Gholami, A., Habibnejad Roshan, M., Shahedi, K., Vafakhah, M., & Solaymani, K. (2016). Hydrological stream flow modeling in the Talar catchment (central section of the Alborz Mountains, north of Iran): Parameterization and uncertainty analysis using SWAT-CUP. *Journal of Water and Land Development*, *30*(1), 57–69. https://doi.org/10.1515/jwld-2016-0022

Gholizadeh, M. H., Melesse, A. M., & Reddi, L. (2016). A comprehensive review on water quality parameters

estimation using remote sensing techniques. *Sensors (Switzerland)*, *16*(8). https://doi.org/10.3390/s16081298

Giardino, Bresciani, M., Villa, P., & Martinelli, A. (2010). Application of Remote Sensing in Water Resource Management: The Case Study of Lake Trasimeno, Italy. *Water Resources Management*, *24*(14), 3885–3899. https://doi.org/10.1007/s11269-010-9639-3

Giordano, M., Petropoulos, S. A., & Rouphael, Y. (2021). The fate of nitrogen from soil to plants: Influence of agricultural practices in modern agriculture. *Agriculture (Switzerland)*, *11*(10). https://doi.org/10.3390/agriculture11100944

Girma, K. (2016). The State of Freshwaters in Ethiopia. In *Freshwater* (pp. 137–188). Mount Holyoke College South Hadley, MA, USA.

Gitelson, A., Mayo, M., Yacobi, Y. Z., Parparov, A., & Berman, T. (1994). The use of high-spectral-resolution radiometer data for detection of low chlorophyll concentrations in Lake Kinneret. *Journal of Plankton Research*, *16*(8), 993–1002. https://doi.org/10.1093/plankt/16.8.993

Glavan, M., & Pintar, M. (2015). *Threats of Catchment Modelling with Soil and Water Assessment Tool (SWAT) Model*.

Godif, G., & Manjunatha, B. R. (2022). Prioritizing sub-watersheds for soil and water conservation via morphometric analysis and the weighted sum approach: A case study of the Geba river basin in Tigray, Ethiopia. *Heliyon*, *8*(12). https://doi.org/10.1016/j.heliyon.2022.e12261

Golmohammadi, G., Prasher, S., Madani, A., & Rudra, R. (2014). Evaluating Three Hydrological Distributed Watershed Models: MIKE-SHE, APEX, SWAT. *Hydrology*, *1*(1), 20–39. https://doi.org/10.3390/hydrology1010020

Gonfa, Z. B. (2016). *Runoff and sediment yield modelling using soil and water assessment tool for management planning of mojo watershed, Ethiopia*. G.B. Pant University of Agriculture & Technology.

Gonfa, Z. B., & Kumar, D. (2016). *Application of Soil and Water Assessment Tool Model to Estimate Runoff and Sediment Yield from Mojo Watershed*. 2081–2091. https://doi.org/10.15680/IJIRSET.2016.0502058

Govedarica, M., & Jakovljevic, G. (2019). Monitoring spatial and temporal variation of water quality parameters using time series of open multispectral data. *Proc. SPIE 11174, Seventh International Conference on Remote Sensing and Geoinformation of the Environment (RSCy2019), 111740Y (27 June 2019), June*, 55. https://doi.org/https://doi.org/10.1117/12.2533708

Gower, J., King, S., Borstad, G., & Brown, L. (2005). Detection of intense plankton blooms using the 709 nm band of the MERIS imaging spectrometer. *International Journal of Remote Sensing*, *26*(9), 2005–2012. https://doi.org/10.1080/01431160500075857

Graham, D. N., & Butts, M. B. (2005). *Flexible, integrated watershed modelling with MIKE SHE*. (pp. 1–25).

Graichen, K. (2011). Lake Water Management in three Ethiopian Rift Valley Watersheds. In *Environmental Policy Review 2011*.

Green, W. H., & Ampt, G. . (2011). Studies on soil physics (Part I): the flow of Air and Water Through Soil. *J Agric Sci*, *4*, 1–24. http://soilphysics.okstate.edu/teaching/soil-6583/references-folder/green and ampt 1911.pdf

Grendaitė, D., Stonevičius, E., Karosienė, J., Savadova, K., & Kasperovičienė, J. (2018). Chlorophyll-a concentration retrieval in eutrophic lakes in Lithuania from Sentinel-2 data. *Geologija. Geografija*, *4*(1). https://doi.org/10.6001/geol-geogr.v4i1.3720

Gumma, M. K., Birhanu, B. Z., Mohammed, I. A., Tabo, R., & Whitbread, A. M. (2016). Prioritization of watersheds across mali using remote sensing data and GIS techniques for agricultural development planning. *Water (Switzerland)*, *8*(6), 1–17. https://doi.org/10.3390/W8060260

Guo, D., Lintern, A., Webb, J. A., Ryu, D., Liu, S., Bende-Michl, U., Leahy, P., Wilson, P., & Western, A. W. (2019). Key Factors Affecting Temporal Variability in Stream Water Quality. *Water Resources Research*, *55*(1), 112–129. https://doi.org/10.1029/2018WR023370

Guttierrez-Magness, A. L., & Raffensperger, J. P. (2003). *Development, Calibration, and Analysis of a Hydrologic and Water-Quality Model of the Delaware Inland Bays Watershed. Water Resources Investigations Report 03-4124* (Issue January 2003).

Ha, N. T. T., Thao, N. T. P., Koike, K., & Nhuan, M. T. (2017). Selecting the best band ratio to estimate chlorophyll-a concentration in a tropical freshwater lake using sentinel 2A images from a case study of Lake Ba Be (Northern Vietnam). *ISPRS International Journal of Geo-Information*, *6*(9). https://doi.org/10.3390/ijgi6090290

Haddis, A., Getahun, T., Mengistie, E., Jemal, A., Smets, I., & Van der Bruggen, B. (2014). Challenges to surface water quality in mid-sized African cities: Conclusions from Awetu-Kito Rivers in Jimma, south-west Ethiopia. *Water and Environment Journal*, *28*(2), 173–182. https://doi.org/10.1111/wej.12021

Haile, M. Z., & Mohammed, E. T. (2019). Evaluation of the current water quality of Lake Hawassa, Ethiopia. *International Journal of Water Resources and Environmental Engineering*, *11*(7), 120–128. https://doi.org/10.5897/ijwree2019.0857

Hailu, D., Negassa, A., & Kebede, B. (2020). *Study on the status of some physico-chemical parameters of Lake Koka and its relation with water hyacinth (Eichhornia crassipes) invasion*. *8*(3), 405–412.

Han, L. X., Huo, F., & Sun, J. (2011). Method for calculating non-point source pollution distribution in plain rivers. *Water Science and Engineering*, *4*(1), 83–91. https://doi.org/10.3882/j.issn.1674-2370.2011.01.008

Han, Y., Liu, Z., Chen, Y., Li, Y., Liu, H., Song, L., & Chen, Y. (2023). Assessing non-point source pollution in an apple-dominant basin and associated best fertilizer management based on SWAT modeling. *International Soil and Water Conservation Research*, *11*(2), 353–364. https://doi.org/10.1016/j.iswcr.2022.10.002

Hargreaves, G. H., & Samani, Z. A. (1985). Reference Crop Evapotranspiration From Ambient Air Temperature. *Paper - American Society of Agricultural Engineers*, 96–99.

Hasan, M. K., Shahriar, A., & Jim, K. U. (2019). Water pollution in Bangladesh and its impact on public health. *Heliyon*, *5*(8), e02145. https://doi.org/10.1016/j.heliyon.2019.e02145

He, C., Demarchi, C., & Croley, T. E. (2008). *Modeling Spatial Distributions of Nonpoint Source Pollution Loadings in the Great Lakes Watersheds by Using the Distributed Large Basin Runoff Model 1*. *2008*, 1–7.

He, C., Zhang, L., Fu, L., Luo, Y., Li, L., & DeMarchi, C. (2012). Streamflow allocation in arid watersheds: a case study in Northwestern China. *Hydrology and Earth System Sciences Discussions*, *9*(7), 8941–8978. https://doi.org/10.5194/hessd-9-8941-2012

He, & Croley, T. E. (2007). Application of a distributed large basin runoff model in the Great Lakes basin. *Control Engineering Practice*, *15*(8), 1001–1011. https://doi.org/10.1016/j.conengprac.2007.01.011

Hesse, C., & Krysanova, V. (2016). Modeling climate and management change impacts on water quality and in-stream processes in the Elbe river basin. *Water (Switzerland)*, *8*(2), 1–31. https://doi.org/10.3390/w8020040

High-, C. E., Vecchi, V. V., & Valdarno, S. G. (2016). *ASSESSMENT OF GULLY EROSION IN THE UPPER AWASH , CENTRAL ETHIOPIAN HIGHLANDS BASED ON A COMPARISON OF ARCHIVED AERIAL PHOTOGRAPHS AND VERY HIGH RESOLUTION SATELLITE IMAGES*. *39*, 161–170.

Hindersah, R., Handyman, Z., Indriani, F. N., Suryatmana, P., & Nurlaeny, N. (2018). JOURNAL OF DEGRADED AND MINING LANDS MANAGEMENT Azotobacter population, soil nitrogen and groundnut growth in mercury-contaminated tailing inoculated with Azotobacter. *J. Degrade. Min. Land Manage*, *5*(53), 2502–2458. https://doi.org/10.15243/jdmlm

Horton, R. E. (1932). Drainage-basin characteristics. *Transactions American Geophysical Union*, *13*(1), 350–361. https://doi.org/10.1029/TR013i001p00350

Horton, R. E. (1945). Erosional development of streams and their drainage basins, hydrophysical approach to quantitative morphology. *Geological Society of America Bulletin*, *37*(12), 555–558. https://doi.org/10.1130/0016-7606(1945)56

Hossain, S., Hewa, A., & Wella-Hewage, S. (2019). A comparison of continuous and event-based rainfall-runoff (RR) modelling using EPA-SWMM. *Water (Switzerland)*, *11*(3). https://doi.org/10.3390/w11030611

Hou, L., Zhou, Z., Wang, R., Li, J., Dong, F., & Liu, J. (2022). Research on the Non-Point Source Pollution Characteristics of Important Drinking Water Sources. *Water (Switzerland)*, *14*(2), 1–14. https://doi.org/10.3390/w14020211

Houser, C., & Hamilton, S. (2009). Reservoir siltation in the semi-arid highlands of northern Ethiopia: sediment yield–catchment area relationship and a semi-quantitative approach for predicting sediment yield. *Earth Surface Processes and Landforms*, *34*(March), 613–628. https://doi.org/10.1002/esp

Huang, H., Roy, D. P., Boschetti, L., Zhang, H. K., Yan, L., Kumar, S. S., Gomez-Dans, J., & Li, J. (2016). Separability analysis of Sentinel-2A Multi-Spectral Instrument (MSI) data for burned area discrimination. *Remote Sensing*, *8*(10). https://doi.org/10.3390/rs8100873

Huang, J. J., Tzeng, G. H., & Liu, H. H. (2009). A revised vikor model for multiple criteria decision making - The perspective of regret theory. *Communications in Computer and Information Science*, *35*, 761–768. https://doi.org/10.1007/978-3-642-02298-2_112

Hurni, H. (1993). Land degradation, famine, and land resource scenarios in Ethiopia. In *World Soil Erosion and conservation* (Issue January, pp. 27–61). https://www.researchgate.net/publication/279605109_Land_degradation_famine_and_land_resource_scenarios_in_Ethiopia#fullTextFileContent

Hurni, K., Zeleke, G., Kassie, M., Tegegne, B., Kassawmar, T., Teferi, E., Moges, A., Tadesse, D., Ahmed, M., Degu, Y., Kebebew, Z., Hodel, E., Amdihun, A., Mekuriaw, A., Debele, B., Deichert, G., & Hurni, H. (2015). The Economics of Land Degradation. Ethiopia Case Study. Soil Degradation and Sustainable Land Management in the Rainfed Agricultural Areas of Ethiopia: An Assessment of the Economic Implications. In *Report for the Economcs of Land Degradation Initiative* (Issue February 2016).

Igwe, P.U., Chukwudi, C.C., Ifenatuorah, F.C., Fagbeja, I.F., Okeke, C. A. (2017). A Review of Environmental Effects of Surface Water Pollution. *International Journal of Advanced Engineering Research and Science*, *4*(12), 128–137. https://doi.org/10.22161/ijaers.4.12.21

Im, S., Brannan, K. M., Mostaghimi, S., & Kim, S. M. (2007). Comparison of HSPF and SWAT models performance for runoff and sediment yield prediction. *Journal of Environmental Science and Health - Part A Toxic/Hazardous Substances and Environmental Engineering*, *42*(11), 1561–1570. https://doi.org/10.1080/10934520701513456

Ingwani, E., Gumbo, T., & Gondo, T. (2010). The general information about the impact of water hyacinth on Aba Samuel dam, Addis Ababa, Ethiopia: Implications for ecohydrologists. *Ecohydrology and Hydrobiology*, *10*(2–4), 341–345. https://doi.org/10.2478/v10104-011-0014-7

Inyinbor Adejumoke A., Adebesin Babatunde O., Oluyori Abimbola P., Adelani-Akande Tabitha A., D. A. O. O. T. A., & Additional. (2018). Water Pollution: Effects, Prevention, and Climatic Impact. In *Water Challenges of an Urbanizing World*. https://doi.org/10.5772/intechopen.72018

Islam, A. R. M. T., Islam, H. M. T., Mia, M. U., Khan, R., Habib, M. A., Bodrud-Doza, M., Siddique, M. A. B., & Chu, R. (2020). Co-distribution, possible origins, status and potential health risk of trace elements in surface water sources from six major river basins, Bangladesh. *Chemosphere*, *249*. https://doi.org/10.1016/j.chemosphere.2020.126180

Islam, M. S., Idris, A. M., Islam, A. R. M. T., Ali, M. M., & Rakib, M. R. J. (2021). Hydrological distribution of physicochemical parameters and heavy metals in surface water and their ecotoxicological implications in the Bay of Bengal coast of Bangladesh. *Environmental Science and Pollution Research*. https://doi.org/10.1007/s11356-021-15353-9

Issaka, S., & Ashraf, M. A. (2017). Impact of soil erosion and degradation on water quality : a review. *Geology, Ecology, and Landscapes*, *9508*, 1–11. https://doi.org/10.1080/24749508.2017.1301053

Itanna, F. (2002). Metals in leafy vegetables grown in Addis Ababa and toxicological implications. *Ethiopian Journal of Health Development*, *16*(3). https://doi.org/10.4314/ejhd.v16i3.9797

Jaber, F. H., & Shukla, S. (2012). *Mike she: MODEL USE, CALIBRATION, AND VALIDATION*. *55*(4), 1479–1489.

Jaelani, L. M., Limehuwey, R., Kurniadin, N., Pamungkas, A., Koenhardono, E. S., & Sulisetyono, A. (2016). Estimation of Total Suspended Sediment and Chlorophyll-A Concentration from Landsat 8-Oli: The Effect of Atmospher and Retrieval Algorithm. *IPTEK The Journal for Technology and Science*, *27*(1), 16–23. https://doi.org/10.12962/j20882033.v27i1.1217

Jajarmizadeh, Harun, & Salarpour. (2012). A Review on Theoretical Consideration and Types of Models in Hydrollogy. *J.Environ. Sci. Technol.*, *5*(5), 249–261. https://doi.org/10.3923/jest.2012.249.261

Javed, A., Khanday, M. Y., & Ahmed, R. (2009). Prioritization of sub-watersheds based on morphometric and land use analysis using Remote Sensing and GIS techniques. *Journal of the Indian Society of Remote Sensing*, *37*(2), 261–274. https://doi.org/10.1007/s12524-009-0016-8

Jayawardena, A. W. (2013). Environmental and hydrological systems modelling. In *Environmental and Hydrological Systems Modelling*. https://doi.org/10.1201/b16395

Jebessa, Z. F., & Bekele, E. (2018). Changes in the Physichochemical Properties of Upper Awash River Caused by Effluents from Anmol product Ethiopia paper factory , Ginchi , Ethiopia . *Scholars Research Library Archives*, *10*(1), 34–50.

Jenkinson, D. S., & Parry, L. C. (1989). The nitrogen cycle in the broadbalk wheat experiment: A model for the turnover of nitrogen through the soil microbial biomass. *Soil Biology and Biochemistry*, *21*(4), 535–541. https://doi.org/10.1016/0038-0717(89)90127-2

Jha, M., Gassman, P. W., Secchi, S., Gu, R., & Arnold, J. (2004). Effect of watershed subdivision on swat flow, sediment, and nutrient predictions. *Journal of the American Water Resources Association*, *40*(3), 811–825. https://doi.org/10.1111/j.1752-1688.2004.tb04460.x

Jilo, N. B., Gebremariam, B., Harka, A. E., Woldemariam, G. W., & Behulu, F. (2019). Evaluation of the impacts of climate change on sediment yield from the Logiya Watershed, Lower Awash Basin, Ethiopia. *Hydrology*, *6*(3). https://doi.org/10.3390/hydrology6030081

Jilo, N. B., Gurara, M. A., Tolche, A. D., & Harka, A. E. (2022). Impacts of Management Scenarios on Sediment Yield Simulation in Upper and Middle Awash River Basin, Ethiopia. *Ecohydrology and Hydrobiology*, *22*(2), 269–282. https://doi.org/10.1016/j.ecohyd.2021.11.003

Jin, L., Whitehead, P. G., Bussi, G., Hirpa, F., Taye, M. T., Abebe, Y., & Charles, K. (2021). Natural and anthropogenic sources of salinity in the Awash River and Lake Beseka (Ethiopia): Modelling impacts of climate change and lake-river interactions. *Journal of Hydrology: Regional Studies*, *36*(January), 100865. https://doi.org/10.1016/j.ejrh.2021.100865

Jonathan M. Abell, Deniz Özkundakci, D. P. H. and J. R. J. (2012). Latitudinal variation in nutrient stoichiometry and chlorophyll-nutrient relationships in lakes: A global study. *Fundamental and Applied Limnology*, *181*(1), 1–14. https://doi.org/10.1127/1863-9135/2012/0272

Jones-lee, A., Lee, G. F., Lee, G. F., Macero, E. El, & Macero, E. (2000). *DEVELOPMENT OF TMDL GOALS*

FOR CONTROL OF ORGANOPHOSPHATE PESTICIDE-CAUSED AQUATIC LIFE TOXICITY IN URBAN STORMWATER RUNOFF. *October 2000*, 1–10.

Jothimani, M., Lawrence, F., & Dawit, Z. (2020). Morphometric Analysis and Prioritization of Sub-watersheds for Soil Erosion using Geomatics Technologies in Megech River Catchment, Lake Tana Basin, North Western Ethiopia. *Ethiopian Journal of Science and Sustainable Development*, *8*(1), 2021. https://doi.org/10.20372/ejssdastu:v8.i1.2021.225

Kaleab, H., Mamo, M., & K. Jain, M. (2013). Runoff and Sediment Modeling Using SWAT in Gumera Catchment, Ethiopia. *Open Journal of Modern Hydrology*, *03*(04), 196–205. https://doi.org/10.4236/ojmh.2013.34024

Kalsido, T., & Berhanu, B. (2020). Impact of Land-Use Changes on Sediment Load and Capacity Reduction of Lake Ziway, Ethiopia. *Natural Resources*, *11*(11), 530–542. https://doi.org/10.4236/nr.2020.1111031

Kang, D., & Park, Y. (2014). Review-based measurement of customer satisfaction in mobile service: Sentiment analysis and VIKOR approach. *Expert Systems with Applications*, *41*(4 PART 1), 1041–1050. https://doi.org/10.1016/j.eswa.2013.07.101

Karamouz, M., Taheriyoun, M., Emami, F., & Rouhanizadeh, B. (2008). Assessment of watershed nutrient load input to reservoir, a case study. *World Environmental and Water Resources Congress 2008: Ahupua'a - Proceedings of the World Environmental and Water Resources Congress 2008*, *316*, 1–10. https://doi.org/10.1061/40976(316)543

Karaoui, I., Arioua, A., Boudhar, A., Hssaisoune, M., Mouatassime, S. El, Ouhamchich, K. A., & Elhamdouni, D. (2019). Evaluating the potential of Sentinel-2 satellite images for water quality characterization of artificial reservoirs: The Bin El Ouidane Reservoir case study (Morocco). *Meteorology Hydrology and Water Management*, *7*(1). https://doi.org/10.26491/mhwm/95087

Karatas, F. U. (2015). *Estimating Sediment and Nutrient Loading in the Davis Creek Watershed Using Soil and Water Assessment Tool (SWAT)* [Western Michigan University]. https://scholarworks.wmich.edu/masters_theses/597%0AThis

Kassegne, A. B., Esho, T. B., Okonkwo, J. O., & Asfaw, S. L. (2018). Distribution and ecological risk assessment of trace metals in surface sediments from Akaki River catchment and Aba Samuel reservoir, Central Ethiopia. *Environmental Systems Research*, *7*(1). https://doi.org/10.1186/s40068-018-0127-8

Kathleen, P. M. (2010). *Expanding Biofuel Production : Sustainability and the Transition to Advanced Biofuels : Summary of a Workshop*. http://site.ebrary.com/lib/uamerica/docDetail.action?docID=10384032&p00=biofuels+review+United+States

Katko, T. S., & Hukka, J. J. (2015). Social and Economic Importance of Water Services in the Built Environment: Need for More Structured Thinking. *Procedia Economics and Finance*, *21*(15), 217–223. https://doi.org/10.1016/s2212-5671(15)00170-7

Katlane, R., Dupouy, C., Kilani, B. El, & Berges, J. C. (2020). Estimation of Chlorophyll and Turbidity Using Sentinel 2A and EO1 Data in Kneiss Archipelago Gulf of Gabes, Tunisia. *International Journal of Geosciences*, *11*(10), 708–728. https://doi.org/10.4236/ijg.2020.1110035

Kebede, N. M., Ambushe, A. A., Chandravanshi, B. S., Abshiro, M. R., & McCrindle, R. I. (2012). Potentially toxic elements in some fresh water bodies in Ethiopia. *Toxicological and Environmental Chemistry*, *94*(10), 1980–1994. https://doi.org/10.1080/02772248.2012.744024

Kefay, T., Abdisa, T., & Tumsa, B. C. (2022). Prioritization of Susceptible Watershed to Sediment Yield and Evaluation of Best Management Practice: A Case Study of Awata River, Southern Ethiopia. *Applied and Environmental Soil Science*, *2022*. https://doi.org/10.1155/2022/1460945

Keraga, A. S., Kiflie, Z., & Engida, A. N. (2017a). Evaluating water quality of Awash River using water quality index. *International Journal of Water Resources and Environmental Engineering*, *9*(11), 243–253.

https://doi.org/10.5897/ijwree2017.0736

Keraga, A. S., Kiflie, Z., & Engida, A. N. (2017b). Spatial and temporal water quality dynamics of Awash River using multivariate statistical techniques. *African Journal of Environmental Science and Technology*, *11*(11), 565–577. https://doi.org/10.5897/ajest2017.2353

Ketema, A., & Dwarakish, G. S. (2020). Prioritization of sub-watersheds for conservation measures based on soil loss rate in Tikur Wuha watershed, Ethiopia. *Arabian Journal of Geosciences*, *13*(19), 1–16. https://doi.org/10.1007/s12517-020-06054-7

Kim, J., Lim, K. J., & Park, Y. S. (2018). Evaluation of Regression Models of LOADEST and Eight-Parameter Model for Nitrogen Load Estimations. *Water, Air, and Soil Pollution*, *229*(6). https://doi.org/10.1007/s11270-018-3844-8

Kılıç, Z. (2020). The importance of water and conscious use of water. *International Journal of Hydrology*, *4*(5), 239–241. https://doi.org/10.15406/ijh.2020.04.00250

Krisper, M. (2021). *Problems with Risk Matrices Using Ordinal Scales*. http://arxiv.org/abs/2103.05440

Kroll, C., Warchold, A., & Pradhan, P. (2019). Sustainable Development Goals (SDGs): Are we successful in turning trade-offs into synergies? *Palgrave Communications*, *5*(1), 1–11. https://doi.org/10.1057/s41599-019-0335-5

Krysanova, V., Müller-Wohlfeil, D. I., & Becker, A. (1998). Development and test of a spatially distributed hydrological/water quality model for mesoscale watersheds. *Ecological Modelling*, *106*(2–3), 261–289. https://doi.org/10.1016/S0304-3800(97)00204-4

Krysanova, V., & Wechsung, F. (2000). *SWIM (Soil and Water Integrated Model) User Manual*. *December*.

Kumar, R., & Ramaraj, M. (2021). *Prioritization of Sub-Watersheds in the Arasalar-Palavar Region using Sediment Production Rate (SPR)*. *48*, 1005–1010.

Kumar, S., Islam, A. R. M. T., Hasanuzzaman, M., Salam, R., Khan, R., & Islam, M. S. (2021). Preliminary assessment of heavy metals in surface water and sediment in Nakuvadra-Rakiraki River, Fiji using indexical and chemometric approaches. *Journal of Environmental Management*, *298*(March), 113517. https://doi.org/10.1016/j.jenvman.2021.113517

Kupssinskü, L. S., Guimarães, T. T., De Souza, E. M., Zanotta, D. C., Veronez, M. R., Gonzaga, L., & Mauad, F. F. (2020). A method for chlorophyll-a and suspended solids prediction through remote sensing and machine learning. *Sensors (Switzerland)*, *20*(7). https://doi.org/10.3390/s20072125

L. Shoemaker, M. Lahlou, M. Bryer D. Kumar, K. K. (1997). *Compendium of Tools for Watershed Assessment and TMDL Development*. *May*.

Lai, Y., Zhang, J., Song, Y., & Gong, Z. (2021). Retrieval and evaluation of chlorophyll-a concentration in reservoirs with main water supply function in beijing, china, based on landsat satellite images. *International Journal of Environmental Research and Public Health*, *18*(9). https://doi.org/10.3390/ijerph18094419

Lake, I. N. C., & Small, F. (1948). *OF WIND ON THE DISTRIBUTION OF CHLOROPHYLL a*. 426–432.

Langbein, W. B. (1947). Topographic Characteristics of Drainage Basins. *US Geological Society Water Supply Paper 968-C*. http://pubs.usgs.gov/wsp/0968c/report.pdf

Lawrence, P. L. (2013). *Geospatial Tools for Urban Water Resources*. Springer Dordrecht Heidelberg New York London.

Lee, G. F., & Jones-Lee, A. (1999). *Water Quality Control TMDL Goals for Urban Stormwater Runoff OP Pesticide-Caused Aquatic Life Toxicity*.

Lee, S., Yeo, I. Y., Sadeghi, A. M., McCarty, G. W., Hively, W. D., Lang, M. W., & Sharifi, A. (2018). Comparative analyses of hydrological responses of two adjacent watersheds to climate variability and change using the SWAT model. *Hydrology and Earth System Sciences*, *22*(1), 689–708. https://doi.org/10.5194/hess-22-689-2018

Legates, G. (2007). *Evaluating the use of "goodness-of- fit" measures in hydrologic and hy- droclimatic model validation. Wa- ter Resources Research. 35*(1), 1–9.

Legese, W., Koricha, D., & Ture, K. (2018). Characteristics of Seasonal Rainfall and its Distribution Over Bale Highland, Southeastern Ethiopia. *Journal of Earth Science & Climatic Change*, *09*(02). https://doi.org/10.4172/2157-7617.1000443

Legesse, E. E., Srivastava, A. K., Kuhn, A., & Gaiser, T. (2019). Household welfare implications of better fertilizer access and lower use inefficiency: Long-term scenarios for Ethiopia. *Sustainability (Switzerland)*, *11*(14). https://doi.org/10.3390/su11143952

Lemma, M. (2018a). *Sediment Yield Modeling Using Swat , Case Study of Upper Awash Basin*.

Lemma, M. (2018b). *Sediment Yield Modeling Using Swat , Case Study of Upper Awash Basin* (Issue June).

Leta, M. K., Ebsa, D. G., & Regasa, M. S. (2022). Parameter Uncertainty Analysis for Streamflow Simulation Using SWAT Model in Nashe Watershed, Blue Nile River Basin, Ethiopia. *Applied and Environmental Soil Science*, *2022*. https://doi.org/10.1155/2022/1826942

Li, C., & Li, G. (2021). Impact of China's water pollution on agricultural economic growth: an empirical analysis based on a dynamic spatial panel lag model. *Environmental Science and Pollution Research*, *28*(6), 6956–6965. https://doi.org/10.1007/s11356-020-11079-2

Li, J., Li, H., Shen, B., & Li, Y. (2011). Effect of non-point source pollution on water quality of the Weihe River. *International Journal of Sediment Research*, *26*(1), 50–61. https://doi.org/10.1016/S1001-6279(11)60075-9

Li, J., & Roy, D. P. (2017). A global analysis of Sentinel-2a, Sentinel-2b and Landsat-8 data revisit intervals and implications for terrestrial monitoring. *Remote Sensing*, *9*(9). https://doi.org/10.3390/rs9090902

Lian, Q., Yao, L., Uddin Ahmad, Z., Lei, X., Islam, F., Zappi, M. E., & Gang, D. D. (2019). Nonpoint source pollution. *Water Environment Research*, *91*(10), 1114–1128. https://doi.org/10.1002/wer.1205

Ligdi, E. E., Kahloun, M. El, & Meire, P. (2010). Ecohydrological status of Lake Tana - A shallow highland lake in the Blue Nile (Abbay) basin in Ethiopia: Review. *Ecohydrology and Hydrobiology*, *10*(2–4), 109–122. https://doi.org/10.2478/v10104-011-0021-8

Lim, K. J., Engel, B. A., Kim, Y., Bhaduri, B., & Harbor, J. (2001). Development of the Long Term Hydrologic Impact Assessment (LTHIA) www Systems. *Sustaining the Global Farm. 10th Interational Soil Convservation Organization Meeting*, 1018–1023.

Lin, B., Chen, X., & Yao, H. (2020). Threshold of sub-watersheds for SWAT to simulate hillslope sediment generation and its spatial variations. *Ecological Indicators*, *111*(8), 106040. https://doi.org/10.1016/j.ecolind.2019.106040

Lin, L., Yang, H., & Xu, X. (2022). Effects of Water Pollution on Human Health and Disease Heterogeneity: A Review. *Frontiers in Environmental Science*, *10*(June). https://doi.org/10.3389/fenvs.2022.880246

Lins, R. C., Martinez, J. M., Marques, D. da M., Cirilo, J. A., & Fragoso, C. R. (2017). Assessment of chlorophyll-a remote sensing algorithms in a productive tropical estuarine-lagoon system. *Remote Sensing*, *9*(6), 1–19. https://doi.org/10.3390/rs9060516

Liu, H., Li, Q., Shi, T., Hu, S., Wu, G., & Zhou, Q. (2017). Application of Sentinel 2 MSI Images to Retrieve Suspended Particulate Matter Concentrations in Poyang Lake. *Remote Sensing*, *9*(7), 761.

https://doi.org/10.3390/rs9070761

Liu, M., Li, C., Hu, Y., Sun, F., Xu, Y., & Chen, T. (2014). Combining CLUE-S and SWAT models to forecast land use change and non-point source pollution impact at a watershed scale in Liaoning Province, China. *Chinese Geographical Science*, *24*(5), 540–550. https://doi.org/10.1007/s11769-014-0661-x

Liu, R., Zhang, P., Wang, X., Wang, J., Yu, W., & Shen, Z. (2014). Cost-effectiveness and cost-benefit analysis of BMPs in controlling agricultural nonpoint source pollution in China based on the SWAT model. *Environmental Monitoring and Assessment*, *186*(12), 9011–9022. https://doi.org/10.1007/s10661-014-4061-6

Liu, X., Li, D., Zhang, H., Cai, S., Li, X., & Ao, T. (2015). Research on Nonpoint Source Pollution Assessment Method in Data Sparse Regions: A Case Study of Xichong River Basin, China. *Advances in Meteorology*, *2015*. https://doi.org/10.1155/2015/519671

Liu, X., Li, H., Zhang, S., Cruse, R. M., & Zhang, X. (2019). Gully erosion control practices in Northeast China: A review. *Sustainability (Switzerland)*, *11*(18). https://doi.org/10.3390/su11185065

Liu, Y., Li, H., Cui, G., & Cao, Y. (2020). Water quality attribution and simulation of non-point source pollution load flux in the Hulan River basin. *Scientific Reports*, *10*(1), 1–15. https://doi.org/10.1038/s41598-020-59980-7

Liu, Y., Li, S., Wallace, C. W., Chaubey, I., Flanagan, D. C., Theller, L. O., & Engel, B. A. (2017). Comparison of Computer Models for Estimating Hydrology and Water Quality in an Agricultural Watershed. *Water Resources Management*, *31*(11), 3641–3665. https://doi.org/10.1007/s11269-017-1691-9

Loiskandl, W., Ruffeis, D., Schönerklee, M., & Spendlingwimmer, R. (2005). Case study review of investigated irrigation projects in Ethiopia. *Water Management*, 357–369.

Luo, C., Li, Z., Li, H., & Chen, X. (2015). Evaluation of the annAGNPS model for predicting runoff and nutrient export in a typical small watershed in the hilly region of taihu lake. *International Journal of Environmental Research and Public Health*, *12*(9), 10955–10973. https://doi.org/10.3390/ijerph120910955

Ma, T., Sun, S., Fu, G., Hall, J. W., Ni, Y., He, L., Yi, J., Zhao, N., Du, Y., Pei, T., Cheng, W., Song, C., Fang, C., & Zhou, C. (2020). Pollution exacerbates China's water scarcity and its regional inequality. *Nature Communications*, *11*(1), 1–9. https://doi.org/10.1038/s41467-020-14532-5

Ma, Y. (2004). *L-THIA : A Useful Hydrologic Impact Assessment Model*. *2*(1), 68–73.

Ma, Y., Song, K., Wen, Z., Liu, G., Shang, Y., Lyu, L., Du, J., Yang, Q., Li, S., Tao, H., & Hou, J. (2021). Remote sensing of turbidity for lakes in Northeast China using sentinel-2 images with machine learning algorithms. *IEEE Journal of Selected Topics in Applied Earth Observations and Remote Sensing*, *14*, 9132–9146. https://doi.org/10.1109/JSTARS.2021.3109292

Makhdumi, W., & Dwarakish, G. S. (2019). *Prioritisation of watersheds using TOPSIS and VIKOR method*. *June 2019*, 6. https://doi.org/10.1117/12.2532024

Malthus, T. J., Hestir, E. L., Dekker, A. G., & Brando, V. E. (2012). The case for a global inland water quality product. *2012 IEEE International Geoscience and Remote Sensing Symposium*, *July*, 5234–5237. https://doi.org/10.1109/IGARSS.2012.6352429

Mamun, M., Ferdous, J., & An, K. G. (2021). Empirical estimation of nutrient, organic matter and algal chlorophyll in a drinking water reservoir using landsat 5 tm data. *Remote Sensing*, *13*(12). https://doi.org/10.3390/rs13122256

Mapanda, F., Mangwayana, E. N., Nyamangara, J., & Giller, K. E. (2005). The effect of long-term irrigation using wastewater on heavy metal contents of soils under vegetables in Harare, Zimbabwe. *Agriculture, Ecosystems and Environment*, *107*(2–3), 151–165. https://doi.org/10.1016/j.agee.2004.11.005

Marcomini, A., II, G. W. S., & Andrea, C. (2001). Decision Support Systems for Risk-Based Management of Contaminated Sites. In *Springer US*. Springer US. https://doi.org/DOI 10.1007/978-0-387-09722-0

Marinho, R. R., Harmel, T., Martinez, J. M., & Junior, N. P. F. (2021). Spatiotemporal dynamics of suspended sediments in the negro river, amazon basin, from in situ and sentinel-2 remote sensing data. *ISPRS International Journal of Geo-Information*, *10*(2). https://doi.org/10.3390/ijgi10020086

Maroneze, M. M., Zepka, L. Q., Vieira, J. G., Queiroz, M. I., & Jacob-Lopes, E. (2014). Sensitivity analysis of the Soil and Water Assessment Tools (SWAT) model in streamflow modeling in a rural river basin. *Revista Ambiente e Agua*, *9*(3), 445–458. https://doi.org/10.4136/1980-993X

Martinez, J. M., Espinoza-Villar, R., Armijos, E., & Silva Moreira, L. (2015). The optical properties of river and floodplain waters in the Amazon River Basin: Implications for satellite-based measurements of suspended particulate matter. *Journal of Geophysical Research F: Earth Surface*, *120*(7), 1274–1287. https://doi.org/10.1002/2014JF003404

Maru, H., Haileslassie, A., Zeleke, T., & Teferi, E. (2023). Analysis of the impacts of land use land cover change on streamflow and surface water availability in Awash Basin, Ethiopia. *Geomatics, Natural Hazards and Risk*, *14*(1), 1–25. https://doi.org/10.1080/19475705.2022.2163193

Masindi, V., & Khathutshelo, L. M. (2018). *Environmental Contamination by Heavy Metals* (pp. 115–133). https://doi.org/10.5772/intechopen.76082

Masresha, A. E., Skipperud, L., Rosseland, B. O., G.M., Z., Meland, S., Teien, H. C., & Salbu, B. (2011). Speciation of selected trace elements in three ethiopian rift valley lakes (koka, ziway, and awassa) and their major inflows. *Science of the Total Environment*, *409*(19), 3955–3970. https://doi.org/10.1016/j.scitotenv.2011.06.051

Matthews, M. W., Bernard, S., & Winter, K. (2010). Remote sensing of cyanobacteria-dominant algal blooms and water quality parameters in Zeekoevlei, a small hypertrophic lake, using MERIS. *Remote Sensing of Environment*, *114*(9), 2070–2087. https://doi.org/10.1016/j.rse.2010.04.013

Matthews, Stewart, B., & Lisl, R. (2012). An algorithm for detecting trophic status (chlorophyll-a), cyanobacterial-dominance, surface scums and floating vegetation in inland and coastal waters. *Remote Sensing of Environment*, *124*, 637–652. https://doi.org/10.1016/j.rse.2012.05.032

Maximus, J. K. (2025). Assessing watershed vulnerability to erosion and sedimentation: Integrating DEM and LULC data in Guyana's diverse landscapes. *HydroResearch*, *8*, 178–193. https://doi.org/10.1016/j.hydres.2024.11.002

McDonald, R. I., Weber, K., Padowski, J., Flörke, M., Schneider, C., Green, P. A., Gleeson, T., Eckman, S., Lehner, B., Balk, D., Boucher, T., Grill, G., & Montgomery, M. (2014). Water on an urban planet: Urbanization and the reach of urban water infrastructure. *Global Environmental Change*, *27*(1), 96–105. https://doi.org/10.1016/j.gloenvcha.2014.04.022

McGrane, S. J. (2016). Impacts of urbanisation on hydrological and water quality dynamics, and urban water management: a review. *Hydrological Sciences Journal*, *61*(13), 2295–2311. https://doi.org/10.1080/02626667.2015.1128084

Mehari, A. K., Gebremedhin, S., & Ayele, B. (2015). Effects of Bahir Dar Textile Factory Effluents on the Water Quality of the Head Waters of Blue Nile River, Ethiopia. *International Journal of Analytical Chemistry*, *2015*. https://doi.org/10.1155/2015/905247

Mekonnen, E. T., Temesgen, S. A., & Wu, Z. (2020). An overview of water pollution status in Ethiopia with a particular emphasis on Akaki River : A Review. *Ethiop. j. Public Health Nutr. An*, *November*, 1–10.

Mekonnen, T. M., Mitiku, A. B., & Woldemichael, A. T. (2023). Flood Hazard Zoning of Upper Awash River Basin, Ethiopia, Using the Analytical Hierarchy Process (AHP) as Compared to Sensitivity Analysis.

Scientific World Journal, *2023*, 15. https://doi.org/10.1155/2023/1675634

Mekuria, D. M., Kassegne, A. B., & Asfaw, S. L. (2021). Assessing pollution profiles along Little Akaki River receiving municipal and industrial wastewaters, Central Ethiopia: implications for environmental and public health safety. *Heliyon*, *7*(7), e07526. https://doi.org/10.1016/j.heliyon.2021.e07526

Melaku, S., Wondimu, T., Dams, R., & Moens, L. (2004). Simultaneous determination of trace elements in tinishu akaki river water sample, Ethiopia, by ICP-MS. *Canadian Journal of Analytical Sciences and Spectroscopy*, *49*(6), 374–384.

Melaku, S., Wondimu, T., Dams, R., & Moens, L. (2007). Pollution status of Tinishu Akaki River and its tributaries (ethiopia) evaluated using physico-chemical parameters, major ions, and nutrients. *Bulletin of the Chemical Society of Ethiopia*, *21*(1), 13–22. https://doi.org/10.4314/bcse.v21i1.61364

Melaku, Worku, L., Seid, T., Geremew, S., & Mary, K.-Q. (2020). Challenges for water quality protection in the greater metropolitan area of Addis Ababa and the upper Awash basin, Ethiopia – time to take stock. *Environmental Reviews*, *5*(1), 43–54. https://doi.org/https://doi.org/10.1139/er-2020-0042

Menbere, M. P. (2019). Industrial Wastes and Their Management Challenges in Ethiopia. *Chemistry and Materials Research*, 1–6. https://doi.org/10.7176/cmr/11-8-01

Mendez, M., Calvo-Valverde, L. A., Imbach, P., Maathuis, B., Hein-Grigg, D., Hidalgo-Madriz, J. A., & Alvarado-Gamboa, L. F. (2022). Hydrological Response of Tropical Catchments to Climate Change as Modeled by the GR2M Model: A Case Study in Costa Rica. *Sustainability (Switzerland)*, *14*(24). https://doi.org/10.3390/su142416938

Mengesha, S. D., Kidane, A. W., & Dinssa, D. A. (2021). Microbial Risk Assessment of Vegetables Irrigated with Akaki River Water in Addis Ababa . *Research Square*, 1–22. https://doi.org/https://doi.org/10.21203/rs.3.rs-492022/v1

Mengesha, S. D., Kidane, A. W., Teklu, K. T., Gizaw, M., Abera, D., Getachew, M., Abate, M., Beyene, Y., Assefa, T., & Alemu, Z. A. (2017). *Pollution status of Akaki river and its contamination effect on surrounding environment and agricultural products: technical report*. http://196.189.110.22/handle/123456789/467?show=full

Mengistie, B. T., Mol, A. P. J., & Oosterveer, P. (2017). Pesticide use practices among smallholder vegetable farmers in Ethiopian Central Rift Valley. *Environment, Development and Sustainability*, *19*(1), 301–324. https://doi.org/10.1007/s10668-015-9728-9

Mengistu, A. G., van Rensburg, L. D., & Woyessa, Y. E. (2019). Techniques for calibration and validation of SWAT model in data scarce arid and semi-arid catchments in South Africa. *Journal of Hydrology: Regional Studies*, *25*(May), 100621. https://doi.org/10.1016/j.ejrh.2019.100621

Menzel, R. G. (1980). CREAMS A Field Scale Model for Chemicals/ Runoff, and Erosion From Agricultural Management Systems. *CREAMS: A Field Scale Model for Chemicals, Runoff, and Erosion from Agricultural Management Systems*, *III*(26), 1–10.

Mersha, A., Masih, I., de Fraiture, C., Wenninger, J., & Alamirew, T. (2018). Evaluating the Impacts of IWRM Policy Actions on Demand Satisfaction and Downstream Water Availability in the Upper Awash Basin, Ethiopia. *Water*, *10*(7), 892. https://doi.org/10.3390/w10070892

Mesfin, M., Tudorancea, C., & Baxter, R. M. (1988). Some limnological observations on two Ethiopian hydroelectric reservoirs: Koka (Shewa administrative district) and Finchaa (Welega administrative district). *Hydrobiologia*, *157*(1), 47–55. https://doi.org/10.1007/BF00008809

Meshram, S. G., & Sharma, S. K. (2017). Prioritization of watershed through morphometric parameters: a PCA-based approach. *Applied Water Science*, *7*(3), 1505–1519. https://doi.org/10.1007/s13201-015-0332-9

Miao, C. Y., Yang, L., Chen, X. H., & Gao, Y. (2012). *THE VEGETATION COVER DYNAMICS (1982 – 2006) IN DIFFERENT EROSION REGIONS OF THE YELLOW RIVER BASIN , CHINA*. *71*(October 2010), 62–71.

Migliaccio, K. W., & Chaubey, I. (2010). Comment on Cao W, Bowden BW, Davie T, Fenemor A. 2006. 'Multi-variable and multi-site calibration and validation of SWAT in a large mountainous catchment with high spatial variability.' *Hydrol. Process.*, *2274*(November 2008), 2267–2274. https://doi.org/10.1002/hyp

Miller, J. D., & Hutchins, M. (2017). The impacts of urbanisation and climate change on urban flooding and urban water quality: A review of the evidence concerning the United Kingdom. *Journal of Hydrology: Regional Studies*, *12*(June), 345–362. https://doi.org/10.1016/j.ejrh.2017.06.006

Mir, A. A., & Ahmed, R. (2021). *SWAT Based Prioritization of Sub- watersheds in Pohru Watershed of Jhelum Basin , Northwestern Himalayas Abaas Ahmad Mir and Rayees Ahmed Research Journal of Agricultural Sciences*. *July*. https://doi.org/10.5281/zenodo.5153487

Mirzaei, M., Solgi, E., & Salman, A. (2017). *Modeling of Non-Point Source Pollution by Long- Term Hydrologic Impact Assessment (L-THIA) (Case Study : Zayandehrood Watershed) in 2015*. *6*(2), 196–205.

Misaghi, F., Nasrabadi, M., & Nouri, M. (2020). Application of swat model to simulate nitrate and phosphate leaching from agricultural lands to the rivers. *Advances in Environmental Technology*, *6*(1), 1–17. https://doi.org/10.22104/AET.2020.4298.1214

Mishra, A., Kar, S., & Singh, V. P. (2007). Prioritizing structural management by quantifying the effect of land use and land cover on watershed runoff and sediment yield. *Water Resources Management*, *21*(11), 1899–1913. https://doi.org/10.1007/s11269-006-9136-x

Mishra, S., & Mishra, D. R. (2012). Normalized difference chlorophyll index : A novel model for remote estimation of chlorophyll- a concentration in turbid productive waters. *Remote Sensing of Environment*, *117*, 394–406. https://doi.org/10.1016/j.rse.2011.10.016

Mitiku, A. B., Meresa, G. A., Mulu, T., & Woldemichael, A. T. (2023). Examining the impacts of climate variabilities and land use change on hydrological responses of Awash River basin, Ethiopia. *HydroResearch*, *6*, 16–28. https://doi.org/10.1016/j.hydres.2022.12.002

Moffitt, A. H. (2019). Better Assessment Science Integrating Point and Nonpoint Sources. BASINS version 4.5 User Manual. *American Journal of Orthodontics and Dentofacial Orthopedics*, *155*(1), 145.e1-145.e2. https://doi.org/10.1016/j.ajodo.2018.11.001

Moges, A. S., Wondimagegn, S. A., & Getahun, Y. S. (2024). Evaluate the effectiveness of soil and water conservation interventions in the upper Awash Basin, Ethiopia. *World Water Policy*, *10*(1), 324–340. https://doi.org/10.1002/wwp2.12165

Moges, M. A., Schmitter, P., Tilahun, S. A., Ayana, E. K., Ketema, A. A., Nigussie, T. E., & Steenhuis, T. S. (2017). Water Quality Assessment by Measuring and Using Landsat 7 ETM+ Images for the Current and Previous Trend Perspective: Lake Tana Ethiopia. *Journal of Water Resource and Protection*, *09*(12), 1564–1585. https://doi.org/10.4236/jwarp.2017.912099

Moges, M. A., Tilahun, S. A., Ayana, E. K., Moges, M. M., Gabye, N., Giri, S., & Steenhuis, T. S. (2016). Non-Point Source Pollution of Dissolved Phosphorus in the Ethiopian Highlands: The Awramba Watershed Near Lake Tana. *Clean - Soil, Air, Water*, *44*(6), 703–709. https://doi.org/10.1002/clen.201500131

Moges, Schmitter, P., Tilahun, S. A., Ayana, E. K., Ketema, A. A., Nigussie, T. E., & Steenhuis, T. S. (2017). Water Quality Assessment by Measuring and Using Landsat 7 ETM+ Images for the Current and Previous Trend Perspective: Lake Tana Ethiopia. *Journal of Water Resource and Protection*, *09*(12), 1564–1585. https://doi.org/10.4236/jwarp.2017.912099

Mohammed, A., & Elias, E. (2017). Domestic waste management and its environmental impacts in Addis Ababa City. *International Scholars Journals*, *4 (3)*(2375–1266). www.internationalscholarsjournals.org

Mohammed, H., Yohannes, F., & Zeleke, G. (2004). Validation of agricultural non-point source (AGNPS) pollution model in Kori watershed, South Wollo, Ethiopia. *International Journal of Applied Earth Observation and Geoinformation*, *6*(2), 97–109. https://doi.org/10.1016/j.jag.2004.08.002

Moher, D., Liberati, A., Tetzlaff, J., & Altman, D. G. (2009). Preferred reporting items for systematic reviews and meta-analyses: The PRISMA statement. *BMJ (Online)*, *339*(7716), 332–336. https://doi.org/10.1136/bmj.b2535

Molkov, A. A., Fedorov, S. V., Pelevin, V. V., & Korchemkina, E. N. (2019). Regional models for high-resolution retrieval of chlorophyll a and TSM concentrations in the Gorky Reservoir by Sentinel-2 imagery. *Remote Sensing*, *11*(10). https://doi.org/10.3390/rs11101215

Moriasi D. N., Arnold J. G., Van Liew M. W., Bingner R. L., Harmel R. D., & Veith T. L. (2007). Model Evaluation Guidelines for Systematic Quantification of Accuracy in Watershed Simulations. *Transactions of the ASABE*, *50*(3), 885–900. https://doi.org/10.13031/2013.23153

Moriasi, D. N., Gitau, M. W., Pai, N., & Daggupati, P. (2015). Hydrologic and water quality models: Performance measures and evaluation criteria. *Transactions of the ASABE*, *58*(6), 1763–1785. https://doi.org/10.13031/trans.58.10715

Morris, B. G. L., & Fan, J. (1997). *RESERVOIR SEDIMENTATION HANDBOOK—DESIGN AND MANAGEMENT OF DAMS,RESERVOIRS, AND WATERSHED FOR SUSTAINABLE USE* (Issue June). McGraw-Hill.

Mortensen, J. (2015). *Final Project: Nitrogen sources in the Rio Grande basin*.

MoWE. (2013). *Water and energy sector development researchable issues/problems and list of research outputs/index*.

MoWIE. (2017). *Awash Basin Water Quality* (Issue June). file:///C:/Users/Endaweke/Downloads/Water Quality Strategic Basin Plan Final - Copy.pdf

MoWIE. (2020). *Existing Water Quality Situation In Ethiopia*.

Mulu, A., Ayenew, T., Berhe, S., & Hailu, A. M. (2013). Impact of Slaughterhouses Effluent on Water Quality of Modjo and Akaki River in Central Ethiopia. *International Journal of Science and Research*, *4*(3), 899–907.

Narsimlu, B., Gosain, A. K., Chahar, B. R., Singh, S. K., & Srivastava, P. K. (2015). SWAT Model Calibration and Uncertainty Analysis for Streamflow Prediction in the Kunwari River Basin, India, Using Sequential Uncertainty Fitting. *Environmental Processes*, *2*(1), 79–95. https://doi.org/10.1007/s40710-015-0064-8

Naser, H., Sultana, S., Haque, M. M., Akhter, S., & Begum, R. (2014). Lead, Cadmium and Nickel Accumulation in Some Common Spices Grown in Industrial Areas of Bangladesh. *The Agriculturists*, *12*(1), 122–130. https://doi.org/10.3329/agric.v12i1.19867

Nasir, M. J., Ahmad, W., Jun, C., Iqbal, J., & Bateni, S. M. (2023). Soil erosion susceptibility assessment of Swat River sub-watersheds using the morphometry-based compound factor approach and GIS. *Environmental Earth Sciences*, *82*(12), 1–28. https://doi.org/10.1007/s12665-023-10982-4

Nautiyal, M. D. (1994). Morphometric analysis of a drainage basin using aerial photographs: A case study of Khairkuli basin, district Dehradun, U.P. *Journal of the Indian Society of Remote Sensing*, *22*(4), 251–261. https://doi.org/10.1007/BF03026526

Neighborhood water quality. (2000). *PROJECT OCEANOGRAPHY*. https://www.marine.usf.edu/pjocean/packets/f00/nwq2.pdf

Neitsch, S. ., Arnold, J. ., Kiniry, J. ., & Williams, J. . (2011). Soil & Water Assessment Tool Theoretical Documentation Version 2009. *Texas Water Resources Institute*, 1–647. https://doi.org/10.1016/j.scitotenv.2015.11.063

Nejadhashemi, A. P., & Woznicki, S. A. (2011). *Comparison of four models (STEPL, PLOAD, L-THIA, AND SWAT) in simulating sediment, nitrogen, and phosphorus loads and pollutant source areas*. *54*(2006), 875–890.

Németh, A., Ainsworth, J., Ravishankar, H., Lens, P. N. L., & Heffernan, B. (2023). Temperature dependence of nitrification in a membrane-aerated biofilm reactor. *Frontiers in Microbiology*, *14*(April), 1–11. https://doi.org/10.3389/fmicb.2023.1114647

Nguyen, T. H. D., Phan, K. D., Nguyen, H. T. T., Tran, S. N., Tran, T. G., Tran, B. L., & Doan, T. N. (2020). TOTAL SUSPENDED SOLID DISTRIBUTION in HAU RIVER USING SENTINEL 2A SATELLITE IMAGERY. *ISPRS Annals of the Photogrammetry, Remote Sensing and Spatial Information Sciences*, *6*(3/W1), 91–97. https://doi.org/10.5194/isprs-annals-VI-3-W1-2020-91-2020

Niazi, M., Nietch, C., Maghrebi, M., Jackson, N., Bennett, B. R., Tryby, M., & Massoudieh, A. (2017). Storm Water Management Model: Performance Review and Gap Analysis. In *Journal of Sustainable Water in the Built Environment* (Vol. 3, Issue 2). https://doi.org/10.1061/JSWBAY.0000817

Niguse, B. D., Yan, X., Wu, H., Colebrooke, L. L., & Wang, J. (2018). Occurrences and Ecotoxicological Risk Assessment of Heavy Metals in Surface Sediments from Awash. *Water*. https://doi.org/10.3390/w10050535

Niguse Bekele Dirbaba, Xue Yan, Hongjuan Wu, L. L. C. and J. W. (2018). Occurrences and Ecotoxicological Risk Assessment of Heavy Metals in Surface Sediments from Awash. *Water*. https://doi.org/10.3390/w10050535

Nitheshnirmal, S., Bhardwaj, A., Dineshkumar, C., & Rahaman, S. A. (2019). *Prioritization of Erosion Prone Micro-Watersheds Using Morphometric Analysis coupled with Multi-Criteria Decision Making*. 11. https://doi.org/10.3390/iecg2019-06207

Noori, N., Kalin, L., & Isik, S. (2020). Water quality prediction using SWAT-ANN coupled approach. *Journal of Hydrology*, *590*, 125220. https://doi.org/10.1016/j.jhydrol.2020.125220

Novem Auyeung, D. S., Martiny, J. B. H., & Dukes, J. S. (2015). Nitrification kinetics and ammonia-oxidizing community respond to warming and altered precipitation. *Ecosphere*, *6*(5), 1–17. https://doi.org/10.1890/ES14-00481.1

Nugusu, S. (2015). *Assessment of surface water quality in upper awash river basin*. Addis Ababa University.

O'Driscoll, M., Clinton, S., Jefferson, A., Manda, A., & McMillan, S. (2010). Urbanization effects on watershed hydrology and in-stream processes in the southern United States. *Water (Switzerland)*, *2*(3), 605–648. https://doi.org/10.3390/w2030605

Okoli, J., Nahazanan, H., Nahas, F., Kalantar, B., Shafri, H. Z. M., & Khuzaimah, Z. (2023). High-Resolution Lidar-Derived DEM for Landslide Susceptibility Assessment Using AHP and Fuzzy Logic in Serdang, Malaysia. *Geosciences (Switzerland)*, *13*(2). https://doi.org/10.3390/geosciences13020034

Olbasa, B. W. (2017). Characterization of Physicochemical Water Quality Parameters of River Gudar (Oromia region, West Shewa Zone, Ethiopia) for Drinking Purpose. *IOSR Journal of Applied Chemistry*, *10*(05), 47–52. https://doi.org/10.9790/5736-1005014752

Ongley, E. D., Xiaolan, Z., & Tao, Y. (2010). Current status of agricultural and rural non-point source Pollution assessment in China. *Environmental Pollution*, *158*(5), 1159–1168. https://doi.org/10.1016/j.envpol.2009.10.047

Opoku, A., Ahmed, V., & Akotia, J. (2016). Choosing an appropriate research methodology and method. *Research Methodology in the Built Environment: A Selection of Case Studies*, *July*, 32–49. https://doi.org/10.4324/9781315725529

Opricovic, S., & Tzeng, G. H. (2004). Compromise solution by MCDM methods: A comparative analysis of VIKOR and TOPSIS. *European Journal of Operational Research*, *156*(2), 445–455. https://doi.org/10.1016/S0377-

2217(03)00020-1

Ouma, Y. (2018). *Analysis of Nonpoint Source Pollution Loading on Water Quality in an Urban- Rural River Catchment Using GIS-PLOAD Model : Case Study of Sosiani River Analysis of Nonpoint Source Pollution Loading on Water Quality in an Urban-Rural River Catchment Using GI*. *10*(March), 70–84.

Ouma, Y. O., Noor, K., & Herbert, K. (2020). Modelling Reservoir Chlorophyll- a, TSS, and Turbidity Using Sentinel-2A MSI and Landsat-8 OLI Satellite Sensors with Empirical Multivariate Regression. *Journal of Sensors*, *2020*. https://doi.org/10.1155/2020/8858408

Ouyang, Y. (2022). A Gap-Filling Tool: Predicting Daily Sediment Loads Based on Sparse Measurements. *Hydrology*, *9*(10). https://doi.org/10.3390/hydrology9100181

Özerol, G., Vinke-De Kruijf, J., Brisbois, M. C., Flores, C. C., Deekshit, P., Girard, C., Knieper, C., Mirnezami, S. J., Ortega-Reig, M., Ranjan, P., Schröder, N. J. S., & Schröter, B. (2018). Comparative studies of water governance: A systematic review. *Ecology and Society*, *23*(4). https://doi.org/10.5751/ES-10548-230443

Öztürk, Ş., Yılmaz, K., Dinçer, A. E., & Kalpakcı, V. (2024). Effect of urbanization on surface runoff and performance of green roofs and permeable pavement for mitigating urban floods. *Natural Hazards*, *120*(13), 12375–12399. https://doi.org/10.1007/s11069-024-06688-w

P. N. Rymbai. (2012). Estimation of sediment production rate of the Umbaniun Micro- watershed, Meghalaya, India. *Journal of Geography and Regional Planning*, *5*(11), 293–297. https://doi.org/10.5897/jgrp11.032

P. W. Gassman, M. R. Reyes, C. H. Green, & J. G. Arnold. (2007). The Soil and Water Assessment Tool: Historical Development, Applications, and Future Research Directions. *Transactions of the ASABE*, *50*(4), 1211–1250. https://doi.org/10.13031/2013.23637

Paghadal, A. M., Rank, H. D., Makavana, J. M., Kukadiya, V. D., & Prajapti, G. V. (2019). Quantitative Analysis of Geomorphometric Parameters of Ozat River Basin Using Remote Sensing and GIS. *International Journal of Current Microbiology and Applied Sciences*, *8*(09), 213–233. https://doi.org/10.20546/ijcmas.2019.809.027

Panagopoulos, Y., Makropoulos, C., Baltas, E., & Mimikou, M. (2011). SWAT parameterization for the identification of critical diffuse pollution source areas under data limitations. *Ecological Modelling*, *222*(19), 3500–3512. https://doi.org/10.1016/j.ecolmodel.2011.08.008

Pandey, A., Chowdary, V. M., & Mal, B. C. (2007). Identification of critical erosion prone areas in the small agricultural watershed using USLE, GIS and remote sensing. *Water Resources Management*, *21*(4), 729–746. https://doi.org/10.1007/s11269-006-9061-z

Pant, S., Kumar, A., Ram, M., Klochkov, Y., & Sharma, H. K. (2022). Consistency Indices in Analytic Hierarchy Process: A Review. *Mathematics*, *10*(8), 1–15. https://doi.org/10.3390/math10081206

Pareek, D. R., Kkahn, D. A. S., & Srivastava, D. P. (2020). Impact on Human Health Due to Ghaggar Water Pollution. *Current World Environment*, *15*, 211–217. https://doi.org/10.12944/cwe.15.2.08

Parker, H., Mosello, B., & Roger Calow, Maria Quattri, Seifu Kebed, Tena Alamirew, Assefa Gudina, A. K. (2016). A thirsty future? Water strategies for Ethiopia's new development era. In *Report* (Issue August). https://www.sdgfund.org/thirsty-future-water-strategies-ethiopias-new-development-era

Patel, D. P., Gajjar, C. A., & Srivastava, P. K. (2013). Prioritization of Malesari mini-watersheds through morphometric analysis: A remote sensing and GIS perspective. *Environmental Earth Sciences*, *69*(8), 2643–2656. https://doi.org/10.1007/s12665-012-2086-0

Patel, M., Nevill, J. T., Hartmann, D. M., Tew, D., Thrall, S., Votaw, G., & Crenshaw, H. C. (2011). Watershed Modeling and its Applications: A State-of-the-Art Review. *The Open Hydrology Journal*, *5*, 1910–1912. https://doi.org/10.2174/1874378101105010026

Patton, P. C., & Baker, V. R. (1976). Morphometry and floods in small drainage basins subject to diverse hydrogeomorphic controls. *Water Resources Research*, *12*(5), 941–952. https://doi.org/10.1029/WR012i005p00941

Peterson, J. R., & Hamlett, J. M. (1997). Hydrologic calibration of the SWAT model in a watershed containing fragipan soils and wetlands. *Paper - American Society of Agricultural Engineers*, *2*(3), 531–544.

Pizani, F. M. C., Maillard, P., Ferreira, A. F. F., Amorim, C. C. De, Federal, U., Gerais, D. M., Horizonte, B., Federal, U., Gerais, D. M., Horizonte, B., Models, S., & Analysis, R. (2020). *ESTIMATION OF WATER QUALITY IN A RESERVOIR FROM SENTINEL-2 MSI AND LANDSAT-8 OLI SENSORS*. *V*, 401–408.

Ploskas, N., & Papathanasiou, J. (2019). A decision support system for multiple criteria alternative ranking using TOPSIS and VIKOR in fuzzy and nonfuzzy environments. *Fuzzy Sets and Systems*, *377*, 1–30. https://doi.org/10.1016/j.fss.2019.01.012

Potsdam Institue for Climate Impact Research. (2013). *SWIM - Soil and Water Integrated Model*. http://www.pik-potsdam.de/research/research-domains/climate-impacts-and-vulnerabilities/models/swim

Prabu, P. C., Wondimu, L., & Tesso, M. (2011). Assessment of water quality of Huluka and Alaltu Rivers of Ambo, Ethiopia. *Journal of Agricultural Science and Technology*, *13*(1), 131–138.

Premkumar, Venkatachalapathy, & Visweswaran. (2021). Mapping of Total Suspended Matter based on Sentinel-2 data on the Hooghly River, India. *Indian J.of Ecology*, *48*(1), 159–165. https://www.researchgate.net/profile/Prem-Kumar-82/publication/349683336_Mapping_of_Total_Suspended_Matter_based_on_Sentinel-2_data_on_the_Hooghly_River_India/links/603c6c98299bf1cc26fbd606/Mapping-of-Total-Suspended-Matter-based-on-Sentinel-2-data-on-the

Preston, S., Alexander, R., & Woodside, M. (2011). *Regional Assessments of the Nation's Water Quality — Improved Understanding of Stream Nutrient Sources Through Enhanced Modeling Capabilities. October*, 1–6.

Program on Sustainable Constraction and Production in the Akaki Rivver Basin: A Situation analysis of the Akaki River. (2005).

Pulighe, G., Bonati, G., Colangeli, M., Traverso, L., Lupia, F., Altobelli, F., Marta, A. D., & Napoli, M. (2020). Predicting streamflow and nutrient loadings in a semi-arid Mediterranean watershed with ephemeral streams using the SWAT model. *Agronomy*, *10*(1). https://doi.org/10.3390/agronomy10010002

Puno, G. R., & Puno, R. C. C. (2019). Watershed conservation prioritization using geomorphometric and land use-land cover parameters. *Global Journal of Environmental Science and Management*, *5*(3), 279–294. https://doi.org/10.22034/gjesm.2019.03.02

Quang, N. H., Sasaki, J., Higa, H., & Huan, N. H. (2017). Spatiotemporal variation of turbidity based on landsat 8 OLI in Cam Ranh Bay and Thuy Trieu Lagoon, Vietnam. *Water (Switzerland)*, *9*(8). https://doi.org/10.3390/w9080570

R. E. Burwell, G. E. Schuman, R. F. Piest, W. E. Larson, & E. E. Alberts. (1975). Sampling Procedures for Nitrogen and Phosphorus in Runoff. *Transactions of the ASAE*, *18*(5), 0912–0917. https://doi.org/10.13031/2013.36706

Rahaman, S. A., Ajeez, S. A., Aruchamy, S., & Jegankumar, R. (2015). Prioritization of Sub Watershed Based on Morphometric Characteristics Using Fuzzy Analytical Hierarchy Process and Geographical Information System – A Study of Kallar Watershed, Tamil Nadu. *Aquatic Procedia*, *4*(Icwrcoe), 1322–1330. https://doi.org/10.1016/j.aqpro.2015.02.172

Rai, Chandel, R. S., Mishra, V. N., & Singh, P. (2018). Hydrological inferences through morphometric analysis of lower Kosi river basin of India for water resource management based on remote sensing data. *Applied Water Science*, *8*(1), 1–16. https://doi.org/10.1007/s13201-018-0660-7

Rai, P., Chaubey, P. K., Mohan, K., & Singh, P. (2017). Geoinformatics for assessing the inferences of quantitative drainage morphometry of the Narmada Basin in India. *Applied Geomatics*, *9*(3), 167–189. https://doi.org/10.1007/s12518-017-0191-1

Rai, P., Mishra, V. N., & Mohan, K. (2017). A study of morphometric evaluation of the Son basin, India using geospatial approach. *Remote Sensing Applications: Society and Environment*, *7*(April 2016), 9–20. https://doi.org/10.1016/j.rsase.2017.05.001

Rakhecha, P. R. (2020). Water environment pollution with its impact on human diseases in India. *International Journal of Hydrology*, *4*(4), 152–158. https://doi.org/10.15406/ijh.2020.04.00240

Ranjan, R., Jhariya, G., & Jaiswal, R. K. (2013). Saaty ' s Analytical Hierarchical Process based Prioritization of Sub-watersheds of Bina River Basin using Remote Sensing and GIS. *American Scientific Research Journal for Engineering, Technology, and Sciences (ASRJETS)*, *3*, 36–55.

Ratnam, K. N., Srivastava, Y. K., Venkateswara Rao, V., Amminedu, E., & Murthy, K. S. R. (2005). Check Dam positioning by prioritization micro-watersheds using SYI model and morphometric analysis - remote sensing and GIS perspective. *Journal of the Indian Society of Remote Sensing*, *33*(1), 25–38. https://doi.org/10.1007/BF02989988

Raynal, J., & Kieffer, G. (2004). Lithology, dynamism and volcanic successions at Melka Kunture (Upper Awash, Ethiopia). … *Site of Melka Kunture, Ethiopia. …*, *March*, 111–135. http://halshs.archives-ouvertes.fr/halshs-00003990/

Razdar, B., Mohammadi, K., Samani, J. M. V., & Pirooz, B. (2011). Determining the best water quality model for the rivers in north of Iran (case study: Pasikhan River). *Comp. Meth. Civil Eng.*, *2*(1), 109–121.

Reddy, R. K., & Mastan, S. A. (2011). Algal toxins and their impact on human health. *Biomedical & Pharmacology Journal*, *4*(1), 129–134. https://doi.org/10.13005/bpj/270

Regulation, C. of M. (2000). *FEDERAL NEGARIT GAZETA OF THE FEDERAL DEMOCRATIC REPUBLIC OF ETHIOPIA*.

Ren, J., Manzardo, A., Mazzi, A., Zuliani, F., & Scipioni, A. (2015). Prioritization of bioethanol production pathways in China based on life cycle sustainability assessment and multicriteria decision-making. *International Journal of Life Cycle Assessment*, *20*(6), 842–853. https://doi.org/10.1007/s11367-015-0877-8

Renard et al., 1997. (1997). *Predicting soil Erosion by Water: A Guide to Conservation Planning With the Revised Universal Soil Loss Equation (RUSLE)*. https://www.ars.usda.gov/arsuserfiles/64080530/rusle/ah_703.pdf

Robertson, D. M., & Saad, D. A. (2013). NUTRIENT INPUTS TO THE LAURENTIAN GREAT LAKES BY SOURCE AND WATERSHED ESTIMATED USING SPARROW WATERSHED MODELS. *Journal of the American Water Resources Association*, *49*(3), 725–734. https://doi.org/10.1111/jawr.12060

Rodríguez-Benito, C. V., Navarro, G., & Caballero, I. (2020). Using Copernicus Sentinel-2 and Sentinel-3 data to monitor harmful algal blooms in Southern Chile during the COVID-19 lockdown. *Marine Pollution Bulletin*, *161*(October). https://doi.org/10.1016/j.marpolbul.2020.111722

Rooijen, D. Van, & Taddesse, G. (2009). Urban sanitation and wastewater treatment in Addis Ababa in the Awash Basin , Ethiopia. *In Water, Sanitation and Hygiene: Sustainable Development and Multisectoral Approaches - Proceedings of the 34th WEDC International Conference, Mcm*, 1–6. https://doi.org/https://hdl.handle.net/2134/28515

Rostamian, R., Jaleh, A., Afyuni, M., Mousavi, S. F., Heidarpour, M., Jalalian, A., & Abbaspour, K. C. (2008). Application of a SWAT model for estimating runoff and sediment in two mountainous basins in central Iran. *Hydrological Sciences Journal*, *53*(5), 977–988. https://doi.org/10.1623/hysj.53.5.977

Rothman, N., Rothstein, D., Foor, F., & Magasanik, B. (1982). Water Quality Assessments - A Guide to Use of

Biota, Sediments and Water in Environmental Monitoring - Second Edition. *Journal of Bacteriology*, *150*(1), 221–230.

Ruddick, K., Nechad, B., Neukermans, G., Park, Y., Doxaran, D., Sirjacobs, D., & Beckers, J.-M. (2008). Remote Sensing of Suspended Particulate Matter in Turbid Waters : State of the Art and Future Perspectives. *The CDROM Proceedings of the Ocean Optics XIX Conference Held in Barga*, 6–10.

Saaty. (1987). The analytic hierarchy process-what it is and how it is used. *Mathematical Modelling*, *9*(3–5), 161–176. https://doi.org/10.1016/0270-0255(87)90473-8

Saaty. (1990). How to make a decision: The analytic hierarchy process. *European Journal of Operational Research*, *48*(1), 9–26. https://doi.org/10.1016/0377-2217(90)90057-I

Saaty, T. L. (1977). A scaling method for priorities in hierarchical structures. *Journal of Mathematical Psychology*, *15*(3), 234–281. https://doi.org/10.1016/0022-2496(77)90033-5

Saaty, & Vargas. (1987). Stimulus-response with reciprocal kernels: The rise and fall of sensation. *Journal of Mathematical Psychology*, *31*(1), 83–92. https://doi.org/10.1016/0022-2496(87)90037-X

Saberioon, M., Brom, J., Nedbal, V., Souček, P., & Císař, P. (2020). Chlorophyll-a and total suspended solids retrieval and mapping using Sentinel-2A and machine learning for inland waters. *Ecological Indicators*, *113*(January 2021). https://doi.org/10.1016/j.ecolind.2020.106236

Saha, S., Gayen, A., Pourghasemi, H. R., & Tiefenbacher, J. P. (2019). Identification of soil erosion-susceptible areas using fuzzy logic and analytical hierarchy process modeling in an agricultural watershed of Burdwan district, India. *Environmental Earth Sciences*, *78*(23). https://doi.org/10.1007/s12665-019-8658-5

Sahour, H., Gholami, V., Vazifedan, M., & Saeedi, S. (2021). Machine learning applications for water-induced soil erosion modeling and mapping. *Soil and Tillage Research*, *211*(April), 105032. https://doi.org/10.1016/j.still.2021.105032

Sajikumar, N., & Remya, R. S. (2015). Impact of land cover and land use change on runoff characteristics. *Journal of Environmental Management*, *161*, 460–468. https://doi.org/10.1016/j.jenvman.2014.12.041

Sakthivel, R., Jawahar Raj, N., Sivasankar, V., Akhila, P., & Omine, K. (2019). Geo-spatial technique-based approach on drainage morphometric analysis at Kalrayan Hills, Tamil Nadu, India. *Applied Water Science*, *9*(1), 1–18. https://doi.org/10.1007/s13201-019-0899-7

Salah, A. M., & Nelson, E. J. (2010). *Water Resources / Quality Modeling using Hydrological Simulation Program-Fortran (HSPF) and Watershed Modeling System (WMS).* 1–13.

Salami, E. B. (2016). *Physicochemical and Bacteriological Analysis of Some Selected Sites From Kebena River and Its Pollution Status in Addis Ababa* [Addis ABaba University]. http://localhost:80/xmlui/handle/123456789/5237

Saleh, A., & Du, B. (2004). Evaluation of SWAT and HSPF within BASINS program for the upper North Bosque River watershed in central Texas. *Transactions of the American Society of Agricultural Engineers*, *47*(4), 1039–1049. https://doi.org/10.13031/2013.16577

Salvini, R., Riccucci, S., & Francioni, M. (2012). Topographic and geological mapping in the prehistoric area of Melka Kunture (Ethiopia). *Journal of Maps*, *8*(2), 169–175. https://doi.org/10.1080/17445647.2012.680779

Sandu, M.-A., & Virsta, A. (2015). Applicability of MIKE SHE to Simulate Hydrology in Argesel River Catchment. *Agriculture and Agricultural Science Procedia*, *6*, 517–524. https://doi.org/10.1016/j.aaspro.2015.08.135

Santhi, C., Arnold, J. G., Williams, J. R., Hauck, L. M., & Dugas, W. A. (2001). Application of a watershed model to evaluate management effects on point and nonpoint source pollution. *TRANSACTIONS OF THE ASAE*.

Santos, F. M., de Oliveira, R. P., & Di Lollo, J. A. (2020). Effects of land use changes on streamflow and sediment yield in Atibaia River Basin-SP, Brazil. *Water (Switzerland)*, *12*(6). https://doi.org/10.3390/W12061711

Sasanka, C. T., & Ravindra, K. (2015). Implementation of VIKOR Method for Selection of Magnesium Alloy to Suit Automotive Applications. *International Journal of Advanced Science and Technology*, *83*, 49–58. https://doi.org/10.14257/ijast.2015.83.05

Sattari, S. Z., Bouwman, A. F., Giller, K. E., & Van Ittersum, M. K. (2012). Residual soil phosphorus as the missing piece in the global phosphorus crisis puzzle. *Proceedings of the National Academy of Sciences of the United States of America*, *109*(16), 6348–6353. https://doi.org/10.1073/pnas.1113675109

Schalles, J. F. (2006). Optical remote sensing techniques to estimate phytoplankton chlorophyll a concentrations in coastal waters with varying suspended matter and cdom concentrations. In *Remote Sensing and Digital Image Processing* (Vol. 9, Issue January 2006, pp. 27–79). https://doi.org/10.1007/1-4020-3968-9

Schiefer, E., Slaymaker, O., & Klinkenberg, B. (2001). Physiographically controlled allometry of specific sediment yield in the Canadian Cordillera: A lake sediment-based approach. *Geografiska Annaler*, *83*(1–2), 55–65. https://doi.org/10.1111/j.0435-3676.2001.00144.x

Schumm, S. A. (1956). EVOLUTION OF DRAINAGE SYSTEMS AND SLOPES IN BADLANDS AT PERTH AMBOY , NEW JERSEY. *Bulletin of the Geological Society of America*, *67*(5), 597–646. https://doi.org/10.1130/0016-7606(1956)67

Schumm, S. A. (1963). Geological Society of America Bulletin Sequences in the Cratonic Interior of North America. *Geological Society of America Bulletin*, *74*(2), 93–114. https://doi.org/10.1130/0016-7606(1963)74

Schwarz, G. E., Hoos, A. B., Alexander, R. B., & Smith, R. A. (2006). The SPARROW Surface Water-Quality Model: Theory, Application and User Documentation. *Techniques and Methods*, *January*, 248. http://pubs.er.usgs.gov/publication/tm6B3

Sebilo, M., Mayer, B., Nicolardot, B., Pinay, G., & Mariotti, A. (2013). Long-term fate of nitrate fertilizer in agricultural soils. *Proceedings of the National Academy of Sciences of the United States of America*, *110*(45), 18185–18189. https://doi.org/10.1073/pnas.1305372110

Sent, G., Biguino, B., Favareto, L., Cruz, J., Sá, C., Dogliotti, A. I., Palma, C., Brotas, V., & Brito, A. C. (2021). Deriving water quality parameters using sentinel-2 imagery: A case study in the Sado Estuary, Portugal. *Remote Sensing*, *13*(5), 1–30. https://doi.org/10.3390/rs13051043

Setegn, S. G., Srinivasan, R., & Dargahi, B. (2008). Hydrological Modelling in the Lake Tana Basin, Ethiopia Using SWAT Model. *The Open Hydrology Journal*, *2*(1), 49–62. https://doi.org/10.2174/1874378100802010049

Sethupathi, A. S., Lakshmi, N., Vasanthamohan, V., & Mohan, S. (2011). Prioritization of mini watersheds based on morphometric analysis using remote sensing and GIS in a drought prone Bargur Mathur sub watersheds, Ponnaiyar River basin, India. *Int J Geomat Geosci*, *2*(2), 403–414.

Sharifinia, M., Adeli, B., & Nafarzadegan, A. R. (2017). Evaluation of water quality trends in the Maroon River Basin, Iran, from 1990 to 2010 by WQI and multivariate analyses. *Environmental Earth Sciences*, *76*(22). https://doi.org/10.1007/s12665-017-7132-5

Sharifinia, M., Zohreh, R., Javid, I., Abbas, M., & Tahsin, R. (2013). Water quality assessment of the Zarivar Lake using physico-chemical parameters and NSF- WQI indicator, Kurdistan Province-Iran. *International Journal of Advanced Biological and Biomedical Research*, *1*(3), 302–312.

Shaver, E., Horner, R., Skupien, J., May, C., & Ridley, G. (2007). Fundamentals of urban runoff management: technical and institutional issues. In N. Rehnby (Ed.), *Change*. North American Lake Management Society. http://agris.fao.org/agris-search/search/display.do?f=1995/US/US95046.xml;US9536404

Shawul, A. A., & Chakma, S. (2019a). Spatiotemporal detection of land use/land cover change in the large basin

using integrated approaches of remote sensing and GIS in the Upper Awash basin, Ethiopia. *Environmental Earth Sciences*, *78*(5), 1–13. https://doi.org/10.1007/s12665-019-8154-y

Shawul, A. A., & Chakma, S. (2019b). Spatiotemporal detection of land use/land cover change in the large basin using integrated approaches of remote sensing and GIS in the Upper Awash basin, Ethiopia. *Environmental Earth Sciences*, *78*(5), 0. https://doi.org/10.1007/s12665-019-8154-y

Shekar, P. R., & Mathew, A. (2022). Morphometric analysis for prioritizing sub-watersheds of Murredu River basin, Telangana State, India, using a geographical information system. *Journal of Engineering and Applied Science*, *69*(1), 1–30. https://doi.org/10.1186/s44147-022-00094-4

Shi, K., Li, Y., Li, L., & Lu, H. (2013). Absorption characteristics of optically complex inland waters: Implications for water optical classification. *Journal of Geophysical Research: Biogeosciences*, *118*(2), 860–874. https://doi.org/10.1002/jgrg.20071

Shoemaker, L., Dai, T., & Koenig, J. (2005). *TMDL Model Evaluation and Research Needs* (Issue November).

Shukla, M. K. (2011). *Soil Hydrology, Land Use and Agriculture*. http://mit.undip.ac.id/ebook/files/508 - Soil_Hydrology_Land_Use_and_Agriculture_184593797X (CABI).pdf#page=209

Sima, S., & Restiani, P. (2017). Water Governance Mapping Report: Textile Industry Water Use in Ethiopia. In *Sweden Textile Water Initiative*. https://www.siwi.org/wp-content/uploads/2017/06/Water-Governance-Mapping-Report-Ethiopia.pdf

Singh, A. P., Arya, A. K., & Singh, D. Sen. (2020). Morphometric Analysis of Ghaghara River Basin, India, Using SRTM Data and GIS. *Journal of the Geological Society of India*, *95*(2), 169–178. https://doi.org/10.1007/s12594-020-1406-3

Singh, J., Knapp, H. V., Arnold, J. G., & Demissie, M. (2005). Hydrological modeling of the Iroquois River watershed using HSPF and SWAT. *Journal of the American Water Resources Association*, *41*(2), 343–360. https://doi.org/10.1111/j.1752-1688.2005.tb03740.x

Singh, K. V., Setia, R., & Sahoo, S. (2014). Evaluation of NDWI and MNDWI for assessment of waterlogging by integrating digital elevation model and groundwater level. *Taylor & Francis*, *January 2015*, 37–41. https://doi.org/10.1080/10106049.2014.965757

Singh, R. M., & Gupta, A. (2017). Water Pollution-Sources , Effects and Control Water Pollution-Sources , Effects and Control. *Research Gate*, *5*(3), 1–17. https://www.researchgate.net/publication/321289637%0AWATER

Sinha, R. K., & Eldho, T. I. (2018). Effects of historical and projected land use/cover change on runoff and sediment yield in the Netravati river basin, Western Ghats, India. *Environmental Earth Sciences*, *77*(3). https://doi.org/10.1007/s12665-018-7317-6

Skahill, B. E. (2004). *Use of the Hydrological Simulation Program - FORTRAN (HSPF) Model for Watershed Studies*. *September*.

Smith, K. G. (1950). Standards for Grading Texture of Erosional Topography. *American Journal of Science*, *248*, 655–668. https://doi.org/https://sci-hub.ru/https://doi.org/10.2475/ajs.248.9.655

Sorando, R., Comín, F. A., Jiménez, J. J., Sánchez-Pérez, J. M., & Sauvage, S. (2019). Water resources and nitrate discharges in relation to agricultural land uses in an intensively irrigated watershed. *Science of the Total Environment*, *659*, 1293–1306. https://doi.org/10.1016/j.scitotenv.2018.12.023

Sòria-Perpinyà, X., Vicente, E., Urrego, P., Pereira-Sandoval, M., Tenjo, C., Ruíz-Verdú, A., Delegido, J., Soria, J. M., Peña, R., & Moreno, J. (2021). Validation of water quality monitoring algorithms for sentinel-2 and sentinel-3 in mediterranean inland waters with in situ reflectance data. *Water (Switzerland)*, *13*(5). https://doi.org/10.3390/w13050686

Srinivasan, J. T., & Reddy, V. R. (2009). Impact of irrigation water quality on human health: A case study in India. *Ecological Economics*, *68*(11), 2800–2807. https://doi.org/10.1016/j.ecolecon.2009.04.019

Srinivasan, R., Santhi, C., Harmel, R. D., & Griensven, A. Van. (2012). *Swat: MODEL USE, CALIBRATION, AND VALIDATION*. *55*(4), 1491–1508.

Stone, C., Windsor, F. M., Munday, M., & Durance, I. (2020). Natural or synthetic – how global trends in textile usage threaten freshwater environments. *Science of the Total Environment*, *718*(xxxx), 134689. https://doi.org/10.1016/j.scitotenv.2019.134689

Strahler, A. N. (1957). Quantitative Analysis of Watershed Geomorphology, Transactions of the American Geophysical Union. *Transactions, American Geophysical Union*, *38*(6), 913–920.

Strahler, A. N. (1973). Geological Society of America Bulletin. *Geological Society Of America Bulletin*, *11*. https://doi.org/10.1130/0016-7606(1952)63

Subiyanto, S., Ramadhanis, Z., & Baktiar, A. H. (2018). Integration of Remote Sensing Technology Using Sentinel-2A Satellite images for Fertilization and Water Pollution Analysis in Estuaries Inlet of Semarang Eastern Flood Canal. *E3S Web of Conferences*, *31*. https://doi.org/10.1051/e3sconf/20183112008

Suh, Y., Park, Y., & Kang, D. (2019). Evaluating mobile services using integrated weighting approach and fuzzy VIKOR. *PLoS ONE*, *14*(6), 1–28. https://doi.org/10.1371/journal.pone.0217786

Suji, V. R., Sheeja, R. V., & Karuppasamy, S. (2015). Prioritization using Morphometric Analysis and Land Use/Land Cover Parameters for Vazhichal Watershed using Remote Sensing and GIS Techniques. *International Journal for Innovative Research in Science & Technology*, *2*(1), 61–68. www.ijirst.org

Sukristiyanti, S., Maria, R., & Lestiana, H. (2018). Watershed-based Morphometric Analysis: A Review. *IOP Conference Series: Earth and Environmental Science*, *118*(1), 1–6. https://doi.org/10.1088/1755-1315/118/1/012028

SWECO. (2008). Review of Hydropower Multipurpose Project Coordination Regimes. In *Nile Basin Initiative* (Issue February). http://nilebasin.org/nileis/system/files/NBI_ Best Practice Compendium_Final.pdf

Szatten, D. A., Obodovskyi, O., & Brzezińska, M. (2024). Erosive stability channel factor for Brda River (Poland): a key assessment of the human impact of the catchment changes. *International Journal of Sediment Research*, *40*, 146–157. https://doi.org/10.1016/j.ijsrc.2024.11.002

Taddese, G. (2019). Irrigation water quality of middle awash river basin ,. *International Journal of Hydrology*, *3*(4), 308–312. https://doi.org/10.15406/ijh.2019.03.00192

Taddese, G., Abegaz, F., & Gidyelew, T. (2007). Evaluation of water quality in middle awash valley, Ethiopia. *Middle East Journal of Scientific Research*, 1–19. https://hdl.handle.net/10568/1493

Taddese, G., McComick, P. G., & Peden, D. (2004). *Economic importance and environmental challenges of the Awash river basin to Ethiopia*. https://mountainscholar.org/bitstream/handle/10217/201659/111_Proceedings 2004 USCID SLC Taddese.pdf?sequence=1&isAllowed=y

Tadese, M., Kumar, L., Koech, R., & Kogo, B. K. (2020). Mapping of land-use/land-cover changes and its dynamics in Awash River Basin using remote sensing and GIS. *Remote Sensing Applications: Society and Environment*, *19*(July), 100352. https://doi.org/10.1016/j.rsase.2020.100352

Tadesse, M., Tsegaye, D., & Girma, G. (2018). *Assessment of the level of some physico-chemical parameters and heavy metals of Rebu river in oromia region , Ethiopia*. *2*(4). https://doi.org/10.15406/mojbm.2018.03.00085

Tafesse, T. B., Yetemegne, A. K., & Kumar, S. (2015). *The Physico-Chemical Studies of Wastewater in Hawassa Textile Industry*. *2*(4), 2–7. https://doi.org/10.4172/2380-2391

Takele, L., & Kebede, M. (2018). Streamflow Modeling of Upper Awash River Basin Using Soil and Water Assessment Tool. In */ Appl. J. Envir. Eng. Sci* (Vol. 4).

Tamene, L., Abera, W., Demissie, B., Desta, G., Woldearegay, K., & Mekonnen, K. (2022). Soil erosion assessment in Ethiopia: A review. *Journal of Soil and Water Conservation*, *77*(2), 144–157. https://doi.org/10.2489/jswc.2022.00002

Tamene, L., & Vlek, P. L. G. (2008). Soil erosion studies in Northern Ethiopia. *Land Use and Soil Resources*, 73–100. https://doi.org/10.1007/978-1-4020-6778-5_5

Tamene, & Seyoum. (2015). Temporal and Spatial Variations on Heavy Metals Concentration in River Mojo, Oromia State, East Ethiopia. *International Journal of Science and Research (IJSR)*, *4*(1), 1424–1432. https://www.ijsr.net/archive/v4i1/SUB141157.pdf

Tamiru. (2001). The impact of uncontrolled waste disposal on surface watwer quality in addis ababa, Ethiopia. In *SINET: Ethiopian Journal of Science 24.1 (2001): 93-104* (Vol. 24, Issue 1, pp. 93–104).

Tang, F. F., Xu, H. S., & Xu, Z. X. (2012). Model calibration and uncertainty analysis for runoff in the Chao River Basin using sequential uncertainty fitting. *Procedia Environmental Sciences*, *13*(December), 1760–1770. https://doi.org/10.1016/j.proenv.2012.01.170

Tarekegn, M. Mm., & Truye, A. Z. (2018). Causes and impacts of shankila river water pollution in Addis Ababa, Ethiopia. *Environ Risk Assess Remediat*, *2*(4), 21–30. http://www.alliedacademies.org/environmental-risk-assessment-and-remediation/

Tassew, A. (2007). *Assessment of biological integrity using physico-chemical parameters and macroinvertebrate community index along sebeta river, Ethiopia* [Addis Ababa University]. http://etd.aau.edu.et/bitstream/handle/123456789/787/Admasu Tassew.pdf?sequence=1&isAllowed=y

Taye, M. T., Dyer, E., Hirpa, F. A., & Charles, K. (2018). Climate change impact on water resources in the Awash basin, Ethiopia. *Water*, *10*(11), 1–16. https://doi.org/10.3390/w10111560

Teffera, F. (2009). *The Status of Harmful Cyanobacteria Bloom in Amuddee (Lake Koka-Ethiopia)*. https://www.waterethiopia.org/wp-content/uploads/2014/03/The-Status-of-Harmful-Cyanobacteria-Bloom-in-Amuddee-Lake-Koka-Ethiopia.pdf

Teklay, A., & Amare, M. (2015). Water quality characteristics and pollution levels of heavy metals in Lake Haiq, Ethiopia. *Ethiopian Journal of Science and Technology*, *8*(1), 15. https://doi.org/10.4314/ejst.v8i1.2

Terefe, B., Melese, T., Temesgen, F., Anagaw, A., Afework, A., & Mitikie, G. (2024). Comparative analysis of RUSLE and SWPT for sub-watershed conservation prioritization in the Ayu watershed, Abay basin, Ethiopia. *Heliyon*, *10*(15), e35132. https://doi.org/10.1016/j.heliyon.2024.e35132

Tesfay, H. (2007). *Spatio-Temporal Variations of the Biomass and Primary Production of Phytoplankton in Koka Reservoir* [Addis Ababa University, collage of Natural Sciences]. http://etd.aau.edu.et/handle/123456789/5359

Teshome, M. (2019, March). The Ethiopian Hearald. *BERHANENA SELAM PRINTING ENTERPRISE*, *LXXV*, 5. https://press.et/english/wp-content/uploads/2019/03/mar27.pdf

Tessema, S. M., Setegn, S. G., & Mörtberg, U. (2015). Watershed modeling as a tool for sustainable water resources management: SWAT model application in the awash river basin, Ethiopia. In *Sustainability of Integrated Water Resources Management: Water Governance, Climate and Ecohydrology* (pp. 579–606). Springer International Publishing. https://doi.org/10.1007/978-3-319-12194-9_30

Tewabe, D. (2015). Preliminary Survey of Water Hyacinth in Lake. *Global Journal of Allergy*, *December*, 013–018. https://doi.org/10.17352/2455-8141.000003

Thavhana, M. P., Savage, M. J., & Moeletsi, M. E. (2018). SWAT model uncertainty analysis, calibration and validation for runoff simulation in the Luvuvhu River catchment, South Africa. *Physics and Chemistry of the Earth*, *105*, 115–124. https://doi.org/10.1016/j.pce.2018.03.012

Tialye, A. (2018). *Field and experimental studies on hytoplankton-zooplankton interaction in Lake Koka, with particular references to control of Microcystis species*. http://etd.aau.edu.et/bitstream/handle/123456789/18705/Aynalem Tialye 2018.pdf?sequence=1&isAllowed=y

Tikkanen, H. (2013). *Hydrological modeling of a large urban catchment using a stormwater management model (SWMM)*. www.aalto.fi

Tilahun, A., Shishaye, H. A., & Gebremariam, B. (2017). Sediment inflow estimation and mapping its spatial distribution at sub-basin scale: the case of Tendaho Dam, Afar Regional State, Ethiopia. *Ethiopian Journal of Environmental Studies and Management*, *10*(3), 315. https://doi.org/10.4314/ejesm.v10i3.4

Tilahun, S., Kifle, D., Zewde, T. W., Johansen, J. A., Demissie, T. B., & Hansen, J. H. (2019). Temporal dynamics of intra-and extra-cellular microcystins concentrations in Koka reservoir (Ethiopia): Implications for public health risk. *Toxicon*, *168*(June), 83–92. https://doi.org/10.1016/j.toxicon.2019.06.217

Tolera, M. B., Chung, I. M., & Chang, S. W. (2018). Evaluation of the climate forecast system reanalysis weather data for watershed modeling in Upper Awash Basin, ethiopia. *Water (Switzerland)*, *10*(6), 725. https://doi.org/10.3390/w10060725

Toming, K., Kutser, T., Laas, A., Sepp, M., Paavel, B., & Nõges, T. (2016). First experiences in mapping lakewater quality parameters with sentinel-2 MSI imagery. *Remote Sensing*, *8*(8), 1–14. https://doi.org/10.3390/rs8080640

Topno, A. R., Job, M., Rusia, D. K., Kumar, V., Bharti, B., & Singh, S. D. (2022). Prioritization and identification of vulnerable sub-watersheds using morphometric analysis and an integrated AHP-VIKOR method. *Water Supply*, *22*(11), 8050–8064. https://doi.org/10.2166/ws.2022.303

Topp, S. N., Pavelsky, T. M., Jensen, D., Simard, M., & Ross, M. R. V. (2020). Research trends in the use of remote sensing for inland water quality science: Moving towards multidisciplinary applications. *Water (Switzerland)*, *12*(1), 1–34. https://doi.org/10.3390/w12010169

Tripathi, M. P., Panda, R. K., & Raghuwanshi, N. S. (2003). Identification and prioritisation of critical sub-watersheds for soil conservation management using the SWAT model. *Biosystems Engineering*, *85*(3), 365–379. https://doi.org/10.1016/S1537-5110(03)00066-7

Tsai, L. Y., Chen, C. F., Fan, C. H., & Lin, J. Y. (2017). Using the HSPF and SWMM models in a high pervious watershed and estimating their parameter sensitivity. *Water (Switzerland)*, *9*(10). https://doi.org/10.3390/w9100780

Tsakiris, G., & Alexakis, D. (2015). *Water quality models : An overview*. 33–46.

Tufa, K. N. (2021). Review on Status , Opportunities and Challenges of Irrigation Practices in Awash River Basin , Ethiopia Agrotechnology. *Agrotechnology*, *10*(4).

Tumsa, B. C., Feyessa, F. F., Tullu, K. T., & Guder, A. C. (2023). Spatiotemporal changes of land use in response to runoff and sediment yield for environmental sustainability in the upper Blue Nile Basin, Oromiyaa, Ethiopia. *H2Open Journal*, *6*(4), 551–575. https://doi.org/10.2166/h2oj.2023.072

Tuppad, P., Mankin, K. R. D., Lee, T., Srinivasan, R., & Arnold, J. G. (2011). *SOIL AND WATER ASSESSMENT TOOL (SWAT) HYDROLOGIC/WATER QUALITY MODEL: EXTENDED CAPABILITY AND WIDER ADOPTION*. *54*(2007), 1677–1684.

Tuppad, S., Shetty, G. R., Souravi, K., Rajasekharan, P. E., Ravi, C. S., & Sandesh, M. S. (2017). Character

association for fruit yield and yield traits in holostemma ada-kodien schult. -A vulnerable medicinal plant. *Indian Journal of Ecology*, *44*(2), 337–339.

Umrikar, B. N. (2017). Morphometric analysis of Andhale watershed, Taluka Mulshi, District Pune, India. *Applied Water Science*, *7*(5), 2231–2243. https://doi.org/10.1007/s13201-016-0390-7

UNEP. (2021). *Progress on ambient water quality. Tracking SDG 6 series: global indicator 6.3.2 updates and acceleration needs*. https://gemstat.org/wp-content/uploads/2018/11/632-progress-on-ambient-water-quality-2018.pdf

Uribe, N., Corzo, G., Quintero, M., van Griensven, A., & Solomatine, D. (2018). Impact of conservation tillage on nitrogen and phosphorus runoff losses in a potato crop system in Fuquene watershed, Colombia. *Agricultural Water Management*, *209*(July), 62–72. https://doi.org/10.1016/j.agwat.2018.07.006

US EPA. (2018). *Nutrient and Sediment Estimation Tools for Watershed Protection EPA*.

USEPA. (2001). *PLOAD version 3.0. GIS Pollutant Loading Application — Users Manual*. *January*, 48. http://water.epa.gov/scitech/datait/models/basins/upload/2002_05_10_BASINS_b3docs_PLOAD_v3.pdf

Usher, B., & van Biljon, W. (2006). The impacts of coal and gold mining on the associated water resources in South Africa. In *Groundwater Pollution in Africa*. https://doi.org/10.1201/9780203963548.ch26

Vagstad, N., Stålnacke, P., Andersen, H. E., Deelstra, J., Jansons, V., Kyllmar, K., Loigu, E., Rekolainen, S., & Tumas, R. (2004). Regional variations in diffuse nitrogen losses from agriculture in the Nordic and Baltic regions. *Hydrology and Earth System Sciences*, *8*(4), 651–662. https://doi.org/10.5194/hess-8-651-2004

van der Werff, H., & van der Meer, F. (2016). Sentinel-2A MSI and Landsat 8 OLI provide data continuity for geological remote sensing. *Remote Sensing*, *8*(11). https://doi.org/10.3390/rs8110883

Vanhellemont, Q. (2019). Adaptation of the dark spectrum fitting atmospheric correction for aquatic applications of the Landsat and Sentinel-2 archives. *Remote Sensing of Environment*, *225*(October 2018), 175–192. https://doi.org/10.1016/j.rse.2019.03.010

Vanhellemont, Q., & Ruddick, K. (2016). Acolite for Sentinel-2: Aquatic applications of MSI imagery. *European Space Agency, (Special Publication) ESA SP*, *SP-740*(May), 9–13.

Vega, M., Pardo, R., Barrado, E., & Debán, L. (1998). Assessment of seasonal and polluting effects on the quality of river water by exploratory data analysis. *Water Research*, *32*(12), 3581–3592. https://doi.org/10.1016/S0043-1354(98)00138-9

Veltman, K., Rotz, C. A., Chase, L., Cooper, J., Ingraham, P., Izaurralde, R. C., Jones, C. D., Gaillard, R., Larson, R. A., Ruark, M., Salas, W., Thoma, G., & Jolliet, O. (2018). A quantitative assessment of Beneficial Management Practices to reduce carbon and reactive nitrogen footprints and phosphorus losses on dairy farms in the US Great Lakes region. *Agricultural Systems*, *166*(July), 10–25. https://doi.org/10.1016/j.agsy.2018.07.005

Verstraeten, G., Poesen, J., de Vente, J., & Koninckx, X. (2003). Sediment yield variability in Spain: A quantitative and semiqualitative analysis using reservoir sedimentation rates. *Geomorphology*, *50*(4), 327–348. https://doi.org/10.1016/S0169-555X(02)00220-9

Vittala, S. S., GOVINDAIAH, S., & GOWDA, H. H. (2004). Using Remote Sensing and Gis Techniques To Assess. *Journal of the Indian Society of Remote Sensing*, *MSc*(August), 351–361.

Walker, D. B., Baumgartner, D. J., Gerba, C. P., & Fitzsimmons, K. (2019). Surface Water Pollution. In *Environmental and Pollution Science* (3rd ed., pp. 261–292). Elsevier Inc. https://doi.org/10.1016/b978-0-12-814719-1.00016-1

Wang, A., Tang, L., & Yang, D. (2016). Spatial and temporal variability of nitrogen load from catchment and

retention along a river network: A case study in the upper Xin'anjiang catchment of China. *Hydrology Research*, *47*(4), 869–887. https://doi.org/10.2166/nh.2015.055

Wang, C., & Pang, C. (2011). Using VIKOR method for evaluating service quality of online auction under fuzzy environment. *Ijcset*, *1*(6), 307–314.

Wang, G., Jager, H. I., Baskaran, L. M., Baker, T. F., & Brandt, C. C. (2016). SWAT Modeling of Water Quantity and Quality in the Tennessee River Basin: Spatiotemporal Calibration and Validation. *Hydrology and Earth System Sciences Discussions*, *2016*(January). https://doi.org/10.5194/hess-2016-34

Wang, M., Yao, Y., Shen, Q., Gao, H., Li, J., Zhang, F., & Wu, Q. (2021). Time-Series Analysis of Surface-Water Quality in Xiong'an New Area, 2016–2019. *Journal of the Indian Society of Remote Sensing*, *49*(4), 857–872. https://doi.org/10.1007/s12524-020-01264-8

Wang, Q., Li, S., Jia, P., Qi, C., & Ding, F. (2013). A Review of Surface Water Quality Models. *The Scientific World Journal*, *2013*, 1–7. https://doi.org/10.1155/2013/231768

Warren, M. A., Simis, S. G. H., Martinez-Vicente, V., Poser, K., Bresciani, M., Alikas, K., Spyrakos, E., Giardino, C., & Ansper, A. (2019). Assessment of atmospheric correction algorithms for the Sentinel-2A MultiSpectral Imager over coastal and inland waters. *Remote Sensing of Environment*, *225*(March), 267–289. https://doi.org/10.1016/j.rse.2019.03.018

WASEEM, M., KACHHOLZ, F., & TRÄNCKNER, J. (2018). Suitability of common models to estimate hydrology and diffuse water pollution in North-eastern German lowland catchments with intensive agricultural land use. *Frontiers of Agricultural Science and Engineering*, *0*(0), 0. https://doi.org/10.15302/j-fase-2018243

Wassie, S. B. (2020). Natural resource degradation tendencies in Ethiopia: a review. *Environmental Systems Research*, *9*(1), 1–29. https://doi.org/10.1186/s40068-020-00194-1

Water Quality Analysis Simulation Progrram (WASP). (2019). https://www.epa.gov/ceam/water-quality-analysis-simulation-program-wasp

Welde, K. (2016). Identification and prioritization of subwatersheds for land and water management in Tekeze dam watershed, Northern Ethiopia. *International Soil and Water Conservation Research*, *4*(1), 30–38. https://doi.org/10.1016/j.iswcr.2016.02.006

Weldegebriel, Y., Chandravanshi, B. S., & Wondimu, T. (2012). Concentration levels of metals in vegetables grown in soils irrigated with river water in Addis Ababa, Ethiopia. *Ecotoxicology and Environmental Safety*, *77*(November), 57–63. https://doi.org/10.1016/j.ecoenv.2011.10.011

WILDCO. (2013). *A Comprehensive Guide to Wildco Water Bottle Samplers* (pp. 1–14). https://wildco.com/wp-content/uploads/2017/05/1200-G-Kemmerer.pdf

Willén, E. (2011). Cyanotoxin production in seven Ethiopian Rift Valley Lakes. *Inland Waters*, *1*(2), 81–91. https://doi.org/10.5268/iw-1.2.391

Williams, B. J. R., Asce, M., Asce, M., & Arnold, J. G. (1985). *Simulator for water resources in rural basins*. *I*(6), 970–986.

Williams, J. R. (1969). Flood Routing With Variable Travel Time or Variable Storage Coefficients. *Transactions of the ASAE*, *12*(1), 0100–0103. https://doi.org/10.13031/2013.38772

Wilson, E. H., Hurd, J. D., Civco, D. L., Prisloe, M. P., & Arnold, C. (2003). Development of a geospatial model to quantify, describe and map urban growth. *Remote Sensing of Environment*, *86*(3), 275–285. https://doi.org/10.1016/S0034-4257(03)00074-9

Winchell, M. F., Peranginangin, N., Srinivasan, R., & Chen, W. (2018). Soil and Water Assessment Tool model predictions of annual maximum pesticide concentrations in high vulnerability watersheds. *Integrated*

Environmental Assessment and Management, *14*(3), 358–368. https://doi.org/10.1002/ieam.2014

Wolde, A. M., Jemal, K., Woldearegay, G. M., & Tullu, K. D. (2020). Quality and safety of municipal drinking water in Addis Ababa City, Ethiopia. *Environmental Health and Preventive Medicine*, *25*(1), 1–6. https://doi.org/10.1186/s12199-020-00847-8

Wondie, A., Mengistu, S., Vijverberg, J., & Dejen, E. (2007). Seasonal variation in primary production of a large high altitude tropical lake (Lake Tana, Ethiopia): Effects of nutrient availability and water transparency. *Aquatic Ecology*, *41*(2), 195–207. https://doi.org/10.1007/s10452-007-9080-8

Wondim, Y. K. (2016). *Water Quality Status of Lake Tana , Ethiopia*. *c*, 39–51.

Wood, R. B., & Talling, J. F. (1988). Chemical and algal relationships in a salinity series of Ethiopian inland waters. *Hydrobiologia*, *158*(1), 29–67. https://doi.org/10.1007/BF00026266

Wool, T., Ambrose, R. B., Martin, J. L., & Comer, A. (2020). WASP 8: The next generation in the 50-year evolution of USEPA's water quality model. *Water (Switzerland)*, *12*(5), 1–33. https://doi.org/10.3390/W12051398

Wool, T., Ambrose, R., Martin, J., Comer, E. A., & Tech, T. (2006). Water quality analysis simulation program (WASP). *User's Manual*, *Version*, *6*. http://env1.kangwon.ac.kr/cyberclass/undergrad/wq/2008/models/wasp/wasp6/WASP6_Manual.pdf

Worako, A. W. (2015). Physicochemical and biological water quality assessment of lake hawassa for multiple designated water uses. *Journal of Urban and Environmental Engineering*, *9*(2), 146–157. https://doi.org/10.4090/juee.2015.v9n2.146157

Worku, & Giweta. (2018). Can We Imagine Pollution Free Rivers around Addis Ababa city, Ethiopia? What were the Wrong-Doings? What Action Should be Taken to Correct Them? *Journal of Pollution Effects & Control*, *06*(03). https://doi.org/10.4172/2375-4397.1000228

Worku, T., Khare, D., & Tripathi, S. K. (2017). Modeling runoff–sediment response to land use/land cover changes using integrated GIS and SWAT model in the Beressa watershed. *Environmental Earth Sciences*, *76*(16), 1–14. https://doi.org/10.1007/s12665-017-6883-3

Xie, H., & Lian, Y. (2013). Uncertainty-based evaluation and comparison of SWAT and HSPF applications to the Illinois River Basin. *Journal of Hydrology*, *481*, 119–131. https://doi.org/10.1016/j.jhydrol.2012.12.027

Xu, H. (2006). Modification of normalised difference water index (NDWI) to enhance open water features in remotely sensed imagery. *International Journal of Remote Sensing*, *27*(14), 3025–3033. https://doi.org/10.1080/01431160600589179

Xue, M., Tang, X., & Feng, N. (2016). An Extended VIKOR Method for Multiple Attribute Decision Analysis with Bidimensional Dual Hesitant Fuzzy Information. *Mathematical Problems in Engineering*, *2016*, 16. https://doi.org/10.1155/2016/4274690

Yang, Y. S., & Wang, L. (2010). A review of modelling tools for implementation of the EU water framework directive in handling diffuse water pollution. *Water Resources Management*, *24*(9), 1819–1843. https://doi.org/10.1007/s11269-009-9526-y

Yard, E., Bayleyegn, T., Abebe, A., Mekonnen, A., Murphy, M., Caldwell, K. L., Luce, R., Hunt, D. R., Tesfaye, K., Abate, M., Assefa, T., Abera, F., Habte, K., Chala, F., Lewis, L., & Kebede, A. (2015). Metals Exposures of Residents Living Near the Akaki River in Addis Ababa, Ethiopia: A Cross-Sectional Study. *Journal of Environmental and Public Health*, *2015*. https://doi.org/10.1155/2015/935297

Yepez, S., Laraque, A., Martinez, J. M., De Sa, J., Carrera, J. M., Castellanos, B., Gallay, M., & Lopez, J. L. (2018). Retrieval of suspended sediment concentrations using Landsat-8 OLI satellite images in the Orinoco River (Venezuela). *Comptes Rendus - Geoscience*, *350*(1–2), 20–30. https://doi.org/10.1016/j.crte.2017.08.004

Yilma, M., Kiflie, Z., Windsperger, A., & Gessese, N. (2019). Assessment and interpretation of river water quality in Little Akaki River using multivariate statistical techniques. *International Journal of Environmental Science and Technology*, *16*(7), 3707–3720. https://doi.org/10.1007/s13762-018-2000-8

Yimer, Y. A., & Jin, L. (2020). Impact of Lake Beseka on the Water Quality of Awash River, Ethiopia. *American Journal of Water Resources*, *8*(1), 21–30. https://doi.org/10.12691/ajwr-8-1-3

Yohannes, H., & Elias, E. (2017). Contamination of Rivers and Water Reservoirs in and Around Addis Ababa City and Actions to Combat It. *Environment Pollution and Climate Change*, *01*(02), 1–12. https://doi.org/10.4172/2753-458x.1000116

Yomo, M., Mourad, K. A., & Gnazou, M. D. T. (2019). Examining water security in the challenging environment in Togo, West Africa. *Water (Switzerland)*, *11*(2), 1–19. https://doi.org/10.3390/w11020231

Young, R. A., Onstad, C. A., Bosch, D. D., & Anderson, W. P. (1989). A nonpoint-source pollution model for evaluating agricultural watersheds. *Journal of Soil and Water Conservation*, *44*(December), 168–173.

Yuceer, M., & Coskun, M. A. (2016). Modeling water quality in rivers: A case study of Beylerderesi river in Turkey. *Applied Ecology and Environmental Research*, *14*(1), 383–395. https://doi.org/10.15666/aeer/1401_383395

Zegeye, M. K., Bekitie, K. T., & Hailu, D. N. (2022). Spatio-temporal variability and trends of hydroclimatic variables at Zarima Sub-Basin North Western Ethiopia. *Environmental Systems Research*, *11*(1). https://doi.org/10.1186/s40068-022-00273-5

Zerihun, F., & Eshetu, B. (2018). Physicochemical Characterization of Upper Awash River of Ethiopia Polluted by Anmol Product Paper Factory. *International Journal of Water and Wastewater Treatment*, *4*(2). https://doi.org/10.16966/2381-5299.154

Zewde, T. W., Johansen, J. A., Kifle, D., Demissie, T. B., Hansen, J. H., & Tadesse, Z. (2018). Concentrations of microcystins in the muscle and liver tissues of fish species from Koka reservoir, Ethiopia: A potential threat to public health. *Toxicon*, *153*(March), 85–95. https://doi.org/10.1016/j.toxicon.2018.08.013

Zhang, L., Jin, X., He, C., Zhang, B., & Zhang, X. (2016). *Comparison of SWAT and DLBRM for Hydrological Modeling of a Mountainous Watershed in Arid Northwest China*. 1–11. https://doi.org/10.1061/(ASCE)HE.1943-5584.0001313.

Zhang, Y., Loiselle, S., Shi, K., Han, T., Zhang, M., Hu, M., Jing, Y., Lai, L., & Zhan, P. (2021). Wind effects for floating algae dynamics in eutrophic lakes. *Remote Sensing*, *13*(4), 1–11. https://doi.org/10.3390/rs13040800

Zhao, J. (2020). Remote Sensing Evaluation of Total Suspended Solids Dynamic with Markov Model : A Case Study of Inland Reservoir across Administrative Boundary in South China. *Sensor*, *20*, 6991. https://doi.org/10.3390/s20236911

Zheng, Y., Han, F., Tian, Y., Wu, B., & Lin, Z. (2014). Addressing the uncertainty in modeling watershed nonpoint source pollution. In *Developments in Environmental Modelling* (1st ed., Vol. 26). © 2014 Elsevier B.V. All rights reserved. https://doi.org/10.1016/B978-0-444-63249-4.00006-3

Zinabu, E., Kelderman, P., Kwast, J. Van Der, & Irvine, K. (2019). *Monitoring river water and sediments within a changing Ethiopian catchment to support sustainable development.*

Zinabu, E., Kelderman, P., van der Kwast, J., & Irvine, K. (2019). Monitoring river water and sediments within a changing Ethiopian catchment to support sustainable development. *Environmental Monitoring and Assessment*, *191*(7). https://doi.org/10.1007/s10661-019-7545-6

Zinabu, Kebede, E., & Desta, Z. (2002). Long-term changes in chemical features of waters of seven Ethiopian rift-valley lakes. *Hydrobiologia*, *477*(1998), 81–91. https://doi.org/10.1023/A:1021061015788

APPENDIX

Appendix A

Appendix A Table 2 The surface water quality investigations with temporal resolution

No of samples	Waterbody	Frequency									
		Random/unknown	Daily	Weekly	Biweekly	Monthly	Quarterly	Seasonally		Yearly	Remark
								Dry	Wet		
1-5	Lake	-	-	-	-	-	-	(Masresha et al., 2011)	(Masresha et al., 2011)	-	(Bedada et al., 2019)[h]
	River	-	-	-	-	-	-	(Jebessa and Bekele, 2018), (Masresha et al., 2011), (Prabu et al., 2011)[5], (Maschal and Zomaneh, 2018)[5], (Kassegne et al., 2018)[5]	(Masresha et al., 2011), (Prabu et al., 2011)[5], (Kassegne et al., 2018)[5]	-	
5-10	Lake	(Teklay and Amare, 2015)[5]	-	-	-	-	-	-	-	-	
	River	-	-	-	(Akalu et al., 2011)	-	-	(Tadesse et al., 2018)[6]	-	-	
10-15	Lake	-	-	-	-	(Degefu et al., 2011) [1]	-	(Haile and Mohammed, 2019)[3], (Gebreyohannes et al., 2015)[6],	-	-	
	River	(Olbasa, 2017),	-	-	-	-	(Degefu et al., 2013)[4]	(Mulu et al., 2013)[*], (Feyissa and Bekele, 2018)[*], (Haile and Mohammed, 2019)		-	
15-20	Lake	-	-	-	-	-	-	-	-	-	
	River	-	-	-	-	-	-	(Keraga et al., 2017a) [8] (Eliku and Leta, 2018), (B.Abate et al., 2015)[6]	(Keraga et al., 2017a) [1] (Eliku and Leta, 2018)	-	
20-25	Lake	-	-	-	-	(Abhachire, 2014)[1]	-			-	(Itanna, 2002)[9]

[8] Twice in each season, [3] – two years, [4] - for one year, [5]- only one time, [6] – Monthly, [7]- from spring and reservoir, [*] - biweekly for two months,

	River	-	-	-	-	(Abhachire, 2014)[1]	-	(Melaku et al., 2007), (Kassegne et al., 2018)[5]	(Kassegne et al., 2018)[5]	-	
> 25	Lake	-	-	-	-	(Tesfay, 2007)[4]	-	-	-	(Cherne t et al., 2001)[3]	(Eskinder, 2019)[8]
	River	(Niguse et al., 2018)	-	-	-	(Keraga et al., 2017b)[9], (Tesfay, 2007)[4] (Dirbaba et al., 2018)[10], (Yimer and Jin 2020)[2]	-	(Adugna et al., 2019)[3], (B.Abate et al., 2015)[6], (Bedada et al., 2019) , (Haddis et al.,2014)[3], (Awoke et al., 2016), (B.Abate et al., 2015)	(Adugna et al., 2019)[3], (Eskinder, 2019), (Awoke et al., 2016), (Eskinder, 2019)[1]	-	
No data	Lake	(Dinka, 2017)[5], (Tafesse et al., 2015)	-	-	-	-	-	(Dsikowitzky et al., 2013), (Mesfin et al., 1988)	-	-	(Awol, 2018)[7],
	River	(Tamiru, 2001) (Amde et al., 2016)[5], (Tafesse et al., 2015)	-	-	-	-	-	(Tadesse et al., 2018),	-	-	

[9] Greater than 10 years, [8] – bimonthly, wet season & industrial, [9] – from vegetables, soil river, [10] – only for one month, [f] – flow in rainy time [h] - Hospital

Appendix A Table3 Summary of major surface water quality studies in different parts of Ethio

Study area/site	Studied surface water quality indicators	Value	Referen
Hawassa Textile Industry	Tem (°C)	17.80-25.75	(Tafesse e al., 2015)
	pH	8.080-11.21	
	EC (µs/cm)	31.01-46.30	
	TDS (mg/l)	277.0-900.4*	
	TSS (mg/l)	90.50-147.0 *	
	BOD (mg/l)	93.00-188.0 *	
	COD (mg/l)	189.6-264.0 *	
Southern eastern part of Ethiopia, Anderacha district, Sheka Zone	Tem (°C)	19.10-24.94 [b]	(Awol, 20
	pH	7.24-8.07	
	EC (µs/cm)	112.36-1626.67	
	TH CaCO3 (mg/l)	393-522*	
	Nitrate (mg/l)	Not detectable - 0.96	
	Nitrite (mg/l)	Not detectable - 0.51	
	Ammonia (mg/l)	0.03-0.84	
	Phosphate (mg/l)	1.32-3.20[b]	
	Chloride (mg/l)	2.13-36.16	
	Carbonate (mg/l)	not detectable	
Lake Hawassa	PH	5.85 to 9.21	(Haile and Mohamme 2019)
	Tem (°C)	20.56 to 28.30	
	DO (mg/l)	4.76 to 8.59	
	TDS (mg/l)	928.3	
	EC (µS/cm)	741.7 to 1956.0	
	turbidity (NTUs)	8.37 to 177.0	
	F^- (mg/l)	15.3[b]	
	nitrate (mg/l)	2.83 to 6.79	
	sulfate (mg/l)	8.4 to 18.5	
	phosphate (mg/l)	0.3 to 1.9[b]	
	fluoride (mg/l)	11.8 to 17.3	
	BOD5 (mg/l)	63.4 to 168.2[b]	
	TH CaCO3 (mg/l)	52.6 to 72.6	
	Alkalinity CaCO3 (mg/l)	10.0 to 19.3	
Lake Hawassa	Tem (°C)	21.23	(B.Abate et 2015), (Worako, 2015)
	pH	7.54	
	DO (mg/l)	17.85	
	TDS (mg/l)	450.1	
	turbidity (NTU)	8.44	
	COD (mg/l)	48.73	
	BOD_5 (mg/l)	117	
	F^- (mg/l)	12.8	
	$NO3^-$ (mg/l)	5.27	
	PO_4^{3-} (mg/l)	1.12	
	NO^{2-} (mg/l)	0.04	
	TN (mg/l)	5.42	
	TP (mg/l)	0.37	

	Cl^- (mg/l)	30.84	
	Chl-a (µg/l)	25.45[10]	
Lake Gudera / Wetland, West Gojjam Zone	Temp (^{0}C)	(21.89, 19.58)[d]	(Brehan, 2017)
	pH	(8.38, 8.17)[d]	
	EC (µS/cm)	(88, 81.5)[d]	
	DO (mg/l)	(7.16, 8.34)[d]	
	TDS (mg/l)	(38.02, 61)[d]	
	salinity	(0.04, 0.04)[d]	
	alkalinity (mg/l)	(72.5, 79)[d]	
	Phosphate (mg/l)	(0.18, 0.17)[d]	
	Ammonia (mg/l)	(0.18, 0.055)[d]	
	Nitrite (mg/l)	(0.018, 0.0216)[d]	
	Nitrate (mg/l)	(1.054,0.665)[d]	
	TH (mg/l)	(56, 45)[d]	
	Sulphate (mg/l)	(13,16.5)[d]	
	turbidity (mg/l)	(54,59)[d]	
Lake Haiq	Tem (°C)	(26.46 ± 2.34)	(Teklay and Amare, 2015)
	pH	(8.83 ± 0.07)[b]	
	turbidity (NTU)	1.26 ± 0.04 924.50 to 66.10±1.84[b]	
	EC (µS/cm)	(2,500 and 10,000)	
	TDS (mg/l)	(458.00 ± 14.14 to 463.00 ± 5.66)	
	Alkalinity (mg/l)	(349.53 ± 4.06 to 627.57 ± 8.15)[b]	
	Chloride (mg/l)	(44.86 ± 1.47 to 49.14 ± 0.72)	
	NH_3 (mg/l)	(0.14 ± 0.02 to 1.35 ± 0.21)	
	NO_3 (mg/l)	(0.04 ± 0.01 to 0.29 ± 0.01)	
	SO_4 (mg/l)	(2.18 ± 0.25 to 5.20 ± 0.85)	
Huluka River, Ambo Area	Tem (^{0}C)	22.4-23 (16.2-17.8)[11]	(Prabu et al., 2011)
	pH	7.91-8.18 (7.42-8.03)[3]	
	EC (µS/cm)	175.1-588.4 (140.2-540.7)[3]	
	TDS (mg/l)	113.8-382.5 (91.1-351.5)[3]	
	$CaCo_3$ (mg/l)	48-91 (38-88)[3]	
	Cl^- (mg/l	18.5-60.8 (13.250.3)[3]	
	Nitrate (mg/l)	0.88-2.8 (1.2-3.5)[3]	
	DO (mg/l)	3.5-6.4 (4.1-7.8)[3b]	
	Phosphate (mg/l)	0.28-1.58 (0.31-1.88)[3e]	
	Sulphate (mg/l)	22.4-40.1 (24.1-48.9)[3]	
Alaltu River, Ambo Area	Tem(^{0}C)	22.5-231 (17.5-18.1)[3]	
	pH	7.26-8.27 (7.01-8.12)[3]	
	EC (µS/cm)	497-788.4 (398.2-712.6)[3]	
	TDS (mg/l)	323.1-512.5 (258.8-463.2)[3]	
	$CaCo_3$ (mg/l)	78-140 (58-121)[3]	
	Cl^- (mg/l)	27.5-73.5 (21.5-65.3)[3]	
	Nitrate (mg/l)	0.95-3.1 (1.22-3.88)[3]	
	DO (mg/l)	3.85-5.55 (4.9-6.2)[3]	

[10] - trophic level is on average hyper eutrophic
[11] Wet season

	Phosphate (mg/l)	0.43-1.75 (0.55-1.9)[3e]	
	Sulphate (mg/l)	28.1-55.9 (32.1-58.9)[3]	
Awetu-Kito Rivers in Jimma	pH	6.57	(Haddis et al.,2014)
	DO (mg/l)	7.4 - 0.8*	
	BOD5 (mg/l)	330 – 480*	
	NO3-N (mg/l)	1.5 - 7	
	NO2-N (mg/l)	0.21	
	PO4 (mg/l)	1*	
	EC (µS/cm)	80-400	
	TDS (mg/l)	120-800	
	chloride (mg/l)	5.5 - 51	
Rebu River in Oromia region	Tem (^{0}C)	22.5[c]	(Tadesse et al., 2018)
	pH	10.5[c]	
	EC (µS/cm)	1592.6 [c]	
	TDS (mg/l)	2359.5[c]	
	Turbidity (NTU)	800[c]	
	Salinity	2440[c]	
	NO_3^- (mg/l)	324.5[c]	
	PO_4^{3-} (mg/l)	163.3[c]	
	NO_2^- (mg/l)	0.58	
	SO_4^{2-} (mg/l)	96	
	NH_3 (mg/l)	15.8[c]	
Elala River, Mekelle, Tigray	EC (µS/cm)	904.11 to 2156.11[b]	(Gebreyohannes et al., 2015)
	Turbidity (NTU)	21.07 to 34.99[b]	
	TDS (mg/l)	700.22 to 1328.22[b]	
	T. alkalinity (mg/l)	131.85 to 267.26[b]	
	TH (mg/l)	198.67 to 478.67[b]	
	chloride (mg/l)	47.32 to 259.43[b]	
	COD (mg/l)	16.02 to 32.53[b]	
	SO_4 (mg/l)	271.82 to 384.07[b]	
	NO_3_N (mg/l)	6.82 to 62.38[b]	
	PO_4 (mg/l)	0.03 to 0.14[b]	
	TP (mg/l)	0.04 to 0.19[b]	
River Gudar, Oromia region	Alkalinity (mg/l)	154±15.556	(Olbasa, 2017)
	pH	8.44	
	EC (µS/cm)	316.47 ± 72.802	
	Turbidity (NTU)	1.23-4.25	
	TDS (mg/l)	149.37 ± 20.64	
	NO_3 (mg/l)	5.23-7.55	
	NH_4 (mg/l)	41.00 ± 1.19	
	SO_4 (mg/l)	35.03-97.05	
	PO_4 (mg/l)	3.50 ± 0.32	
	TSS (mg/l)	121.80-130.00	
	Chloride (mg/l)	3.72-5.32	
	Carbonate (mg/l)	2.65-4.70	
	Bicarbonate (mg/l)	117.66-138.74	
	TH CaCO3 (mg/l)	156.87 ± 8.46	

Blue Nile, Omo-Gibe, Tekeze, and Awash river basins[12]	TN (mg/L)	7.3, 20.3, 2.6, 1.5 (< 0.3 concern level)	(Aymer et al., 2016)
	TP (mg/L)	0.4, 0.3, 0.9, 0.2 (< 0.015 concern level)	
	DO (mg/L)	6.2, 6.1, 6.8, 6.8 (> 7 concern level)	
	BOD5 (mg/L)	12.2, 2.7, 6.9, 13.3 (< 3 concern level)	
	pH	7.4, 7.2, 7.8, 7.6 (6.5 – 9 concern level)	
	EC (µS/cm)	122, 117, 192, 560	
Blue Nile, Omo-Gibe, Tekeze, and Awash river basins[13]	TN (mg/L)	11.1, 17, 30.8, 3.1 (< 0.3 concern level)	
	TP (mg/L)	1, 0.2, 12.5, 2 (< 0.015 concern level)	
	DO (mg/L)	4.9, 5.7, 2.6, 4.9 (> 7 concern level)	
	BOD5 (mg/L)	18.4, 108, 508, 29 (< 3 concern level)	
	pH	7.2, 7.3, 7.2, 6.3 (6.5 – 9 concern level)	
	EC (µS/cm)	92, 140, 580, 514	
Blue Nile and Omo-Gibe river basins[14]	TN (mg/L)	9.3, 22 (< 0.3 concern level)	
	TP (mg/L)	1.3, 0.3 (< 0.015 concern level)	
	DO (mg/L)	5.9, 4.7 (> 7 concern level)	
	BOD5 (mg/L)	17.6, 64 (< 3 concern level)	
	pH	7.1, 6.8 (6.5 – 9 concern level)	
	EC (µS/cm)	95, 101	

b - exceed WHO standard; # - exceed FAO standard; * - exceed Ethiopian EPA standard; c - exceed EDWQ (2010); *d* - exceed USEPA 2015 freshwater bodies
e - exceed (EC) European community standard, *a* - exceeds EEPA and UNIDO slaughterhouse effluent discharge limit, *f*- Australia-New Zealand (ANZE 2000)

[12] Agriculture impacted river basins (the value is in their respected order)
[13] Urban impacted river basins (the value is in their respected order)
[14] Coffee impacted river basins (the value is in their respected order)

Appendix B

Appendix B Table 1 Summary of surface water quality studies in different parts of Awash Basin

Study area/site	Parameters analyzed/results		Remark	Reference
Awash in late, koka reservoir, Awash out late	Tem (°C)	19.1 to 23.6	highest during dry season and the lowest during wet season, no significant spatial variation	(Eliku and Leta, 2018)
	pH	6.08 to 8.47	highest during dry season and the lowest during dry season, significant variation in mean among the sampling sites	
	turbidity (NTU)	29.27 to 159.51	highest during wet season and the lowest during dry season, significant spatial and seasonal variation	
	EC (µS/cm)	261.7–742.62		
	NO3-N (mg/l)	0.28 to 28.8	highest during dry season and the lowest during wet season, significant spatial variation	
	NO2-N (mg/l)	0.06 to 0.92	highest during dry season and the lowest during wet season	
	NH4-N (mg/l)	0.11 and 1.47	highest during dry season and the lowest during wet season	
	TN (mg/l)	0.82 to 84.53	highest during dry season and the lowest during wet season	
	TP (mg/l)	0.02 to 0.31	no a significant spatial and seasonal variation	
	DO (mg/l)	3.02 to 13.51	higher in wet season than in dry season	
	BOD (mg/l)	13.69 to 83.37	significant spatial variation; no significant seasonal variation	
	COD (mg/l)	16.13 to 150.38	the mean is a significant spatial variation but no seasonal variation	
Tinishu Akaki River, Addis Ababa	Tem °C	12.4 to 22.1	above the maximum permissible limit of CCME guidelines	(Melaku et al., 2007)
	pH	7.1 to 8.9	within the limit of the CCME guidelines	
	EC (µS/cm)	56 to1268	within permissible limits of the WHO	
	TDS (mg/l)	0 to 639	negligible temporal and considerable spatial variations, marked increase from upstream to downstream	
	DO (mg/l)	0.1 to 6.7	decreasing in downstream of the river	
	COD (mg/l)	4.0 to 533	spatially varied along the river course	
	BOD5 (mg/l)	2.7 to 204.5	decreasing in downstream of the river	
	HCO_3^- (mg/l)	48 to 168	exceeded common natural concentrations world rivers by 9.2	
	SO_4^{2-} (mg/l)	4.8 to 70.8	exceeded common natural concentrations world rivers by 6.8	
	NO_3^- (mg/l)	1.7 to 9.2	exceeded common natural concentrations world rivers by 19	
	NO_2^- (mg/l)	0.1 to 1.2	decreasing in downstream of the river	

	PO_4^{3-} (mg/l)	0.04 to 15	exceeded common natural concentrations world rivers by 390/ decreasing in downstream of the river	
	Cl^- (mg/l)	3.9 to 193	exceeded common natural concentrations world rivers by 27.2	
	NH_3 (mg/l)	0.4 to 35	decreasing in downstream of the river	
Shegole, Tinishu Akaki and Jemo rivers, Addis Ababa …(Dry season)	DO (mg/l)	(0.18, 3.16, 2.49)		(Adugna et al., 2019)
	pH	(7.76, 7.94, 8.01)		
	PO_4–P (mg/l)	(45.55, 20.97, 41.46) [a,e,d,f]		
	NO_3–N (mg/l)	(2.39, 1.31, 1.46) [a,e,d,f]		
	NO2–N (mg/l)	(0.9, 2.74, 2.62) [a,e,d,f]		
	NH4–N (mg/l)	(2.56, 2.24, 3.16) [a,e,d,f]		
	Turbidity (NTU)	(239, 35, 54)		
Shegole, Little Akaki and Jemo rivers, Addis Ababa …(Wet season)	DO (mg/l)	(5.43, 7.29, 5.16) [a,e,d,f]		
	pH	(8.18, 8.27, 8.47)		
	PO_4–P (mg/l)	(14.77, 8.92, 16.55) [a,e,d,f]		
	NO_3–N (mg/l)	(1.88, 2.05, 2.36)		
	NO2–N (mg/l)	(5.37, 10.26, 11) [a,e,d,f]		
	NH4–N (mg/l)	(0.97, 0.75, 1.76)		
	Turbidity (NTU)	(376, 661, 302)		
Shankela River, Addis Ababa	Turbidity (NTU)	83.14 [b]*		(Maschal and Zomaneh, 2018)
	TSS (mg/l)	142.2 [b]*		
	COD (mg/l)	81.6 [b]*		
	BOD (mg/l)	91.52 [b]*		
	NO_3^- (mg/l)	0.34		
	NH_3 (mg/l)	18 [b]*		
	NO_2^- (mg/l)	0.38 [b]*		
	PO_4^{-3} (mg/l)	19.44 [b]*		
(Kera, Luna)[15] slaughter houses	pH	(7.30, 6.81)		(Mulu et al., 2013)
	Tem (°C)	(26.55; 22.09)		
	EC (µs/cm)	(1614.6; 3850) [a]		
	turbidity (NTU)	(566.66 160.33) [a]		
	TS (mg/l)	(7885.3; 1176) [a]		
	TSS (mg/l)	(3835.3; 125.66) [a]		
	TP (mg/l)	(202; 61.7) [a]		

[15] Their value is in their respected order

	PO_4^{-3} (gm/l)	(67.3; 28.3) [a]		
	Nitrite (gm/l)	(1513.3; 49.33) [a]		
	Nitrate (mg/l)	(1450 ; 13.7) [a]		
	Ammonia (mg/l)	(103.3; 345.7) [a]		
	Sulfate (mg/l)	(693.3; 31.3) [a]		
	Sulfide (mg/l)	(1.83; 0.14) [a]		
	DO (mg/l)	(3.75; 0.97) [a]		
	COD (mg/l)	(11546.7; 431.7) [a]		
	BOD5 (mg/l)	(3980; 177.3) [a]		
(Mojo and Akaki)[4] River	pH	(6.91 - 7.46); (6.84 - 7.47)		(Mulu et al., 2013)
	Tem (°C)	(21.50 - 22.45);(23.71 23.20)		
	EC (µs/cm)	(1564.66-2930);(1235.33-1290.33)		
	Turbidity (NTU)	(134.66-416.66);(350-483.33)		
	TS (mg/l)	(932-2331.33); (725.33-1248.66)		
	TSS (mg/l)	(154-886); (304.33-456)		
	TP (mg/l)	(0.85-46.13);(20.50-75.33)		
	PO_4^{-3} (mg/l)	(0.46-28); (9.6-16.70)		
	Nitrite (mg/l)	(220-26.66);(153.33- 597.0)		
	Nitrate (mg/l)	(6.26-42.66);(140-140.33)		
	Ammonia gm/l	(10.66-212.33);(41.25-47.91)		
	Sulfate (mg/l)	(22.660-103.33); (52-61.33)		
	Sulfide (mg/l)	(0.11-0.2); (0.37-0.38)		
	DO (mg/l)	(3.75; 0.97)		
	COD (mg/l)	(295-1080);(260-1373.33)		
	BOD5 (mg/l)	(84-265.67); (95.66-555.33)		
Anmol Paper Factory, Ginchi area	BOD5 (mg/L)	470-2499.3[b]*		(Feyissa and Bekele, 2018)
	COD (mg/L)	2969 - 5848.6[b]*		
	TP(mg/L)	0.37 - 0.42[b]		
	TN (mg/L)	7.79 - 20[b]		
	Turbidity (NTU)	118.28 - 499.32[b]*		

	TS (mg/L)	1512 - 3432[b]		
	TDS (mg/L)	1032 - 3134[b]*		
	TSS (mg/L)	298 - 726[b]*		
	EC (µS/cm)	1576 - 4720[b]*		
	PH	3.23 – 10.66[b]*		
	T. Hardness (mg/L)	49.5 - 3335		
	Alkalinity (mg/L)	ND – 2000		
	CO3 2- (mg/L)	ND _ 281		
	HCO3- (mg/L)	ND - 2440		
	Chloride (mg/L)	186.22 - 3818.7[b]*		
	Sulphate (mg/L)	26.7 - 282.32		

The table considers the physico-chemical and nutrients. b - exceed WHO standard; # - exceed FAO standard; * - exceed Ethiopian EPA standard; c - exceed EDWQ (2010); *d* - exceed USEPA 2015 freshwater bodies, e - exceed (EC) European community standard, *a* - exceeds EEPA and UNIDO slaughterhouse effluent discharge limit, *f*- Australia-New Zealand (ANZE 2000).

Appendix B Table 2 Summary of major water quality studies from different parts of Ethiopia

Study area/site	Studied water quality indicators		Reference
Leyole river, Kombolcha	Sediments (mg/kg)	maximum 740[l]	(Zinabu et al., 2019)
	Cr (µg/l)	Median 2660, max 36,600 (mg/kg) [l]	
	Cu (µg/l)	median 63[l]	
	Zn (µg/l)	median 521[l]	
	Pb (mg/kg)	maximum 3640	
Lake Hawassa	Fe (mg/l)	0.12 to 0.75[a]	(Haile & Mohammed, 2019)
	Mg (mg/l)	19.8 to 32.2 [b]	
	K (mg/l)	32.2 to 84.3[a]	
	Cr (mg/l)	0.17 to 0.58[a]	
	Cu (mg/l)	0.03 to 0.07[a]	
	Zn (mg/l)	0.2 to 7.4[a]	
	Mn (mg/l)	0.13 to 1.8[a]	
	Pb and Cd	Below detection limit (BDL)	
Rebu River in Oromia region	Fe (mg/l)	2.02[ac]	(Tadesse et al., 2018)
	Pb (mg/l)	0.16[ac]	
	Na (mg/l)	1557.6 [ac]	
	K (mg/l)	22.3 [ac]	
	Cu (mg/l)	0.08[j]	
	Fe (mg/l)	2.02 [ac]	
	Zn (mg/l)	0.21 [ac]	
	Mn (mg/l)	0.23 [ac]	
Lake Hawassa	Mn (mg/l)	0.489[d]	(Abate and Fitamo 2015) (Worako, 2015)
	Zn(mg/l)	0.317[d]	
	Cu(mg/l)	0.046[d]	
	Fe(mg/l)	0.18[d]	
	Cr, Cd, Ni & Pb	non-detectable	
	Na^{+} (mg/l)	300.95 to 414.11[e]	
	Ca (mg/l)	2.34 to 2.92[f]	
	Mg (mg/l)	24.25–31.92[f]	
	K^{++} (mg/l)	70.54 to 85.04[e]	
	Total Coliform	11,883MPN/100ml[g]	
	Fecal Coliform	99.67MPN/100ml [h]	
Lake Haiq	Pb (mg/l)	0.064±0.008 to 0.108±0.001[a]	(Teklay & Amare, 2015)
	Cd (mg/l)	BDL	
	Cu (mg/l)	0.260 ±0.072 to 1.940±0.398 [k]	
	Zn (mg/l)	0.150 ±0.002 to 0.160 ± 0.002[k]	
Southern eastern part of Ethiopia, Anderacha district, Sheka Zone	Ca (mg/l)	4.53-10.49[i]	(Awol, 2018)
	Cd (mg/l)	0.0068-0.0349[i]	
	Cu (mg/l)	0.11-0.70 [a]	
	Zn (mg/l)	0.28-1.16[i]	

	Mn (mg/l)	0.10-0.73 [a]	
	Fe (mg/l)	0.4-1.7 [a]	
	Mg (mg/l)	2.45-9.45[i]	
	Cr (mg/l)	BDL	
	Ni (mg/l)	BDL	
	Pb (mg/l)	BDL	

[a]-above WHO standard (2008); [b]- within WHO and FAO standard except one sampling site; [c]- above the EDWQ (2010); [d]- Within acceptable limit of USEPA (1998); WHO (1993 and 1998) guideline; [e]- above permissible limit of WHO (1984); [f]- below the permissible limit of WHO (1984); [g]- above acceptable limit of WHO (1983) and CCME (1999) standards; [h]- above acceptable limit of USEPA (1976) guideline; [i]- below the WHO standards (2008); [j]- within the EDWQ (2010) and WHO (2008) standards; [k]-within WHO standard, [l]- above WHO (2011) Guidelines

Appendix B Table 3 Some surface water quality studies in different parts of the Awash Basin

Study area/site	Parameters analyzed/results		Status/standard	Reference
Tinishu and Tiliku Akaki River, Addis Ababa[16]	Cd (mg/L)	0.009±0.003; 0.0076±0.01	In potato surpassed naturally expected levels	(G. Gebre, 2009)
	Cr (mg/L)	0.029±0.03; 0.09±0.05	In potato and onion surpassed naturally expected levels	
	Cu (mg/L)	0.028±0.05; 0.069±0.12	In potato surpassed naturally expected levels	
	Co (mg/L)	0.048±0.03; 0.067±0.05	Poorly to badly polluted water, STN[17] Classification (1998)	
	E.Coli (CFU 100ml/1)	$6.68*10^9$; $6.61*10^9$	Very badly polluted water, STN Classification (1998)	
Tinishu Akaki River/TAR, Addis Ababa	Ca^{2+} (mg/L)	19 to 67	concentrations exceeded their most common natural concentrations in world rivers by a factor of 6.3 and 7.6 respectively	(Melaku et al., 2007)
	Mg^{2+}(mg/L)	3.4 to 36		
Akaki River catchment and Aba Samuel reservoir[18]	Mn (mg/kg)	464; 701.4; 787.4 - 1089.1	decreasing order of trace metal concentrations in the dry season: Mn > Fe > Pb > Cr > Zn > Ni > Cu > Cd and in the rainy season: Mn > Fe > Pb > Cr > Ni > Zn > Cu > Cd	(Kassegne et al., 2018)
	Fe (mg/kg)	469.3; 612.7; 508.3 - 30,475.2		
	Pb (mg/kg)	136.8; 137.7; 45.4 - 183.9		
	Cr (mg/kg)	25; 24.5; 28.9 - 262.1		
	Zn (mg/kg)	10; 21.8; 23.9 - 108.6		
	Ni (mg/kg)	20.6; 19.8; 21 - 31.2		
	Cu (mg/kg)	4.5; 4.2; 6.4 – 32.0		
	Cd (mg/kg)	2.6; 2.6; 0.2 - 2.6		
Awash in late, koka reservoir, Awash out late	Fe (mg/l)	1.85 to 3.87 #		(Eliku & Leta, 2018)
	Zn (mg/l)	0.47 to 2.95*		
	Cu (mg/l)	0.82 to 1.69 *		
	Pb (mg/l)	0.41–1.36 *		

[16] Level of metals in potato, cabbage and onion
[17] Slovak Technical Standard
[18] Heavy metal values are in the order of Abasamuel lake, big Akaki and Tinishu Akaki

	Cr (mg/l)	0.36–1.16 *		
	Cd (mg/l)	0.18 to 0.29*		
	Ni (mg/l)	0.02–0.2 *		
Awash River[19]	Pb (mg/l)	1.25 – 4 ^{e}		(Amare et al., 2017)
	Ca^{2+} (mg/l)	98.9 – 163$^{@}$		
	Zn (mg/l)	0.03 - 0.07$^{@}$		
	Cr (mg/l)	0.02 – 0.03$^{@}$		
	Mg^{2+} (mg/l)	78.6 - 50.9 ^{e}		
	K^{+} (mg/l)	4.02 - 8.17 ^{e}		
	Fe (mg/l)	1.15 – 2.55 ^{e}		
	Cu (mg/l)	6 – 15.2$^{♦}$		
	Mn (mg/l)	0.17 – 0.75$^{♦}$		

The table considers metals; $^{\#}$- highest concentration during wet season; *- highest concentration during dry season; $^{@}$-Within FAO (IWQG) and meet the WHO DWQG; $^{♦}$- failed to meet the WHO DWQG and FAO (IWQG); ^{e}- failed to meet the WHO DWQG

[19] Mean values of water quality parameters in the four sites of upper basin (Awash river after Lake Koka, Awash river at Koka Dam, Awash river before Lake Koka and Awash river at Awash Melka Kuntire). TNTC (Too numerous to count)

Appendix C

Appendix C Table 1 LULC change from 2003 to 2023

Sub-watershed ID	2023								2003							
	Bare land	**Built-up area**	**Crop land**	**Forest**	**Grass land**	**Shrub land**	**Water body**	**Wetland**	**Bare land**	**Built-up area**	**Crop land**	**Forest**	**Grass land**	**Shrub land**	**Water body**	**Wetland**
WS01		337.9	25208.8	2988.4	18.9	3457.1				211.8	8409.6	3067.6	557.9	19746.9		
WS02		123.7	10229.9	356.7	97.4	2262.2					759.8	310.8	1342.3	10649.6		
WS03	6.4	5173.1	663.2	2034.9	24.5	2247.4	1.8			6154.8	2.9	2495.6	264.2	1223.9		
WS04	45.7	9160.8	38163.8	2907.4	137.0	17245.9	508.1		3.6	3672.2	211733.0	5469.3	1730.7	35059.9	468.1	
WS05	9.4	426.1	29761.5	654.3	368.8	5388.1				72.5	9250.9	113.4	3693.8	23459.0		
WS06	14.3	100.5	16333.8	142.1	92.5	1822.0	0.1				8298.7	3.5	401.4	9792.4		
WS07		42.4	26407.3		10.2	1051.1	0.0		0.1		13243.9	30.2	163.9	14070.5		
WS08		96.5	15128.8			108.1				33.9	11678.5		34.0	3579.9		6.0
WS09	32.8	1446.1	33109.2	4036.7	6.8	8625.2	2.7			85.2	5850.0	5358.8	1739.4	34214.6		0.5
WS10	22.6	199.4	12051.0			1430.2		1.8			9165.4	97.8	78.3	4359.1		
WS11	28.8	3262.7	10148.8			3250.6	2.1	49.7		824.8	12378.0	617.0	127.1	2162.0		632.7
WS12	14.8	15486.1	11674.2	2678.1	21.7	9481.8	142.6	83.9	0.2	11155.4	4860.9	4839.7	1355.8	16507.4	112.0	740.0
WS13	1.0	127.6	25242.5			2960.3	93.4	37.9	0.4		13453.7	10.1	45.1	14740.2	106.1	85.2
WS14		26.9	15218.0	7.2		418.1	1.3				10750.4		4.7	4915.3		
WS15		117.7	16434.1			3756.7					2898.2	481.8	838.6	16081.5		
WS16		368.7	10960.8	9.5		1668.5	59.1			34.5	4769.5	167.9	1.8	8082.3		9.6
WS17	1.5	473.8	25289.4	581.6		4125.7	330.9	38.8	0.3	181.3	16827.3	917.8	77.3	12424.1	405.3	1.6
WS18	2.8	2604.0	9885.2	546.0		3249.0	367.0	8.9	1.2	1625.2	4991.8	1118.4	99.2	8212.5	401.0	212.5
WS19		1584.3	24573.6	567.4		3372.3	6.8	8.7		97.0	16034.0	1572.2	41.4	12311.5		54.9
WS20		37.1	12563.7			1043.1	0.1				5335.0		23.7	8282.6		
WS21		45.1	20259.3			1560.7	5.4				7576.9	862.4	561.9	12867.8		
WS22		206.6	28712.4	0.2		2743.2	0.1			69.2	11881.6	26.2	958.7	18720.3		
WS23	2.9	114.2	20308.2			4798.4	15.6		4.8		11494.3	2389.7	23.4	11325.5		

WS24	10.6	107.0	8834.7	6.0		877.6			0.5		2606.3	167.9	0.6	7059.8		
WS25	5.1	101.6	13628.3	101.8		1281.8	0.3		10.9		3292.7	78.8	75.3	11648.2		
WS26	0.7	132.8	27689.6	29.3		3073.3	0.3	7.5	0.1		8466.4	216.4	2503.6	19744.9		
WS27		34.2	21229.3	38.3		3087.0	51.9	76.3			14591.1	308.1	211.7	8819.8		584.7
WS28		954.5	27767.6	791.4		4290.5	2.5		3.2	0.2	22126.0	1489.6	198.4	9986.7		
WS29	6.3	191.0	16940.0	93.2	11.6	6878.8			0.1		842.2	371.8	2096.7	20803.0		
WS30		386.4	56690.3	691.8	14.5	7879.2	0.9		0.7	184.5	22731.6	984.1	3069.0	38670.6		
WS31	27.3	82.5	21572.6	25.2	4.5	6744.0	20.2		12.9	7.2	2844.1	1223.4	639.4	23740.2		
WS32	198.6	155.3	27151.5	349.0		6644.8	14.8	583.3			8340.1	1599.7	625.3	23495.5	126.2	906.1
WS33	358.2	956.9	26896.7	1.4		4456.6	4.2	133.2	312.0	531.7	1618.0	732.4	69.4	28791.6	12.8	728.2
WS34	0.8	4.4	10034.2	20.7		2625.3	13.5	316.5	0.3			1248.2	455.3	10873.8	7.1	427.5
WS35	169.9	24.8	26286.0	9.3		11226.9	38.5	1.4	568.9		1119.4	348.6	294.4	35036.7		376.0
WS36	0.1	91.9	24699.1			1791.1	405.8	139.6	6.8	58.5			88.0	26332.8	319.3	295.8
WS37		252.7	23748.3	1455.2		1636.9	3.4	222.3			11751.9	1554.3	0.1	11761.6		2240.1
Total	**960.5**	**45037.1**	**771496.1**	**21123.2**	**808.1**	**148559.5**	**2093.5**	**1709.7**	**926.9**	**25000.1**	**311974.3**	**40273.5**	**24491.7**	**579553.8**	**1957.7**	**7301.5**
Min	**0.1**	**4.4**	**663.2**	**0.2**	**4.5**	**108.1**	**0.0**	**1.4**	**0.1**	**0.2**	**2.9**	**3.5**	**0.1**	**1223.9**	**7.1**	**0.5**
Max	**358.2**	**15486.1**	**56690.3**	**4036.7**	**368.8**	**17245.9**	**508.1**	**583.3**	**568.9**	**11155.4**	**22731.6**	**5469.3**	**3693.8**	**38670.6**	**468.1**	**2240.1**
Aver.	**43.7**	**1217.2**	**20851.2**	**782.3**	**67.3**	**4015.1**	**72.2**	**114.0**	**51.5**	**1388.9**	**8913.6**	**1220.4**	**661.9**	**15663.6**	**217.5**	**456.3**

Appendix D

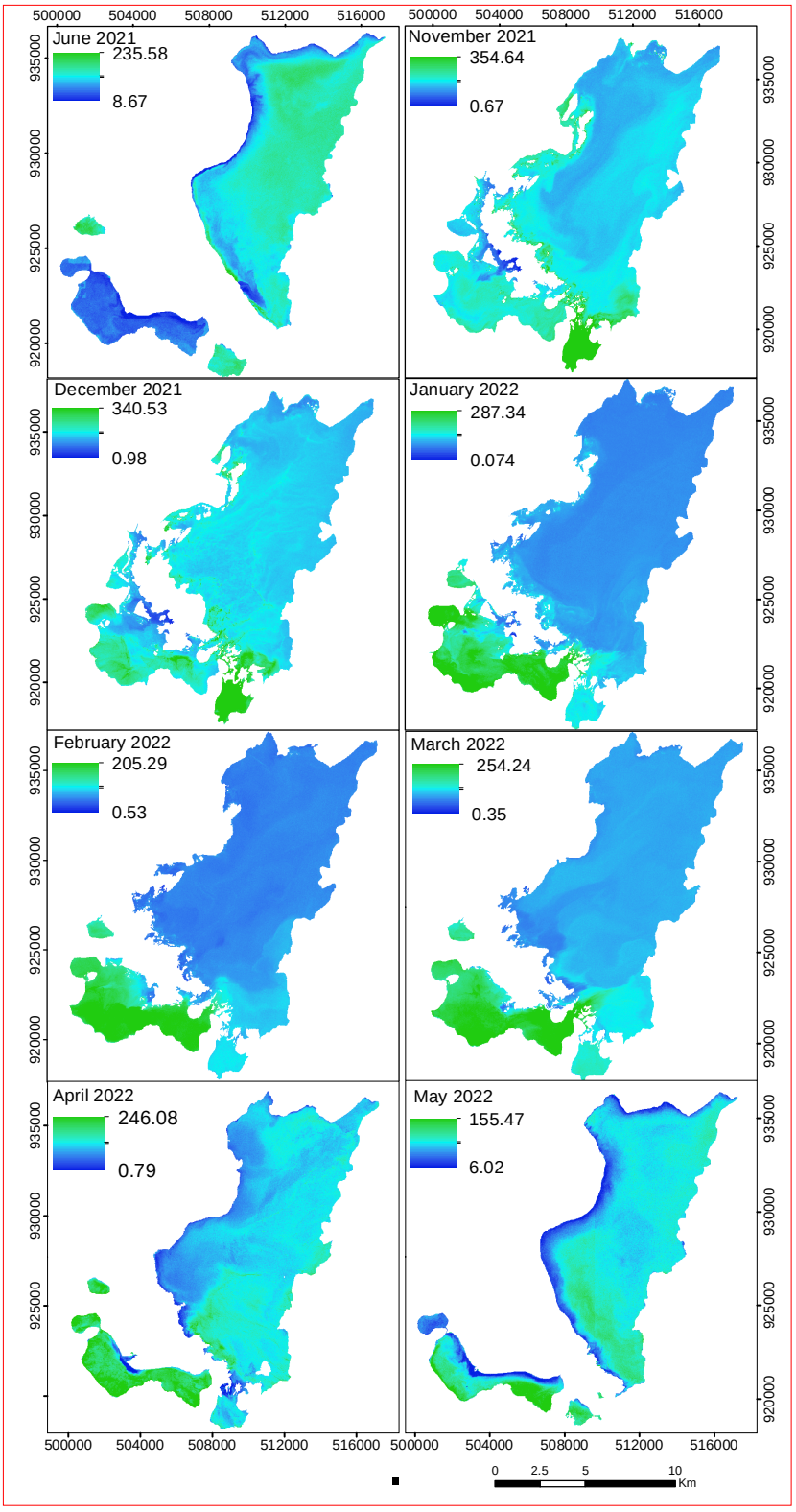

Appendix D Figure 1 Monthly chlorophyll a (in µg/L) spatial distribution

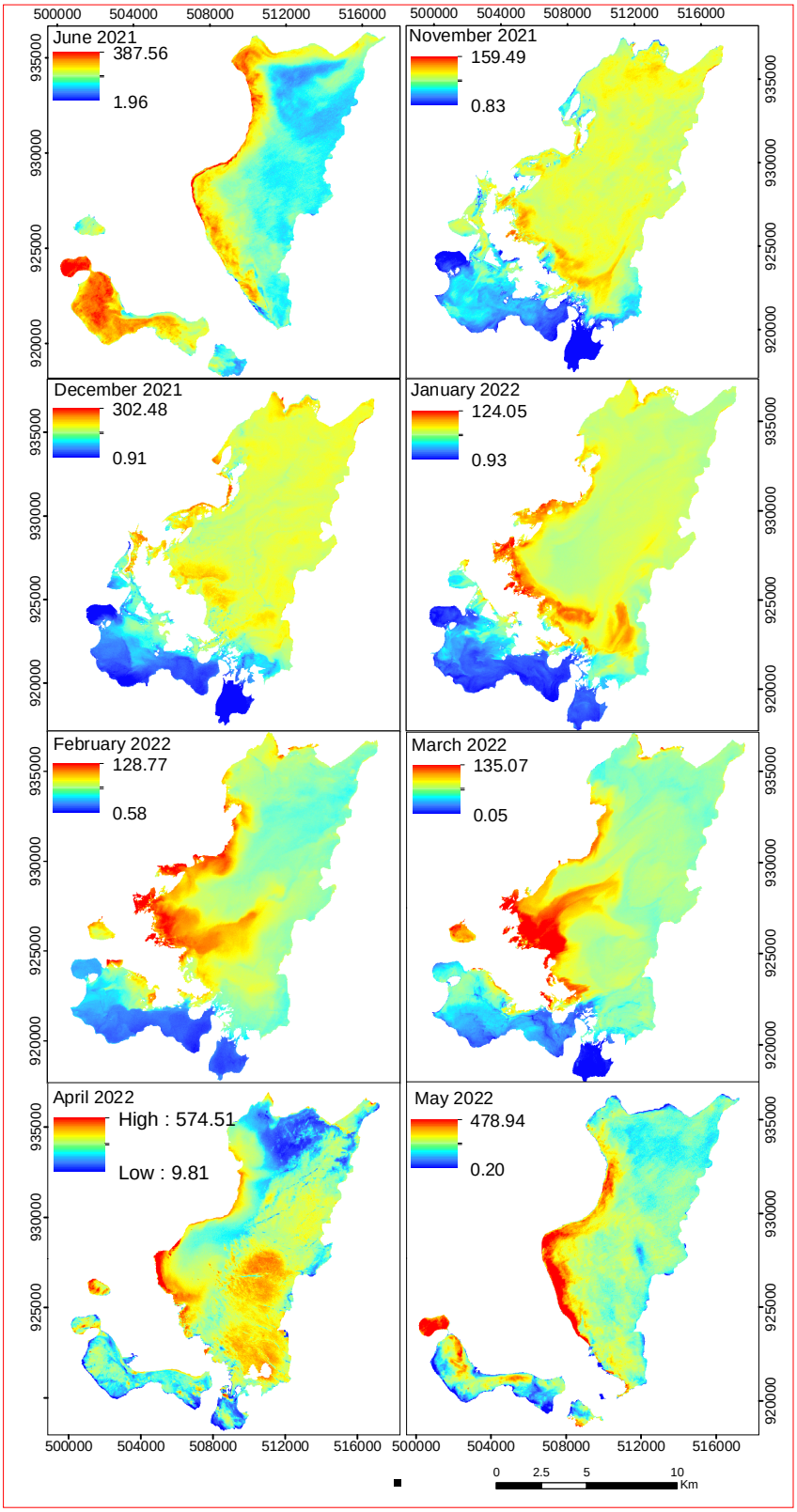

Appendix D Figure 2 Monthly TSS (in mg/L) spatial distribution

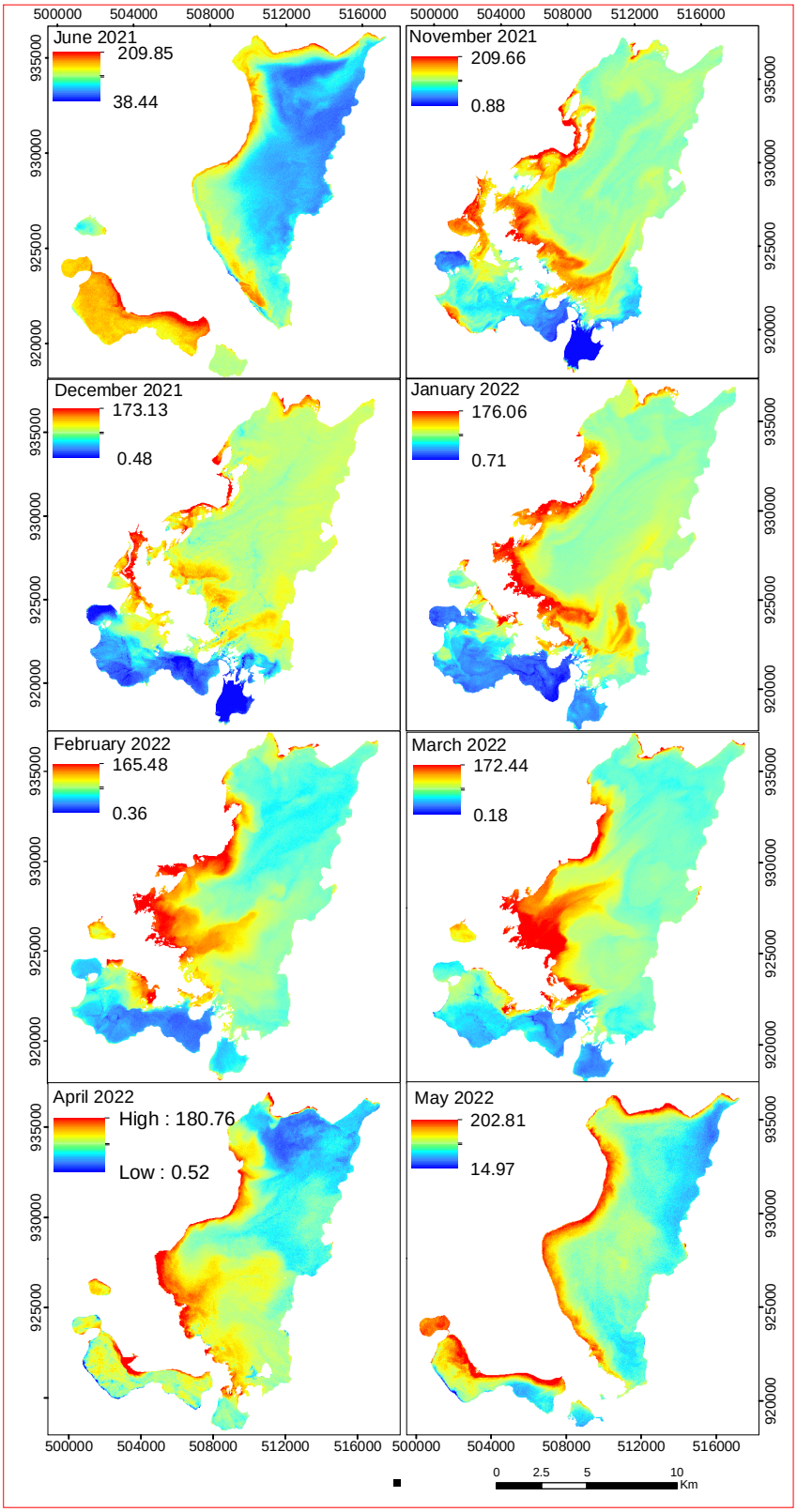

Appendix D Figure 3 Monthly TU (NTU) spatial distribution

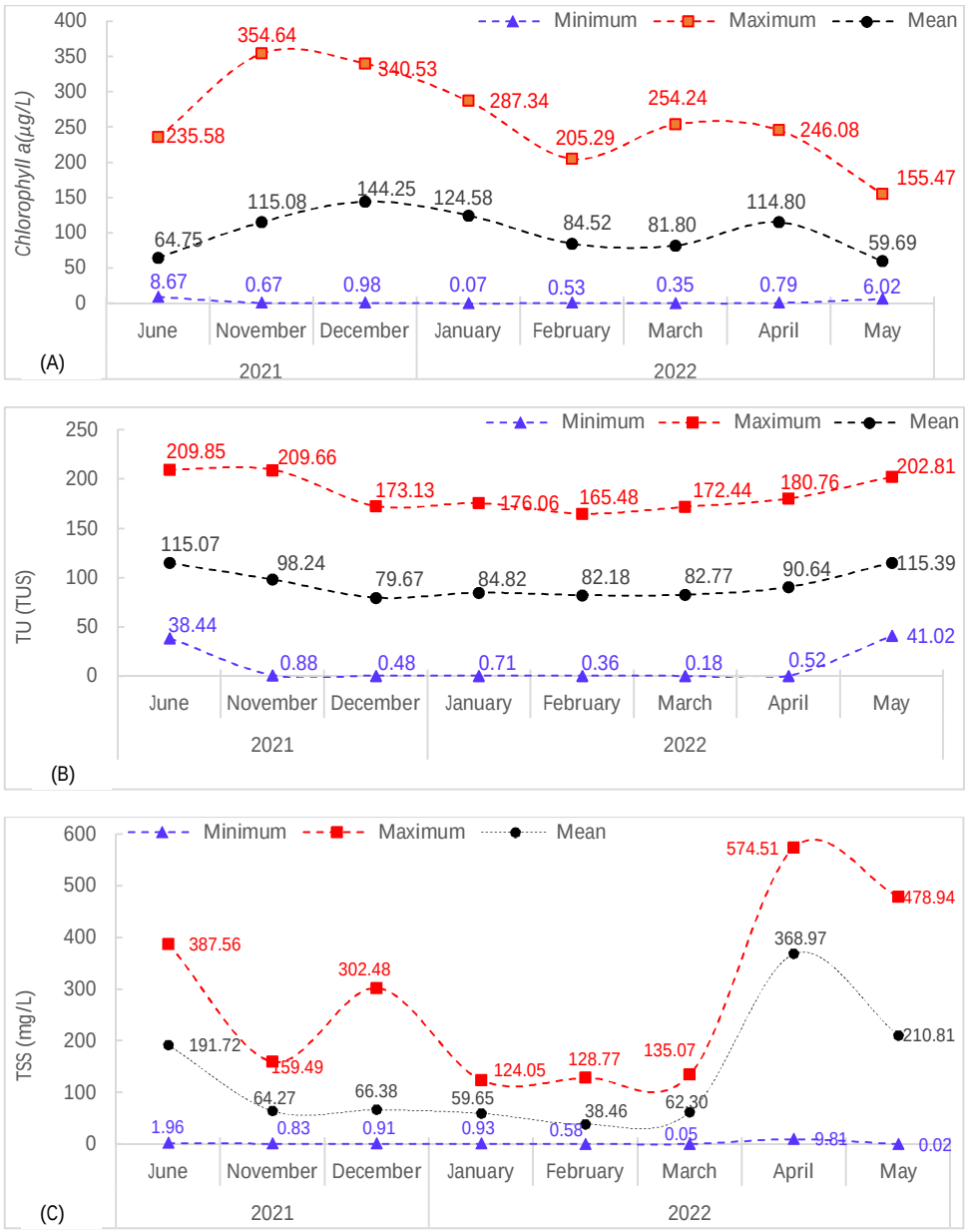

Appendix D Figure 4 Monthly bases temporal WQPs

Monthly bases temporal WQPs from Sentinel 2A satellite image using linear regression models equation 8, 9 and 10. (A)-chlorophyll a (µg/L), (B)-Turbidity (NTU), (C)- Total Suspended Sediment (mg/L)

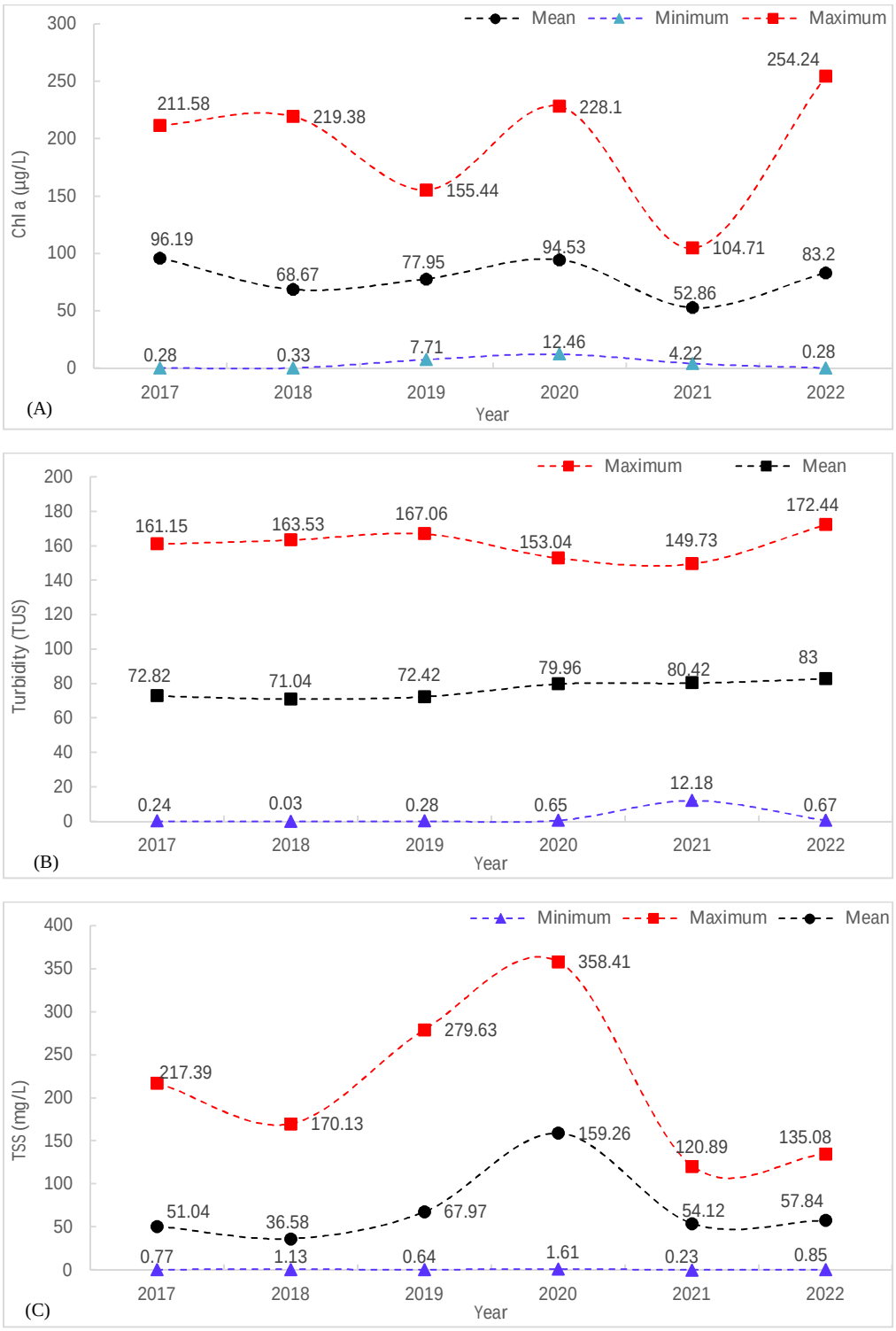

Appendix D Figure 5 Yearly temporal WQPs

Yearly temporal WQPs from Sentinel 2A satellite image using linear regression models. (A)-chlorophyll a (µg/L), (B)-Turbidity (NTU), (C)- Total Suspended Sediment (mg/L)

Turnitin Originality Report

Processed on: 09-Feb-2024 8:53 PM EAT
ID: 2290543120
Word Count: 108611
Submitted: 1

PhD Endaweke By Endaweke E.

Similarity Index	Similarity by Source
14%	Internet Sources: 9% Publications: 9% Student Papers: 3%

2% match (Internet from 28-Jan-2023)
https://www.researchgate.net/publication/321395102_Evaluating_water_quality_of_Awash_River_using_water_quality_index

1% match (Sustainability of Integrated Water Resources Management, 2015.)
Sustainability of Integrated Water Resources Management, 2015.

1% match (Internet from 22-Oct-2022)
http://etd.aau.edu.et/bitstream/handle/123456789/19494/Amare%20Shiberu.pdf?isAllowed=y&sequence=1

1% match (Alireza Arab Ameri, Hamid Reza Pourghasemi, Artemi Cerda. "Erodibility prioritization of sub-watersheds using morphometric parameters analysis and its mapping: A comparison among TOPSIS, VIKOR, SAW, and CF multi-criteria decision making models", Science of The Total Environment, 2018)
Alireza Arab Ameri, Hamid Reza Pourghasemi, Artemi Cerda. "Erodibility prioritization of sub-watersheds using morphometric parameters analysis and its mapping: A comparison among TOPSIS, VIKOR, SAW, and CF multi-criteria decision making models", Science of The Total Environment, 2018

< 1% match (Internet from 03-Feb-2023)
https://www.researchgate.net/publication/334486444_Virological_Quality_of_Urban_Rivers_and_Hospitals_Wastewaters_in_Addis_Ababa_Ethio

< 1% match (Internet from 17-Feb-2023)
https://www.researchgate.net/publication/343620749_Physicochemical_characterization_of_effluents_from_industries_in_Sabata_town_of_Ethi

< 1% match (Internet from 31-Jan-2022)
http://etd.aau.edu.et/bitstream/handle/123456789/22502/Achenafi%27s%20PhD%20Dissertation.pdf?isAllowed=y&sequence=1

< 1% match (Internet from 14-Jul-2023)
https://ouci.dntb.gov.ua/works/4OnXxXq7/

< 1% match (Internet from 11-Jun-2022)
https://ouci.dntb.gov.ua/works/4wAxnE89/

< 1% match (Internet from 24-Aug-2018)
https://swat.tamu.edu/media/69009/swat-proceedings-2012-india.pdf

< 1% match (Internet from 16-Dec-2022)
https://swat.tamu.edu/media/49257/conference-proceedings.pdf

< 1% match (Internet from 24-Sep-2022)
http://real-j.mtak.hu/22934/4/AEER_2020_18_4_.pdf

< 1% match (student papers from 17-Feb-2021)
Submitted to University of Sheffield on 2021-02-17

< 1% match ("Drainage Basin Dynamics", Springer Science and Business Media LLC, 2022)
"Drainage Basin Dynamics", Springer Science and Business Media LLC, 2022

< 1% match ()
Angello, Zelalem Abera (gnd: 1273351061), "Selection of optimal pollution management strategy for the Little Akaki River, Ethiopia, based on determination of spatio-temporal pollutant dynamics and water quality modeling", Universität Rostock, Agrar- und Umweltwissenschaftliche Fakultät, Professur Wasserwirtschaft Rostock, 2022

< 1% match (Internet from 11-Jan-2022)
http://sutir.sut.ac.th:8080/jspui/bitstream/123456789/8750/2/Fulltext.pdf

< 1% match (Abdulkerim Bedewi Serur, Kero Arigaw Adi. "Multi-site calibration of hydrological model and the response of water balance components to land use land cover change in a rift valley Lake Basin in Ethiopia", Scientific African, 2022)
Abdulkerim Bedewi Serur, Kero Arigaw Adi. "Multi-site calibration of hydrological model and the response of water balance components to land use land cover change in a rift valley Lake Basin in Ethiopia", Scientific African, 2022

< 1% match (Springer Earth System Sciences, 2015.)
Springer Earth System Sciences, 2015.

< 1% match ()
Rahman, Md. Masihur, "Hydrologic Modelling of Great Lakes Basin in Southern Ontario and Climate Change Impact Assessment", 'University of Windsor Leddy Library', 2021

< 1% match ()